ISSN 1007-9327 (print)
ISSN 2219-2840 (online)

World Journal of *Gastroenterology*

World J Gastroenterol 2022 August 21; 28(31): 4235-4474

Published by Baishideng Publishing Group Inc

World Journal of Gastroenterology

Contents

Weekly Volume 28 Number 31 August 21, 2022

REVIEW

MINIREVIEWS

ORIGINAL ARTICLE

Basic Study

Retrospective Study

World Journal of Gastroenterology

Weekly Volume 28 Number 31 August 21, 2022

Contents

ABOUT COVER

Editorial Board Member of *World Journal of Gastroenterology*, Mortada H F El-Shabrawi, MD, FAASLD, Professor, Department of Paediatrics, Kasr Alainy School of Medicine, Cairo University, Cairo 11562, Egypt. melshabrawi@kasralainy.edu.eg

AIMS AND SCOPE

The primary aim of *World Journal of Gastroenterology* (*WJG*, *World J Gastroenterol*) is to provide scholars and readers from various fields of gastroenterology and hepatology with a platform to publish high-quality basic and clinical research articles and communicate their research findings online. *WJG* mainly publishes articles reporting research results and findings obtained in the field of gastroenterology and hepatology and covering a wide range of topics including gastroenterology, hepatology, gastrointestinal endoscopy, gastrointestinal surgery, gastrointestinal oncology, and pediatric gastroenterology.

INDEXING/ABSTRACTING

The *WJG* is now abstracted and indexed in Science Citation Index Expanded (SCIE, also known as SciSearch®), Current Contents/Clinical Medicine, Journal Citation Reports, Index Medicus, MEDLINE, PubMed, PubMed Central, Scopus, Reference Citation Analysis, China National Knowledge Infrastructure, China Science and Technology Journal Database, and Superstar Journals Database. The 2022 edition of Journal Citation Reports® cites the 2021 impact factor (IF) for *WJG* as 5.374; IF without journal self cites: 5.187; 5-year IF: 5.715; Journal Citation Indicator: 0.84; Ranking: 31 among 93 journals in gastroenterology and hepatology; and Quartile category: Q2. The *WJG*'s CiteScore for 2021 is 8.1 and Scopus CiteScore rank 2021: Gastroenterology is 18/149.

RESPONSIBLE EDITORS FOR THIS ISSUE

Production Editor: *Yi-Xuan Cai*; **Production Department Director:** *Xiang Li*; **Editorial Office Director:** *Jia-Ru Fan.*

NAME OF JOURNAL
World Journal of Gastroenterology

ISSN
ISSN 1007-9327 (print) ISSN 2219-2840 (online)

LAUNCH DATE
October 1, 1995

FREQUENCY
Weekly

EDITORS-IN-CHIEF
Andrzej S Tarnawski

EDITORIAL BOARD MEMBERS
http://www.wjgnet.com/1007-9327/editorialboard.htm

PUBLICATION DATE
August 21, 2022

INSTRUCTIONS TO AUTHORS
https://www.wjgnet.com/bpg/gerinfo/204

GUIDELINES FOR ETHICS DOCUMENTS
https://www.wjgnet.com/bpg/GerInfo/287

GUIDELINES FOR NON-NATIVE SPEAKERS OF ENGLISH
https://www.wjgnet.com/bpg/gerinfo/240

PUBLICATION ETHICS
https://www.wjgnet.com/bpg/GerInfo/288

PUBLICATION MISCONDUCT
https://www.wjgnet.com/bpg/gerinfo/208

ARTICLE PROCESSING CHARGE
https://www.wjgnet.com/bpg/gerinfo/242

STEPS FOR SUBMITTING MANUSCRIPTS
https://www.wjgnet.com/bpg/GerInfo/239

ONLINE SUBMISSION
https://www.f6publishing.com

World Journal of Gastroenterology

Submit a Manuscript: https://www.f6publishing.com

World J Gastroenterol 2022 August 21; 28(31): 4235-4248

DOI: 10.3748/wjg.v28.i31.4235

ISSN 1007-9327 (print) ISSN 2219-2840 (online)

REVIEW

Early diagnosis of pancreatic cancer: What strategies to avoid a foretold catastrophe

Valeria Tonini, Manuel Zanni

Specialty type: Oncology

Provenance and peer review: Invited article; Externally peer reviewed.

Peer-review model: Single blind

Peer-review report's scientific quality classification

Grade A (Excellent): 0
Grade B (Very good): B
Grade C (Good): C
Grade D (Fair): 0
Grade E (Poor): 0

P-Reviewer: Jeong KY, South Korea; Khalil MTASH, Egypt

Received: March 24, 2022
Peer-review started: March 24, 2022
First decision: May 9, 2022
Revised: May 18, 2022
Accepted: July 24, 2022
Article in press: July 24, 2022
Published online: August 21, 2022

Valeria Tonini, Manuel Zanni, Department of Medical and Surgical Sciences, University of Bologna, Bologna 40138, Italy

Corresponding author: Valeria Tonini, MD, PhD, Adjunct Associate Professor, Professor, Surgeon, Surgical Oncologist, Department of Medical and Surgical Sciences, University of Bologna, Via Massarenti 9, Bologna 40138, Italy. valeria.tonini@unibo.it

Abstract

While great strides in improving survival rates have been made for most cancers in recent years, pancreatic ductal adenocarcinoma (PDAC) remains one of the solid tumors with the worst prognosis. PDAC mortality often overlaps with incidence. Surgical resection is the only potentially curative treatment, but it can be performed in a very limited number of cases. In order to improve the prognosis of PDAC, there are ideally two possible ways: the discovery of new strategies or drugs that will make it possible to treat the tumor more successfully or an earlier diagnosis that will allow patients to be operated on at a less advanced stage. The aim of this review was to summarize all the possible strategies available today for the early diagnosis of PDAC and the paths that research needs to take to make this goal ever closer. All the most recent studies on risk factors and screening modalities, new laboratory tests including liquid biopsy, new imaging methods and possible applications of artificial intelligence and machine learning were reviewed and commented on. Unfortunately, in 2022 the results for this type of cancer still remain discouraging, while a catastrophic increase in cases is expected in the coming years. The article was also written with the aim of highlighting the urgency of devoting more attention and resources to this pathology in order to reach a solution that seems more and more unreachable every day.

Key Words: Pancreatic cancer; Pancreatic ductal adenocarcinoma; Early diagnosis; Liquid biopsy; Pancreatic cancer biomarkers; Artificial intelligence; Pancreatic cancer screening

Core Tip: Pancreatic ductal adenocarcinoma is one of the solid neoplasms with the worst prognosis. Surgical resection is the only potentially curative treatment. In 80% of patients, pancreatic ductal adenocarcinoma is discovered at a stage too advanced for surgery. The aim of this review was to summarize all the possible strategies available today for the early diagnosis of pancreatic ductal adenocarcinoma and the paths that research must take to make this goal ever closer. The article highlights the urgency of devoting more attention and resources to this pathology in order to reach a solution that seems more and more unreachable every day.

Citation: Tonini V, Zanni M. Early diagnosis of pancreatic cancer: What strategies to avoid a foretold catastrophe. *World J Gastroenterol* 2022; 28(31): 4235-4248
URL: https://www.wjgnet.com/1007-9327/full/v28/i31/4235.htm
DOI: https://dx.doi.org/10.3748/wjg.v28.i31.4235

INTRODUCTION

Pancreatic ductal adenocarcinoma (PDAC) is ranked as the seventh leading cause of cancer deaths worldwide, while it ranks fourth in the Western world, just behind lung, colorectal and breast cancers. Rahib *et al*[1] estimated that it will become the second leading cause of cancer death by 2030. The 2020 global cancer statistics reported a total of nearly 496000 new cases of PDAC and more than 466000 related deaths. PDAC mortality is almost overlapping with incidence[2].

The 5-year survival rate of PDAC is less than 10%[3]. A study that included 84275 patients showed that the 5-year survival rate increased from 0.9% in 1975 to 4.2% in 2011, considering all stages of PDAC. In patients undergoing surgical resection, it increased from 1.5% to 17.4%[4], while in unresected patients by 0.8% in 1975 and 0.9% in 2011. The high mortality and poor improvement in survival rates over the years are due to several factors. First, the retroperitoneal location of the pancreas results in the appearance of symptoms only when the neoplasm has reached considerable size, and diagnosis is often made at an advanced stage of the disease. Second, PDAC is inherently characterized by a fierce biology with early metastasis, and in fact about half of patients have metastatic disease at the time of presentation. Third, PDAC drastically weakens patients, limiting the possibility of aggressive treatments. Finally, through the desmoplastic reaction, it shows resistance to many antineoplastic therapies[5,6].

The 5-year survival rate for patients with stage 0 (in situ) according to the Union for International Cancer Control classification is 85.8%, while that of patients with stage IA is 68.7%. In the early stages of the disease, therefore, the prognosis is relatively good[7,8]. Early diagnosis of the disease is therefore essential.

Our efforts should focus on recognizing risk factors that contribute to the development of the disease in order to define the population at risk that could benefit from a screening protocol and on researching new techniques for early diagnosis[9-12].

RISK FACTORS AND STRATIFICATION

Several non-modifiable and modifiable risk factors are correlated with PDAC. Non-modifiable risk factors include the patient's age, ethnicity, gender, blood type, microbiota, diabetes mellitus, family history and genetic predisposition, while modifiable risk factors include tobacco use, alcohol consumption, diet, pancreatitis, obesity and socioeconomic status[12]. According to some studies, one-third of all cancers could be prevented through lifestyle improvement. The EPIC study, for example, evaluated the association between healthy lifestyle index score and pancreatic cancer[13,14]. A three-point increase in this score, achieved through adherence to healthy behaviors, is associated with a 16%-23% lower risk[15]. No smoking, making your home/workplace smoke-free, maintaining a normal body weight, having a diet rich in grains, legumes, and vegetables and limiting alcohol intake are key factors in the prevention of PDAC.

According to several studies, the new onset of diabetes in an elderly patient should suggest PDAC, especially if such a finding is associated with unintentional weight loss[16-18]. A study by Pelaez-Luna *et al*[19] evaluated the use of computed tomography (CT) scans in asymptomatic patients at the time of diabetes diagnosis and found a higher likelihood of detecting potentially resectable tumors compared with scans performed 6 mo later. However, CT-based screening of all elderly patients with new-onset diabetes (NOD) is not feasible[18]. Screening programs and guidelines will likely be updated when the features that differentiate pancreatic cancer-associated diabetes from other cases of NOD are identified.

The creation of a pancreatic cancer risk prediction model based on the integration of multiple risk factors could contribute to its early detection[20]. Sharma *et al*[21] developed a model called Enriching New-Onset Diabetes for Pancreatic Cancer that weights the scores of three factors including weight change, blood glucose change and age at diabetes onset in patients with NOD. A score of at least three points in the Enriching New-Onset Diabetes for Pancreatic Cancer model was able to identify individuals who developed PDAC within 3 years of the onset of diabetes with good sensitivity and specificity[21].

In addition to the strictly environmental risk factors, familial pancreatic cancer and genetic syndromes (hereditary breast and ovarian cancer syndrome, Lynch syndrome, familial atypical multiple melanoma, Peutz-Jegher syndrome, Li-Fraumeni syndrome and hereditary pancreatitis) are added. Familial pancreatic cancer is defined by the occurrence of PDAC in at least two first-degree relatives and accounts for up to 10% of all cases of PDAC[22].

Patients at high risk for developing PDAC include those with inherited risk factors (both genetic syndromes and familial pancreatic cancer), those with NOD and those with cystic lesions of the pancreas.

Pancreatic cysts are found in approximately 8% of individuals over the age of 70 years[23] and include intraductal papillary mucinous neoplasms (IPMN) and mucinous cystic neoplasms, both of which are precursors to PDAC. IPMN and mucinous cystic neoplasms are collectively referred to as mucinous cystic lesions. In contrast to the third precursor lesion, pancreatic intraepithelial neoplasia, which can be identified only at surgical histopathology, mucinous cystic lesions are easy to detect and are found incidentally in 3% of CT subjects[23]. Therefore, their identification offers the potential for early diagnosis of PDAC. However, there are two problems. First, not all pancreatic cystic lesions are IPMN or mucinous cystic neoplasms. Many are cystic lesions without risk of malignant transformation, and therefore do not require surveillance. Second, most IPMN and mucinous cystic neoplasms do not progress to PDAC. Over the years, evidence has been found to predict the possibility of progression to PDAC[23].

In mucinous cystic neoplasms the presence of eggshell calcification, larger tumor size or a mural nodule on cross-sectional imaging is suggestive of malignancy[24]. Regarding IPMN, worrisome (main duct 5-9 mm, enhancing mural nodule < 5 mm, thickened, enhancing cyst wall, branch duct IPMN > 3 cm, abrupt caliber change in main duct with upstream atrophy, lymphadenopathy, pancreatitis, increased serum 19-9, cyst growth > 5 mm over 2 years) and high-risk features (main duct > 1 cm, enhancing, mural nodule > 5 mm, jaundice) have been defined[25].

However, these clinical features are still imperfect in differentiating between benign cysts and mucinous cystic lesions that harbor high-grade dysplasia or PDAC and require surgical resection and mucinous cystic lesions that have low-grade dysplasia and are safe to look at.

For the time being, a screening program is offered to individuals with a strong family history and/or genetic predisposition to develop pancreatic cancer and subjects with mucinous cystic lesions of the pancreas. The primary goals of screening are the detection of high-grade dysplastic precancerous lesions (IPMN and pancreatic intraepithelial neoplasia) and T1N0M0 pancreatic cancer that are more amenable to potentially curative resection[26].

The current recommendation is to perform endoscopic ultrasound (EUS) or magnetic resonance imaging (MRI)/magnetic resonance cholangiopancreatography. Screening is recommended at age 50 years or 10 years before the youngest relative with PDAC in familial pancreatic cancer cases. In other settings, screening is performed between the ages of 35 years and 45 years. In case the patient had a normal pancreas on imaging, it is recommended to repeat the procedure every year alternating EUS and magnetic resonance cholangiopancreatography. However, no consensus has been found on the preferred modality and optimal timing/frequency. This reflects the absence of robust data in the literature and underscores the lack of biological tools to detect precancerous lesions early.

IMAGING

There are several imaging methods that can identify pancreatic cancer at an early stage. Contrast-enhanced CT and MRI according to Japanese guidelines[27] are the first methods to be performed in patients with suspected PDAC based on clinical symptoms, serum pancreatic enzymes, tumor markers and transabdominal US. They are supplemented by EUS and endoscopic retrograde cholangiopancreatography (ERCP).

A study evaluated the diagnostic accuracy of US, CT, MRI, and EUS in 200 cases of PDAC stage 0/1. Only 20% of patients were symptomatic[28]. The diagnostic accuracy was 67.5%, 98.0%, 86.5%, and 86.5%, respectively. According to some authors, CT and US are procedures with limitations in the early detection of pancreatic cancer because only indirect signs, such as pancreatic duct dilatation, localized pancreatic atrophy or local fat changes in the pancreatic parenchyma, can be detected with these methods[20].

Two systematic reviews[29,30] evaluated the performance of EUS in the diagnosis of pancreatic cancer. In the first review, EUS was shown to have higher sensitivity than CT (91%-100% *vs* 53%-91%),

while in the second review, Kitano *et al*[30] reported that EUS was more sensitive than US and CT (94% *vs* 67% and 98% *vs* 74%, respectively).

However, conventional EUS does not distinguish carcinoma from other etiologies very well because most pancreatic tumors, including benign ones, have a hypoechogenic appearance. Contrast-enhanced EUS can improve imaging of parenchymal perfusion and microvessels in pancreatic pathology. This method has higher sensitivity (94.5% *vs* 83.1%) and specificity (84.1% *vs* 78.6%) than conventional EUS [31,32].

Endoscopic ultrasonography guided fine needle aspiration (EUS-FNA) represents the first-line method for pathological diagnosis. In relation to lesion size, the accuracy of EUS-FNA is 93.4% for lesions ≥ 20 mm, 83.5% for lesions of 10-20 mm and 82.5% for lesions of 10 mm or less[33]. Sometimes CT, MRI and EUS fail to detect early stage pancreatic tumors and it is difficult to collect specimens with EUS-FNA. In this situation, especially with regard to PDAC in situ, the only available imaging finding is localized stenosis of the main pancreatic duct. Detailed evaluation of the pancreatic duct by ERCP and subsequent cytology of pancreatic juice become extremely important for diagnosis. In this context, ERCP has a sensitivity and specificity of 57.9% and 90.6%[34]. The sensitivity of pancreatic juice cytology in the diagnosis of PDAC in situ is 72.2%-100%[28,35].

ERCP is particularly useful in distinguishing autoimmune pancreatitis from PDAC, especially in patients[36] with atypical pancreatic parenchymal findings, such as focal enlargement of the pancreas and mass formation.

Ikemoto *et al*[37] proposed a recent algorithm for early diagnosis of PDAC in stage 0 and IA, with a promising long-term prognosis. In addition to pancreatic laboratory tests, US should be performed earlier in patients with risk factors in order to identify asymptomatic patients. Patients with an obvious tumor are managed according to conventional algorithms. Patients who do not have an overt pancreatic tumor but have indirect findings, such as abnormalities of the main pancreatic duct, cystic lesions or pancreatic atrophy, should be evaluated by MRI with magnetic resonance cholangiopancreatography. If the MRI shows abnormalities suggestive for PDAC, EUS-FNA is performed[37].

ARTIFICIAL INTELLIGENCE APPLIED TO IMAGING

Great hopes are now pinned on artificial intelligence (AI) for solving the most difficult problems in medicine, and these include the early diagnosis of PDAC. AI is the ability of a computer to perform functions and reasoning typical of the human mind completely autonomously. In the deepest sense, it is the ability of a machine to learn and improve automatically based on experience, provided directly through data. In this way, AI becomes a powerful tool for discovering signals that are difficult for humans to infer or describe and for expanding the frontiers of our scientific capabilities.

Muhammad *et al*[38] used AI to predict the risk of developing PDAC. By analyzing variables such as demographic data, comorbidities and family history, they built a model capable of predicting the development of PDAC with good accuracy [area under the curve (AUC) of 0.85][38,39].

The application of AI in the field of radiology is also very promising, as AI is capable of analyzing thousands of images on a pixel-by-pixel level, does not make human errors and achieves data processing in a short time[40]. Several studies have reported the application of AI in EUS image analysis of pancreatic diseases. Das *et al*[41] evaluated the performance of AI in differentiating PDAC from normal pancreas and chronic pancreatitis. The algorithm they used identified neoplasia with an AUC of 0.93. A recent study by Zhu *et al*[42] reported an overall accuracy of 94% by AI in distinguishing pancreatic cancer from chronic inflammation. CT is the most explored medical imaging modality with AI. Liu *et al*[43] reported an AUC of 0.963 for the diagnosis of PDAC using CT with the AI platform. In addition, the time to diagnosis was 20 s/case, certainly less than the time needed by radiologists. The same authors, in more recent work, found 99% accuracy for analysis based on the use of AI. In this study, AI provided higher sensitivity than radiologists (0.983 *vs* 0.929, respectively)[44]. AI missed 3 (1.7%) of 176 PDACs (1.1-1.2 cm), while radiologists missed 12 (7%) of 168 PDACs (1.0-3.3 cm), of which 11 (92%) were correctly detected by AI.

Two important ongoing projects should be noted. Project Felix is a multidisciplinary study led by Johns Hopkins University, which compared 156 PDAC cases and 300 healthy controls using deep learning computer models with manually segmented images. In an initial report, they reported a sensitivity and specificity of 94% and 99%, respectively[45]. The analysis was subsequently expanded to 575 normal patients and 750 patients with PDAC. The second ongoing project is being conducted by the Alliance of Pancreatic Cancer Consortium Imaging Working Group[46]. The goal of the project is to create a shared repository by collecting pre- and post-diagnosis CT, MRI and US images of patients with PDAC to develop AI that can predict the onset of pancreatic cancer and/or diagnose it at an early stage [47].

LIQUID BIOPSY

Serum biomarkers

Carbohydrate antigens: The most validated serum tumor marker in terms of diagnostic, prognostic and surveillance capacity for pancreatic cancer is CA19-9. The sensitivity and specificity of elevated CA19-9 to detect PDAC are 79% and 82%, respectively[48,49].

However, the use of CA19-9 has several limitations. Approximately 10% of the Caucasian population has reduced CA19-9 production due to Lewis antigen dependence. In addition, there are several conditions that result in the increase of the biomarker, such as obstructive jaundice, liver cirrhosis, chronic pancreatitis and cholangitis. The low positive predictive value of CA19-9 limits its application as a screening tool for larger populations[48,50-52]. Other carbohydrate antigens have been evaluated for early diagnosis of pancreatic cancer, such as CA125, CA72-4[53], CA50, CA199 and CA242[48,54]. The solitary diagnostic potential of these biomarkers could not be verified; however, they could help in discriminating between benign and malignant pancreatic lesions in combination with CA19-9[48].

Circulating tumor DNA and circulating tumor cells: New and interesting diagnostic tools in the field of pancreatic cancer are circulating tumor DNA (ctDNA) and circulating tumor cells (CTCs). In patients with malignancies, cell-free circulating DNA (cfDNA) molecules are released from tumor cells by apoptosis, necrosis or active release and are called ctDNA. The ctDNA contains mutations specific to the cancer cells from which they are released[55,56]. Thanks to these DNA molecules, it is therefore possible to trace the presence or absence of cancer.

However, a recent meta-analysis evaluated the role of ctDNA in the diagnosis of PDAC and found a rather low sensitivity[57]. This happens because in the early stages the rate of necrosis and apoptosis is lower and not enough ctDNA is released into the circulation (in the early stages of PDAC, only one molecule of circulating tumor DNA can be detected for every 5 mL of plasma)[57]. This challenge could be solved with technological advances, and ctDNA could become an important tool for early diagnosis.

CtDNA has been studied together with other biomarkers to improve its sensitivity and specificity. The combination of KRAS mutations in ctDNA and CA19-9 proved to be particularly interesting. Indeed, it showed a sensitivity and specificity of 0.98 and 0.77, respectively, to differentiate PDAC from chronic pancreatitis and sensitivity and specificity of 0.82 and 0.81 to differentiate PDAC from benign pancreatic tumors[56,58]. Combining the KRAS mutation in ctDNA with four protein biomarkers (CEA, CA19-9, hepatocyte growth factor and osteopontin) identified 64% of patients with pancreatic cancer with a specificity of 0.99[59]. This strategy seems to be very promising; however, it needs validation through studies on large populations.

Analysis of epigenetic alterations in cfDNA also seems to play an important role. By assessing the methylation status of two genes (*ADAMTS1* and *BNC1*) in cfDNA, it seems possible to identify pancreatic cancer early with a sensitivity of 0.95 and specificity of 0.92[60]. In a pilot study, it was reported that a model combining changes in 5-methylcytosine and 5-hydroxymethylcytosine in cfDNA achieved a sensitivity of 0.94 and specificity of 0.95, with an AUC of 0.99 for the diagnosis of PDAC[61].

The ability of targeted cfDNA methylation analysis to detect and localize multiple cancer types at all stages was evaluated. Among patients included with PDAC at different stages, a sensitivity of 0.63 in stage I, 0.83 in stage II, 0.75 in stage III and 1.0 in stage IV was found[62]. These changes in cfDNA methylation could be very useful for monitoring risk groups[63].

CTCs can be isolated tumor cells or cells organized in a group to form a tumor microthrombus[64] and are detected in 21%-100% of patients with PDAC[65]. According to some studies, they can be detected in 75%-80% of patients with early-stage tumors[66] and up to 88% of patients with precursor lesions, predominantly IPMNs[67-69]. Notably, CTCs identify patients with high-grade dysplasia, indicating its potential to stratify high-grade IPMNs against low-grade IPMNs and other benign cysts [67]. In a meta-analysis, the sensitivity, specificity and AUC for PDAC diagnosis of ctDNA, exosomes and CTCs were evaluated. They were 0.64, 0.92 and 0.94 for ctDNA, 0.93, 0.92 and 0.98 for exosomes and 0.74, 0.83 and 0.81 for CTCs, respectively[57]. This lower AUC of CTCs is due to the possibility that CTCs become trapped in the liver when traveling through the portal vein[57]. The ability to detect CTCs by analyzing portal vein blood is greatly increased. They can be found in 100% of patients with metastatic PDAC[70] and in 58% of resectable patients[71]. As with ctDNA, the low amount of CTCs in the early stages is the main factor hindering their use as biomarkers[57].

RNA, metabolites and exosomes: The most significant microRNAs are *miR-21*, *miR-25* and *miR-233*. *miR-21* has a sensitivity for early diagnosis of 0.90 and a specificity of 0.72, while *miR-25* has a sensitivity of 0.75 and 0.93, respectively[72,73]. In contrast, *miR-233* has proven useful in the differential diagnosis between benign and malignant IPMNs[74]. The microRNAs offer a cumulative sensitivity for early-stage pancreatic cancer of 0.79 and a specificity of 0.74[75]. The combined use of CA19-9 and microRNAs can improve diagnostic accuracy, especially *miR-216*[76-77].

Potentially useful biomarkers also include long non-coding (lnc)RNAs. *SNHG15* lncRNA expression is found to be increased in patients with pancreatic cancer compared to healthy controls[78]. Permuth *et al*[79] demonstrated that the differential diagnosis between malignant and nonmalignant IPMNs can be made through the combination of eight lncRNAs. In addition, some lncRNAs (*HAND2-AS1*, *CTD-*

2033D15.2 and *lncRNA-TGF*) are early markers of IPMNs[80]. Other lncRNAs that might be useful in the early detection of pancreatic cancer and IPMN are *HOTAIR*, *MALAT1*, *MEG3*, *H19*, *PVT1*, *HOTTIP*[81], *HAND2-AS1*, *CTD-2033D15.2* and *lncRNA-TGF*[82].

The role of serum metabolites in pancreatic cancer has become of interest with the advent of metabolomic technologies involving nuclear magnetic resonance and mass spectrometry[83]. An important study was performed by Michálková *et al*[84], who developed a nuclear magnetic resonance-based model that included 12 metabolites (3-hydroxybutyrate, lactate, glutamine, alanine, valine, lysine, citrate, histidine, isoleucine, glutamate, acetone and dimethylamine). The model has 94% accuracy, 100% sensitivity and 90% specificity in distinguishing patients with PDAC from healthy individuals[84].

Another study compared the metabolomic profiles of serum samples from patients with NOD and those with PDAC and NOD[85]. This identified 62 different metabolites and found that a panel including N-succinyl-L-diaminopimelic and PE (18:2) had high sensitivity (93.3%) and specificity (93.1%). Currently, studies focusing on metabolomics are expensive and consequently rare; however, it is offering great results on the early diagnosis of PDAC. Further studies are desperately needed.

Recent studies are focusing on multimarker panels in combination with CA19-9. The combined use of eight proteins (S100A11, ITGB5, PPY, ERBB3, SCAMP3, RET, 5-NT, CEACAM1) discriminated with fair accuracy between patients with early stage I/II PDAC and healthy individuals[48,86].

A new and still much to be studied chapter in PDAC concerns the study of exosomes. Kitagawa *et al*[87] studied molecules of exosomal mRNA (*CCDC88A*, *ARF6*, *Vav3* and *WASF2*) and nucleolar RNA (*SNORA14B*, *SNORA18*, *SNORA25*, *SNORA74A* and *SNORD22*) and obtained excellent results for early-stage neoplasia. Tumor-specific expression of exosome surface proteins, the so-called tumor-specific surfaceome, can also be analyzed. Castillo *et al*[88] characterized six PDAC-specific surfaceome proteins, such as CLDN4, EPCAM, CD151, LGALS3BP, HIST2H2BE and HIST2H2BF. These proteins were suggested as promising biomarkers for PDAC diagnosis by the authors. Yu *et al*[89] developed a signature with long RNAs from plasma extracellular vesicles. This signature identified stage I/II pancreatic cancer with very high accuracy and performed better than CA19-9 in distinguishing PDAC from chronic pancreatitis (AUC 0.931 *vs* 0.873)[89]. Serum biomarkers are summarized in Table 1.

Pancreatic juice and pancreatic cyst fluid

In addition to blood, other body materials can be exploited to diagnose PDAC. For example, pancreatic juice collected during ERCP and cyst fluid obtained by EUS-FNA can be analyzed for specific markers. They include KRAS and GNAS mutants (the latter specific for IPMNs) as well as TP53, SMAD4, PIK3CA, PTEN and AKT1, which are generally related to IPMN-associated tumors[90-92].

Biomarkers still under study include mucins (MUCs). Normal pancreatic tissue expresses low levels of MUCs, whereas in branch duct IPMNs there is upregulation of the mucin gene and even more pronounced changes in PDAC[93-95]. MUC4 and MUC16 are 100% specific for pancreatic cancer but have sensitivities of 63% and 67%, respectively[95]. The combined biomarker panel consisting of MUC5AC and CA19-9 also showed excellent performance in distinguishing pancreatic cancer subjects from healthy controls[96].

It also seems possible to distinguish pancreatic cystic lesions with high-grade dysplasia or malignancy by assessing interleukins (IL-1b, IL-5 and IL-8) present in pancreatic juice or by using the monoclonal antibody Das-1. Das-1 can detect pancreatic cysts at risk of malignancy with a sensitivity of 88% and specificity of 98%[97-99].

In recent work by Majumder *et al*[100], a panel of three methylated DNA markers (C13orf18, FER1L4 and BMP3) in pancreatic juice discriminated cases from controls with good accuracy. Using a specificity cutoff value of 86%, the panel distinguished patients with any stage of pancreatic cancer from controls with a sensitivity of 83% and identified patients with stage I or II PDAC or IPMN with high-grade dysplasia with a sensitivity of 80%[100].

Saliva

Progress has also been made in saliva evaluation. A recent study[101] identified seven upregulated genes (*MBD3L2*, *KRAS*, *STIM2*, *DMXL2*, *ACRV1*, *DMD* and *CABLES1*) and five downregulated genes (*TK2*, *GLTSCR2*, *CDKL3*, *TPT1* and *DPM1*) in subjects with PDAC compared with healthy controls or those with chronic pancreatitis. It was possible to discriminate patients with pancreatic cancer with sensitivity and specificity greater than 90% by combining the mRNAs of *MBD3L2*, *KRAS*, *ACRV1* and *DPM1*[101]. Xie *et al*[102] evaluated the expression of lncRNAs and found an upregulation of *HOTAIR* and *PV1T* in the PDAC group compared with controls and benign pancreatic cancers. The combination of salivary *HOTAIR* and *PVT1* differentiated PDAC from healthy controls with a sensitivity of 78.2% and specificity of 90.9% and PDAC from benign tumors with a sensitivity of 81.8% and specificity of 95%[103].

Urine

Radon *et al*[104] used three protein biomarkers (REG1A, TFF1 and LYVE1) to form a powerful urinary panel that could detect patients with stage I-II PDAC with an accuracy of more than 90%. Brezgyte *et al*[105] found increased levels of *miR-143*, *miR-204* and *miR-223* and reduced levels of *miR-30e* in the urine

Table 1 Serum biomarkers

Carbohydrate antigens	CtDNA	miRNA	lncRNA	Metabolites
CA19-9	KRAS	*miR21*	*SNHG15*	3-hydroxybutyrate
CA125	ADAMTS1	*miR25*	*HOTAIR*	Lactate
CA72-4	BNC1	*miR233*	*MALAT1*	Glutamine
CA50	5-methylcytosine	*miR216*	*MEG3*	Alanine
CA242	5-hydroxymethylcytosine	*miR-92-a-5p*	*H19*	Valine
		miR-125b-3p	*PVT1*	Lysine
		miR-532e5p	*HOTTIP*	Citrate
		miR-663	*HAND2-AS1*	Histidine
		miR-1469	*CTD-2033D15.2*	Isoleucine
				Glutamate
				Acetone
				Dimethylamine
				N-succinyl-L-diaminopimelic
				PE (18:2)
Exosomal mRNA molecules	**Exosomal small nucleolar RNA molecules**	**Exosome surfaceome**	**Exosomal long RNAs**	**Others**
CCDC88A	*SNORA14B*	*CLDN4*	*FGA*	CTCs
ARF6	*SNORA18*	*EPCAM*	*KRT19*	ITGB5
Vav3	*SNORA25*	*CD151*	*HIST1H2BK*	PPY
WASF2	*SNORA74A*	*LGAL53BP*	*ITIH2*	ERBB3
	SNORD22	*HIST2H2BE*	*MARCH2*	SCAMP3
		HIST2H2BF	*CLDN1*	RET
			MAL2	5-NT
			TIMP1	CEACAM1
				S100A11

CtDNA: Circulation tumor DNA; miRNA: MicroRNA; lncRNA: Long non-coding RNA; CTC: Circulating tumor cells.

of patients with stage I PDAC compared with the healthy population. However, further studies are needed to validate their clinical utility.

A case-control study that included 914 PDAC patients found the superiority of a panel of metabolites (proline, sphingomyelin, phosphatidylcholine, isocitrate, sphinganine-1-phosphate, histidine, pyruvate, ceramide, sphingomyelin) over CA19-9 in discriminating early-stage PDAC from chronic pancreatitis [106]. According to the authors, the metabolic panel could result in changes in the diagnostic pathway and treatment stratification for one-third of the included patients[106]. Biomarkers of pancreatic juice and cystic fluid, saliva and urine are listed in Table 2.

ARTIFICIAL INTELLIGENCE AND BIOMARKERS

AI can be applied to the identification of biomarkers. Zhang *et al*[107] identified a nine gene pair signature that can distinguish PDAC patients from non-PDAC patients. Alizadeh Savareh *et al*[108] evaluated the best miRNAs using a machine learning method to aid in the early detection of PDAC. The final model included *miR-92a-2-5p*, *miR-125b-3p*, *miR-532e5p*, *miR-663a and miR-1469* with a high performance in differentiating PDAC from controls (accuracy, 0.93; sensitivity, 0.93 and specificity, 0.92).

Table 2 Pancreatic juice and cyst fluid biomarkers, saliva biomarkers, urine biomarkers

Pancreatic juice and cyst fluid biomarkers			
Mutant genes	**Mucins**	**Interleukins**	**Methylated DNA markers**
GNAS	MUC4	IL-1b	C13orf18
KRAS	MUC16	IL-5	FER1L4
TP53	MUC5AC	IL-8	BMP3
SMAD4			
PIK3CA			
PTEN			
AKT1			
Saliva biomarkers			
Upregulated genes	**Downregulated genes**	**LncRNA**	
MBD3L2	*TK2*	*HOTAIR*	
KRAS	*GLTSCR2*	*PVT1*	
STIM2	*CDKL3*		
DMXL2	*TPT1*		
ACRV1	*DPM1*		
DMD			
CABLES1			
Urine biomarkers			
Protein markers	**MiRNA**	**Metabolites**	
REG1A	*miR-143*	CA19.9	
TFF1	*miR-204*	Proline	
LYVE1	*miR-223*	Sphingomyelin (d18:2, C17:0)	
	miR-30e	Phosphatidylcholine	
		Isocitrate	
		Sphinganine-1-phosphate	
		Histidine	
		Pyruvate	
		Sphingomyelin (d17:1, C18:0)	

miRNA: MicroRNA; lncRNA: Long non-coding RNA.

WHAT STRATEGIES TO AVOID A FORETOLD CATASTROPHE

As we have already mentioned in the introduction, the current predictions for PDAC give us a glimpse of a catastrophe on the horizon. If the increase in annual PDAC cases continues at the current rate, we will soon have a staggering number of cases without the weapons to stem this foretold catastrophe. The only option is to arm ourselves and not arrive unprepared for this hard battle. What strategies should we adopt to prepare for this ordeal? Undoubtedly first, we need to make academia, industry and the politics/economic world understand the urgency of finding solutions quickly, trying to interact with each other according to specific competencies. On the one hand, academia and industry will have to move forward together, as quickly as possible, in those research paths that we have broadly summarized in this article. On the other hand, the political/economic world, made aware of the emergency to be faced, will have to commit itself both to allocating more funding for research in this field and to lavishing more funding on public health. If public health had sufficient funds to subject all patients of a certain age to a simple screening ultrasound of the abdomen, perhaps many patients could be saved. But at present, with current resources, this scenario remains a pipe dream.

CONCLUSION

In this article, we have summarized all the possible strategies we have available today for the early detection of PDAC and the paths that research must pursue to make this goal ever closer. Unfortunately, in 2022 the results for this type of cancer still remain discouraging, while a catastrophic increase in cases is expected in the coming years. The article has been written with the aim of highlighting the urgency of devoting more attention and resources to this pathology in order to reach a solution that seems more and more unreachable every day.

FOOTNOTES

Author contributions: Tonini V and Zanni M contributed equally to this work; Both authors designed the research study, wrote the manuscript and read and approved the final manuscript.

Conflict-of-interest statement: All authors report no relevant conflicts of interest for this article.

Country/Territory of origin: Italy

ORCID number: Valeria Tonini 0000-0003-3130-2928; Manuel Zanni 0000-0001-7732-7739.

S-Editor: Ma YJ
L-Editor: Filipodia
P-Editor: Ma YJ

REFERENCES

1 **Rahib L**, Smith BD, Aizenberg R, Rosenzweig AB, Fleshman JM, Matrisian LM. Projecting cancer incidence and deaths to 2030: the unexpected burden of thyroid, liver, and pancreas cancers in the United States. *Cancer Res* 2014; **74**: 2913-2921 [PMID: 24840647 DOI: 10.1158/0008-5472.CAN-14-0155]
2 **Sung H**, Ferlay J, Siegel RL, Laversanne M, Soerjomataram I, Jemal A, Bray F. Global Cancer Statistics 2020: GLOBOCAN Estimates of Incidence and Mortality Worldwide for 36 Cancers in 185 Countries. *CA Cancer J Clin* 2021; **71**: 209-249 [PMID: 33538338 DOI: 10.3322/caac.21660]
3 **Oldfield LE**, Connor AA, Gallinger S. Molecular Events in the Natural History of Pancreatic Cancer. *Trends Cancer* 2017; **3**: 336-346 [PMID: 28718411 DOI: 10.1016/j.trecan.2017.04.005]
4 **Bengtsson A**, Andersson R, Ansari D. The actual 5-year survivors of pancreatic ductal adenocarcinoma based on real-world data. *Sci Rep* 2020; **10**: 16425 [PMID: 33009477 DOI: 10.1038/s41598-020-73525-y]
5 **Siegel RL**, Miller KD, Jemal A. Cancer statistics, 2020. *CA Cancer J Clin* 2020; **70**: 7-30 [PMID: 31912902 DOI: 10.3322/caac.21590]
6 **Grasso C**, Jansen G, Giovannetti E. Drug resistance in pancreatic cancer: Impact of altered energy metabolism. *Crit Rev Oncol Hematol* 2017; **114**: 139-152 [PMID: 28477742 DOI: 10.1016/j.critrevonc.2017.03.026]
7 **Ishii Y**, Serikawa M, Tsuboi T, Kawamura R, Tsushima K, Nakamura S, Hirano T, Fukiage A, Mori T, Ikemoto J, Kiyoshita Y, Saeki S, Tamura Y, Miyamoto S, Chayama K. Role of Endoscopic Ultrasonography and Endoscopic Retrograde Cholangiopancreatography in the Diagnosis of Pancreatic Cancer. *Diagnostics (Basel)* 2021; **11** [PMID: 33557084 DOI: 10.3390/diagnostics11020238]
8 **Egawa S**, Toma H, Ohigashi H, Okusaka T, Nakao A, Hatori T, Maguchi H, Yanagisawa A, Tanaka M. Japan Pancreatic Cancer Registry; 30th year anniversary: Japan Pancreas Society. *Pancreas* 2012; **41**: 985-992 [PMID: 22750974 DOI: 10.1097/MPA.0b013e318258055c]
9 **Singhi AD**, Koay EJ, Chari ST, Maitra A. Early Detection of Pancreatic Cancer: Opportunities and Challenges. *Gastroenterology* 2019; **156**: 2024-2040 [PMID: 30721664 DOI: 10.1053/j.gastro.2019.01.259]
10 **Carreras-Torres R**, Johansson M, Gaborieau V, Haycock PC, Wade KH, Relton CL, Martin RM, Davey Smith G, Brennan P. The Role of Obesity, Type 2 Diabetes, and Metabolic Factors in Pancreatic Cancer: A Mendelian Randomization Study. *J Natl Cancer Inst* 2017; **109** [PMID: 28954281 DOI: 10.1093/jnci/djx012]
11 **Michl P**, Löhr M, Neoptolemos JP, Capurso G, Rebours V, Malats N, Ollivier M, Ricciardiello L. UEG position paper on pancreatic cancer. Bringing pancreatic cancer to the 21st century: Prevent, detect, and treat the disease earlier and better. *United European Gastroenterol J* 2021; **9**: 860-871 [PMID: 34431604 DOI: 10.1002/ueg2.12123]
12 **Hu JX**, Zhao CF, Chen WB, Liu QC, Li QW, Lin YY, Gao F. Pancreatic cancer: A review of epidemiology, trend, and risk factors. *World J Gastroenterol* 2021; **27**: 4298-4321 [PMID: 34366606 DOI: 10.3748/wjg.v27.i27.4298]
13 **Klein AP**. Pancreatic cancer epidemiology: understanding the role of lifestyle and inherited risk factors. *Nat Rev*

Gastroenterol Hepatol 2021; **18**: 493-502 [PMID: 34002083 DOI: 10.1038/s41575-021-00457-x]

14 **McKenzie F**, Biessy C, Ferrari P, Freisling H, Rinaldi S, Chajès V, Dahm CC, Overvad K, Dossus L, Lagiou P, Trichopoulos D, Trichopoulou A, Bueno-de-Mesquita HB, May A, Peeters PH, Weiderpass E, Sanchez MJ, Navarro C, Ardanaz E, Ericson U, Wirfält E, Travis RC, Romieu I. Healthy Lifestyle and Risk of Cancer in the European Prospective Investigation Into Cancer and Nutrition Cohort Study. *Medicine (Baltimore)* 2016; **95**: e2850 [PMID: 27100409 DOI: 10.1097/MD.0000000000002850]

15 **Ferrari P**, Licaj I, Muller DC, Kragh Andersen P, Johansson M, Boeing H, Weiderpass E, Dossus L, Dartois L, Fagherazzi G, Bradbury KE, Khaw KT, Wareham N, Duell EJ, Barricarte A, Molina-Montes E, Sanchez CN, Arriola L, Wallström P, Tjønneland A, Olsen A, Trichopoulou A, Benetou V, Trichopoulos D, Tumino R, Agnoli C, Sacerdote C, Palli D, Li K, Kaaks R, Peeters P, Beulens JW, Nunes L, Gunter M, Norat T, Overvad K, Brennan P, Riboli E, Romieu I. Lifetime alcohol use and overall and cause-specific mortality in the European Prospective Investigation into Cancer and nutrition (EPIC) study. *BMJ Open* 2014; **4**: e005245 [PMID: 24993766 DOI: 10.1136/bmjopen-2014-005245]

16 **Yuan C**, Babic A, Khalaf N, Nowak JA, Brais LK, Rubinson DA, Ng K, Aguirre AJ, Pandharipande PV, Fuchs CS, Giovannucci EL, Stampfer MJ, Rosenthal MH, Sander C, Kraft P, Wolpin BM. Diabetes, Weight Change, and Pancreatic Cancer Risk. *JAMA Oncol* 2020; **6**: e202948 [PMID: 32789511 DOI: 10.1001/jamaoncol.2020.2948]

17 **Roy A**, Sahoo J, Kamalanathan S, Naik D, Mohan P, Kalayarasan R. Diabetes and pancreatic cancer: Exploring the two-way traffic. *World J Gastroenterol* 2021; **27**: 4939-4962 [PMID: 34497428 DOI: 10.3748/wjg.v27.i30.4939]

18 **US Preventive Services Task Force**, Owens DK, Davidson KW, Krist AH, Barry MJ, Cabana M, Caughey AB, Curry SJ, Doubeni CA, Epling JW Jr, Kubik M, Landefeld CS, Mangione CM, Pbert L, Silverstein M, Simon MA, Tseng CW, Wong JB. Screening for Pancreatic Cancer: US Preventive Services Task Force Reaffirmation Recommendation Statement. *JAMA* 2019; **322**: 438-444 [PMID: 31386141 DOI: 10.1001/jama.2019.10232]

19 **Pelaez-Luna M**, Takahashi N, Fletcher JG, Chari ST. Resectability of presymptomatic pancreatic cancer and its relationship to onset of diabetes: a retrospective review of CT scans and fasting glucose values prior to diagnosis. *Am J Gastroenterol* 2007; **102**: 2157-2163 [PMID: 17897335 DOI: 10.1111/j.1572-0241.2007.01480.x]

20 **Yang J**, Xu R, Wang C, Qiu J, Ren B, You L. Early screening and diagnosis strategies of pancreatic cancer: a comprehensive review. *Cancer Commun (Lond)* 2021; **41**: 1257-1274 [PMID: 34331845 DOI: 10.1002/cac2.12204]

21 **Sharma A**, Kandlakunta H, Nagpal SJS, Feng Z, Hoos W, Petersen GM, Chari ST. Model to Determine Risk of Pancreatic Cancer in Patients With New-Onset Diabetes. *Gastroenterology* 2018; **155**: 730-739.e3 [PMID: 29775599 DOI: 10.1053/j.gastro.2018.05.023]

22 **Goggins M**, Overbeek KA, Brand R, Syngal S, Del Chiaro M, Bartsch DK, Bassi C, Carrato A, Farrell J, Fishman EK, Fockens P, Gress TM, van Hooft JE, Hruban RH, Kastrinos F, Klein A, Lennon AM, Lucas A, Park W, Rustgi A, Simeone D, Stoffel E, Vasen HFA, Cahen DL, Canto MI, Bruno M; International Cancer of the Pancreas Screening (CAPS) consortium. Management of patients with increased risk for familial pancreatic cancer: updated recommendations from the International Cancer of the Pancreas Screening (CAPS) Consortium. *Gut* 2020; **69**: 7-17 [PMID: 31672839 DOI: 10.1136/gutjnl-2019-319352]

23 **Pereira SP**, Oldfield L, Ney A, Hart PA, Keane MG, Pandol SJ, Li D, Greenhalf W, Jeon CY, Koay EJ, Almario CV, Halloran C, Lennon AM, Costello E. Early detection of pancreatic cancer. *Lancet Gastroenterol Hepatol* 2020; **5**: 698-710 [PMID: 32135127 DOI: 10.1016/S2468-1253(19)30416-9]

24 **European Study Group on Cystic Tumours of the Pancreas**. European evidence-based guidelines on pancreatic cystic neoplasms. *Gut* 2018; **67**: 789-804 [PMID: 29574408 DOI: 10.1136/gutjnl-2018-316027]

25 **Tanaka M**, Fernández-Del Castillo C, Kamisawa T, Jang JY, Levy P, Ohtsuka T, Salvia R, Shimizu Y, Tada M, Wolfgang CL. Revisions of international consensus Fukuoka guidelines for the management of IPMN of the pancreas. *Pancreatology* 2017; **17**: 738-753 [PMID: 28735806 DOI: 10.1016/j.pan.2017.07.007]

26 **Aslanian HR**, Lee JH, Canto MI. AGA Clinical Practice Update on Pancreas Cancer Screening in High-Risk Individuals: Expert Review. *Gastroenterology* 2020; **159**: 358-362 [PMID: 32416142 DOI: 10.1053/j.gastro.2020.03.088]

27 **Okusaka T**, Nakamura M, Yoshida M, Kitano M, Uesaka K, Ito Y, Furuse J, Hanada K, Okazaki K; Committee for Revision of Clinical Guidelines for Pancreatic Cancer of the Japan Pancreas Society. Clinical Practice Guidelines for Pancreatic Cancer 2019 From the Japan Pancreas Society: A Synopsis. *Pancreas* 2020; **49**: 326-335 [PMID: 32132516 DOI: 10.1097/MPA.0000000000001513]

28 **Kanno A**, Masamune A, Hanada K, Maguchi H, Shimizu Y, Ueki T, Hasebe O, Ohtsuka T, Nakamura M, Takenaka M, Kitano M, Kikuyama M, Gabata T, Yoshida K, Sasaki T, Serikawa M, Furukawa T, Yanagisawa A, Shimosegawa T; Japan Study Group on the Early Detection of Pancreatic Cancer (JEDPAC). Multicenter study of early pancreatic cancer in Japan. *Pancreatology* 2018; **18**: 61-67 [PMID: 29170051 DOI: 10.1016/j.pan.2017.11.007]

29 **Dewitt J**, Devereaux BM, Lehman GA, Sherman S, Imperiale TF. Comparison of endoscopic ultrasound and computed tomography for the preoperative evaluation of pancreatic cancer: a systematic review. *Clin Gastroenterol Hepatol* 2006; **4**: 717-25; quiz 664 [PMID: 16675307 DOI: 10.1016/j.cgh.2006.02.020]

30 **Kitano M**, Yoshida T, Itonaga M, Tamura T, Hatamaru K, Yamashita Y. Impact of endoscopic ultrasonography on diagnosis of pancreatic cancer. *J Gastroenterol* 2019; **54**: 19-32 [PMID: 30406288 DOI: 10.1007/s00535-018-1519-2]

31 **Bunganič B**, Laclav M, Dvořáková T, Bradáč O, Traboulsi E, Suchánek Š, Frič P, Zavoral M. Accuracy of EUS and CEH EUS for the diagnosis of pancreatic tumours. *Scand J Gastroenterol* 2018; **53**: 1411-1417 [PMID: 30394143 DOI: 10.1080/00365521.2018.1524023]

32 **Yamashita Y**, Shimokawa T, Napoléon B, Fusaroli P, Gincul R, Kudo M, Kitano M. Value of contrast-enhanced harmonic endoscopic ultrasonography with enhancement pattern for diagnosis of pancreatic cancer: A meta-analysis. *Dig Endosc* 2019; **31**: 125-133 [PMID: 30338569 DOI: 10.1111/den.13290]

33 **Haba S**, Yamao K, Bhatia V, Mizuno N, Hara K, Hijioka S, Imaoka H, Niwa Y, Tajika M, Kondo S, Tanaka T, Shimizu Y, Yatabe Y, Hosoda W, Kawakami H, Sakamoto N. Diagnostic ability and factors affecting accuracy of endoscopic ultrasound-guided fine needle aspiration for pancreatic solid lesions: Japanese large single center experience. *J Gastroenterol* 2013; **48**: 973-981 [PMID: 23090002 DOI: 10.1007/s00535-012-0695-8]

34 **Li H**, Hu Z, Chen J, Guo X. Comparison of ERCP, EUS, and ERCP combined with EUS in diagnosing pancreatic

neoplasms: a systematic review and meta-analysis. *Tumour Biol* 2014; **35**: 8867-8874 [PMID: 24891188 DOI: 10.1007/s13277-014-2154-z]

35 **Kawamura R**, Ishii Y, Serikawa M, Tsuboi T, Tsushima K, Nakamura S, Hirano T, Ikemoto J, Kiyoshita Y, Saeki S, Tamura Y, Miyamoto S, Nakamura K, Furukawa M, Ishida K, Arihiro K, Uemura K, Aikata H. Optimal indication of endoscopic retrograde pancreatography-based cytology in the preoperative pathological diagnosis of pancreatic ductal adenocarcinoma. *Pancreatology* 2022; **22**: 414-420 [PMID: 35219581 DOI: 10.1016/j.pan.2022.02.001]

36 **Kawa S**, Kamisawa T, Notohara K, Fujinaga Y, Inoue D, Koyama T, Okazaki K. Japanese Clinical Diagnostic Criteria for Autoimmune Pancreatitis, 2018: Revision of Japanese Clinical Diagnostic Criteria for Autoimmune Pancreatitis, 2011. *Pancreas* 2020; **49**: e13-e14 [PMID: 31856100 DOI: 10.1097/MPA.0000000000001443]

37 **Ikemoto J**, Serikawa M, Hanada K, Eguchi N, Sasaki T, Fujimoto Y, Sugiyama S, Yamaguchi A, Noma B, Kamigaki M, Minami T, Okazaki A, Yukutake M, Ishii Y, Mouri T, Shimizu A, Tsuboi T, Arihiro K, Chayama K. Clinical Analysis of Early-Stage Pancreatic Cancer and Proposal for a New Diagnostic Algorithm: A Multicenter Observational Study. *Diagnostics (Basel)* 2021; **11** [PMID: 33673151 DOI: 10.3390/diagnostics11020287]

38 **Muhammad W**, Hart GR, Nartowt B, Farrell JJ, Johung K, Liang Y, Deng J. Pancreatic Cancer Prediction Through an Artificial Neural Network. *Front Artif Intell* 2019; **2**: 2 [PMID: 33733091 DOI: 10.3389/frai.2019.00002]

39 **Hayashi H**, Uemura N, Matsumura K, Zhao L, Sato H, Shiraishi Y, Yamashita YI, Baba H. Recent advances in artificial intelligence for pancreatic ductal adenocarcinoma. *World J Gastroenterol* 2021; **27**: 7480-7496 [PMID: 34887644 DOI: 10.3748/wjg.v27.i43.7480]

40 **Mendoza Ladd A**, Diehl DL. Artificial intelligence for early detection of pancreatic adenocarcinoma: The future is promising. *World J Gastroenterol* 2021; **27**: 1283-1295 [PMID: 33833482 DOI: 10.3748/wjg.v27.i13.1283]

41 **Das A**, Nguyen CC, Li F, Li B. Digital image analysis of EUS images accurately differentiates pancreatic cancer from chronic pancreatitis and normal tissue. *Gastrointest Endosc* 2008; **67**: 861-867 [PMID: 18179797 DOI: 10.1016/j.gie.2007.08.036]

42 **Zhu M**, Xu C, Yu J, Wu Y, Li C, Zhang M, Jin Z, Li Z. Differentiation of pancreatic cancer and chronic pancreatitis using computer-aided diagnosis of endoscopic ultrasound (EUS) images: a diagnostic test. *PLoS One* 2013; **8**: e63820 [PMID: 23704940 DOI: 10.1371/journal.pone.0063820]

43 **Liu SL**, Li S, Guo YT, Zhou YP, Zhang ZD, Lu Y. Establishment and application of an artificial intelligence diagnosis system for pancreatic cancer with a faster region-based convolutional neural network. *Chin Med J (Engl)* 2019; **132**: 2795-2803 [PMID: 31856050 DOI: 10.1097/CM9.0000000000000544]

44 **Liu KL**, Wu T, Chen PT, Tsai YM, Roth H, Wu MS, Liao WC, Wang W. Deep learning to distinguish pancreatic cancer tissue from non-cancerous pancreatic tissue: a retrospective study with cross-racial external validation. *Lancet Digit Health* 2020; **2**: e303-e313 [PMID: 33328124 DOI: 10.1016/S2589-7500(20)30078-9]

45 **Chu LC**, Park S, Kawamoto S, Wang Y, Zhou Y, Shen W, Zhu Z, Xia Y, Xie L, Liu F, Yu Q, Fouladi DF, Shayesteh S, Zinreich E, Graves JS, Horton KM, Yuille AL, Hruban RH, Kinzler KW, Vogelstein B, Fishman EK. Application of Deep Learning to Pancreatic Cancer Detection: Lessons Learned From Our Initial Experience. *J Am Coll Radiol* 2019; **16**: 1338-1342 [PMID: 31492412 DOI: 10.1016/j.jacr.2019.05.034]

46 **Young MR**, Abrams N, Ghosh S, Rinaudo JAS, Marquez G, Srivastava S. Prediagnostic Image Data, Artificial Intelligence, and Pancreatic Cancer: A Tell-Tale Sign to Early Detection. *Pancreas* 2020; **49**: 882-886 [PMID: 32675784 DOI: 10.1097/MPA.0000000000001603]

47 **Kenner B**, Chari ST, Kelsen D, Klimstra DS, Pandol SJ, Rosenthal M, Rustgi AK, Taylor JA, Yala A, Abul-Husn N, Andersen DK, Bernstein D, Brunak S, Canto MI, Eldar YC, Fishman EK, Fleshman J, Go VLW, Holt JM, Field B, Goldberg A, Hoos W, Iacobuzio-Donahue C, Li D, Lidgard G, Maitra A, Matrisian LM, Poblete S, Rothschild L, Sander C, Schwartz LH, Shalit U, Srivastava S, Wolpin B. Artificial Intelligence and Early Detection of Pancreatic Cancer: 2020 Summative Review. *Pancreas* 2021; **50**: 251-279 [PMID: 33835956 DOI: 10.1097/MPA.0000000000001762]

48 **Sturm N**, Ettrich TJ, Perkhofer L. The Impact of Biomarkers in Pancreatic Ductal Adenocarcinoma on Diagnosis, Surveillance and Therapy. *Cancers (Basel)* 2022; **14** [PMID: 35008381 DOI: 10.3390/cancers14010217]

49 **Fahrmann JF**, Schmidt CM, Mao X, Irajizad E, Loftus M, Zhang J, Patel N, Vykoukal J, Dennison JB, Long JP, Do KA, Chabot JA, Kluger MD, Kastrinos F, Brais L, Babic A, Jajoo K, Lee LS, Clancy TE, Ng K, Bullock A, Genkinger J, Yip-Schneider MT, Maitra A, Wolpin BM, Hanash S. Lead-Time Trajectory of CA19-9 as an Anchor Marker for Pancreatic Cancer Early Detection. *Gastroenterology* 2021; **160**: 1373-1383.e6 [PMID: 33333055 DOI: 10.1053/j.gastro.2020.11.052]

50 **Luo G**, Fan Z, Cheng H, Jin K, Guo M, Lu Y, Yang C, Fan K, Huang Q, Long J, Liu L, Xu J, Lu R, Ni Q, Warshaw AL, Liu C, Yu X. New observations on the utility of CA19-9 as a biomarker in Lewis negative patients with pancreatic cancer. *Pancreatology* 2018; **18**: 971-976 [PMID: 30131287 DOI: 10.1016/j.pan.2018.08.003]

51 **Loosen SH**, Neumann UP, Trautwein C, Roderburg C, Luedde T. Current and future biomarkers for pancreatic adenocarcinoma. *Tumour Biol* 2017; **39**: 1010428317692231 [PMID: 28618958 DOI: 10.1177/1010428317692231]

52 **Lee T**, Teng TZJ, Shelat VG. Carbohydrate antigen 19-9 - tumor marker: Past, present, and future. *World J Gastrointest Surg* 2020; **12**: 468-490 [PMID: 33437400 DOI: 10.4240/wjgs.v12.i12.468]

53 **Wang Z**, Tian YP. Clinical value of serum tumor markers CA19-9, CA125 and CA72-4 in the diagnosis of pancreatic carcinoma. *Mol Clin Oncol* 2014; **2**: 265-268 [PMID: 24649344 DOI: 10.3892/mco.2013.226]

54 **Dou H**, Sun G, Zhang L. CA242 as a biomarker for pancreatic cancer and other diseases. *Prog Mol Biol Transl Sci* 2019; **162**: 229-239 [PMID: 30905452 DOI: 10.1016/bs.pmbts.2018.12.007]

55 **Buscail E**, Maulat C, Muscari F, Chiche L, Cordelier P, Dabernat S, Alix-Panabières C, Buscail L. Liquid Biopsy Approach for Pancreatic Ductal Adenocarcinoma. *Cancers (Basel)* 2019; **11** [PMID: 31248203 DOI: 10.3390/cancers11060852]

56 **Heredia-Soto V**, Rodríguez-Salas N, Feliu J. Liquid Biopsy in Pancreatic Cancer: Are We Ready to Apply It in the Clinical Practice? *Cancers (Basel)* 2021; **13** [PMID: 33924143 DOI: 10.3390/cancers13081986]

57 **Zhu Y**, Zhang H, Chen N, Hao J, Jin H, Ma X. Diagnostic value of various liquid biopsy methods for pancreatic cancer: A systematic review and meta-analysis. *Medicine (Baltimore)* 2020; **99**: e18581 [PMID: 32011436 DOI:

10.1097/MD.0000000000018581]
58 **Wang ZY**, Ding XQ, Zhu H, Wang RX, Pan XR, Tong JH. *KRAS* Mutant Allele Fraction in Circulating Cell-Free DNA Correlates With Clinical Stage in Pancreatic Cancer Patients. *Front Oncol* 2019; **9**: 1295 [PMID: 31850201 DOI: 10.3389/fonc.2019.01295]
59 **Cohen JD**, Javed AA, Thoburn C, Wong F, Tie J, Gibbs P, Schmidt CM, Yip-Schneider MT, Allen PJ, Schattner M, Brand RE, Singhi AD, Petersen GM, Hong SM, Kim SC, Falconi M, Doglioni C, Weiss MJ, Ahuja N, He J, Makary MA, Maitra A, Hanash SM, Dal Molin M, Wang Y, Li L, Ptak J, Dobbyn L, Schaefer J, Silliman N, Popoli M, Goggins MG, Hruban RH, Wolfgang CL, Klein AP, Tomasetti C, Papadopoulos N, Kinzler KW, Vogelstein B, Lennon AM. Combined circulating tumor DNA and protein biomarker-based liquid biopsy for the earlier detection of pancreatic cancers. *Proc Natl Acad Sci U S A* 2017; **114**: 10202-10207 [PMID: 28874546 DOI: 10.1073/pnas.1704961114]
60 **Eissa MAL**, Lerner L, Abdelfatah E, Shankar N, Canner JK, Hasan NM, Yaghoobi V, Huang B, Kerner Z, Takaesu F, Wolfgang C, Kwak R, Ruiz M, Tam M, Pisanic TR 2nd, Iacobuzio-Donahue CA, Hruban RH, He J, Wang TH, Wood LD, Sharma A, Ahuja N. Promoter methylation of ADAMTS1 and BNC1 as potential biomarkers for early detection of pancreatic cancer in blood. *Clin Epigenetics* 2019; **11**: 59 [PMID: 30953539 DOI: 10.1186/s13148-019-0650-0]
61 **Cao F**, Wei A, Hu X, He Y, Zhang J, Xia L, Tu K, Yuan J, Guo Z, Liu H, Xie D, Li A. Integrated epigenetic biomarkers in circulating cell-free DNA as a robust classifier for pancreatic cancer. *Clin Epigenetics* 2020; **12**: 112 [PMID: 32703318 DOI: 10.1186/s13148-020-00898-2]
62 **Liu MC**, Oxnard GR, Klein EA, Swanton C, Seiden MV; CCGA Consortium. Sensitive and specific multi-cancer detection and localization using methylation signatures in cell-free DNA. *Ann Oncol* 2020; **31**: 745-759 [PMID: 33506766 DOI: 10.1016/j.annonc.2020.02.011]
63 **Brancaccio M**, Natale F, Falco G, Angrisano T. Cell-Free DNA Methylation: The New Frontiers of Pancreatic Cancer Biomarkers' Discovery. *Genes (Basel)* 2019; **11** [PMID: 31877923 DOI: 10.3390/genes11010014]
64 **Yeo D**, Bastian A, Strauss H, Saxena P, Grimison P, Rasko JEJ. Exploring the Clinical Utility of Pancreatic Cancer Circulating Tumor Cells. *Int J Mol Sci* 2022; **23** [PMID: 35163592 DOI: 10.3390/ijms23031671]
65 **Kaczor-Urbanowicz KE**, Cheng J, King JC, Sedarat A, Pandol SJ, Farrell JJ, Wong DTW, Kim Y. Reviews on Current Liquid Biopsy for Detection and Management of Pancreatic Cancers. *Pancreas* 2020; **49**: 1141-1152 [PMID: 33003085 DOI: 10.1097/MPA.0000000000001662]
66 **Ankeny JS**, Court CM, Hou S, Li Q, Song M, Wu D, Chen JF, Lee T, Lin M, Sho S, Rochefort MM, Girgis MD, Yao J, Wainberg ZA, Muthusamy VR, Watson RR, Donahue TR, Hines OJ, Reber HA, Graeber TG, Tseng HR, Tomlinson JS. Circulating tumour cells as a biomarker for diagnosis and staging in pancreatic cancer. *Br J Cancer* 2016; **114**: 1367-1375 [PMID: 27300108 DOI: 10.1038/bjc.2016.121]
67 **Poruk KE**, Valero V 3rd, He J, Ahuja N, Cameron JL, Weiss MJ, Lennon AM, Goggins M, Wood LD, Wolfgang CL. Circulating Epithelial Cells in Intraductal Papillary Mucinous Neoplasms and Cystic Pancreatic Lesions. *Pancreas* 2017; **46**: 943-947 [PMID: 28697136 DOI: 10.1097/MPA.0000000000000869]
68 **Franses JW**, Basar O, Kadayifci A, Yuksel O, Choz M, Kulkarni AS, Tai E, Vo KD, Arora KS, Desai N, Licausi JA, Toner M, Maheswaran S, Haber DA, Ryan DP, Brugge WR, Ting DT. Improved Detection of Circulating Epithelial Cells in Patients with Intraductal Papillary Mucinous Neoplasms. *Oncologist* 2018; **23**: 121-127 [PMID: 28860411 DOI: 10.1634/theoncologist.2017-0234]
69 **Vasseur A**, Kiavue N, Bidard FC, Pierga JY, Cabel L. Clinical utility of circulating tumor cells: an update. *Mol Oncol* 2021; **15**: 1647-1666 [PMID: 33289351 DOI: 10.1002/1878-0261.12869]
70 **Catenacci DV**, Chapman CG, Xu P, Koons A, Konda VJ, Siddiqui UD, Waxman I. Acquisition of Portal Venous Circulating Tumor Cells From Patients With Pancreaticobiliary Cancers by Endoscopic Ultrasound. *Gastroenterology* 2015; **149**: 1794-1803.e4 [PMID: 26341722 DOI: 10.1053/j.gastro.2015.08.050]
71 **Tien YW**, Kuo HC, Ho BI, Chang MC, Chang YT, Cheng MF, Chen HL, Liang TY, Wang CF, Huang CY, Shew JY, Chang YC, Lee EY, Lee WH. A High Circulating Tumor Cell Count in Portal Vein Predicts Liver Metastasis From Periampullary or Pancreatic Cancer: A High Portal Venous CTC Count Predicts Liver Metastases. *Medicine (Baltimore)* 2016; **95**: e3407 [PMID: 27100430 DOI: 10.1097/MD.0000000000003407]
72 **Deng T**, Yuan Y, Zhang C, Yao W, Wang C, Liu R, Ba Y. Identification of Circulating MiR-25 as a Potential Biomarker for Pancreatic Cancer Diagnosis. *Cell Physiol Biochem* 2016; **39**: 1716-1722 [PMID: 27639768 DOI: 10.1159/000447872]
73 **Li X**, Gao P, Wang Y, Wang X. Blood-Derived microRNAs for Pancreatic Cancer Diagnosis: A Narrative Review and Meta-Analysis. *Front Physiol* 2018; **9**: 685 [PMID: 29922178 DOI: 10.3389/fphys.2018.00685]
74 **Komatsu S**, Ichikawa D, Miyamae M, Kawaguchi T, Morimura R, Hirajima S, Okajima W, Ohashi T, Imamura T, Konishi H, Shiozaki A, Ikoma H, Okamoto K, Taniguchi H, Otsuji E. Malignant potential in pancreatic neoplasm; new insights provided by circulating miR-223 in plasma. *Expert Opin Biol Ther* 2015; **15**: 773-785 [PMID: 25819175 DOI: 10.1517/14712598.2015.1029914]
75 **Peng C**, Wang J, Gao W, Huang L, Liu Y, Li X, Li Z, Yu X. Meta-analysis of the Diagnostic Performance of Circulating MicroRNAs for Pancreatic Cancer. *Int J Med Sci* 2021; **18**: 660-671 [PMID: 33437201 DOI: 10.7150/ijms.52706]
76 **Shen SY**, Singhania R, Fehringer G, Chakravarthy A, Roehrl MHA, Chadwick D, Zuzarte PC, Borgida A, Wang TT, Li T, Kis O, Zhao Z, Spreafico A, Medina TDS, Wang Y, Roulois D, Ettayebi I, Chen Z, Chow S, Murphy T, Arruda A, O'Kane GM, Liu J, Mansour M, McPherson JD, O'Brien C, Leighl N, Bedard PL, Fleshner N, Liu G, Minden MD, Gallinger S, Goldenberg A, Pugh TJ, Hoffman MM, Bratman SV, Hung RJ, De Carvalho DD. Sensitive tumour detection and classification using plasma cell-free DNA methylomes. *Nature* 2018; **563**: 579-583 [PMID: 30429608 DOI: 10.1038/s41586-018-0703-0]
77 **Cirmena G**, Dameri M, Ravera F, Fregatti P, Ballestrero A, Zoppoli G. Assessment of Circulating Nucleic Acids in Cancer: From Current Status to Future Perspectives and Potential Clinical Applications. *Cancers (Basel)* 2021; **13** [PMID: 34298675 DOI: 10.3390/cancers13143460]
78 **Guo XB**, Yin HS, Wang JY. Evaluating the diagnostic and prognostic value of long non-coding RNA SNHG15 in pancreatic ductal adenocarcinoma. *Eur Rev Med Pharmacol Sci* 2018; **22**: 5892-5898 [PMID: 30280769 DOI:

10.26355/eurrev_201809_15917]
79 **Permuth JB**, Chen DT, Yoder SJ, Li J, Smith AT, Choi JW, Kim J, Balagurunathan Y, Jiang K, Coppola D, Centeno BA, Klapman J, Hodul P, Karreth FA, Trevino JG, Merchant N, Magliocco A, Malafa MP, Gillies R. Linc-ing Circulating Long Non-coding RNAs to the Diagnosis and Malignant Prediction of Intraductal Papillary Mucinous Neoplasms of the Pancreas. *Sci Rep* 2017; **7**: 10484 [PMID: 28874676 DOI: 10.1038/s41598-017-09754-5]
80 **Satoh K**. Molecular Approaches Using Body Fluid for the Early Detection of Pancreatic Cancer. *Diagnostics (Basel)* 2021; **11** [PMID: 33671729 DOI: 10.3390/diagnostics11020375]
81 **Li Y**, Al Hallak MN, Philip PA, Azmi AS, Mohammad RM. Non-Coding RNAs in Pancreatic Cancer Diagnostics and Therapy: Focus on lncRNAs, circRNAs, and piRNAs. *Cancers (Basel)* 2021; **13** [PMID: 34439315 DOI: 10.3390/cancers13164161]
82 **Ding J**, Li Y, Zhang Y, Fan B, Li Q, Zhang J. Identification of key lncRNAs in the tumorigenesis of intraductal pancreatic mucinous neoplasm by coexpression network analysis. *Cancer Med* 2020; **9**: 3840-3851 [PMID: 32239802 DOI: 10.1002/cam4.2927]
83 **Schmidt DR**, Patel R, Kirsch DG, Lewis CA, Vander Heiden MG, Locasale JW. Metabolomics in cancer research and emerging applications in clinical oncology. *CA Cancer J Clin* 2021; **71**: 333-358 [PMID: 33982817 DOI: 10.3322/caac.21670]
84 **Michálková L**, Horník Š, Sýkora J, Habartová L, Setnička V. Diagnosis of pancreatic cancer via^{1}H NMR metabolomics of human plasma. *Analyst* 2018; **143**: 5974-5978 [PMID: 30270368 DOI: 10.1039/c8an01310a]
85 **He X**, Zhong J, Wang S, Zhou Y, Wang L, Zhang Y, Yuan Y. Serum metabolomics differentiating pancreatic cancer from new-onset diabetes. *Oncotarget* 2017; **8**: 29116-29124 [PMID: 28418859 DOI: 10.18632/oncotarget.16249]
86 **Yu J**, Ploner A, Kordes M, Löhr M, Nilsson M, de Maturana MEL, Estudillo L, Renz H, Carrato A, Molero X, Real FX, Malats N, Ye W. Plasma protein biomarkers for early detection of pancreatic ductal adenocarcinoma. *Int J Cancer* 2021; **148**: 2048-2058 [PMID: 33411965 DOI: 10.1002/ijc.33464]
87 **Kitagawa T**, Taniuchi K, Tsuboi M, Sakaguchi M, Kohsaki T, Okabayashi T, Saibara T. Circulating pancreatic cancer exosomal RNAs for detection of pancreatic cancer. *Mol Oncol* 2019; **13**: 212-227 [PMID: 30358104 DOI: 10.1002/1878-0261.12398]
88 **Castillo J**, Bernard V, San Lucas FA, Allenson K, Capello M, Kim DU, Gascoyne P, Mulu FC, Stephens BM, Huang J, Wang H, Momin AA, Jacamo RO, Katz M, Wolff R, Javle M, Varadhachary G, Wistuba II, Hanash S, Maitra A, Alvarez H. Surfaceome profiling enables isolation of cancer-specific exosomal cargo in liquid biopsies from pancreatic cancer patients. *Ann Oncol* 2018; **29**: 223-229 [PMID: 29045505 DOI: 10.1093/annonc/mdx542]
89 **Yu S**, Li Y, Liao Z, Wang Z, Qian L, Zhao J, Zong H, Kang B, Zou WB, Chen K, He X, Meng Z, Chen Z, Huang S, Wang P. Plasma extracellular vesicle long RNA profiling identifies a diagnostic signature for the detection of pancreatic ductal adenocarcinoma. *Gut* 2020; **69**: 540-550 [PMID: 31562239 DOI: 10.1136/gutjnl-2019-318860]
90 **Kanda M**, Knight S, Topazian M, Syngal S, Farrell J, Lee J, Kamel I, Lennon AM, Borges M, Young A, Fujiwara S, Seike J, Eshleman J, Hruban RH, Canto MI, Goggins M. Mutant GNAS detected in duodenal collections of secretin-stimulated pancreatic juice indicates the presence or emergence of pancreatic cysts. *Gut* 2013; **62**: 1024-1033 [PMID: 22859495 DOI: 10.1136/gutjnl-2012-302823]
91 **Kanda M**, Sadakari Y, Borges M, Topazian M, Farrell J, Syngal S, Lee J, Kamel I, Lennon AM, Knight S, Fujiwara S, Hruban RH, Canto MI, Goggins M. Mutant TP53 in duodenal samples of pancreatic juice from patients with pancreatic cancer or high-grade dysplasia. *Clin Gastroenterol Hepatol* 2013; **11**: 719-30.e5 [PMID: 23200980 DOI: 10.1016/j.cgh.2012.11.016]
92 **Singhi AD**, McGrath K, Brand RE, Khalid A, Zeh HJ, Chennat JS, Fasanella KE, Papachristou GI, Slivka A, Bartlett DL, Dasyam AK, Hogg M, Lee KK, Marsh JW, Monaco SE, Ohori NP, Pingpank JF, Tsung A, Zureikat AH, Wald AI, Nikiforova MN. Preoperative next-generation sequencing of pancreatic cyst fluid is highly accurate in cyst classification and detection of advanced neoplasia. *Gut* 2018; **67**: 2131-2141 [PMID: 28970292 DOI: 10.1136/gutjnl-2016-313586]
93 **Garcia-Carracedo D**, Chen ZM, Qiu W, Huang AS, Tang SM, Hruban RH, Su GH. PIK3CA mutations in mucinous cystic neoplasms of the pancreas. *Pancreas* 2014; **43**: 245-249 [PMID: 24518503 DOI: 10.1097/MPA.0000000000000034]
94 **Kaur S**, Kumar S, Momi N, Sasson AR, Batra SK. Mucins in pancreatic cancer and its microenvironment. *Nat Rev Gastroenterol Hepatol* 2013; **10**: 607-620 [PMID: 23856888 DOI: 10.1038/nrgastro.2013.120]
95 **Nagata K**, Horinouchi M, Saitou M, Higashi M, Nomoto M, Goto M, Yonezawa S. Mucin expression profile in pancreatic cancer and the precursor lesions. *J Hepatobiliary Pancreat Surg* 2007; **14**: 243-254 [PMID: 17520199 DOI: 10.1007/s00534-006-1169-2]
96 **Henry KE**, Shaffer TM, Mack KN, Ring J, Ogirala A, Klein-Scory S, Eilert-Micus C, Schmiegel W, Bracht T, Sitek B, Clyne M, Reid CJ, Sipos B, Lewis JS, Kalthoff H, Grimm J. Exploiting the MUC5AC Antigen for Noninvasive Identification of Pancreatic Cancer. *J Nucl Med* 2021; **62**: 1384-1390 [PMID: 33712530 DOI: 10.2967/jnumed.120.256776]
97 **Maker AV**, Katabi N, Qin LX, Klimstra DS, Schattner M, Brennan MF, Jarnagin WR, Allen PJ. Cyst fluid interleukin-1beta (IL1beta) levels predict the risk of carcinoma in intraductal papillary mucinous neoplasms of the pancreas. *Clin Cancer Res* 2011; **17**: 1502-1508 [PMID: 21266527 DOI: 10.1158/1078-0432.CCR-10-1561]
98 **Hao S**, Takahashi C, Snyder RA, Parikh AA. Stratifying Intraductal Papillary Mucinous Neoplasms by Cyst Fluid Analysis: Present and Future. *Int J Mol Sci* 2020; **21** [PMID: 32050465 DOI: 10.3390/ijms21031147]
99 **Das KK**, Geng X, Brown JW, Morales-Oyarvide V, Huynh T, Pergolini I, Pitman MB, Ferrone C, Al Efishat M, Haviland D, Thompson E, Wolfgang C, Lennon AM, Allen P, Lillemoe KD, Fields RC, Hawkins WG, Liu J, Castillo CF, Das KM, Mino-Kenudson M. Cross Validation of the Monoclonal Antibody Das-1 in Identification of High-Risk Mucinous Pancreatic Cystic Lesions. *Gastroenterology* 2019; **157**: 720-730.e2 [PMID: 31175863 DOI: 10.1053/j.gastro.2019.05.014]
100 **Majumder S**, Raimondo M, Taylor WR, Yab TC, Berger CK, Dukek BA, Cao X, Foote PH, Wu CW, Devens ME, Mahoney DW, Smyrk TC, Pannala R, Chari ST, Vege SS, Topazian MD, Petersen BT, Levy MJ, Rajan E, Gleeson FC,

Abu Dayyeh B, Nguyen CC, Faigel DO, Woodward TA, Wallace MB, Petersen G, Allawi HT, Lidgard GP, Kisiel JB, Ahlquist DA. Methylated DNA in Pancreatic Juice Distinguishes Patients With Pancreatic Cancer From Controls. *Clin Gastroenterol Hepatol* 2020; **18**: 676-683.e3 [PMID: 31323382 DOI: 10.1016/j.cgh.2019.07.017]

101 **Zhang L**, Farrell JJ, Zhou H, Elashoff D, Akin D, Park NH, Chia D, Wong DT. Salivary transcriptomic biomarkers for detection of resectable pancreatic cancer. *Gastroenterology* 2010; **138**: 949-57.e1 [PMID: 19931263 DOI: 10.1053/j.gastro.2009.11.010]

102 **Xie Z**, Yin X, Gong B, Nie W, Wu B, Zhang X, Huang J, Zhang P, Zhou Z, Li Z. Salivary microRNAs show potential as a noninvasive biomarker for detecting resectable pancreatic cancer. *Cancer Prev Res (Phila)* 2015; **8**: 165-173 [PMID: 25538087 DOI: 10.1158/1940-6207.CAPR-14-0192]

103 **Ghafouri-Fard S**, Fathi M, Zhai T, Taheri M, Dong P. LncRNAs: Novel Biomarkers for Pancreatic Cancer. *Biomolecules* 2021; **11** [PMID: 34827663 DOI: 10.3390/biom11111665]

104 **Radon TP**, Massat NJ, Jones R, Alrawashdeh W, Dumartin L, Ennis D, Duffy SW, Kocher HM, Pereira SP, Guarner posthumous L, Murta-Nascimento C, Real FX, Malats N, Neoptolemos J, Costello E, Greenhalf W, Lemoine NR, Crnogorac-Jurcevic T. Identification of a Three-Biomarker Panel in Urine for Early Detection of Pancreatic Adenocarcinoma. *Clin Cancer Res* 2015; **21**: 3512-3521 [PMID: 26240291 DOI: 10.1158/1078-0432.CCR-14-2467]

105 **Brezgyte G**, Shah V, Jach D, Crnogorac-Jurcevic T. Non-Invasive Biomarkers for Earlier Detection of Pancreatic Cancer-A Comprehensive Review. *Cancers (Basel)* 2021; **13** [PMID: 34072842 DOI: 10.3390/cancers13112722]

106 **Mayerle J**, Kalthoff H, Reszka R, Kamlage B, Peter E, Schniewind B, González Maldonado S, Pilarsky C, Heidecke CD, Schatz P, Distler M, Scheiber JA, Mahajan UM, Weiss FU, Grützmann R, Lerch MM. Metabolic biomarker signature to differentiate pancreatic ductal adenocarcinoma from chronic pancreatitis. *Gut* 2018; **67**: 128-137 [PMID: 28108468 DOI: 10.1136/gutjnl-2016-312432]

107 **Zhang ZM**, Wang JS, Zulfiqar H, Lv H, Dao FY, Lin H. Early Diagnosis of Pancreatic Ductal Adenocarcinoma by Combining Relative Expression Orderings With Machine-Learning Method. *Front Cell Dev Biol* 2020; **8**: 582864 [PMID: 33178697 DOI: 10.3389/fcell.2020.582864]

108 **Alizadeh Savareh B**, Asadzadeh Aghdaie H, Behmanesh A, Bashiri A, Sadeghi A, Zali M, Shams R. A machine learning approach identified a diagnostic model for pancreatic cancer through using circulating microRNA signatures. *Pancreatology* 2020; **20**: 1195-1204 [PMID: 32800647 DOI: 10.1016/j.pan.2020.07.399]

World Journal of Gastroenterology

Submit a Manuscript: https://www.f6publishing.com

World J Gastroenterol 2022 August 21; 28(31): 4249-4262

DOI: 10.3748/wjg.v28.i31.4249

ISSN 1007-9327 (print) ISSN 2219-2840 (online)

REVIEW

Insights into induction of the immune response by the hepatitis B vaccine

Federico Alejandro Di Lello, Alfredo Pedro Martínez, Diego Martín Flichman

Specialty type: Gastroenterology and hepatology

Provenance and peer review: Invited article; Externally peer reviewed.

Peer-review model: Single blind

Peer-review report's scientific quality classification

Grade A (Excellent): 0
Grade B (Very good): B
Grade C (Good): C, C
Grade D (Fair): 0
Grade E (Poor): 0

P-Reviewer: JAN CFJ, Taiwan; Kumar R, India; Maslennikov R, Russia

Received: January 16, 2022
Peer-review started: January 16, 2022
First decision: May 10, 2022
Revised: May 21, 2022
Accepted: July 24, 2022
Article in press: July 24, 2022
Published online: August 21, 2022

Federico Alejandro Di Lello, Microbiology, Universidad de Buenos Aires. Facultad de Farmacia y Bioquímica. Instituto de Investigaciones en Bacteriología y Virología Molecular, Buenos Aires C1113AAD, Argentina

Federico Alejandro Di Lello, Diego Martín Flichman, Consejo Nacional de Investigaciones Científicas y Técnicas, Buenos Aires C1425FQB, Argentina

Alfredo Pedro Martínez, Virology Section, Centro de Educación Médica e Investigaciones Clínicas Norberto Quirno "CEMIC", Buenos Aires C1431FWO, Argentina

Diego Martín Flichman, Microbiology, Universidad de Buenos Aires, Instituto de Investigaciones Biomédicas en Retrovirus y Síndrome de Inmunodeficiencia Adquirida, Buenos Aires C1121ABG, Argentina

Corresponding author: Diego Martín Flichman, PhD, Adjunct Professor, Research Scientist, Microbiology, Universidad de Buenos Aires, Instituto de Investigaciones Biomédicas en Retrovirus y Síndrome de Inmunodeficiencia Adquirida, Paraguay 2155, Buenos Aires C1121ABG, Argentina. dflichman@ffyb.uba.ar

Abstract

After more than four decades of hepatitis B virus (HBV) vaccine implementation, its safety and efficacy in preventing HBV infection have been proven and several milestones have been achieved. Most countries have included HBV immunization schedules in their health policies and progress has been made regarding universalization of the first HBV vaccine dose at birth. All of these actions have significantly contributed to reducing both the incidence of HBV infection and its related complications. However, there are still many drawbacks to overcome. The main concerns are the deficient coverage rate of the dose at birth and the large adult population that has not been reached timely by universal immunization. Additionally, the current most widely used second-generation vaccines do not induce protective immunity in 5% to 10% of the population, particularly in people over 40-years-old, obese (body mass index > 25 kg/m^2), heavy smokers, and patients undergoing dialysis or infection with human immunodeficiency virus. Recently developed and approved novel vaccine formulations using more potent adjuvants or multiple antigens have shown better performance, particularly in difficult settings. These advances re-launch the expectations of achieving the World Health Organization's objective of completing hepatitis control by 2030.

Key Words: Hepatitis B virus; Vaccine; Immune response; Antibodies; Neutralizing

Core Tip: Second-generation vaccines induce the production of anti-hepatitis B surface antibodies (anti-HBs). Anti-HBs levels ≥ 10 mIU/mL prevent against infection. More than 90% of immunized persons achieve protective anti-HBs levels 1 mo after completing the three-dose vaccination schedule. Although antibody titers significantly drop during the 1st years after vaccination, memory immunity is sufficient to prevent infection regardless of the antibody levels. In some specific settings showing lower immune response rates, schemes with larger or additional doses and novel vaccine formulations are recommended.

Citation: Di Lello FA, Martínez AP, Flichman DM. Insights into induction of the immune response by the hepatitis B vaccine. *World J Gastroenterol* 2022; 28(31): 4249-4262
URL: https://www.wjgnet.com/1007-9327/full/v28/i31/4249.htm
DOI: https://dx.doi.org/10.3748/wjg.v28.i31.4249

INTRODUCTION

Hepatitis B infection has been a major public health concern for a long time. Identification of the hepatitis B virus (HBV) in the 1960s and the subsequent development of a safe and effective vaccine were the kickoff to begin to retrace the path and achieve the desired control of this health problem.

First-generation vaccines based on heat-treated plasma derived from hepatitis B surface antigen (HBsAg)-positive donors raised concerns about its safety and availability to meet the vaccine manufacturer's needs. Shortly afterwards, second-generation DNA vaccines prepared in yeast transfected with recombinant plasmids encoding small HBV surface proteins (SHBs) were developed and approved in 1986[1]. Lastly, third-generation vaccines have been produced in mammalian cells that express and secrete SHBs and middle pre-S2 proteins (MHBs) or the three HBV envelope proteins (SHBs, MHBs, and large HBs).

It is worth noting that several studies have compared the immune response to plasma-derived first-generation vaccines to the recombinant second-generation ones. Most of the studies showed that the lowering rate of anti-HBs was higher in people receiving the recombinant HBV vaccine. However, plasma-derived vaccines were replaced by the recombinant ones due to safety concerns about human blood-derived products[2-5]. In addition, it has been shown that third-generation vaccines containing the pre-S2 and pre-S1 antigens would induce a higher anti-HBs response than second-generation ones, particularly in people ≥ 45-years-old[6-8]. Moreover, compared to plasma-derived vaccines, it has been observed that the HBsAg seropositive rate drops by about 71% and that the anti-HBc seropositive rate decreases by approximately 65% when recombinant HBV vaccines are used, supporting their higher effectiveness[4].

The HBV vaccine has been introduced progressively in the national vaccination calendars. Currently, second-generation HBV vaccines have been widely implemented for newborns in most countries. The pentavalent vaccine formulation protecting against diphtheria, pertussis, tetanus, hepatitis B, and *Haemophilus influenzae* type B is administered in three doses, 4 wk apart (recommended dosing at 6, 10, and 14 postnatal wk), and aims to lessen horizontal transmission. In addition, a monovalent single dose of the HBV vaccine (HepB-BD) administered within 24 h after delivery is also recommended to reduce mother-to-child transmission (Figure 1). The advised immunization schedule for the adult population includes three vaccine doses (HepB3) according to the individuals' age. Immunocompromised adults or patients on dialysis treatment require higher or additional doses of HBV vaccines. Recently, a novel vaccine (Heplisav-B) with a different adjuvant was approved for adult immunization with a recommended schedule of two doses 1 mo apart.

Since 1990, the proportion of children receiving all three doses of the HBV vaccine has increased globally from 1% to 85%. By 2020, the HBV vaccine was introduced to 190 countries with 83% of three-dose coverage rate. Few countries with very low endemicity that consider HBV infection as a limited public health problem provide the HBV vaccine to only well-defined risk groups. Likewise, a dose of HepB-BD has been introduced in the national calendar of 113 countries. Figure 2 shows the HBV worldwide three-dose infant vaccine coverage and the HBsAg seroprevalence[2,9]. However, the at birth dose coverage rate is poor (estimated at 43%) with remarkable disparities according to region and development level[10-12].

Universal vaccination is the most effective strategy to prevent and control HBV infection. In 2016, the World Health Organization (WHO) set the goal of controlling HBV by 2030. The proposed targets include the 90% global coverage of three-dose infant vaccination by 2020, birth-dose vaccination of 50%

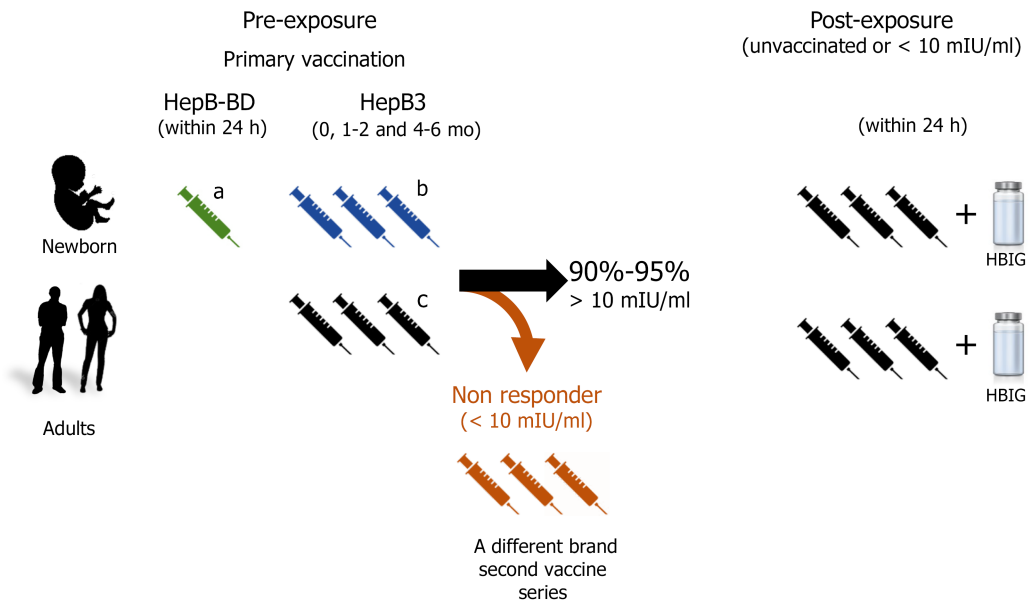

DOI: 10.3748/wjg.v28.i31.4249 **Copyright** ©The Author(s) 2022.

Figure 1 Recommended hepatitis B virus vaccination schemes. The hepatitis B immunization schedule is flexible, but minimal intervals and ages need to be observed. The recommended dose varies (5-40 μg of hepatitis B surface antigen protein/mL) depending on the individuals' age and the vaccine brand. [a]Monovalent hepatitis B vaccine 0.5 mL must be used for the at birth immunization (HepB-BD). Immunocompromised adults or patients under dialysis require larger or additional doses of the hepatitis B vaccine; [b]Combined hepatitis B, diphtheria, tetanus, adsorbed acellular pertussis, inactivated poliovirus vaccine. This vaccine cannot be administered at birth, before 6 postnatal weeks, or at age ≥ 7 years; [c]Heplisav-B is a vaccine recently approved for adults; it has a novel adjuvant and its recommended schedule is two doses 1 mo apart. HepB3: Three doses of hepatitis B vaccine; HepB-BD: Monovalent single dose of the hepatitis B virus vaccine; HBIG: Hepatitis B Immunoglobulin.

of infants by 2020, and of 90% of them by 2030[13].

MILESTONES ACHIEVED WITH THE HBV VACCINE

One of the goals of the strategy to achieve HBV control by 2030 is to reduce HBsAg prevalence to 0.1% in 5-year-old children and many countries are already on track to that milestone[14].

The global implementation of the HBV vaccine as part of the national health policies has contributed to directly reducing the global burden of infection, and indirectly, the HBV-related mortality. After the inclusion of HBV vaccination schedules, several surveillance studies have shown an overtime global HBsAg prevalence decrease in most countries[15], either in hyperendemic ones or in those with low or medium HBV infection prevalence[16-20].

Taiwan was the first country to implement a mass vaccination program against HBV in 1984 and it is the paradigm of its impact on the control of hepatitis. After 30 years of sustained immunization programs, the prevalence of HBsAg has decreased from 9.8% in the pre-vaccination period to 0.5% in the cohort reached by HBV vaccination protocols[21]. The main reason for Taiwan's success was its high three-dose hepatitis infant vaccine coverage rate, which increased from 88.9% in 1985[22,23] to 98.1% in 2018[21].

In the United States, since first HBV vaccine recommendations, the infection incidence has decreased by approximately 90%, from 9.6/100000 cases in 1982 to 1.0/100000 cases in 2018[24]. Similarly, in China, where the coverage of the three-dose vaccine schedule has increased from 30.0% to 93.4% and the at birth dose increased from 22.2% to 82.6%, the HBsAg prevalence decreased from 5.5% to 0.9% between 1992 and 2005[25]. In Argentina, a country with low HBV endemicity, the HBV vaccine was included in newborns' schedules in 2000 and, later in 2003, the catch-up strategy was implemented in 11-year-old adolescents. Currently, the coverage rate of protective antibodies is significantly higher in persons born after 1992 than in those born previously (Figure 3A)[26,27]. In fact, new infections generally occur in the population over 20-years-old not reached by vaccination[28]. These results emphasize the need to raise awareness among people not reached by universal HBV immunization programs and to focus vaccination campaigns on this group.

However, the most outstanding HBV preventive action impact has been detected in regions that were hyperendemic before introduction of the vaccine. In a Southern Italian area, where the vaccine was introduced in 1991, the HBsAg prevalence dropped from 13.4% in 1978 to 0.91% in 2006[29]. Likewise, in Alaska, where one of the highest HBV infection incidences has been reported, universal childhood

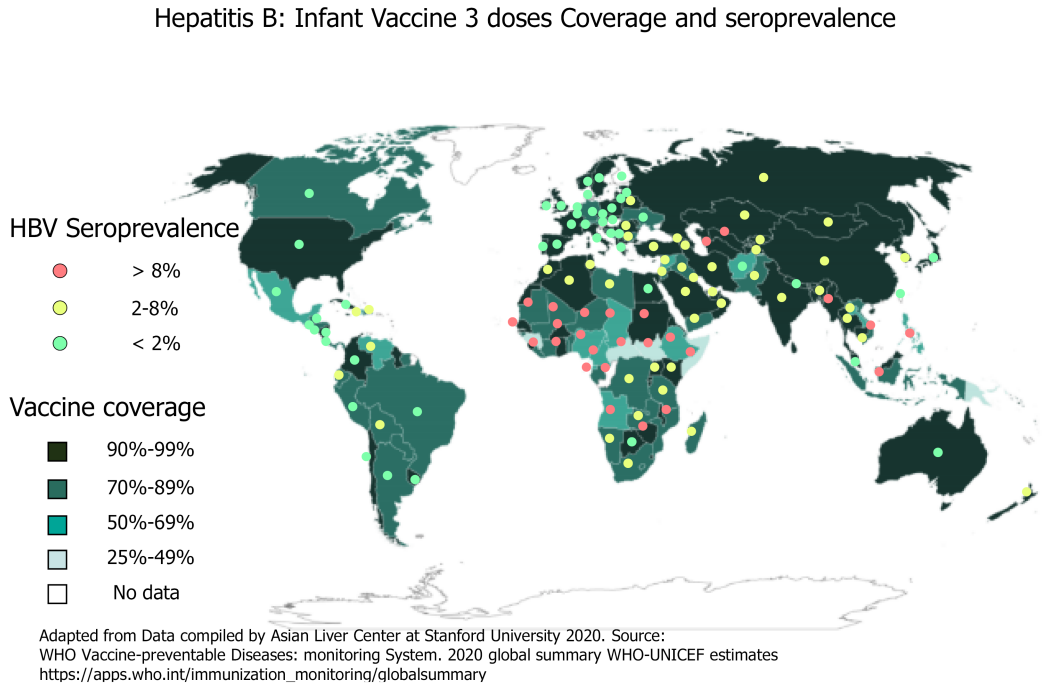

Figure 2 Hepatitis B three doses of infant vaccine coverage and seroprevalence. Hepatitis B virus seroprevalence data is from Polaris Observatory Collaborators: Global Prevalence, Treatment, and Prevention of Hepatitis B Virus Infection in 2016: A Modelling Study. Lancet Gastroenterol Hepatol 2018; 3: 383–403. HBV: Hepatitis B virus.

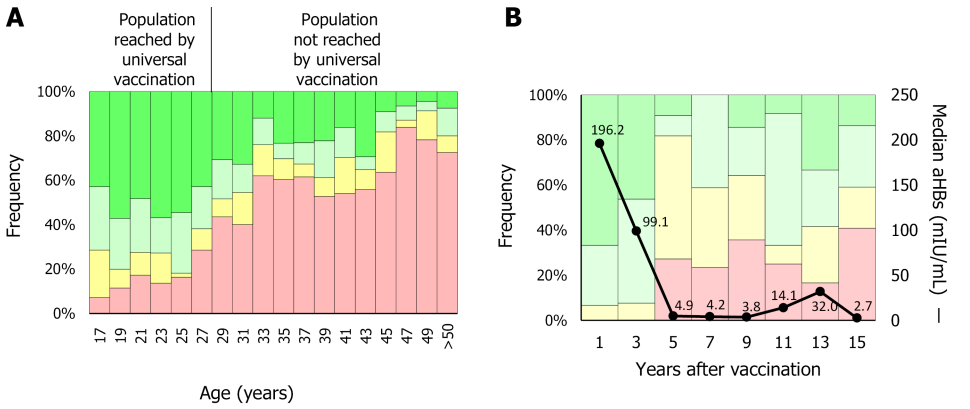

DOI: 10.3748/wjg.v28.i31.4249 **Copyright** ©The Author(s) 2022.

Figure 3 Anti-hepatitis B surface antibodies titers by age. A: The anti-hepatitis B surface antibodies (anti-HBs) titer was determined in 765 blood donors. In 2000, vaccination against hepatitis B virus was included in the Argentine newborns' National Vaccination Calendar. In 2003, the catch-up strategy for 11-year-old children was implemented. Therefore, individuals under 28-years-old are reached currently by the universal vaccine implementation. On average, protective levels of anti-HBs (> 10 mIU/mL) were detected in 75.2% of the population reached by universal vaccination (< 28-years-old) and in 32.2% of the not reached population (> 28-years-old); B: Anti-HBs kinetics. The anti-HBs titer was determined in 132 children born after 2000. In the first 2 years, the median anti-HBs titer fell from 196.2 mIU/mL to less than 10 mIU/mL (black line). Five years post-vaccination, about 20% of the population showed anti-HBs levels below 10 mIU/mL. aHBs: Anti-hepatitis B surface antibodies.

vaccination was implemented for newborns in 1993. The HBsAg prevalence dropped from 13% detected before the HBV vaccination program, to 0% HBsAg-positive children less than 10-years-old[30].

Although slowly and delayed, a significant reduction in the hepatocellular carcinoma annual average incidence has been observed concomitantly with the HBV infection incidence decline, particularly in those countries where early vaccine protocols have been introduced[31-33].

IMMUNITY

HBV vaccine-induced protective immunity

Several studies have shown that HBV vaccines induced both humoral and cellular immunity providing long-term protection[34,35]. On the one hand, neutralizing antibodies are elicited and two types of them have been identified. The first type targets the "a" determinant and neutralizes cell viral penetration by blocking the interaction with heparan sulfate[36], required by the virus at an early stage of hepatocyte entrance[37]. The second type targets the high-affinity receptor-binding site of the HBV pre-S1 domain and blocks the binding to the Na^+-taurocholate cotransporting polypeptide receptor preventing the infection of hepatocytes[38,39]. On the other hand, immune memory cells are generated, which upon contact with the HBV can be activated to expand rapidly. This response has been well demonstrated in studies that administered a booster dose to previously vaccinated persons whose antibody titers had fallen below protective titers[16,40-42].

Pre-exposure: Efficacy and effectiveness studies carried out in animal models first and then in human beings have shown that the HBV vaccine induces the production of neutralizing antibodies against HBV surface antigen (anti-HBs)[43]. Two main questions raised suddenly once the HBV vaccine was developed: What are the levels of antibodies that protect against infection and how long does immunity last? Soon after the release of the vaccine, several studies have shown that anti-HBs levels ≥ 10 mIU/mL, determined 1 to 3 mo after the complete three-dose vaccination scheme administration, were a surrogate marker for vaccine-induced protective immunity[44-46].

The overall response rate to the HBV vaccine, defined as individuals achieving anti-HBs levels > 10 mIU/mL, is 90% to 95% of immunized persons. Different factors such as host genetics, age, body weight, smoking, and concomitant disease have been shown to affect the response rate to the vaccine [47]. These variations probably rely on the strength of the cellular immune response. Velu *et al*[48] have characterized the cellular immune response and the cytokine profile of vaccine responders and non-responders to investigate the immunization outcome underlying mechanisms. The authors reported that HBsAg-specific interferon gamma, interleukin 10, and tumor necrosis factor alpha secretion correlated with the HBV vaccine-induced humoral immune response. Likewise, non-responders had lower levels of T helper type 1 (Th1) and Th2 cytokines. In addition, Körber *et al*[49] observed a higher frequency of regulatory B cells in HBV vaccine non-responders. Regulatory B cells suppress immunopathology by skewing T-cell differentiation. Overall, these results suggest that impaired lymphocyte activation is associated with a weak or no response to HBV vaccination.

Notably, although the HBV vaccine induces protective immunity against infection it would not be sterilizing. Consequently, vaccinated people can become infected although episodes are usually asymptomatic and self-limited[50-52]. These benign infection results are possibly due to long-lasting HBV cellular immunity induced by the vaccine despite antibody loss against HBV surface antigens[53].

Post-exposure: Immunization with HBV vaccines combined with different injection sites of HBV immunoglobulin administration, within 12 h after birth, showed a greater than 85% efficacy in preventing infection in infants born to HBsAg-positive mothers[54]. In adult persons, post-exposure prophylaxis is also recommended depending on the individual's vaccination and anti-HBs status. In unvaccinated subjects or with non-protective levels of anti-HBs, the HBV vaccine has shown high efficacy in preventing infection when administered within 24 h after percutaneous or mucosal exposure to HBV-positive blood. Additional post-exposure immunoprophylaxis is not suggested in individuals who achieved anti-HBs protective levels after vaccination.

Although, as previously mentioned, the massive implementation of the HBV vaccine substantially reduced the incidence and prevalence of the infection, few works have addressed the effectiveness of the vaccine and most of them have been carried out in high endemic countries. In general, a 70% to 94% effectiveness range has been reported, depending mainly on the follow-up time, the exposure risk rate (HBsAg prevalence of the population), and the studied cohort age[18,23,55]. A recent study showed an approximately 58% effectiveness in a birth cohort (mean age, 12 years) and 85% in participants at least 20-years-old[56]. The lower efficacy observed in the birth cohort could be a consequence of a lower level of exposure.

HOW LONG DO THE ANTIBODIES LAST?

Protective antibodies levels tend to decrease over time, especially during the 1st years after vaccination [57]. In a study carried out by our group, including 132 children born after infants' vaccine implementation, we observed that anti-HBs titers were significantly higher 1 year post-vaccination compared to the 2 years and 3 years earliest vaccinated population (Figure 3B). In addition, approximately 20% of the 5-year post-vaccination cohort showed anti-HBs levels lower than 10 mIU/mL[27]. These results are in line with a study conducted in Germany, where anti-HBs levels were determined in 106 teenagers, mean age 13.7-years-old, after primary vaccination. Forty percent of cases had anti-HBs levels < 10 mIU/mL. However, almost all (97%) teenagers who received a booster vaccine achieved anti-

HBs levels ≥ 100 mIU/mL regardless of their pre-booster levels[58]. Besides time elapsed since primary vaccination, a systematic meta-analysis including 46 studies analyzed the anti-HBs levels from 5 years to 20 years after the primary vaccination and identified the vaccination dose and the less than 6-mo interval between the last dose and the previous one as the main factors associated with anti-HBs titer loss[59]. On the other hand, the duration of antibody levels is directly correlated with the titers reached when completing the vaccination scheme[60].

Another interesting issue regarding antibodies duration refers to the subjects' age at the time of vaccination. Numerous studies have shown that vaccination in adolescence generates higher and long-lasting titers compared to children vaccinated at birth[61-64], being the age at the time of vaccination an independent variable associated with an anti-HBs titer < 10 mIU/mL. However, childhood HBV vaccination, together with other vaccines, guarantees a higher coverage rate.

Overall, it is widely accepted that a large proportion of vaccinated individuals, particularly those immunized during childhood, rapidly lose their anti-HBs titers below protective levels[40]. However, it has also been extensively described that individuals who achieved anti-HBs protective titers at the time of vaccination, show a rapid anamnestic response when boosted[41,42], suggesting that memory immunity plays a decisive role in the protection against clinical disease and the development of a carrier state regardless of anti-HBs antibody levels[35]. In this regard, it has been observed that even in the lack of anti-HBs, a significant amount of HBsAg-specific memory T and B cells are detected in vaccine responders. For this reason, although it remains a controversial issue, vaccine booster doses are not recommended currently for children and adults with normal immune status, despite the overtime drop of anti-HBs antibody titers[35,65]. Nonetheless, the anti-HBs titer decline could represent a problem for high-risk groups.

MANAGEMENT OF SPECIAL POPULATIONS

Adult persons with increased risk factors for infection are one of the WHO identified obstacles to HBV elimination as a public health problem[66,67]. These groups mainly include health care providers, illicit injected drug users, sexually active individuals (more than 1 partner in the past 6 mo), persons with diabetes, dialysis patients, and people living with human immunodeficiency virus (HIV). The last two groups, in addition to showing a higher risk of HBV infection compared to the general population[68-70] due to the frequent use of percutaneous materials and the common route of HBV and HIV transmission, have shown suboptimal responses to HBV immunization[71,72]. Patients on dialysis have also shown a diminished response to the HBV vaccine probably due to a uremic-associated suppression of the immune system that leads to a significant progressive reduction of the percentage and count of lymphocytes CD3+, CD4+, and CD8+ and a disturbance of antigen-presenting cells that results in an inability to sustain a satisfactory antibody titer over time[73-76]. In fact, in this population subset, the rate of seroprotection level ranges from 33.3% to 86%[77].

It has been reported that patients living with HIV present a poor initial HBV immunization response, lower seroconversion rates, and difficulty in maintaining immunity over time, mainly due to B-cell dysfunction[67,71,78,79]. For this group, the efficacy of the standard vaccine scheme in the era of the highly active antiretroviral therapy ranges from 17.5% to 71%[80-83].

Consequently, for patients on dialysis and/or living with HIV, other approaches are recommended to enhance the HBV vaccine immune response. For patients undergoing dialysis therapy, alternative strategies include the use of adjuvants, additional vaccination cycles, different vaccine formulations, greater number and concentration of doses, greater frequency of doses, dual vaccination, alternative administration routes, and/or use of booster vaccines[67,72,84-86]. On the other hand, for HIV-infected individuals with negative or < 10 mIU/mL anti-HBs levels after a primary vaccine series, a second HBV vaccine series using larger or additional doses is recommended[71,87]. Furthermore, revaccination should be attempted after HIV viral load suppression and CD4 cell count improvement[83].

RATE OF RESPONSE TO HBV VACCINE

As mentioned above, the average response rate to the HBV vaccine is greater than 90% with 5% to 10% vaccinated persons failing to mount a protective immunity level once the vaccination schedule is completed. The response to the vaccine ultimately relies on the individual immune system; however, different factors impairing the response rate have been identified. Response rates can drop drastically when more than one of these factors are present.

Host genetics

Several studies have addressed, through different experimental approaches, the role of genetic polymorphisms in the response to the HBV vaccine. Single nucleotide polymorphisms in HLA loci[88-92], ILs (with a key role in the cellular and humoral response interplay)[93,94], or even other genes have

been associated with the response rate to HBV vaccination[90,95,96]. However, these findings have not been widely validated in different cohorts and should be considered with caution.

Age

One of the most recognized consequences of aging is the declination of the immune function and the concomitant vaccination response reduction. The HBV vaccine response rate decreases in people 40-years-old and even more in people older than 60 years[97,98]. This highlights the need to vaccinate the population not covered by health policies before they reach 40-years-old, which will result in important cost-benefit profits.

Body weight

Overweight and obesity are a growing public health problem worldwide that affects all age groups[99]. They are caused by the deposition of lipids into the adipose tissue and are defined as a body mass index ≥ 25 kg/m.

Shortly after the HBV vaccine was developed and implemented, obesity was found to be a factor impairing the strength of the immune response[100]. This finding has been widely validated in subsequent studies[101,102]. This drawback is not only attributed to the HBV vaccine but has also been described for other vaccines[103,104]. Adipose tissue has a role in modulating the immune system through different pathways, inducing a chronic pro-inflammatory state[105,106], which in the end is associated with immune system dysfunction. This includes the chronic activation of cells of the innate immune system and consequent local and systemic inflammation[107]. In addition, Frasca *et al*[108] described a percentage decrease of switched memory and transitional B cells and an increase of late/exhausted memory B cells with the consequent impaired response to the vaccine.

Smoking

As described for obesity, the link between tobacco smoking and impaired vaccine response has been proposed to be mediated by inflammation[109]. However, data from different studies are less robust. Some studies have reported lower responses to vaccination while others showed no association[110]. This controversy could be based on the level of daily cigarette intake. A recent study reported that subjects in the non-responder group were almost exclusively 'heavy smokers' defined as consumers of ≥ 10 cigarettes per day[111]. The development of new vaccine formulations including either additional antigens or more potent adjuvants could represent a solution to improve the response rate of individuals affected by these factors as well as for dialyzed or immunosuppressed patients.

NEW FORMULATIONS

As previously mentioned, one of the main drawbacks of the second-generation vaccines is the poor induction of immune response in 5% to 10% of the general population and individuals presenting detrimental factors that impair vaccine response. Therefore, efforts have been made to find more effective formulations to overcome this limitation. Two advances have been reported in recent years. One of them is the development and evaluation of new and more powerful adjuvants to enhance immunogenicity[112,113].

Heplisav-B (HepB-CpG), a single-antigen vaccine with a novel immunostimulatory adjuvant, has been approved for its use in people at least 18-years-old. This vaccine is administered in two doses, 1 mo apart[114]. The new adjuvant is a small synthetic cytidine-phosphate-guanosine oligodeoxynucleotide containing non-methylated CpG patterns, similar to those present in microbial DNA. This structure acts as an agonist of the toll-like receptor 9 that enhances the immune response. Several studies have shown higher response rates to other second-generation vaccines both in general population[115-117] and in persons with detrimental factors for vaccination response[118-120]. In addition, the two doses-1 mo apart-simplified schedule could help increase patient compliance and raise the coverage rate.

Alternatively, third-generation vaccines derived from mammalian cells, containing the medium and large HBV envelope proteins have been developed. The advantage of this approach is that antigens display the same *in vivo* post-translational modifications and protein folding.

In 2021, Sci-B-Vac was licensed, and phase III trials showed faster seroprotection and higher response rates than the second-generation vaccines[8,121]. These data making turn Sci-B-Vac of particular interest for its use in people with poor or no response. Particularly, Sci-B-Vac has shown greater efficacy in HIV-infected individuals' immunization and in the prevention of vertical infection transmission[122,123]. Furthermore, the multiple antigen display of the third-generation vaccines would protect against HBV vaccine breakthrough infections caused by the HBV S gene mutants widely described[124-126]. The results obtained through novel vaccine formulation approaches suppose a contribution to the prophylaxis of HBV infection and represent a promising future.

CURRENT CHALLENGE

Beyond significant advances in the prevention of HBV infection, several pitfalls have been identified that need to be overcome in order to eliminate HBV as a health problem[127]. Particularly, in developing countries, sustainable financial mechanisms are required to scale up screening interventions and ensure access to vaccines.

Regarding the at birth dose, out-of-hospital deliveries, shortage of monovalent vaccine formulation in some regions, insufficient training of health care providers, weak monitoring and reporting systems, and low government commitment impair its implementation. On the other hand, in the adult population not covered by universal vaccination, promoting information, raising consciousness about risk, and finally focusing and promoting vaccination campaigns should improve immunization strategies for this group.

CONCLUSION

The worldwide application of HBV vaccines has led to a significant decrease in HBV infection incidence and its related death rates. As a general strategy, surveys are necessary to identify local constraints (in regions or countries) in order to achieve the implementation of WHO guidelines, both at the prophylaxis and diagnostic levels. Increasing efforts to improve vaccination coverage and raise awareness among populations not reached by universal vaccination will contribute significantly to achieving the WHO goals by 2030. Although HBV vaccines induce protective immunity in more than 90% of immunized people, there are particular settings where the efficacy is lower. In recent years, new formulations containing new adjuvants or other HBV antigens in addition to HBs, that could overcome the limitations of current presentations.

ACKNOWLEDGEMENTS

To Silvina Heisecke, from CEMIC-CONICET, for the copyediting of the manuscript.

FOOTNOTES

Author contributions: Di Lello FA and Flichman DM contributed to the review concept, and designed and drafted the manuscript; Martínez AP contributed to critical revisions of the manuscript for important intellectual content and gave final approval of the version to be submitted.

Conflict-of-interest statement: The authors have no conflicts of interest to declare.

Country/Territory of origin: Argentina

ORCID number: Federico Alejandro Di Lello 0000-0001-9771-9705; Alfredo Pedro Martínez 0000-0002-1807-0598; Diego Martín Flichman 0000-0001-5730-154X.

S-Editor: Chang KL
L-Editor: Filipodia
P-Editor: Chang KL

REFERENCES

1 **Beasley RP**. Development of hepatitis B vaccine. *JAMA* 2009; **302**: 322-324 [PMID: 19602694 DOI: 10.1001/jama.2009.1024]
2 **Kao JT**, Wang JH, Hung CH, Yen YH, Hung SF, Hu TH, Lee CM, Lu SN. Long-term efficacy of plasma-derived and recombinant hepatitis B vaccines in a rural township of Central Taiwan. *Vaccine* 2009; **27**: 1858-1862 [PMID: 19186203 DOI: 10.1016/j.vaccine.2009.01.027]
3 **Kim YJ**, Li P, Hong JM, Ryu KH, Nam E, Chang MS. A Single Center Analysis of the Positivity of Hepatitis B Antibody

after Neonatal Vaccination Program in Korea. *J Korean Med Sci* 2017; **32**: 810-816 [PMID: 28378555 DOI: 10.3346/jkms.2017.32.5.810]

4 **Hsu SH**, Chih AH, Lee YC, Huang KC, Jan CF. Higher disappearance rate of anti-HBs in Taiwanese freshers neonatally vaccinated with recombinant yeast hepatitis B vaccine. *Liver Int* 2017; **37**: 1780-1787 [PMID: 28374906 DOI: 10.1111/liv.13437]

5 **Hu YC**, Yeh CC, Chen RY, Su CT, Wang WC, Bai CH, Chan CF, Su FH. Seroprevalence of hepatitis B virus in Taiwan 30 years after the commencement of the national vaccination program. *PeerJ* 2018; **6**: e4297 [PMID: 29472994 DOI: 10.7717/peerj.4297]

6 **Shouval D**, Roggendorf H, Roggendorf M. Enhanced immune response to hepatitis B vaccination through immunization with a Pre-S1/Pre-S2/S vaccine. *Med Microbiol Immunol* 2015; **204**: 57-68 [PMID: 25557605 DOI: 10.1007/s00430-014-0374-x]

7 **Krawczyk A**, Ludwig C, Jochum C, Fiedler M, Heinemann FM, Shouval D, Roggendorf M, Roggendorf H, Lindemann M. Induction of a robust T- and B-cell immune response in non- and low-responders to conventional vaccination against hepatitis B by using a third generation PreS/S vaccine. *Vaccine* 2014; **32**: 5077-5082 [PMID: 24975813 DOI: 10.1016/j.vaccine.2014.06.076]

8 **Vesikari T**, Langley JM, Segall N, Ward BJ, Cooper C, Poliquin G, Smith B, Gantt S, McElhaney JE, Dionne M, van Damme P, Leroux-Roels I, Leroux-Roels G, Machluf N, Spaans JN, Yassin-Rajkumar B, Anderson DE, Popovic V, Diaz-Mitoma F; PROTECT Study Group. Immunogenicity and safety of a tri-antigenic *vs* a mono-antigenic hepatitis B vaccine in adults (PROTECT): a randomised, double-blind, phase 3 trial. *Lancet Infect Dis* 2021; **21**: 1271-1281 [PMID: 33989539 DOI: 10.1016/S1473-3099(20)30780-5]

9 **Polaris Observatory Collaborators**. Global prevalence, treatment, and prevention of hepatitis B virus infection in 2016: a modelling study. *Lancet Gastroenterol Hepatol* 2018; **3**: 383-403 [PMID: 29599078 DOI: 10.1016/S2468-1253(18)30056-6]

10 **World Health Organization**. Hepatitis B Control Through Immunization: A Reference Guide. [cited 5 February 2021]. In: World Health Organization [Internet]. Available from: http://iris.wpro.who.int/bitstream/handle/10665.1/10820/9789290616696_eng.pdf;jsessionid=FEDDD4672274909D7E6998B86BED45C8?sequence=3%0Ahttp://www.who.int/immunization/sage/meetings/2015/october/8_WPRO_Hepatitis_B_Prevention_Through_Immunization_Regional_R

11 **de Villiers MJ**, Nayagam S, Hallett TB. The impact of the timely birth dose vaccine on the global elimination of hepatitis B. *Nat Commun* 2021; **12**: 6223 [PMID: 34711822 DOI: 10.1038/s41467-021-26475-6]

12 **World Health Organization**. Progress Towards Global Immunization Goals – 2019. Summary presentations of key indicators, Updated July 2020. [cited 5 February 2021]. In: World Health Organization [Internet]. Available from: https://cdn.who.int/media/docs/default-source/immunization/global_monitoring/slidesglobalimmunization.pdf?sfvrsn=25385c3b_7

13 **World Health Organization**. Combating hepatitis B and C to reach elimination by 2030: advocacy brief (World Health Organization, Geneva, 2016). [cited 5 February 2021]. In: World Health Organization [Internet]. Available from: https://www.who.int/publications/i/item/combating-hepatitis-b-and-c-to-reach-elimination-by-2030

14 **World Health Organization**. Global health sector strategy on viral hepatitis 2016–2021. Towards ending viral hepatitis. [cited 5 February 2021]. In: World Health Organization [Internet]. Available from: https://www.who.int/publications/i/item/WHO-HIV-2016.06

15 **Zanetti AR**, Van Damme P, Shouval D. The global impact of vaccination against hepatitis B: a historical overview. *Vaccine* 2008; **26**: 6266-6273 [PMID: 18848855 DOI: 10.1016/j.vaccine.2008.09.056]

16 **McMahon BJ**, Dentinger CM, Bruden D, Zanis C, Peters H, Hurlburt D, Bulkow L, Fiore AE, Bell BP, Hennessy TW. Antibody levels and protection after hepatitis B vaccine: results of a 22-year follow-up study and response to a booster dose. *J Infect Dis* 2009; **200**: 1390-1396 [PMID: 19785526 DOI: 10.1086/606119]

17 **Mohaghegh Shelmani H**, Karayiannis P, Ashtari S, Mahmanzar MA, Khanabadi B, Modami N, Gholipour F, Zare F, Zali MR. Demographic changes of hepatitis B virus infection in Iran for the last two decades. *Gastroenterol Hepatol Bed Bench* 2017; **10**: S38-S43 [PMID: 29511470]

18 **Garcia D**, Porras A, Rico Mendoza A, Alvis N, Navas MC, De La Hoz F, De Neira M, Osorio E, Valderrama JF. Hepatitis B infection control in Colombian Amazon after 15 years of hepatitis B vaccination. Effectiveness of birth dose and current prevalence. *Vaccine* 2018; **36**: 2721-2726 [PMID: 29609968 DOI: 10.1016/j.vaccine.2017.11.004]

19 **Stroffolini T**, Guadagnino V, Rapicetta M, Menniti Ippolito F, Caroleo B, De Sarro G, Focà A, Liberto MC, Giancotti A, Barreca GS, Marascio N, Lombardo F, Staltari O; Sersale's Study Collaborating Group. The impact of a vaccination campaign against hepatitis B on the further decrease of hepatitis B virus infection in a southern Italian town over 14 years. *Eur J Intern Med* 2012; **23**: e190-e192 [PMID: 22981290 DOI: 10.1016/j.ejim.2012.08.009]

20 **Huynh C**, Minuk GY, Uhanova J, Baikie M, Wong T, Osiowy C. Serological and molecular epidemiological outcomes after two decades of universal infant hepatitis B virus (HBV) vaccination in Nunavut, Canada. *Vaccine* 2017; **35**: 4515-4522 [PMID: 28736196 DOI: 10.1016/j.vaccine.2017.07.040]

21 **Lu FT**, Ni YH. Elimination of Mother-to-Infant Transmission of Hepatitis B Virus: 35 Years of Experience. *Pediatr Gastroenterol Hepatol Nutr* 2020; **23**: 311-318 [PMID: 32704492 DOI: 10.5223/pghn.2020.23.4.311]

22 **Gust ID**. Immunisation against hepatitis B in Taiwan. *Gut* 1996; **38** Suppl 2: S67-S68 [PMID: 8786059 DOI: 10.1136/gut.38.suppl_2.s67]

23 **Chien YC**, Jan CF, Kuo HS, Chen CJ. Nationwide hepatitis B vaccination program in Taiwan: effectiveness in the 20 years after it was launched. *Epidemiol Rev* 2006; **28**: 126-135 [PMID: 16782778 DOI: 10.1093/epirev/mxj010]

24 **Centers for Diseases Control and Prevention**. Epidemiology and Prevention of Vaccine-Preventable Diseases, Chapter 10: Hepatitis B. [cited 5 February 2021]. Available From: https://www.cdc.gov/vaccines/pubs/pinkbook/hepb.html

25 **Liang X**, Bi S, Yang W, Wang L, Cui G, Cui F, Zhang Y, Liu J, Gong X, Chen Y, Wang F, Zheng H, Guo J, Jia Z, Ma J, Wang H, Luo H, Li L, Jin S, Hadler SC, Wang Y. Evaluation of the impact of hepatitis B vaccination among children born during 1992-2005 in China. *J Infect Dis* 2009; **200**: 39-47 [PMID: 19469708 DOI: 10.1086/599332]

26 **Stecher D**, Katz N, Vizzotti C. Hepatitis B en Argentina. Situación actual y estrategia de vacunación universal para su

control y eliminación. *Actualizaciones en Sida e Infectología* 2014; **22**: 18-21

27 **Di Lello FA**, Blejer J, Alter A, Bartoli S, Vargas F, Ruiz R, Galli C, Blanco S, Gallego S, Fernández R, Martínez AP, Flichman DM. Hepatitis B surface antibodies seroprevalence among people born before and after implementation of universal HBV vaccination. *Vaccine* 2020; **38**: 2678-2682 [PMID: 32061386 DOI: 10.1016/j.vaccine.2020.02.014]

28 **Ministerio de Salud y desarrollo Social**. Boletín sobre las Hepatitis Virales en Argentina, N 1, AÑO 1, Octubre 2019. [cited 5 February 2021]. Available from: https://bancos.salud.gob.ar/sites/default/files/2020-01/0000001592cnt-2019-10_boletin-hepatitis.pdf

29 **Da Villa G**, Romanò L, Sepe A, Iorio R, Paribello N, Zappa A, Zanetti AR. Impact of hepatitis B vaccination in a highly endemic area of south Italy and long-term duration of anti-HBs antibody in two cohorts of vaccinated individuals. *Vaccine* 2007; **25**: 3133-3136 [PMID: 17280750 DOI: 10.1016/j.vaccine.2007.01.044]

30 **Harpaz R**, McMahon BJ, Margolis HS, Shapiro CN, Havron D, Carpenter G, Bulkow LR, Wainwright RB. Elimination of new chronic hepatitis B virus infections: results of the Alaska immunization program. *J Infect Dis* 2000; **181**: 413-418 [PMID: 10669320 DOI: 10.1086/315259]

31 **Lin CL**, Kao JH. Hepatitis B: Immunization and Impact on Natural History and Cancer Incidence. *Gastroenterol Clin North Am* 2020; **49**: 201-214 [PMID: 32389359 DOI: 10.1016/j.gtc.2020.01.010]

32 **Chang MH**, Chen CJ, Lai MS, Hsu HM, Wu TC, Kong MS, Liang DC, Shau WY, Chen DS. Universal hepatitis B vaccination in Taiwan and the incidence of hepatocellular carcinoma in children. Taiwan Childhood Hepatoma Study Group. *N Engl J Med* 1997; **336**: 1855-1859 [PMID: 9197213 DOI: 10.1056/NEJM199706263362602]

33 **Chang MH**, You SL, Chen CJ, Liu CJ, Lee CM, Lin SM, Chu HC, Wu TC, Yang SS, Kuo HS, Chen DS; Taiwan Hepatoma Study Group. Decreased incidence of hepatocellular carcinoma in hepatitis B vaccinees: a 20-year follow-up study. *J Natl Cancer Inst* 2009; **101**: 1348-1355 [PMID: 19759364 DOI: 10.1093/jnci/djp288]

34 **Said ZN**, Abdelwahab KS. Induced immunity against hepatitis B virus. *World J Hepatol* 2015; **7**: 1660-1670 [PMID: 26140085 DOI: 10.4254/wjh.v7.i12.1660]

35 **Van Damme P**, Dionne M, Leroux-Roels G, Van Der Meeren O, Di Paolo E, Salaun B, Surya Kiran P, Folschweiller N. Persistence of HBsAg-specific antibodies and immune memory two to three decades after hepatitis B vaccination in adults. *J Viral Hepat* 2019; **26**: 1066-1075 [PMID: 31087382 DOI: 10.1111/jvh.13125]

36 **Sureau C**, Salisse J. A conformational heparan sulfate binding site essential to infectivity overlaps with the conserved hepatitis B virus a-determinant. *Hepatology* 2013; **57**: 985-994 [PMID: 23161433 DOI: 10.1002/hep.26125]

37 **Schulze A**, Gripon P, Urban S. Hepatitis B virus infection initiates with a large surface protein-dependent binding to heparan sulfate proteoglycans. *Hepatology* 2007; **46**: 1759-1768 [PMID: 18046710 DOI: 10.1002/hep.21896]

38 **Urban S**, Bartenschlager R, Kubitz R, Zoulim F. Strategies to inhibit entry of HBV and HDV into hepatocytes. *Gastroenterology* 2014; **147**: 48-64 [PMID: 24768844 DOI: 10.1053/j.gastro.2014.04.030]

39 **Yan H**, Zhong G, Xu G, He W, Jing Z, Gao Z, Huang Y, Qi Y, Peng B, Wang H, Fu L, Song M, Chen P, Gao W, Ren B, Sun Y, Cai T, Feng X, Sui J, Li W. Sodium taurocholate cotransporting polypeptide is a functional receptor for human hepatitis B and D virus. *Elife* 2012; **1**: e00049 [PMID: 23150796 DOI: 10.7554/eLife.00049]

40 **Lu CY**, Ni YH, Chiang BL, Chen PJ, Chang MH, Chang LY, Su IJ, Kuo HS, Huang LM, Chen DS, Lee CY. Humoral and cellular immune responses to a hepatitis B vaccine booster 15-18 years after neonatal immunization. *J Infect Dis* 2008; **197**: 1419-1426 [PMID: 18444799 DOI: 10.1086/587695]

41 **Bruce MG**, Bruden D, Hurlburt D, Zanis C, Thompson G, Rea L, Toomey M, Townshend-Bulson L, Rudolph K, Bulkow L, Spradling PR, Baum R, Hennessy T, McMahon BJ. Antibody Levels and Protection After Hepatitis B Vaccine: Results of a 30-Year Follow-up Study and Response to a Booster Dose. *J Infect Dis* 2016; **214**: 16-22 [PMID: 26802139 DOI: 10.1093/infdis/jiv748]

42 **Wang ZZ**, Gao YH, Lu W, Jin CD, Zeng Y, Yan L, Ding F, Li T, Liu XE, Zhuang H. Long-term persistence in protection and response to a hepatitis B vaccine booster among adolescents immunized in infancy in the western region of China. *Hum Vaccin Immunother* 2017; **13**: 909-915 [PMID: 27874311 DOI: 10.1080/21645515.2016.1250990]

43 **Bitter GA**, Egan KM, Burnette WN, Samal B, Fieschko JC, Peterson DL, Downing MR, Wypych J, Langley KE. Hepatitis B vaccine produced in yeast. *J Med Virol* 1988; **25**: 123-140 [PMID: 3292698 DOI: 10.1002/jmv.1890250202]

44 **Jack AD**, Hall AJ, Maine N, Mendy M, Whittle HC. What level of hepatitis B antibody is protective? *J Infect Dis* 1999; **179**: 489-492 [PMID: 9878036 DOI: 10.1086/314578]

45 **Hall AJ**. Hepatitis B vaccination: protection for how long and against what? *BMJ* 1993; **307**: 276-277 [PMID: 8374369 DOI: 10.1136/bmj.307.6899.276]

46 Immunisation against hepatitis B. *Lancet* 1988; **1**: 875-876 [PMID: 2895375]

47 **Yang S**, Tian G, Cui Y, Ding C, Deng M, Yu C, Xu K, Ren J, Yao J, Li Y, Cao Q, Chen P, Xie T, Wang C, Wang B, Mao C, Ruan B, Jiang T, Li L. Factors influencing immunologic response to hepatitis B vaccine in adults. *Sci Rep* 2016; **6**: 27251 [PMID: 27324884 DOI: 10.1038/srep27251]

48 **Velu V**, Saravanan S, Nandakumar S, Shankar EM, Vengatesan A, Jadhav SS, Kulkarni PS, Thyagarajan SP. Relationship between T-lymphocyte cytokine levels and sero-response to hepatitis B vaccines. *World J Gastroenterol* 2008; **14**: 3534-3540 [PMID: 18567083 DOI: 10.3748/wjg.14.3534]

49 **Körber N**, Pohl L, Weinberger B, Grubeck-Loebenstein B, Wawer A, Knolle PA, Roggendorf H, Protzer U, Bauer T. Hepatitis B Vaccine Non-Responders Show Higher Frequencies of $CD24^{high}CD38^{high}$ Regulatory B Cells and Lower Levels of IL-10 Expression Compared to Responders. *Front Immunol* 2021; **12**: 713351 [PMID: 34566969 DOI: 10.3389/fimmu.2021.713351]

50 **Werner JM**, Abdalla A, Gara N, Ghany MG, Rehermann B. The hepatitis B vaccine protects re-exposed health care workers, but does not provide sterilizing immunity. *Gastroenterology* 2013; **145**: 1026-1034 [PMID: 23916846 DOI: 10.1053/j.gastro.2013.07.044]

51 **Su TH**, Chen PJ. Emerging hepatitis B virus infection in vaccinated populations: a rising concern? *Emerg Microbes Infect* 2012; **1**: e27 [PMID: 26038431 DOI: 10.1038/emi.2012.28]

52 **Poovorawan Y**, Chongsrisawat V, Theamboonlers A, Leroux-Roels G, Kuriyakose S, Leyssen M, Jacquet JM. Evidence

of protection against clinical and chronic hepatitis B infection 20 years after infant vaccination in a high endemicity region. *J Viral Hepat* 2011; **18**: 369-375 [PMID: 20384962 DOI: 10.1111/j.1365-2893.2010.01312.x]

53 **Simons BC**, Spradling PR, Bruden DJ, Zanis C, Case S, Choromanski TL, Apodaca M, Brogdon HD, Dwyer G, Snowball M, Negus S, Bruce MG, Morishima C, Knall C, McMahon BJ. A Longitudinal Hepatitis B Vaccine Cohort Demonstrates Long-lasting Hepatitis B Virus (HBV) Cellular Immunity Despite Loss of Antibody Against HBV Surface Antigen. *J Infect Dis* 2016; **214**: 273-280 [PMID: 27056956 DOI: 10.1093/infdis/jiw142]

54 **Yu AS**, Cheung RC, Keeffe EB. Hepatitis B vaccines. *Clin Liver Dis* 2004; **8**: 283-300 [PMID: 15481341 DOI: 10.1016/j.cld.2004.02.010]

55 **Peto TJ**, Mendy ME, Lowe Y, Webb EL, Whittle HC, Hall AJ. Efficacy and effectiveness of infant vaccination against chronic hepatitis B in the Gambia Hepatitis Intervention Study (1986-90) and in the nationwide immunisation program. *BMC Infect Dis* 2014; **14**: 7 [PMID: 24397793 DOI: 10.1186/1471-2334-14-7]

56 **He WQ**, Guo GN, Li C. The impact of hepatitis B vaccination in the United States, 1999-2018. *Hepatology* 2022; **75**: 1566-1578 [PMID: 34855999 DOI: 10.1002/hep.32265]

57 **Jilg W**, Schmidt M, Deinhardt F. Four-year experience with a recombinant hepatitis B vaccine. *Infection* 1989; **17**: 70-76 [PMID: 2714860 DOI: 10.1007/BF01646879]

58 **Anderson CL**, Remschmidt C, Drobnitzky FP, Falkenhorst G, Zimmermann R, Wichmann O, Harder T. Hepatitis B immune status in adolescents vaccinated during infancy: A retrospective cohort study from a pediatric practice in Germany. *Hum Vaccin Immunother* 2016; **12**: 779-784 [PMID: 26633195 DOI: 10.1080/21645515.2015.1105414]

59 **Schönberger K**, Riedel C, Rückinger S, Mansmann U, Jilg W, Kries RV. Determinants of Long-term protection after hepatitis B vaccination in infancy: a meta-analysis. *Pediatr Infect Dis J* 2013; **32**: 307-313 [PMID: 23249904 DOI: 10.1097/INF.0b013e31827bd1b0]

60 **Mendy M**, Peterson I, Hossin S, Peto T, Jobarteh ML, Jeng-Barry A, Sidibeh M, Jatta A, Moore SE, Hall AJ, Whittle H. Observational study of vaccine efficacy 24 years after the start of hepatitis B vaccination in two Gambian villages: no need for a booster dose. *PLoS One* 2013; **8**: e58029 [PMID: 23533578 DOI: 10.1371/journal.pone.0058029]

61 **Coppola N**, Corvino AR, De Pascalis S, Signoriello G, Di Fiore E, Nienhaus A, Sagnelli E, Lamberti M. The long-term immunogenicity of recombinant hepatitis B virus (HBV) vaccine: contribution of universal HBV vaccination in Italy. *BMC Infect Dis* 2015; **15**: 149 [PMID: 25884719 DOI: 10.1186/s12879-015-0874-3]

62 **Trevisan A**, Mason P, Nicolli A, Maso S, Fonzo M, Scarpa B, Bertoncello C. Future Healthcare Workers and Hepatitis B Vaccination: A New Generation. *Int J Environ Res Public Health* 2021; **18** [PMID: 34360071 DOI: 10.3390/ijerph18157783]

63 **Pileggi C**, Papadopoli R, Bianco A, Pavia M. Hepatitis B vaccine and the need for a booster dose after primary vaccination. *Vaccine* 2017; **35**: 6302-6307 [PMID: 28988867 DOI: 10.1016/j.vaccine.2017.09.076]

64 **Stefanati A**, Bolognesi N, Sandri F, Dini G, Massa E, Montecucco A, Lupi S, Gabutti G. Long-term persistency of hepatitis B immunity: an observational cross-sectional study on medical students and resident doctors. *J Prev Med Hyg* 2019; **60**: E184-E190 [PMID: 31650052 DOI: 10.15167/2421-4248/jpmh2019.60.3.1315]

65 **Bauer T**, Jilg W. Hepatitis B surface antigen-specific T and B cell memory in individuals who had lost protective antibodies after hepatitis B vaccination. *Vaccine* 2006; **24**: 572-577 [PMID: 16171909 DOI: 10.1016/j.vaccine.2005.08.058]

66 World Health Organization. Hepatitis B vaccines: WHO position paper – July 2017. [cited 5 February 2021]. In: World Health Organization [Internet]. Available from: https://www.who.int/immunization/policy/position_papers/hepatitis_b/en/

67 **Schillie S**, Harris A, Link-Gelles R, Romero J, Ward J, Nelson N. Recommendations of the Advisory Committee on Immunization Practices for Use of a Hepatitis B Vaccine with a Novel Adjuvant. *MMWR Morb Mortal Wkly Rep* 2018; **67**: 455-458 [PMID: 29672472 DOI: 10.15585/mmwr.mm6715a5]

68 **Burdick RA**, Bragg-Gresham JL, Woods JD, Hedderwick SA, Kurokawa K, Combe C, Saito A, LaBrecque J, Port FK, Young EW. Patterns of hepatitis B prevalence and seroconversion in hemodialysis units from three continents: the DOPPS. *Kidney Int* 2003; **63**: 2222-2229 [PMID: 12753311 DOI: 10.1046/j.1523-1755.2003.00017.x]

69 **Thio CL**. Hepatitis B and human immunodeficiency virus coinfection. *Hepatology* 2009; **49**: S138-S145 [PMID: 19399813 DOI: 10.1002/hep.22883]

70 **Pereson MJ**, Martínez AP, Isaac K, Laham G, Ridruejo E, Garcia GH, Flichman DM, Di Lello FA. Seroprevalence of hepatitis B, hepatitis C and HIV infection among patients undergoing haemodialysis in Buenos Aires, Argentina. *J Med Microbiol* 2021; **70** [PMID: 33180017 DOI: 10.1099/jmm.0.001278]

71 **Whitaker JA**, Rouphael NG, Edupuganti S, Lai L, Mulligan MJ. Strategies to increase responsiveness to hepatitis B vaccination in adults with HIV-1. *Lancet Infect Dis* 2012; **12**: 966-976 [PMID: 23174382 DOI: 10.1016/S1473-3099(12)70243-8]

72 **Fabrizi F**, Cerutti R, Alfieri CM, Ridruejo E. An Update on Hepatocellular Carcinoma in Chronic Kidney Disease. *Cancers (Basel)* 2021; **13** [PMID: 34298832 DOI: 10.3390/cancers13143617]

73 **Fabrizi F**, Martin P. Hepatitis B virus infection in dialysis patients. *Am J Nephrol* 2000; **20**: 1-11 [PMID: 10644861 DOI: 10.1159/000013548]

74 **Cohen G**, Hörl WH. Immune dysfunction in uremia—an update. *Toxins (Basel)* 2012; **4**: 962-990 [PMID: 23202302 DOI: 10.3390/toxins4110962]

75 **Sampani E**, Vagiotas L, Daikidou DV, Nikolaidou V, Xochelli A, Kasimatis E, Lioulios G, Dimitriadis C, Fylaktou A, Papagianni A, Stangou M. End stage renal disease has an early and continuous detrimental effect on regulatory T cells. *Nephrology (Carlton)* 2022; **27**: 281-287 [PMID: 34781412 DOI: 10.1111/nep.13996]

76 **Sampani E**, Stangou M, Daikidou DV, Nikolaidou V, Asouchidou D, Dimitriadis C, Lioulios G, Xochelli A, Fylaktou A, Papagianni A. Influence of end stage renal disease on CD28 expression and T-cell immunity. *Nephrology (Carlton)* 2021; **26**: 185-196 [PMID: 32935413 DOI: 10.1111/nep.13784]

77 **Fabrizi F**, Lunghi G, Martin P. Treatment of HBV-related liver disease in the dialysis population: reality and promises. *Int J Artif Organs* 2001; **24**: 598-605 [PMID: 11693415]

78 **Kernéis S**, Launay O, Turbelin C, Batteux F, Hanslik T, Boëlle PY. Long-term immune responses to vaccination in HIV-

infected patients: a systematic review and meta-analysis. *Clin Infect Dis* 2014; **58**: 1130-1139 [PMID: 24415637 DOI: 10.1093/cid/cit937]

79 **Moretto F**, Catherine FX, Esteve C, Blot M, Piroth L. Isolated Anti-HBc: Significance and Management. *J Clin Med* 2020; **9** [PMID: 31940817 DOI: 10.3390/jcm9010202]

80 **Rey D**, Krantz V, Partisani M, Schmitt MP, Meyer P, Libbrecht E, Wendling MJ, Vetter D, Nicolle M, Kempf-Durepaire G, Lang JM. Increasing the number of hepatitis B vaccine injections augments anti-HBs response rate in HIV-infected patients. Effects on HIV-1 viral load. *Vaccine* 2000; **18**: 1161-1165 [PMID: 10649616 DOI: 10.1097/00002030-199911120-00016]

81 **Overton ET**, Sungkanuparph S, Powderly WG, Seyfried W, Groger RK, Aberg JA. Undetectable plasma HIV RNA load predicts success after hepatitis B vaccination in HIV-infected persons. *Clin Infect Dis* 2005; **41**: 1045-1048 [PMID: 16142673 DOI: 10.1086/433180]

82 **Paitoonpong L**, Suankratay C. Immunological response to hepatitis B vaccination in patients with AIDS and virological response to highly active antiretroviral therapy. *Scand J Infect Dis* 2008; **40**: 54-58 [PMID: 17852939 DOI: 10.1080/00365540701522975]

83 **Landrum ML**, Huppler Hullsiek K, Ganesan A, Weintrob AC, Crum-Cianflone NF, Barthel RV, Peel S, Agan BK. Hepatitis B vaccine responses in a large U.S. military cohort of HIV-infected individuals: another benefit of HAART in those with preserved CD4 count. *Vaccine* 2009; **27**: 4731-4738 [PMID: 19540026 DOI: 10.1016/j.vaccine.2009.04.016]

84 **Janus N**, Vacher LV, Karie S, Ledneva E, Deray G. Vaccination and chronic kidney disease. *Nephrol Dial Transplant* 2008; **23**: 800-807 [PMID: 18065804]

85 **Zhang W**, Du X, Zhao G, Jin H, Kang Y, Xiao C, Liu M, Wang B. Levamisole is a potential facilitator for the activation of Th1 responses of the subunit HBV vaccination. *Vaccine* 2009; **27**: 4938-4946 [PMID: 19549606 DOI: 10.1016/j.vaccine.2009.06.012]

86 **Haddiya I**. Current Knowledge of Vaccinations in Chronic Kidney Disease Patients. *Int J Nephrol Renovasc Dis* 2020; **13**: 179-185 [PMID: 32801834 DOI: 10.2147/IJNRD.S231142]

87 **Vargas JI**, Jensen D, Martínez F, Sarmiento V, Peirano F, Acuña P, Provoste F, Bustos V, Cornejo F, Fuster A, Acuña M, Fuster F, Soto S, Estay D, Jensen W, Ahumada R, Arab JP, Soza A. Comparative Efficacy of a High-Dose *vs* Standard-Dose Hepatitis B Revaccination Schedule Among Patients With HIV: A Randomized Clinical Trial. *JAMA Netw Open* 2021; **4**: e2120929 [PMID: 34424307 DOI: 10.1001/jamanetworkopen.2021.20929]

88 **Wang C**, Tang J, Song W, Lobashevsky E, Wilson CM, Kaslow RA. HLA and cytokine gene polymorphisms are independently associated with responses to hepatitis B vaccination. *Hepatology* 2004; **39**: 978-988 [PMID: 15057902 DOI: 10.1002/hep.20142]

89 **Davila S**, Froeling FE, Tan A, Bonnard C, Boland GJ, Snippe H, Hibberd ML, Seielstad M. New genetic associations detected in a host response study to hepatitis B vaccine. *Genes Immun* 2010; **11**: 232-238 [PMID: 20237496 DOI: 10.1038/gene.2010.1]

90 **Pan LP**, Zhang W, Zhang L, Wu XP, Zhu XL, Yan BY, Li JY, Xu AQ, Liu Y, Li H. CD3Z genetic polymorphism in immune response to hepatitis B vaccination in two independent Chinese populations. *PLoS One* 2012; **7**: e35303 [PMID: 22536368 DOI: 10.1371/journal.pone.0035303]

91 **Pan L**, Zhang L, Zhang W, Wu X, Li Y, Yan B, Zhu X, Liu X, Yang C, Xu J, Zhou G, Xu A, Li H, Liu Y. A genome-wide association study identifies polymorphisms in the HLA-DR region associated with non-response to hepatitis B vaccination in Chinese Han populations. *Hum Mol Genet* 2014; **23**: 2210-2219 [PMID: 24282030 DOI: 10.1093/hmg/ddt586]

92 **Ou G**, Liu X, Jiang Y. HLA-DPB1 alleles in hepatitis B vaccine response: A meta-analysis. *Medicine (Baltimore)* 2021; **100**: e24904 [PMID: 33832070 DOI: 10.1097/MD.0000000000024904]

93 **Cui W**, Sun CM, Deng BC, Liu P. Association of polymorphisms in the interleukin-4 gene with response to hepatitis B vaccine and susceptibility to hepatitis B virus infection: a meta-analysis. *Gene* 2013; **525**: 35-40 [PMID: 23651591 DOI: 10.1016/j.gene.2013.04.065]

94 **Höhler T**, Reuss E, Freitag CM, Schneider PM. A functional polymorphism in the IL-10 promoter influences the response after vaccination with HBsAg and hepatitis A. *Hepatology* 2005; **42**: 72-76 [PMID: 15918171 DOI: 10.1002/hep.20740]

95 **Duan Z**, Chen X, Liang Z, Zeng Y, Zhu F, Long L, McCrae MA, Zhuang H, Shen T, Lu F. Genetic polymorphisms of CXCR5 and CXCL13 are associated with non-responsiveness to the hepatitis B vaccine. *Vaccine* 2014; **32**: 5316-5322 [PMID: 25077417 DOI: 10.1016/j.vaccine.2014.07.064]

96 **Höhler T**, Reuss E, Evers N, Dietrich E, Rittner C, Freitag CM, Vollmar J, Schneider PM, Fimmers R. Differential genetic determination of immune responsiveness to hepatitis B surface antigen and to hepatitis A virus: a vaccination study in twins. *Lancet* 2002; **360**: 991-995 [PMID: 12383669 DOI: 10.1016/S0140-6736(02)11083-X]

97 **Van Der Meeren O**, Crasta P, Cheuvart B, De Ridder M. Characterization of an age-response relationship to GSK's recombinant hepatitis B vaccine in healthy adults: An integrated analysis. *Hum Vaccin Immunother* 2015; **11**: 1726-1729 [PMID: 25996260 DOI: 10.1080/21645515.2015.1039758]

98 **Weinberger B**, Haks MC, de Paus RA, Ottenhoff THM, Bauer T, Grubeck-Loebenstein B. Impaired Immune Response to Primary but Not to Booster Vaccination Against Hepatitis B in Older Adults. *Front Immunol* 2018; **9**: 1035 [PMID: 29868000 DOI: 10.3389/fimmu.2018.01035]

99 **Ng M**, Fleming T, Robinson M, Thomson B, Graetz N, Margono C, Mullany EC, Biryukov S, Abbafati C, Abera SF, Abraham JP, Abu-Rmeileh NM, Achoki T, AlBuhairan FS, Alemu ZA, Alfonso R, Ali MK, Ali R, Guzman NA, Ammar W, Anwari P, Banerjee A, Barquera S, Basu S, Bennett DA, Bhutta Z, Blore J, Cabral N, Nonato IC, Chang JC, Chowdhury R, Courville KJ, Criqui MH, Cundiff DK, Dabhadkar KC, Dandona L, Davis A, Dayama A, Dharmaratne SD, Ding EL, Durrani AM, Esteghamati A, Farzadfar F, Fay DF, Feigin VL, Flaxman A, Forouzanfar MH, Goto A, Green MA, Gupta R, Hafezi-Nejad N, Hankey GJ, Harewood HC, Havmoeller R, Hay S, Hernandez L, Husseini A, Idrisov BT, Ikeda N, Islami F, Jahangir E, Jassal SK, Jee SH, Jeffreys M, Jonas JB, Kabagambe EK, Khalifa SE, Kengne AP, Khader YS, Khang YH, Kim D, Kimokoti RW, Kinge JM, Kokubo Y, Kosen S, Kwan G, Lai T, Leinsalu M, Li Y, Liang X, Liu S, Logroscino G, Lotufo PA, Lu Y, Ma J, Mainoo NK, Mensah GA, Merriman TR, Mokdad AH, Moschandreas J,

Naghavi M, Naheed A, Nand D, Narayan KM, Nelson EL, Neuhouser ML, Nisar MI, Ohkubo T, Oti SO, Pedroza A, Prabhakaran D, Roy N, Sampson U, Seo H, Sepanlou SG, Shibuya K, Shiri R, Shiue I, Singh GM, Singh JA, Skirbekk V, Stapelberg NJ, Sturua L, Sykes BL, Tobias M, Tran BX, Trasande L, Toyoshima H, van de Vijver S, Vasankari TJ, Veerman JL, Velasquez-Melendez G, Vlassov VV, Vollset SE, Vos T, Wang C, Wang X, Weiderpass E, Werdecker A, Wright JL, Yang YC, Yatsuya H, Yoon J, Yoon SJ, Zhao Y, Zhou M, Zhu S, Lopez AD, Murray CJ, Gakidou E. Global, regional, and national prevalence of overweight and obesity in children and adults during 1980-2013: a systematic analysis for the Global Burden of Disease Study 2013. *Lancet* 2014; **384**: 766-781 [PMID: 24880830 DOI: 10.1016/S0140-6736(14)60460-8]

100 **Weber DJ**, Rutala WA, Samsa GP, Santimaw JE, Lemon SM. Obesity as a predictor of poor antibody response to hepatitis B plasma vaccine. *JAMA* 1985; **254**: 3187-3189 [PMID: 2933532]

101 **Young KM**, Gray CM, Bekker LG. Is obesity a risk factor for vaccine non-responsiveness? *PLoS One* 2013; **8**: e82779 [PMID: 24349359 DOI: 10.1371/journal.pone.0082779]

102 **Liu F**, Guo Z, Dong C. Influences of obesity on the immunogenicity of Hepatitis B vaccine. *Hum Vaccin Immunother* 2017; **13**: 1014-1017 [PMID: 28059607 DOI: 10.1080/21645515.2016.1274475]

103 **Painter SD**, Ovsyannikova IG, Poland GA. The weight of obesity on the human immune response to vaccination. *Vaccine* 2015; **33**: 4422-4429 [PMID: 26163925 DOI: 10.1016/j.vaccine.2015.06.101]

104 **Tagliabue C**, Principi N, Giavoli C, Esposito S. Obesity: impact of infections and response to vaccines. *Eur J Clin Microbiol Infect Dis* 2016; **35**: 325-331 [PMID: 26718941 DOI: 10.1007/s10096-015-2558-8]

105 **Ellulu MS**, Patimah I, Khaza'ai H, Rahmat A, Abed Y. Obesity and inflammation: the linking mechanism and the complications. *Arch Med Sci* 2017; **13**: 851-863 [PMID: 28721154 DOI: 10.5114/aoms.2016.58928]

106 **de Heredia FP**, Gómez-Martínez S, Marcos A. Obesity, inflammation and the immune system. *Proc Nutr Soc* 2012; **71**: 332-338 [PMID: 22429824 DOI: 10.1017/S0029665112000092]

107 **Thomas AL**, Alarcon PC, Divanovic S, Chougne CA, Hildeman DA, Moreno-Fernandez ME. Implications of Inflammatory States on Dysfunctional Immune Responses in Aging and Obesity. *Front Aging* 2021; **2**: 732414 [DOI: 10.3389/fragi.2021.732414]

108 **Frasca D**, Ferracci F, Diaz A, Romero M, Lechner S, Blomberg BB. Obesity decreases B cell responses in young and elderly individuals. *Obesity (Silver Spring)* 2016; **24**: 615-625 [PMID: 26857091 DOI: 10.1002/oby.21383]

109 **Younas M**, Carrat F, Desaint C, Launay O, Corbeau P; ANRS HB03 VIHVAC-B Trial Group. Immune activation, smoking, and vaccine response. *AIDS* 2017; **31**: 171-173 [PMID: 27835620 DOI: 10.1097/QAD.0000000000001311]

110 **Zimmermann P**, Curtis N. Factors That Influence the Immune Response to Vaccination. *Clin Microbiol Rev* 2019; **32** [PMID: 30867162 DOI: 10.1128/CMR.00084-18]

111 **Meier MA**, Berger CT. A simple clinical score to identify likely hepatitis B vaccination non-responders - data from a retrospective single center study. *BMC Infect Dis* 2020; **20**: 891 [PMID: 33238923 DOI: 10.1186/s12879-020-05634-y]

112 **Leroux-Roels G**. Old and new adjuvants for hepatitis B vaccines. *Med Microbiol Immunol* 2015; **204**: 69-78 [PMID: 25523196 DOI: 10.1007/s00430-014-0375-9]

113 **Lee S**, Nguyen MT. Recent advances of vaccine adjuvants for infectious diseases. *Immune Netw* 2015; **15**: 51-57 [PMID: 25922593 DOI: 10.4110/in.2015.15.2.51]

114 **Food and Drug Administration**. Product approval information: package insert. Heplisav-B. Silver Spring, MD: US Department of Health and Human Services, Food and Drug Administration; 2018. [cited 5 February 2021]. Available from: https://www.fda.gov/BiologicsBloodVaccines/Vaccines/ApprovedProducts/ucm584752.htm

115 **Jackson S**, Lentino J, Kopp J, Murray L, Ellison W, Rhee M, Shockey G, Akella L, Erby K, Heyward WL, Janssen RS; HBV-23 Study Group. Immunogenicity of a two-dose investigational hepatitis B vaccine, HBsAg-1018, using a toll-like receptor 9 agonist adjuvant compared with a licensed hepatitis B vaccine in adults. *Vaccine* 2018; **36**: 668-674 [PMID: 29289383 DOI: 10.1016/j.vaccine.2017.12.038]

116 **Splawn LM**, Bailey CA, Medina JP, Cho JC. Heplisav-B vaccination for the prevention of hepatitis B virus infection in adults in the United States. *Drugs Today (Barc)* 2018; **54**: 399-405 [PMID: 30090877 DOI: 10.1358/dot.2018.54.7.2833984]

117 **Halperin SA**, Ward B, Cooper C, Predy G, Diaz-Mitoma F, Dionne M, Embree J, McGeer A, Zickler P, Moltz KH, Martz R, Meyer I, McNeil S, Langley JM, Martins E, Heyward WL, Martin JT. Comparison of safety and immunogenicity of two doses of investigational hepatitis B virus surface antigen co-administered with an immunostimulatory phosphorothioate oligodeoxyribonucleotide and three doses of a licensed hepatitis B vaccine in healthy adults 18-55 years of age. *Vaccine* 2012; **30**: 2556-2563 [PMID: 22326642 DOI: 10.1016/j.vaccine.2012.01.087]

118 **Heyward WL**, Kyle M, Blumenau J, Davis M, Reisinger K, Kabongo ML, Bennett S, Janssen RS, Namini H, Martin JT. Immunogenicity and safety of an investigational hepatitis B vaccine with a Toll-like receptor 9 agonist adjuvant (HBsAg-1018) compared to a licensed hepatitis B vaccine in healthy adults 40-70 years of age. *Vaccine* 2013; **31**: 5300-5305 [PMID: 23727002 DOI: 10.1016/j.vaccine.2013.05.068]

119 **Halperin SA**, Ward BJ, Dionne M, Langley JM, McNeil SA, Smith B, Mackinnon-Cameron D, Heyward WL, Martin JT. Immunogenicity of an investigational hepatitis B vaccine (hepatitis B surface antigen co-administered with an immunostimulatory phosphorothioate oligodeoxyribonucleotide) in nonresponders to licensed hepatitis B vaccine. *Hum Vaccin Immunother* 2013; **9**: 1438-1444 [PMID: 23571179 DOI: 10.4161/hv.24256]

120 **Champion CR**. Heplisav-B: A Hepatitis B Vaccine With a Novel Adjuvant. *Ann Pharmacother* 2021; **55**: 783-791 [PMID: 32988213 DOI: 10.1177/1060028020962050]

121 **Vesikari T**, Finn A, van Damme P, Leroux-Roels I, Leroux-Roels G, Segall N, Toma A, Vallieres G, Aronson R, Reich D, Arora S, Ruane PJ, Cone CL, Manns M, Cosgrove C, Faust SN, Ramasamy MN, Machluf N, Spaans JN, Yassin-Rajkumar B, Anderson D, Popovic V, Diaz-Mitoma F; CONSTANT Study Group. Immunogenicity and Safety of a 3-Antigen Hepatitis B Vaccine *vs* a Single-Antigen Hepatitis B Vaccine: A Phase 3 Randomized Clinical Trial. *JAMA Netw Open* 2021; **4**: e2128652 [PMID: 34636914 DOI: 10.1001/jamanetworkopen.2021.28652]

122 **Alon D**, Stein GY, Hadas-Golan V, Tau L, Brosh T, Turner D. Immunogenicity of Sci-B-Vac (a Third-Generation Hepatitis B Vaccine) in HIV-Positive Adults. *Isr Med Assoc J* 2017; **19**: 143-146 [PMID: 28457089]

123 **Safadi R**, Khoury T, Saed N, Hakim M, Jamalia J, Nijim Y, Farah N, Nuser T, Natur N, Mahamid M, Amer J, Roppert PL, Gerlich WH, Glebe D. Efficacy of Birth Dose Vaccination in Preventing Mother-to-Child Transmission of Hepatitis B: A Randomized Controlled Trial Comparing Engerix-B and Sci-B-Vac. *Vaccines (Basel)* 2021; **9** [PMID: 33915943 DOI: 10.3390/vaccines9040331]

124 **Di Lello FA**, Ridruejo E, Martínez AP, Pérez PS, Campos RH, Flichman DM. Molecular epidemiology of hepatitis B virus mutants associated with vaccine escape, drug resistance and diagnosis failure. *J Viral Hepat* 2019; **26**: 552-560 [PMID: 30576055 DOI: 10.1111/jvh.13052]

125 **Campos-Valdez M**, Monroy-Ramírez HC, Armendáriz-Borunda J, Sánchez-Orozco LV. Molecular Mechanisms during Hepatitis B Infection and the Effects of the Virus Variability. *Viruses* 2021; **13** [PMID: 34207116 DOI: 10.3390/v13061167]

126 **Qin Y**, Liao P. Hepatitis B virus vaccine breakthrough infection: surveillance of S gene mutants of HBV. *Acta Virol* 2018; **62**: 115-121 [PMID: 29895151 DOI: 10.4149/av_2018_210]

127 **Ropero Alvarez AM**, Vilajeliu A, Magariños M, Jauregui B, Guzmán L, Whittembury A, Cain E, Garcia O, Montesanos R, Ruiz Matus C; PAHO MNI working group. Enablers and barriers of maternal and neonatal immunization programs in Latin America. *Vaccine* 2021; **39** Suppl 2: B34-B43 [PMID: 32943263 DOI: 10.1016/j.vaccine.2020.07.051]

World Journal of Gastroenterology

Submit a Manuscript: https://www.f6publishing.com

World J Gastroenterol 2022 August 21; 28(31): 4263-4298

DOI: 10.3748/wjg.v28.i31.4263

ISSN 1007-9327 (print) ISSN 2219-2840 (online)

REVIEW

Evidence-based pathogenesis and treatment of ulcerative colitis: A causal role for colonic epithelial hydrogen peroxide

Jay Pravda

Specialty type: Gastroenterology and hepatology

Provenance and peer review: Unsolicited article; Externally peer reviewed

Peer-review model: Single blind

Peer-review report's scientific quality classification

Grade A (Excellent): 0
Grade B (Very good): 0
Grade C (Good): C, C
Grade D (Fair): 0
Grade E (Poor): 0

P-Reviewer: Iizuka M, Japan; Zhao G, China

Received: January 25, 2022
Peer-review started: January 25, 2022
First decision: April 10, 2022
Revised: April 19, 2022
Accepted: July 20, 2022
Article in press: July 20, 2022
Published online: August 21, 2022

Jay Pravda, Disease Pathogenesis, Inflammatory Disease Research Centre, Palm Beach Gardens, FL 33410, United States

Corresponding author: Jay Pravda, MD, Research Scientist, Senior Researcher, Disease Pathogenesis, Inflammatory Disease Research Centre, 4371 Northlake Blvd No. 247, Palm Beach Gardens, FL 33410, United States. jay.pravda@protonmail.com

Abstract

In this comprehensive evidence-based analysis of ulcerative colitis (UC), a causal role is identified for colonic epithelial hydrogen peroxide (H_2O_2) in both the pathogenesis and relapse of this debilitating inflammatory bowel disease. Studies have shown that H_2O_2 production is significantly increased in the non-inflamed colonic epithelium of individuals with UC. H_2O_2 is a powerful neutrophilic chemo-tactic agent that can diffuse through colonic epithelial cell membranes creating an interstitial chemotactic molecular "trail" that attracts adjacent intra-vascular neutrophils into the colonic epithelium leading to mucosal inflammation and UC. A novel therapy aimed at removing the inappropriate H_2O_2 mediated chemotactic signal has been highly effective in achieving complete histologic resolution of colitis in patients experiencing refractory disease with at least one (biopsy-proven) histologic remission lasting 14 years to date. The evidence implies that therapeutic intervention to prevent the re-establishment of a pathologic H_2O_2 mediated chemotactic signaling gradient will indefinitely preclude neutrophilic migration into the colonic epithelium constituting a functional cure for this disease. Cumulative data indicate that individuals with UC have normal immune systems and current treatment guidelines calling for the suppression of the immune response based on the belief that UC is caused by an underlying immune dysfunction are not supported by the evidence and may cause serious adverse effects. It is the aim of this paper to present experimental and clinical evidence that identifies H_2O_2 produced by the colonic epithelium as the causal agent in the pathogenesis of UC. A detailed explanation of a novel therapeutic intervention to normalize colonic H_2O_2, its rationale, components, and formulation is also provided.

Key Words: Ulcerative colitis; Pathogenesis, Treatment; Hydrogen peroxide

Core Tip: Ulcerative colitis (UC) is a chronic inflammatory bowel disease that has resisted all efforts to uncover its cause and cure. However, an evidence-based systems medicine approach has provided compelling evidence that the secretion of hydrogen peroxide (H_2O_2) from colonic epithelial cells is the etiological agent responsible for this debilitating illness. H_2O_2 is a highly potent chemotactic agent that can attract neutrophils into the colonic epithelium, and significantly elevated production of H_2O_2 has been documented in the non-inflamed colonic epithelium of individuals with UC. Treatment to normalize colonic H_2O_2 leads to long-lasting histologic remission.

Citation: Pravda J. Evidence-based pathogenesis and treatment of ulcerative colitis: A causal role for colonic epithelial hydrogen peroxide. *World J Gastroenterol* 2022; 28(31): 4263-4298
URL: https://www.wjgnet.com/1007-9327/full/v28/i31/4263.htm
DOI: https://dx.doi.org/10.3748/wjg.v28.i31.4263

INTRODUCTION

Treating ulcerative colitis (UC) has never been easy. The natural history of UC is one of worsening and progressive disease, and no currently available approved medication can cure the life-long repeating episodes of rectal bleeding, diarrhea, and abdominal pain that are experienced by individuals suffering from this illness[1]. The difficulty in choosing from currently available non-curative therapies was underscored by a recent study, which concluded that the majority of clinical guidelines for the treatment of UC are based on low or very low-quality evidence[2]. Thus, we are left with therapies that cannot cure and have a disappointing track record when it comes to treatment.

The distress engendered by the lack of effective treatment is universal with the majority of UC patients in a 10-country global survey reporting poor disease control, mental exhaustion, and adverse impact on quality of life[3]. This is consistent with other multi-country studies reporting that UC was not controlled in over 87% of participants[4]. The real-world effects of non-curative low-quality therapy are evident by the high degree of medical treatment failure that is responsible for up to a 30% colectomy rate in patients with this illness[5]. With a dismal 40% one-year clinical remission rate for current drugs that alter the immune response, and similar upcoming drugs no more effective, there is no reason to believe that any treatment focused on modifying the immune response will improve current patient outcomes[6]. We are thus left to conclude that this class of therapeutics has reached the limit of clinical effectiveness, and any hope for effective therapy or a cure can only arrive with a fundamentally new approach in our understanding and treatment of this disease.

Almost all treatments for UC consist of agents that modify, alter, or suppress the immune response[7, 8]. This is based on the belief that an underlying immune abnormality is the cause of this condition. But is this assumption evidence-based? Unfortunately not, despite extensive research conducted since the mid-20th century, no evidence of a causal antecedent immune vulnerability has been uncovered in individuals with UC or their first-degree relatives[9]. Additionally, studies in UC patients have revealed normal immune responses when compared to healthy controls[10,11]. Thus, the evidence indicates that an immune abnormality is not the cause of UC, and treatment directed against the immune response cannot bring about a cure, restore healthy colonic functionality, or a normal quality of life.

Faced with these facts, we must consider that the immune response in UC is an accompanying effect of a separate underlying phenomenon that has a causal role in the development of this disease. In other words, the immune system is doing what it's programed to do given the stimulus it is subjected to. But if there's nothing wrong with the immune system then what stimulus could cause inflammation of the colon leading to UC and how can we treat it? The next section describes a novel evidence-based pathogenesis that provides answers to these questions.

UC: AN EVIDENCE-BASED PATHOGENESIS

A causal role for colonic epithelial cell hydrogen peroxide in the pathogenesis of UC

In order to understand the pathogenesis of UC and develop an effective treatment, we need to answer several questions. Starting with what we can see, we must explain why the inflammation typically begins in the rectum and advances contiguously to more proximal regions of the colon without sparing intervening mucosa. We also need to identify the molecular mechanism that initiates the inflammation in the first place. In other words, how the inflammation begins. This raises the question of what causes this mechanism to initially appear and reappear over and over again after (apparently) successful treatment leading to life-long relapse. Finally, we need to derive the genetic predisposition that makes this all possible. Understanding the overlapping lineal sequence of events leading up to UC and the

mechanism of relapse is crucial for effective therapeutic intervention and long-term remission so as to permanently alter the natural history of disease. Stated differently, we will start with what we can see (the inflammation) and work our way upstream until we arrive at the inception of disease, which originates from the interaction of a shared genetic predisposition with exposomal elements giving rise to a final common pathway that must be present among all individuals with UC; at all times basing our conclusions on the known experimental evidence.

Neutrophils are the first responders into the colonic epithelium in UC with the formation of neutrophilic cryptitis and neutrophilic crypt abscesses, which are hallmarks of active inflammation[12-14]. This typically begins in the rectum causing mucosal inflammation, which advances proximally and contiguously (without skipping). Once in contact with bacteria in the rectal epithelium, neutrophils are activated to release large amounts of hydrogen peroxide (H_2O_2). Studies have shown that a single neutrophil can produce enough H_2O_2 to diffuse into and oxidize nearly all the hemoglobin contained in ten intact surrounding red blood cells[15].

H_2O_2 is a cell-membrane permeable, highly potent neutrophilic chemotactic factor that attracts neutrophils into the colonic epithelium[16]. Studies have demonstrated that neutrophils can respond to and migrate towards an H_2O_2 concentration variation of 100 picomolar, which is a difference of approximately five molecules of H_2O_2 between the leading and trailing halves of the neutrophil[17]. H_2O_2 is also a powerful oxidizing agent that disintegrates tight junctional proteins[18-21]. This leads to increased paracellular permeability and decreased epithelial resistance, which is characteristically observed in UC[22-25].

The resulting H_2O_2 mediated increase in paracellular permeability facilitates antigenic translocation across the colonic epithelium while simultaneously creating an H_2O_2 chemotactic gradient, both of which act cooperatively to attract other neutrophils into the advancing proximal edge of the inflammatory field thereby extending colonic inflammation from the rectum, in a contiguous fashion, to more proximal regions of the colon. The inflammation only halting upon encountering sufficient circumferential epithelial reductive capacity to neutralize the advancing wave of neutrophil released H_2O_2, resulting in a sharp demarcation between healthy and diseased tissue. This redox tug-of-war between epithelial reductive capacity and neutrophilic H_2O_2 explains the characteristic proximal migratory behavior of colonic mucosal inflammation in UC. This interpretation is supported by studies showing that neutrophil accumulation within epithelial crypts and in the intestinal mucosa directly correlates with clinical disease activity and epithelial injury in individuals with UC[26]. Stated differently, neutrophils in the crypts of Lieberkühn secrete large amounts of H_2O_2 that attracts other neutrophils into the epithelium. Continuous secretion of H_2O_2 by neutrophils overwhelms epithelial reductive (antioxidant) capacity causing additional neutrophils to enter the inflammatory field. This advances the inflammation in a proximal direction until sufficient epithelial reductive (antioxidant) capacity is encountered to stop further proximal advance.

On a cellular level, neutrophils in the colonic epithelium can be thought of as microscopic H_2O_2 factories, whose function can be replaced by exogenous H_2O_2. This interpretation is supported by rectal H_2O_2 infusion studies in mice resulting in sharp inflammatory tissue delineation from normal tissue, contiguous inflammatory proximal extension, and rectal inflammatory persistence (discussed below), which are also characteristic of human UC[27]. Additionally, the colonic introduction of H_2O_2 in humans results in classic UC[28]. Although this explains proximal extension, the next step is to explicate what causes these white blood cells (neutrophils) to move into the colonic epithelium in the first place causing inflammation and why it typically starts in the rectum?

Neutrophils are attracted into the colonic epithelium by H_2O_2 secreted by the colonic epithelium

Neutrophils are not the only cells in the body that produce H_2O_2. All living cells in the body generate H_2O_2 from metabolic reactions, including colonic epithelial cells (colonocytes)[29]. Studies have shown increased production of H_2O_2 in ascending non-inflamed colonic epithelium from patients with UC[30]. This indicates a pre-inflammatory build-up of H_2O_2 within colonocytes. In other words, H_2O_2 builds up in colonic epithelial cells prior to the appearance of inflammation satisfying the absolute requirement of chronology for the cause (H_2O_2) to precede the effect (colitis).

H_2O_2 is membrane permeable and can easily diffuse through the colonic epithelial cell membrane to the extracellular space[29]. Once outside the colonocyte, H_2O_2 initiates inflammation *via* the same mechanism as H_2O_2 secreted by neutrophils, *i.e.*, oxidative disintegration of tight junctions and neutrophilic chemotaxis. Other studies have shown that reductive capacity (ability to neutralize H_2O_2) progressively decreases from proximal to distal regions of the colon with rectal epithelial cells having the least protection against the buildup of H_2O_2[31]. This causes the rectum to be the initial location in the colonic epithelium where H_2O_2 will build up and, upon diffusion to the colonocyte extracellular space, attract neutrophils into the rectal epithelium causing inflammation and colitis. And due to its diminished reductive capacity, the rectum will be the last colonic region to heal resulting in a persistent ulcerative proctitis that is experienced by many patients.

Studies in genetically engineered mice that are unable to neutralize colonic H_2O_2 [glutathione (GSH) peroxidase knock-out mice] develop colitis analogous to human UC[32]. This indicates that colonic epithelial cells can generate enough H_2O_2, which upon extracellular diffusion, can initiate colonic inflammation and colitis. The mechanism behind the initial increase in colonocyte H_2O_2 giving rise to

human UC will be discussed below in the section on oxidative stressors.

In other words, H_2O_2 is a normal immune signaling molecule that attracts neutrophils. Neutrophils cannot determine which cell is secreting H_2O_2; whether it's another neutrophil calling for help fighting an infection or a colonic epithelial cell leaking H_2O_2. In the latter case, neutrophils are simply doing what they are programmed to do given the stimulus (H_2O_2) they are exposed to. The development of UC indicates a healthy functioning innate immune system responding to a normal immune chemotactic factor (H_2O_2) being inappropriately secreted by the colonic epithelium. The correct treatment (discussed below) is not to abrogate this normal response with drugs that suppress essential innate normal immune reactivity but to restore colonic redox homeostasis so as to prevent colonocyte secretion of H_2O_2.

In summary, H_2O_2's unique properties of cell membrane permeability, long life, potent oxidizing potential, and neutrophilic chemotactic capability combine to promote colonocyte extracellular diffusion followed by oxidative disintegration of colonic epithelial tight junctional proteins, which facilitates bacterial translocation from the colonic lumen into the sterile subjacent lamina propria while simultaneously (and chemotactically) attracting neutrophils into the colonic epithelium, both of which lead to colonic inflammation, and eventual UC (Figures 1A and 1B). H_2O_2 initially accumulates in colonocytes and diffuses to the extra-cellular space in the rectal epithelium, which has the least tissue reductive capacity of the entire colon.

Neutrophils in the subjacent epithelial vasculature migrate along the interstitial H_2O_2 concentration gradient to the source of the H_2O_2 in the rectal epithelium. Once exposed to lumenal antigens, neutrophils are activated to secrete large amounts of H_2O_2, which promotes further neutrophilic infiltration while migrating the advancing edge of the inflammatory field to more proximal regions of the colon as described above. H_2O_2 also causes vasodilation and severe damage to blood vessels with destruction of endothelial cells and disruption of endothelial cell tight junctions[33-35]. This leads to erythrocyte extravasation and bleeding into the colonic lumen as commonly observed in UC. Thus, the effects of H_2O_2 on the innate immune system and vasculature explain both the microscopic and macroscopic features that characterize UC. The next section provides an evidence-based explanation for relapse. Following this, the concept of oxidative stress is discussed, which provides an evidence-based mechanism to explicate why H_2O_2 builds up in the colonic epithelium to begin with.

Relapse: An acquired "hard-wired" vicious cycle of inflammation

Once complete histologic remission has been achieved and the colonic epithelium is free of inflammatory cells, neutrophils can, once again, migrate back into the colonic epithelium after medication is withdrawn. This resumption of inflammation after a period of quiescent disease is called relapse, also known as a flare. Stated differently, if UC were simply a function of exposure to environmental factors, neutrophils would not migrate back into the colonic epithelium causing mucosal inflammation and relapse after exposure has ceased and medication is withdrawn.

Relapse indicates that a fundamental change has occurred in colonic epithelial cells before and/or during mucosal inflammation leading to increased production of H_2O_2, which continues to diffuse throughout the extracellular space resulting in neutrophilic chemotactic migration into the colonic epithelium and eventual relapse. This is consistent with the significantly elevated intracellular colonocyte H_2O_2 production observed in the non-involved colonic epithelium in patients with UC[30]. The question is why do colonocytes in individuals with UC produce more H_2O_2 than normal?

The answer is suggested by the susceptibility of mitochondrial DNA (mtDNA) to H_2O_2-induced oxidative damage. Due to their lack of histones, limited repair capability, and high single strand exposure time, mtDNA is highly susceptible to H_2O_2-induced oxidative damage[36,37]. H_2O_2 induced oxidative damage to mtDNA introduces base mutations into the mitochondrial genome, which miscode during transcription of electron transport chain (ETC) complexes resulting in nucleotide mispairing and the incorporation of faulty protein subunits into the ETC. These acquired mitochondrial ETC mutations cause increased ETC electron leakage that produces increased amounts of superoxide, which is converted to excess H_2O_2. The end result is a dysfunctional mitochondrial ETC that generates higher levels of cellular H_2O_2, which upon extracellular diffusion initiates a relapse of colonic inflammation (Figure 1C)[38].

The elevated colonocyte H_2O_2 resulting in mtDNA mutations originates from two sources. The initial increase in colonocyte H_2O_2 is intracellular and originates from oxidative stress exposure (discussed in the next section). This is augmented by a large exogenous source of H_2O_2 supplied by neutrophils that stream into the colonic epithelium and fill up the crypts of Lieberkühn. Being cell membrane permeable, H_2O_2 can easily diffuse into surrounding epithelial stem cells and transition amplification cells, which give rise to the surface epithelium. This "back flow" of H_2O_2 into colonocytes would ordinarily be neutralized by the cell. However, colonocyte reductive capacity has already been compromised by the initial rise in cellular H_2O_2 due to oxidative stress exposure. This allows intracellular H_2O_2 to diffuse unimpeded throughout the colonocyte into mitochondria leading to mtDNA oxidative damage and acquired mutations.

A causal role for mitochondrial ETC generated H_2O_2 in the development of relapse is consistent with the onset of impaired mitochondrial beta-oxidation in the weeks leading up to relapse, which is reported to be caused by H_2O_2 induced oxidative inhibition of mitochondrial thiolase, a necessary

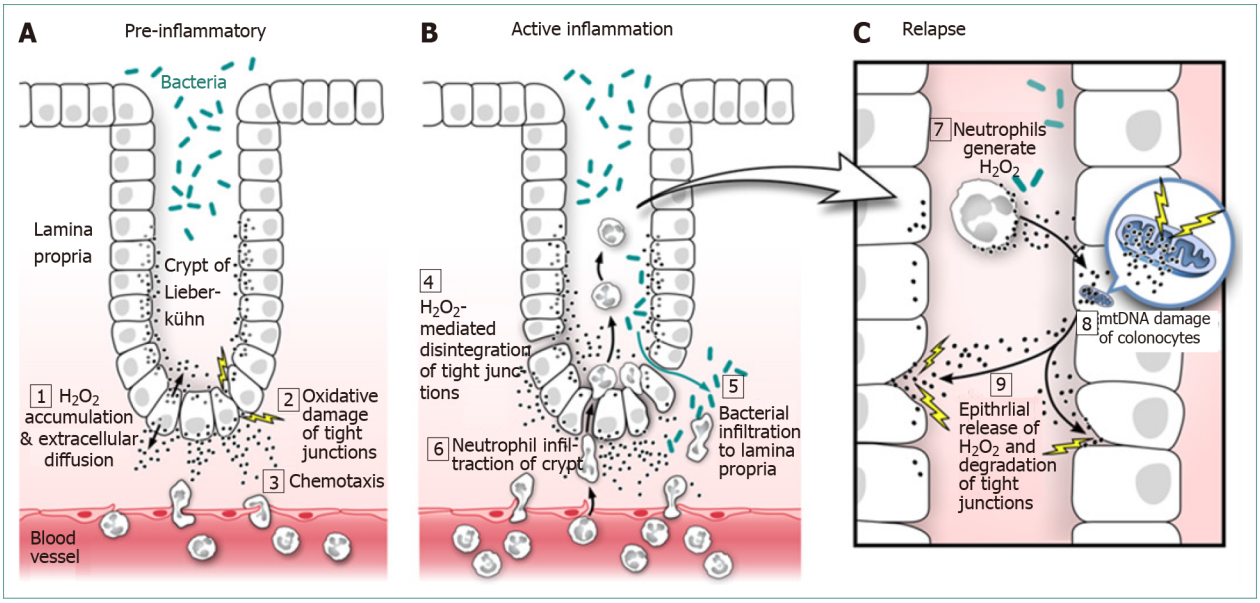

DOI: 10.3748/wjg.v28.i31.4263 **Copyright** ©The Author(s) 2022.

Figure 1 Ulcerative colitis: Evidence-based pathogenesis and relapse. A: Pre-inflammatory; B: Active inflammation; C: Relapse. Hydrogen peroxide (H_2O_2) is produced by all cells of the body, mainly as a toxic by-product of cellular metabolism and must be immediately neutralized to prevent cell damage. If produced in excess by colonocytes (colonic epithelial cells), H_2O_2 easily diffuses through the cell membrane; 1: To the extracellular space where its unique properties of long life, potent oxidizing power, and the ability to attract neutrophils (neutrophilic chemotaxis) combine to promote oxidative damage of colonocyte tight junctions; 2: While attracting neutrophils into the colonic epithelium; 3: Continued H_2O_2 exposure leads to oxidative disintegration of tight junctional proteins and increased colonic epithelial paracellular permeability; 4: Increased paracellular permeability promotes bacterial translocation into the sterile lamina propria; 5: And facilitates neutrophil migration up the H_2O_2 concentration gradient into the crypts of Lieberkühn; 6: Both of which lead to colonic inflammation and eventual ulcerative colitis. Neutrophils exposed to bacteria in the crypts become activated and produce large amounts of H_2O_2 that diffuses into colonic epithelial cells; 7: Which adds to the already high colonocyte H_2O_2 load. The increased colonocyte H_2O_2 oxidizes mitochondrial DNA (mtDNA) introducing genetic mutations that miscode when transcribing for electron transport chain (ETC) proteins; 8: Faulty ETC proteins exhibit additional electron leakage leading to greater H_2O_2 production creating a vicious cycle of mtDNA damage and ever greater H_2O_2 production, which contributes to and increases the frequency and severity of relapse; 9: This amounts to a "hard-wired" genetic reprogramming that promotes colonic inflammation as discussed below. H_2O_2: Hydrogen peroxide; mtDNA: Mitochondrial DNA.

enzyme in the mitochondrial beta-oxidation pathway[39-41]. The involvement of ETC-generated H_2O_2 in UC relapse is supported by reports of intractable UC in the setting of inherited ETC disfunction[42]. At birth, all mtDNA is normally identical. This is called homoplasmy. After H_2O_2-induced base mutations are introduced into the mitochondrial genome, all mtDNA is no longer identical. The simultaneous occurrence of genetically dissimilar cellular mtDNA (normal and mutated) is called mitochondrial heteroplasmy[43]. Studies have shown a significant degree of heteroplasmic mtDNA in the colonic epithelium of individuals with UC[44,45]. The presence of colonocyte mitochondrial heteroplasmy in UC will constitutively generate higher amounts of H_2O_2 leading to additional mtDNA damage and greater H_2O_2 production creating a self-amplifying vicious cycle of ever-increasing colonocyte H_2O_2[46]. This constitutive internally reinforcing production of colonocyte H_2O_2 perpetuates mucosal inflammation leading to relapse upon withdrawal of medication. The increased basal production of colonocyte H_2O_2 promotes more frequent episodes of relapse and leads to refractory disease as colonocyte H_2O_2 increases and UC becomes less responsive to medication.

Up until now, we have an H_2O_2-based mechanism that explains how UC begins, why inflammation extends proximally throughout the colon, and how mitochondrial heteroplasmy promotes a constitutive increase in colonocyte H_2O_2 that contributes to relapse. What we are missing is why colonocyte H_2O_2 becomes elevated in the first place. To understand this, we need to discuss the concept of oxidative stress as outlined in the next section for it is exposure to oxidative stress that initiates *de novo* development (and relapse) of UC.

OXIDATIVE STRESS

The invisible force that increases H_2O_2 and leads to UC

We are all subjected to oxidative stress since the moment of conception. But what is oxidative stress? More importantly, how can we define oxidative stress in a manner that is relevant for diagnosing disease, understanding pathogenesis, and advancing therapeutic intervention. Since most biological effects of reactive oxidant species are mediated by H_2O_2[47], and since cellular GSH is principally responsible for supplying the reducing equivalents (electrons) needed to neutralize H_2O_2[48,49], a

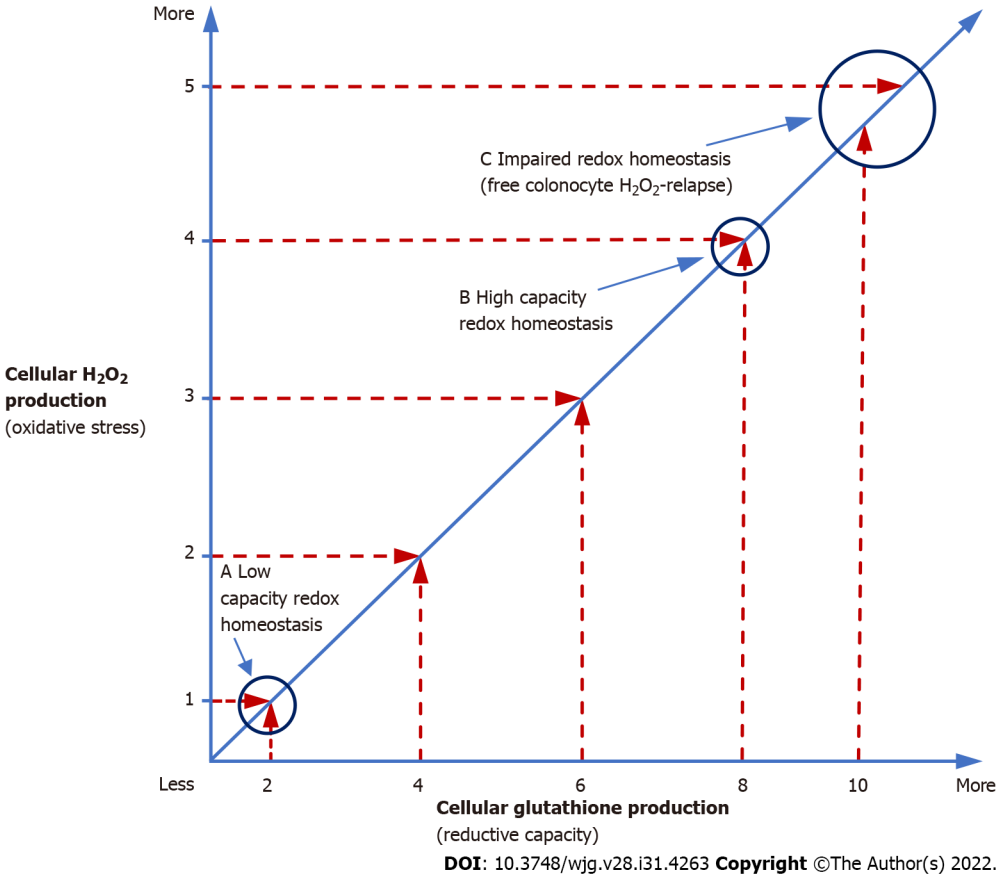

DOI: 10.3748/wjg.v28.i31.4263

Figure 2 Redox homeostasis. Redox homeostasis is more than just a balance between oxidizing [hydrogen peroxide (H_2O_2)] and reducing agents (glutathione). In the above graph, redox homeostasis (slanted line) is maintained at both low and high H_2O_2 production rates (a and b), but the cell is functioning at a higher oxidative capacity (high capacity redox homeostasis) (b), when more H_2O_2 is being produced compared to times when lesser amounts of H_2O_2 are being generated (a). Mitochondria, the site of most cellular H_2O_2 production, do not synthesize their own glutathione and only contain 10% of the total cellular supply of this vital reducing equivalent that must be generated in the cytoplasm and imported into mitochondria, which takes time[53]. Once depleted, mitochondrial glutathione can take several hours to restore to normal levels[46]. In contrast to the limited supply of mitochondrial glutathione, studies have shown that mitochondrial electron transport chain production of H_2O_2 can increase up to 15 × during periods of high metabolic demand[54]. Any increase in H_2O_2 production forces the cell to utilize additional glutathione in order to maintain redox balance which may lead to high capacity redox homeostasis (b). Since about 30% of cell thiols (*i.e.*, glutathione) normally undergo oxidation per hour[55], the additional oxidative stress imposed by high capacity redox homeostasis can, over time, deplete available glutathione and overwhelm colonocyte reductive capacity creating a state of impaired redox homeostasis (c) followed by H_2O_2 build-up and extracellular diffusion, which can lead to *de novo* ulcerative colitis or relapse. High capacity redox homeostasis is consistent with increased H_2O_2 production observed in the non-inflamed ascending colonic epithelium of individuals with ulcerative colitis[30]. H_2O_2: Hydrogen peroxide.

clinical working definition of oxidative stress can be summarized as any stimulus that increases the amount or production of H_2O_2 or elevates the risk of its occurrence by decreasing cellular reductive (antioxidant) capacity (*i.e.*, GSH). Stimuli that fulfill this definition are called oxidative stressors.

Oxidative stressors can be external (*i.e.*, environmental) or internal (originating in the body). Many oxidative stressors can be identified by the medical history and targeted for elimination by changes in diet and lifestyle. Clinically assessing the risk that oxidative stress will increase H_2O_2 leading to worsening disease requires a working understanding of redox homeostasis. Redox homeostasis refers to the balance that is achieved when there is sufficient cellular reductive capacity (GSH) to neutralize the H_2O_2 being produced. Thus, an oxidative stressor is a stimulus that places additional demands on the cell's capacity to neutralize H_2O_2 and maintain redox homeostasis. Over time, oxidative stress can disrupt the cell's ability to maintain this critical balance. When this occurs it is called impaired redox homeostasis, which can lead to the build-up of colonocyte H_2O_2 resulting in extracellular diffusion, mucosal inflammation, and UC as described above. Thus, identifying and eliminating oxidative stressors in order to assist in restoring colonic redox homeostasis is critical for the maintenance of long-term remission in UC. In order to maintain redox homeostasis, colonocytes utilize as much GSH as needed to neutralize the H_2O_2 that is being produced by the cell. In this reaction, two molecules of GSH react with one molecule of H_2O_2 *via* the action of GSH peroxidase (GPx) to yield one molecule of GSH disulfide (GSSG) and one molecule of water, as illustrated below.

$$2\,GSH + H_2O_2 \xrightarrow{GPx} GSSG + H_2O_2$$

At higher levels of H_2O_2 production significantly more GSH is consumed compared to lower levels of H_2O_2 production in order to maintain a 2 (GSH) to 1 (H_2O_2) balance or redox homeostasis. However, higher levels of GSH consumption enhance the risk of GSH depletion after which free H_2O_2 can begin to accumulate within the cell[50].

Thus, all redox homeostasis is not the same. Redox homeostasis maintained at high levels of H_2O_2 production [high capacity redox homeostasis (HCRH)] increases the risk of GSH depletion and subsequent accumulation of intracellular H_2O_2 (Figure 2). HCRH indicates that the cell has a greater capacity to oxidize substrate such as GSH and is consuming GSH at greater rates than normal. As long as the substrate being oxidized is GSH, redox homeostasis can be maintained and the cell is protected from the toxic effects of H_2O_2 buildup. However, if GSH is depleted due to excessive utilization by HCRH, H_2O_2 is free to diffuse throughout the cell and oxidize other molecules in the colonocyte such as enzymes and DNA. This can lead to metabolic disturbances such as impaired mitochondrial beta-oxidation in addition to oxidative nuclear DNA mutations in tumor suppression and oncogenes that promote colorectal cancer as well as mtDNA mutations (mitochondrial heteroplasmy) that increase cellular H_2O_2 production and facilitate disease relapse[30,51,52] (Figure 2).

Even if redox homeostasis is maintained during HCRH, the high demand for GSH may sequester this vital reducing agent away from other critical metabolic functions that depend upon GSH such as elimination of toxic xenobiotics and electrophiles, regulation of apoptosis and cell division, GSH dependent enzymes, maintenance of reduced vitamins C and E for cell membrane protection, and glutathionylation of proteins/enzymes to protect against irreversible oxidative damage[56-58]. Thus, HCRH may consume GSH needed for other cellular activity and compromise colonocyte and colonic functionality independent of the development of UC.

Exposure to multiple contemporaneous oxidative stressors facilitates progressively greater production of H_2O_2 that increases the risk of reaching HCRH, which can lead to impaired redox homeostasis with the development of symptomatic UC (Figure 2C). This explains why the initial appearance of UC can be very explosive since HCRH may lead to sudden depletion of GSH causing significant acute increases in cellular H_2O_2, which can lead to severe mucosal inflammation as large amounts of colonocyte H_2O_2 diffuse to the cell exterior. Lesser amounts of colonocyte extracellular H_2O_2 can account for the pre-symptomatic systemic inflammation observed in individuals who go on to develop UC[59]. Seemingly insignificant oxidative stressors can lead to relapse for individuals functioning at HCRH. This should prompt a search for other unrecognized oxidative stress exposures to prevent relapse. Lastly, an important distinction to keep in mind is that oxidative stress is not the same as oxidative damage. Oxidative stress appears before oxidative damage occurs, while oxidative damage always indicates previous or ongoing oxidative stress. Rectal bleeding in UC is an indication of severe concurrent oxidative (H_2O_2 induced) tissue damage caused by exposure to oxidative stress.

In summary, oxidative stress increases H_2O_2 in the body. Oxidative stressors mediate the effects of oxidative stress on the body. As H_2O_2 increases, colonocytes utilize greater amounts of GSH to maintain redox balance leading to HCRH, which can deplete cellular GSH leading to *de novo* UC or relapse. The increased H_2O_2 production rates observed in the non-inflamed colonic epithelium of individuals with UC indicate the presence of HCRH[30]. The effects of multiple oxidative stressors are additive, each contributing to the cellular H_2O_2 load. HCRH may lead to a GSH deficiency state and cellular disfunction**.** In the next section, we put it all together and derive the genetic susceptibility that predisposes to the development of UC.

PUTTING IT ALL TOGETHER

Predisposition, pathogenesis, pathophysiology, and relapse

Based on the cumulative data, we can now construct an evidence-based natural history of UC. The disease begins with exposure to one or more oxidative stressors, which increase the production of colonocyte H_2O_2. Over time, cellular reductive capacity is overwhelmed as the colonocyte is no longer able to maintain HCRH and H_2O_2 accumulates in the cell. This is followed by H_2O_2 diffusion through the cell membrane to the extracellular space within the crypts of Lieberkühn and the surrounding cellular microenvironment. This results in oxidative damage to interepithelial tight junctions and increased paracellular permeability accompanied by the creation of an H_2O_2 diffusion gradient that envelops the subjacent microvasculature.

The combined effect of colonic epithelial antigenic translocation due to increased paracellular permeability and H_2O_2 gradient-guided neutrophilic chemotaxis results in directed migration of neutrophils from the subjacent vasculature into the crypts of Lieberkühn along with the formation of neutrophilic cryptitis and crypt abscesses. Continued neutrophilic infiltration into the colonic epithelium leads to mucosal inflammation and UC (Figures 3A-E).

The rectum, having the lowest reductive capacity of the intestinal tract, is the initial site of H_2O_2 accumulation and the first region to experience inflammation, which proceeds in a proximal direction as continuous secretion of large amounts of neutrophil released H_2O_2 overcomes colonic epithelial reductive capacity in a circumferential manner resulting in a sharp demarcation between healthy and

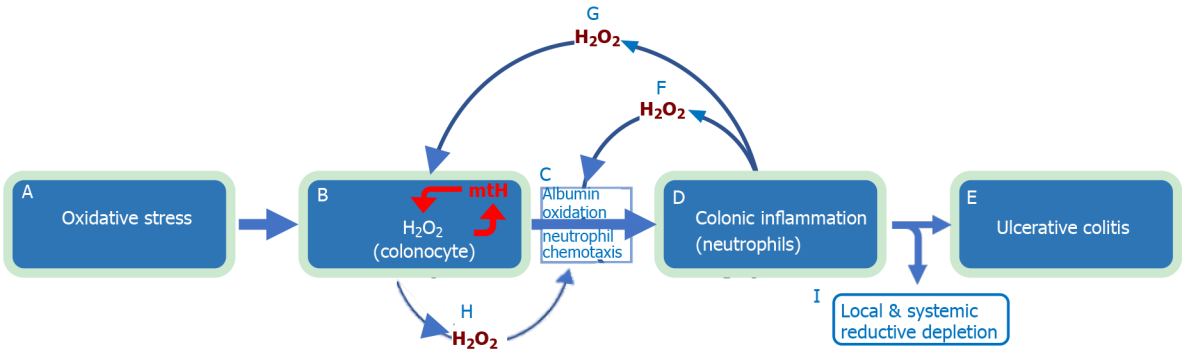

DOI: 10.3748/wjg.v28.i31.4263 **Copyright** ©The Author(s) 2022.

Figure 3 Natural history of ulcerative colitis. The evidence-based natural history of ulcerative colitis begins with exposure to oxidative stressors (a), which increases colonocyte hydrogen peroxide (H_2O_2) (b). The increase in colonocyte H_2O_2 facilitates extracellular diffusion which overwhelms (oxidizes) local interstitial serum albumin antioxidant defense (60% of serum albumin is interstitial), leading to directed migration of neutrophils (chemotaxis) into the colonic epithelium (c) and mucosal inflammation (d) with subsequent development of ulcerative colitis (e). Large amounts of H_2O_2 are released by neutrophils into the extracellular space (f) with further oxidation of interstitial albumin and exhaustion of tissue antioxidant capacity (c). This worsens colonic inflammation (d) leading to local and systemic reductive depletion (i) as albumin is circulated through the colonic interstitium into tissue lymphatics and back into the systemic circulation. Neutrophil released H_2O_2 "back flows" into colonocytes (g) adding to the already elevated intracellular H_2O_2 levels resulting in mitochondrial DNA damage and mitochondrial heteroplasmy (b, red mtH). Mitochondrial heteroplasmy introduces mutations into the electron transport chain protein subunits, which generate additional H_2O_2 *via* enhanced electron leakage setting up a vicious cycle of ever increasing colonocyte H_2O_2 (b, red arrows). Increased colonocyte H_2O_2 diffuses into the extracellular space (h) causing disease relapse (c, d, e). The combination of local and systemic reductive depletion along with a ready supply of H_2O_2 from colonocytes and neutrophils (b and d) creates a mucosal inflammation that is self-amplifying, forward propagating, and auto-initiating (relapsing). Elimination of neutrophilic inflammation (d) by any means (*i.e.*, immunosuppressive agents) will not stop relapse from occurring as colonocyte H_2O_2 continues to diffuse into the extracellular space (c, h). Conversely, normalizing colonocyte H_2O_2 alone will not stop the inflammation, which has become self-sustaining. This indicates that simultaneous elimination of all pathological sources contributing H_2O_2 to the inflammatory field must be achieved to ensure long-term remission and normal colonic functionality. Systemic reductive depletion may contribute to other serious health hazards as detailed below. H_2O_2: Hydrogen peroxide.

diseased tissue (epithelial cells at the same circumferential level have the same reductive capacity). Mucosal inflammation may reach more proximally and regress distally over time as a result of fluctuations in colonic epithelial reductive capacity due to changes in oxidative stress exposure (diet, stress, *etc.*) and epithelial repopulation.

The large amount of H_2O_2 released by neutrophils in the inflammatory field is chemotactic for other neutrophils in the subjacent vascular bed. This causes epithelial inflammation to become self-propagating and auto-amplifying (Figure 3F), which enables prolonged contact between neutrophils and surrounding colonocytes. This close contact facilitates the back-flow of neutrophil-derived H_2O_2 into adjacent colonocytes that adds to the already high colonocyte H_2O_2 load due to oxidative stress exposure (Figure 3G).

High intracellular colonocyte H_2O_2 promotes diffusion into mitochondria leading to mtDNA oxidation and the formation of acquired mtDNA mutations (mitochondrial heteroplasmy-mtH) (Figure 3B red arrows), which miscode during translation of ETC protein subunits. The resulting ETC mutations facilitate a higher degree of electron leakage and greater H_2O_2 formation causing additional mtDNA damage and the creation of a vicious cycle, which maintains a high intracellular colonocyte H_2O production that facilitates spontaneous relapse upon withdrawal of medication or exposure to ever-present oxidative stressors (Figure 3H).

Thus, based on the data, the derived genetic predisposition leading to UC is the inability of the colonic epithelium to cope with (neutralize) an oxidant (H_2O_2) load forcing the colonocyte into a state of impaired redox homeostasis after which free H_2O_2 begins to accumulate in the cell (Figure 2C). Pathogenesis begins with impaired colonocyte redox homeostasis leading to the intracellular accumulation of H_2O_2 after HCRH has exhausted cellular reductive capacity (Figure 2C). The pathophysiology commences with the influx of neutrophils into the colonic mucosa, which defines the beginning of what will eventually become the symptomatic phase of the illness. However, extracellular colonocyte diffusion of H_2O_2 does not inexorably lead to UC due to the presence of a secondary "back-up" system of antioxidant defense provided by human serum albumin (HSA) (Figure 3C) as discussed in the following section.

HSA: The link between colonocyte and systemic redox homeostasis

Although UC is traditionally thought of being limited to the colon, the significant decrease reported in total blood antioxidant capacity (erythrocytes and plasma) in individuals with UC suggests that excess colonic production of H_2O_2 is causing impaired systemic redox homeostasis as well[60-62]. In other words, the capacity of the blood to remove H_2O_2 in UC patients is compromised. Why would colonic production of H_2O_2 affect systemic redox homeostasis and what effect might this have on the severity of UC and overall patient health?

Systemic redox homeostasis is provided by HSA and erythrocytes, both of which are highly effective scavengers of H_2O_2. Their combined action maintains blood H_2O_2 at very low levels, in the range of 0.8-6 μM for healthy individuals[63]. HSA can directly scavenge H_2O_2 *via* a reduced surface cysteine thiol (cys34)[64]. In addition, the HSA molecule itself has a GSH-linked thiol peroxidase activity that can remove circulating H_2O_2[65]. The significant anti-oxidant scavenging ability of HSA represents approximately 70% of the free radical trapping ability of human serum[64]. Since 60% of HSA is present in the interstitial space, this indicates that HSA acts as an extracellular backup anti-oxidant defensive layer (after intracellular colonocyte GSH) that protects against the development of UC by preventing the interstitial accumulation and diffusion of colonocyte released H_2O_2 from reaching the subjacent epithelial blood vessels and attracting neutrophils into the colonic epithelium leading to colonic mucosal inflammation and UC. Interstitial albumin has a turnover of 4% per hour after which it recycles back to the systemic circulation[66]. This suggests that each day the entire blood supply of reduced albumin is exposed to excess colonic H_2O_2 with a significant portion becoming oxidized.

Red blood cells also provide a significant level of systemic anti-oxidant defense. Erythrocytes contribute up to 30% of whole blood reductive capacity. Erythrocytes are highly permeable to H_2O_2[67]. With a normal mean inter-erythrocytic distance of 3 μm, a molecule of H_2O_2 in the circulation will encounter a red blood cell before it encounters HSA[68]. Free serum H_2O_2 will diffuse into red blood cells where it is neutralized by significant anti-oxidant enzymatic defenses comprised of catalase and GSH[67]. Whereas H_2O_2 released by colonocytes or infiltrating epithelial neutrophils during active UC can oxidize HSA in the interstitial space, decreased red blood cell reductive capacity (*i.e.*, decreased erythrocyte GSH) implies that colonic H_2O_2 is diffusing directly into the systemic circulation and into erythrocytes with depletion of total blood reductive capacity. The inability of interstitial HSA to completely remove colonic H_2O_2 will lead to H_2O_2 accumulation and a greater degree of tissue damage accompanied by neutrophilic infiltration resulting in increased severity of disease, which contributes to relapse (Figure 3F). This is supported by studies showing that the loss of blood reductive capacity (inability to remove H_2O_2) is associated with worsening UC[62]. The critical role of reduced albumin for the maintenance of colonic interstitial redox homeostasis is illustrated by studies showing that the onset and progression of experimental murine colitis were prevented by reduced (reductively enhanced) albumin, which, in turn, was strongly associated with an improved systemic reductive capacity[69].

Reduced albumin also directly neutralized H_2O_2 and prevented the *in vitro* loss of tight junctional proteins in human intestinal cell tissue treated with H_2O_2[69]. This indicates that reduced albumin can act as an interstitial reducing agent (antioxidant) and delay/prevent the onset of UC by neutralizing interstitial H_2O_2 released by colonocytes before the H_2O_2 can initiate chemotactic directed migration of neutrophils into the colonic epithelium. This implies that oxidized, or decreased albumin levels would offer less protection and hasten the development of UC. This is consistent with worsening UC observed in association with anemia and hypoalbuminemia[70,71]. Other studies report a significant inverse relationship between low serum albumin and risk of colectomy[72]. Conversely, studies in UC patients have shown that mucosal healing is positively associated with high (> 4.4 mg/dL) serum albumin[73].

Although low HSA can be secondary to colonic protein loss, and improved HSA levels may follow mucosal healing, the association of high HSA levels with a protective effect in conditions without colitis such as Bell's palsy and coronary artery disease implies an independent association with an intrinsic property of HSA such as oxidation status and not just as a biomarker for worsening colitis[74,75]. Thus, it is reasonable to assume that it is not just worsening colitis that causes low albumin but low serum albumin reductive capacity causing worsening colitis that increases albumin loss. HSA oxidation status should be part of screening lab work as oxidized albumin is inherently proinflammatory and associated with the progression of other diseases in addition to UC[76,77]. The proinflammatory nature of oxidized albumin and subsequent loss of systemic reductive capacity may be reflected in the worsening health and the high healthcare resource utilization in the year leading up to the diagnosis of UC[78]. This insight provides a critical therapeutic window of opportunity to restore systemic redox homeostasis and prevent UC if HSA is found to be significantly oxidized. In summary, once symptomatic UC develops, local and systemic reductive depletion is likely. At this point, colonocytes have already been exposed to genotoxic levels of H_2O_2 for many months or years setting the stage for molecular oxidative alterations that lead to life-long relapse (Figures 3A-H). However, the oxidative nature of these changes offers the possibility of reversal with a therapeutic reducing agent (detailed in treatment section below).

HOW OXIDATIVE STRESSORS GENERATE H_2O_2 IN THE BODY

Oxidative stress: Sources, classification, and definition

H_2O_2 is produced by many different cellular enzymatic reactions. Using the advanced search option in the BRENDA enzyme database limited to "homo sapiens" as the organism and "H_2O_2" as the product in the subitem text field returned 29 different enzymes acting upon 188 distinct molecular substrates[79]. This does not include non-enzymatic reactions such as the auto-oxidation of oxyhemoglobin or subunits of the mitochondrial ETC, which is considered the principal source of H_2O_2 in the body. Oxidative stressors are extremely diverse in their mechanism of action with some increasing the substrate for a

single enzyme while others can affect every H_2O_2 generating system in the body by inhibiting critical anti-oxidant enzyme systems needed for H_2O_2 removal. Individuals with UC are usually contemporaneously affected by more than one oxidative stressor but the commonality among all oxidative stressors, however, is the production of H_2O_2. Consequently, oxidative stressors are additive since they all increase the H_2O_2 load in the body. This may cause different individuals with UC to be more or less affected by the same oxidative stressor depending on the pre-existing H_2O_2 load in the colonocyte and state of redox homeostasis, which can change over time (Figure 2).

This can also result in the individual tolerance for the same oxidative stressor to vary with age, comorbidity, lifestyle and exposure duration and intensity. Thus, based on the evidence, it is reasonable to conclude that all factors that increase the risk of relapse or developing *de novo* UC are oxidative stressors that increase H_2O_2 in the body. Conversely, all oxidative stressors are risk factors for relapse or the development of UC. A convenient method of classification is grouping oxidative stressors as exogenous (originating external to the body) or endogenous (originating inside the body). The following section details the mechanism of action for several reported and/or common oxidative stressors associated with UC.

Exogenous oxidative stressors

Diet has been implicated in the pathogenesis and pathophysiology of UC[80]. 65% of surveyed individuals with UC believe that food is a significant trigger for relapse with 50% asserting that diet contributed to the initial development of disease[81]. This suggests that dietary factors exert their effect on the pathogenesis of UC by means of a common mechanism within the molecular chain of events leading to the onset of disease.

Dietary fat

Studies have shown that a high-fat low-fiber "westernized" type diet is associated with the development of UC, and high-fiber low-fat diets reduce systemic inflammatory biomarkers in patients with this illness[82,83]. Additionally, diets high in total fat and certain fatty acids are associated with exacerbation of UC[82,84,85]. But how does dietary fat initiate or worsen UC? Peroxisomes play an indispensable role in the metabolism of fatty acids obtained from dietary fat[86]. Peroxisomes are involved in the metabolism of dietary lipids such as medium chain, long chain, and very long chain fatty acids and cholesterol in addition to pristanic and phytanic acids[86,87]. Peroxisomal metabolism of fatty acids generates large amounts of H_2O_2, which is estimated to be about 35% of total cellular H_2O_2 production[88]. This is in line with data implicating peroxisomal H_2O_2 as an important source of cellular oxidative stress[89]. This implies that excess peroxisomal generated H_2O_2 can overwhelm the cell's reductive (antioxidant) capacity and accumulate to the point of causing cellular dysfunction. This is consistent with previous data ascribing a causal role for H_2O_2 in the pathogenesis of UC and implies that high fat diets contribute to the pathogenesis and relapse of UC by generating large amounts of peroxisomal H_2O_2. Excess peroxisomal generated H_2O_2 can diffuse into the cytoplasm and overwhelm the colonocyte's ability for its removal leading to extracellular diffusion and the development or relapse of UC as described above. Thus, high fat diets are risk factors for the development of UC because they are oxidative stressors that generate large amounts of peroxisomal H_2O_2[89]. Low fat diets ameliorate colonocyte oxidative stress by decreasing production of peroxisomal H_2O_2 and in so doing promote remission of UC.

Fiber

As mentioned above, low fiber diets are associated with the development and worsening of UC. But how does fiber interface with the pathogenesis and relapse of this illness? The colonic epithelium utilizes short chain fatty acids (*i.e.*, butyrate) for most of its energy requirements[90]. The production of butyrate starts with the fermentation of dietary soluble fiber by colonic bacteria. Butyrate is rapidly absorbed by colonic epithelial cells *via* passive diffusion and cell membrane transport proteins[91]. Once in the cytoplasm, butyrate is transported *via* the carnitine shuttle into mitochondria where it undergoes beta-oxidation. The resulting acetyl-coenzyme A (CoA) enters the Krebs cycle, which generates reducing equivalents (NADH, FADH2) that provide the energy for oxidative phosphorylation and ATP production[92]. This process provides up to 70% of colonocyte energy supplies (Figure 4A)[93,94].

A decrease in the available dietary soluble fiber will diminish the amount of butyrate absorbed by colonic epithelial cells and less butyrate will be available to undergo mitochondrial beta-oxidation. With decreased beta-oxidation of butyrate generating less acetyl-CoA, the colonocyte may not have enough fuel for the Krebs cycle to produce sufficient reducing equivalents (NADH, FADH2) in order to power oxidative phosphorylation and provide the energy for the biosynthesis of ATP. Without sufficient ATP to fuel critical cellular functions, the colonocyte will die. To increase ATP production, the colonocyte diverts glutamate into the Krebs cycle (*via* alpha keto-glutarate) in order to replace Krebs cycle intermediary metabolites that would otherwise be supplied by dietary fiber, which is in low supply (Figure 4B). Glutamate (an amino acid) is derived from the amino acid glutamine (the storage form of glutamate), and studies have shown cellular diversion of glutamine into the Krebs cycle as a consequence of impaired mitochondrial pyruvate transport underscoring glutamine's role as a backup

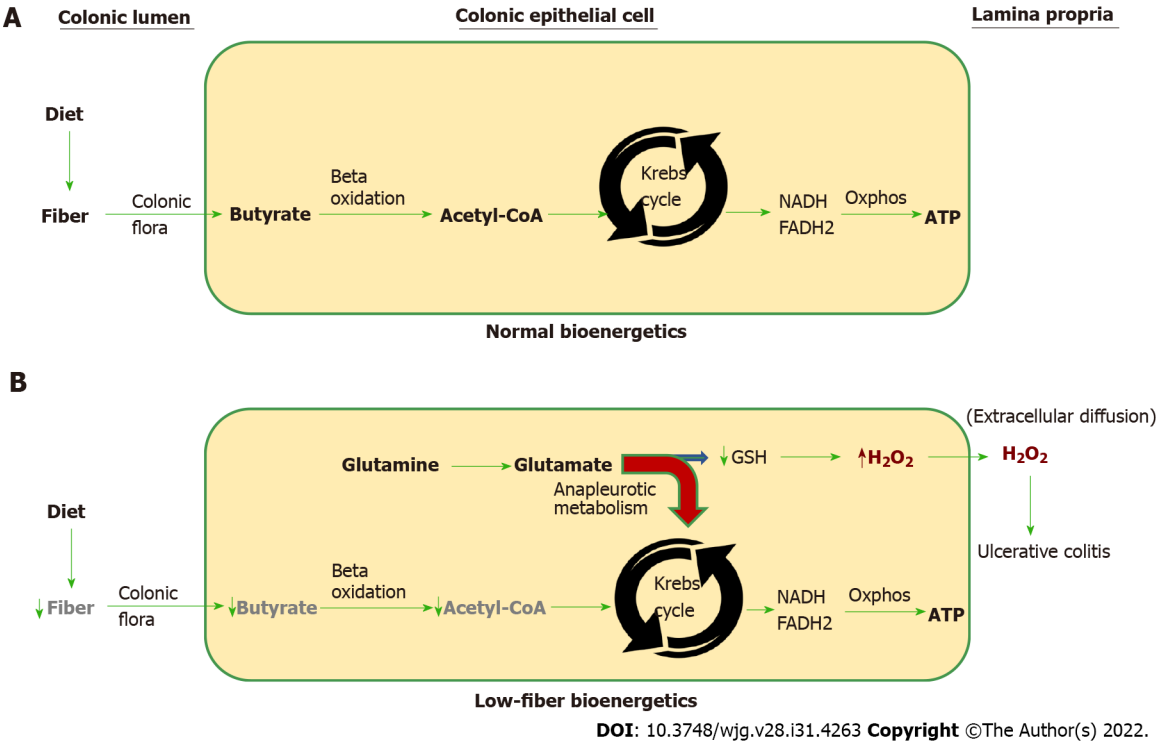

DOI: 10.3748/wjg.v28.i31.4263 **Copyright** ©The Author(s) 2022.

Figure 4 Normal *vs* low-fiber colonocyte bioenergetics. A: The normal vectorial bioenergetic flux beginning with soluble dietary fiber that is converted to short-chain fatty acids (*i.e.*, butyrate) by bacteria in the colonic lumen. Butyrate is rapidly absorbed by colonic epithelial cells (colonocytes). Once inside the colonocyte, butyrate undergoes mitochondrial beta-oxidation to generate acetyl-coenzyme A (CoA), which is processed by the Krebs cycle that produces NADH and FADH2. The high-energy electrons present in NADH and FADH2 are used to drive oxidative phosphorylation (Oxphos) resulting in the biosynthesis of ATP, which fuels most of the cell's energy needs; B: Low fiber intake decreases available butyrate needed for acetyl-CoA production. Under these energy-restricted conditions, glutamate is diverted into the Krebs cycle and away from the synthesis of glutathione (GSH). Diversion of glutamate into the Krebs cycle is called anapleurotic metabolism (red curved arrow) and is needed to replenish depleted Krebs cycle intermediary metabolites that would otherwise be supplied by dietary soluble fiber, which can no longer perform this role due to a low fiber diet. Since glutamate is needed for the synthesis of GSH, the sequestration of glutamate as a replacement energy source restricts the amount of glutathione the cell is able to synthesize. GSH is the principal reducing equivalent required to neutralize cellular hydrogen peroxide (H_2O_2). Insufficient glutathione will cause cellular H_2O_2 to increase, which upon extracellular diffusion may initiate neutrophil chemotaxis into the colonic epithelium and *de novo* ulcerative colitis or disease relapse. Interruption of colonocyte bioenergetic flux anywhere along the pathway from the microbiome to acetyl CoA will increase colonocyte anapleurotic metabolism and cellular H_2O_2, which can lead to ulcerative colitis. H_2O_2: Hydrogen peroxide; CoA: Coenzyme A.

energy supply during times of limited acetyl-CoA availability[95].

Studies on isolated colonocytes from germ-free rats (that cannot produce butyrate) report a 45% increase in glutamine use by these cells compared to conventionally reared animals[96]. Other studies using isolated colonocytes from germ-free mice demonstrated 16-fold lower NADH/NAD+ ratios as well as 56% lower ATP levels[97]. Colonization of germ-free mice with flora from conventional mice or butyrate-producing bacteria rescued the colonocyte energy deficit as did butyrate exposure to isolated colonocytes from germ-free mice[97]. This indicates that butyrate is a critical source of energy for colonocyte ATP production and colonocytes will compensate for the loss of butyrate by diverting glutamine (*via* glutamate) into the Krebs cycle to maintain the production of ATP.

However, the continued Krebs-cycle oxidation of glutamine as a backup energy source (*i.e.*, during prolonged low-fiber diets) entails significant consequences for the colonocyte. Glutamine is the precursor to glutamate, which is necessary for GSH synthesis. The diversion of glutamate into the Krebs cycle (called anapleurotic metabolism) to sustain cellular energy requirements restricts glutamate's availability for the biosynthesis of GSH, which is critical for the elimination of cellular H_2O_2[98]. Studies have shown that disrupting mitochondrial pyruvate uptake directs glutamine into the Krebs cycle and away from GSH synthesis[99]. Because GSH is critical for the elimination of cellular H_2O_2, a decrease in GSH synthesis will lead to increased colonocyte H_2O_2 and subsequent diffusion through the cell membrane to the extracellular space, which may precipitate *de novo* UC, worsen existing UC, or contribute to relapse (Figure 1B). Thus, low fiber diets are oxidative stressors because they increase the risk of colonocyte intracellular H_2O_2 buildup.

The critical importance of (soluble) dietary fiber for colonic bioenergetics and redox homeostasis is underscored by what occurs with the complete absence of colonic fiber. Diversion colitis is a reactive colonic inflammatory response in the by-passed segment of the large intestine as a result of fecal stream diversion secondary to colostomy or ileostomy. Under these circumstances, there is no dietary fiber entering the defunctioned segment of the large intestine. This results in a colitis affecting nearly all individuals undergoing this procedure within 1 to 3 years after colonic diversion[90]. Histopathology

soon after onset shows an influx of neutrophils into the colonic epithelium (analogous to UC)[100]. This suggests the alternate use of glutamate to compensate for the complete lack of lumenal butyrate decreases colonocyte GSH enough to raise cellular H_2O_2 to levels that facilitate extracellular diffusion and the development of colitis. It also implies that H_2O_2 plays a prominent causal role in the development of diversion colitis as well[101].

This interpretation is consistent with a case report of a healthy 36-year-old male who developed UC after following an extremely low carbohydrate diet for weight loss, which resolved without medication upon the institution of a semi-vegetarian diet[102]. Studies have demonstrated significant declines in fecal butyrate and butyrate-producing bacteria in individuals with reduced dietary carbohydrates[103]. The decrease in colonocyte butyrate can be reversed with butyrate enemas that significantly increased colonic epithelial GSH, which is consistent with a GSH sparing effect of butyrate inferred from Figure 4B[104].

Butyrate enemas also significantly reduced mucosal inflammation in patients with refractory UC [105]. This can be attributed to the butyrate-mediated increase in colonocyte GSH and subsequent reduction in colonic epithelial H_2O_2. This is supported by studies showing that butyrate prevents H_2O_2-induced DNA damage in isolated human colonocytes[106]. Thus, colonic butyrate has a critical role in maintaining colonocyte redox-homeostasis by preventing the anapleurotic metabolism of glutamate and subsequent decrease in colonic epithelial GSH, which leads to elevated colonocyte H_2O_2 and UC[107].

The crucial role of GSH in the elimination of cellular H_2O_2 can be seen in GPx knockout mice that lack this key enzyme needed to utilize GSH for the elimination of H_2O_2. Knockout mice lacking GPx develop colitis[32]. Colitis also occurs concomitantly with experimental beta-oxidation inhibition in mice, and in pigs subsequent to vitamin B-5 (pantothenic acid) deficiency. Vitamin B-5 is necessary for CoA synthesis, without which there is no acetyl CoA[108,109]. This suggests that disruption of bioenergetic flux at any point along the metabolic pathway from lumenal fiber to the formation of acetyl CoA will result in increased colonocyte H_2O_2 and colitis (Figure 4B).

Based on these data, we can reasonably predict that alterations in the colonic flora (microbiome dysbiosis) that lead to impaired short-chain fatty acid (*i.e.*, butyrate) production will contribute to the development and relapse of UC by increasing colonocyte H_2O_2. A diverse set of adverse environmental exposures can shift the colonic microbiome towards dysbiosis and impaired butyrate production. These include high fat/low fiber/high protein diets, food additives in processed food, smoking and alcohol ingestion[110-113]. Other diverse factors such as infant delivery and feeding methods, medications, enteric endocrine disruptors, psychological stress can also facilitate microbiome dysbiosis[114-117]. Long term dietary patterns that include soft drinks and artificial sweeteners may tip the balance towards dysbiosis[118,119]. Thus, microbiome dysbiosis is an oxidative stressor that can increase colonocyte H_2O_2 and contribute to the onset of UC[120].

Lastly, as mentioned above, H_2O_2, being membrane permeable, can diffuse into the colonocyte nucleus leading to oxidative nuclear DNA mutations in tumor suppression and oncogenes that promote colorectal cancer[51,52]. Studies have shown that mice fed a total western diet develop a neutrophil predominant colitis and colorectal cancer[121]. This is analogous to histological findings in human UC, which also carries an enhanced risk of colorectal cancer. Taken together, when the evidence supporting a causal role for H_2O_2 in UC and its associated colon cancer is viewed in light of biological mechanisms leading to increased colonocyte H_2O_2 subsequent to low-fiber high-fat diets, it is reasonable to conclude that the increased incidence of UC and colorectal cancer associated with the (low-fiber high-fat) western diet[9,97,122] is mediated through elevated colonocyte H_2O_2. This raises the possibility of primary prevention *via* changes to reduce dietary oxidative stress (*i.e.*, high fiber, low fat *etc*) and/or the administration of an oral reducing agent (detailed in the treatment section below).

Alcohol

Several studies have found that alcohol consumption increases the risk of onset, relapse, and gastrointestinal symptoms in individuals with UC[123]. Alcohol is biomembrane permeable, and after ingestion is distributed to all tissues in the body[124]. Alcohol metabolizing enzymes in the colonic epithelium can generate large amounts of H_2O_2[124]. Alcohol metabolism by alcohol dehydrogenase generates acetaldehyde, which is converted to acetic acid by aldehyde dehydrogenase. Both these reactions generate NADH, which feeds into the mitochondrial ETC causing increased electron leakage and enhanced generation of H_2O_2[124]. The increased amount of colonocyte H_2O_2 can overwhelm cellular reductive capacity and diffuse to the extracellular space leading to relapse or the onset of UC.

Cytochrome P450 2E1 (CYP2E1) is a second alcohol oxidizing enzyme that is highly expressed in the human intestine and is upregulated by chronic alcohol exposure[125]. CYP2E1 has the highest catalytic activity among the members of CYP enzymes in metabolizing ethanol[126]. CYP2E1 consumes NADPH when metabolizing ethanol to acetaldehyde and in the process generates large amounts of H_2O_2[126, 127]. NADPH is also required for the recycling of oxidized GSH (GSSG) back to reduced GSH by GSSG reductase[49]. This can reduce the availability of GSH for the elimination of H_2O_2 and contribute to increased colonocyte H_2O_2 levels. The total combined effect of alcohol metabolism is excess production of colonocyte H_2O_2 that can overwhelm cellular reductive capacity leading to extracellular H_2O_2 diffusion and *de novo* UC or relapse by the mechanisms detailed above. CYP2E1 is also upregulated by ethanol, which magnifies the oxidative stress caused by this alcohol metabolizing enzyme.

Antibiotics

Due to their widespread use, antibiotics represent a significant source of oxidative stress within the population. Studies have shown an association between antibiotic use and the development of UC[128]. Although antibiotics are administered to eradicate pathogenic bacteria they also indiscriminately kill beneficial commensal bacteria that make up the colonic microbiome leading to a decrease in species diversity including a reduction in bacterial species that produce butyrate[129]. A decrease in colonic butyrate can lead to metabolic changes favoring increased colonocyte production of H_2O_2 (Figure 4). Antibiotic-induced microbiome depletion (dysbiosis) can last for years and act cooperatively with other oxidative stressors such as a high-fat diet[130,131]. This can hasten colonocyte H_2O_2 build-up (HCRH) and the development of UC.

However, microbiome depletion is not the only mechanism by which antibiotics generate excess colonocyte H_2O_2. Studies have shown that antibiotics induce the production of significant amounts of H_2O_2 in both bacteria and human intestinal epithelial cells, which in the latter was caused by an alteration to the ETC[132-135]. Since H_2O_2 is cell membrane permeable, bacterial H_2O_2 can diffuse across epithelial cell membranes and add to the already increased antibiotic-induced colonic epithelial cell H_2O_2 load. This can lead to mtDNA oxidative damage with the formation of colonocyte mitochondrial heteroplasmy and ever-increasing production of intracellular H_2O_2 resulting in HCRH (Figure 2). Increased cellular production of H_2O_2 can overwhelm colonocyte reductive (antioxidant) capacity and lead to a buildup of colonocyte H_2O_2 that will facilitate the development of UC years later. Because virtually everyone is exposed to antibiotics at one time or another, they exert a selective oxidative pressure that can manifest as UC in individuals with a predisposing genetic makeup encoding for a diminished reductive capacity that facilitates the buildup of H_2O_2.

Psychological stress: A common oxidative stressor leading to H_2O_2 production

Stress is a significant risk factor for UC. Up to 40% of patients with UC report psychological stress as an exacerbating factor[136]. Psychological stress can cause *de novo* UC and worsen existing disease[137-141]. Psychological stress exposure is reported to induce mucosal inflammatory responses and can result in colonic hypermotility that may be sufficient to occlude the lumen[142,143]. But why is psychological stress pro-inflammatory in the colon and how does stress initiate or worsen UC?

The coordinated movement of food along the gastrointestinal (GI) tract is dependent on 5-hydroxytryptamine (serotonin) mediated regulation of smooth muscle tone, motility, and peristalsis[144]. 95% of serotonin is stored in enterochromaffin cells (EC) that are present in the GI tract mucosa[145]. Serotonin is released from EC cells and stimulates enteric nerve terminals to initiate a peristaltic wave[144,146]. However, the amount released is much more than needed and the excess serotonin is rapidly taken up by colonic epithelial cells and metabolized by colonocyte monoamine oxidase (EC#1.4.3.4)[144]. This prevents hyper-stimulation and excessive bowel motility that can lead to colonic spasms. Mono-amine oxidase catalyzes the oxidative deamination of serotonin in a process that generates H_2O_2; the reaction catalyzed is $RCH2NHR' + H_2O + O_2 \rightarrow RCHO + R'NH_2 + H_2O_2$[147].

Studies have shown that psychological stress causes prolonged increases in colonic motility[148]. Stress-induced colonic hypermobility and spasm will release large amounts of serotonin into the colonic mucosa that is metabolized to H_2O_2 within colonocytes. The excess colonocyte H_2O_2 can acutely overwhelm the enterocyte's antioxidant capacity resulting in H_2O_2 accumulation and eventual UC after extracellular diffusion. This mechanism is supported by studies showing that serotonin has a key role in the pathogenesis of experimental colitis[149].

Thus, psychological stress has a pernicious effect on the course of UC but UC is also psychologically stressful with studies reporting that patients with UC are engaged in a continuous "fight" to maintain health-related normality[150]. This sets up a self-sustaining bidirectional cycle of continuous psychological stress that contributes to increased frequency and severity of disease[151]. Although stress can cause or worsen UC, stress reduction is generally not effective at altering the activity or course of disease sufficiently to induce remission[152,153]. This is not surprising since the principal driving force behind the auto-propagating nature of inflammation in UC is H_2O_2 release by activated infiltrating mucosal neutrophils and not the metabolism of serotonin, which has its principal effect as a contributing factor in the stress-induced pathogenesis and relapse of UC[26,149].

Cigarette smoking: Releasing the brakes

Since reports in the early 1980s, numerous studies included in three meta-analyses (1989, 2006 and 2021) have established that cigarette smoking is significantly protective against the development of UC compared to non-smokers while smoking cessation is a significant risk factor for developing UC or experiencing disease relapse with increased severity of illness[154-158]. Additionally, as noted below, cigarette smoking also affects the therapeutic response after smoking cessation. But why is cigarette smoking protective against the onset of UC?

Nicotine, an addictive chemical present in tobacco, was initially considered as a possible protective factor. Nicotine is effective at inducing remission when begun at the time of or soon (up to 4 wk) after smoking cessation (early relapse)[159,160] However, nicotine is largely ineffective when therapy is administered for disease relapse several months or years after smoking cessation (late relapse) with

studies concluding that nicotine therapy is of minimal value in the treatment of UC and questions whether nicotine is the active protective component of smoking that decreases risk and inflammation in UC[161-164]. In contrast, the resumption of smoking is reported to be an effective therapy for induction and long-term maintenance of remission in patients with early or late relapse[159,160,165]. Indeed, studies have reported that resumption of smoking is highly effective for induction of remission in refractory disease years after smoking cessation; with nicotine being effective if treatment is begun at the same time as smoking cessation[160]. Thus, in ex-smokers, nicotine is effective for remission induction in early relapse while the resumption of smoking is effective in both early and late relapse.

Taken together, the data indicate that there are two distinct oxidative stressors with distinct short and long-term mechanisms of action both of which are caused by the latent and repressed effects of active smoking and are only unmasked by smoking cessation. The initial mechanism manifests soon after smoking cessation and lasts for days to under a month. In contrast, the second mechanism becomes predominant many months to years later reaching a peak of the highest risk of relapse within 2 to 5 years of smoking cessation[166].

The initial oxidative stressor is the physiological and psychological stress of nicotine withdrawal, which is manifest shortly after smoking cessation and peaks within the first week, and lasts up to one month[167]. Nicotine withdrawal symptoms can include anger, irritability, frustration, anxiety, depression, insomnia, restlessness, and constipation[167]. These same psychological emotions of anger, resentment, emotional conflict, hostility, anxiety, and psychological tension were observed under direct observation to cause significant colonic hypermotility and spasm[168]. Thus, it is reasonable to conclude that nicotine withdrawal secondary to smoking cessation can result in colonic hypermotility with increased colonic serotonin secretion and enhanced monoamine oxidase production of H_2O_2 (see above section-psychological stress). Under these circumstances, the administration of nicotine will decrease colonic hypermotility and lower colonic serotonin production, which decreases colonocyte H_2O_2 leading to remission. Resumption of cigarette smoking also provides the nicotine needed to treat early relapse due to nicotine withdrawal.

In other words, nicotine-induced remission is due to the relief of nicotine withdrawal symptoms (and accompanying colonic hypermotility) during early relapse after smoking cessation. Nicotine treatment is rendered minimally effective after nicotine withdrawal symptoms (and colonic hypermotility) have subsided. Colonic hypermotility (from any cause) is an oxidative stressor that increases colonocyte H_2O_2, which can overwhelm colonocyte reductive (antioxidant) capacity leading to extracellular diffusion and UC.

The second oxidative stressor caused by cigarette smoking cessation is due to disinhibition of the colonocyte ETC. Studies quantifying the effect of cigarette tar on mitochondrial ETC activity report an 82% inhibition rate on whole chain respiration[169]. Under normal conditions, the ETC is fueled by electron flux provided by reducing equivalents (NADH and FADH2) generated by the multi-enzyme Krebs cycle[170]. H_2O_2 is produced by spontaneous auto-oxidation of the ETC (electron leakage). These leaked electrons combine with vicinal oxygen within the mitochondrial matrix to form superoxide, which is converted to H_2O_2 by superoxide dismutase. H_2O_2 is subsequently neutralized by GPx using GSH as a reducing co-factor.

Under conditions of ETC inhibition during active smoking, less ETC-generated H_2O_2 is produced, which affords protection against the development of UC. However, while smoking, upregulation of bioenergetic enzyme systems can be expected as the colonocyte attempts to overcome the smoking-induced inhibition and restore normal mitochondrial bioenergetics[171]. Upon smoking cessation, the inhibition is slowly lifted and increased production of ETC "fuel" is metabolized producing supraphysiological amounts of H_2O_2 as a result of increased ETC auto-oxidation (electron leakage). Colonocytes respond to this oxidative stress by producing additional GSH for H_2O_2 neutralization. This creates a condition of HCRH (Figure 2) that can eventually overwhelm colonocyte reductive capacity leading to cellular H_2O_2 build-up and eventual *de novo* UC as H_2O_2 diffuses to the extracellular interstitial space attracting neutrophils into the colonic epithelium from the subjacent microvasculature.

Smoking resumption inhibits ETC activity, which decreases colonic epithelial cell H_2O_2 leading to remission. Nicotine does not inhibit the ETC and cannot induce remission of late UC relapse (years after smoking cessation). This interpretation is supported by studies that demonstrated significantly improved clinical manifestations such as bloody stool, diarrhea, and abdominal pain in UC patients treated with metformin[172]. Further, UC patients treated with metformin showed a significant decrease in histological and endoscopic disease scores in addition to significantly diminished erythrocyte sedimentation rate (a biomarker of systemic inflammation) and significantly decreased indices of colonic local oxidative stress (tissue malonaldehyde and myeloperoxidase)[172].

But how does metformin improve UC and how is it related to cigarette smoking? Metformin is a biguanide antihyperglycemic agent used to treat type 2 diabetes. Its mechanism of action includes inhibition of mitochondrial glycerol 3-phosphate dehydrogenase (of the glycerolphosphate shuttle-EC 1.1.5.3) and inhibition of ETC complex I both of which are major contributors of electrons to the ETC in mitochondria[173-175]. Inhibition of electron flux by metformin is analogous to the ETC inhibitory effects of cigarette smoking. This implies that both smoking and metformin improve UC by decreasing mitochondrial production of H_2O_2. This is supported by studies showing that targeted inhibition of glycerol 3-phosphate dehydrogenase decreases cellular production of H_2O_2[176].

In summary, the evidence supports two distinct oxidative stress mechanisms to explain the effects of smoking cessation on UC. Early relapse after smoking cessation (within days) is mediated by the oxidative stress induced by the physiological effects of nicotine withdrawal while late relapse (months to years) is mediated by a slow rise in colonocyte H_2O_2 due to disinhibition of mitochondrial H_2O_2-generating metabolic pathways. Conversely, cigarette smoking affords protection against early and late UC relapse by providing nicotine and decreasing colonocyte production of H_2O_2, respectively.

Mercury

Mercury is a major environmental contaminant and a significant source of occupational exposure[177]. Occupational inhalation of mercury vapor is reported to cause a recurrent relapse of UC[178]. Mercury forms stable bonds with thiol groups present on GSH in addition to inhibiting GPx, both of which are critical for the removal of cellular H_2O_2[179-181]. This results in the inactivation of the entire GSH-based antioxidant system. The compromise of this critical system by mercury prevents neutralization of H_2O_2, which can accumulate to excessive levels inside colonocytes leading to extracellular diffusion and UC relapse as described above. Thus, mercury is an oxidative stressor that increases cellular H_2O_2 by preventing its elimination from the cell. Mercury is a pervasive contaminating xenobiotic whose exposure is likely to be insidious, bio-accumulative, and additive to other contemporaneous oxidative stress exposures.

PERFLUOROOCTANOIC ACID

Perfluorooctanoic acid (PFOA) is a ubiquitous environmental contaminant that was used to manufacture non-stick pans in addition to other commercial products such as stain and water-resistant fabrics. Introduced into the environment in the 1950s, PFOA can be found in the serum of virtually all residents of industrialized countries. Human exposure occurs *via* many sources including contaminated drinking water, food, and house dust. Due to the high dissociation energy of its carbon-fluorine bond, PFOA is resistant to vertebrate metabolism and environmental degradation[182]. As a result, PFOA is called a "forever-chemical" because it is not biodegradable and has a long elimination half-life of 3.5 years[183].

Studies have demonstrated a significant exposure-response relationship between PFOA serum levels and subsequent UC but no association with Crohn's disease (CD)[183]. Other studies have reported significantly increased serum PFOA in UC patients compared to a combined group of CD (positive control for intestinal inflammation) and normal individuals (negative non-diseased control)[184]. The specific association of PFOA with UC suggests that PFOA's effect is acting in concert with a unique predisposing genetic makeup to select a subset of individuals for the development of UC. In other words, PFOA's mechanism of action in all exposed individuals is the same but the genetic predisposition in a subset of individuals is permissive for the development of UC.

A related halogenated chemical, 2-bromooctanoic acid, after conversion to the sodium salt 2-bromooctanoate, is reported to cause an acute murine colitis analogous to human UC after rectal installation[108]. This suggests the possibility that PFOA might be acting in the same manner as 2-bromooctanoate since halogenated carbon compounds, as a group, have a high resistance to degradation[185].

In human UC, beta-oxidation is inhibited as a secondary effect caused by rising levels of colonocyte H_2O_2[30]. Since 2-bromooctanoate causes murine UC accompanied by inhibition of beta-oxidation and the related halogenated chemical PFOA causes UC and is not biodegradable this suggests that intracellular H_2O_2 is increased as a result of the colonocyte's high expenditure of energy (ATP) in a futile attempt to metabolize and remove these non-biodegradable halogenated xenobiotics from the cell. Since almost all cellular ATP is produced as a result of mitochondrial ETC activity, which also generates most of the cell's H_2O_2, this implies that the initial buildup of H_2O_2 occurs in mitochondria where beta-oxidation is also located. Increased mitochondrial H_2O_2 will inhibit mitochondrial thiolase, the last enzyme in the beta-oxidation cascade, leading to inhibition of mitochondrial beta-oxidation[30].

In other words, the colonocyte's persistent metabolic response in an attempt to eliminate these non-biodegradable chemicals leads to increased H_2O_2 generated by the ETC, which inhibits mitochondrial beta-oxidation followed, sometime later, by UC as H_2O_2 diffuses out of the colonocyte into the extra cellular space. This mechanism is consistent with studies showing inhibition of beta-oxidation in UC patients is followed shortly after by a relapse of disease[41]. H_2O_2-induced inhibition of mitochondrial beta-oxidation (*via* mitochondrial thiolase inhibition) increases the anapleurotic metabolism of glutamine, which decreases the biosynthesis of GSH contributing to the excess colonocyte H_2O_2 load (Figure 4). This mechanism is also consistent with a genetic predisposition that impairs the colonocyte's ability to neutralize an H_2O_2 load. Within this redox framework, inhibition of colonocyte beta-oxidation is a secondary effect of colonocyte xenobiotic (PFOA or bromooctanoate) metabolism, which generates excess ETC H_2O_2 that impairs mitochondrial beta-oxidation *via* H_2O_2 induced inhibition of mitochondrial thiolase. This raises the possibility of primary prevention with an oral reducing agent for communities at risk for the adverse effects of PFOA exposure. A causal role for H_2O_2 can be tested in the

laboratory by the prevention of PFOA (or 2-bromooctanoate) induced murine colitis with an oral reducing agent (see treatment section below).

Lastly, PFOA's adverse effects are not limited to UC. Lymphocytes are highly sensitive to the toxic effects of H_2O_2 and undergo apoptosis at very low levels of H_2O_2 exposure of less than 1 μm[186]. Studies showing a significant association between PFOA serum levels and decreased antibody response to vaccination are consistent with this mechanism of action[182]. Thus, PFOA resistance to cellular metabolism and degradation is likely to result in excess H_2O_2 production in any cell contaminated by this xenobiotic.

Endogenous oxidative stressors: A look inside

In UC, lifelong episodes of relapsing inflammation affecting the same colonic regions previously inflamed indicate that inflammation has fundamentally changed the colonic epithelium compared to the pre-morbid state. Since the character of the inflammation does not change over time and neutrophils continue to be the first responders streaming into the colonic epithelium, this suggests that H_2O_2 is still the chemotactic agent involved but from a new source. The evidence points to new endogenous sources of H_2O_2 that combine with pre-existing sources of H_2O_2 to increase the likelihood of relapse.

Microbiome: An oxidative dysbiosis

Although disruption of the colonic microbiome can contribute to the onset of UC by decreasing butyrate production, which leads to increased colonocyte H_2O_2 (Figure 4), UC can also adversely affect the microbiome. Studies have shown a 10 × increase in H_2O_2 producing bacteria in biopsies of inflamed colonic tissue in individuals with UC compared to normal controls[120]. These H_2O_2-producing bacteria are adherent to the colonic mucosa. This suggests that chronically high levels of H_2O_2 in the inflammatory field create an environment that selects for bacteria that produce H_2O_2, which are those able to tolerate the abnormally high levels of lumenal oxidative stress. Over time, this oxidative dysbiosis may replace large portions of the normal microbiome, which may not be able to survive under conditions of high H_2O_2-induced oxidative stress. The H_2O_2 released by bacteria can contribute to relapse by diffusing through the epithelium to the subjacent vascular layer where it serves as a chemotactic agent to attract neutrophils into the colonic epithelium. This creates a microbiome, which is a pro-inflammatory endogenous oxidative stressor that contributes to the onset or relapse of UC by continuous H_2O_2 production. A recent analysis examining the pathogenesis of UC concluded that "*disease onset is triggered by events that alter the healthy balance of the gut microbiota, perturb the mucosal barrier, and abnormally stimulate gut immune responses*"[12]. H_2O_2 does all three.

CYP2E1 induction: A vicious cycle

As explained above CYP2E1 is an alcohol inducible enzyme that is involved in the metabolism of ethanol and other xenobiotics entering the body. H_2O_2 is within the chain of molecular events that upregulate inducible CYP2E1[187]. This implies that chronically elevated colonocyte H_2O_2 from any source (*i.e.*, ethanol or xenobiotic metabolism, oxidative stress exposure, *etc*) can upregulate CYP2E1. In other words, elevated colonocyte H_2O_2 can upregulate CYP2E1 without ethanol exposure. This can cause increased sensitivity to CYP2E1 substrates, which can lead to heightened H_2O_2 production in areas of previous inflammation when exposed to ethanol or other xenobiotics metabolized by this enzyme. Studies have shown the cells with upregulated CYP2E1 produced higher amounts of H_2O_2 that can exit the cell[188]. This can cause increased H_2O_2 production upon exposure to CYP2E1 substrates such as alcohol and other xenobiotics, which increases the risk of relapse or *de novo* UC. Under these circumstances, upregulated CYP2E1 becomes an endogenous oxidative stressor.

Mitochondrial heteroplasmy: Hard-wired for inflammation

Intracellular H_2O_2 is normally kept within a very low picomolar range to prevent oxidative damage from this very powerful oxidizing agent[186,189]. Over time, colonocytes from individuals with UC are exposed to higher levels of H_2O_2 due to multiple oxidative stressors including infiltrating epithelial neutrophils (mucosal inflammation), microbiome (oxidative dysbiosis), CYP2E1 induction (alcohol and xenobiotic exposure), peroxisomal beta-oxidation (high-fat diet) and ETC hyperactivity (smoking cessation), *etc.* The increase in colonocyte H_2O_2 can overwhelm cellular antioxidant systems resulting in mitochondrial genetic damage[44,45]. This occurs because mtDNA is highly susceptible to H_2O_2-induced oxidative damage due to a lack of introns or histones, proximity to the ETC where H_2O_2 is produced, and inefficient DNA repair mechanisms compared to nuclear DNA[37,38].

As mentioned above, H_2O_2-induced mitochondrial genetic damage introduces mutations into mtDNA resulting in a different genetic sequence for some of the hundreds of mitochondrial chromosomes present in a cell. The simultaneous occurrence of normal and mutated mtDNA is called mitochondrial heteroplasmy. The presence of mitochondrial heteroplasmy (mtDNA mutations) causes miscoding during the transcription of ETC proteins leading to the biosynthesis of faulty and mutated ETC subunits. The mutated ETC disrupts electron flow causing electron loss at a greater rate than normal (increased electron leakage). These electrons combine with vicinal molecular oxygen to form superoxide that is converted to H_2O_2 by superoxide dismutase. Since the ETC and mtDNA are both in close

proximity to each other within the mitochondrial matrix, any excess H_2O_2 produced by the ETC can easily diffuse over to any one of the 2-10 chromosomes contained within a mitochondrion leading to additional mtDNA mutations and greater H_2O_2 production[190]. This positive biofeedback mechanism establishes a vicious cycle that leads to ever-increasing levels of colonocyte H_2O_2.

The presence of mitochondrial heteroplasmy (and the resulting increase in colonocyte H_2O_2) can contribute to the tendency of UC to worsen over time with more frequent and severe episodes of relapse [7]. Relapse may occur in response to increasingly minor (oxidative) stressors due to the already high intracellular colonocyte H_2O_2. Thus, the accumulation of colonocyte H_2O_2 transforms otherwise innocuous insults into 'second hit' stimuli. The "first hit" being the pre-existing excess of colonocyte H_2O_2. For example, in individuals with inactive UC, low to moderate red wine consumption (1-3 glasses daily) increased colonic epithelial paracellular permeability in areas previously affected by mucosal inflammation[123,191]. Increased colonic paracellular permeability is characteristic of individuals with UC[24,25]. And H_2O_2 is reported to increase paracellular permeability by disrupting cellular tight junctions[20,22,192-194]. Under these circumstances, it takes less alcohol to increase colonocyte H_2O_2 to the point where it diffuses out of the cell causing oxidative damage to tight junctions with subsequent increases in colonic paracellular permeability. This explains the second hit phenomenon in UC. In summary, mitochondrial heteroplasmy is unique because it is an ever-present self-amplifying intracellular oxidative stressor that facilitates the establishment of HCRH (Figure 2), which contributes to both the increased frequency of relapse and/or severity of disease.

Homocysteine: Inhibition of GPx

Several studies have reported significantly elevated levels of tissue and serum homocysteine in children and adults with UC[195-198]. A significant positive association between elevated homocysteine and UC was confirmed by two meta-analyses in 2011 and 2018[199,200]. Homocysteine inhibits GPx, the principal antioxidant enzyme system used by the cell to remove (neutralize) H_2O_2[201,202]. Furthermore, homocysteine-induced inhibition of GPx occurs at physiologic levels of serum homocysteine[203]. Inhibition of GPx can increase cellular H_2O_2, especially during oxidative stress exposure, which acutely increases cellular H_2O_2 production. Thus, homocysteine is a significant endogenous oxidative stressor that can increase colonocyte H_2O_2 and contribute to *de novo* UC or disease relapse.

EVIDENCE-BASED TREATMENT

Therapy: Targeting H_2O_2

A causal role for H_2O_2 in the pathogenesis of UC implies that induction of remission can be achieved by eliminating extracellular colonocyte H_2O_2 while maintenance of remission is attained by normalizing intracellular levels of colonocyte H_2O_2. The overall objective is to abrogate the H_2O_2 molecular chemotactic "trail" that is guiding the directed migration of subjacent intravascular neutrophils to the source of H_2O_2 emanating from the colonic epithelium. Without an interstitial H_2O_2 gradient signal to follow, neutrophils are no longer attracted into the colonic epithelium, which effectively terminates the inflammatory response. These were the goals that guided the formulation of a novel therapy, which consists of a topical multicomponent enema (described below) administered with a systemic oral reducing agent [R-dihydrolipoic acid (RDLA)] that targets extracellular and intracellular colonocyte H_2O_2 respectively. RDLA is the reduced form of the biologically active 'R' enantiomer of lipoic acid and is the only form that should be administered as the oxidized form (described below) might worsen UC.

We administered the enema once daily (usually at bedtime) for 2 wk followed by once every other day for two weeks. Oral RDLA 300 mg twice daily was initiated when enema therapy was begun. Treatment with RDLA was continued for 4-6 mo. The components of the enema are mesalamine [5-aminosalicylic acid (5-ASA)], budesonide, sodium cromolyn, and sodium butyrate. The enema formulation and evidence-based rationale for the inclusion of each component of the entire therapy are discussed below. The severity or extension of the disease was not a consideration when initiating therapy since, in theory, all patients with UC should respond to a reduction of colonic H_2O_2. Our only consideration was whether the patient could tolerate the therapy.

Enema formulation

The enema was formulated by adding the following components to a standard 60-milliliter enema bottle containing 4 g of mesalamine (5-ASA) from which 20 milliliters were removed (and discarded): (1) 15 milliliters of 1 molar sodium butyrate (1.7 g); (2) 5 milliliters of sodium cromolyn (total 100 mg); and (3) 1 milliliter of budesonide (5 mg/mL). Gentle swirling should follow the addition of each component to ensure uniform dispersal. The total ending volume is 61 milliliters. The combination enema is easily made by a compounding pharmacist. We only used the original enema bottle containing mesalamine to formulate this therapy as other bottles may have residual chemicals that can worsen UC.

Results of treatment

The novel treatment was offered to 36 patients with refractory UC as part of the practice of medicine (average MAYO score 8.6, range 3-12) and the results were published as a case series in which 85% achieved complete histologic remission in under 8 wk[204]. Although long-term follow-up was not part of the case series, a case report was generated after I was contacted by a patient included in this case series[205]. The patient had a 39-year history of refractory UC, which had progressed to severe pancolitis at the time of treatment when he was being considered for a total colectomy. His follow-up colonoscopy, which was performed 12 years later in 2019, showed completely normal colonic biopsies with no signs of UC. To date, (14 years after treatment) the patient relates having uninterrupted completely normal bowel movements. Based on the available data, this appears to be the first documented cure of UC. The video of an in-house clinical presentation of the first five patients to receive this new therapy with before-and-after treatment histology presented by the attending physician and attending pathologist is available[206].

Within this evidence-based redox framework, the general therapeutic intervention for all UC patients is the same regardless of duration or severity of illness, course, relapsing frequency, mucosal inflammatory distribution, age of onset, previous medications, or extra intestinal manifestations. Modifications may be required for those patients who are intolerant to any of the components in the therapy. In patients who are intolerant of topical (enema) therapy, treatment can be initiated with RDLA alone, which as an amphipathic membrane-permeable antioxidant (H_2O_2 neutralizing) and reducing (cellular electron-donating) agent may restore colonocyte redox homeostasis and resolve mild-moderate cases of UC with more severe cases improving enough to begin topical (enema) therapy if needed.

Severe UC

Up to 25% of patients with UC will experience severe disease requiring hospitalization either on initial presentation or during the course of their illness[207]. Severe UC presenting with multiple daily episodes of bloody diarrhea and signs of systemic toxicity is a life-threatening emergency with significant morbidity, high risk of colectomy, and a pre- and post-operative mortality of up to 3% and 5% respectively[8,207,208]. In these individuals, oral and/or topical therapy may not be possible or advisable. The evolution of UC to this extreme degree indicates severe depletion of both colonic and systemic reductive capacity[61,62]. The exceptionally high rate of current medical treatment failure for severe UC and the observation that remission is associated with restoration of colonic redox homeostasis[208,209], suggests that patients with severe UC should be considered for therapy with an intravenous reducing agent such as sodium thiosulfate (STS) as part of their overall treatment regimen in order to rapidly reduce systemic and colonic H_2O_2, restore redox homeostasis and promote mucosal healing. Given that current management of acute severe UC is not based on high-quality evidence, the need for effective therapy is all the more pressing[210].

STS is an odorless, water-soluble, small inorganic molecule (MW-158.11 g/mol) that is normally produced in mitochondria as a product of sulfide oxidation pathways[211]. STS is on the World Health Organization's (WHO) list of essential medicines and is supplied for intravenous use due to rapid gastric degradation[211]. STS is a direct-acting reducing agent that can donate two electrons to chemically neutralize H_2O_2 upon contact[212]. STS will also reduce the oxidized form of GSH (GSSG) back to reduced GSH, which is needed to neutralize H_2O_2 and maintain cellular redox homeostasis[213]. The advantage of STS is that it does not depend upon biological antioxidant enzyme systems for its therapeutic action. This is beneficial in critical settings when rapid reduction of H_2O_2 and restoration of redox homeostasis are required.

The basic chemical reaction for the reduction of H_2O_2 with STS is: $4\ H_2O_2 + S_2O_3^{2-} \rightarrow 2\ SO_4^{2-} + 2\ H^+ + 3\ H_2O$[212]. Based on the above chemical reaction and evidence implicating a causal role for H_2O_2 in the pathogenesis of UC, STS is expected to abrogate the interstitial neutrophilic chemotactic effect being exerted by H_2O_2 and thus prevent neutrophil migration into the colonic epithelium, which perpetuates colonic inflammation. The reduction of extracellular colonic mucosal H_2O_2 by STS can act as a sink that will facilitate the diffusion of intracellular colonocyte H_2O_2 to the extracellular space where it can be neutralized by STS.

H_2O_2 can impair smooth muscle contraction and interrupt neuromuscular transmission leading to reduced colonic muscle tone and lowered colonic lumenal pressure, which is postulated to play an essential role in the development of toxic megacolon, a life-threatening complication of UC[214-218]. Thus, reducing agents such as STS or RDLA may have a role in treating or preventing toxic megacolon. Once severe UC is resolved, patients should be discharged on an oral reducing agent such as RDLA for an indefinite period of time to lower the risk of relapse.

STS is well tolerated and approved for use in cyanide poisoning with a recommended dose of 12.5 g over slow IV infusion (10-20 min) in adults and 250 mg/kg in children[219,220]. Similar dosing regimens can be considered in UC with repeat dosing guided by clinical status. STS is an accepted therapy for calciphylaxis due to chronic renal failure and is administered to mitigate the adverse effects of cisplatin toxicity during the treatment of solid tumors[213].

MAINTENANCE: TARGETING OXIDATIVE STRESSORS

Although therapeutic intervention to lower H_2O_2 and restore colonic redox homeostasis is a critical part of overall therapy, elimination of contributing lifestyle and dietary habits that increase cellular H_2O_2 (environmental oxidative stressors, Figure 3A) must be part of the long term strategy to maintain remission. A complete list of environmental oxidative stressors and their mechanisms is beyond the scope of this paper however, some general evidence-based guidelines can be made. Stress and alcohol ingestion are major oxidative stressors and should be avoided. A low-fat diet with adequate amounts of dietary fiber, especially soluble fiber, is extremely important to minimize colonic oxidative stress[83,221-223].

Eating food that is free of pesticides, chemicals and additives is critical for maintaining a healthy microbiome. High levels of iron in red meat and some tap water are oxidative stressors and should be avoided[224,225]. Certain fish contain high levels of mercury[226,227]. Mercury is an oxidative stressor and therefore it is prudent to minimize ingestion of fish containing high levels of mercury. Studies have shown that sugar and sugar-sweetened drinks are also associated with UC[228,229]. So it is best to avoid high sugar-containing foods and drinks.

Carrageenan is a non-nutritive food additive that is used as a thickening agent in many foods. Although considered safe, food-grade carrageenan can be converted to a colitis-promoting small-molecular (degraded) carrageenan when exposed to H_2O_2[230,231]. Since H_2O_2 is present in the inflammatory field it (H_2O_2) can convert food-grade carrageenan to the degraded variety in the colon of individuals with UC. Studies report that degraded carrageenan can penetrate colonocytes and generate superoxide, which is converted to H_2O_2[232]. Thus, carrageenan is an oxidative stressor that generates intracellular colonic H_2O_2 and should avoid by individuals with UC.

Smoking cessation is a strong oxidative stressor and should be undertaken very slowly in patients with UC to avoid relapse. RDLA can be administered during smoking cessation to counteract oxidative stress. Patients should be very cautious with vitamin supplementation because studies have shown that certain vitamins such as vitamin B6 (pyridoxine) have been associated with the development of UC [233]. Pyridoxine used in supplements and food fortification is converted to the biologically active pyridoxal by pyridoxine 4-oxidase (EC1.1.3.12), which produces H_2O_2 as a by-product[234]. Adequate sleep (at least 6 h) and regular moderate exercise are very important for individuals with UC to reduce stress[235,236]. Based on the data indicating a compromised reductive capacity, all UC patients should be maintained on an oral reducing agent (*i.e.*, RDLA) for an indefinite period of time. The following section provides a detailed explanation regarding the scientific basis for each component of the therapy.

Rationale for multicomponent enema therapy

As mentioned above, the compound enema contains four components: Mesalamine (5-ASA), budesonide, sodium cromolyn, and sodium butyrate. The therapeutic rationale for the compound enema is based on the mechanism of action for each component to act in an additive fashion in order to decrease colonic H_2O_2 as indicated below. The base component, 5-ASA has an anti-inflammatory effect that is limited to the specific type of inflammation present in UC and does not have a positive therapeutic action on colonic inflammation in general[237]. This suggests that 5-ASA's mechanism of action is directed at the causal agent responsible for the inflammation in UC. This is in contrast to other currently available therapeutic agents used to treat UC, which have a more general immunosuppressive action in the colon. 5-ASA's mechanism of action is that of a topically-acting extracellular tetra-valent reducing agent capable of donating up to 4 electrons per molecule for the reduction (neutralization) of H_2O_2 and other oxygen radials[238,239]. Since 5-ASA is able to induce and maintain histologic remission in active UC, this indicates that 5-ASA can neutralize extracellular neutrophil-derived H_2O_2 in the inflammatory field leading to induction of remission while the sustained topical epithelial presence of 5-ASA maintains remission by neutralizing H_2O_2 diffusing from colonocytes.

Neutralization of colonocyte-derived H_2O_2 by 5-ASA prevents the establishment of an H_2O_2 mediated neutrophilic chemotactic gradient, which attracts neutrophils into the colonic epithelium leading to relapse. This is supported by the observation that 5-ASA's histologic remission rate of nearly 45% is the highest of any currently available therapeutic approved to treat UC suggesting 5-ASA's ability to neutralize colonic H_2O_2 is interrupting a fundamental underlying biological process (*i.e.*, neutrophilic chemotaxis) in the molecular chain of events leading to UC[240].

Butyrate, a short-chain fatty acid normally produced by the colonic microbiome as a colonocyte fuel source, is the second component. Butyrate reduces the anapleurotic metabolism of glutamine, which increases colonocyte GSH. This augments the colonocyte's capacity to neutralize intracellular H_2O_2 (Figure 4). Studies have shown significantly increased colonic epithelial GSH after topical butyrate administration, and high fiber diets that generate increased fecal butyrate are reported to maintain prolonged remission in patients with UC[104,241].

The third component, cromolyn sodium, is a mast cell stabilizer that inhibits the secretion of histamine by mast cells, which accumulate in large amounts at sites of tissue injury in UC[242-244]. Mast cells are significantly activated in UC and undergo intense degranulation resulting in the secretion of significantly greater amounts of histamine that is concentrated at sites of colonic inflammation in UC [245-248]. Rectal biopsies of patients with UC contained significantly higher amounts of histamine

compared to normal controls[249,250]. Histamine is degraded by diamine oxidase (EC 1.4.3.22) whose activity is especially high in the intestinal mucosa and the inflammatory field with H_2O_2 being the product of this reaction[245,251,252]. Thus, cromolyn prevents histamine from being secreted from mucosal mast cells, which precludes its conversion to H_2O_2 that can significantly contribute to the intensity and persistence of colonic inflammation in UC. This is consistent with studies reporting that histamine drives the severity of inflammation in a murine model of experimental UC[253].

Budesonide is the fourth component and is a topically acting corticosteroid that inhibits neutrophil infiltration into the colon by down-regulating neutrophil and endothelial surface adhesion molecules, which prevents neutrophil attachment to the endothelium and subsequent directed migration into the colonic epithelium[254]. Neutrophils produce a large amount of H_2O_2 *via* surface NADPH oxidase[255]. Corticosteroids reduce the expression of neutrophil surface NADPH oxidase thus decreasing neutrophil production of H_2O_2[254]. The combination of inhibited neutrophilic epithelial migration and decreased production of H_2O_2 significantly reduces this large source of H_2O_2, which is a significant driving factor of mucosal inflammation in UC.

RATIONALE FOR RDLA

Targeting H_2O_2 with RDLA

RDLA, the oral component of the therapy, is the biologically active (dextrorotatory) reduced enantiomer of alpha-lipoic acid (the oxidized form)[256]. Alpha-lipoic acid is synthesized in mitochondria and plays an essential role as a co-factor for several multi-enzymatic complexes involved in mitochondrial energy metabolism[257]. Alpha-lipoic acid is enzymatically reduced to RDLA (the reduced form) *via* dihydrolipoamide dehydrogenase (E.C. 1.8.1.4) in mitochondria. Thus, alpha-lipoic acid acts as an oxidizing agent that may worsen colonocyte redox homeostasis and should not be administered to patients with UC (Figure 5).

Aside from its enzymatic role in energy metabolism, RDLA is a powerful biological reducing (antioxidant) agent that can be administered orally[263]. RDLA's dithiol group can donate electrons to reduce (reactivate) oxidized forms of other cellular antioxidants such as vitamin-C, vitamin-E, and GSH [264]. RDLA is both a water and lipid-soluble (amphipathic) molecule so it is delivered *via* the bloodstream to all cells of the body where it diffuses through cell membranes to deliver needed reducing equivalents for the reduction of H_2O_2 and synthesis of GSH[265]. Studies in mice demonstrate that the recycling of GSH is critical for cell survival when exposed to oxidative stress (*i.e.*, H_2O_2)[266]. Other studies show that GSH protects rat intestinal epithelial cells from H_2O_2-induced injury[267]. RDLA's capacity to directly react with H_2O_2 combined with its ability to significantly increase cellular GSH, the principal cellular H_2O_2 reducing agent, underlie RDLA's ability to combat the high levels of colonocyte H_2O_2 in UC.

RDLA significantly increases nuclear factor E2-related factor 2, a master antioxidant transcription factor that mediates the expression of antioxidant genes, including those for GSH synthesis[268]. This significantly increases the cellular capacity to synthesize GSH and neutralize H_2O_2. RDLA is reported to reduce nuclear transcription factor-kappa B and adhesion molecule expression[268], which downregulates the inflammatory response and decreases neutrophilic infiltration into the colonic epithelium contributing to the resolution of inflammation and colitis. Thus, RDLA prevents colonocyte cell death during periods of oxidative stress (H_2O_2 exposure) and promotes *de novo* synthesis and recycling of GSH in order to keep cellular GSH high and H_2O_2 low. Hence, RDLA's mechanism of action indicates that it can significantly contribute to inducing and achieving remission in UC.

Studies have shown that restoration of depleted mitochondrial GSH can reverse oxidant (*i.e.*, H_2O_2) induced mtDNA damage, which leads to mitochondrial heteroplasmy[46]. Since RDLA is highly effective at increasing cellular GSH, this suggests that RDLA will be also effective at reversing H_2O_2 induced mtDNA oxidative damage and subsequent mitochondrial heteroplasmy that is postulated to contribute to life-long relapse. This is supported by the continuous 14-year biopsy-proven histologic remission in a patient with a 39-year history of severe refractory UC after treatment with a regimen containing RDLA[205].

RDLA is generally considered safe and is approved for the treatment of diabetic peripheral neuropathy in Europe[269]. Oral lipoic acid at doses as high as 1800 mg/d for 6 mo and 1200 mg/d for 2 years did not result in serious adverse effects when used to treat diabetic peripheral neuropathy[270,271]. Studies indicate that 40% of RDLA is quickly absorbed systemically after oral dosing and rapidly distributed to tissues[263]. RDLA undergoes renal excretion and intracellular beta-oxidation[268,272], which provides a second pathway to increase cellular GSH by decreasing the anapleurotic metabolism of glutamate (Figure 4).

RDLA is the only amphipathic orally administered therapeutic that is both an intracellular and extracellular anti-oxidant (H_2O_2 neutralizing) and reducing agent (electron-donating for maintenance of redox homeostasis). Given these highly unique and desirable therapeutic properties, which are essential for long-term remission in UC, RDLA should be made widely available and be included on the WHO's list of essential medications. STS, an intravenous reducing agent, is already on the WHO's list of

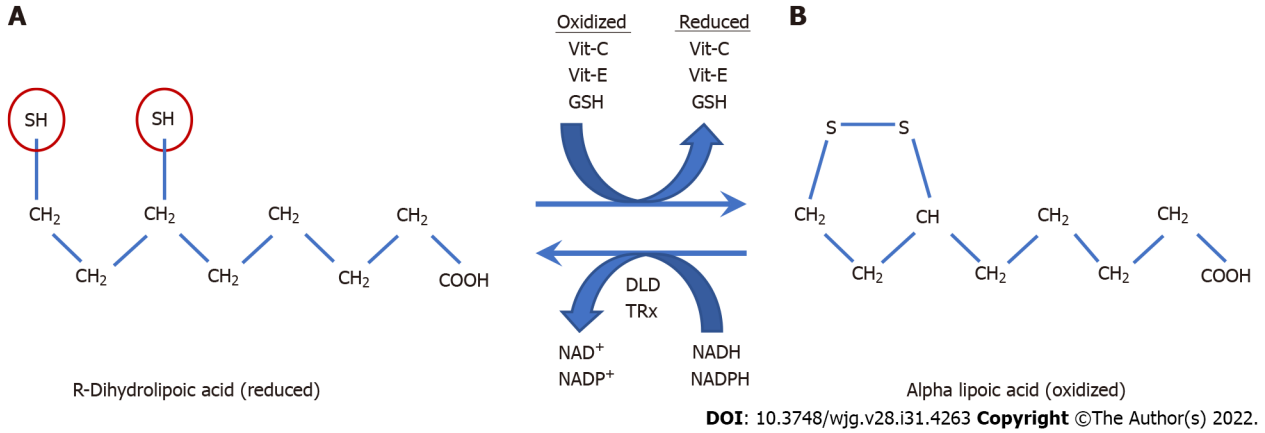

DOI: 10.3748/wjg.v28.i31.4263

Figure 5 R-dihydrolipoic acid. A: R-dihydrolipoic acid (RDLA) is the reduced form of alpha lipoic acid (the oxidized form); B: The reducing equivalents of RDLA are provided by its two thiol groups (red circles) that are each capable of donating one electron. RDLA has a redox potential of -290 millivolts which is only exceeded by NADH and NADPH with a redox potential of -320 and -400 millivolts respectively[258]. Due to its very low (more negative) redox potential, RDLA can directly or indirectly reduce all other cellular antioxidants and many types of oxygen radicals[256]. These include vitamin-C, vitamin-E, glutathione, thioredoxin, glutaredoxin, catalase, glutathione peroxidase, and peroxiredoxin[258-261]. Alpha-lipoic acid is reduced by dehydrolipoamide dehydrogenase and Thioredoxin reductase, which use NADH and NADPH as reducing co-factors respectively[262]. The amphipathic nature of RDLA (lipid and water-soluble) allows it to diffuse throughout cellular compartments to transport reducing equivalents where needed and assist in neutralizing excess hydrogen peroxide. The elimination of excess intracellular cellular hydrogen peroxide is essential in order to restore cellular redox homeostasis and prevent ulcerative colitis relapse caused by extracellular diffusion of colonocyte hydrogen peroxide. Vit: Vitamin; DLD: Dehydrolipoamide dehydrogenase; TRx: Thioredoxin reductase; GSH: Glutathione.

essential medications and thus RDLA, a therapeutically active oral reducing agent should also be included. In addition to UC, emerging evidence suggests that RDLA (and STS) may have a preventive and/or therapeutic role in other diseases in which the evidence indicates a causal role for H_2O_2 such as systemic lupus erythematosus, sepsis, and diabetes[273-275].

In summary, an evidence-based analysis of the pathogenesis and therapy of UC indicates that treatment of inflammation is no longer the main objective of this illness. Instead, the primary goal is the restoration of colonic and systemic redox homeostasis by therapeutic normalization of colonic H_2O_2, which removes the molecular chemotactic signal that initiates and maintains colonic inflammation and is responsible for disease relapse.

DISCUSSION

The existence of an unpredictable, unexplainable, and incurable disease such as UC indicates that we are guided by the wrong theory of pathogenesis in our quest to develop effective treatment and find causes and cures. Currently, there are two, mutually exclusive, mechanisms of disease that have been put forward to explain how UC develops and guide therapeutic development. Both mechanisms attempt to answer the same question; why do white blood cells (neutrophils) suddenly leave the surrounding blood vessels and head straight into the epithelial lining of the large intestine causing inflammation, bleeding, and UC?

The first hypothesis is consensus-based, agreed upon among researchers in the field, and posits an immune abnormality as a primary event in the development of UC while the second mechanism is evidence-based and maintains that the immune system is completely normal but only appears to be "attacking" the colon due to the inappropriate secretion of a neutrophilic chemoattractant, H_2O_2, by the colonic epithelium, which draws neutrophils into the epithelial lining. Despite decades of intensive research, no evidence of any antecedent immune abnormality has ever been identified in individuals with UC or their immediate relatives, and studies of basic immune functionality in UC patients are normal[10,11]. Due to the absence of a biologically plausible mechanism, the term "immune dysregulation" has been coined to explain the presence of neutrophils in the colonic epithelium. In contrast, studies have demonstrated significantly increased H_2O_2 production in non-inflamed colonic epithelium prior to the appearance of mucosal inflammation, satisfying the absolute chronological requirement that the cause (H_2O_2) must precede the effect (inflammation). Since H_2O_2 is cell membrane permeable, once it leaves the colonocyte H_2O_2 can establish a chemotactic gradient "trail" that neutrophils can follow right into the colonic epithelium after exiting the subjacent vasculature. Hence, within this framework and in line with previous data, the immune system in UC is normal. Neutrophils are just doing what they are biologically programmed to do when exposed to H_2O_2; a normal chemotactic immune signaling agent being inappropriately secreted by the colonic epithelium.

On a clinical level, immune dysregulation cannot explain any of the basic characteristics that define UC such as why people develop this disease to begin with, what is the genetic predisposition, why it always starts in the rectum, what causes proximal inflammatory progression, why the loss of intestinal hemostasis leading to bloody diarrhea, what is the mechanism behind relapse, what causes colonic epithelial crypt abscesses, why are smoking cessation, low fiber and high-fat diets risk factors for UC, what dietary and lifestyle changes will help prevent relapse, what therapeutic intervention will provide long-lasting remission and how can we effectuate a cure, to name a few. In other words, immune dysregulation, as a mechanism of disease, has no explanatory power, which is essential for understanding a disease process. In comparison, a redox mechanism of disease based on colonocyte buildup of H_2O_2 explains these basic observations and provides a consistent and clear mechanistic foundation to understand the hereto-forth puzzling observations that characterize UC.

Despite the absence of any hard evidence for an immune abnormality, this hypothesis continues to be the main focus of ongoing investigation by "leading researchers" in the field who have issued consensus statements asserting that a "dysregulated immune response" is the "widely accepted" cause of UC[276, 277]. A consequence of leading researcher support for immune dysregulation is the near-total focus of therapeutic development on proprietary and costly drugs that alter the immune response in a limited number of commercially viable but non-curative ways[6]. As a result, induction trials for new drug development have reached an unsurpassable therapeutic ceiling of 20%-30% indicating that treatment aimed solely at modifying the immune response cannot alter the natural history of the disease, which is essential for achieving universal long-lasting remission in patients with UC[278]. In other words, immune dysregulation as a mechanism of disease has no predictive power to identify a discreet causal agent, which can be targeted for effective treatment and curative potential.

In contrast, the evidence-based identification of H_2O_2 as a causal agent in UC has guided the development of highly effective treatment with at least one documented, biopsy-proven, histologic remission lasting 14 years to date without any episodes of intervening relapse, in a patient with a 39-year history of refractory UC[205]. This is the basis of bench-to-bedside translational medicine that integrates basic science discoveries into predictable effective treatments and potential cures. A causal therapeutic target eliminates much of the "trial and error" that defines the history of current UC therapeutic development[279].

Nevertheless, what leading researchers think is highly relevant for patients with UC. A consensus mechanism of disease put forth and agreed upon among researchers means that clinicians do not have an evidence-based pathogenesis to guide clinical decision-making. This forces clinicians to rely on a variety of clinical variables including the severity of disease, colonic inflammatory distribution, age of onset, previous medication, disease duration, disease course, relapse frequency, and extra-intestinal manifestations to make bedside patient care determinations[7]. Since each one of these variables can be different for every patient, the number of treatment guidelines must be numerous enough to encompass all these different patient combinations. These treatment guidelines, in turn, are not founded on evidence that defines the pathogenesis but instead rely on an ever-growing and changing database of empirical studies incorporating one or more of these myriad clinical variables. The interpretation of these clinical studies is consensus-driven by committee and thus inherently subjective, leading to numerous clinical recommendations for UC that range in number from 32 to 124 treatment guidelines depending on the country of origin[2].

Committee members may also disagree about the relevance of any particular study for the treatment of UC leading to differences in the number of treatment guidelines between medical societies in the same country with the American Gastroenterological Association espousing 24 treatment recommendations while the American College of Gastroenterology supports 49 clinical treatment guidelines for the treatment of this highly debilitating inflammatory bowel disease[280-282]. Moreover, due to the "inconsistencies regarding recommendations" between the two societies, a "Guide to Guidelines in UC" was published in an effort to reconcile the differences among leading clinicians in the field[283]. In contrast, an evidence-based H_2O_2 mechanism of disease only has one guideline for the treatment of UC that does not change, which is to normalize colonic H_2O_2.

The current degree of therapeutic uncertainty when treating patients with UC is the inevitable result of not having an evidence-based mechanism of disease as the foundation for clinical decision-making and therapeutic development. In other words, since there is no evidence for an antecedent immune vulnerability in UC, treatment with the sole aim of suppressing the immune response is not anchored in an evidence-based pathogenesis. The end result is subjective and malleable clinical guidelines with shifting therapeutic targets generating different empirical treatments, the majority of which are based on low or very low-quality evidence while being permeated by high degrees of conflict of interest[2]. Patients ultimately bear the brunt of these fluid upstream decisions because treatments based on low-quality evidence cannot alter the natural history of disease leading to a high degree of medical treatment failure and a 30% colectomy rate[5]. The high degree of medical treatment failure, in turn, fuels endless fund-raising to pay for research in order to find a more effective therapy. And research, unfortunately, continues to be guided by the same consensus immune dysregulation hypothesis ultimately degenerating into a perpetual sisyphean iterative endeavor.

Perhaps the most relevant outcome when applying the predictive power of an H_2O_2 evidence-based mechanism of disease to UC is the expectation of indefinite remission and normal colon functionality once excess colonic H_2O_2 is neutralized. Given a causal role for H_2O_2 in UC, the elimination of excess colonic H_2O_2 would abrogate the molecular signal for directed neutrophil migration into the colonic epithelium leading to long-term histologic (and biochemical) remission. Accordingly, colonic inflammation is not the principal focus of treatment, instead, the primary therapeutic goal is to remove the H_2O_2 mediated chemotactic signal attracting neutrophils into the colonic epithelium.

This represents a functional cure as long as intracellular colonocyte H_2O_2 remains normal and unable to diffuse into the extracellular microenvironment. Treatment limited to reducing inflammation does not address H_2O_2 emanating from colonocytes, and thus cannot cure. The continued build-up of colonocyte H_2O_2 while being treated with these drugs can increase mitochondrial heteroplasmy with worsening disease and/or lead to colon cancer due to the genotoxic effects of H_2O_2[50,51].

From a redox medicine perspective, inflammation (neutrophil infiltration) is just one source of H_2O_2 that must be addressed. Other sources contributing H_2O_2 to the colonic inflammatory field in UC such as mast cells (histamine), EC (serotonin), and microbiome oxidative dysbiosis must also be considered for optimal therapeutic intervention to induce remission. Environmental oxidative stressors and mitochondrial heteroplasmy, which channel H_2O_2 *via* the colonocyte into the colonic epithelium have a crucial role in provoking relapse and must be addressed in order to achieve long-lasting remission.

Additionally, the common metabolic origin of cellular H_2O_2 suggests that H_2O_2-mediated intestinal inflammation is not solely confined to the colon. A recent analysis concluded that a shared mechanism underlies UC and UC-associated ileitis, which develops in up to 35% of patients with UC[284]. This is supported by studies in UC patients showing impaired ileal butyrate oxidation in both terminal ileum and colon, which in the latter was associated with H_2O_2 induced inhibition of mitochondrial thiolase, the last enzyme in the butyrate beta-oxidation cascade[30,285]. This suggests that excess H_2O_2 is responsible for impaired ileal butyrate oxidation in the small intestine as well. Moreover, the neutrophilic epithelial infiltration, cryptitis, and crypt abscesses that characterize UC-associated ileitis is analogous to the typical histopathological changes observed in UC[286]. This strongly implies that H_2O_2 is also elevated in the small intestine leading to mucosal inflammation and metabolic derangements. Thus, treatments that simply target colonic inflammation do not address the consequences of elevated ileal H_2O_2, which may lead to small bowel inflammation and interfere with the absorption of nutrients. In contrast, treatment with a systemic reducing agent such as RDLA has the potential of resolving UC-associated ileitis.

The interdisciplinary nature of evidence-based analysis can provide clues to understanding and effectively treating other serious conditions that are linked to UC whose medical therapy has so far been suboptimal. Studies have shown that H_2O_2 can effectively inhibit neuromuscular transmission[216]. Protection against H_2O_2-induced inhibition of neuromuscular transmission was associated with the cellular ability to eliminate H_2O_2[287]. Other studies have demonstrated that H_2O_2 contributes to motor disfunction in human UC[218]. This suggests a potential causal role for H_2O_2 in the motility dysfunction that is thought to underlie toxic mega colon and small bowel bacterial overgrowth, both of which are associated with symptomatic UC[214,288]. It also implies that therapeutic intervention with reducing agents (STS or RDLA) to reduce colonic H_2O_2 may be an effective therapeutic option in treating or preventing these serious conditions.

At the other end of the clinical spectrum, up to 2% of asymptomatic individuals undergoing screening colonoscopy were shown to have typical histologic inflammatory features of UC with two-thirds developing symptomatic disease (rectal bleeding) within 5 years[289,290]. Despite having a high probability of developing symptomatic UC and the possibility of increased risk of colon cancer, clinicians are in a quandary regarding the appropriate treatment for these asymptomatic individuals since all medications used to treat UC can have serious side effects and there are no data regarding their effectiveness at this very early asymptomatic stage[291-293]. However, the presence of preclinical neutrophilic inflammation implies that H_2O_2 has begun "leaking" out of colonocytes and is attracting neutrophils into the colonic epithelium. The use of an oral reducing agent (RDLA) to normalize colonocyte H_2O_2 and restore redox homeostasis would be a logical choice at this stage due to its recognized safety profile and ability to enhance cellular reductive capacity in order to reduce colonic H_2O_2. If future studies show that this is an effective treatment, it will be possible to prevent symptomatic disease from developing while UC is still in a preclinical asymptomatic stage.

All things considered, with current therapy and under the best of circumstances, UC patients must undergo life-long surveillance colonoscopy for colon cancer, which cannot detect all neoplastic lesions leading to a high mortality rate[29,294,295]. And although total colectomy has been touted as a cure for the approximately 30% of UC patients who fail medical therapy or develop colon cancer, studies have shown that patients who have undergone ileal pouch/anal anastomosis have higher disability scores than patients with active UC[296]. In contrast, maintenance therapy with an oral reducing agent has the potential of eliminating the need for colectomy, lifelong colonoscopies, and, by removing excess colonic H_2O_2, may significantly reduce the incidence of UC-associated colorectal cancer.

An evidence-based theory of UC identifying H_2O_2 as a causal therapeutic target not only has the potential of highly effective and inexpensive treatment that may be curative but opens the door to population-wide primary prevention by increasing total reducing equivalents (antioxidants) in our food

supply. This is supported by studies demonstrating a decreased risk of developing UC with diets high in anti-oxidants (reducing agents)[297]. Dietary intervention can be successful in reducing the incidence of UC because, in contrast to established disease with high levels of colonic H_2O_2 that require treatment with powerful reducing agents, intervention before colonocytes develop HCRH (while intracellular H_2O_2 is still low) requires much less reductive capacity, which can be supplied by increasing the amount of reducing equivalents (antioxidants) in the food supply. This public health level intervention may prevent UC from developing in the entire population before it even starts.

CONCLUSION

The evidence supports a causal role for colonocyte H_2O_2 in the pathogenesis and pathophysiology of UC. Treatment to reduce and maintain normal colonic H_2O_2 levels leads to long-term histologic remission (complete mucosal healing) in patients with refractory disease. The treatment is inexpensive and well tolerated. Lifestyle modifications to reduce oxidative stress exposure will help maintain remission. This is the first time that a causal evidence-based therapeutic target with curative potential has been identified for UC. The inclusion of multiple components to address the different sources of H_2O_2 within the colitic inflammatory field contributes to its singular effectiveness but also slows its acceptance by a healthcare system dominated by single molecular therapeutics.

H_2O_2 is a normal by-product of cellular metabolism that can accumulate within colonic epithelial cells. H_2O_2's unique properties of cell membrane permeability, long life, potent oxidizing potential, and the ability to attract white blood cells combine to promote colonocyte extracellular diffusion followed by oxidative disintegration of colonic epithelial tight junctional proteins while simultaneously attracting white blood cells into the colonic epithelium, both of which lead to colonic inflammation and eventual UC. This makes it appear as if the immune system is "attacking" the colon when in reality the immune response is behaving as it is normally programmed to respond. The abnormality is the inappropriate secretion of H_2O_2 by the colonic epithelium and not the immune response.

The pleiotropic effects of H_2O_2 have misdirected the careers of multiple generations of researchers into searching for a non-existent primary immune abnormality as the cause of UC. Extensive research since the mid-20th century has failed to uncover a primary immune vulnerability to explicate this illness. Cumulative evidence does not support any form of immune dysregulation in the pathogenesis of UC. This line of research is not evidence-based and should be abandoned. The continued search for immune dysregulation as the cause of UC leads to enormous research waste and endless fundraising that will never find the cause or cure for this disease while at the same time encouraging the treatment of UC with expensive immune altering agents that drive up healthcare costs, do not cure and are associated with lower quality of life, higher rates of colon cancer and other serious adverse effects. Continued research to uncover a primary immune abnormality as the cause of UC reinforces a false sense of hope for millions of individuals suffering from this illness who are desperately waiting for a cure that will never materialize with this line of research. Only by following the evidence can we cure disease.

Evidence-based medical research will eventually displace consensus-driven hypothesis in the highly competitive race for research funding as the National Institute of General Medical Sciences begins to shift funding priorities to grant applications that can clearly explicate falsifiable disease mechanisms that are "associated with the pathogenesis and resolution" of disease[298]. This pathogenesis initiative has begun with sepsis in July 2019 and is likely to be expanded as a requirement to obtain scarce research funding for other diseases as well. Under these guidelines, the current consensus-based immune dysregulation hypothesis invoked to explain UC does not meet this threshold for Federal research funding since it neither provides a coherent falsifiable pathogenesis nor a means of disease resolution.

A causal role for colonic H_2O_2 in the pathogenesis of UC is biologically plausible and supported by both experimental and clinical evidence. H_2O_2 satisfies all the basic requirements for an etiological agent leading to the development of UC and is worthy of continued and expanded research to confirm a potential causal role in the pathogenesis of this debilitating inflammatory bowel disease affecting millions worldwide. It is incumbent upon the research community to follow up on this highly promising line of research that raises the real possibility of targeted and highly effective treatment with curative potential.

Future directions

Complex diseases such as UC arise as an emergent systems property of its individual, *in vivo*, interacting constituent elements. The physical proximity of the colonic epithelium, innate immune system, and colonic lumenal contents gives rise to the disease phenotype we call UC in response to colonocyte extracellular diffusion of H_2O_2. Complex chronic diseases such as UC are not amenable to a reductionist analytical laboratory approach that examines each contributing element outside of its disease-producing *in vivo* context[299]. The prevalence of "incurable" complex chronic diseases continues to rise because they have slipped through the cracks of our current reductionist methodology of medical research that is not designed to detect emergent systems diseases such as UC. The shortcoming of laboratory research

to deal with chronic complex diseases can be overcome with graduate programs dedicated to theoretical (systems) medicine, which looks at the big picture to help guide laboratory researchers down a focused experimental pathway to discovering causes and cures of disease[300]. With chronic disease mortality accounting for 60% of all global deaths as well as 70% of all deaths in the United States, and 60% of Americans suffering from at least one chronic disease with 40% afflicted with two or more chronic ailments, chronic disease has become the leading driver of the United States' $3.5 trillion in annual health care cost[301-303]. We simply cannot win the war against encroaching chronic disease by experimentation alone. This underscores the critical need for collaboration between systems medicine (theoretical systems pathogenesis) and laboratory-based experimentalists (reductionist medical research) before the financial, emotional, and familial burden becomes too much to bear and society begins to destabilize under the weight of too many sick people.

FOOTNOTES

Author contributions: Pravda J is the sole author of this manuscript and solely responsible for its content; Pravda J performed all the research, collected, analyzed, and interpreted all the data; Pravda J conceived of and developed the hydrogen peroxide-based pathogenesis of ulcerative colitis; Pravda J prepared and wrote the manuscript and performed all critical revisions; Pravda J certifies that this manuscript is the product of his original research; and Pravda J has overall responsibility for this manuscript.

Conflict-of-interest statement: The author reported no relevant conflicts of interest for this article.

Country/Territory of origin: United States

ORCID number: Jay Pravda 0000-0001-5737-5506.

S-Editor: Wang JJ
L-Editor: A
P-Editor: Wang JJ

REFERENCES

1 **Fumery M**, Singh S, Dulai PS, Gower-Rousseau C, Peyrin-Biroulet L, Sandborn WJ. Natural History of Adult Ulcerative Colitis in Population-based Cohorts: A Systematic Review. *Clin Gastroenterol Hepatol* 2018; **16**: 343-356.e3 [PMID: 28625817 DOI: 10.1016/j.cgh.2017.06.016]
2 **Goldowsky A**, Sen R, Hoffman G, Feuerstein JD. Is there a standardized practice for the development of international ulcerative colitis and Crohn's disease treatment guidelines? *Gastroenterol Rep (Oxf)* 2021; **9**: 408-417 [PMID: 34733526 DOI: 10.1093/gastro/goab009]
3 **Rubin DT**, Hart A, Panaccione R, Armuzzi A, Suvanto U, Deuring JJ, Woolcott J, Cappelleri JC, Steinberg K, Wingate L, Schreiber S. Ulcerative Colitis Narrative Global Survey Findings: Communication Gaps and Agreements Between Patients and Physicians. *Inflamm Bowel Dis* 2021; **27**: 1096-1106 [PMID: 33057598 DOI: 10.1093/ibd/izaa257]
4 **Peyrin-Biroulet L**, Van Assche G, Sturm A, Gisbert JP, Gaya DR, Bokemeyer B, Mantzaris GJ, Armuzzi A, Sebastian S, Lara N, Lynam M, Rojas-Farreras S, Fan T, Ding Q, Black CM, Kachroo S. Treatment satisfaction, preferences and perception gaps between patients and physicians in the ulcerative colitis CARES study: A real world-based study. *Dig Liver Dis* 2016; **48**: 601-607 [PMID: 27012447 DOI: 10.1016/j.dld.2016.01.013]
5 **Wong DJ**, Roth EM, Feuerstein JD, Poylin VY. Surgery in the age of biologics. *Gastroenterol Rep (Oxf)* 2019; **7**: 77-90 [PMID: 30976420 DOI: 10.1093/gastro/goz004]
6 **Hirten RP**, Sands BE. New Therapeutics for Ulcerative Colitis. *Annu Rev Med* 2021; **72**: 199-213 [PMID: 33502898 DOI: 10.1146/annurev-med-052919-120048]
7 **Gajendran M**, Loganathan P, Jimenez G, Catinella AP, Ng N, Umapathy C, Ziade N, Hashash JG. A comprehensive review and update on ulcerative colitis. *Dis Mon* 2019; **65**: 100851 [PMID: 30837080 DOI: 10.1016/j.disamonth.2019.02.004]
8 **Kayal M**, Shah S. Ulcerative Colitis: Current and Emerging Treatment Strategies. *J Clin Med* 2019; **9** [PMID: 31905945 DOI: 10.3390/jcm9010094]
9 **Kirsner JB**. Historical origins of current IBD concepts. *World J Gastroenterol* 2001; **7**: 175-184 [PMID: 11819757 DOI: 10.3748/wjg.v7.i2.175]
10 **Jewell DP**, Truelove SC. Reaginic hypersensitivity in ulcerative colitis. *Gut* 1972; **13**: 903-906 [PMID: 4646293 DOI: 10.1136/gut.13.11.903]
11 **Triantafillidis JK**, Economidou J, Manousos ON, Efthymiou P. Cutaneous delayed hypersensitivity in Crohn's disease

and ulcerative colitis. Application of multi-test. *Dis Colon Rectum* 1987; **30**: 536-539 [PMID: 3595375 DOI: 10.1007/BF02554785]
12 **Porter RJ**, Kalla R, Ho GT. Ulcerative colitis: Recent advances in the understanding of disease pathogenesis. *F1000Res* 2020; **9** [PMID: 32399194 DOI: 10.12688/f1000research.20805.1]
13 **Petri B**, Sanz MJ. Neutrophil chemotaxis. *Cell Tissue Res* 2018; **371**: 425-436 [PMID: 29350282 DOI: 10.1007/s00441-017-2776-8]
14 **Kővári B**, Báthori Á, Friedman MS, Lauwers GY. Histologic Diagnosis of Inflammatory Bowel Diseases. *Adv Anat Pathol* 2022; **29**: 48-61 [PMID: 34879038 DOI: 10.1097/PAP.0000000000000325]
15 **Weiss SJ**. Neutrophil-mediated methemoglobin formation in the erythrocyte. The role of superoxide and hydrogen peroxide. *J Biol Chem* 1982; **257**: 2947-2953 [PMID: 6277918 DOI: 10.1016/S0021-9258(19)81056-6]
16 **Klyubin IV**, Kirpichnikova KM, Gamaley IA. Hydrogen peroxide-induced chemotaxis of mouse peritoneal neutrophils. *Eur J Cell Biol* 1996; **70**: 347-351 [PMID: 8864663]
17 **Morad H**, Luqman S, Tan CH, Swann V, McNaughton PA. TRPM2 ion channels steer neutrophils towards a source of hydrogen peroxide. *Sci Rep* 2021; **11**: 9339 [PMID: 33927223 DOI: 10.1038/s41598-021-88224-5]
18 **Gangwar R**, Meena AS, Shukla PK, Nagaraja AS, Dorniak PL, Pallikuth S, Waters CM, Sood A, Rao R. Calcium-mediated oxidative stress: a common mechanism in tight junction disruption by different types of cellular stress. *Biochem J* 2017; **474**: 731-749 [PMID: 28057718 DOI: 10.1042/BCJ20160679]
19 **Rao RK**, Baker RD, Baker SS, Gupta A, Holycross M. Oxidant-induced disruption of intestinal epithelial barrier function: role of protein tyrosine phosphorylation. *Am J Physiol* 1997; **273**: G812-G823 [PMID: 9357822 DOI: 10.1152/ajpgi.1997.273.4.G812]
20 **Parrish AR**, Catania JM, Orozco J, Gandolfi AJ. Chemically induced oxidative stress disrupts the E-cadherin/catenin cell adhesion complex. *Toxicol Sci* 1999; **51**: 80-86 [PMID: 10496679 DOI: 10.1093/toxsci/51.1.80]
21 **Grisham MB**, Gaginella TS, von Ritter C, Tamai H, Be RM, Granger DN. Effects of neutrophil-derived oxidants on intestinal permeability, electrolyte transport, and epithelial cell viability. *Inflammation* 1990; **14**: 531-542 [PMID: 2174408 DOI: 10.1007/BF00914274]
22 **Katinios G**, Casado-Bedmar M, Walter SA, Vicario M, González-Castro AM, Bednarska O, Söderholm JD, Hjortswang H, Keita ÅV. Increased Colonic Epithelial Permeability and Mucosal Eosinophilia in Ulcerative Colitis in Remission Compared With Irritable Bowel Syndrome and Health. *Inflamm Bowel Dis* 2020; **26**: 974-984 [PMID: 31944236 DOI: 10.1093/ibd/izz328]
23 **Bienert GP**, Chaumont F. Aquaporin-facilitated transmembrane diffusion of hydrogen peroxide. *Biochim Biophys Acta* 2014; **1840**: 1596-1604 [PMID: 24060746 DOI: 10.1016/j.bbagen.2013.09.017]
24 **Rao RK**, Li L, Baker RD, Baker SS, Gupta A. Glutathione oxidation and PTPase inhibition by hydrogen peroxide in Caco-2 cell monolayer. *Am J Physiol Gastrointest Liver Physiol* 2000; **279**: G332-G340 [PMID: 10915642 DOI: 10.1152/ajpgi.2000.279.2.G332]
25 **Hu JE**, Weiß F, Bojarski C, Branchi F, Schulzke JD, Fromm M, Krug SM. Expression of tricellular tight junction proteins and the paracellular macromolecule barrier are recovered in remission of ulcerative colitis. *BMC Gastroenterol* 2021; **21**: 141 [PMID: 33789594 DOI: 10.1186/s12876-021-01723-7]
26 **Naito Y**, Takagi T, Yoshikawa T. Molecular fingerprints of neutrophil-dependent oxidative stress in inflammatory bowel disease. *J Gastroenterol* 2007; **42**: 787-798 [PMID: 17940831 DOI: 10.1007/s00535-007-2096-y]
27 **Sheehan JF**, Brynjolfsson G. Ulcerative colitis following hydrogen peroxide enema: case report and experimental production with transient emphysema of colonic wall and gas embolism. *Lab Invest* 1960; **9**: 150-168 [PMID: 14445720]
28 **Meyer CT**, Brand M, DeLuca VA, Spiro HM. Hydrogen peroxide colitis: a report of three patients. *J Clin Gastroenterol* 1981; **3**: 31-35 [PMID: 7276490 DOI: 10.1097/00004836-198103000-00008]
29 **Hopkins RZ**. Hydrogen peroxide in biology and medicine: an overview. *React Oxyg Species* 2017; **3**: 26-37
30 **Santhanam S**, Venkatraman A, Ramakrishna BS. Impairment of mitochondrial acetoacetyl CoA thiolase activity in the colonic mucosa of patients with ulcerative colitis. *Gut* 2007; **56**: 1543-1549 [PMID: 17483192 DOI: 10.1136/gut.2006.108449]
31 **Hoensch H**, Peters WH, Roelofs HM, Kirch W. Expression of the glutathione enzyme system of human colon mucosa by localisation, gender and age. *Curr Med Res Opin* 2006; **22**: 1075-1083 [PMID: 16846540 DOI: 10.1185/030079906X112480]
32 **Esworthy RS**, Aranda R, Martín MG, Doroshow JH, Binder SW, Chu FF. Mice with combined disruption of Gpx1 and Gpx2 genes have colitis. *Am J Physiol Gastrointest Liver Physiol* 2001; **281**: G848-G855 [PMID: 11518697 DOI: 10.1152/ajpgi.2001.281.3.G848]
33 **Harrison GJ**, Jordan LR, Willis RJ. Deleterious effects of hydrogen peroxide on the function and ultrastructure of cardiac muscle and the coronary vasculature of perfused rat hearts. *Can J Cardiol* 1994; **10**: 843-849 [PMID: 7954020]
34 **Wittenburg AL**, Phillips SA, Gutterman DD. The role of catalase and endothelium in hydrogen peroxide induced vasodilatation of human adipose arterioles. *FASEB J* 2007; **21**
35 **Weiss SJ**, Young J, LoBuglio AF, Slivka A, Nimeh NF. Role of hydrogen peroxide in neutrophil-mediated destruction of cultured endothelial cells. *J Clin Invest* 1981; **68**: 714-721 [PMID: 6268662 DOI: 10.1172/JCI110307]
36 **Yakes FM**, Van Houten B. Mitochondrial DNA damage is more extensive and persists longer than nuclear DNA damage in human cells following oxidative stress. *Proc Natl Acad Sci U S A* 1997; **94**: 514-519 [PMID: 9012815 DOI: 10.1073/pnas.94.2.514]
37 **Wu Z**, Sainz AG, Shadel GS. Mitochondrial DNA: cellular genotoxic stress sentinel. *Trends Biochem Sci* 2021; **46**: 812-821 [PMID: 34088564 DOI: 10.1016/j.tibs.2021.05.004]
38 **Hahn A**, Zuryn S. Mitochondrial Genome (mtDNA) Mutations that Generate Reactive Oxygen Species. *Antioxidants (Basel)* 2019; **8** [PMID: 31514455 DOI: 10.3390/antiox8090392]
39 **Dlasková A**, Hlavatá L, Jezek P. Oxidative stress caused by blocking of mitochondrial complex I H(+) pumping as a link in aging/disease vicious cycle. *Int J Biochem Cell Biol* 2008; **40**: 1792-1805 [PMID: 18291703 DOI: 10.1016/j.biocel.2008.01.012]

40 **Den Hond E**, Hiele M, Evenepoel P, Peeters M, Ghoos Y, Rutgeerts P. In vivo butyrate metabolism and colonic permeability in extensive ulcerative colitis. *Gastroenterology* 1998; **115**: 584-590 [PMID: 9721155 DOI: 10.1016/S0016-5085(98)70137-4]

41 **Chapman MA**, Grahn MF, Boyle MA, Hutton M, Rogers J, Williams NS. Butyrate oxidation is impaired in the colonic mucosa of sufferers of quiescent ulcerative colitis. *Gut* 1994; **35**: 73-76 [PMID: 8307454 DOI: 10.1136/gut.35.1.73]

42 **Vanderborght M**, Nassogne MC, Hermans D, Moniotte S, Seneca S, Van Coster R, Buts JP, Sokal EM. Intractable ulcerative colitis of infancy in a child with mitochondrial respiratory chain disorder. *J Pediatr Gastroenterol Nutr* 2004; **38**: 355-357 [PMID: 15076640 DOI: 10.1097/00005176-200403000-00023]

43 **Dimauro S**, Davidzon G. Mitochondrial DNA and disease. *Ann Med* 2005; **37**: 222-232 [PMID: 16019721 DOI: 10.1080/07853890510007368]

44 **Nishikawa M**, Oshitani N, Matsumoto T, Nishigami T, Arakawa T, Inoue M. Accumulation of mitochondrial DNA mutation with colorectal carcinogenesis in ulcerative colitis. *Br J Cancer* 2005; **93**: 331-337 [PMID: 15956973 DOI: 10.1038/sj.bjc.6602664]

45 **Sifroni KG**, Damiani CR, Stoffel C, Cardoso MR, Ferreira GK, Jeremias IC, Rezin GT, Scaini G, Schuck PF, Dal-Pizzol F, Streck EL. Mitochondrial respiratory chain in the colonic mucosal of patients with ulcerative colitis. *Mol Cell Biochem* 2010; **342**: 111-115 [PMID: 20440543 DOI: 10.1007/s11010-010-0474-x]

46 **Circu ML**, Moyer MP, Harrison L, Aw TY. Contribution of glutathione status to oxidant-induced mitochondrial DNA damage in colonic epithelial cells. *Free Radic Biol Med* 2009; **47**: 1190-1198 [PMID: 19647792 DOI: 10.1016/j.freeradbiomed.2009.07.032]

47 **Martínez-Reyes I**, Cuezva JM. The H(+)-ATP synthase: a gate to ROS-mediated cell death or cell survival. *Biochim Biophys Acta* 2014; **1837**: 1099-1112 [PMID: 24685430 DOI: 10.1016/j.bbabio.2014.03.010]

48 **Schafer FQ**, Buettner GR. Redox environment of the cell as viewed through the redox state of the glutathione disulfide/glutathione couple. *Free Radic Biol Med* 2001; **30**: 1191-1212 [PMID: 11368918 DOI: 10.1016/s0891-5849(01)00480-4]

49 **Marí M**, de Gregorio E, de Dios C, Roca-Agujetas V, Cucarull B, Tutusaus A, Morales A, Colell A. Mitochondrial Glutathione: Recent Insights and Role in Disease. *Antioxidants (Basel)* 2020; **9** [PMID: 32987701 DOI: 10.3390/antiox9100909]

50 **Han D**, Canali R, Rettori D, Kaplowitz N. Effect of glutathione depletion on sites and topology of superoxide and hydrogen peroxide production in mitochondria. *Mol Pharmacol* 2003; **64**: 1136-1144 [PMID: 14573763 DOI: 10.1124/mol.64.5.1136]

51 **Lu SC**. Regulation of glutathione synthesis. *Mol Aspects Med* 2009; **30**: 42-59 [PMID: 18601945 DOI: 10.1016/j.mam.2008.05.005]

52 **Aon MA**, Stanley BA, Sivakumaran V, Kembro JM, O'Rourke B, Paolocci N, Cortassa S. Glutathione/thioredoxin systems modulate mitochondrial H2O2 emission: an experimental-computational study. *J Gen Physiol* 2012; **139**: 479-491 [PMID: 22585969 DOI: 10.1085/jgp.201210772]

53 **Seril DN**, Liao J, Yang GY, Yang CS. Oxidative stress and ulcerative colitis-associated carcinogenesis: studies in humans and animal models. *Carcinogenesis* 2003; **24**: 353-362 [PMID: 12663492 DOI: 10.1093/carcin/24.3.353]

54 **Qi L**, Wu XC, Zheng DQ. Hydrogen peroxide, a potent inducer of global genomic instability. *Curr Genet* 2019; **65**: 913-917 [PMID: 30963245 DOI: 10.1007/s00294-019-00969-9]

55 **Jones DP**. Radical-free biology of oxidative stress. *Am J Physiol Cell Physiol* 2008; **295**: C849-C868 [PMID: 18684987 DOI: 10.1152/ajpcell.00283.2008]

56 **Forman HJ**, Zhang H, Rinna A. Glutathione: overview of its protective roles, measurement, and biosynthesis. *Mol Aspects Med* 2009; **30**: 1-12 [PMID: 18796312 DOI: 10.1016/j.mam.2008.08.006]

57 **Deponte M**. The Incomplete Glutathione Puzzle: Just Guessing at Numbers and Figures? *Antioxid Redox Signal* 2017; **27**: 1130-1161 [PMID: 28540740 DOI: 10.1089/ars.2017.7123]

58 **Musaogullari A**, Chai YC. Redox Regulation by Protein S-Glutathionylation: From Molecular Mechanisms to Implications in Health and Disease. *Int J Mol Sci* 2020; **21** [PMID: 33143095 DOI: 10.3390/ijms21218113]

59 **Bergemalm D**, Andersson E, Hultdin J, Eriksson C, Rush ST, Kalla R, Adams AT, Keita ÅV, D'Amato M, Gomollon F, Jahnsen J; IBD Character Consortium, Ricanek P, Satsangi J, Repsilber D, Karling P, Halfvarson J. Systemic Inflammation in Preclinical Ulcerative Colitis. *Gastroenterology* 2021; **161**: 1526-1539.e9 [PMID: 34298022 DOI: 10.1053/j.gastro.2021.07.026]

60 **Blázovics A**, Kovács A, Lugasi A, Hagymási K, Bíró L, Fehér J. Antioxidant defense in erythrocytes and plasma of patients with active and quiescent Crohn disease and ulcerative colitis: a chemiluminescent study. *Clin Chem* 1999; **45**: 895-896 [PMID: 10351999 DOI: 10.1093/clinchem/45.6.895]

61 **Rana SV**, Sharma S, Prasad KK, Sinha SK, Singh K. Role of oxidative stress & antioxidant defence in ulcerative colitis patients from north India. *Indian J Med Res* 2014; **139**: 568-571 [PMID: 24927343]

62 **Neselioglu S**, Keske PB, Senat AA, Yurekli OT, Erdogan S, Alisik M, Ergin MS, Koseoglu H, Ersoy O, Erel O. The relationship between severity of ulcerative colitis and thiol-disulphide homeostasis. *Bratisl Lek Listy* 2018; **119**: 498-502 [PMID: 30160158 DOI: 10.4149/BLL_2018_091]

63 **Gaikwad R**, Thangaraj PR, Sen AK. Direct and rapid measurement of hydrogen peroxide in human blood using a microfluidic device. *Sci Rep* 2021; **11**: 2960 [PMID: 33536535 DOI: 10.1038/s41598-021-82623-4]

64 **Roche M**, Rondeau P, Singh NR, Tarnus E, Bourdon E. The antioxidant properties of serum albumin. *FEBS Lett* 2008; **582**: 1783-1787 [PMID: 18474236 DOI: 10.1016/j.febslet.2008.04.057]

65 **Cha MK**, Kim IH. Glutathione-linked thiol peroxidase activity of human serum albumin: a possible antioxidant role of serum albumin in blood plasma. *Biochem Biophys Res Commun* 1996; **222**: 619-625 [PMID: 8670254 DOI: 10.1006/bbrc.1996.0793]

66 **Turell L**, Botti H, Carballal S, Radi R, Alvarez B. Sulfenic acid--a key intermediate in albumin thiol oxidation. *J Chromatogr B Analyt Technol Biomed Life Sci* 2009; **877**: 3384-3392 [PMID: 19386559 DOI: 10.1016/j.jchromb.2009.03.035]

67 **Tozzi-Ciancarelli MG**, Di Massimo C, D'Orazio MC, Mascioli A, Di Giulio A, Tozzi E. Effect of exogenous hydrogen peroxide on human erythrocytes. *Cell Mol Biol* 1990; **36**: 57-64 [PMID: 2337915]

68 **Turell L**, Radi R, Alvarez B. The thiol pool in human plasma: the central contribution of albumin to redox processes. *Free Radic Biol Med* 2013; **65**: 244-253 [PMID: 23747983 DOI: 10.1016/j.freeradbiomed.2013.05.050]

69 **Yang X**, Mao Z, Huang Y, Yan H, Yan Q, Hong J, Fan J, Yao J. Reductively modified albumin attenuates DSS-Induced mouse colitis through rebalancing systemic redox state. *Redox Biol* 2021; **41**: 101881 [PMID: 33601276 DOI: 10.1016/j.redox.2021.101881]

70 **Koutroubakis IE**, Ramos-Rivers C, Regueiro M, Koutroumpakis E, Click B, Schoen RE, Hashash JG, Schwartz M, Swoger J, Baidoo L, Barrie A, Dunn MA, Binion DG. Persistent or Recurrent Anemia Is Associated With Severe and Disabling Inflammatory Bowel Disease. *Clin Gastroenterol Hepatol* 2015; **13**: 1760-1766 [PMID: 25862987 DOI: 10.1016/j.cgh.2015.03.029]

71 **Khan N**, Patel D, Shah Y, Trivedi C, Yang YX. Albumin as a prognostic marker for ulcerative colitis. *World J Gastroenterol* 2017; **23**: 8008-8016 [PMID: 29259376 DOI: 10.3748/wjg.v23.i45.8008]

72 **Tanaka M**, Takagi T, Naito Y, Uchiyama K, Hotta Y, Toyokawa Y, Kashiwagi S, Kamada K, Ishikawa T, Yasuda H, Konishi H, Itoh Y. Low serum albumin at admission is a predictor of early colectomy in patients with moderate to severe ulcerative colitis. *JGH Open* 2021; **5**: 377-381 [PMID: 33732885 DOI: 10.1002/jgh3.12506]

73 **Yagi S**, Furukawa S, Shiraishi K, Hashimoto Y, Tange K, Mori K, Ninomiya T, Suzuki S, Shibata N, Murakami H, Ohashi K, Hasebe A, Tomida H, Yamamoto Y, Takeshita E, Ikeda Y, Hiasa Y. Effect of disease duration on the association between serum albumin and mucosal healing in patients with ulcerative colitis. *BMJ Open Gastroenterol* 2021; **8** [PMID: 34099464 DOI: 10.1136/bmjgast-2021-000662]

74 **Suzuki S**, Hashizume N, Kanzaki Y, Maruyama T, Kozuka A, Yahikozawa K. Prognostic significance of serum albumin in patients with stable coronary artery disease treated by percutaneous coronary intervention. *PLoS One* 2019; **14**: e0219044 [PMID: 31269058 DOI: 10.1371/journal.pone.0219044]

75 **Shang W**, Hu H, Shen M, Wu J, Yu Z, Xuan L. Investigating the correlation between serum albumin level and the prognosis of Bell's palsy. *Medicine (Baltimore)* 2021; **100**: e26726 [PMID: 34398047 DOI: 10.1097/MD.0000000000026726]

76 **Tabata F**, Wada Y, Kawakami S, Miyaji K. Serum Albumin Redox States: More Than Oxidative Stress Biomarker. *Antioxidants (Basel)* 2021; **10** [PMID: 33804859 DOI: 10.3390/antiox10040503]

77 **Magzal F**, Sela S, Szuchman-Sapir A, Tamir S, Michelis R, Kristal B. In-vivo oxidized albumin- a pro-inflammatory agent in hypoalbuminemia. *PLoS One* 2017; **12**: e0177799 [PMID: 28542419 DOI: 10.1371/journal.pone.0177799]

78 **Rodríguez-Lago I**, Zabana Y, Barreiro-de Acosta M. Diagnosis and natural history of preclinical and early inflammatory bowel disease. *Ann Gastroenterol* 2020; **33**: 443-452 [PMID: 32879589 DOI: 10.20524/aog.2020.0508]

79 BRENDA Enzyme Database. [cited 24 December 2021]. Available from: https://www.brenda-enzymes.org/advanced.php

80 **Keshteli AH**, Madsen KL, Dieleman LA. Diet in the Pathogenesis and Management of Ulcerative Colitis; A Review of Randomized Controlled Dietary Interventions. *Nutrients* 2019; **11** [PMID: 31262022 DOI: 10.3390/nu11071498]

81 **Casanova MJ**, Chaparro M, Molina B, Merino O, Batanero R, Dueñas-Sadornil C, Robledo P, Garcia-Albert AM, Gómez-Sánchez MB, Calvet X, Trallero MDR, Montoro M, Vázquez I, Charro M, Barragán A, Martínez-Cerezo F, Megias-Rangil I, Huguet JM, Marti-Bonmati E, Calvo M, Campderá M, Muñoz-Vicente M, Merchante A, Ávila AD, Serrano-Aguayo P, De Francisco R, Hervías D, Bujanda L, Rodriguez GE, Castro-Laria L, Barreiro-de Acosta M, Van Domselaar M, Ramirez de la Piscina P, Santos-Fernández J, Algaba A, Torra S, Pozzati L, López-Serrano P, Arribas MDR, Rincón ML, Peláez AC, Castro E, García-Herola A, Santander C, Hernández-Alonso M, Martín-Noguerol E, Gómez-Lozano M, Monedero T, Villoria A, Figuerola A, Castaño-García A, Banales JM, Díaz-Hernández L, Argüelles-Arias F, López-Díaz J, Pérez-Martínez I, García-Talavera N, Nuevo-Siguairo OK, Riestra S, Gisbert JP. Prevalence of Malnutrition and Nutritional Characteristics of Patients With Inflammatory Bowel Disease. *J Crohns Colitis* 2017; **11**: 1430-1439 [PMID: 28981652 DOI: 10.1093/ecco-jcc/jjx102]

82 **Hou JK**, Abraham B, El-Serag H. Dietary intake and risk of developing inflammatory bowel disease: a systematic review of the literature. *Am J Gastroenterol* 2011; **106**: 563-573 [PMID: 21468064 DOI: 10.1038/ajg.2011.44]

83 **Fritsch J**, Garces L, Quintero MA, Pignac-Kobinger J, Santander AM, Fernández I, Ban YJ, Kwon D, Phillips MC, Knight K, Mao Q, Santaolalla R, Chen XS, Maruthamuthu M, Solis N, Damas OM, Kerman DH, Deshpande AR, Lewis JE, Chen C, Abreu MT. Low-Fat, High-Fiber Diet Reduces Markers of Inflammation and Dysbiosis and Improves Quality of Life in Patients With Ulcerative Colitis. *Clin Gastroenterol Hepatol* 2021; **19**: 1189-1199.e30 [PMID: 32445952 DOI: 10.1016/j.cgh.2020.05.026]

84 **Barnes EL**, Nestor M, Onyewadume L, de Silva PS, Korzenik JR; DREAM Investigators. High Dietary Intake of Specific Fatty Acids Increases Risk of Flares in Patients With Ulcerative Colitis in Remission During Treatment With Aminosalicylates. *Clin Gastroenterol Hepatol* 2017; **15**: 1390-1396.e1 [PMID: 28110099 DOI: 10.1016/j.cgh.2016.12.036]

85 **Gu P**, Feagins LA. Dining With Inflammatory Bowel Disease: A Review of the Literature on Diet in the Pathogenesis and Management of IBD. *Inflamm Bowel Dis* 2020; **26**: 181-191 [PMID: 31670372 DOI: 10.1093/ibd/izz268]

86 **Waterham HR**, Ferdinandusse S, Wanders RJ. Human disorders of peroxisome metabolism and biogenesis. *Biochim Biophys Acta* 2016; **1863**: 922-933 [PMID: 26611709 DOI: 10.1016/j.bbamcr.2015.11.015]

87 **Poirier Y**, Antonenkov VD, Glumoff T, Hiltunen JK. Peroxisomal beta-oxidation--a metabolic pathway with multiple functions. *Biochim Biophys Acta* 2006; **1763**: 1413-1426 [PMID: 17028011 DOI: 10.1016/j.bbamcr.2006.08.034]

88 **Jo DS**, Park NY, Cho DH. Peroxisome quality control and dysregulated lipid metabolism in neurodegenerative diseases. *Exp Mol Med* 2020; **52**: 1486-1495 [PMID: 32917959 DOI: 10.1038/s12276-020-00503-9]

89 **Nordgren M**, Fransen M. Peroxisomal metabolism and oxidative stress. *Biochimie* 2014; **98**: 56-62 [PMID: 23933092 DOI: 10.1016/j.biochi.2013.07.026]

90 **Tominaga K**, Kamimura K, Takahashi K, Yokoyama J, Yamagiwa S, Terai S. Diversion colitis and pouchitis: A mini-review. *World J Gastroenterol* 2018; **24**: 1734-1747 [PMID: 29713128 DOI: 10.3748/wjg.v24.i16.1734]

91 **Leonel AJ**, Alvarez-Leite JI. Butyrate: implications for intestinal function. *Curr Opin Clin Nutr Metab Care* 2012; **15**:

474-479 [PMID: 22797568 DOI: 10.1097/MCO.0b013e32835665fa]
92 **Houten SM**, Wanders RJ. A general introduction to the biochemistry of mitochondrial fatty acid β-oxidation. *J Inherit Metab Dis* 2010; **33**: 469-477 [PMID: 20195903 DOI: 10.1007/s10545-010-9061-2]
93 **De Preter V**, Arijs I, Windey K, Vanhove W, Vermeire S, Schuit F, Rutgeerts P, Verbeke K. Impaired butyrate oxidation in ulcerative colitis is due to decreased butyrate uptake and a defect in the oxidation pathway. *Inflamm Bowel Dis* 2012; **18**: 1127-1136 [PMID: 21987487 DOI: 10.1002/ibd.21894]
94 **McNabney SM**, Henagan TM. Short Chain Fatty Acids in the Colon and Peripheral Tissues: A Focus on Butyrate, Colon Cancer, Obesity and Insulin Resistance. *Nutrients* 2017; **9** [PMID: 29231905 DOI: 10.3390/nu9121348]
95 **Yang C**, Ko B, Hensley CT, Jiang L, Wasti AT, Kim J, Sudderth J, Calvaruso MA, Lumata L, Mitsche M, Rutter J, Merritt ME, DeBerardinis RJ. Glutamine oxidation maintains the TCA cycle and cell survival during impaired mitochondrial pyruvate transport. *Mol Cell* 2014; **56**: 414-424 [PMID: 25458842 DOI: 10.1016/j.molcel.2014.09.025]
96 **Cherbuy C**, Darcy-Vrillon B, Morel MT, Pégorier JP, Duée PH. Effect of germfree state on the capacities of isolated rat colonocytes to metabolize n-butyrate, glucose, and glutamine. *Gastroenterology* 1995; **109**: 1890-1899 [PMID: 7498654 DOI: 10.1016/0016-5085(95)90756-4]
97 **Donohoe DR**, Garge N, Zhang X, Sun W, O'Connell TM, Bunger MK, Bultman SJ. The microbiome and butyrate regulate energy metabolism and autophagy in the mammalian colon. *Cell Metab* 2011; **13**: 517-526 [PMID: 21531334 DOI: 10.1016/j.cmet.2011.02.018]
98 **Kim MH**, Kim H. The Roles of Glutamine in the Intestine and Its Implication in Intestinal Diseases. *Int J Mol Sci* 2017; **18** [PMID: 28498331 DOI: 10.3390/ijms18051051]
99 **Tompkins SC**, Sheldon RD, Rauckhorst AJ, Noterman MF, Solst SR, Buchanan JL, Mapuskar KA, Pewa AD, Gray LR, Oonthonpan L, Sharma A, Scerbo DA, Dupuy AJ, Spitz DR, Taylor EB. Disrupting Mitochondrial Pyruvate Uptake Directs Glutamine into the TCA Cycle away from Glutathione Synthesis and Impairs Hepatocellular Tumorigenesis. *Cell Rep* 2019; **28**: 2608-2619.e6 [PMID: 31484072 DOI: 10.1016/j.celrep.2019.07.098]
100 **Lane A**, Dalkie N, Henderson L, Irwin J, Rostami K. An elemental diet is effective in the management of diversion colitis. *Gastroenterol Hepatol Bed Bench* 2021; **14**: 81-84 [PMID: 33868614]
101 **Pravda J**. Diversion Colitis: A Bioenergetic Model of Pathogenesis. *Japanese J Gastroenterol Hepatol* 2019; **2**: 1-11
102 **Chiba M**, Tsuda S, Komatsu M, Tozawa H, Takayama Y. Onset of Ulcerative Colitis during a Low-Carbohydrate Weight-Loss Diet and Treatment with a Plant-Based Diet: A Case Report. *Perm J* 2016; **20**: 80-84 [PMID: 26824967 DOI: 10.7812/TPP/15-038]
103 **Duncan SH**, Belenguer A, Holtrop G, Johnstone AM, Flint HJ, Lobley GE. Reduced dietary intake of carbohydrates by obese subjects results in decreased concentrations of butyrate and butyrate-producing bacteria in feces. *Appl Environ Microbiol* 2007; **73**: 1073-1078 [PMID: 17189447 DOI: 10.1128/AEM.02340-06]
104 **Hamer HM**, Jonkers DM, Bast A, Vanhoutvin SA, Fischer MA, Kodde A, Troost FJ, Venema K, Brummer RJ. Butyrate modulates oxidative stress in the colonic mucosa of healthy humans. *Clin Nutr* 2009; **28**: 88-93 [PMID: 19108937 DOI: 10.1016/j.clnu.2008.11.002]
105 **Scheppach W**, Sommer H, Kirchner T, Paganelli GM, Bartram P, Christl S, Richter F, Dusel G, Kasper H. Effect of butyrate enemas on the colonic mucosa in distal ulcerative colitis. *Gastroenterology* 1992; **103**: 51-56 [PMID: 1612357 DOI: 10.1016/0016-5085(92)91094-k]
106 **Rosignoli P**, Fabiani R, De Bartolomeo A, Spinozzi F, Agea E, Pelli MA, Morozzi G. Protective activity of butyrate on hydrogen peroxide-induced DNA damage in isolated human colonocytes and HT29 tumour cells. *Carcinogenesis* 2001; **22**: 1675-1680 [PMID: 11577008 DOI: 10.1093/carcin/22.10.1675]
107 **Blachier F**, Boutry C, Bos C, Tomé D. Metabolism and functions of L-glutamate in the epithelial cells of the small and large intestines. *Am J Clin Nutr* 2009; **90**: 814S-821S [PMID: 19571215 DOI: 10.3945/ajcn.2009.27462S]
108 **Roediger WE**, Nance S. Metabolic induction of experimental ulcerative colitis by inhibition of fatty acid oxidation. *Br J Exp Pathol* 1986; **67**: 773-782 [PMID: 3099821]
109 **Nelson RA**. Intestinal transport, coenzyme A, and colitis in pantothenic acid deficiency. *Am J Clin Nutr* 1968; **21**: 495-501 [PMID: 5649470 DOI: 10.1093/ajcn/21.5.495]
110 **Martinez JE**, Kahana DD, Ghuman S, Wilson HP, Wilson J, Kim SCJ, Lagishetty V, Jacobs JP, Sinha-Hikim AP, Friedman TC. Unhealthy Lifestyle and Gut Dysbiosis: A Better Understanding of the Effects of Poor Diet and Nicotine on the Intestinal Microbiome. *Front Endocrinol (Lausanne)* 2021; **12**: 667066 [PMID: 34168615 DOI: 10.3389/fendo.2021.667066]
111 **Losso JN**. Food Processing, Dysbiosis, Gastrointestinal Inflammatory Diseases, and Antiangiogenic Functional Foods or Beverages. *Annu Rev Food Sci Technol* 2021; **12**: 235-258 [PMID: 33467906 DOI: 10.1146/annurev-food-062520-090235]
112 **Kamm MA**. Processed food affects the gut microbiota: The revolution has started. *J Gastroenterol Hepatol* 2020; **35**: 6-7 [PMID: 31965661 DOI: 10.1111/jgh.14976]
113 **Defois C**, Ratel J, Garrait G, Denis S, Le Goff O, Talvas J, Mosoni P, Engel E, Peyret P. Food Chemicals Disrupt Human Gut Microbiota Activity And Impact Intestinal Homeostasis As Revealed By In Vitro Systems. *Sci Rep* 2018; **8**: 11006 [PMID: 30030472 DOI: 10.1038/s41598-018-29376-9]
114 **Gálvez-Ontiveros Y**, Páez S, Monteagudo C, Rivas A. Endocrine Disruptors in Food: Impact on Gut Microbiota and Metabolic Diseases. *Nutrients* 2020; **12** [PMID: 32326280 DOI: 10.3390/nu12041158]
115 **Bajinka O**, Tan Y, Abdelhalim KA, Özdemir G, Qiu X. Extrinsic factors influencing gut microbes, the immediate consequences and restoring eubiosis. *AMB Express* 2020; **10**: 130 [PMID: 32710186 DOI: 10.1186/s13568-020-01066-8]
116 **Vich Vila A**, Collij V, Sanna S, Sinha T, Imhann F, Bourgonje AR, Mujagic Z, Jonkers DMAE, Masclee AAM, Fu J, Kurilshikov A, Wijmenga C, Zhernakova A, Weersma RK. Impact of commonly used drugs on the composition and metabolic function of the gut microbiota. *Nat Commun* 2020; **11**: 362 [PMID: 31953381 DOI: 10.1038/s41467-019-14177-z]
117 **Karl JP**, Hatch AM, Arcidiacono SM, Pearce SC, Pantoja-Feliciano IG, Doherty LA, Soares JW. Effects of Psychological, Environmental and Physical Stressors on the Gut Microbiota. *Front Microbiol* 2018; **9**: 2013 [PMID:

30258412 DOI: 10.3389/fmicb.2018.02013]
118 **Bolte LA**, Vich Vila A, Imhann F, Collij V, Gacesa R, Peters V, Wijmenga C, Kurilshikov A, Campmans-Kuijpers MJE, Fu J, Dijkstra G, Zhernakova A, Weersma RK. Long-term dietary patterns are associated with pro-inflammatory and anti-inflammatory features of the gut microbiome. *Gut* 2021; **70**: 1287-1298 [PMID: 33811041 DOI: 10.1136/gutjnl-2020-322670]
119 **Laudisi F**, Stolfi C, Monteleone G. Impact of Food Additives on Gut Homeostasis. *Nutrients* 2019; **11** [PMID: 31581570 DOI: 10.3390/nu11102334]
120 **Strus M**, Gosiewski T, Fyderek K, Wedrychowicz A, Kowalska-Duplaga K, Kochan P, Adamski P, Heczko PB. A role of hydrogen peroxide producing commensal bacteria present in colon of adolescents with inflammatory bowel disease in perpetuation of the inflammatory process. *J Physiol Pharmacol* 2009; **60** Suppl 6: 49-54 [PMID: 20224151]
121 **Benninghoff AD**, Hintze KJ, Monsanto SP, Rodriguez DM, Hunter AH, Phatak S, Pestka JJ, Wettere AJV, Ward RE. Consumption of the Total Western Diet Promotes Colitis and Inflammation-Associated Colorectal Cancer in Mice. *Nutrients* 2020; **12** [PMID: 32093192 DOI: 10.3390/nu12020544]
122 **Rizzello F**, Spisni E, Giovanardi E, Imbesi V, Salice M, Alvisi P, Valerii MC, Gionchetti P. Implications of the Westernized Diet in the Onset and Progression of IBD. *Nutrients* 2019; **11** [PMID: 31072001 DOI: 10.3390/nu11051033]
123 **White BA**, Ramos GP, Kane S. The Impact of Alcohol in Inflammatory Bowel Diseases. *Inflamm Bowel Dis* 2022; **28**: 466-473 [PMID: 33988227 DOI: 10.1093/ibd/izab089]
124 **Cederbaum AI**. Alcohol metabolism. *Clin Liver Dis* 2012; **16**: 667-685 [PMID: 23101976 DOI: 10.1016/j.cld.2012.08.002]
125 **Forsyth CB**, Voigt RM, Keshavarzian A. Intestinal CYP2E1: A mediator of alcohol-induced gut leakiness. *Redox Biol* 2014; **3**: 40-46 [PMID: 25462064 DOI: 10.1016/j.redox.2014.10.002]
126 **Abdelmegeed MA**, Ha SK, Choi Y, Akbar M, Song BJ. Role of CYP2E1 in Mitochondrial Dysfunction and Hepatic Injury by Alcohol and Non-Alcoholic Substances. *Curr Mol Pharmacol* 2017; **10**: 207-225 [PMID: 26278393 DOI: 10.2174/1874467208666150817111114]
127 **García-Suástegui WA**, Ramos-Chávez LA, Rubio-Osornio M, Calvillo-Velasco M, Atzin-Méndez JA, Guevara J, Silva-Adaya D. The Role of CYP2E1 in the Drug Metabolism or Bioactivation in the Brain. *Oxid Med Cell Longev* 2017; **2017**: 4680732 [PMID: 28163821 DOI: 10.1155/2017/4680732]
128 **Nguyen LH**, Örtqvist AK, Cao Y, Simon TG, Roelstraete B, Song M, Joshi AD, Staller K, Chan AT, Khalili H, Olén O, Ludvigsson JF. Antibiotic use and the development of inflammatory bowel disease: a national case-control study in Sweden. *Lancet Gastroenterol Hepatol* 2020; **5**: 986-995 [PMID: 32818437 DOI: 10.1016/S2468-1253(20)30267-3]
129 **Ramirez J**, Guarner F, Bustos Fernandez L, Maruy A, Sdepanian VL, Cohen H. Antibiotics as Major Disruptors of Gut Microbiota. *Front Cell Infect Microbiol* 2020; **10**: 572912 [PMID: 33330122 DOI: 10.3389/fcimb.2020.572912]
130 **Korpela K**, Salonen A, Virta LJ, Kekkonen RA, Forslund K, Bork P, de Vos WM. Intestinal microbiome is related to lifetime antibiotic use in Finnish pre-school children. *Nat Commun* 2016; **7**: 10410 [PMID: 26811868 DOI: 10.1038/ncomms10410]
131 **Lee JY**, Cevallos SA, Byndloss MX, Tiffany CR, Olsan EE, Butler BP, Young BM, Rogers AWL, Nguyen H, Kim K, Choi SW, Bae E, Lee JH, Min UG, Lee DC, Bäumler AJ. High-Fat Diet and Antibiotics Cooperatively Impair Mitochondrial Bioenergetics to Trigger Dysbiosis that Exacerbates Pre-inflammatory Bowel Disease. *Cell Host Microbe* 2020; **28**: 273-284.e6 [PMID: 32668218 DOI: 10.1016/j.chom.2020.06.001]
132 **Dwyer DJ**, Belenky PA, Yang JH, MacDonald IC, Martell JD, Takahashi N, Chan CT, Lobritz MA, Braff D, Schwarz EG, Ye JD, Pati M, Vercruysse M, Ralifo PS, Allison KR, Khalil AS, Ting AY, Walker GC, Collins JJ. Antibiotics induce redox-related physiological alterations as part of their lethality. *Proc Natl Acad Sci U S A* 2014; **111**: E2100-E2109 [PMID: 24803433 DOI: 10.1073/pnas.1401876111]
133 **Kalghatgi S**, Spina CS, Costello JC, Liesa M, Morones-Ramirez JR, Slomovic S, Molina A, Shirihai OS, Collins JJ. Bactericidal antibiotics induce mitochondrial dysfunction and oxidative damage in Mammalian cells. *Sci Transl Med* 2013; **5**: 192ra85 [PMID: 23825301 DOI: 10.1126/scitranslmed.3006055]
134 **Guillouzo A**, Guguen-Guillouzo C. Antibiotics-induced oxidative stress. *Cure Opin Tox* 2020; **20-21**: 23-28 [DOI: 10.1016/j.cotox.2020.03.004]
135 **Singh R**, Sripada L, Singh R. Side effects of antibiotics during bacterial infection: mitochondria, the main target in host cell. *Mitochondrion* 2014; **16**: 50-54 [PMID: 24246912 DOI: 10.1016/j.mito.2013.10.005]
136 **Theis MK**, Boyko EJ. Patient perceptions of causes of inflammatory bowel disease. *Am J Gastroenterol* 1994; **89**: 1920 [PMID: 7942711]
137 **Crohn BB**. The clinical use of succinyl sulfathiazole (Sulfasuxidine). *Gastroenterology* 1943; **1**: 140-146
138 **Salem SN**, Shubair KS. Non-specific ulcerative colitis in Bedouin Arabs. *Lancet* 1967; **1**: 473-475 [PMID: 4164069 DOI: 10.1016/s0140-6736(67)91094-x]
139 **Araki M**, Shinzaki S, Yamada T, Arimitsu S, Komori M, Shibukawa N, Mukai A, Nakajima S, Kinoshita K, Kitamura S, Murayama Y, Ogawa H, Yasunaga Y, Oshita M, Fukui H, Masuda E, Tsujii M, Kawai S, Hiyama S, Inoue T, Tanimukai H, Iijima H, Takehara T. Psychologic stress and disease activity in patients with inflammatory bowel disease: A multicenter cross-sectional study. *PLoS One* 2020; **15**: e0233365 [PMID: 32453762 DOI: 10.1371/journal.pone.0233365]
140 **Levenstein S**, Prantera C, Varvo V, Scribano ML, Andreoli A, Luzi C, Arcà M, Berto E, Milite G, Marcheggiano A. Stress and exacerbation in ulcerative colitis: a prospective study of patients enrolled in remission. *Am J Gastroenterol* 2000; **95**: 1213-1220 [PMID: 10811330 DOI: 10.1111/j.1572-0241.2000.02012.x]
141 **Maunder RG**, Levenstein S. The role of stress in the development and clinical course of inflammatory bowel disease: epidemiological evidence. *Curr Mol Med* 2008; **8**: 247-252 [PMID: 18537632 DOI: 10.2174/156652408784533832]
142 **Mawdsley JE**, Macey MG, Feakins RM, Langmead L, Rampton DS. The effect of acute psychologic stress on systemic and rectal mucosal measures of inflammation in ulcerative colitis. *Gastroenterology* 2006; **131**: 410-419 [PMID: 16890594 DOI: 10.1053/j.gastro.2006.05.017]
143 **Almy TP**, Tulin M. Alterations in colonic function in man under stress; experimental production of changes simulating the irritable colon. *Gastroenterology* 1947; **8**: 616-626 [PMID: 20238757]

144 **Beattie DT**, Smith JA. Serotonin pharmacology in the gastrointestinal tract: a review. *Naunyn Schmiedebergs Arch Pharmacol* 2008; **377**: 181-203 [PMID: 18398601 DOI: 10.1007/s00210-008-0276-9]

145 **Gershon MD**. 5-Hydroxytryptamine (serotonin) in the gastrointestinal tract. *Curr Opin Endocrinol Diabetes Obes* 2013; **20**: 14-21 [PMID: 23222853 DOI: 10.1097/MED.0b013e32835bc703]

146 **Nozawa K**, Kawabata-Shoda E, Doihara H, Kojima R, Okada H, Mochizuki S, Sano Y, Inamura K, Matsushime H, Koizumi T, Yokoyama T, Ito H. TRPA1 regulates gastrointestinal motility through serotonin release from enterochromaffin cells. *Proc Natl Acad Sci U S A* 2009; **106**: 3408-3413 [PMID: 19211797 DOI: 10.1073/pnas.0805323106]

147 **BRENDA**. Information on EC 1.4.3.4 - monoamine oxidase. [cited 24 December 2021]. Available from: https://www.brenda-enzymes.org/enzyme.php?ecno=1.4.3.4

148 **Rao SS**, Hatfield RA, Suls JM, Chamberlain MJ. Psychological and physical stress induce differential effects on human colonic motility. *Am J Gastroenterol* 1998; **93**: 985-990 [PMID: 9647034 DOI: 10.1111/j.1572-0241.1998.00293.x]

149 **Ghia JE**, Li N, Wang H, Collins M, Deng Y, El-Sharkawy RT, Côté F, Mallet J, Khan WI. Serotonin has a key role in pathogenesis of experimental colitis. *Gastroenterology* 2009; **137**: 1649-1660 [PMID: 19706294 DOI: 10.1053/j.gastro.2009.08.041]

150 **McMullan C**, Pinkney TD, Jones LL, Magill L, Nepogodiev D, Pathmakanthan S, Cooney R, Mathers JM. Adapting to ulcerative colitis to try to live a 'normal' life: a qualitative study of patients' experiences in the Midlands region of England. *BMJ Open* 2017; **7**: e017544 [PMID: 28827271 DOI: 10.1136/bmjopen-2017-017544]

151 **Kobayashi T**, Siegmund B, Le Berre C, Wei SC, Ferrante M, Shen B, Bernstein CN, Danese S, Peyrin-Biroulet L, Hibi T. Ulcerative colitis. *Nat Rev Dis Primers* 2020; **6**: 74 [PMID: 32913180 DOI: 10.1038/s41572-020-0205-x]

152 **Jedel S**, Hoffman A, Merriman P, Swanson B, Voigt R, Rajan KB, Shaikh M, Li H, Keshavarzian A. A randomized controlled trial of mindfulness-based stress reduction to prevent flare-up in patients with inactive ulcerative colitis. *Digestion* 2014; **89**: 142-155 [PMID: 24557009 DOI: 10.1159/000356316]

153 **Boye B**, Lundin KE, Jantschek G, Leganger S, Mokleby K, Tangen T, Jantschek I, Pripp AH, Wojniusz S, Dahlstroem A, Rivenes AC, Benninghoven D, Hausken T, Roseth A, Kunzendorf S, Wilhelmsen I, Sharpe M, Blomhoff S, Malt UF, Jahnsen J. INSPIRE study: does stress management improve the course of inflammatory bowel disease and disease-specific quality of life in distressed patients with ulcerative colitis or Crohn's disease? *Inflamm Bowel Dis* 2011; **17**: 1863-1873 [PMID: 21287660 DOI: 10.1002/ibd.21575]

154 **Harries AD**, Baird A, Rhodes J. Non-smoking: a feature of ulcerative colitis. *Br Med J (Clin Res Ed)* 1982; **284**: 706 [PMID: 6802296 DOI: 10.1136/bmj.284.6317.706]

155 **Mahid SS**, Minor KS, Soto RE, Hornung CA, Galandiuk S. Smoking and inflammatory bowel disease: a meta-analysis. *Mayo Clin Proc* 2006; **81**: 1462-1471 [PMID: 17120402 DOI: 10.4065/81.11.1462]

156 **Calkins BM**. A meta-analysis of the role of smoking in inflammatory bowel disease. *Dig Dis Sci* 1989; **34**: 1841-1854 [PMID: 2598752 DOI: 10.1007/BF01536701]

157 **Piovani D**, Pansieri C, Kotha SRR, Piazza AC, Comberg CL, Peyrin-Biroulet L, Danese S, Bonovas S. Ethnic Differences in the Smoking-related Risk of Inflammatory Bowel Disease: A Systematic Review and Meta-analysis. *J Crohns Colitis* 2021; **15**: 1658-1678 [PMID: 33721889 DOI: 10.1093/ecco-jcc/jjab047]

158 **Du L**, Ha C. Epidemiology and Pathogenesis of Ulcerative Colitis. *Gastroenterol Clin North Am* 2020; **49**: 643-654 [PMID: 33121686 DOI: 10.1016/j.gtc.2020.07.005]

159 Non-smoking: a feature of ulcerative colitis. *Br Med J (Clin Res Ed)* 1982; **285**: 440 [PMID: 6809118 DOI: 10.1136/bmj.285.6339.440-a]

160 **Calabrese E**, Yanai H, Shuster D, Rubin DT, Hanauer SB. Low-dose smoking resumption in ex-smokers with refractory ulcerative colitis. *J Crohns Colitis* 2012; **6**: 756-762 [PMID: 22398093 DOI: 10.1016/j.crohns.2011.12.010]

161 **Kannichamy V**, Antony I, Mishra V, Banerjee A, Gandhi AB, Kaleem I, Alexander J, Hisbulla M, Khan S. Transdermal Nicotine as a Treatment Option for Ulcerative Colitis: A Review. *Cureus* 2020; **12**: e11096 [PMID: 33240692 DOI: 10.7759/cureus.11096]

162 **Lunney PC**, Leong RW. Review article: Ulcerative colitis, smoking and nicotine therapy. *Aliment Pharmacol Ther* 2012; **36**: 997-1008 [PMID: 23072629 DOI: 10.1111/apt.12086]

163 **Carlens C**, Hergens MP, Grunewald J, Ekbom A, Eklund A, Höglund CO, Askling J. Smoking, use of moist snuff, and risk of chronic inflammatory diseases. *Am J Respir Crit Care Med* 2010; **181**: 1217-1222 [PMID: 20203245 DOI: 10.1164/rccm.200909-1338OC]

164 **Salih A**, Widbom L, Hultdin J, Karling P. Smoking is associated with risk for developing inflammatory bowel disease including late onset ulcerative colitis: a prospective study. *Scand J Gastroenterol* 2018; **53**: 173-178 [PMID: 29262738 DOI: 10.1080/00365521.2017.1418904]

165 **de Castella H**. Non-smoking: a feature of ulcerative colitis. *Br Med J (Clin Res Ed)* 1982; **284**: 1706 [PMID: 6805664 DOI: 10.1136/bmj.284.6330.1706]

166 **Higuchi LM**, Khalili H, Chan AT, Richter JM, Bousvaros A, Fuchs CS. A prospective study of cigarette smoking and the risk of inflammatory bowel disease in women. *Am J Gastroenterol* 2012; **107**: 1399-1406 [PMID: 22777340 DOI: 10.1038/ajg.2012.196]

167 **Hughes JR**. Effects of abstinence from tobacco: valid symptoms and time course. *Nicotine Tob Res* 2007; **9**: 315-327 [PMID: 17365764 DOI: 10.1080/14622200701188919]

168 **Grace WJ**. Life stress and chronic ulcerative colitis. *Ann of NY Acad Sci* 2006; **58**: 389-397 [DOI: 10.1111/j.1749-6632.1954.tb45851.x]

169 **Pryor WA**, Arbour NC, Upham B, Church DF. The inhibitory effect of extracts of cigarette tar on electron transport of mitochondria and submitochondrial particles. *Free Radic Biol Med* 1992; **12**: 365-372 [PMID: 1317324 DOI: 10.1016/0891-5849(92)90085-u]

170 **Murphy MP**. How mitochondria produce reactive oxygen species. *Biochem J* 2009; **417**: 1-13 [PMID: 19061483 DOI: 10.1042/BJ20081386]

171 **Miró O**, Alonso JR, Jarreta D, Casademont J, Urbano-Márquez A, Cardellach F. Smoking disturbs mitochondrial

respiratory chain function and enhances lipid peroxidation on human circulating lymphocytes. *Carcinogenesis* 1999; **20**: 1331-1336 [PMID: 10383908 DOI: 10.1093/carcin/20.7.1331]

172 **Kabel A**, Omar MS, Alotaibi SN, Baali MH. Effect of Indole-3-carbinol and/or Metformin on Female Patients with Ulcerative Colitis (Premalignant Condition): Role of Oxidative Stress, Apoptosis and Proinflammatory Cytokines. *J Cancer Res Treat* 2017; **5**: 1-8 [DOI: 10.12691/jcrt-5-1-1]

173 **Vancura A**, Bu P, Bhagwat M, Zeng J, Vancurova I. Metformin as an Anticancer Agent. *Trends Pharmacol Sci* 2018; **39**: 867-878 [PMID: 30150001 DOI: 10.1016/j.tips.2018.07.006]

174 **LaMoia TE**, Shulman GI. Cellular and Molecular Mechanisms of Metformin Action. *Endocr Rev* 2021; **42**: 77-96 [PMID: 32897388 DOI: 10.1210/endrev/bnaa023]

175 **Mráček T**, Drahota Z, Houštěk J. The function and the role of the mitochondrial glycerol-3-phosphate dehydrogenase in mammalian tissues. *Biochim Biophys Acta* 2013; **1827**: 401-410 [PMID: 23220394 DOI: 10.1016/j.bbabio.2012.11.014]

176 **Singh G**. Mitochondrial FAD-linked Glycerol-3-phosphate Dehydrogenase: A Target for Cancer Therapeutics. *Pharmaceuticals (Basel)* 2014; **7**: 192-206 [PMID: 24521925 DOI: 10.3390/ph7020192]

177 **Shirkhanloo H**, Golbabaei F, Hassani H, Eftekhar F, Kian MJ. Occupational Exposure to Mercury: Air Exposure Assessment and Biological Monitoring based on Dispersive Ionic Liquid-Liquid Microextraction. *Iran J Public Health* 2014; **43**: 793-799 [PMID: 26110150]

178 **Schmoldt A**, Benthe HF, Haberland G. Digitoxin metabolism by rat liver microsomes. *Biochem Pharmacol* 1975; **24**: 1639-1641 [PMID: 10]

179 **Bagger S**, Breddam K, Byberg BR. Binding of mercury(II) to protein thiol groups: a study of proteinase K and carboxypeptidase Y. *J Inorg Biochem* 1991; **42**: 97-103 [PMID: 1856724 DOI: 10.1016/0162-0134(91)80036-h]

180 **Franco JL**, Posser T, Dunkley PR, Dickson PW, Mattos JJ, Martins R, Bainy AC, Marques MR, Dafre AL, Farina M. Methylmercury neurotoxicity is associated with inhibition of the antioxidant enzyme glutathione peroxidase. *Free Radic Biol Med* 2009; **47**: 449-457 [PMID: 19450679 DOI: 10.1016/j.freeradbiomed.2009.05.013]

181 **Bose-O'Reilly S**, McCarty KM, Steckling N, Lettmeier B. Mercury exposure and children's health. *Curr Probl Pediatr Adolesc Health Care* 2010; **40**: 186-215 [PMID: 20816346 DOI: 10.1016/j.cppeds.2010.07.002]

182 **Liang L**, Pan Y, Bin L, Liu Y, Huang W, Li R, Lai KP. Immunotoxicity mechanisms of perfluorinated compounds PFOA and PFOS. *Chemosphere* 2022; **291**: 132892 [PMID: 34780734 DOI: 10.1016/j.chemosphere.2021.132892]

183 **Steenland K**, Zhao L, Winquist A, Parks C. Ulcerative colitis and perfluorooctanoic acid (PFOA) in a highly exposed population of community residents and workers in the mid-Ohio valley. *Environ Health Perspect* 2013; **121**: 900-905 [PMID: 23735465 DOI: 10.1289/ehp.1206449]

184 **Steenland K**, Kugathasan S, Barr DB. PFOA and ulcerative colitis. *Environ Res* 2018; **165**: 317-321 [PMID: 29777922 DOI: 10.1016/j.envres.2018.05.007]

185 **Balaban N**, Gelman F, Taylor AA, Walker SL, Bernstein A, Ronen Z. Degradation of Brominated Organic Compounds (Flame Retardants) by a Four-Strain Consortium Isolated from Contaminated Groundwater. *Applied Sci* 2021; **11**: 6263 [DOI: 10.3390/app11146263]

186 **Antunes F**, Cadenas E. Cellular titration of apoptosis with steady state concentrations of H(2)O(2): submicromolar levels of H(2)O(2) induce apoptosis through Fenton chemistry independent of the cellular thiol state. *Free Radic Biol Med* 2001; **30**: 1008-1018 [PMID: 11316581 DOI: 10.1016/s0891-5849(01)00493-2]

187 **Jin M**, Ande A, Kumar A, Kumar S. Regulation of cytochrome P450 2e1 expression by ethanol: role of oxidative stress-mediated pkc/jnk/sp1 pathway. *Cell Death Dis* 2013; **4**: e554 [PMID: 23519123 DOI: 10.1038/cddis.2013.78]

188 **Wu D**, Cederbaum AI. Oxidative stress mediated toxicity exerted by ethanol-inducible CYP2E1. *Toxicol Appl Pharmacol* 2005; **207**: 70-76 [PMID: 16019049 DOI: 10.1016/j.taap.2005.01.057]

189 **Halliwell B**, Clement MV, Long LH. Hydrogen peroxide in the human body. *FEBS Lett* 2000; **486**: 10-13 [PMID: 11108833 DOI: 10.1016/s0014-5793(00)02197-9]

190 **Fazzini F**, Schöpf B, Blatzer M, Coassin S, Hicks AA, Kronenberg F, Fendt L. Plasmid-normalized quantification of relative mitochondrial DNA copy number. *Sci Rep* 2018; **8**: 15347 [PMID: 30337569 DOI: 10.1038/s41598-018-33684-5]

191 **Swanson GR**, Tieu V, Shaikh M, Forsyth C, Keshavarzian A. Is moderate red wine consumption safe in inactive inflammatory bowel disease? *Digestion* 2011; **84**: 238-244 [PMID: 21876358 DOI: 10.1159/000329403]

192 **Seth A**, Yan F, Polk DB, Rao RK. Probiotics ameliorate the hydrogen peroxide-induced epithelial barrier disruption by a PKC- and MAP kinase-dependent mechanism. *Am J Physiol Gastrointest Liver Physiol* 2008; **294**: G1060-G1069 [PMID: 18292183 DOI: 10.1152/ajpgi.00202.2007]

193 **Chuenkitiyanon S**, Pengsuparp T, Jianmongkol S. Protective effect of quercetin on hydrogen peroxide-induced tight junction disruption. *Int J Toxicol* 2010; **29**: 418-424 [PMID: 20445016 DOI: 10.1177/1091581810366487]

194 **Katsube T**, Tsuji H, Onoda M. Nitric oxide attenuates hydrogen peroxide-induced barrier disruption and protein tyrosine phosphorylation in monolayers of intestinal epithelial cell. *Biochim Biophys Acta* 2007; **1773**: 794-803 [PMID: 17451824 DOI: 10.1016/j.bbamcr.2007.03.002]

195 **Nakano E**, Taylor CJ, Chada L, McGaw J, Powers HJ. Hyperhomocystinemia in children with inflammatory bowel disease. *J Pediatr Gastroenterol Nutr* 2003; **37**: 586-590 [PMID: 14581802 DOI: 10.1097/00005176-200311000-00016]

196 **Akbulut S**, Altiparmak E, Topal F, Ozaslan E, Kucukazman M, Yonem O. Increased levels of homocysteine in patients with ulcerative colitis. *World J Gastroenterol* 2010; **16**: 2411-2416 [PMID: 20480528 DOI: 10.3748/wjg.v16.i19.2411]

197 **Morgenstern I**, Raijmakers MT, Peters WH, Hoensch H, Kirch W. Homocysteine, cysteine, and glutathione in human colonic mucosa: elevated levels of homocysteine in patients with inflammatory bowel disease. *Dig Dis Sci* 2003; **48**: 2083-2090 [PMID: 14627359 DOI: 10.1023/A:1026338812708]

198 **Drzewoski J**, Gasiorowska A, Małecka-Panas E, Bald E, Czupryniak L. Plasma total homocysteine in the active stage of ulcerative colitis. *J Gastroenterol Hepatol* 2006; **21**: 739-743 [PMID: 16677162 DOI: 10.1111/j.1440-1746.2006.04255.x]

199 **Oussalah A**, Guéant JL, Peyrin-Biroulet L. Meta-analysis: hyperhomocysteinaemia in inflammatory bowel diseases. *Aliment Pharmacol Ther* 2011; **34**: 1173-1184 [PMID: 21967576 DOI: 10.1111/j.1365-2036.2011.04864.x]

200 **Zhong Y**, Yan F, Jie W, Zhou Y, Fang F. Correlation between serum homocysteine level and ulcerative colitis: A meta-

analysis. *Pteridines* 2019; **30**: 114-120 [DOI: 10.1515/pteridines-2019-0013]
201 **Handy DE**, Zhang Y, Loscalzo J. Homocysteine down-regulates cellular glutathione peroxidase (GPx1) by decreasing translation. *J Biol Chem* 2005; **280**: 15518-15525 [PMID: 15734734 DOI: 10.1074/jbc.M501452200]
202 **Upchurch GR Jr**, Welch GN, Fabian AJ, Freedman JE, Johnson JL, Keaney JF Jr, Loscalzo J. Homocyst(e)ine decreases bioavailable nitric oxide by a mechanism involving glutathione peroxidase. *J Biol Chem* 1997; **272**: 17012-17017 [PMID: 9202015 DOI: 10.1074/jbc.272.27.17012]
203 **Chen N**, Liu Y, Greiner CD, Holtzman JL. Physiologic concentrations of homocysteine inhibit the human plasma GSH peroxidase that reduces organic hydroperoxides. *J Lab Clin Med* 2000; **136**: 58-65 [PMID: 10882228 DOI: 10.1067/mlc.2000.107692]
204 **Pravda J**, Weickert MJ, Wruble LD. Novel Combination Therapy Induced Histological Remission in Patients with Refractory Ulcerative Colitis. *J Inflam Bowel Dis Disor* 2019; **4**: 1-8
205 **Pravda J**, Gordon R, Sylvestre P. Sustained Histologic Remission (Complete Mucosal Healing) 12 Years after One-Time Treatment of Refractory Ulcerative Colitis with Novel Combination Therapy: A Case Report. *J Inflamm Bowel Dis Disorder* 2020; **5**: 1-5 [DOI: 10.37421/2476-1958.2020.5.132]
206 Clinical presentation: Novel therapy induced Complete histologic remission in refractory ulcerative colitis. [cited 12 December 2021]. Available from: https://www.youtube.com/watch?v=oQYwUMFAraA
207 **Dong C**, Metzger M, Holsbø E, Perduca V, Carbonnel F. Systematic review with meta-analysis: mortality in acute severe ulcerative colitis. *Aliment Pharmacol Ther* 2020; **51**: 8-33 [PMID: 31821584 DOI: 10.1111/apt.15592]
208 **Rosiou K**, Selinger CP. Acute severe ulcerative colitis: management advice for internal medicine and emergency physicians. *Intern Emerg Med* 2021; **16**: 1433-1442 [PMID: 33754227 DOI: 10.1007/s11739-021-02704-0]
209 **Tsunada S**, Iwakiri R, Ootani H, Aw TY, Fujimoto K. Redox imbalance in the colonic mucosa of ulcerative colitis. *Scand J Gastroenterol* 2003; **38**: 1002-1003 [PMID: 14531541 DOI: 10.1080/00365520310005055]
210 **Holvoet T**, Lobaton T, Hindryckx P. Optimal Management of Acute Severe Ulcerative Colitis (ASUC): Challenges and Solutions. *Clin Exp Gastroenterol* 2021; **14**: 71-81 [PMID: 33727846 DOI: 10.2147/CEG.S197719]
211 **Zhang MY**, Dugbartey GJ, Juriasingani S, Sener A. Hydrogen Sulfide Metabolite, Sodium Thiosulfate: Clinical Applications and Underlying Molecular Mechanisms. *Int J Mol Sci* 2021; **22** [PMID: 34208631 DOI: 10.3390/ijms22126452]
212 **Bijarnia RK**, Bachtler M, Chandak PG, van Goor H, Pasch A. Sodium thiosulfate ameliorates oxidative stress and preserves renal function in hyperoxaluric rats. *PLoS One* 2015; **10**: e0124881 [PMID: 25928142 DOI: 10.1371/journal.pone.0124881]
213 **McGeer PL**, McGeer EG, Lee M. Medical uses of Sodium thiosulfate. *J Neurol Neuromed* 2016 [DOI: 10.29245/2572.942X/2016/3.1032]
214 **Desai J**, Elnaggar M, Hanfy AA, Doshi R. Toxic Megacolon: Background, Pathophysiology, Management Challenges and Solutions. *Clin Exp Gastroenterol* 2020; **13**: 203-210 [PMID: 32547151 DOI: 10.2147/CEG.S200760]
215 **Shi XZ**, Winston JH, Sarna SK. Differential immune and genetic responses in rat models of Crohn's colitis and ulcerative colitis. *Am J Physiol Gastrointest Liver Physiol* 2011; **300**: G41-G51 [PMID: 20947704 DOI: 10.1152/ajpgi.00358.2010]
216 **Giniatullin A**, Petrov A, Giniatullin R. Action of Hydrogen Peroxide on Synaptic Transmission at the Mouse Neuromuscular Junction. *Neuroscience* 2019; **399**: 135-145 [PMID: 30593920 DOI: 10.1016/j.neuroscience.2018.12.027]
217 **Colton CA**, Colton JS, Gilbert DL. Changes in synaptic transmission produced by hydrogen peroxide. *J Free Radic Biol Med* 1986; **2**: 141-148 [PMID: 3029210 DOI: 10.1016/s0748-5514(86)80063-0]
218 **Cao W**, Vrees MD, Kirber MT, Fiocchi C, Pricolo VE. Hydrogen peroxide contributes to motor dysfunction in ulcerative colitis. *Am J Physiol Gastrointest Liver Physiol* 2004; **286**: G833-G843 [PMID: 14670823 DOI: 10.1152/ajpgi.00414.2003]
219 **Electronic medicines compendium**. Sodium Thiosulfate Solution for Injection. [cited 24 December 2021]. Available from: https://www2.medicines.org.uk/emc/product/7354/smpc
220 US Department of Health and Human Services. Chemical Hazards emergency medical management. [cited 24 December 2021]. Available from: https://chemm.hhs.gov/
221 **De Angelis M**, Garruti G, Minervini F, Bonfrate L, Portincasa P, Gobbetti M. The Food-gut Human Axis: The Effects of Diet on Gut Microbiota and Metabolome. *Curr Med Chem* 2019; **26**: 3567-3583 [PMID: 28462705 DOI: 10.2174/0929867324666170428103848]
222 **Pituch-Zdanowska A**, Banaszkiewicz A, Albrecht P. The role of dietary fibre in inflammatory bowel disease. *Prz Gastroenterol* 2015; **10**: 135-141 [PMID: 26516378 DOI: 10.5114/pg.2015.52753]
223 **Wagenaar CA**, van de Put M, Bisschops M, Walrabenstein W, de Jonge CS, Herrema H, van Schaardenburg D. The Effect of Dietary Interventions on Chronic Inflammatory Diseases in Relation to the Microbiome: A Systematic Review. *Nutrients* 2021; **13** [PMID: 34579085 DOI: 10.3390/nu13093208]
224 **Aamodt G**, Bukholm G, Jahnsen J, Moum B, Vatn MH; IBSEN Study Group. The association between water supply and inflammatory bowel disease based on a 1990-1993 cohort study in southeastern Norway. *Am J Epidemiol* 2008; **168**: 1065-1072 [PMID: 18801890 DOI: 10.1093/aje/kwn218]
225 **Jowett SL**, Seal CJ, Pearce MS, Phillips E, Gregory W, Barton JR, Welfare MR. Influence of dietary factors on the clinical course of ulcerative colitis: a prospective cohort study. *Gut* 2004; **53**: 1479-1484 [PMID: 15361498 DOI: 10.1136/gut.2003.024828]
226 **United States Environmental Protection Agency**. EPA-FDA Advice about Eating Fish and Shellfish. [cited 26 December 2021]. Available from: https://www.epa.gov/fish-tech/epa-fda-advice-about-eating-fish-and-shellfish
227 EPA-2: Fish Advice. [cited 24 December 2021]. Available from: https://www.fda.gov/food/metals-and-your-food/mercury-levels-commercial-fish-and-shellfish-1990-2012
228 **Wang F**, Feng J, Gao Q, Ma M, Lin X, Liu J, Li J, Zhao Q. Carbohydrate and protein intake and risk of ulcerative colitis: Systematic review and dose-response meta-analysis of epidemiological studies. *Clin Nutr* 2017; **36**: 1259-1265 [PMID: 27776925 DOI: 10.1016/j.clnu.2016.10.009]
229 **Nie JY**, Zhao Q. Beverage consumption and risk of ulcerative colitis: Systematic review and meta-analysis of

epidemiological studies. *Medicine (Baltimore)* 2017; **96**: e9070 [PMID: 29245319 DOI: 10.1097/MD.0000000000009070]

230 **Benitz KF**, Golberg L, Coulston F. Intestinal effects of carrageenans in the rhesus monkey (*Macaca mulatta*). *Food Cosmet Toxicol* 1973; **11**: 565-575 [DOI: 10.1016/S0015-6264(73)80327-X]

231 **Siregar RF**, Santoso J, Uju U. Physico Chemical Characteristic of Kappa Carrageenan Degraded Using Hydrogen Peroxide. *JPHPI* 2017; **19**: 256 [DOI: 10.17844/jphpi.v19i3.14532]

232 **Bhattacharyya S**, Dudeja PK, Tobacman JK. Carrageenan-induced NFkappaB activation depends on distinct pathways mediated by reactive oxygen species and Hsp27 or by Bcl10. *Biochim Biophys Acta* 2008; **1780**: 973-982 [PMID: 18452717 DOI: 10.1016/j.bbagen.2008.03.019]

233 **Geerling BJ**, Dagnelie PC, Badart-Smook A, Russel MG, Stockbrügger RW, Brummer RJ. Diet as a risk factor for the development of ulcerative colitis. *Am J Gastroenterol* 2000; **95**: 1008-1013 [PMID: 10763951 DOI: 10.1111/j.1572-0241.2000.01942.x]

234 **BRENDA**. Information on EC 1.1.3.12 - pyridoxine 4-oxidase. [cited 24 December 2021]. Available from: https://www.brenda-enzymes.org/enzyme.php?ecno=1.1.3.12

235 **Everson CA**, Laatsch CD, Hogg N. Antioxidant defense responses to sleep loss and sleep recovery. *Am J Physiol Regul Integr Comp Physiol* 2005; **288**: R374-R383 [PMID: 15472007 DOI: 10.1152/ajpregu.00565.2004]

236 **Ananthakrishnan AN**, Khalili H, Konijeti GG, Higuchi LM, de Silva P, Fuchs CS, Richter JM, Schernhammer ES, Chan AT. Sleep duration affects risk for ulcerative colitis: a prospective cohort study. *Clin Gastroenterol Hepatol* 2014; **12**: 1879-1886 [PMID: 24780288 DOI: 10.1016/j.cgh.2014.04.021]

237 **Hauso Ø**, Martinsen TC, Waldum H. 5-Aminosalicylic acid, a specific drug for ulcerative colitis. *Scand J Gastroenterol* 2015; **50**: 933-941 [PMID: 25733192 DOI: 10.3109/00365521.2015.1018937]

238 **Couto D**, Ribeiro D, Freitas M, Gomes A, Lima JL, Fernandes E. Scavenging of reactive oxygen and nitrogen species by the prodrug sulfasalazine and its metabolites 5-aminosalicylic acid and sulfapyridine. *Redox Rep* 2010; **15**: 259-267 [PMID: 21208525 DOI: 10.1179/135100010X12826446921707]

239 **Ahnfelt-Rønne I**, Nielsen OH. The antiinflammatory moiety of sulfasalazine, 5-aminosalicylic acid, is a radical scavenger. *Agents Actions* 1987; **21**: 191-194 [PMID: 2888280 DOI: 10.1007/BF01974941]

240 **Battat R**, Duijvestein M, Guizzetti L, Choudhary D, Boland BS, Dulai PS, Parker CE, Nguyen TM, Singh S, Vande Casteele N, Pai RK, Feagan BG, Sandborn WJ, Jairath V. Histologic Healing Rates of Medical Therapies for Ulcerative Colitis: A Systematic Review and Meta-Analysis of Randomized Controlled Trials. *Am J Gastroenterol* 2019; **114**: 733-745 [PMID: 30694863 DOI: 10.14309/ajg.0000000000000111]

241 **Hallert C**, Björck I, Nyman M, Pousette A, Grännö C, Svensson H. Increasing fecal butyrate in ulcerative colitis patients by diet: controlled pilot study. *Inflamm Bowel Dis* 2003; **9**: 116-121 [PMID: 12769445 DOI: 10.1097/00054725-200303000-00005]

242 **Minutello K**, Gupta V. Cromolyn Sodium. 2022 Jan 12. In: StatPearls [Internet]. Treasure Island (FL): StatPearls Publishing; 2022 Jan- [PMID: 32491405]

243 **Chen E**, Chuang LS, Giri M, Villaverde N, Hsu NY, Sabic K, Joshowitz S, Gettler K, Nayar S, Chai Z, Alter IL, Chasteau CC, Korie UM, Dzedzik S, Thin TH, Jain A, Moscati A, Bongers G, Duerr RH, Silverberg MS, Brant SR, Rioux JD, Peter I, Schumm LP, Haritunians T, McGovern DP, Itan Y, Cho JH. Inflamed Ulcerative Colitis Regions Associated With MRGPRX2-Mediated Mast Cell Degranulation and Cell Activation Modules, Defining a New Therapeutic Target. *Gastroenterology* 2021; **160**: 1709-1724 [PMID: 33421512 DOI: 10.1053/j.gastro.2020.12.076]

244 **van Hoboken EA**, Thijssen AY, Verhaaren R, van der Veek PP, Prins FA, Verspaget HW, Masclee AA. Symptoms in patients with ulcerative colitis in remission are associated with visceral hypersensitivity and mast cell activity. *Scand J Gastroenterol* 2011; **46**: 981-987 [PMID: 21623672 DOI: 10.3109/00365521.2011.579156]

245 **Schirmer B**, Neumann D. The Function of the Histamine H4 Receptor in Inflammatory and Inflammation-Associated Diseases of the Gut. *Int J Mol Sci* 2021; **22** [PMID: 34204101 DOI: 10.3390/ijms22116116]

246 **Fox CC**, Lazenby AJ, Moore WC, Yardley JH, Bayless TM, Lichtenstein LM. Enhancement of human intestinal mast cell mediator release in active ulcerative colitis. *Gastroenterology* 1990; **99**: 119-124 [PMID: 1693122 DOI: 10.1016/0016-5085(90)91238-2]

247 **Balázs M**, Illyés G, Vadász G. Mast cells in ulcerative colitis. Quantitative and ultrastructural studies. *Virchows Arch B Cell Pathol Incl Mol Pathol* 1989; **57**: 353-360 [PMID: 2575298 DOI: 10.1007/BF02899101]

248 **Youngblood BA**, Butuci M, Davis T, Schanin J, Brock EC, Singh B, Rasmussen HS, Holman A, Drake R, Peterson K, Flynn AD. Mast Cells Are Significantly Activated In Patients with Ulcerative Colitis and Are Inhibited by an Anti-Siglec-8 Antibody, Antolimab (AK002). Proceedings of the Digestive Disease Week; 2020 May 2-5; Leeds, US. Chicago: Springer, 2020

249 **Baenkler HW**, Lux G, Günthner R, Kohlhäufl M, Matek W. Biopsy histamine in ulcerative colitis and Crohn's disease. *Hepatogastroenterology* 1987; **34**: 289-290 [PMID: 3428863]

250 **Raithel M**, Matek M, Baenkler HW, Jorde W, Hahn EG. Mucosal histamine content and histamine secretion in Crohn's disease, ulcerative colitis and allergic enteropathy. *Int Arch Allergy Immunol* 1995; **108**: 127-133 [PMID: 7549499 DOI: 10.1159/000237129]

251 **McGrath AP**, Hilmer KM, Collyer CA, Shepard EM, Elmore BO, Brown DE, Dooley DM, Guss JM. Structure and inhibition of human diamine oxidase. *Biochemistry* 2009; **48**: 9810-9822 [PMID: 19764817 DOI: 10.1021/bi9014192]

252 **Wolvekamp MC**, de Bruin RW. Diamine oxidase: an overview of historical, biochemical and functional aspects. *Dig Dis* 1994; **12**: 2-14 [PMID: 8200121 DOI: 10.1159/000171432]

253 **Wechsler JB**, Szabo A, Hsu CL, Krier-Burris RA, Schroeder HA, Wang MY, Carter RG, Velez TE, Aguiniga LM, Brown JB, Miller ML, Wershil BK, Barrett TA, Bryce PJ. Histamine drives severity of innate inflammation *via* histamine 4 receptor in murine experimental colitis. *Mucosal Immunol* 2018; **11**: 861-870 [PMID: 29363669 DOI: 10.1038/mi.2017.121]

254 **Ronchetti S**, Ricci E, Migliorati G, Gentili M, Riccardi C. How Glucocorticoids Affect the Neutrophil Life. *Int J Mol Sci* 2018; **19** [PMID: 30563002 DOI: 10.3390/ijms19124090]

255 **Winterbourn CC**, Kettle AJ, Hampton MB. Reactive Oxygen Species and Neutrophil Function. *Annu Rev Biochem* 2016; **85**: 765-792 [PMID: 27050287 DOI: 10.1146/annurev-biochem-060815-014442]

256 **Bilska A**, Włodek L. Lipoic acid - the drug of the future? *Pharmacol Rep* 2005; **57**: 570-577 [PMID: 16227639]

257 **Tort F**, Ferrer-Cortes X, Ribes A. Differential diagnosis of lipoic acid synthesis defects. *J Inherit Metab Dis* 2016; **39**: 781-793 [PMID: 27586888 DOI: 10.1007/s10545-016-9975-4]

258 **Xiao W**, Wang RS, Handy DE, Loscalzo J. NAD(H) and NADP(H) Redox Couples and Cellular Energy Metabolism. *Antioxid Redox Signal* 2018; **28**: 251-272 [PMID: 28648096 DOI: 10.1089/ars.2017.7216]

259 **Rampon C**, Volovitch M, Joliot A, Vriz S. Hydrogen Peroxide and Redox Regulation of Developments. *Antioxidants (Basel)* 2018; **7** [PMID: 30404180 DOI: 10.3390/antiox7110159]

260 **Packer L**, Kraemer K, Rimbach G. Molecular aspects of lipoic acid in the prevention of diabetes complications. *Nutrition* 2001; **17**: 888-895 [PMID: 11684397 DOI: 10.1016/s0899-9007(01)00658-x]

261 **Rochette L**, Ghibu S, Richard C, Zeller M, Cottin Y, Vergely C. Direct and indirect antioxidant properties of α-lipoic acid and therapeutic potential. *Mol Nutr Food Res* 2013; **57**: 114-125 [PMID: 23293044 DOI: 10.1002/mnfr.201200608]

262 **Arnér ES**, Nordberg J, Holmgren A. Efficient reduction of lipoamide and lipoic acid by mammalian thioredoxin reductase. *Biochem Biophys Res Commun* 1996; **225**: 268-274 [PMID: 8769129 DOI: 10.1006/bbrc.1996.1165]

263 **Smith AR**, Shenvi SV, Widlansky M, Suh JH, Hagen TM. Lipoic acid as a potential therapy for chronic diseases associated with oxidative stress. *Curr Med Chem* 2004; **11**: 1135-1146 [PMID: 15134511 DOI: 10.2174/0929867043365387]

264 **Nguyen H**, Gupta V. Alpha-Lipoic Acid. 2021 Nov 20. In: StatPearls [Internet]. Treasure Island (FL): StatPearls Publishing; 2022 Jan- [PMID: 33231971]

265 **Moura FA**, de Andrade KQ, dos Santos JC, Goulart MO. Lipoic Acid: its antioxidant and anti-inflammatory role and clinical applications. *Curr Top Med Chem* 2015; **15**: 458-483 [PMID: 25620240 DOI: 10.2174/1568026615666150114161358]

266 **Harvey CJ**, Thimmulappa RK, Singh A, Blake DJ, Ling G, Wakabayashi N, Fujii J, Myers A, Biswal S. Nrf2-regulated glutathione recycling independent of biosynthesis is critical for cell survival during oxidative stress. *Free Radic Biol Med* 2009; **46**: 443-453 [PMID: 19028565 DOI: 10.1016/j.freeradbiomed.2008.10.040]

267 **Ren H**, Meng Q, Yepuri N, Du X, Sarpong JO, Cooney RN. Protective effects of glutathione on oxidative injury induced by hydrogen peroxide in intestinal epithelial cells. *J Surg Res* 2018; **222**: 39-47 [PMID: 29273374 DOI: 10.1016/j.jss.2017.09.041]

268 **Petersen Shay K**, Moreau RF, Smith EJ, Hagen TM. Is alpha-lipoic acid a scavenger of reactive oxygen species in vivo? *IUBMB Life* 2008; **60**: 362-367 [PMID: 18409172 DOI: 10.1002/iub.40]

269 **Nguyen N**, Takemoto JK. A Case for Alpha-Lipoic Acid as an Alternative Treatment for Diabetic Polyneuropathy. *J Pharm Pharm Sci* 2018; **21**: 177s-191s [PMID: 30139425 DOI: 10.18433/jpps30100]

270 **Reljanovic M**, Reichel G, Rett K, Lobisch M, Schuette K, Möller W, Tritschler HJ, Mehnert H. Treatment of diabetic polyneuropathy with the antioxidant thioctic acid (alpha-lipoic acid): a two year multicenter randomized double-blind placebo-controlled trial (ALADIN II). Alpha Lipoic Acid in Diabetic Neuropathy. *Free Radic Res* 1999; **31**: 171-179 [PMID: 10499773 DOI: 10.1080/10715769900300721]

271 **Ziegler D**, Hanefeld M, Ruhnau KJ, Hasche H, Lobisch M, Schütte K, Kerum G, Malessa R. Treatment of symptomatic diabetic polyneuropathy with the antioxidant alpha-lipoic acid: a 7-month multicenter randomized controlled trial (ALADIN III Study). ALADIN III Study Group. Alpha-Lipoic Acid in Diabetic Neuropathy. *Diabetes Care* 1999; **22**: 1296-1301 [PMID: 10480774 DOI: 10.2337/diacare.22.8.1296]

272 **Moini H**, Packer L, Saris NE. Antioxidant and prooxidant activities of alpha-lipoic acid and dihydrolipoic acid. *Toxicol Appl Pharmacol* 2002; **182**: 84-90 [PMID: 12127266 DOI: 10.1006/taap.2002.9437]

273 **Pravda J**. Hydrogen peroxide and disease: towards a unified system of pathogenesis and therapeutics. *Mol Med* 2020; **26**: 41 [PMID: 32380940 DOI: 10.1186/s10020-020-00165-3]

274 **Elsner M**, Gehrmann W, Lenzen S. Peroxisome-generated hydrogen peroxide as important mediator of lipotoxicity in insulin-producing cells. *Diabetes* 2011; **60**: 200-208 [PMID: 20971967 DOI: 10.2337/db09-1401]

275 **Lenzen S**. The pancreatic beta cell: an intricate relation between anatomical structure, the signalling mechanism of glucose-induced insulin secretion, the low antioxidative defence, the high vulnerability and sensitivity to diabetic stress. *ChemTexts* 2021; **7**: 13 [DOI: 10.1007/s40828-021-00140-3]

276 Challenges in IBD Research. *Inflamm Bowel Dis* 2019; **25** Suppl 2: S1-S4 [PMID: 31095705 DOI: 10.1093/ibd/izz074]

277 **Pizarro TT**, Stappenbeck TS, Rieder F, Rosen MJ, Colombel JF, Donowitz M, Towne J, Mazmanian SK, Faith JJ, Hodin RA, Garrett WS, Fichera A, Poritz LS, Cortes CJ, Shtraizent N, Honig G, Snapper SB, Hurtado-Lorenzo A, Salzman NH, Chang EB. Challenges in IBD Research: Preclinical Human IBD Mechanisms. *Inflamm Bowel Dis* 2019; **25**: S5-S12 [PMID: 31095706 DOI: 10.1093/ibd/izz075]

278 **Alsoud D**, Verstockt B, Fiocchi C, Vermeire S. Breaking the therapeutic ceiling in drug development in ulcerative colitis. *Lancet Gastroenterol Hepatol* 2021; **6**: 589-595 [PMID: 34019798 DOI: 10.1016/S2468-1253(21)00065-0]

279 **Truelove SC**. Ulcerative colitis provoked by milk. *Br Med J* 1961; **1**: 154-160 [PMID: 13778258 DOI: 10.1136/bmj.1.5220.154]

280 **Ko CW**, Singh S, Feuerstein JD, Falck-Ytter C, Falck-Ytter Y, Cross RK; American Gastroenterological Association Institute Clinical Guidelines Committee. AGA Clinical Practice Guidelines on the Management of Mild-to-Moderate Ulcerative Colitis. *Gastroenterology* 2019; **156**: 748-764 [PMID: 30576644 DOI: 10.1053/j.gastro.2018.12.009]

281 **Feuerstein JD**, Isaacs KL, Schneider Y, Siddique SM, Falck-Ytter Y, Singh S; AGA Institute Clinical Guidelines Committee. AGA Clinical Practice Guidelines on the Management of Moderate to Severe Ulcerative Colitis. *Gastroenterology* 2020; **158**: 1450-1461 [PMID: 31945371 DOI: 10.1053/j.gastro.2020.01.006]

282 **Rubin DT**, Ananthakrishnan AN, Siegel CA, Sauer BG, Long MD. ACG Clinical Guideline: Ulcerative Colitis in Adults. *Am J Gastroenterol* 2019; **114**: 384-413 [PMID: 30840605 DOI: 10.14309/ajg.0000000000000152]

283 **Sandborn WJ**, Feagan BG, Hanauer SB, Lichtenstein GR. The Guide to Guidelines in Ulcerative Colitis: Interpretation

and Appropriate Use in Clinical Practice. *Gastroenterol Hepatol (N Y)* 2021; **17**: 3-13 [PMID: 34135718]
284 **Patil DT**, Odze RD. Backwash Is Hogwash: The Clinical Significance of Ileitis in Ulcerative Colitis. *Am J Gastroenterol* 2017; **112**: 1211-1214 [PMID: 28631729 DOI: 10.1038/ajg.2017.182]
285 **Chapman MA**, Grahn MF, Hutton M, Williams NS. Butyrate metabolism in the terminal ileal mucosa of patients with ulcerative colitis. *Br J Surg* 1995; **82**: 36-38 [PMID: 7881952 DOI: 10.1002/bjs.1800820115]
286 **DeRoche TC**, Xiao SY, Liu X. Histological evaluation in ulcerative colitis. *Gastroenterol Rep (Oxf)* 2014; **2**: 178-192 [PMID: 24942757 DOI: 10.1093/gastro/gou031]
287 **Shakirzyanova A**, Valeeva G, Giniatullin A, Naumenko N, Fulle S, Akulov A, Atalay M, Nikolsky E, Giniatullin R. Age-dependent action of reactive oxygen species on transmitter release in mammalian neuromuscular junctions. *Neurobiol Aging* 2016; **38**: 73-81 [PMID: 26827645 DOI: 10.1016/j.neurobiolaging.2015.10.023]
288 **Yang C**, Zhang X, Wang S, Huo X, Wang J. Small intestinal bacterial overgrowth and evaluation of intestinal barrier function in patients with ulcerative colitis. *Am J Transl Res* 2021; **13**: 6605-6610 [PMID: 34306403]
289 **Park SK**, Ye BD, Yang SK, Kim SO, Kim J, Kim JW, Park SH, Yang DH, Jung KW, Kim KJ, Byeon JS, Myung SJ, Kim JH. Clinical features and course of ulcerative colitis diagnosed in asymptomatic subjects. *J Crohns Colitis* 2014; **8**: 1254-1260 [PMID: 24662395 DOI: 10.1016/j.crohns.2014.03.002]
290 **Rodríguez-Lago I**, Ramírez C, Merino O, Azagra I, Maiz A, Zapata E, Higuera R, Montalvo I, Fernández-Calderón M, Arreba P, Carrascosa J, Iriarte A, Muñoz-Navas M, Cabriada JL, Barreiro-de Acosta M. Early microscopic findings in preclinical inflammatory bowel disease. *Dig Liver Dis* 2020; **52**: 1467-1472 [PMID: 32601034 DOI: 10.1016/j.dld.2020.05.052]
291 **Farrukh A**, Mayberry JF. Asymptomatic inflammatory bowel disease and colorectal cancer screening programs: how common is it and what should be done about it? *Gastrointest Disord* 2019; **1**: 261-265 [DOI: 10.3390/gidisord1020021]
292 **Howarth GF**, Robinson MH, Jenkins D, Hardcastle JD, Logan RF. High prevalence of undetected ulcerative colitis: data from the Nottingham fecal occult blood screening trial. *Am J Gastroenterol* 2002; **97**: 690-694 [PMID: 11926210 DOI: 10.1111/j.1572-0241.2002.05586.x]
293 **Sheriff MZ**, Mansoor E, Luther J, Ananthakrishnan AN, Abou Saleh M, Ho E, Briggs FBS, Dave M. Opportunistic Infections Are More Prevalent in Crohn's Disease and Ulcerative Colitis: A Large Population-Based Study. *Inflamm Bowel Dis* 2020; **26**: 291-300 [PMID: 31314891 DOI: 10.1093/ibd/izz147]
294 **Reznicek E**, Arfeen M, Shen B, Ghouri YA. Colorectal Dysplasia and Cancer Surveillance in Ulcerative Colitis. *Diseases* 2021; **9** [PMID: 34842672 DOI: 10.3390/diseases9040086]
295 **Narula N**, Hu A, Nguyen GC, Rangrej J, Marshall JK. Periodic Colonoscopies Are Associated with Improved Survival and Prognosis of Colorectal Cancer in Ulcerative Colitis. *Dig Dis Sci* 2021 [PMID: 34318355 DOI: 10.1007/s10620-021-07151-7]
296 **Kayal M**, Ungaro RC, Riggs A, Kamal K, Agrawal M, Cohen-Mekelburg S, Axelrad J, Faye A, Scherl E, Lawlor G, Sultan K, Lukin D, Dubinsky MC, Colombel JF; New York Crohn's and Colitis Organization (NYCCO). Ileal Pouch Anal Anastomosis for the Management of Ulcerative Colitis Is Associated With Significant Disability. *Clin Gastroenterol Hepatol* 2022; **20**: e761-e769 [PMID: 34033922 DOI: 10.1016/j.cgh.2021.05.033]
297 **Rahmani J**, Kord-Varkaneh H, Ryan PM, Rashvand S, Clark C, Day AS, Hekmatdoost A. Dietary total antioxidant capacity and risk of ulcerative colitis: A case-control study. *J Dig Dis* 2019; **20**: 636-641 [PMID: 31571400 DOI: 10.1111/1751-2980.12823]
298 **National Institutes of Health**. Notice of information: NIGMS Priorities for Sepsis Research. [cited 23 December 2021]. Available from: https://grants.nih.gov/grants/guide/notice-files/NOT-GM-19-054.html
299 **Finzer P**. How we become ill: Investigating emergent properties of biological systems could help to better understand the pathology of diseases. *EMBO Rep* 2017; **18**: 515-518 [PMID: 28242749 DOI: 10.15252/embr.201743948]
300 **Pravda J**. Can Medical Research Do Its Job? *Med Sci Ed* 2017; **27**: 1-2 [DOI: 10.1007/s40670-017-0481-6]
301 **World Health Organization**. Chronic Disease Mortality. [cited 26 December 2021]. Available from: https://www.who.int/chp/chronic_disease_report/part1/en/index1.html
302 **Raghupathi W**, Raghupathi V. An Empirical Study of Chronic Diseases in the United States: A Visual Analytics Approach. *Int J Environ Res Public Health* 2018; **15** [PMID: 29494555 DOI: 10.3390/ijerph15030431]
303 **Centers for Disease Control and Prevention**. Chronic Diseases in America. [cited 24 December 2021]. Available from: https://www.cdc.gov/chronicdisease/resources/infographic/chronic-diseases.htm

World Journal of Gastroenterology

Submit a Manuscript: https://www.f6publishing.com

World J Gastroenterol 2022 August 21; 28(31): 4299-4309

DOI: 10.3748/wjg.v28.i31.4299

ISSN 1007-9327 (print) ISSN 2219-2840 (online)

MINIREVIEWS

Recent advances in multidisciplinary therapy for adenocarcinoma of the esophagus and esophagogastric junction

Yi-Han Zheng, En-Hao Zhao

Specialty type: Gastroenterology and hepatology

Provenance and peer review: Invited article; Externally peer reviewed.

Peer-review model: Single blind

Peer-review report's scientific quality classification

Grade A (Excellent): 0
Grade B (Very good): B, B
Grade C (Good): 0
Grade D (Fair): 0
Grade E (Poor): 0

P-Reviewer: Oguma J, Japan; Ono T, Japan

Received: January 17, 2022
Peer-review started: January 17, 2022
First decision: March 8, 2022
Revised: March 22, 2022
Accepted: July 20, 2022
Article in press: July 20, 2022
Published online: August 21, 2022

Yi-Han Zheng, En-Hao Zhao, Department of Gastrointestinal Surgery, Renji Hospital, Shanghai Jiao Tong University School of Medicine, Shanghai 200127, China

Corresponding author: En-Hao Zhao, PhD, Associate Professor, Doctor, Department of Gastrointestinal Surgery, Renji Hospital, Shanghai Jiao Tong University School of Medicine, No. 160 Pujian Road, Shanghai 200127, China. microzhaoenhao@hotmail.com

Abstract

Esophageal adenocarcinoma (EAC) and adenocarcinoma of the esophagogastric junction (EGJA) have long been associated with poor prognosis. With changes in the spectrum of the disease caused by economic development and demographic changes, the incidence of EAC and EGJA continues to increase, making them worthy of more attention from clinicians. For a long time, surgery has been the mainstay treatment for EAC and EGJA. With advanced techniques, endoscopic therapy, radiotherapy, chemotherapy, and other treatment methods have been developed, providing additional treatment options for patients with EAC and EGJA. In recent decades, the emergence of multidisciplinary therapy (MDT) has enabled the comprehensive treatment of tumors and made the treatment more flexible and diversified, which is conducive to achieving standardized and individualized treatment of EAC and EGJA to obtain a better prognosis. This review discusses recent advances in EAC and EGJA treatment in the surgical-centered MDT mode in recent years.

Key Words: Multidisciplinary therapy; Esophageal adenocarcinoma; Adenocarcinoma of esophagogastric junction; Endoscopic resection; Surgery

Core Tip: Worldwide, esophageal adenocarcinoma (EAC) and adenocarcinoma of the esophagogastric junction (EGJA) have long been associated with poor prognosis, and their incidence continues to increase. For a long time, surgery has been the mainstay treatment for EAC and EGJA. With the advent of advanced techniques, other treatment methods have been developed. In recent decades, the emergence of multidisciplinary therapy (MDT) has enabled the comprehensive treatment of tumors, which is conducive to achieving standardized and individualized treatment. This review discusses recent advances in EAC and EGJA treatment in the surgical-centered MDT mode in recent years.

Citation: Zheng YH, Zhao EH. Recent advances in multidisciplinary therapy for adenocarcinoma of the esophagus and esophagogastric junction. *World J Gastroenterol* 2022; 28(31): 4299-4309
URL: https://www.wjgnet.com/1007-9327/full/v28/i31/4299.htm
DOI: https://dx.doi.org/10.3748/wjg.v28.i31.4299

INTRODUCTION

Currently, esophageal cancer is ranked 7th in incidence and 6th in overall mortality worldwide, with approximately 70% of cases occurring in males[1]. The most common subtypes of esophageal cancer are esophageal adenocarcinoma (EAC) and esophageal squamous cell carcinoma (ESCC). The two subtypes have very different etiologies; therefore, their incidence varies greatly in different countries and regions. Although its morbidity is much lower than that of ESCC in low-income countries, EAC accounts for two-thirds of esophageal cancer cases in high-income countries. Furthermore, owing to demographic changes, the burden of EAC is expected to increase in the future[2]. Obesity, gastroesophageal reflux disease (GERD), and Barrett's esophagus are some of the main risk factors for EAC. The increasing incidences of obesity and GERD are likely responsible for the continuing increase in the incidence of EAC. Additionally, reduction in chronic *Helicobacter pylori* (*H. pylori*) infection has been shown to be negatively correlated with EAC[2].

Adenocarcinoma of the esophagogastric junction (EGJA) is a type of cancer that develops at the junction of the esophagus and stomach, and is traditionally known as cardia cancer. According to the standard set by Siewert *et al*[3] in 1987, esophagogastric carcinoma is defined as a tumor located within 5 cm of the esophagogastric junction (EGJ). Type I was defined when the tumor center was located 1-5 cm above the EGJ, Type II when located from 1 cm above to 2 cm below the EGJ, and Type III when located 2-5 cm below the EGJ. Type II is also known as "real" carcinoma of the cardia. This classification also coincides with the distribution of the cardiac glands[4]. The American Joint Committee on Cancer 8th edition suggests that when the tumor center is located 2 cm below the EGJ or within 2 cm without invasion, it should be staged according to the TNM staging of gastric cancer. When the tumor center is located within 2 cm below the EGJ or with invasion, it should be staged according to the TNM staging of esophageal cancer[5]. Siewert type I EGJA is treated as esophageal cancer, Siewert type III EGJA is classified as gastric cancer, while controversies still exist in the treatment principles for Siewert type II EGJA[6,7]. Evidence indicates that the etiology of EGJA, which is negatively related to *H. pylori* infection and correlates with obesity and GERD injury, is similar to the risk factors for EAC[8].

Currently, surgery remains the primary treatment method for EAC and EGJA. However, due to the anatomical location, gastrointestinal surgeons and thoracic surgeons have different opinions regarding the treatment options. Perioperative therapies, including neoadjuvant and adjuvant therapies, are also gaining attention in the treatment of EAC and EGJA. The importance of multidisciplinary therapy (MDT) in the diagnosis and treatment of tumors has been increasingly emphasized. Clinicians from multiple departments, including radiologists, endoscopists, surgeons, and oncologists, have joined the MDT team to participate in clinical decision making, which has been conducive to the individualization of the diagnosis and treatment of EAC and EGJA.

ENDOSCOPIC RESECTION: GROWING IN IMPORTANCE

For years, surgery has been the only radical treatment for esophageal and EGJ cancer. However, in recent decades, with the development of techniques, endoscopic therapy has gained popularity. Endoscopy has already been used for the early diagnosis of malignant tumors of the esophagus and EGJ, and in suitable patients, endoscopic treatment can be performed. However, endoscopic resection still has limitations and is more commonly used as a diagnostic method than a treatment. A retrospective cohort study demonstrated that, compared to patients who did not undergo continuous endoscopic examination, patients who underwent continuous endoscopy before the diagnosis of EAC were associated with less advanced locoregional staging, better prognosis and survival[9].

Endoscopic radical therapy includes endoscopic tumor resection and ablation of surrounding precancerous tissues to prevent recurrence. The most widely used techniques are endoscopic mucosal resection (EMR) and endoscopic submucosal dissection (ESD). EMR is a relatively safe procedure, with a low risk of postoperative complications. However, it should be noted that during EMR operations, the involved Barrett's esophagus requires treatment; otherwise, locoregional EMR operations may lead to a high rate of recurrence[10]. Research has shown that the prognosis is relatively acceptable, with approximately 96% of patients achieving complete remission, with a 10-year survival rate of 75%[11]. ESD technology is more demanding than EMR technology. Both EMR and ESD have similar postoperative adverse events, but their incidence is higher following ESD[12]. The most common complications are stenosis, perforation, and bleeding[10]. According to a study, in the postoperative assessment, the recurrence rate after radical resection at 22.9 mo of follow-up was 0.17%[13].

The risk of lymphatic metastasis is relatively low in T1a cancer, but appears to increase with the depth of submucosal infiltration[14]. For EAC, the lymphatic metastasis rate is 0-2% in T1a cancer, and 0-22%, 0-30%, 20%-70% when T1b cancers infiltrate the upper third, the middle third, and the lower third of the submucosa, respectively[15-17]. Therefore, patient selection is essential for endoscopic therapy. EAC endoscopic resection is indicated in T1 carcinomas of differentiation grade G1/G2 without lymphatic invasion, venous invasion, or ulceration. In addition to these criteria, for T1b, infiltration less than 500 μm in depth and less than 20 mm in size is required[14]. Current guidelines usually recommend that additional surgery should be performed after endoscopic resection when the risk of lymphatic metastasis or residual cancer is too high to cure[18]. Meanwhile, if the specimen resected by endoscopic therapy reveals a positive margin on histological examination, additional esophagectomy is also required. Based on some cases of T1 carcinoma that underwent esophageal endoscopic resection with additional esophagectomy, among which 17/30 were cases of EAC, researchers concluded that esophagectomy could achieve further removal of residual advanced cancer or lymphatic metastases in 13% of patients. However, postoperative severe morbidity was 43% and mortality was 7%; therefore, the benefits and risks of close follow-up *vs* surgery should be considered[19].

In addition, Barrett's esophagus has been demonstrated to be a significant risk factor for esophageal and EGJ carcinomas. The pathological basis of Barrett's esophagus is the change in mucosal cells caused by long-term exposure to gastric acid, which can develop into adenocarcinoma. Compared to the normal population, patients with Barrett's esophagus have a relative risk of 11.3 of developing adenocarcinoma[20]. Due to the relatively high rate of 25% developing into carcinoma, precursor intraepithelial neoplasia in Barrett's esophagus is usually necessary for endoscopic resection[21]. Additionally, removal of low-grade intraepithelial neoplasia is recommended[22].

SURGERY: REMAINS THE MAINSTAY OF TREATMENT

Surgical options for esophagus adenocarcinoma

According to the guidelines, the transthoracic approach is usually recommended for the treatment of esophageal carcinoma. For cancers located in the proximal one-third of the esophagus, thoracic esophagectomy can be expanded to three fields, including cervical lymph node dissection. However, controversy remains between transthoracic esophagectomy combined with intrathoracic anastomosis (Ivor-Lewis esophagectomy) and three-field esophagectomy combined with esophagogastrostomy (McKeown esophagectomy); the recommendations of concerned guidelines vary from country to country[7]. It is recommended that the absence of suspicious lymph node enlargement indicates a preference for extended two-field thoracoabdominal lymphadenectomy (conventional thoracoabdominal and upper mediastinal lymphadenectomy), whereas, suspicious lymph node enlargement supports the option of three-field cervical and thoracoabdominal lymphadenectomy (cervical and thoracoabdominal lymphadenectomy and upper mediastinal lymphadenectomy)[23]. Furthermore, to investigate the precise lymphatic staging, at least 15 Lymph nodes should be obtained[24]. In recent years, studies have compared two-field approach lymphadenectomy with three-field approach lymphadenectomy for postoperative overall survival (OS) and disease-free survival. The results suggest that there are no significant differences in prognosis between the two approaches[25].

Additionally, studies have shown that lymph node harvest during esophagectomy is associated with improved postoperative survival. A study by Lutfi *et al*[26] demonstrated that during lymphadenectomy, when 7 lymph nodes were harvested, OS improved significantly, and when 25 Lymph nodes were harvested, it showed maximum OS benefits. Other researchers also came to a similar conclusion regarding the influence of lymphadenectomy on postoperative survival after neoadjuvant therapy; when the number of lymph node dissections reached 25, postoperative life expectancy was the highest [27].

Surgical options for adenocarcinoma of EGJ

Although many studies have compared the transthoracic approach to the transhiatal approach, because of the special anatomical location of EGJA, the optimal surgical option is still under debate and recommendations are inconsistent[7]. Based on 14 studies published over the last 30 years, Tseng *et al*

[28] concluded that the Siewert classification had a significant influence on the surgical options. The transthoracic approach was recommended for Siewert type I EGJA, and extended gastrectomy for Siewert type III EGJA. Siewert type II EGJA can be resected using a transthoracic or transhiatal approach, and each approach has similar effects on surgical results and overall prognosis. The surgical method should be determined according to patient factors, such as risk factors and general condition, and also depends on the preference of the surgeon[28]. The advantages of the transthoracic approach are better mediastinal lymph node dissection and better proximal resection margin, as it has the advantages of better para-celiac and para-aortic lymph node dissection, avoidance of thoracotomy-associated morbidity, and preferable postoperative quality of life[28].

Based on the analysis of the results of the Siewert type II EGJ carcinoma surgical treatment conducted by the JCOG9502 trial, the consensus of Chinese experts suggested that the transhiatal approach is recommended for esophageal invasion < 3 cm, and the right thoracoabdominal two-incision surgical approach is preferred for esophageal invasion ≥ 3 cm[29]. Currently, surgical treatment for true EGJA in Japan is generally determined by esophageal invasion of 3 cm and gastric invasion of the upper one-third as a demarcation[4]. Ivor-Lewis esophagectomy combined with upper or middle mediastinal lymphadenectomy is recommended for esophageal invasion ≥ 3 cm. For esophageal invasion < 3 cm, an extended proximal transdiaphragmatic gastrectomy was performed for distal invasion within the upper third of the stomach, and an extended total transdiaphragmatic gastrectomy was performed for invasion that exceeded the upper third of the stomach; meanwhile, a lower mediastinal lymphadenectomy was also required[4]. Nishiwaki *et al*[30] proposed that the distance from the EGJ to the proximal margin of the primary tumor (esophageal invasion) could be an indicator of mediastinal lymph node metastasis in Siewert type II tumors. The results showed that a distance ≥ 2 cm in esophageal invasion was associated with a higher risk of mediastinal lymph node metastasis. When esophageal infiltrates reach 3 cm, the risk was even higher, and the transthoracic approach should be considered for upper and middle mediastinal lymphatic dissection[30]. These results are consistent with the guidelines and current surgical options (Figure 1).

The optimum range of lymphatic dissection has not reached a consensus. According to previous studies, for Siewert type III EGJA, the incidence of lymphatic metastasis in groups No. 1, 2, 3, and 7 was higher than 20 %, metastasis in groups No. 5, 6, 11d, and 12a was less than 5 %, and metastasis in groups No. 107, 111, and 112 was much lower and close to zero. Compared with Siewert type III EGJA, the incidence of lymphatic metastasis in Siewert type II EGJA was significantly lower in the abdominal lymph nodes and higher in the lower mediastinal lymph nodes[31].

To date, only retrospective trials have been conducted on the surgical choice of Siewert type II EGJA, and research has not indicated any difference between the two surgical approaches. The CARDIA trial is the first randomized trial to compare transthoracic esophagectomy with transhiatal extended gastrectomy for Siewert type II EGJA, and the trial is ongoing (DRKS00016923). Esophagectomy is expected to achieve better radical resection and thorough mediastinal lymphatic dissection, leading to better OS, while the quality of life is still acceptable[32].

PERIOPERATIVE CHEMOTHERAPY AND RADIOTHERAPY: EXIST CONTROVERSY

Perioperative treatment includes multiple options, among which chemotherapy (CT), radiotherapy (RT), and chemoradiotherapy (CRT) are the most commonly used regimens. Neoadjuvant therapies benefit tumors by reducing tumor volume, tumor stage, *etc*., and therefore improve the surgical resection rate and prognosis. Postoperative therapies are mainly used to eliminate tumors that have not been completely resected and possible metastases, prolong postoperative survival and reduce the recurrence rate. Over the years, many researchers have made efforts to explore the best perioperative therapy for adenocarcinoma of esophagus and EGJ (Table 1).

RT in adenocarcinoma of esophagus and EGJ

Compared to many other tumors, including gastric carcinoma, RT plays a more important role in the treatment of EAC and EGJA. A Chinese research group included 4160 patients with Siewert type II EGJA to investigate whether perioperative RT benefits patients. The results indicate that neoadjuvant RT improves prognosis in more advanced patients (T3 or with lymphatic metastases) and is more effective in T4 tumors. For stage T1-2, surgery alone is preferred[33]. Furthermore, studies have shown that CRT is superior to RT alone in many aspects, such as tumor downstaging, R0 resection, and pathological complete response (pCR)[34,35], especially in patients with fairly good tolerance for CT. A study analyzed 101 patients with esophageal cancer who underwent CRT or RT alone. The primary endpoints were OS, progression-free survival, local control rate, and toxicity. The results showed that RT was safe and feasible and could partially compensate for the absence of CT[36]. However, because many elderly patients included in the cohort were not eligible for CT, the conclusion has limitations.

CT in adenocarcinoma of esophagus and EGJ

The validity of perioperative CT and concurrent CRT has been widely discussed and is considered the

Table 1 Some clinical studies of perioperative therapy in recent years

Ref.	Cancer	Cases	Groups	Conclusion
RT in EAC and EGJA				
Zhou *et al*[33], 2021	EGJA (Siewert II)	4160	nRT *vs* RT	nRT improves prognosis in patients with more advanced tumors
Klevebro *et al*[35], 2016	Esophageal or EGJ cancer	181	nCRT *vs* nCT	nCRT group had higher complete response rate, R0 resection rate, and lower lymph-node metastases, without significantly affecting survival
Ristau *et al*[36], 2021	EC	101	RT *vs* CT	RT could partially compensate for CT
CT in EAC and EGJA				
Mokdad *et al*[37], 2018	Lower EAC or EGJA	10086	CT *vs* observation	Most patients benefited from adjuvant CT for OS
Papaxoinis *et al*[38], 2019	Lower EAC or EGJA	312	nCT *vs* CT	No significant differences; only patients with postoperative microscopic residual disease benefited from postoperative CT
Davies *et al*[39], 2014	EAC or EGJA	584	Downstaging after nCT *vs* no response	Tumor stage after nCT is more closely associated with prognosis and eligibility for surgery
Bunting *et al*[41], 2018	EAC	286	Toxicity of nCT *vs* no toxicity	Toxicity can lead to adverse consequences, such as failure to complete CT, loss of opportunity for surgical resection, and poor OS
CRT in EAC and EGJA				
Shapiro *et al*[44], 2015	Esophageal or EGJ cancer	368	nCT + surgery *vs* surgery alone	Patients with resectable esophageal or EGJ carcinoma benefited more from nCRT plus surgery than surgery alone
Zafar *et al*[46], 2020	Lower EAC or EGJA	13783	nCRT *vs* nCT	nCRT group was more likely to achieve pCR; OS was not statistically different
Al-Sukhni *et al*[47], 2016	EAC or EGJA	6986	nCRT *vs* nCT	nCRT group showed no difference in improving survival in resectable tumor
Samson *et al*[48], 2016	EC	7338	nCRT *vs* nCT	nCRT lead to more downstaging of tumor, but it is not an individual prognostic factor
Li *et al*[50], 2021	EGJA (Siewert II/III)	170	nCRT *vs* nCT	nCRT provided better survival and improved R0 removal and pCR rates more than nCT in patients with locally advanced EJGA
Tian *et al*[51], 2020	Gastric or EGJ adenocarcinoma	1048	Perioperative CRT *vs* perioperative CT	Perioperative CRT was associated with a higher pCR rate but increase the risk of mortality
Noordman *et al*[52], 2018	Esophageal or EGJ cancer	368	nCRT + surgery *vs* surgery alone	Physical function and frailty remained relatively low in nCRT group, but no adverse effects on long-term HRQoL were observed
Noordman *et al*[53], 2019	Esophageal or EGJ cancer	96	nCRT	HRQoL reduced in short-term, but would return to baseline
Noordman *et al*[54], 2018	Esophageal or EGJ cancer	363	nCRT + surgery *vs* surgery alone	nCRT had no significant effect on postoperative HRQoL
Nilsson *et al*[55], 2020	Esophageal or EGJ cancer	249	Standard TTS *vs* prolonged TTS	Time to surgery (TTS) after nCRT had no significant effect on short-term prognosis

RT: Radiotherapy; EAC: Esophageal adenocarcinoma; EGJA: Adenocarcinoma of the esophagogastric junction; EGJ: Esophagogastric junction; TTS: Time to surgery; HRQoL: Health-related quality of life; CT: Chemotherapy; CRT: Chemoradiotherapy; pCR: Pathological complete response; OS: Overall survival; nRT: Neoadjuvant radiotherapy; nCT: Neoadjuvant chemotherapy; nCRT: Neoadjuvant chemoradiotherapy.

standard treatment option. Mokdad *et al*[37] included 10086 patients with EGJ cancer who received adjuvant CT or postoperative observation. Patients who underwent adjuvant CT were relatively younger and more likely to have advanced disease. In the long-term, the OS of patients who received CT was clearly better at 1 year (94% *vs* 88%), 3 years (54% *vs* 47%), and 5 years (38% *vs* 34%). In other words, most patients benefited from adjuvant CT for OS[37]. Another group included 312 patients (210 with EGJA and 102 with EAC) who underwent radical surgery after neoadjuvant CT (nCT). The experimental group received postoperative CT based on ECX (epirubicin, cisplatin, and capecitabine) regimen, while the control group did not. No significant differences were found in the primary prognostic data between the two groups. Only patients with postoperative microscopic residual disease (R1) benefited from postoperative CT[38].

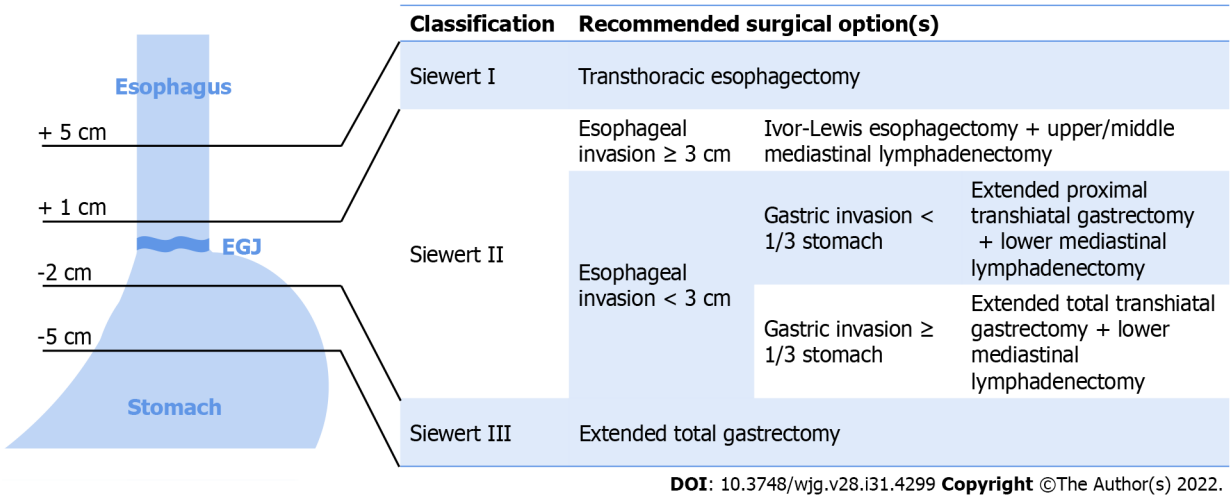

DOI: 10.3748/wjg.v28.i31.4299

Figure 1 Siewert classification of adenocarcinoma of the esophagogastric junction and recommended surgical options[3,4,28,29]. The tumors that centered 1-5 cm above esophagogastric junction (EGJ) are defined as Siewert type I, transthoracic esophagectomy is recommended. the tumors centered from 1 cm above to 2 cm below the EGJ are Siewert type II. For Siewert type II tumor with esophageal invasion ≥ 3 cm, Ivor-Lewis esophagectomy with upper/middle mediastinal lymphadenectomy is propriate surgical option; for esophageal invasion < 3 cm, extended proximal transhiatal gastrectomy or extended total trashiatal gastrectomy with lower mediastinal lymphadenectomy are recommended according to whether gastric invasion exceeded 1/3 of the stomach. The tumors that centered 2-5 cm below EGJ are defined as Siewert type III and extended total gastrectomy is the optimal surgical option. EGJ: Esophagogastric junction.

The purpose of nCT in tumor downstaging is to facilitate resection and improve the postoperative prognosis. Compared with the clinical stage before nCT, the tumor stage after nCT is more closely associated with prognosis and eligibility for surgery[39]. For borderline resectable cancers of the esophagus and EGJ, neoadjuvant therapy is usually recommended, followed by evaluation of the tumor stage according to the guidelines. Davies *et al*[39] reported that patients who received neoadjuvant therapy had a lower local recurrence rate (6% *vs* 13%) and systemic recurrence rate (19% *vs* 29%), along with improved survival. Predictors of postoperative survival after nCT have also been discussed. The results showed that pT staging, pN staging, and resection status were strong predictors of survival, including patients who underwent surgery alone or who received neoadjuvant therapy. Patients who achieved R1 resection or pT3/4 stage after neoadjuvant therapy had better OS than those who achieved the same outcome after surgery alone[40]. In addition, the adverse effects associated with neoadjuvant therapy, also known as toxicity, require attention. Bunting *et al*[41] reported 67 (23.4% of 286 cases) patients who experienced toxicity during nCT. Toxicity can lead to adverse consequences, such as failure to complete CT (47% *vs* 17%), loss of opportunity for surgical resection (17.9% *vs* 7.8%), and poor OS (median survival of 20.7 mo *vs* 37.8 mo). Even if patients who missed surgery were excluded, median survival was shorter in patients with toxicity responses (26.2 mo *vs* 47.8 mo)[41].

CRT in adenocarcinoma of esophagus and EGJ

Perioperative concurrent CRT is widely used to treat EAC and EGJA. The INT0116 trial, the first randomized controlled study of postoperative adjuvant CRT for gastric and EGJ carcinoma, showed that postoperative 5-FU and tetrahydrofolic acid combined with RT significantly extended OS and relapse-free survival in patients with advanced gastric and EGJ carcinoma[42]. This illustrates the importance of CRT in perioperative adjuvant therapy. Currently, adjuvant CRT is the standard treatment for gastric and EGJ carcinoma in the United States[43]. The CROSS study conducted by a Netherlands group in 2015 concluded that the OS of the long-term follow-up of 368 patients with resectable esophageal or EGJ carcinoma benefited more from neoadjuvant CRT (nCRT) followed by surgery than surgery alone. For patients with adenocarcinoma, the median OS of the group that received nCRT plus surgery was 43.2 mo, longer than 27.1 mo of the group that received surgery alone. Therefore, nCRT followed by surgery could be considered the standard treatment for patients with resectable locally advanced EAC or EGJA [44]. The importance of nCRT in the treatment of esophageal and EGJ carcinoma has been widely recognized. After sufficient evaluation of perioperative treatment options, the American Radium Society gastrointestinal expert panel established appropriate criteria that recommended nCRT for patients with resectable non-metastatic EAC or EGJA, cT3 or lymphatic metastasis, and high-risk manifestations. In patients with pathological evidence of lymphatic metastasis without neoadjuvant treatment, adjuvant CRT is recommended[45].

Compared with surgery alone, CT and CRT promote the survival of patients with EAC and EGJA. However, whether CRT is superior to CT remains under debate. Among the 13738 patients with EAC and EGJA who received nCT or nCRT and eventually underwent surgery, patients who underwent nCRT were 2.7 times more likely to achieve pCR than those who underwent nCT; however, OS was not statistically different[46]. Similarly, many studies have shown that nCRT is associated with a higher

pCR rate, higher R0 resection rate, lower lymphatic metastasis rate, and is more likely to achieve downstaging before surgery than nCT; however, previous studies have not been able to reveal the effect on postoperative survival[35,47,48]. Several studies have suggested improvements in postoperative survival in patients treated with nCRT compared with those treated with nCT. Smyth *et al*[49] showed a 4% increase in the 3-year OS in patients who received adjuvant CT after CRT plus surgery. Since most recurrent EGJAs occur within three years after surgery, this may indicate an increase in the curative ratio and that postoperative CT improves survival even after neoadjuvant therapy[49]. In another study of 170 patients with Siewert type II/III EGJA, Li *et al*[50] showed that nCRT provided better survival and improved R0 removal and pCR rates more than nCT in patients with locally advanced EJGA. However, Tian *et al*[51] drew the opposite conclusion after retrospectively reviewing 1048 patients with gastric adenocarcinoma and EGJA who underwent preoperative CT or CRT. While perioperative CRT was associated with a higher pCR rate (13.1% *vs* 8.2%), preoperative CRT appeared to increase the risk of mortality[51].

In addition to the effectiveness of nCRT, its adverse effects and impact on the postoperative quality of life are also factors that must be considered. In the postoperative follow-up, a total of 386 patients with EAC who underwent surgery alone or nCRT plus surgery were followed up for 105 mo. Although the physical function and frailty of the patients remained relatively low, no adverse effects on long-term health-related quality of life (HRQoL) were observed in patients with preoperative nCRT. This finding supports the application of nCRT in patients with EAC[52]. Other similar trials conducted by the same group showed a significant reduction in HRQoL, but eventually HRQoL returned to baseline within eight weeks[53], and nCRT had no significant effect on postoperative HRQoL compared with patients who received surgery alone[54]. That is, nCRT did not cause irreversible long-term changes in HRQoL, which confirmed the safety of nCRT.

Further, there has been some discussion regarding the timing of surgery after neoadjuvant therapy. The current routine is 4-6 wk. Nilsson *et al*[55] randomly assigned 249 patients with esophageal or EGJ cancer into two groups: standard timing of surgery (4-6 wk) or prolonged timing of surgery (10-12 wk). The primary endpoint was overall postoperative complications, and the secondary endpoints were severity of complications, 90-d mortality, and inpatient stay. Data analysis showed that the timing of surgery after nCRT had no significant effect on short-term prognosis[55], while a meta-analysis in 2018 suggested a different opinion. A total of 15086 patients from 13 studies were included. Enrolled patients were divided into two groups based on the time of surgery (shorter or longer than the 7-8 wk interval). A subgroup analysis of patients with adenocarcinoma did not show significant differences in pCR rates, and a prolonged interval was significantly associated with increased mortality. An extended interval was also detrimental to the 2-year and 5-year OS[56].

Furthermore, researchers have compared the prognosis of patients with EAC after surgery alone and in combination with neoadjuvant therapy to clarify whether current treatment strategies could obtain any benefit. Although many patients are predicted to benefit from neoadjuvant therapy, their responses to therapy vary. It is estimated that the total restricted mean survival time would have a 7% gain if optimal therapy was applied instead of actual therapy[57]. This suggests that individualized treatment could benefit patients the most, but how to select individuals with better reactions to specific treatment options and achieve such benefits remains to be further studied.

DEFINITIVE CRT: FOR UNRESECTABLE TUMORS

At diagnosis, tumors in a considerable proportion of patients are no longer indicated for surgery because of tumor invasion of vital organs, main vessels, or nerves (T4b) or the occurrence of distant metastasis (M1)[5]. Neoadjuvant therapy might achieve tumor downstaging in some cases; however, for patients who refuse surgery or have unresectable tumors, definitive CRT (dCRT) remains the only option[23]. With the improvement in concurrent CRT, the 5-year survival of patients with unresectable tumors significantly improved from 0-14% to 20%-25%, indicating that the aim was transformed from palliative to efficient treatment[58]. It was about three decades ago when dCRT first attracted attention. Early randomized trials have shown that the median survival and 5-year survival of patients who received CRT were superior to those who received RT alone[59], and subsequent research confirmed the superiority of CRT over RT[58].

Locoregional recurrence was the main cause of treatment failure in patients who underwent dCRT. In a retrospective study of 184 patients with esophageal carcinoma, locoregional recurrences occurred in 41% of the cases, mostly within 12 mo after cessation of dCRT, and almost all occurred in 24 mo. Among the cases that recurred at the primary tumor site, only 57% occurred within the scope of radiation, which suggests that RT is valid in reducing locoregional recurrences[60]. However, the therapeutic doses of dCRT are still under discussion. In a cohort study, 12638 patients with metastatic esophageal cancer were divided into three groups: CT alone, combined with palliative RT, and combined with definitive RT. The median OS of the patients treated with CRT was 11.3 mo for the definitive dose radiation group and 7.5 mo for the palliative dose group. Thus, in CRT, compared to a lower dose of radiation, patients benefit more from definitive dose radiation[61]. In contrast, another study compared

RT of standard dose with high dose in dCRT, which enrolled 260 patients with esophageal cancer. The results showed that the 3-year local progression-free survival rates were 70% and 73%, respectively, which suggested that higher doses of RT did not necessarily improve the clinical outcome, as assumed [62]. Therefore, the current recommended dose of radiation for dCRT benefits clinical outcomes more than higher or lower doses.

CONCLUSION

Surgery has long been the only radical treatment available for EAC and EGJA. In recent decades, with the development of various other techniques as well as the concept of MDT, increased treatment options could be applied in patients with EAC or EGJA. There is no doubt that surgery is always one of the most important treatments; however, it is no longer the only solution. Clinicians with MDT teams can tailor the regimens for patients. At the same time, more options face more challenges. There are still many controversies, such as the optimal treatment for specific patient groups and the proper timing for applying certain treatments. Moreover, the implementation of MDT is also problematic because not every region or medical center can perform every treatment independently. It is worth exploring and discussing how to make MDT a useful and efficient method to guide treatment. It should be clarified that the final goal is to provide a standardized, efficient, and individualized treatment to each patient to improve OS and quality of life.

FOOTNOTES

Author contributions: Zheng YH wrote the manuscript; Zhao EH reviewed and revised the manuscript; and both authors proofed the manuscript.

Conflict-of-interest statement: The authors have nothing to disclose.

Country/Territory of origin: China

ORCID number: Yi-Han Zheng 0000-0003-2664-0535; En-Hao Zhao 0000-0003-1112-0043.

S-Editor: Yan JP
L-Editor: A
P-Editor: Yan JP

REFERENCES

1 **Sung H**, Ferlay J, Siegel RL, Laversanne M, Soerjomataram I, Jemal A, Bray F. Global Cancer Statistics 2020: GLOBOCAN Estimates of Incidence and Mortality Worldwide for 36 Cancers in 185 Countries. *CA Cancer J Clin* 2021; **71**: 209-249 [PMID: 33538338 DOI: 10.3322/caac.21660]
2 **Arnold M**, Laversanne M, Brown LM, Devesa SS, Bray F. Predicting the Future Burden of Esophageal Cancer by Histological Subtype: International Trends in Incidence up to 2030. *Am J Gastroenterol* 2017; **112**: 1247-1255 [PMID: 28585555 DOI: 10.1038/ajg.2017.155]
3 **Siewert JR**, Hölscher AH, Becker K, Gössner W. [Cardia cancer: attempt at a therapeutically relevant classification]. *Chirurg* 1987; **58**: 25-32 [PMID: 3829805]
4 **Kumamoto T**, Kurahashi Y, Niwa H, Nakanishi Y, Okumura K, Ozawa R, Ishida Y, Shinohara H. True esophagogastric junction adenocarcinoma: background of its definition and current surgical trends. *Surg Today* 2020; **50**: 809-814 [PMID: 31278583 DOI: 10.1007/s00595-019-01843-4]
5 **Rice TW**, Ishwaran H, Hofstetter WL, Kelsen DP, Apperson-Hansen C, Blackstone EH; Worldwide Esophageal Cancer Collaboration Investigators. Recommendations for pathologic staging (pTNM) of cancer of the esophagus and esophagogastric junction for the 8th edition AJCC/UICC staging manuals. *Dis Esophagus* 2016; **29**: 897-905 [PMID: 27905172 DOI: 10.1111/dote.12533]
6 **Chevallay M**, Bollschweiler E, Chandramohan SM, Schmidt T, Koch O, Demanzoni G, Mönig S, Allum W. Cancer of the gastroesophageal junction: a diagnosis, classification, and management review. *Ann N Y Acad Sci* 2018; **1434**: 132-138 [PMID: 30138540 DOI: 10.1111/nyas.13954]
7 **Jung MK**, Schmidt T, Chon SH, Chevallay M, Berlth F, Akiyama J, Gutschow CA, Mönig SP. Current surgical treatment

standards for esophageal and esophagogastric junction cancer. *Ann N Y Acad Sci* 2020; **1482**: 77-84 [PMID: 32798235 DOI: 10.1111/nyas.14454]

8 **Kamangar F**, Dawsey SM, Blaser MJ, Perez-Perez GI, Pietinen P, Newschaffer CJ, Abnet CC, Albanes D, Virtamo J, Taylor PR. Opposing risks of gastric cardia and noncardia gastric adenocarcinomas associated with Helicobacter pylori seropositivity. *J Natl Cancer Inst* 2006; **98**: 1445-1452 [PMID: 17047193 DOI: 10.1093/jnci/djj393]

9 **Cummings LC**, Kou TD, Chak A, Schluchter MD, Margevicius S, Cooper GS. Receipt of Serial Endoscopy Procedures Prior to Esophageal Adenocarcinoma Diagnosis Is Associated with Better Survival. *Dig Dis Sci* 2022; **67**: 1036-1044 [PMID: 33881677 DOI: 10.1007/s10620-021-06927-1]

10 **Malik S**, Sharma G, Sanaka MR, Thota PN. Role of endoscopic therapy in early esophageal cancer. *World J Gastroenterol* 2018; **24**: 3965-3973 [PMID: 30254401 DOI: 10.3748/wjg.v24.i35.3965]

11 **Pech O**, May A, Manner H, Behrens A, Pohl J, Weferling M, Hartmann U, Manner N, Huijsmans J, Gossner L, Rabenstein T, Vieth M, Stolte M, Ell C. Long-term efficacy and safety of endoscopic resection for patients with mucosal adenocarcinoma of the esophagus. *Gastroenterology* 2014; **146**: 652-660.e1 [PMID: 24269290 DOI: 10.1053/j.gastro.2013.11.006]

12 **Terheggen G**, Horn EM, Vieth M, Gabbert H, Enderle M, Neugebauer A, Schumacher B, Neuhaus H. A randomised trial of endoscopic submucosal dissection *vs* endoscopic mucosal resection for early Barrett's neoplasia. *Gut* 2017; **66**: 783-793 [PMID: 26801885 DOI: 10.1136/gutjnl-2015-310126]

13 **Yang D**, Zou F, Xiong S, Forde JJ, Wang Y, Draganov PV. Endoscopic submucosal dissection for early Barrett's neoplasia: a meta-analysis. *Gastrointest Endosc* 2018; **87**: 1383-1393 [PMID: 28993137 DOI: 10.1016/j.gie.2017.09.038]

14 **Gockel I**, Hoffmeister A. Endoscopic or Surgical Resection for Gastro-Esophageal Cancer. *Dtsch Arztebl Int* 2018; **115**: 513-519 [PMID: 30149830 DOI: 10.3238/arztebl.2018.0513]

15 **Cho JW**, Choi SC, Jang JY, Shin SK, Choi KD, Lee JH, Kim SG, Sung JK, Jeon SW, Choi IJ, Kim GH, Jee SR, Lee WS, Jung HY; Korean ESD Study Group. Lymph Node Metastases in Esophageal Carcinoma: An Endoscopist's View. *Clin Endosc* 2014; **47**: 523-529 [PMID: 25505718 DOI: 10.5946/ce.2014.47.6.523]

16 **Japan Esophageal Society**. Japanese Classification of Esophageal Cancer, 11th Edition: part I. *Esophagus* 2017; **14**: 1-36 [PMID: 28111535 DOI: 10.1007/s10388-016-0551-7]

17 **Japan Esophageal Society**. Japanese Classification of Esophageal Cancer, 11th Edition: part II and III. *Esophagus* 2017; **14**: 37-65 [PMID: 28111536 DOI: 10.1007/s10388-016-0556-2]

18 **Pimentel-Nunes P**, Dinis-Ribeiro M, Ponchon T, Repici A, Vieth M, De Ceglie A, Amato A, Berr F, Bhandari P, Bialek A, Conio M, Haringsma J, Langner C, Meisner S, Messmann H, Morino M, Neuhaus H, Piessevaux H, Rugge M, Saunders BP, Robaszkiewicz M, Seewald S, Kashin S, Dumonceau JM, Hassan C, Deprez PH. Endoscopic submucosal dissection: European Society of Gastrointestinal Endoscopy (ESGE) Guideline. *Endoscopy* 2015; **47**: 829-854 [PMID: 26317585 DOI: 10.1055/s-0034-1392882]

19 **Dermine S**, Leconte M, Leblanc S, Dousset B, Terris B, Berger A, Rahmi G, Lepilliez V, Plomteux O, Leclercq P, Coriat R, Chaussade S, Prat F, Barret M. Outcomes of esophagectomy after noncurative endoscopic resection of early esophageal cancer. *Therap Adv Gastroenterol* 2019; **12**: 1756284819892556 [PMID: 31839807 DOI: 10.1177/1756284819892556]

20 **Hvid-Jensen F**, Pedersen L, Drewes AM, Sørensen HT, Funch-Jensen P. Incidence of adenocarcinoma among patients with Barrett's esophagus. *N Engl J Med* 2011; **365**: 1375-1383 [PMID: 21995385 DOI: 10.1056/NEJMoa1103042]

21 **Kastelein F**, van Olphen S, Steyerberg EW, Sikkema M, Spaander MC, Looman CW, Kuipers EJ, Siersema PD, Bruno MJ, de Bekker-Grob EW; ProBar-study group. Surveillance in patients with long-segment Barrett's oesophagus: a cost-effectiveness analysis. *Gut* 2015; **64**: 864-871 [PMID: 25037191 DOI: 10.1136/gutjnl-2014-307197]

22 **Phoa KN**, van Vilsteren FG, Weusten BL, Bisschops R, Schoon EJ, Ragunath K, Fullarton G, Di Pietro M, Ravi N, Visser M, Offerhaus GJ, Seldenrijk CA, Meijer SL, ten Kate FJ, Tijssen JG, Bergman JJ. Radiofrequency ablation *vs* endoscopic surveillance for patients with Barrett esophagus and low-grade dysplasia: a randomized clinical trial. *JAMA* 2014; **311**: 1209-1217 [PMID: 24668102 DOI: 10.1001/jama.2014.2511]

23 **Ajani JA**, D'Amico TA, Bentrem DJ, Chao J, Corvera C, Das P, Denlinger CS, Enzinger PC, Fanta P, Farjah F, Gerdes H, Gibson M, Glasgow RE, Hayman JA, Hochwald S, Hofstetter WL, Ilson DH, Jaroszewski D, Johung KL, Keswani RN, Kleinberg LR, Leong S, Ly QP, Matkowskyj KA, McNamara M, Mulcahy MF, Paluri RK, Park H, Perry KA, Pimiento J, Poultsides GA, Roses R, Strong VE, Wiesner G, Willett CG, Wright CD, McMillian NR, Pluchino LA. Esophageal and Esophagogastric Junction Cancers, Version 2.2019, NCCN Clinical Practice Guidelines in Oncology. *J Natl Compr Canc Netw* 2019; **17**: 855-883 [PMID: 31319389 DOI: 10.6004/jnccn.2019.0033]

24 **Isono K**, Sato H, Nakayama K. Results of a nationwide study on the three-field lymph node dissection of esophageal cancer. *Oncology* 1991; **48**: 411-420 [PMID: 1745490 DOI: 10.1159/000226971]

25 **Li B**, Zhang Y, Miao L, Ma L, Luo X, Ye T, Li H, Zhang J, Li Y, Zhao K, Fan M, Zhu Z, Wang J, Xu J, Deng Y, Lu Q, Pan Y, Liu S, Shao L, Sun Y, Xiang J, Hu H, Chen H. Esophagectomy With Three-Field Versus Two-Field Lymphadenectomy for Middle and Lower Thoracic Esophageal Cancer: Long-Term Outcomes of a Randomized Clinical Trial. *J Thorac Oncol* 2021; **16**: 310-317 [PMID: 33307192 DOI: 10.1016/j.jtho.2020.10.157]

26 **Lutfi W**, Martinez-Meehan D, Dhupar R, Christie N, Sarkaria I, Ekeke C, Baker N, Luketich JD, Okusanya OT. Higher lymph node harvest in patients with a pathologic complete response after neoadjuvant therapy for esophageal cancer is associated with improved survival. *J Surg Oncol* 2020; **121**: 654-661 [PMID: 31970776 DOI: 10.1002/jso.25846]

27 **Raja S**, Rice TW, Murthy SC, Ahmad U, Semple ME, Blackstone EH, Ishwaran H; Worldwide Esophageal Cancer Collaboration Investigators. Value of Lymphadenectomy in Patients Receiving Neoadjuvant Therapy for Esophageal Adenocarcinoma. *Ann Surg* 2021; **274**: e320-e327 [PMID: 31850981 DOI: 10.1097/SLA.0000000000003598]

28 **Tseng J**, Posner MC. For Gastroesophageal Junction Cancers, Does an "Esophageal" or "Gastric" Surgical Approach Offer Better Perioperative and Oncologic Outcomes? *Ann Surg Oncol* 2020; **27**: 511-517 [PMID: 31571057 DOI: 10.1245/s10434-019-07732-x]

29 **Kurokawa Y**, Yamaguchi T, Sasako M, Sano T, Mizusawa J, Nakamura K, Fukuda H. Institutional variation in short- and long-term outcomes after surgery for gastric or esophagogastric junction adenocarcinoma: correlative study of two randomized phase III trials (JCOG9501 and JCOG9502). *Gastric Cancer* 2017; **20**: 508-516 [PMID: 27568321 DOI:

10.1007/s10120-016-0636-y]
30 **Nishiwaki N**, Noma K, Matsuda T, Maeda N, Tanabe S, Sakurama K, Shirakawa Y, Fujiwara T. Risk factor of mediastinal lymph node metastasis of Siewert type I and II esophagogastric junction carcinomas. *Langenbecks Arch Surg* 2020; **405**: 1101-1109 [PMID: 33155069 DOI: 10.1007/s00423-020-02017-4]
31 **Chen XD**, He FQ, Chen M, Zhao FZ. Incidence of lymph node metastasis at each station in Siewert types II/III adenocarcinoma of the esophagogastric junction: A systematic review and meta-analysis. *Surg Oncol* 2020; **35**: 62-70 [PMID: 32835903 DOI: 10.1016/j.suronc.2020.08.001]
32 **Leers JM**, Knepper L, van der Veen A, Schröder W, Fuchs H, Schiller P, Hellmich M, Zettelmeyer U, Brosens LAA, Quaas A, Ruurda JP, van Hillegersberg R, Bruns CJ. The CARDIA-trial protocol: a multinational, prospective, randomized, clinical trial comparing transthoracic esophagectomy with transhiatal extended gastrectomy in adenocarcinoma of the gastroesophageal junction (GEJ) type II. *BMC Cancer* 2020; **20**: 781 [PMID: 32819399 DOI: 10.1186/s12885-020-07152-1]
33 **Zhou Y**, Tian M, Güngör C, Wang D. Neoadjuvant radiotherapy for locoregional Siewert type II gastroesophageal junction adenocarcinoma: A propensity scores matching analysis. *PLoS One* 2021; **16**: e0251555 [PMID: 33979405 DOI: 10.1371/journal.pone.0251555]
34 **Herskovic A**, Martz K, al-Sarraf M, Leichman L, Brindle J, Vaitkevicius V, Cooper J, Byhardt R, Davis L, Emami B. Combined chemotherapy and radiotherapy compared with radiotherapy alone in patients with cancer of the esophagus. *N Engl J Med* 1992; **326**: 1593-1598 [PMID: 1584260 DOI: 10.1056/NEJM199206113262403]
35 **Klevebro F**, Alexandersson von Döbeln G, Wang N, Johnsen G, Jacobsen AB, Friesland S, Hatlevoll I, Glenjen NI, Lind P, Tsai JA, Lundell L, Nilsson M. A randomized clinical trial of neoadjuvant chemotherapy versus neoadjuvant chemoradiotherapy for cancer of the oesophagus or gastro-oesophageal junction. *Ann Oncol* 2016; **27**: 660-667 [PMID: 26782957 DOI: 10.1093/annonc/mdw010]
36 **Ristau J**, Thiel M, Katayama S, Schlampp I, Lang K, Häfner MF, Herfarth K, Debus J, Koerber SA. Simultaneous integrated boost concepts in definitive radiation therapy for esophageal cancer: outcomes and toxicity. *Radiat Oncol* 2021; **16**: 23 [PMID: 33522923 DOI: 10.1186/s13014-021-01749-x]
37 **Mokdad AA**, Yopp AC, Polanco PM, Mansour JC, Reznik SI, Heitjan DF, Choti MA, Minter RR, Wang SC, Porembka MR. Adjuvant Chemotherapy *vs* Postoperative Observation Following Preoperative Chemoradiotherapy and Resection in Gastroesophageal Cancer: A Propensity Score-Matched Analysis. *JAMA Oncol* 2018; **4**: 31-38 [PMID: 28975352 DOI: 10.1001/jamaoncol.2017.2805]
38 **Papaxoinis G**, Kamposioras K, Weaver JMJ, Kordatou Z, Stamatopoulou S, Germetaki T, Nasralla M, Owen-Holt V, Anthoney A, Mansoor W. The Role of Continuing Perioperative Chemotherapy Post Surgery in Patients with Esophageal or Gastroesophageal Junction Adenocarcinoma: a Multicenter Cohort Study. *J Gastrointest Surg* 2019; **23**: 1729-1741 [PMID: 30671799 DOI: 10.1007/s11605-018-04087-8]
39 **Davies AR**, Gossage JA, Zylstra J, Mattsson F, Lagergren J, Maisey N, Smyth EC, Cunningham D, Allum WH, Mason RC. Tumor stage after neoadjuvant chemotherapy determines survival after surgery for adenocarcinoma of the esophagus and esophagogastric junction. *J Clin Oncol* 2014; **32**: 2983-2990 [PMID: 25071104 DOI: 10.1200/JCO.2014.55.9070]
40 **Ronellenfitsch U**, Schwarzbach M, Hofheinz R, Kienle P, Nowak K, Kieser M, Slanger TE, Burmeister B, Kelsen D, Niedzwiecki D, Schuhmacher C, Urba S, van de Velde C, Walsh TN, Ychou M, Jensen K. Predictors of overall and recurrence-free survival after neoadjuvant chemotherapy for gastroesophageal adenocarcinoma: Pooled analysis of individual patient data (IPD) from randomized controlled trials (RCTs). *Eur J Surg Oncol* 2017; **43**: 1550-1558 [PMID: 28551325 DOI: 10.1016/j.ejso.2017.05.005]
41 **Bunting D**, Berrisford R, Wheatley T, Humphreys L, Ariyarathenam A, Sanders G. Prospective cohort study of neoadjuvant therapy toxicity in the treatment of oesophageal adenocarcinoma. *Int J Surg* 2018; **52**: 126-130 [PMID: 29455047 DOI: 10.1016/j.ijsu.2018.02.023]
42 **Macdonald JS**, Smalley SR, Benedetti J, Hundahl SA, Estes NC, Stemmermann GN, Haller DG, Ajani JA, Gunderson LL, Jessup JM, Martenson JA. Chemoradiotherapy after surgery compared with surgery alone for adenocarcinoma of the stomach or gastroesophageal junction. *N Engl J Med* 2001; **345**: 725-730 [PMID: 11547741 DOI: 10.1056/NEJMoa010187]
43 **Moorcraft SY**, Smyth EC, Cunningham D. Adjuvant or neoadjuvant therapy for operable esophagogastric cancer? *Gastric Cancer* 2015; **18**: 1-10 [PMID: 24638977 DOI: 10.1007/s10120-014-0356-0]
44 **Shapiro J**, van Lanschot JJB, Hulshof MCCM, van Hagen P, van Berge Henegouwen MI, Wijnhoven BPL, van Laarhoven HWM, Nieuwenhuijzen GAP, Hospers GAP, Bonenkamp JJ, Cuesta MA, Blaisse RJB, Busch ORC, Ten Kate FJW, Creemers GM, Punt CJA, Plukker JTM, Verheul HMW, Bilgen EJS, van Dekken H, van der Sangen MJC, Rozema T, Biermann K, Beukema JC, Piet AHM, van Rij CM, Reinders JG, Tilanus HW, Steyerberg EW, van der Gaast A; CROSS study group. Neoadjuvant chemoradiotherapy plus surgery *vs* surgery alone for oesophageal or junctional cancer (CROSS): long-term results of a randomised controlled trial. *Lancet Oncol* 2015; **16**: 1090-1098 [PMID: 26254683 DOI: 10.1016/S1470-2045(15)00040-6]
45 **Anker CJ**, Dragovic J, Herman JM, Bianchi NA, Goodman KA, Jones WE 3rd, Kennedy TJ, Kumar R, Lee P, Russo S, Sharma N, Small W, Suh WW, Tchelebi LT, Jabbour SK. Executive Summary of the American Radium Society Appropriate Use Criteria for Operable Esophageal and Gastroesophageal Junction Adenocarcinoma: Systematic Review and Guidelines. *Int J Radiat Oncol Biol Phys* 2021; **109**: 186-200 [PMID: 32858113 DOI: 10.1016/j.ijrobp.2020.08.050]
46 **Zafar SN**, Blum M, Chiang YJ, Ajani JA, Estrella JS, Das P, Minsky BD, Hofstetter WL, Mansfield P, Badgwell BD, Ikoma N. Preoperative Chemoradiation Versus Chemotherapy in Gastroesophageal Junction Adenocarcinoma. *Ann Thorac Surg* 2020; **110**: 398-405 [PMID: 32289300 DOI: 10.1016/j.athoracsur.2020.03.024]
47 **Al-Sukhni E**, Gabriel E, Attwood K, Kukar M, Nurkin SJ, Hochwald SN. No Survival Difference with Neoadjuvant Chemoradiotherapy Compared with Chemotherapy in Resectable Esophageal and Gastroesophageal Junction Adenocarcinoma: Results from the National Cancer Data Base. *J Am Coll Surg* 2016; **223**: 784-792.e1 [PMID: 27641320 DOI: 10.1016/j.jamcollsurg.2016.09.002]
48 **Samson P**, Robinson C, Bradley J, Lockhart AC, Puri V, Broderick S, Kreisel D, Krupnick AS, Patterson GA, Meyers B,

Crabtree T. Neoadjuvant Chemotherapy *vs* Chemoradiation Prior to Esophagectomy: Impact on Rate of Complete Pathologic Response and Survival in Esophageal Cancer Patients. *J Thorac Oncol* 2016; **11**: 2227-2237 [PMID: 27544058 DOI: 10.1016/j.jtho.2016.07.031]

49 **Smyth EC**, Cunningham D. Adjuvant Chemotherapy Following Neoadjuvant Chemotherapy Plus Surgery for Patients With Gastroesophageal Cancer-Is There Room for Improvement? *JAMA Oncol* 2018; **4**: 38-39 [PMID: 28975190 DOI: 10.1001/jamaoncol.2017.2792]

50 **Li J**, Zhao Q, Ge X, Song Y, Tian Y, Wang S, Liu M, Qiao X. Neoadjuvant chemoradiotherapy improves survival in locally advanced adenocarcinoma of esophagogastric junction compared with neoadjuvant chemotherapy: a propensity score matching analysis. *BMC Surg* 2021; **21**: 137 [PMID: 33731072 DOI: 10.1186/s12893-021-01136-z]

51 **Tian S**, Jiang R, Madden NA, Ferris MJ, Buchwald ZS, Xu KM, Cardona K, Maithel SK, McDonald MW, Lin JY, Curran WJ, El-Rayes BF, Behera M, Patel PR. Survival outcomes in patients with gastric and gastroesophageal junction adenocarcinomas treated with perioperative chemotherapy with or without preoperative radiotherapy. *Cancer* 2020; **126**: 37-45 [PMID: 31532544 DOI: 10.1002/cncr.32516]

52 **Noordman BJ**, Verdam MGE, Lagarde SM, Shapiro J, Hulshof MCCM, van Berge Henegouwen MI, Wijnhoven BPL, Nieuwenhuijzen GAP, Bonenkamp JJ, Cuesta MA, Plukker JTM, Spillenaar Bilgen EJ, Steyerberg EW, van der Gaast A, Sprangers MAG, van Lanschot JJB; CROSS Study Group. Impact of neoadjuvant chemoradiotherapy on health-related quality of life in long-term survivors of esophageal or junctional cancer: results from the randomized CROSS trial. *Ann Oncol* 2018; **29**: 445-451 [PMID: 29126244 DOI: 10.1093/annonc/mdx726]

53 **Noordman BJ**, Verdam MGE, Onstenk B, Heisterkamp J, Jansen WJBM, Martijnse IS, Lagarde SM, Wijnhoven BPL, Acosta CMM, van der Gaast A, Sprangers MAG, van Lanschot JJB. Quality of Life During and After Completion of Neoadjuvant Chemoradiotherapy for Esophageal and Junctional Cancer. *Ann Surg Oncol* 2019; **26**: 4765-4772 [PMID: 31620943 DOI: 10.1245/s10434-019-07779-w]

54 **Noordman BJ**, Verdam MGE, Lagarde SM, Hulshof MCCM, van Hagen P, van Berge Henegouwen MI, Wijnhoven BPL, van Laarhoven HWM, Nieuwenhuijzen GAP, Hospers GAP, Bonenkamp JJ, Cuesta MA, Blaisse RJB, Busch OR, Ten Kate FJW, Creemers GM, Punt CJA, Plukker JTM, Verheul HMW, Spillenaar Bilgen EJ, van Dekken H, van der Sangen MJC, Rozema T, Biermann K, Beukema JC, Piet AHM, van Rij CM, Reinders JG, Tilanus HW, Steyerberg EW, van der Gaast A, Sprangers MAG, van Lanschot JJB. Effect of Neoadjuvant Chemoradiotherapy on Health-Related Quality of Life in Esophageal or Junctional Cancer: Results From the Randomized CROSS Trial. *J Clin Oncol* 2018; **36**: 268-275 [PMID: 29161204 DOI: 10.1200/JCO.2017.73.7718]

55 **Nilsson K**, Klevebro F, Rouvelas I, Lindblad M, Szabo E, Halldestam I, Smedh U, Wallner B, Johansson J, Johnsen G, Aahlin EK, Johannessen HO, Hjortland GO, Bartella I, Schröder W, Bruns C, Nilsson M. Surgical Morbidity and Mortality From the Multicenter Randomized Controlled NeoRes II Trial: Standard Versus Prolonged Time to Surgery After Neoadjuvant Chemoradiotherapy for Esophageal Cancer. *Ann Surg* 2020; **272**: 684-689 [PMID: 32833767 DOI: 10.1097/SLA.0000000000004340]

56 **Qin Q**, Xu H, Liu J, Zhang C, Xu L, Di X, Zhang X, Sun X. Does timing of esophagectomy following neoadjuvant chemoradiation affect outcomes? *Int J Surg* 2018; **59**: 11-18 [PMID: 30261331 DOI: 10.1016/j.ijsu.2018.09.013]

57 **Rice TW**, Lu M, Ishwaran H, Blackstone EH; Worldwide Esophageal Cancer Collaboration Investigators. Precision Surgical Therapy for Adenocarcinoma of the Esophagus and Esophagogastric Junction. *J Thorac Oncol* 2019; **14**: 2164-2175 [PMID: 31442498 DOI: 10.1016/j.jtho.2019.08.004]

58 **van Rossum PSN**, Mohammad NH, Vleggaar FP, van Hillegersberg R. Treatment for unresectable or metastatic oesophageal cancer: current evidence and trends. *Nat Rev Gastroenterol Hepatol* 2018; **15**: 235-249 [PMID: 29235549 DOI: 10.1038/nrgastro.2017.162]

59 **Cooper JS**, Guo MD, Herskovic A, Macdonald JS, Martenson JA Jr, Al-Sarraf M, Byhardt R, Russell AH, Beitler JJ, Spencer S, Asbell SO, Graham MV, Leichman LL. Chemoradiotherapy of locally advanced esophageal cancer: long-term follow-up of a prospective randomized trial (RTOG 85-01). Radiation Therapy Oncology Group. *JAMA* 1999; **281**: 1623-1627 [PMID: 10235156 DOI: 10.1001/jama.281.17.1623]

60 **Versteijne E**, van Laarhoven HW, van Hooft JE, van Os RM, Geijsen ED, van Berge Henegouwen MI, Hulshof MC. Definitive chemoradiation for patients with inoperable and/or unresectable esophageal cancer: locoregional recurrence pattern. *Dis Esophagus* 2015; **28**: 453-459 [PMID: 24725186 DOI: 10.1111/dote.12215]

61 **Guttmann DM**, Mitra N, Bekelman J, Metz JM, Plastaras J, Feng W, Swisher-McClure S. Improved Overall Survival with Aggressive Primary Tumor Radiotherapy for Patients with Metastatic Esophageal Cancer. *J Thorac Oncol* 2017; **12**: 1131-1142 [PMID: 28461255 DOI: 10.1016/j.jtho.2017.03.026]

62 **Hulshof MCCM**, Geijsen ED, Rozema T, Oppedijk V, Buijsen J, Neelis KJ, Nuyttens JJME, van der Sangen MJC, Jeene PM, Reinders JG, van Berge Henegouwen MI, Thano A, van Hooft JE, van Laarhoven HWM, van der Gaast A. Randomized Study on Dose Escalation in Definitive Chemoradiation for Patients With Locally Advanced Esophageal Cancer (ARTDECO Study). *J Clin Oncol* 2021; **39**: 2816-2824 [PMID: 34101496 DOI: 10.1200/JCO.20.03697]

World Journal of Gastroenterology

Submit a Manuscript: https://www.f6publishing.com

World J Gastroenterol 2022 August 21; 28(31): 4310-4327

DOI: 10.3748/wjg.v28.i31.4310

ISSN 1007-9327 (print) ISSN 2219-2840 (online)

ORIGINAL ARTICLE

Basic Study

Exosomal glypican-1 is elevated in pancreatic cancer precursors and can signal genetic predisposition in the absence of endoscopic ultrasound abnormalities

Pedro Moutinho-Ribeiro, Ines A Batista, Sofia T Quintas, Bárbara Adem, Marco Silva, Rui Morais, Armando Peixoto, Rosa Coelho, Pedro Costa-Moreira, Renato Medas, Susana Lopes, Filipe Vilas-Boas, Manuela Baptista, Diogo Dias-Silva, Ana L Esteves, Filipa Martins, Joanne Lopes, Helena Barroca, Fátima Carneiro, Guilherme Macedo, Sonia A Melo

Specialty type: Gastroenterology and hepatology

Provenance and peer review: Unsolicited article; Externally peer reviewed.

Peer-review model: Single blind

Peer-review report's scientific quality classification

Grade A (Excellent): A
Grade B (Very good): B
Grade C (Good): 0
Grade D (Fair): 0
Grade E (Poor): 0

P-Reviewer: Chen SY, China; Villa E, United States

Received: February 17, 2022
Peer-review started: February 17, 2022
First decision: April 16, 2022
Revised: April 30, 2022
Accepted: June 24, 2022
Article in press: June 24, 2022
Published online: August 21, 2022

Pedro Moutinho-Ribeiro, Marco Silva, Rui Morais, Armando Peixoto, Rosa Coelho, Pedro Costa-Moreira, Renato Medas, Susana Lopes, Filipe Vilas-Boas, Guilherme Macedo, Serviço de Gastrenterologia, Centro Hospitalar Universitário de São João, Porto 4200, Portugal

Pedro Moutinho-Ribeiro, Marco Silva, Rui Morais, Armando Peixoto, Rosa Coelho, Pedro Costa-Moreira, Renato Medas, Susana Lopes, Filipe Vilas-Boas, Fátima Carneiro, Guilherme Macedo, Sonia A Melo, Faculty of Medicine, University of Porto, Porto 4200, Portugal

Ines A Batista, Sofia T Quintas, Bárbara Adem, Fátima Carneiro, Sonia A Melo, Instituto de Investigação e Inovação em Saúde (i3S), Universidade do Porto, Porto 4200, Portugal

Ines A Batista, Sofia T Quintas, Fátima Carneiro, Sonia A Melo, IPATIMUP–Institute of Molecular Pathology and Immunology, University of Porto, Porto 4200, Portugal

Ines A Batista, Bárbara Adem, Instituto de Ciências Biomédicas Abel Salazar (ICBAS), University of Porto, Porto 4050, Portugal

Manuela Baptista, Serviço de Cirurgia Geral, Centro Hospitalar Universitário de São João, Porto 4200, Portugal

Diogo Dias-Silva, Ana L Esteves, Filipa Martins, Unidade de Saúde Familiar Serpa Pinto, ACeS Porto Ocidental, Porto 4250, Portugal

Joanne Lopes, Helena Barroca, Fátima Carneiro, Serviço de Anatomia Patológica, Centro Hospitalar Universitário de São João, Porto 4200, Portugal

Corresponding author: Sonia A Melo, PhD, Academic Research, Assistant Professor, Instituto de Investigação e Inovação em Saúde (i3S), Universidade do Porto, R. Alfredo Allen 208, Porto 4200, Portugal. smelo@i3s.up.pt

Abstract

BACKGROUND

Individuals within specific risk groups for pancreatic ductal adenocarcinoma

(PDAC) [mucinous cystic lesions (MCLs), hereditary risk (HR), and new-late onset diabetes mellitus (NLOD)] represent an opportunity for early cancer detection. Endoscopic ultrasound (EUS) is a premium image modality for PDAC screening and precursor lesion characterization. While no specific biomarker is currently clinically available for this purpose, glypican-1 (GPC1) is overexpressed in the circulating exosomes (crExos) of patients with PDAC compared with healthy subjects or those harboring benign pancreatic diseases.

AIM

To evaluate the capacity of GPC1$^+$ crExos to identify individuals at higher risk within these specific groups, all characterized by EUS.

METHODS

This cross-sectional study with a prospective unicentric cohort included 88 subjects: 40 patients with MCL, 20 individuals with HR, and 20 patients with NLOD. A control group (CG) was submitted to EUS for other reasons than pancreatic pathology, with normal pancreas and absence of hereditary risk factors (n = 8). The inclusion period was between October 2016 and January 2019, and the study was approved by the Ethics Committee of Centro Hospitalar Universitário de São João, Porto, Portugal. All patients provided written informed consent. EUS and blood tests for quantification of GPC1$^+$ crExos by flow cytometry and carbohydrate antigen 19-9 (CA 19-9) levels by ELISA were performed in all subjects. EUS-guided tissue acquisition was done whenever necessary. For statistical analysis, SPSS® 27.0 (IBM Corp., Armonk, NY, United States) version was used. All graphs were created using GraphPad Prism 7.00 (GraphPad Software, San Diego, CA, United States).

RESULTS

Half of MCLs harbored worrisome features (WF) or high-risk stigmata (HRS). Pancreatic abnormalities were detected by EUS in 10.0% and 35.0% in HR and NLOD individuals, respectively, all considered non-malignant and "harmless." Median levels of GPC1$^+$ crExos were statistically different: MCL [99.4%, interquartile range (IQR): 94.9%-99.8%], HR (82.0%, IQR: 28.9%-98.2%), NLOD (12.6%, IQR: 5.2%-63.4%), and CG (16.2%, IQR: 6.6%-20.1%) (P < 0.0001). Median levels of CA 19-9 were within the normal range in all groups (standard clinical cut-off of 37 U/mL). Within HR, individuals with a positive history of cancer had higher median levels of GPC1$^+$ crExos (97.9%; IQR: 61.7%-99.5%), compared to those without (59.7%; IQR: 26.3%-96.4%), despite no statistical significance (P = 0.21). Pancreatic cysts with WF/HRS were statistically associated with higher median levels of GPC1$^+$ crExos (99.6%; IQR: 97.6%-99.8%) compared to those without (96.5%; IQR: 81.3%-99.5%) (P = 0.011), presenting an area under the receiver operating characteristic curve value of 0.723 (sensitivity 75.0% and specificity 67.7%, using a cut-off of 98.5%; P = 0.012).

CONCLUSION

GPC1$^+$ crExos may act as biomarker to support the diagnosis and stratification of PDAC precursor lesions, and in signaling individuals with genetic predisposition in the absence of EUS abnormalities.

Key Words: Glypican-1; Circulating exosomes; Endoscopic ultrasound; Pancreatic cancer risk groups; Pancreatic cancer precursor lesions; Genetic predisposition

Core Tip: Patients with mucinous cystic lesions (MCLs), hereditary risk (HR), and new-late onset diabetes mellitus represent a target for early pancreatic ductal adenocarcinoma (PDAC) detection. Within these groups, we evaluated the capacity of glypican-1 positive (GPC1$^+$) circulating exosomes (crExos) to identify individuals at higher risk, all characterized by endoscopic ultrasound (EUS). High levels of GPC1$^+$ crExos were present in MCL and in individuals with HR (predominantly in those with history of cancer), even in the absence of EUS abnormalities. GPC1 may represent a biomarker to support the diagnosis and stratification of PDAC precursor lesions, and indicate genetic predisposition.

Citation: Moutinho-Ribeiro P, Batista IA, Quintas ST, Adem B, Silva M, Morais R, Peixoto A, Coelho R, Costa-Moreira P, Medas R, Lopes S, Vilas-Boas F, Baptista M, Dias-Silva D, Esteves AL, Martins F, Lopes J, Barroca H, Carneiro F, Macedo G, Melo SA. Exosomal glypican-1 is elevated in pancreatic cancer precursors and can signal genetic predisposition in the absence of endoscopic ultrasound abnormalities. *World J Gastroenterol* 2022; 28(31): 4310-4327
URL: https://www.wjgnet.com/1007-9327/full/v28/i31/4310.htm
DOI: https://dx.doi.org/10.3748/wjg.v28.i31.4310

INTRODUCTION

Pancreatic ductal adenocarcinoma (PDAC) is considered one of the deadliest malignant diseases around the world, and is estimated to become the second leading cause of cancer-related deaths in the United States in 2030[1]. Most patients present with advanced disease at diagnosis, with only 20% being candidates for surgical treatment, the only chance for cure[2,3].

In its early stages, PDAC usually develops with few or no symptoms, and current sectional imaging modalities are inadequate to detect early small lesions[3]. Endoscopic ultrasound (EUS) is a highly accurate diagnostic technique for pancreatic lesions, with its role majored by the possibility of performing EUS-guided tissue acquisition[4-6].

Among PDAC precursor lesions are pancreatic intraepithelial neoplasias (PanINs) and mucinous cystic lesions (MCLs)[7,8]. While the former are very difficult to identify by available imaging modalities, the latter can be more clearly detected and characterized, specially by magnetic resonance imaging (MRI)/magnetic resonance cholangiopancreatography (MRCP) and EUS[5,9].

Along with the improvement of imaging diagnostic accuracy, the search for a biomarker that could adequately identify PDAC at early stages or its high-risk precursor lesions is a top research priority. The only biomarker approved for clinical use is carbohydrate antigen 19-9 (CA 19-9), but it lacks sensitivity and specificity for PDAC early detection, being mostly reserved for monitoring response to therapy and disease progression[10]. In recent years, several molecules have been tested to serve this purpose[11,12]. Among these, membrane-anchored proteoglycan glypican-1 (GPC1) has been shown to be a good candidate. We previously studied GPC1 in circulating exosomes (crExos) and found that it could identify PDAC patients among healthy individuals with perfect accuracy[13]. In addition, $GPC1^+$ crExos correlated with tumor burden and patients' survival. Moreover, in a genetically engineered mouse model of PDAC, GPC1 was overexpressed in crExos even before the tumor could be detected by MRI [13]. Finally, we also showed higher levels of $GPC1^+$ crExos in MCL compared to controls, although the number of patients was very limited[13]. Several studies have demonstrated the role of GPC1 in PDAC [14-18]. Considering the distinct methodologies that some of the studies adopted to study GPC1 in circulation, some support the potential of $GPC1^+$ crExos as a biomarker for early detection of PDAC[14, 15,19], while others only demonstrate their correlation with disease burden[16-18].

At present, while 90% of PDAC cases are sporadic, only individuals harboring increased hereditary risk (HR), either kindreds of familial pancreatic cancer (FPC) (7%) or belonging to other cancer syndromes with increased risk of PDAC (3%), are candidates for screening[20-22]. Nevertheless, there are other well-defined PDAC-associated risk groups that deserve special attention and can constitute a refined population to be surveilled in order to increase the rate of early detection and improve overall survival. One of these groups is composed by individuals older than 50 years with a recent (< 36 mo) diagnosis of type II diabetes mellitus (DM). Increasing epidemiological, clinical, and experimental evidence shows that new-onset DM can be a clinical manifestation of asymptomatic PDAC or harbinger the disease and offers the promise for early detection in these individuals[3,23-26]. In fact, although the complex and multidirectional relationship between the two entities is not fully understood, new-late onset DM (NLOD) has been recognized as an entity signaling a 6- to 8-fold increased risk of developing PDAC in 3 years[27].

We previously showed that levels of $GPC1^+$ crExos discriminate PDAC from chronic pancreatitis (CP) with high accuracy[28]. In this work, we aimed to determine the capacity of $GPC1^+$ crExos to identify individuals at higher risk of developing PDAC, comparing its levels with EUS pancreatic abnormalities (PA) within specific risk groups: MCL, HR, and NLOD.

MATERIALS AND METHODS

Design of the study and population

This cross-sectional study with a prospective unicentric cohort included 88 subjects: 40 patients with MCLs, 20 individuals with HR, 20 patients with NLOD, and 8 individuals in the control group (CG). The inclusion period was between October 2016 and January 2019, and the study was approved by the Ethics Committee of Centro Hospitalar Universitário de São João (CHUSJ) (ID No. CES 327-15), Porto,

Portugal. All patients provided written informed consent and underwent blood sample collection at the time of EUS.

In the MCL group, we considered for inclusion both intraductal papillary mucinous neoplasms (IPMNs) and mucinous cystic neoplasms (MCNs). For its diagnosis, we used both imagiological and cyst fluid analysis criteria. We have assumed IPMN etiology when EUS and/or MRCP clearly showed communication of the cyst(s) with the pancreatic ductal system. In this situation, branch-duct type (BD-IPMN) were presumed if multiple and no dominant main pancreatic duct (MPD) dilation was seen. Main-duct IPMN (MD-IPMN) was considered if a segmental or diffuse dilatation of the main duct > 5 mm was observed without any other cause of obstruction. Mixed-type IPMN (MT-IPMN) was defined when features of MD-IPMN and BD-IPMN coexisted[29]. MCN was assumed when a mucin-producing cyst forming epithelial neoplasia of the pancreas with a distinctive ovarian-type stroma was present, typically with no communication with the ductal system[30].

We performed EUS-guided fine needle aspiration (FNA) in almost all cystic lesions included. Mucinous nature was supported by a fluid carcinoembryonic antigen (CEA) > 192 ng/mL and/or fluid glucose < 50 mg/dL[31]. In relation to amylase content, if > 250 U/L, a diagnosis of IPMN was likely, whereas levels < 250 U/L suggested MCN. If the aspirated content was sufficient, a sample was also evaluated by experienced cytopathologists.

In the HR group, we considered for inclusion FPC (family history of PDAC in at least two first-degree, or in three or more first- and second-degree relatives) and PDAC susceptibility gene mutation carriers[20,22,32,33]. All of these individuals had a clinically and genetically established diagnosis and have been followed in a dedicated consultation for hereditary digestive cancers in our institution. They underwent detailed evaluation of family history, and verification of cancer diagnoses by review of medical records and genetic testing.

In the NLOD group, we included patients aged ≥ 50 years who had been diagnosed with type II DM within a period of 36 mo[23,24]. Diagnosis of type II DM was made according to the American Diabetes Association and consisted of: Fasting plasma glucose level ≥ 126 mg/dL, a 2-h plasma glucose level of ≥ 200 mg/dL during a 75-g oral glucose tolerance test, a random plasma glucose level of ≥ 200 mg/dL in a patient with classic symptoms of hyperglycemia or hyperglycemic crisis, or a hemoglobin A1c level of ≥ 6.5%[34].

In the CG, individuals who underwent EUS for other reasons than pancreatic pathology were included with a normal pancreas and absence of hereditary/familial risk factors. The exclusion criteria were patients unable or unwilling to give informed consent, individuals younger than 18 years of age, pregnancy or breast feeding, contraindications to endoscopic procedures or contrast administration, contraindications to computed tomography (CT) or MRI, coagulopathy (prothrombin time > 50% of control, activated partial thromboplastin time > 50 s, or international normalized ratio > 1.5), patients on chronic anticoagulation, platelet count < 50000/μL, and inability to tolerate sedated upper endoscopy due to cardiopulmonary instability or other contraindication to endoscopic procedures.

At the time of inclusion, immediately before EUS examination, a blood sample was collected for complete blood count as well as renal, liver, and pancreatic chemistry at the CHUSJ laboratory. A separate blood sample collected at the same time was used to quantify CA 19-9 serum levels (ab108642, CA 19-9 Human ELISA Kit; Abcam, Cambridge, MA, United States) and GPC1 expression in crExos by fluorescence-activated cell sorting (FACS) (Figure 1). For CA 19-9, the standard clinical cut-off of 37 U/mL was used. A complete personal and family clinical history was registered, and demographic data was recorded [age, body mass index (BMI)], previous history of pancreatic disease, smoking and drinking habits, history of diabetes and duration since diagnosis, digestive and systemic symptoms. Laboratory values and previous results of cross-sectional imaging (CT, MRI, or magnetic resonance cholangiopancreatography) were registered. The results of the EUS evaluation at the time of inclusion in the study as well as transechoendoscopic or surgically collected specimens were also recorded.

All subjects were observed, examined, and followed-up at the Department of Gastroenterology of CHUSJ (Porto, Portugal) until death or July 2021.

EUS, tissue acquisition techniques, and fluid/specimen analyses

All EUS evaluations were performed by three experienced endoscopists under deep sedation (propofol or pethidine plus midazolam as assisted by an anesthesiologist). Linear scopes from Olympus® (GT-UCT140, GT-UCT180; Tokyo, Japan) and Pentax® (EG-3670UTK, EG-3870UTK; Tokyo, Japan) along with Olympus® EU-ME2 and Hitachi Avius® (Tokyo, Japan) image processors were used.

PA were classified into major and minor changes. Major changes comprised cystic lesions, CP-like parenchymal changes, and solid lesions. Minor ones constituted changes in pancreatic echogenicity compatible with lipomatous transformation[35,36]. EUS high-risk stigmata (HRS) and worrisome features (WF) were categorized according to the International consensus of Fukuoka guidelines for the management of IPMN of the pancreas[29]. A main duct dilatation ≥ 10 mm or an enhancing mural nodule > 5 mm were classified as HRS, whereas a main duct dilatation between 5 and 9 mm, an enhancing mural nodule < 5 mm, a cyst diameter > 3 cm, the presence of thickened/enhancing cyst walls, an abrupt change in pancreatic duct caliber with distal pancreatic atrophy, and lymphadenopathy were considered WF.

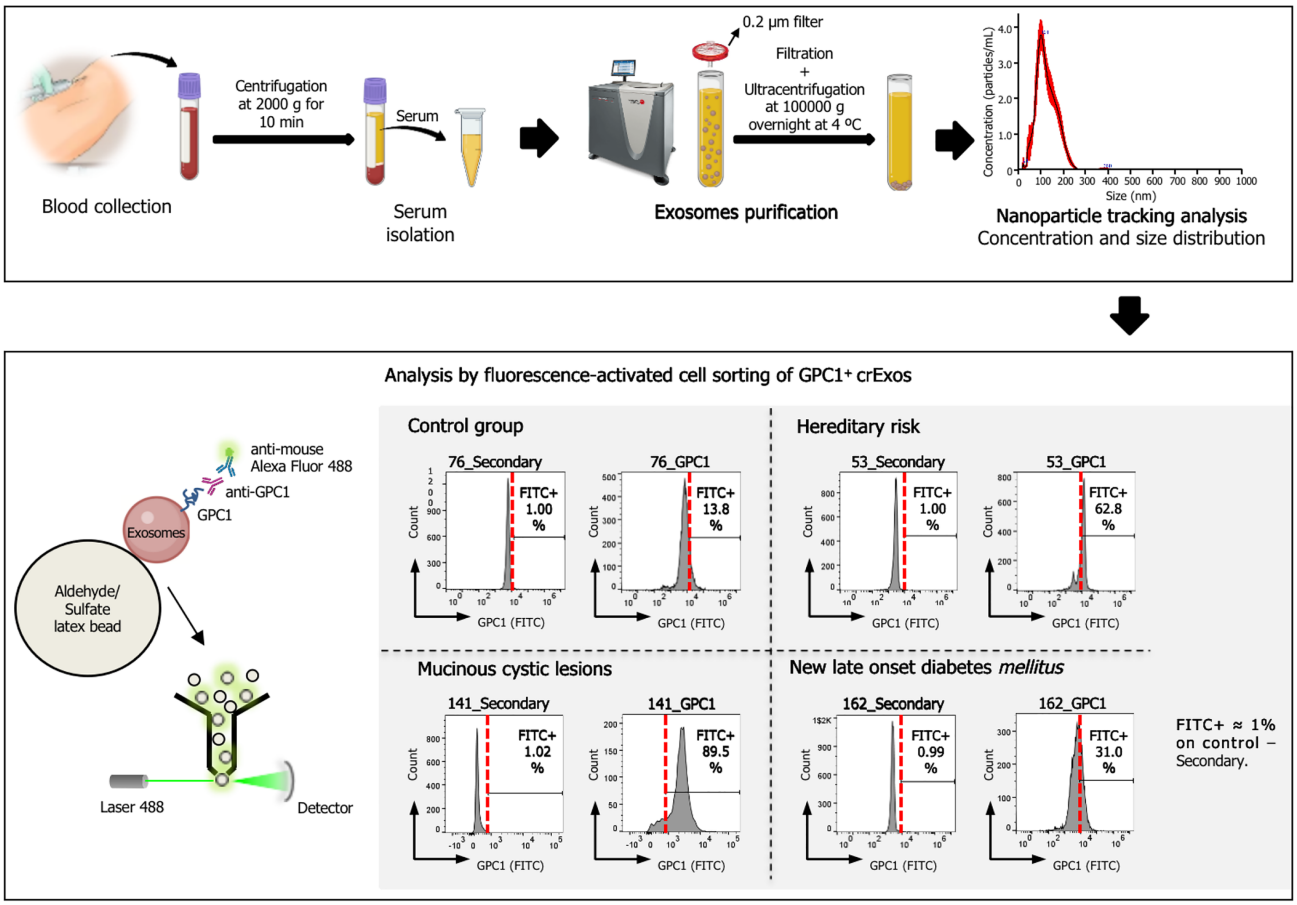

DOI: 10.3748/wjg.v28.i31.4310 **Copyright** ©The Author(s) 2022.

Figure 1 Schematic representation of the workflow for the analysis of circulating exosomes from control group, mucinous cystic lesions, hereditary risk and new-late onset diabetes mellitus patients for the expression of glypican-1. Scheme illustrating the workflow of our study of the expression of glypican-1 (GPC1) on exosomes retrieved from patients' blood samples, from blood collection to the analysis by flow cytometry of GPC1$^+$ circulating exosomes (crExos). A representative histogram of the percentage of beads bound to GPC1-positive crExos (GPC1$^+$ crExos) that were isolated from the serum of a control group, composed by individuals submitted to endoscopic ultrasound for other reasons than pancreatic pathology, as well as the following pancreatic ductal adenocarcinoma risk groups: Mucinous cystic lesions, hereditary risk, and new-late onset diabetes mellitus. Red dashed lines in each histogram depict the start of the fluorescein isothiocyanate (FITC)-positive gate (anti-immunoglobulin G) Alexa Fluor 488), which was determined for each patient separately by considering FITC+ approximately 1% on control–secondary–but maintained between control and GPC1 samples. GPC1: Glypican-1; FITC: Fluorescein isothiocyanate; crExos: Circulating exosomes.

Doppler, elastography, and contrast-enhanced EUS image acquisition (sulphur hexafluoride microbubbles; SonoVue®, Bracco, Italy) were used for assistance in the characterization of mural nodules and thickened cyst walls.

EUS-FNA was performed in almost all cystic lesions, preferably with a 22 G needle (Wilson-Cook Medical, Winston, NC, United States and Boston Scientific, Natick MA, United States) in a single pass, and along with antibiotic prophylaxis (single intravenous infusion of 200 mg ciprofloxacin). The fluid collected was sent for amylase, glucose, and CEA quantification, and also, if in enough volume, for cytological examination. Solid or indeterminate lesions, mural nodules, or suspicious thickenings of the cyst wall or septa were punctured in a distinct pass, preferably with a 22 G fine needle biopsy. Adverse events related to EUS procedures were registered and monitored.

Microscopic examinations of specimens resulting from EUS-FNA/B and/or surgical resection were analyzed by experienced pathologists in pancreatic diseases and contextualized to patients' clinical history and imaging findings. Cytological evaluation was performed according to the Papanicolaou Society of Cytopathology System for Reporting Pancreaticobiliary Cytology[37].

Collection of human blood samples

At the same time of EUS performance, blood samples were collected at the Department of Gastroenterology of CHUSJ. Serum samples were obtained by centrifugation of the whole blood sample at 2000 g for 10 min at 4 °C and collection of the supernatant. The resultant serum samples were then aliquoted and stored at -80 °C prior to analysis.

Isolation of exosomes by ultracentrifugation of serum samples and nanoparticle tracking analysis

Human serum samples were allowed to thaw on ice with periodic agitation to avoid degradation. A volume of 200 µL serum was retrieved into a new tube and centrifuged at 10000 rpm for 2 min at 4 ºC. The recovered supernatant was diluted in 200 µL NaCl prior to filtration into 14 mL Open-Top Thinwall Ultra-Clear Tubes (Beckman Coulter, Inc., Brea, CA, United States) using a 0.2 µm pore filter (Whatman International Ltd., England, United Kingdom). The tubes were filled with NaCl, and the samples were ultracentrifuged at 100000 g overnight at 4 °C. The next day, the supernatant was carefully and thoroughly discarded and the exosomes' pellet was resuspended in 300 µL of 1 × phosphate-buffered saline (PBS). To determine particle concentration and size distribution, nanoparticle tracking (NTA) (NanoSight NS300) was performed using 10 µL of the exosomes sample dissolved in 1 × PBS at a 1:100 dilution. The remaining exosomes sample was saved at -20 ºC for downstream analysis.

GPC1 analysis by FACS of exosomes coupled to beads

Using the exosomes concentration previously obtained by NTA analysis as a reference, an equal number of exosomes was used for downstream FACS analysis. A total of 3.0×10^9 exosomes were coupled to 4 µm aldehyde/sulfate latex beads (A37304; Thermo Fisher Scientific, Waltham, MA, United States) that had been previously equilibrated at room temperature (through resuspension of 5 µL beads in 100 µL of 1 × PBS and rotation at room temperature for 15 min). The sample volume was adjusted to 300 µL with 1 × PBS. Upon incubation in a rotator at room temperature for 15 min and then at 4 ºC for 30 min to allow the formation of exosomes-bead complexes, 300 µL glycine 1 M in 1 × PBS was added to the sample, followed by incubation at room temperature for 1 h with continuous rotation. Samples were centrifuged at 12000 rpm for 2 min and the supernatant was discarded. The pellet containing the exosomes-bead complexes was subjected to a blocking step with 100 µL of 10% bovine serum albumin (BSA) in 1 × PBS and then incubated with continuous rotation at room temperature for 45 min. The samples were centrifuged at 12000 rpm for 2 min and divided into two tubes: Control and GPC1-incubated samples. Control samples were incubated with a solution of 2% BSA in 1 × PBS, whereas experimental samples were incubated with anti-GPC1 (1:240 dilution in a solution of 2% BSA in 1 × PBS, MAB8351; Abnova, Taipei, Taiwan) overnight in a rotator at 4 ºC. The next morning, the samples were spun at 12000 rpm for 2 min and the pellet was washed twice with 2% BSA in 1 × PBS, with centrifugation at 12000 rpm for 2 min between washes. Following incubation with an Alexa-488-tagged secondary antibody (anti-mouse A-21202; Thermo Fisher Scientific) for 30 min with continuous rotation at room temperature of both control and experimental samples, samples were washed again twice with 2% BSA in 1 × PBS. Finally, samples were resuspended in 300 µL of 2% BSA in 1 × PBS for BD Accuri C6 or BD FACS Canto II analysis (BD Biosciences, Haryana, IN, United States). Using the control samples of each patient (*i.e.* exosomes-bead complexes from each patient only incubated with secondary antibody) as a reference, the fluorescein isothiocyanate (FITC) voltage was adjusted until the percentage of FITC+ beads was 1%. Then, using the same gate and FITC voltage, the percentage of beads bound with $GPC1^+$ crExos in the experimental sample was determined for each patient separately. Data were analyzed using FlowJo software.

Statistical analyses

Categorical variables are described as absolute and relative frequencies and continuous variables as mean and standard deviation, median, percentiles, minimum, and maximum. Hypotheses were tested regarding the distribution of continuous variables *via* the independent samples *t*-test/one-way analysis of variance (ANOVA) or nonparametric Mann-Whitney and Kruskal-Wallis test depending on normal or non-normal distribution, respectively, and considering the nature of the hypothesis. The chi-squared and ANOVA tests were used for categorical variables analysis. Pearson's correlation coefficient was used to assess the statistical relationship/association between two continuous variables. The diagnostic accuracy of $GPC1^+$ crExos was assessed by receiver operating characteristic curve (ROC) considering 95% confidence intervals. Area under the ROC curve (AUROC) was calculated. SPSS® 27.0 (IBM Corp., Armonk, NY, United States) version was used. All graphs were created using GraphPad Prism 7.00 (GraphPad Software, San Diego, CA, United States). The statistical review of the study was performed by a biomedical statistician.

RESULTS

Population demographic characteristics

The baseline demographic characteristics of the 88 individuals included in the study (40 MCL, 20 HR, 20 NLOD, and 8 CG) are summarized in Table 1. The overall female:male ratio was 1.6:1 and did not differ statistically among groups. The mean age of the population was 60.3 ± 12.6 years. The older individuals belonged to the MCL group, with a median age of 67.2 ± 8.9 years, whereas the younger individuals were in the HR group, with a median age of 48.7 ± 10.8 years ($P < 0.001$). Patients in the NLOD group presented with a significantly higher BMI (29.9 ± 4.5 kg/m^2; $P < 0.001$).

Table 1 Baseline demographic characteristics of the study population, *n* = 88

Cohort characteristics	MCL, *n* = 40	HR, *n* = 20	NLOD, *n* = 20	CG, *n* = 8	Total, *n* = 88	*P* value
Sex						NS
Male	14 (35.0)	9 (45.0)	9 (45.0)	2 (25.0)	34 (38.6)	
Female	26 (65.0)	11 (55.0)	11 (55.0)	6 (75.0)	54 (61.4)	
Age in yr	67.2 ± 8.9	48.7 ± 10.8	60.8 ± 7.4	53.8 ± 18.7	60.3 ± 12.6	< 0.001
BMI in kg/m^2	24.9 ± 3.8	24.2 ± 3.9	29.9 ± 4.5	25.0 ± 4.0	25.9 ± 4.5	< 0.001
Smoking habits						NS
Never	27 (67.5)	13 (65.0)	12 (60.0)	7 (87.5)	59 (67.1)	
Ex-smoker, > 5 yr	8 (20.0)	4 (20.0)	7 (35.0)	1 (12.5)	20 (22.7)	
Active	5 (12.5)	3 (15.0)	1 (5.0)	0 (0.0)	9 (10.2)	
Alcohol habits						NS
No	22 (55.0)	11 (55.0)	10 (50.0)	7 (87.5)	50 (56.8)	
Yes	18 (45.0)	9 (45.0)	10 (50.0)	1 (12.5)	38 (43.2)	
Family history of PDAC						< 0.001
No	34 (85.0)	7 (35.0)	18 (90.0)	8 (100.0)	67 (76.1)	
Yes	6 (15.0)	13 (65.0)	2 (10.0)	0 (0.0)	21 (23.9)	

Data are presented as *n* (%) or mean ± SD. BMI: Body mass index; CG: Control group; HR: Hereditary risk; MCL: Mucinous cystic lesion; NLOD: New-late onset diabetes mellitus; NS: Non-significant; PDAC: Pancreatic ductal adenocarcinoma; SD: Standard deviation.

No statistically significant differences were observed in relation to smoking or drinking habits among the studied groups. Overall, 10.2% of the population were active smokers and 22.7% ex-smokers (more than 5 years of abstinence). In relation to alcohol consumption, 43.2% were considered active drinkers (average ingesting amounts of > 30 g or > 40 g alcohol *per* day, in case of female or male individuals, respectively).

Family history of PDAC was present in 23.9% of the entire population, with the highest proportion observed in the HR group (65.0%; $P < 0.001$). In the HR group, 17 (85.0%) individuals were diagnosed with Lynch Syndrome, 1 (5.0%) with Peutz-Jeghers syndrome, and the remaining 2 (10%) with FPC. Six individuals with Lynch Syndrome had a previous personal history of cancer, mostly colorectal ($n = 5$), but all were disease-free at the time of inclusion. Detailed information about this group, including the type of harbored mutation(s), can be found in Table 2. In the NLOD group, the mean time between inclusion in the study and establishment of DM diagnosis was 20.9 ± 8.6 mo.

EUS findings and other clinicopathological features

Main PA detected by EUS is illustrated in Figure 2A-F and constituted cystic lesions (with or without WF/HRS), CP-like parenchymal changes, and lipomatous transformation of pancreatic parenchyma. The EUS features of cystic lesions in the MCL group are described in Table 3. Of the 40 cases included, 39 (97.5%) were IPMNs, and most (89.8%) were classified as BD-IPMNs. Sixty percent of patients presented with multiple cysts, with a mean size of the dominant lesion of 28.1 ± 14.1 mm. In respect to WF and/or HRS, mural nodules, wall thickening, and a dilated MPD were identified in 10%, 7.5%, and 15% of the lesions, respectively. Nineteen of the forty MCL patients (47.5%) underwent additional study with MRCP.

The clinicopathological characteristics of the study population, particularly the type of PA found in EUS among the different groups, the results of EUS-guided tissue acquisition, surgical treatment and specimen analysis, as well as information on cancer detection during follow-up and mortality rate, are summarized in Table 4. Besides the MCL group, where PA in the form of cyst(s) were present in all patients by definition, PA were also detected during the EUS exam in 10.0% and 35.0% of the subjects belonging to HR and NLOD groups, respectively. Half of the lesions in the MCL group were considered to harbor WF or HRS, in contrast to the PA found in the other groups that were all "harmless" in terms of ultrasonographic appearance (CP-like parenchymal changes, lipomatous transformation and infracentimetric simple cystic lesions). EUS-FNA/B was performed only in the MCL group in 35 of the 40 patients (87.5%), either to confirm the diagnosis or in the presence of WF or HRS (Figure 2G and H). Malignancy was detected in 3 patients; in 1, the malignancy was detected in a subsequent EUS exam performed during follow-up (this case was previously reported by our team[38]). The result of cytological exam was considered inconclusive in 37.1% of the procedures. Of the 88 patients of the

Table 2 Characterization of hereditary risk group: Germline mutations and personal history of cancer, *n* = 20

	Lynch syndrome, *n* = 17 (85.0%)	Peutz-Jeghers syndrome, *n* = 1 (5.0%)	FPC, *n* = 2 (10.0%)
Germline mutation(s)			
MLH1	7 (41.2)	-	-
MSH2	6 (35.3)	-	-
MLH1 + *MSH2*	1 (5.9)	-	-
MSH2 + *MSH6*	2 (11.7)	-	-
MSH6	1 (5.9)	-	-
STK11	-	1 (100.0)	-
Not identified	-		2 (100.0)
Personal history of cancer			
No	11 (64.7)	1 (100.0)	2 (100.0)
Yes	6 (35.3)	0 (0.0)	0 (0.0)
Type of cancer			
Colon and rectum	5 (83.3%)	-	-
Endometrium	1 (16.7)	-	-

FPC: Familial pancreatic cancer.

Table 3 Endoscopic ultrasound features of cystic lesions among the mucinous cystic lesions group, *n* = 40

Type of mucinous cyst, *n* (%)	MCN	1 (2.5)
	IPMN	39 (97.5)
Type of IPMN, *n* (%)	MD-IPMN	2 (5.1)
	BD-IPMN	35 (89.8)
	MT-IPMN	2 (5.1)
Number of cysts, *n* (%)	Single	16 (40.0)
	Multiple	24 (60.0)
Main cyst size in mm, mean ± SD		28.1 ± 14.4
Main cyst size in mm, median (IQR)		21.5 (16.3-40.5)
Septa, *n* (%)	Absent	10 (25.0)
	Present	30 (75.0)
Mural nodules, *n* (%)	Absent	36 (90.0)
	Present	4 (10.0)
Wall thickening, *n* (%)	Absent	37 (92.5)
	Present	3 (7.5)
MPD caliber, *n* (%)	Normal	34 (85.0)
	Dilated	6 (15.0)

BD-IPMN: Branch-duct IPMN; IPMN: Intraductal papillary mucinous neoplasm; IQR: Interquartile range; MCN: Mucinous cystic neoplasm; MD-IPMN: Main-duct IPMN; MPD: Main pancreatic duct; MT-IPMN: Mixed type.

cohort, 15 (17.0%) were submitted to surgical resection, and all belonged to the MCL group. These 15 patients either harbored MD or MT-IPMNs or presented a cyst with WF/HRS with suspicious or positive cytology. Malignancy was confirmed in the surgical specimen in all 3 patients with a previous positive cytological exam, and the remaining 12 had a definitive histopathological diagnosis of a low grade dysplastic MCL.

Table 4 Clinical-pathological findings, treatment and follow-up of the study population, *n* = 88

	MCL, *n* = 40	HR, *n* = 20	NLOD, *n* = 20	CG, *n* = 8	Total, *n* = 88
PA in EUS					
No	0 (0.0)	18 (90.0)	13 (65.0)	8 (100.0)	39 (44.3)
Yes	40 (100.0)	2 (10.0)	7 (35.0)	0 (0.0)	49 (55.7)
Type of PA					
Cystic lesions	40 (100.0)	2 (100.0)	2 (28.6)	-	44 (89.8)
CP-like parenchymal changes	0 (0.0)	0 (0.0)	2 (28.6)	-	2 (4.1)
Solid lesions	0 (0.0)	0 (0.0)	0 (0.0)	-	0 (0.0)
Lipomatous transformation	0 (0.0)	0 (0.0)	3 (42.8)	-	3 (6.1)
PA with HRS / WF					
No	20 (50.0)	2 (100.0)	7 (100.0)	-	29 (59.2)
Yes	20 (50.0)	0 (0.0)	0 (0.0)	-	20 (40.8)
EUS FNA/B					
No	5 (12.5)	20 (100.0)	20 (100)	8 (100)	53 (60.2)
Yes	35 (87.5)	0 (0.0)	0 (0.0)	0 (0.0)	35 (39.8)
Inconclusive	13 (37.1)	-	-	-	13 (37.1)
Benign	19 (54.3)	-	-	-	19 (54.3)
Malignant	3 (8.6)[1]	-	-	-	3 (8.6)[1]
Surgery					
No	25 (62.5)	20 (100)	20 (100)	8 (100)	73 (83.0)
Yes	15 (37.5)	0 (0.0)	0 (0.0)	0 (0.0)	15 (17.0)
Benign/Malignant	12 (80.0)/3 (20.0)	-/-	-/-	-/-	12 (80.0)/3 (20.0)
F-up in mo	33.3 ± 12.8	34.9 ± 7.1	27.7 ± 4.7	36.1 ± 5.1	32.6 ± 10.0
Cancer detection during F-up	1 (2.5)	0 (0.0)	0 (0.0)	0 (0.0)	1 (1.1)
Mortality	5 (12.5)	0 (0.0)	0 (0.0)	0 (0.0)	5 (5.7)

Data are presented as *n* (%) or mean ± SD.

[1]One of 3 patients with malignant cytology was diagnosed during follow-up.

CG: Control group; CP: Chronic pancreatitis; EUS: Endoscopic ultrasound; FNA/B: Fine needle aspiration/biopsy; F-up: Follow up; HR: Hereditary risk; HRS: High risk stigmata; MCL: Mucinous cystic lesion; NLOD: New-late onset diabetes mellitus; NS: Non-significant; PA: Pancreatic abnormality; WF: Worrisome features.

The mean follow-up period of the entire cohort was 32 ± 8.6 mo and did not differ statistically among groups (*P* = NS). Five of the 88 individuals (5.7%) died during follow-up, but only one of these due to cancer progression. Two of the other deaths were related to post-operative complications in a 74-year-old and 75-year-old patients, one was related to a pulmonary carcinoma that developed 1 year after inclusion in a 72-year-old patient, and the remaining one corresponded to an 85-year-old patient that did not survive to an infectious respiratory insufficiency. The 2 other patients submitted to surgical resection of malignant cysts were alive and disease-free after 45 mo of follow-up.

Exosomal GPC1 levels are elevated in MCL lesions with WF/HRS and HR groups

The overall median levels of $GPC1^+$ crExos coupled to beads were statistically different among the studied groups: MCL [99.4%, interquartile range (IQR): 94.9%-99.8%], HR (82.0%, IQR: 28.9%-98.2%), and NLOD and CG groups (12.6%, IQR: 5.2%-63.4% and 16.2%, IQR: 6.6%-20.1%, respectively) ($P < 0.0001$) (Figure 3A and Table 5).

The crExos concentration and their median size were significantly higher in NLOD patients (6.05E+10/mL; IQR: 4.83-7.22 and 100.7 nm; IQR: 89.2-110.1, respectively) compared to all other groups ($P < 0.001$ and $P = 0.012$, respectively) (Figure 3B and C and Table 6).

In turn, overall median levels of CA 19-9 were 18.4 U/mL (IQR: 8.3-206) and did not differ statistically between groups: MCL: 20.4 U/mL (IQR: 14.0-35.8), HR: 16.9 U/mL (IQR: 11.7-18.1), NLOD: 18.8

Table 5 Biomarkers (glypican-1-positive circulating exosomes and carbohydrate antigen 19-9) profiles in the study groups, *n* = 88

Biomarker	MCL, *n* = 40	HR, *n* = 20	NLOD, *n* = 20	CG, *n* = 8	Total, *n* = 88	*P* value
$GPC1^+$ crExos, %						< 0.001
Median	99.4	82.0	12.6	16.2	86.8	
Min/Max	6.4/99.9	1.1/99.0	2.1/93.9	1.2/24.5	1.1/99.9	
IQR	94.9-99.8	28.9-98.2	5.2-63.4	6.6-20.1	18.6-99.4	
CA 19-9 in U/mL						NS
Median	20.4	16.9	18.8	30.6	18.4	
Min/Max	8.5/206.6	8.3/28.0	12.8-48.7	13.7-69.6	8.3/206.6	
IQR	14.0-35.8	11.7-18.1	16.6-23.4	15.0-40.8	14.2-27.7	

P value for Kruskal-Wallis test. CA 19-9: Carbohydrate antigen 19-9; CG: Control group; HR: Hereditary risk; IQR: Interquartile range; $GPC1^+$ crExos: Glypican-1 positive circulating exosomes; Max: Maximum; MCL: Mucinous cystic lesion; Min: Minimum; NLOD: New-late onset diabetes mellitus; NS: Non-significant.

Table 6 Size and concentration of exosomes according to the study groups, *n* = 88

	MCL, *n* = 40	HR, *n* = 20	NLOD, *n* = 20	CG, *n* = 8	Total, *n* = 88	*P* value
Size in nm						0.012
Median	82.5	94.7	100.7	72.8	90.5	
IQR	72.8-97.6	83.0-109.7	89.2-110.1	67.0-102.8	77.9-103.2	
Concentration as particles E + 10/mL						< 0.001
Median	3.48	3.36	6.05	3.30	4.10	
IQR	1.88-5.08	2.51-4.37	4.83-7.22	2.91-4.20	2.60-5.69	

P value for Kruskal-Wallis test. CG: Control group; HR: Hereditary risk; IQR: Interquartile range; MCL: Mucinous cystic lesion; NLOD: New-late onset diabetes mellitus.

U/mL (IQR: 12.8-48.7) and CG: 30.6 U/mL (IQR: 13.7-69.6) (*P* = NS) (Figure 3D and Table 5). All CA 19-9 median levels were considered in the normal range considering the clinical standard cut-off (37 U/mL).

We further investigated the profile of both biomarkers in a sub-analysis in two distinct settings. First, among the HR group, we evaluated $GPC1^+$ crExos and CA 19-9 levels according to the presence or absence of personal cancer history (Figure 4A and B). In the individuals with a positive history of cancer (5 colorectal and 1 cancer of the endometrium), although not statistically significant, we observed higher median levels of $GPC1^+$ crExos (97.9%; IQR: 61.7%-99.5%) compared to those with a negative history (*n* = 14) (59.7%; IQR: 26.3%-96.4%) (*P* = 0.21). In relation to CA 19-9 median levels, they did not differ among these two subgroups (17.5 U/mL; IQR: 10.7%-20.1% and 16.3 U/mL; IQR: 12.2%-19.5%, respectively) (*P* = NS).

Second, in the total number of patients harboring pancreatic cystic lesions (40 in the MCL group, 2 diagnosed in the HR group, and 2 in the NLOD group), we studied the levels of $GPC1^+$ crExos and CA 19-9 according to the presence or absence of WF/HRS in the EUS examination (Figure 4C and D). When WF or HRS were present (*n* = 20), patients presented with statistically significant higher median levels of $GPC1^+$ crExos (99.6%; IQR: 97.6%-99.8%) compared to those with endosonographic "harmless" lesions (*n* = 24) (96.5%; IQR: 81.3%-99.5%) (*P* = 0.011) (Figure 4C). The levels of $GPC1^+$ crExos presented an AUROC value of 0.723 in differentiating the group of cystic lesions with WF/HRS from those without (sensitivity 75.0% and specificity 67.7% for a cut-off of 98.5% (*P* = 0.012) (Figure 4E). CA 19-9 median levels did not statistically differ between these two subgroups (22.9 U/mL; IQR: 14.1-35.8 and 17.4 U/mL; IQR: 13.7-29.8, respectively) (*P* = NS) (Figure 4D).

DISCUSSION

MCLs are established as PDAC precursor lesions, with different risks considering morphologic

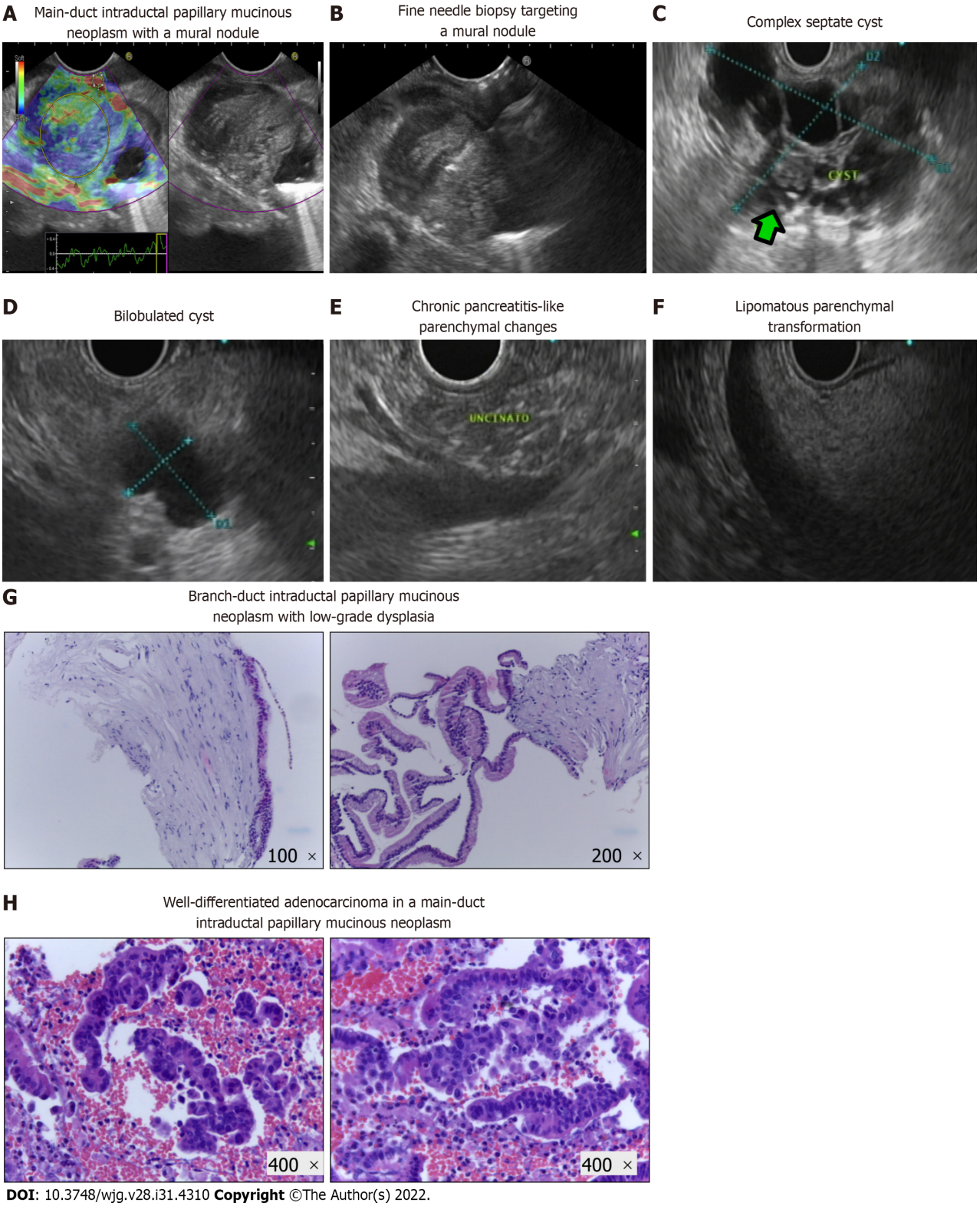

DOI: 10.3748/wjg.v28.i31.4310 **Copyright** ©The Author(s) 2022.

Figure 2 Pancreatic abnormalities in endoscopy ultrasound examination and pathological exams of endoscopic ultrasound-guided fine needle aspiration/biopsy specimens from intraductal papillary mucinous neoplasms. A: Main-duct intraductal papillary mucinous neoplasm (MD-IPMN) with a large mural nodule, visualized in B-mode (right panel) and characterized with qualitative elastography (left panel) that revealed areas of hard consistency (blue color); B: Endoscopic ultrasound-guided fine needle biopsy with a 22 G needle targeting the harder lesions in the described mural nodule (pathological exam showed malignant degeneration); C: Complex septate cyst with areas of wall focal thickenings and a mural nodule (green arrow); D: Simple bilobulated cyst without worrisome features or high-risk stigmata; E: Chronic pancreatitis-like parenchymal changes (lobulation, hyperechoic foci, and strands); F: Homogenous hyperechogenic appearance of pancreatic parenchyma suggestive of lipomatous transformation; G: Branch-duct IPMN with low-grade dysplasia [hematoxylin and eosin (H&E)-stained cellblock]. These images show the wall of a cystic lesion, partly lined by a cylindrical mucosecretory epithelium with low-grade atypia (left: 100 ×; right: 200 ×); H: Well-differentiated adenocarcinoma originated in a MD-IPMN (H&E-stained cellblock: 400 ×). These images show an epithelial neoplasm with marked architectural disorganization and severe cytological atypia. The cells have a high nucleus-cytoplasmic ratio, with anisokaryosis, irregular nuclei

with coarse chromatin and some with an exuberant nucleolus.

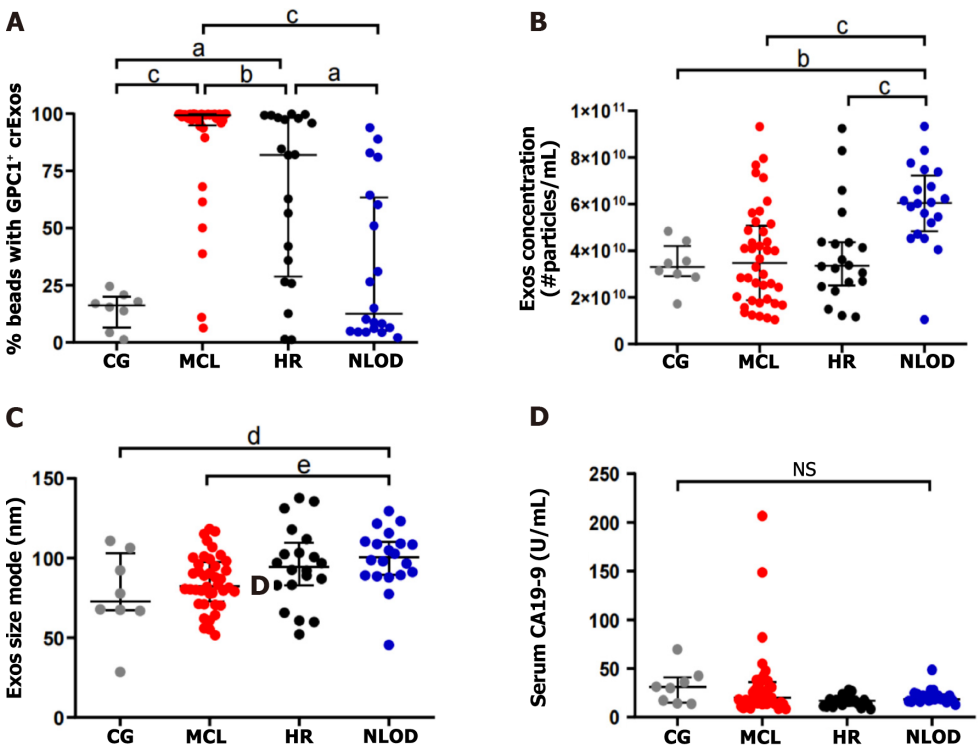

DOI: 10.3748/wjg.v28.i31.4310

Figure 3 Glypican-1-positive circulating exosomes levels are different among the studied groups, whereas the levels of carbohydrate antigen 19-9 do not differ and are within the normal range in the entire population. A: Scatter dot plot representing the percentage of beads bound to glypican-1-positive exosomes (GPC1$^+$ crExos) in the control group (CG) (n = 8), mucinous cystic lesions (MCLs) (n = 40), hereditary risk (HR) (n = 20) and new-late onset diabetes mellitus (NLOD) (n = 20), (Mann-Whitney U Test, $^aP < 0.02$, $^bP = 0.005$, $^cP < 0.001$); B: Scatter dot plot representing exosomes concentration measured by nanoparticle tracking analysis depicting the number of exosomes/0.666 mL serum derived from CG (n = 8), MCL (n = 40), HR (n = 20), and NLOD (n = 20) donors (Mann-Whitney U Test, $^bP = 0.005$, $^cP < 0.001$); C: Scatter dot plot representing exosomes mode size distribution determined by nanoparticle tracking analysis from CG (n = 8), MCL (n = 40), HR (n = 20), and NLOD (n = 20) donors (Mann-Whitney U Test, $^dP = 0.018$, $^eP = 0.04$); D: Scatter dot plot representing the serum carbohydrate antigen 19-9 concentration (U/mL) as determined by enzyme-linked immunoassay in CG (n = 8), MCL (n = 40), HR (n = 20), and NLOD (n = 20), (Kruskal-Wallis Test, P = NS). Data are shown as the median ± interquartile range. NS: Non-significant; GPC1: Glypican-1; CA 19-9: Carbohydrate antigen 19-9; crExos: Circulating exosomes.

appearance as well as cytological findings resulting from guided tissue acquisition. While the diagnostic and management of pancreatic cysts differs between international guidelines[29,39-42], they all agree that the risk of malignancy should be based, essentially, in the assessment of the classical WF/HRS, which was initially defined in the Fukuoka consensus[43].

Our cohort mainly constituted IPMNs, most of which were BD-IPMN type and half of the lesions presented with WF and/or HRS[29]. Malignancy was suspected by EUS in two advanced lesions with main duct involvement, which were confirmed by cytology. Interestingly, the third confirmed malignant cyst corresponded to a case we have previously reported[38], and was diagnosed during a follow-up examination of an apparently "inoffensive" cystic lesion in the index EUS. Our results have confirmed the limited utility of the use of cytology alone for cyst etiological characterization[44,45], as 37% of the results of EUS-FNA of the cyst fluid were considered inconclusive by pathologists. This limitation of cyst fluid cytological analysis tends to be overwhelmed by the referral for surgical resection of indeterminate suspicious lesions. In fact, 15 of the 40 patients with MCL proposed for surgical treatment, after evaluation by a multidisciplinary team, corresponded to 3 cases with a positive cytology for malignancy and 12 patients with indeterminate/inconclusive results of EUS-FNA. The surgical specimen confirmed malignancy in all 3 cases with previous diagnosis and in the remaining 12 revealed benign IPMNs with low grade dysplasia. The overtreatment of some of these patients is an important issue, as the morbidity and mortality of pancreatic surgery is not negligible[46,47]. In the present cohort, 2 of the 5 deaths recorded were precisely due to complications after surgery, both in patients harboring benign lesions. This observation supports the drive of research, justifying the need to evaluate the role of upcoming biomarkers, like exosomal GPC1, in complement with EUS evaluation, for the stratification of MCL, ultimately contributing to refine the criteria for surgical treatment or continued surveillance. In

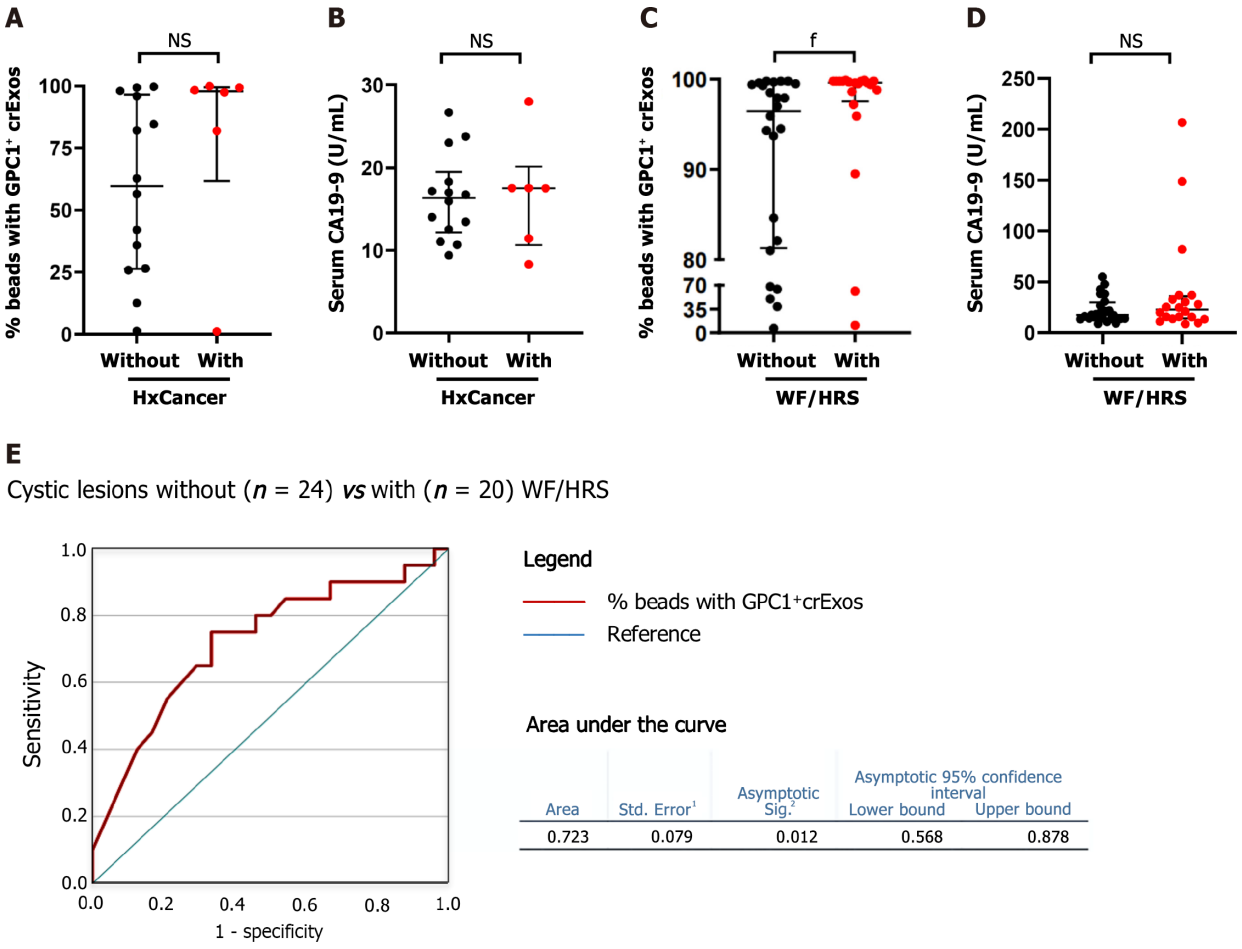

DOI: 10.3748/wjg.v28.i31.4310

Figure 4 Glypican-1-positive circulating exosomes are higher in individuals with personal history of cancer within the hereditary risk group, and among patients harboring pancreatic cystic lesions when worrisome features/high-risk stigmata are present. A: Scatter dot plot representing the percentage of beads bound to glypican-1 (GPC1)-positive circulating exosomes (GPC1⁺ crExos) in subjects in the hereditary risk (HR) group, without (n = 14) and with (n = 6) a personal history of cancer (HxCancer) [Mann-Whitney U Test, P = non-significant (NS)]; B: Scatter dot plot representing the serum carbohydrate antigen 19-9 (CA 19-9) concentration (U/mL) as determined by enzyme-linked immunoassay (ELISA) in subjects in the HR group, without (n = 14) and with (n = 6) HxCancer (Mann-Whitney U Test, P = 0.21); C: Scatter dot plot representing the percentage of GPC1⁺ crExos coupled to beads in subjects harboring pancreatic cystic lesions, without (n = 24) and with (n = 20) worrisome features (WF) or high-risk stigmata (HRS) (Mann-Whitney U Test, [f]P = 0.011); D: Scatter dot plot representing the serum CA 19-9 concentration (U/mL) as determined by ELISA in subjects harboring pancreatic cystic lesions, without (n = 24) and with (n = 20) WF/HRS (Mann-Whitney U Test, P = NS); E: Receiver operating characteristic curve of the cohort of pancreatic cystic lesions without (n = 24) or with (n = 20) WF/HRS, regarding the GPC1⁺ crExos levels (% beads with GPC1⁺ crExos). [1]Under nonparametric assumption; [2]Null hypothesis: True area = 0.5. Data are shown as the median ± interquartile range. NS: Non-significant; GPC1: Glypican-1; crExos: Circulating exosomes; WF: Worrisome features; HRS: High-risk stigmata.

this setting, our preliminary results initially reported were promising, as the levels of GPC1⁺ crExos were equally elevated in patients with PDAC and with MCLs[48,49]. The findings in the present study confirm these observations, as the median levels of GPC1⁺ crExos observed in the MCL group (significantly higher than in the other studied groups) were in the same magnitude as the ones registered for PDAC patients, that we have recently reported using the same methodology[28]. Moreover, when we analyzed the levels GPC1⁺ crExos among all pancreatic cystic lesions (MCL group plus those detected in the screening EUS in HR and NLOD groups), we found that they were statistically more elevated when WF/HRS were present, suggesting that this biomarker can, in fact, have a role in the risk stratification of these PDAC precursor lesions.

This is the first study to access the profile of GPC1⁺ crExos in HR and NLOD individuals, and our results showed that the median levels of this biomarker were statistically more elevated among the HR group when compared to NLOD patients and controls. Considering our previous published observations[28], these levels of GPC1⁺ crExos in HR individuals were also higher than those registered among patients with CP (28.4%), but not as elevated as in those with PDAC (99.7%). Interestingly, our results also showed a tendency of the individuals with a history of previous cancer (mainly colorectal) to present higher levels of GPC1⁺ crExos when compared to those without. While PA were detected in only 10% among HR individuals, all representing simple cystic lesions, these observations may suggest a potential role of GPC1⁺ crExos as a marker of genetically determined predisposition for cancer development, even in the absence of "harmful" pancreatic lesions.

Important studies have recently been published[24-26] and prospective investigational projects are ongoing[50] demonstrating the importance to access the magnitude of the risk to develop PDAC among NLOD patients and to define PDAC incidence during long-term follow-up. This justified the inclusion of NLOD patients in our investigation cohort. We found PA in EUS in 35% of the NLOD patients, comprising simple cystic lesions, CP-like changes and lipomatous parenchymal transformations, all of them considered "harmless", not requiring further investigation. Despite the highest median values of exosomes' size and particle concentration being registered in this group, the percentage of crExos positive for GPC1 was low and not statistically different from the CG. This finding is in accordance with the lack of sufficient evidence, at the present, to include these patients in regular screening programs for PDAC early detection.

Some limitations of this study should be pointed out, namely the sample size, the possibility of a referral bias giving the nature of our tertiary center, the relatively short period of patients' follow-up, and the cut-off found to stratify patients with cystic lesions and WF/HRS from those without. Also, the impossibility to include PanIN lesions in the study that would certainly power the analysis of GPC1 profile among PDAC pathological precursors. Lastly, the technique of exosomes isolation and analysis can still hamper its translation to clinical use. Despite these restraints, our results open the door for future studies to determine the value of this biomarker in the stratification of risk groups.

CONCLUSION

In summary, we demonstrate that GPC1$^+$ crExos levels are elevated in MCL, in the same magnitude of PDAC patients. These levels were statistically higher in cysts harboring WF/HRS. High levels were also registered among individuals with HR for PDAC (predominantly in those with history of previous cancer). Longitudinal studies will clarify the potential of exosomal GPC1 as a biomarker for the diagnosis and stratification of PDAC precursor lesions, as well as in signaling individuals with genetic predisposition for this neoplasia, ultimately contributing to refine screening and surveillance strategies.

ARTICLE HIGHLIGHTS

Research background

Most of the patients with pancreatic ductal adenocarcinoma (PDAC) are diagnosed with advanced disease at which stage treatment is inefficient. In order to improve survival, new strategies to identify and stratify individuals at risk of developing PDAC [*i.e.* individuals with hereditary risk (HR), mucinous cystic lesions (MCLs) and new-late onset diabetes mellitus (NLOD)] are urgently needed. Endoscopic ultrasound (EUS) is one of the imaging modalities with better performance for the study of the pancreas. In turn, carbohydrate antigen 19-9 (CA 19-9), the only biomarker approved for clinical use, is still imperfect as it lacks sensitivity and specificity. Glypican-1 (GPC1) represents a promising candidate since it has been demonstrated to be overexpressed in circulating exosomes (crExos) of patients with PDAC, possibly allowing early detection.

Research motivation

To contribute to further evaluate the capacity of GPC1$^+$ crExos to act as a potential biomarker for the investigation of individuals at risk for PDAC development, allowing for the early detection of the disease or its high-grade precursor lesions. Ultimately, we aim to contribute to improve patient's survival.

Research objectives

We aimed to determine the capacity of GPC1$^+$ crExos to identify individuals at higher risk to develop PDAC by comparing EUS pancreatic abnormalities (PA) with its levels within specific risk groups: HR, MCL and NLOD.

Research methods

We conducted a cross-sectional study with a prospective unicentric cohort including individuals with HR, MCL and NLOD, along with a control group (CG). All subjects were submitted to EUS at time of inclusion, with detailed characterization of detected PA. At the same time, blood samples were analyzed for GPC1$^+$ crExos and CA 19-9 by flow cytometry and ELISA, respectively. EUS-guided tissue acquisition was performed whenever necessary. SPSS® 27.0 version was used for statistical analysis and all graphs were created using GraphPad Prism 7.

Research results

We found that: Individuals harboring MCL globally presented with the highest levels of GPC1$^+$ crExos;

these levels were increased in the presence of worrisome features and or high-risk stigmata characterized by EUS; GPC1$^+$ crExos levels were also elevated among individuals with HR for PDAC (predominantly in those with personal history of cancer), even in absence of harmful PA in EUS examination; and NLOD patients presented with GPC1$^+$ crExos levels as low as those observed in the CG.

Research conclusions

Our study supports the role of GPC1$^+$ crExos in the diagnosis and stratification of PDAC precursor lesions, namely MCL, and its eventual capacity in signaling individuals with genetic predisposition for this neoplasia, even when no harmful PA are detected by EUS.

Research perspectives

Our data encourage longitudinal studies to confirm the potential of exosomal GPC1 as a biomarker to be used in the future in the management of individuals at risk for PDAC.

ACKNOWLEDGEMENTS

The authors acknowledge the support of the Translational Cytometry i3S Scientific Platform and the collaboration of Catarina Meireles MD, Elvira Sampaio MD, Liliana Silva MD and Mariana Santos MD in patient management.

FOOTNOTES

Author contributions: Moutinho-Ribeiro P was the main project investigator, was responsible for patient selection and sample collection, performed pancreatic endoscopic ultrasound, and wrote the initial manuscript; Batista IA participated in the sample processing, supervised and collected the data, performed the data analyses, and supported the manuscript writing; Quintas ST participated in the sample processing, data collection and analyses, assembled the figures, and supported the manuscript writing; Adem B participated in the sample processing and supported the data analyses; Silva M participated in the data collection and performed the statistical analyses; Morais R, Peixoto A, Coelho R, Costa-Moreira P, and Medas R participated in patient observation, data collection, and database management; Medas R performed the statistical analyses; Lopes S and Vilas-Boas F performed the pancreatic endoscopic ultrasound; Baptista M, Dias-Silva D, Esteves AL, and Martins F participated in patient observation and data collection; Lopes J, Barroca H, and Carneiro F performed the cytological and histological examination of the pancreatic specimens; Macedo G conceived and designed the study, interpreted the data analyses, and critically reviewed the manuscript; Melo SA conceived and designed the study, supervised the data analyses, and critically reviewed the manuscript; All authors approved the final version to be published.

Supported by Guilherme Macedo team was supported by the Portuguese Society of Digestive Endoscopy (SPED) 2017 Research Grant, No. SG/CHSJ-A2017; Norte Portugal Regional Programme (NORTE 2020) under the PORTUGAL 2020 Partnership Agreement through the European Regional Development Fund (ERDF) to Sonia A Melo, No. NORTE-01-0145-FEDER-000029; National Funds through Foundation for Science and Technology (FCT) to Sonia A Melo, No. POCI-01-0145-FEDER-32189; and Foundation for Science and Technology (FCT) to Bárbara Adem and Ines A Batista, No. PD/BD/135546/2018 and No. SFRH/BD/144854/2019.

Institutional review board statement: This study was reviewed and approved by the Ethics Committee of *Centro Hospitalar Universitário de São João* (CHUSJ), Porto, Portugal, No. CES 327-15.

Informed consent statement: All study participants or their legal guardian provided informed written consent about personal and medical data collection prior to study enrolment.

Conflict-of-interest statement: Sónia A Melo holds patents in the field of exosomes biology and are licensed to Codiak Biosciences, Inc. All other authors have no conflicts of interest to declare.

Data sharing statement: No additional data are available.

Country/Territory of origin: Portugal

ORCID number: Pedro Moutinho-Ribeiro 0000-0002-4782-6489; Ines A Batista 0000-0003-0321-7902; Sofia T Quintas 0000-0002-4190-3527; Bárbara Adem 0000-0003-0398-1185; Marco Silva 0000-0001-8215-1213; Rui Morais 0000-0003-1293-3353;

Armando Peixoto 0000-0003-3994-2882; Rosa Coelho 0000-0003-2706-2351; Pedro Costa-Moreira 0000-0003-0981-2497; Renato Medas 0000-0002-1892-2666; Susana Lopes 0000-0002-0407-6016; Filipe Vilas-Boas 0000-0001-7041-0863; Manuela Baptista 0000-0002-4306-769X; Diogo Dias-Silva 0000-0001-7367-6915; Ana L Esteves 0000-0001-8844-7939; Filipa Martins 0000-0002-5753-9811; Joanne Lopes 0000-0002-2339-2823; Helena Barroca 0000-0001-5684-3523; Fátima Carneiro 0000-0002-1964-1006; Guilherme Macedo 0000-0002-9387-9872; Sonia A Melo 0000-0002-2291-4263.

S-Editor: Fan JR
L-Editor: Filipodia
P-Editor: Fan JR

REFERENCES

1 **Sung H**, Ferlay J, Siegel RL, Laversanne M, Soerjomataram I, Jemal A, Bray F. Global Cancer Statistics 2020: GLOBOCAN Estimates of Incidence and Mortality Worldwide for 36 Cancers in 185 Countries. *CA Cancer J Clin* 2021; **71**: 209-249 [PMID: 33538338 DOI: 10.3322/caac.21660]
2 **Moutinho-Ribeiro P**, Coelho R, Giovannini M, Macedo G. Pancreatic cancer screening: Still a delusion? *Pancreatology* 2017; **17**: 754-765 [PMID: 28739291 DOI: 10.1016/j.pan.2017.07.001]
3 **Singhi AD**, Koay EJ, Chari ST, Maitra A. Early Detection of Pancreatic Cancer: Opportunities and Challenges. *Gastroenterology* 2019; **156**: 2024-2040 [PMID: 30721664 DOI: 10.1053/j.gastro.2019.01.259]
4 **Moutinho-Ribeiro P**, Iglesias-Garcia J, Gaspar R, Macedo G. Early pancreatic cancer - The role of endoscopic ultrasound with or without tissue acquisition in diagnosis and staging. *Dig Liver Dis* 2019; **51**: 4-9 [PMID: 30337098 DOI: 10.1016/j.dld.2018.09.027]
5 **Bhutani MS**, Koduru P, Joshi V, Saxena P, Suzuki R, Irisawa A, Yamao K. The role of endoscopic ultrasound in pancreatic cancer screening. *Endosc Ultrasound* 2016; **5**: 8-16 [PMID: 26879161 DOI: 10.4103/2303-9027.175876]
6 **Luz LP**, Al-Haddad MA, Sey MS, DeWitt JM. Applications of endoscopic ultrasound in pancreatic cancer. *World J Gastroenterol* 2014; **20**: 7808-7818 [PMID: 24976719 DOI: 10.3748/wjg.v20.i24.7808]
7 **Hruban RH**, Maitra A, Kern SE, Goggins M. Precursors to pancreatic cancer. *Gastroenterol Clin North Am* 2007; **36**: 831-849, vi [PMID: 17996793 DOI: 10.1016/j.gtc.2007.08.012]
8 **Pereira SP**, Oldfield L, Ney A, Hart PA, Keane MG, Pandol SJ, Li D, Greenhalf W, Jeon CY, Koay EJ, Almario CV, Halloran C, Lennon AM, Costello E. Early detection of pancreatic cancer. *Lancet Gastroenterol Hepatol* 2020; **5**: 698-710 [PMID: 32135127 DOI: 10.1016/S2468-1253(19)30416-9]
9 **Al-Hawary MM**, Francis IR, Chari ST, Fishman EK, Hough DM, Lu DS, Macari M, Megibow AJ, Miller FH, Mortele KJ, Merchant NB, Minter RM, Tamm EP, Sahani DV, Simeone DM. Pancreatic ductal adenocarcinoma radiology reporting template: consensus statement of the society of abdominal radiology and the american pancreatic association. *Gastroenterology* 2014; **146**: 291-304.e1 [PMID: 24355035 DOI: 10.1053/j.gastro.2013.11.004]
10 **Ballehaninna UK**, Chamberlain RS. The clinical utility of serum CA 19-9 in the diagnosis, prognosis and management of pancreatic adenocarcinoma: An evidence based appraisal. *J Gastrointest Oncol* 2012; **3**: 105-119 [PMID: 22811878 DOI: 10.3978/j.issn.2078-6891.2011.021]
11 **Yadav DK**, Bai X, Yadav RK, Singh A, Li G, Ma T, Chen W, Liang T. Liquid biopsy in pancreatic cancer: the beginning of a new era. *Oncotarget* 2018; **9**: 26900-26933 [PMID: 29928492 DOI: 10.18632/oncotarget.24809]
12 **Buscail E**, Maulat C, Muscari F, Chiche L, Cordelier P, Dabernat S, Alix-Panabières C, Buscail L. Liquid Biopsy Approach for Pancreatic Ductal Adenocarcinoma. *Cancers (Basel)* 2019; **11** [PMID: 31248203 DOI: 10.3390/cancers11060852]
13 **Melo SA**, Luecke LB, Kahlert C, Fernandez AF, Gammon ST, Kaye J, LeBleu VS, Mittendorf EA, Weitz J, Rahbari N, Reissfelder C, Pilarsky C, Fraga MF, Piwnica-Worms D, Kalluri R. Glypican-1 identifies cancer exosomes and detects early pancreatic cancer. *Nature* 2015; **523**: 177-182 [PMID: 26106858 DOI: 10.1038/nature14581]
14 **Lewis JM**, Vyas AD, Qiu Y, Messer KS, White R, Heller MJ. Integrated Analysis of Exosomal Protein Biomarkers on Alternating Current Electrokinetic Chips Enables Rapid Detection of Pancreatic Cancer in Patient Blood. *ACS Nano* 2018; **12**: 3311-3320 [PMID: 29570265 DOI: 10.1021/acsnano.7b08199]
15 **Xiao D**, Dong Z, Zhen L, Xia G, Huang X, Wang T, Guo H, Yang B, Xu C, Wu W, Zhao X, Xu H. Combined Exosomal GPC1, CD82, and Serum CA19-9 as Multiplex Targets: A Specific, Sensitive, and Reproducible Detection Panel for the Diagnosis of Pancreatic Cancer. *Mol Cancer Res* 2020; **18**: 300-310 [PMID: 31662449 DOI: 10.1158/1541-7786.MCR-19-0588]
16 **Qian JY**, Tan YL, Zhang Y, Yang YF, Li XQ. Prognostic value of glypican-1 for patients with advanced pancreatic cancer following regional intra-arterial chemotherapy. *Oncol Lett* 2018; **16**: 1253-1258 [PMID: 29963198 DOI: 10.3892/ol.2018.8701]
17 **Zhou CY**, Dong YP, Sun X, Sui X, Zhu H, Zhao YQ, Zhang YY, Mason C, Zhu Q, Han SX. High levels of serum glypican-1 indicate poor prognosis in pancreatic ductal adenocarcinoma. *Cancer Med* 2018; **7**: 5525-5533 [PMID: 30358133 DOI: 10.1002/cam4.1833]
18 **Frampton AE**, Prado MM, López-Jiménez E, Fajardo-Puerta AB, Jawad ZAR, Lawton P, Giovannetti E, Habib NA, Castellano L, Stebbing J, Krell J, Jiao LR. Glypican-1 is enriched in circulating-exosomes in pancreatic cancer and correlates with tumor burden. *Oncotarget* 2018; **9**: 19006-19013 [PMID: 29721179 DOI: 10.18632/oncotarget.24873]
19 **Lucien F**, Lac V, Billadeau DD, Borgida A, Gallinger S, Leong HS. Glypican-1 and glycoprotein 2 bearing extracellular vesicles do not discern pancreatic cancer from benign pancreatic diseases. *Oncotarget* 2019; **10**: 1045-1055 [PMID: 30800217 DOI: 10.18632/oncotarget.26620]
20 **Canto MI**, Harinck F, Hruban RH, Offerhaus GJ, Poley JW, Kamel I, Nio Y, Schulick RS, Bassi C, Kluijt I, Levy MJ,

Chak A, Fockens P, Goggins M, Bruno M; International Cancer of Pancreas Screening (CAPS) Consortium. International Cancer of the Pancreas Screening (CAPS) Consortium summit on the management of patients with increased risk for familial pancreatic cancer. *Gut* 2013; **62**: 339-347 [PMID: 23135763 DOI: 10.1136/gutjnl-2012-303108]

21 **Goggins M**, Overbeek KA, Brand R, Syngal S, Del Chiaro M, Bartsch DK, Bassi C, Carrato A, Farrell J, Fishman EK, Fockens P, Gress TM, van Hooft JE, Hruban RH, Kastrinos F, Klein A, Lennon AM, Lucas A, Park W, Rustgi A, Simeone D, Stoffel E, Vasen HFA, Cahen DL, Canto MI, Bruno M; International Cancer of the Pancreas Screening (CAPS) consortium. Management of patients with increased risk for familial pancreatic cancer: updated recommendations from the International Cancer of the Pancreas Screening (CAPS) Consortium. *Gut* 2020; **69**: 7-17 [PMID: 31672839 DOI: 10.1136/gutjnl-2019-319352]

22 **Aslanian HR**, Lee JH, Canto MI. AGA Clinical Practice Update on Pancreas Cancer Screening in High-Risk Individuals: Expert Review. *Gastroenterology* 2020; **159**: 358-362 [PMID: 32416142 DOI: 10.1053/j.gastro.2020.03.088]

23 **Pannala R**, Leirness JB, Bamlet WR, Basu A, Petersen GM, Chari ST. Prevalence and clinical profile of pancreatic cancer-associated diabetes mellitus. *Gastroenterology* 2008; **134**: 981-987 [PMID: 18395079 DOI: 10.1053/j.gastro.2008.01.039]

24 **Sharma A**, Smyrk TC, Levy MJ, Topazian MA, Chari ST. Fasting Blood Glucose Levels Provide Estimate of Duration and Progression of Pancreatic Cancer Before Diagnosis. *Gastroenterology* 2018; **155**: 490-500.e2 [PMID: 29723506 DOI: 10.1053/j.gastro.2018.04.025]

25 **Sharma A**, Kandlakunta H, Nagpal SJS, Feng Z, Hoos W, Petersen GM, Chari ST. Model to Determine Risk of Pancreatic Cancer in Patients With New-Onset Diabetes. *Gastroenterology* 2018; **155**: 730-739.e3 [PMID: 29775599 DOI: 10.1053/j.gastro.2018.05.023]

26 **Boursi B**, Finkelman B, Giantonio BJ, Haynes K, Rustgi AK, Rhim AD, Mamtani R, Yang YX. A Clinical Prediction Model to Assess Risk for Pancreatic Cancer Among Patients With New-Onset Diabetes. *Gastroenterology* 2017; **152**: 840-850.e3 [PMID: 27923728 DOI: 10.1053/j.gastro.2016.11.046]

27 **Chari ST**, Leibson CL, Rabe KG, Ransom J, de Andrade M, Petersen GM. Probability of pancreatic cancer following diabetes: a population-based study. *Gastroenterology* 2005; **129**: 504-511 [PMID: 16083707 DOI: 10.1016/j.gastro.2005.05.007]

28 **Moutinho-Ribeiro P**, Adem B, Batista I, Silva M, Silva S, Ruivo CF, Morais R, Peixoto A, Coelho R, Costa-Moreira P, Lopes S, Vilas-Boas F, Durães C, Lopes J, Barroca H, Carneiro F, Melo SA, Macedo G. Exosomal glypican-1 discriminates pancreatic ductal adenocarcinoma from chronic pancreatitis. *Dig Liver Dis* 2021 [PMID: 34840127 DOI: 10.1016/j.dld.2021.10.012]

29 **Tanaka M**, Fernández-Del Castillo C, Kamisawa T, Jang JY, Levy P, Ohtsuka T, Salvia R, Shimizu Y, Tada M, Wolfgang CL. Revisions of international consensus Fukuoka guidelines for the management of IPMN of the pancreas. *Pancreatology* 2017; **17**: 738-753 [PMID: 28735806 DOI: 10.1016/j.pan.2017.07.007]

30 **Reddy RP**, Smyrk TC, Zapiach M, Levy MJ, Pearson RK, Clain JE, Farnell MB, Sarr MG, Chari ST. Pancreatic mucinous cystic neoplasm defined by ovarian stroma: demographics, clinical features, and prevalence of cancer. *Clin Gastroenterol Hepatol* 2004; **2**: 1026-1031 [PMID: 15551256 DOI: 10.1016/s1542-3565(04)00450-1]

31 **McCarty TR**, Garg R, Rustagi T. Pancreatic cyst fluid glucose in differentiating mucinous from nonmucinous pancreatic cysts: a systematic review and meta-analysis. *Gastrointest Endosc* 2021; **94**: 698-712.e6 [PMID: 33964311 DOI: 10.1016/j.gie.2021.04.025]

32 **Overbeek KA**, Levink IJM, Koopmann BDM, Harinck F, Konings ICAW, Ausems MGEM, Wagner A, Fockens P, van Eijck CH, Groot Koerkamp B, Busch ORC, Besselink MG, Bastiaansen BAJ, van Driel LMJW, Erler NS, Vleggaar FP, Poley JW, Cahen DL, van Hooft JE, Bruno MJ; Dutch Familial Pancreatic Cancer Surveillance Study Group. Long-term yield of pancreatic cancer surveillance in high-risk individuals. *Gut* 2022; **71**: 1152-1160 [PMID: 33820756 DOI: 10.1136/gutjnl-2020-323611]

33 **DaVee T**, Coronel E, Papafragkakis C, Thaiudom S, Lanke G, Chakinala RC, Nogueras González GM, Bhutani MS, Ross WA, Weston BR, Lee JH. Pancreatic cancer screening in high-risk individuals with germline genetic mutations. *Gastrointest Endosc* 2018; **87**: 1443-1450 [PMID: 29309780 DOI: 10.1016/j.gie.2017.12.019]

34 **American Diabetes Association**. 2. Classification and Diagnosis of Diabetes: *Standards of Medical Care in Diabetes-2021 . Diabetes Care* 2021; **44**: S15-S33 [PMID: 33298413 DOI: 10.2337/dc21-S002]

35 **Lorenzo D**, Rebours V, Maire F, Palazzo M, Gonzalez JM, Vullierme MP, Aubert A, Hammel P, Lévy P, de Mestier L. Role of endoscopic ultrasound in the screening and follow-up of high-risk individuals for familial pancreatic cancer. *World J Gastroenterol* 2019; **25**: 5082-5096 [PMID: 31558858 DOI: 10.3748/wjg.v25.i34.5082]

36 **Canto MI**, Hruban RH, Fishman EK, Kamel IR, Schulick R, Zhang Z, Topazian M, Takahashi N, Fletcher J, Petersen G, Klein AP, Axilbund J, Griffin C, Syngal S, Saltzman JR, Mortele KJ, Lee J, Tamm E, Vikram R, Bhosale P, Margolis D, Farrell J, Goggins M; American Cancer of the Pancreas Screening (CAPS) Consortium. Frequent detection of pancreatic lesions in asymptomatic high-risk individuals. *Gastroenterology* 2012; **142**: 796-804; quiz e14 [PMID: 22245846 DOI: 10.1053/j.gastro.2012.01.005]

37 **Pitman MB**, Centeno BA, Ali SZ, Genevay M, Stelow E, Mino-Kenudson M, Castillo CF, Schmidt CM, Brugge WR, Layfield LJ. Standardized terminology and nomenclature for pancreatobiliary cytology: The Papanicolaou Society of Cytopathology Guidelines. *Cytojournal* 2014; **11**: 3 [PMID: 25191517 DOI: 10.4103/1742-6413.133343]

38 **Moutinho-Ribeiro P**, Costa-Moreira P, Adem B, Batista I, Almeida M, Barroca H, Lopes J, Carneiro F, Melo SA, Macedo G. Exosomal glypican-1 for risk stratification of pancreatic cystic lesions: A case of pathological progression in the absence of any suspicious imaging finding. *Pancreatology* 2020; **20**: 571-575 [PMID: 32024605 DOI: 10.1016/j.pan.2020.01.015]

39 **Vege SS**, Ziring B, Jain R, Moayyedi P; Clinical Guidelines Committee; American Gastroenterology Association. American gastroenterological association institute guideline on the diagnosis and management of asymptomatic neoplastic pancreatic cysts. *Gastroenterology* 2015; **148**: 819-22; quize12 [PMID: 25805375 DOI: 10.1053/j.gastro.2015.01.015]

40 **Elta GH**, Enestvedt BK, Sauer BG, Lennon AM. ACG Clinical Guideline: Diagnosis and Management of Pancreatic Cysts. *Am J Gastroenterol* 2018; **113**: 464-479 [PMID: 29485131 DOI: 10.1038/ajg.2018.14]

41 **Megibow AJ**, Baker ME, Morgan DE, Kamel IR, Sahani DV, Newman E, Brugge WR, Berland LL, Pandharipande PV. Management of Incidental Pancreatic Cysts: A White Paper of the ACR Incidental Findings Committee. *J Am Coll Radiol*

2017; **14**: 911-923 [PMID: 28533111 DOI: 10.1016/j.jacr.2017.03.010]

42 **European Study Group on Cystic Tumours of the Pancreas**. European evidence-based guidelines on pancreatic cystic neoplasms. *Gut* 2018; **67**: 789-804 [PMID: 29574408 DOI: 10.1136/gutjnl-2018-316027]

43 **Tanaka M**, Fernández-del Castillo C, Adsay V, Chari S, Falconi M, Jang JY, Kimura W, Levy P, Pitman MB, Schmidt CM, Shimizu M, Wolfgang CL, Yamaguchi K, Yamao K; International Association of Pancreatology. International consensus guidelines 2012 for the management of IPMN and MCN of the pancreas. *Pancreatology* 2012; **12**: 183-197 [PMID: 22687371 DOI: 10.1016/j.pan.2012.04.004]

44 **Thornton GD**, McPhail MJ, Nayagam S, Hewitt MJ, Vlavianos P, Monahan KJ. Endoscopic ultrasound guided fine needle aspiration for the diagnosis of pancreatic cystic neoplasms: a meta-analysis. *Pancreatology* 2013; **13**: 48-57 [PMID: 23395570 DOI: 10.1016/j.pan.2012.11.313]

45 **Brugge WR**, Lewandrowski K, Lee-Lewandrowski E, Centeno BA, Szydlo T, Regan S, del Castillo CF, Warshaw AL. Diagnosis of pancreatic cystic neoplasms: a report of the cooperative pancreatic cyst study. *Gastroenterology* 2004; **126**: 1330-1336 [PMID: 15131794 DOI: 10.1053/j.gastro.2004.02.013]

46 **Nimptsch U**, Krautz C, Weber GF, Mansky T, Grützmann R. Nationwide In-hospital Mortality Following Pancreatic Surgery in Germany is Higher than Anticipated. *Ann Surg* 2016; **264**: 1082-1090 [PMID: 26978570 DOI: 10.1097/SLA.0000000000001693]

47 **Kimura W**, Miyata H, Gotoh M, Hirai I, Kenjo A, Kitagawa Y, Shimada M, Baba H, Tomita N, Nakagoe T, Sugihara K, Mori M. A pancreaticoduodenectomy risk model derived from 8575 cases from a national single-race population (Japanese) using a web-based data entry system: the 30-day and in-hospital mortality rates for pancreaticoduodenectomy. *Ann Surg* 2014; **259**: 773-780 [PMID: 24253151 DOI: 10.1097/SLA.0000000000000263]

48 **Moutinho-Ribeiro P**, Santos A, Batista I, Adem B, Silva S, Morais R, Coelho R, Lopes S, Vilas-Boas F, Baptista M, Barroca H, Machado J, Carneiro F, Melo SA, Macedo G. Exosomal Glypican-1 and Pancreatic Adenocarcinoma: Prime Time for Early Diagnosis? *Am J Gastroenterol* 2018; **113**: S44 [DOI: 10.14309/00000434-201810001-00079]

49 **Moutinho-Ribeiro P**, Silva S, Adem B, Silva M, Lopes S, Vilas-Boas F, Melo S, Macedo G. Glipican-1 circulating exosomes levels are higher in pancreatic adenocarcinoma and cystic mucinous neoplasms than in other associated risk groups for pancreatic cancer: Clues for early diagnosis? *Pancreatology* 2017; **17**: S63-S64 [DOI: 10.1016/j.pan.2017.07.219]

50 **Maitra A**, Sharma A, Brand RE, Van Den Eeden SK, Fisher WE, Hart PA, Hughes SJ, Mather KJ, Pandol SJ, Park WG, Feng Z, Serrano J, Rinaudo JAS, Srivastava S, Chari ST; Consortium for the Study of Chronic Pancreatitis, Diabetes, and Pancreatic Cancer (CPDPC). A Prospective Study to Establish a New-Onset Diabetes Cohort: From the Consortium for the Study of Chronic Pancreatitis, Diabetes, and Pancreatic Cancer. *Pancreas* 2018; **47**: 1244-1248 [PMID: 30325864 DOI: 10.1097/MPA.0000000000001169]

World Journal of Gastroenterology

Submit a Manuscript: https://www.f6publishing.com

World J Gastroenterol 2022 August 21; 28(31): 4328-4337

DOI: 10.3748/wjg.v28.i31.4328

ISSN 1007-9327 (print) ISSN 2219-2840 (online)

ORIGINAL ARTICLE

Basic Study

Duodenal-jejunal bypass reduces serum ceramides *via* inhibiting intestinal bile acid-farnesoid X receptor pathway

Zhi-Qiang Cheng, Tong-Ming Liu, Peng-Fei Ren, Chang Chen, Yan-Lei Wang, Yong Dai, Xiang Zhang

Specialty type: Gastroenterology and hepatology

Provenance and peer review: Unsolicited article; Externally peer reviewed

Peer-review model: Single blind

Peer-review report's scientific quality classification

Grade A (Excellent): 0
Grade B (Very good): B, B, B
Grade C (Good): 0
Grade D (Fair): 0
Grade E (Poor): 0

P-Reviewer: Becchetti C, Switzerland; Cereatti F, Italy; Pazos F, Spain

Received: March 11, 2022
Peer-review started: March 11, 2022
First decision: May 10, 2022
Revised: May 12, 2022
Accepted: July 25, 2022
Article in press: July 25, 2022
Published online: August 21, 2022

Zhi-Qiang Cheng, Chang Chen, Yan-Lei Wang, Yong Dai, Xiang Zhang, Department of General Surgery, Qilu Hospital of Shandong University, Jinan 250012, Shandong Province, China

Tong-Ming Liu, Department of Colorectal and Anal Surgery, Feicheng Hospital Affiliated to Shandong First Medical University, Feicheng 271600, Shandong Province, China

Peng-Fei Ren, Department of General Surgery, Lincheng People's Hospital, Dezhou 253500, Shandong Province, China

Corresponding author: Xiang Zhang, MD, PhD, Surgeon, Surgical Oncologist, Department of General Surgery, Qilu Hospital of Shandong University, No. 107 West Wenhua Road, Jinan 250012, Shandong Province, China. xiang.zhang02@hotmail.com

Abstract

BACKGROUND

Bile acids play an important role in the amelioration of type 2 diabetes following duodenal-jejunal bypass (DJB). Serum bile acids are elevated postoperatively. However, the clinical relevance is not known. Bile acids in the peripheral circulation reflect the amount of bile acids in the gut. Therefore, a further investigation of luminal bile acids following DJB is of great significance.

AIM

To investigate changes of luminal bile acids following DJB.

METHODS

Salicylhydroxamic acid (SHAM), DJB, and DJB with oral chenodeoxycholic acid (CDCA) supplementation were performed in a high-fat-diet/streptozotocin-induced diabetic rat model. Body weight, energy intake, oral glucose tolerance test, luminal bile acids, serum ceramides and intestinal ceramide synthesis were analyzed at week 12 postoperatively.

RESULTS

Compared to SHAM, DJB achieved rapid and durable improvement in glucose tolerance and led to increased total luminal bile acid concentrations with preferentially increased proportion of farnesoid X receptor (FXR) - inhibitory bile acids within the common limb. Intestinal ceramide synthesis was repressed with decreased serum ceramides, and this phenomenon could be partially antagonized by luminal supplementation of FXR activating bile acid CDCA.

CONCLUSION
DJB significantly changes luminal bile acid composition with increased proportion FXR-inhibitory bile acids and reduces serum ceramide levels. There observations suggest a novel mechanism of bile acids in metabolic regulation after DJB.

Key Words: Bariatric surgery; Duodenal-jejunal bypass; Farnesoid X receptor; Ceramide; Bile acids; Liver fat accumulation

Core Tip: Bile acids play an important role in the amelioration of type 2 diabetes following duodenal-jejunal bypass (DJB), and are elevated significantly in the serum postoperatively. Bile acids in the peripheral circulation reflect the amount of bile acids in the gut. Therefore, a further investigation of luminal bile acids following DJB is of great significance. Here we performed DJB in a high-fat diet/streptozotocin-induced diabetic rat model and demonstrated that DJB achieved rapid and durable improvement in glucose tolerance and led to increased total luminal bile acid concentrations with preferentially increased proportion of farnesoid X receptor (FXR) - inhibitory bile acids within the common limb. Intestinal ceramide synthesis was repressed with decreased serum ceramides, and this phenomenon could be partially antagonized by luminal supplementation of FXR activating bile acid (chenodeoxycholic acid). There observations suggest a novel mechanism of bile acids in metabolic regulation after DJB.

Citation: Cheng ZQ, Liu TM, Ren PF, Chen C, Wang YL, Dai Y, Zhang X. Duodenal-jejunal bypass reduces serum ceramides *via* inhibiting intestinal bile acid-farnesoid X receptor pathway. *World J Gastroenterol* 2022; 28(31): 4328-4337
URL: https://www.wjgnet.com/1007-9327/full/v28/i31/4328.htm
DOI: https://dx.doi.org/10.3748/wjg.v28.i31.4328

INTRODUCTION

Duodenal-jejunal bypass (DJB) can induce rapid and durable amelioration of type 2 diabetes mellitus[1-3]. The underlying mechanisms remain incompletely understood. Our previous research has proved that bile acids play an important role in the amelioration of type 2 diabetes following DJB[4], and found that serum taurine-conjugated bile acids are preferentially elevated postoperatively[5]. However, the clinical relevance of the specific alterations of serum bile acids is still not known. Bile acids in the peripheral circulation reflect the amount of bile acids that could not be totally reabsorbed by hepatocytes during the enterohepatic circulation[6]. Therefore, the alterations of serum bile acids might be a secondary change of the bile acids within the gut, and a further investigation of luminal bile acids following DJB is of great significance.

Bile acids are traditionally known as lipid absorption-facilitating agents. It was not until recent years that the role of bile acids as signaling molecules in modulating metabolism has be unveiled. The intestinal lumina, where bile acid concentrations are high, is the main place for bile acid signaling. Two major receptors, including Takeda G-protein-coupled receptor 5 (TGR5) and nuclear farnesoid X receptor (FXR) are responsible for luminal bile acid sensing. TGR5 expression is detected in a variety of enteroendocrine cells and acute exposure of TGR5 to luminal bile acids lead to significant secretion of glucagon-like peptide 1 (GLP-1), which is a vital hormone for maintaining normal incretin effect in type 2 diabetes[7,8]. The interaction between bile acids and FXR is more complicated, as different subtypes of bile acids have distinct effect on the downstream pathway of FXR[9]. Chenodeoxycholic acid (CDCA) represents the most potent FXR stimulator while ursodeoxycholic acid (UDCA) and β-muricholic acid (β MCA) are FXR inhibitors[9-11]. Therefore, the net effect of luminal bile acids on FXR depends on the proportion of FXR-stimulating bile acids rather than the total amount of bile acids.

Intestinal FXR could affect lipid metabolism and this process is closely related to ceramide synthesis. Intestine-selective FXR inhibition downregulates the expression of ceramide synthesis-related genes sphingomyelin phosphodiesterase 3 (Smpd3) and serine palmitoyltransferase long chain base subunit 2 (Sptlc2), resulting in decreased concentrations of ceramides within the small intestine, portal system and peripheral circulation[12]. Decreased ceramides inhibit the expression of sterol regulatory element binding protein-1 (SREBP-1) in the liver[12], which is a key enzyme in the process of hepatic fat accumulation. Coincidentally, the changes in lipid metabolism after intestine-selective FXR inhibition is similar to the changes following DJB that hepatic fat accumulation is alleviated and the key transcriptional regulators and enzymes involved in hepatic *de novo* lipogenesis are downregulated[13]. Therefore, we

hypothesized that the net effect of luminal bile acids on intestinal FXR might be inhibitory after DJB which leads to decreased ceramide synthesis. To test this hypothesis, we measure the changes of individual luminal bile acid and ceramide concentrations within the enterohepatic circulation after DJB in a high-fat diet (HFD)/streptozotocin (STZ)-induced diabetic rat model.

MATERIALS AND METHODS

Animals and surgical procedures

Eight-week-old male Wistar rats (220 g on average, purchased from Huafukang Biotech, China) were individually housed with a 12 h light/dark cycle under constant temperature (24-26 °C) and humidity (50%-70%). All rats were fed with HFD (42% carbohydrate, 18% protein and 40% fat, as a total percentage of calories, Huafukang Biotech, China) with no restriction to tap water for 1 mo to induce insulin resistance. After fasting for 12 h, 30 mg/kg STZ (Sigma Aldrich, United States) dissolved in sodium citrate buffer (pH 4.2) was injected into the peritoneal cavity. Random blood glucose concentrations were measured with a glucometer (Roche Diagnostics, Germany) from tail veins 72 h later. Thirty rats with random blood glucose ≥ 16.7 mmol/L were considered diabetic and were matched into salicylhydroxamic acid (SHAM) group (n = 10), DJB group (n = 10) and DJB + CDCA group (n = 10). One month later, surgery was performed as we previously reported[5]. Body weight and calorie intake were recorded daily. All rats were sacrificed after 12 h fasting at week 12 postoperatively. All procedures involving animals were reviewed and approved by the Ethics Committee on Animal Experiment of Shandong University Qilu Hospital.

CDCA gavage

Without fasting, rats in the DJB + CDCA group were administrated with CDCA suspension (100 mg/kg suspended in 3 mL tap water) by intragastric gavage three times a week since week 5 postoperatively. The gavage procedure ceased after week 11.

Oral glucose tolerance test

At week 4 and week 12, after 12 h fasting, the rats were administrated with 20% of glucose (1 g/kg) by intragastric gavage. Blood glucose concentrations were measured at t = 0, 10, 30, 60 and 120 min.

Blood sample preparation

Peripheral blood samples were collected from the retrobulbar venous plexus after 12 h fasting before sacrificing. Portal venous blood samples were collected directly from the portal vein. After centrifugation, the supernatant was stored at -80 °C until analysis.

Luminal bile acid detection

Three independent intestinal segments (3 cm each) was excised at the proximal, medium and distal sites within the common limb, respectively, without prior flushing. The control intestinal segments from SHAM group were excised at the corresponding anatomic location. Total luminal bile acids from intestinal segments were extracted by 9 mL 50 % tert-butyl alcohol for 1 h at 37 °C. After centrifugation, the supernatant was collected for bile acid analysis. Total bile acids were measured by Roche Cobas 8000 system using enzyme cycling method and individual bile acid species was measured using high-pressure liquid chromatography coupled with tandem mass spectrometry as we previously described [5].

Western blot

Small intestinal mucosa were flushed with saline and then scratched. Total protein was extracted by RIPA lysis buffer (KeyGEN, China) with protease and phosphatase inhibitor cocktail (KeyGEN, China) and was quantified using bicinchoninic acid protein assay kit (Beyotime, China). Equivalent amount of small intestinal mucosal protein were loaded on 10% sodium dodecyl sulfate-polyacrylamide gel electrophoresis gels (Bio-Rad, United States) and separated by electrophoresis. Then, proteins were transferred onto 0.45 μm polyvinylidene fluoride membranes (Millipore, Ireland). After being blocked in 5 % skim milk powder (Beyotime, China) for 2 h, the membranes were incubated with primary antibodies to Smpd3 (Abcam, United Kingdom) and Sptlc2 (Invitrogen, United States) overnight, followed by incubation in horseradish peroxidase-conjugated secondary antibodies (Proteintech, China) for 60 min. The protein bands were visualized by ECL solution (Millipore, United States) and their density was assessed with LI-COR Odyssey Imager (LI-COR Biosciences, United States).

RNA analysis

The expression of smpd3 and sptlc2 in the small intestine was analyzed by real-ime quantitative polymerase chain reaction (RT-qPCR). RNA was isolated using Trizol reagent (Invitrogen, United States), and the concentration of RNA was measured using the NanoDrop spectrophotometer

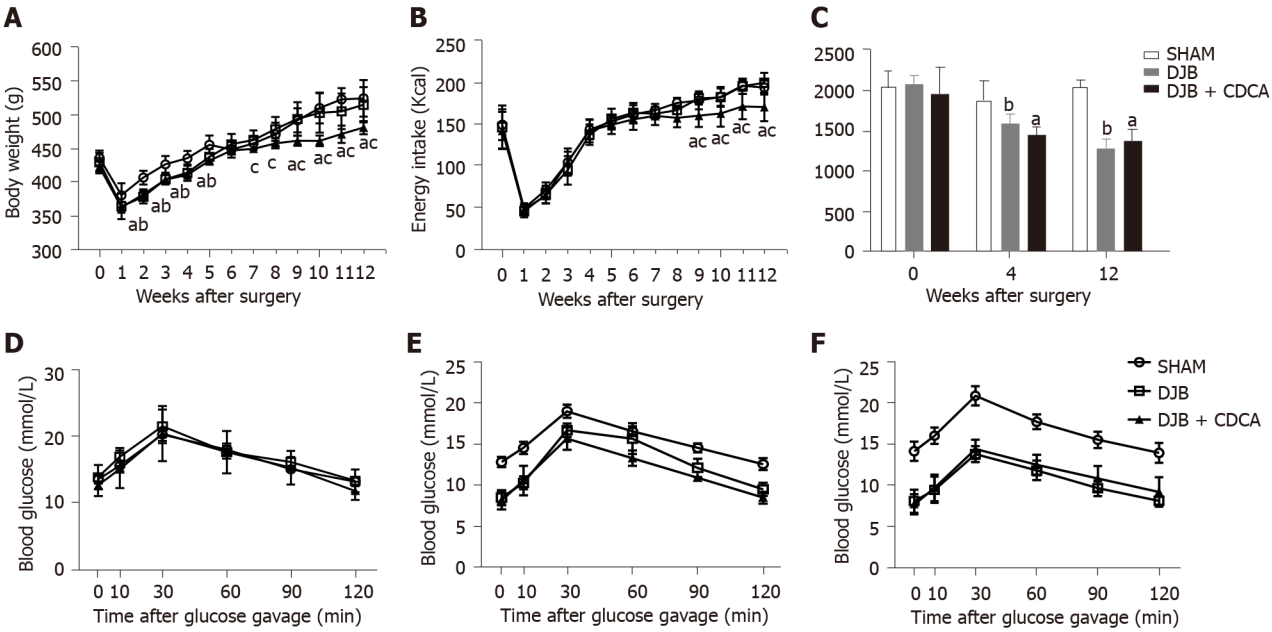

DOI: 10.3748/wjg.v28.i31.4328

Figure 1 Body weight and energy intake from baseline to week 12 after operations as well as oral glucose tolerance test and the corresponding areas under the curves at baseline, week 4 and week 12 after operations. A: Body weight; B: Energy intake; C: Area under the curve of oral glucose tolerance test; D: Oral glucose tolerance test at baseline; E: Oral glucose tolerance test at week 4; F: Oral glucose tolerance test at week 12. $^{a}P < 0.05$, salicylhydroxamic acid *vs* duodenal-jejunal bypass + chenodeoxycholic acid; $^{b}P < 0.05$, salicylhydroxamic acid *vs* duodenal-jejunal bypass. SHAM: Salicylhydroxamic acid; DJB: Duodenal-jejunal bypass; CDCA: Chenodeoxycholic acid.

(NanoDrop Technologies, United States). RNA was then reverse transcribed into complementary DNA (cDNA) using a ReverTra Ace qPCR RT Kit (TOYOBO, Japan). Amplification of messenger RNA (mRNA) was carried out using SYBR Green Real-time PCR Master Mix Kit (TOYOBO, Japan) at a range of temperatures in a Roche Lightcycle 2.0 system (Roche, Switzerland). The housekeeping gene gapdh was used as an internal reference, and mRNA levels for each target were then calculated by the $2^{-\Delta\Delta Ct}$ method. The primers were smpd3 (forward primer: 5′-ACTCGCTCGCAAGGCTCAATAATG-3′, reverse primer: 5′-CTGAAGCTGGCTGCACTGATGG-3′), sptlc2 (forward primer: 5′-CGCCTTCCT-GAAGTGATTGCTCTC-3′, reverse primer: 5′-AGTCTACTACACCACGCCCTGAAG-3′), and gapdh (forward primer: 5′-ACCCTGTTGCTGTAGCCATATTC-3′; reverse primer: 5′-ACCCTGTTGCTGTAGC-CATATTC-3′).

Ceramide detection

Ceramide concentrations peripheral circulation and the portal vein were measured as previously described using Ceramide LIPIDOMIX Mass Spec Standard (#330712X-1EA, Avanti, United States) as standards[14].

Statistical analysis

Data are mean ± SEM. Area under the curve (AUC) for oral glucose tolerance test (OGTT) was calculated by trapezoidal integration. Intergroup comparisons were performed by one-way analysis of variance followed by Bonferroni *post hoc* comparisons. $P < 0.05$ was considered statistically significant. All calculations were performed using SPSS version 25.0.

RESULTS

One rat in SHAM group died of intestinal obstruction. Two rats in DJB group and 2 rats in DJB + CDCA group died of anastomotic leak. At the end of the study, the number of rats alive in SHAM, DJB and DJB + CDCA groups were 9, 8 and 8, respectively.

Body weight and energy intake

At baseline, both body weight and energy intake were comparable between three groups. After surgery, both body weight and energy intake decreased sharply in all three groups and increased gradually thereafter. At week 2-5 postoperatively, body weight of the rats in DJB and DJB + CDCA groups was significantly less than that in SHAM group ($P < 0.05$ all). At week 7-12 postoperatively, body weight of

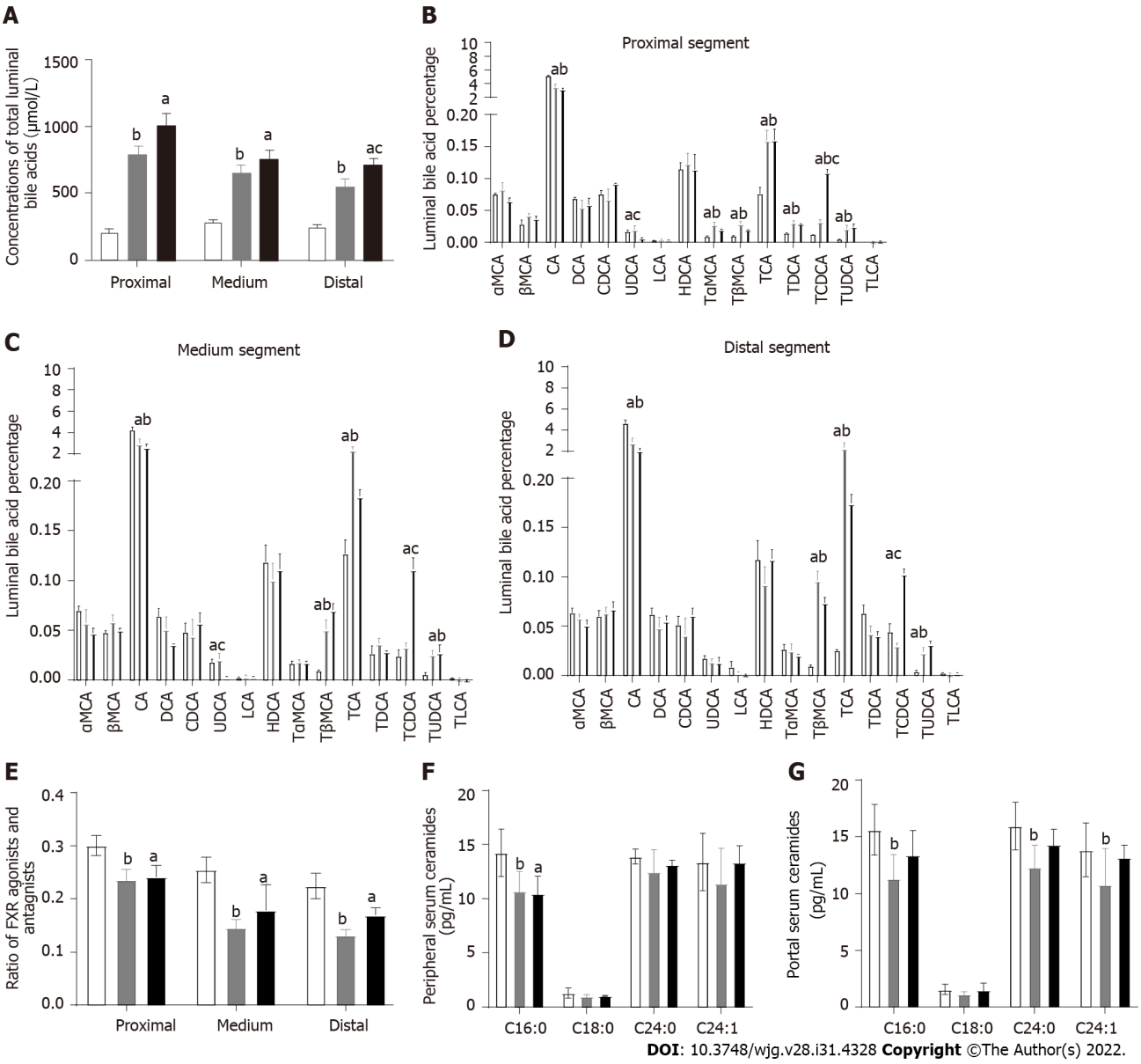

DOI: 10.3748/wjg.v28.i31.4328

Figure 2 Luminal total and individual bile acid concentrations and ceramide concentrations within the peripheral and portal circulations.
A: Total amount of luminal bile acids; B: Luminal individual bile acid percentage in the proximal; C: Medium segment within the common limb; D: Distal segment within the common limb; E: Ratio of farnesoid X receptor agonist and antagnist within the common limb; F: Peripheral serum ceramides; G: Portal serum ceramides. $^{a}P < 0.05$, salicylhydroxamic acid *vs* duodenal-jejunal bypass + chenodeoxycholic acid; $^{b}P < 0.05$, salicylhydroxamic acid *vs* duodenal-jejunal bypass; $^{c}P < 0.05$, duodenal-jejunal bypass *vs* duodenal-jejunal bypass + chenodeoxycholic acid. FXR: Farnesoid X receptor; SHAM: Salicylhydroxamic acid; DJB: Duodenal-jejunal bypass; CDCA: Chenodeoxycholic acid; αMCA: α-muricholic acid; UDCA: Ursodeoxycholic acid; LCA: Lithocholic acid; HDCA: Hyocholic acid; TLCA: Taurine-conjugated lithocholic acid.

the rats in DJB + CDCA group was significantly less than that in DJB group ($P < 0.05$ all) (Figure 1A). At week 9-12 postoperatively, body weight of the rats in DJB + CDCA group was significantly less than that in SHAM group ($P < 0.05$ all). At week 9-12 postoperatively, energy intake of the rats in DJB + CDCA group was significantly less than that in SHAM and DJB groups ($P < 0.05$ all) (Figure 1B).

OGTT

There was no difference in glucose tolerance between three groups at baseline based on AUC_{OGTT}. At week 4 and 12, glucose tolerance was significantly improved with DJB and DJB + CDCA groups compared to SHAM group based on AUC_{OGTT} ($P < 0.05$ each). There was no difference between DJB and DJB + CDCA groups, or between week 4 and week 12 within each group (Figures 1C-F).

Luminal bile acids

Total luminal bile acid concentrations were significantly less with SHAM group compared to both DJB and DJB + CDCA groups in either proximal, medium or distal segment in the common limb ($P < 0.05$ all). In the distal segment, luminal total bile acid concentrations were significantly greater with DJB +

CDCA group than DJB group ($P < 0.05$), while this difference was not significant in the proximal or medium segment (Figure 2A).

In the proximal segment (Figure 2B), CA accounted for over 20% of the total luminal bile acids in all three groups, and was significantly greater with SHAM group than DJB and DJB + CDCA groups ($P < 0.05$). The percentages of α-muricholic acid (αMCA), βMCA, deoxycholic acid, CDCA, lithocholic acid (LCA), hyocholic acid (HDCA), and taurine-conjugated LCA (TLCA) were comparable between all three groups. The percentage of UDCA was less with DJB + CDCA group compared to SHAM and DJB groups ($P < 0.05$). The percentages of taurine-conjugated forms of αMCA, βMCA, CA, DCA, CDCA and UDCA were all greater with DJB and DJB + CDCA groups compared to SHAM group ($P < 0.05$). The percentage of TCDCA was greater with DJB + CDCA group than DJB group ($P < 0.05$).

In the medium segment (Figure 2C), the difference in TαMCA and TDCA between three groups was no longer significant compared to the proximal segment. The percentage of TβMCA increased to more than 5% in DJB and DJB + CDCA groups which was significantly greater than SHAM group ($P < 0.05$). The percentage of TCDCA was comparable between SHAM and DJB groups, which was significantly less than DJB + CDCA group ($P < 0.05$).

In the distal segment (Figure 2D), the percentage of TβMCA, TCA and TUDCA was significantly greater with DJB and DJB + CDCA groups compared to SHAM group ($P < 0.05$), without any difference between the former two groups. The percentage of CA was significantly less with DJB and DJB + CDCA groups compared to SHAM group ($P < 0.05$). There was no difference in the percentage of UDCA between three groups. The percentage of other individual bile acids was comparable to that in the medium segment. The ratio of FXR agonists (including CA, TCA, DCA, TDCA, CDCA, TCDCA, LCA, and TLCA) and antagonists (including αMCA, TαMCA, βMCA, TβMCA, UDCA, TUDCA and HDCA) in DJB and DJB + CDCA groups was decreased compared to SHAM group in either proximal, medium or distal segment ($P < 0.05$). No difference was observed between DJB group and DJB + CDCA group (Figure 2E).

Ceramides

At week 12, in the peripheral circulation, serum C16:0 ceramide concentrations were lower with DJB and DJB + CDCA groups compared to SHAM group ($P < 0.05$); no difference in C18:0, C24:0 or C24:1 ceramides between three groups (Figure 2F). In the portal vein, serum C16:0, C24:0 and C24:1 ceramide concentrations were lower with DJB group compared to SHAM group ($P < 0.05$); there was no difference in either ceramide species between DJB and DJB + CDCA groups or between DJB + CDCA and SHAM groups (Figure 2G).

Expression of Smpd3 and Sptlc2

At week 12, the expression of Smpd3 and Sptlc2 were lower with DJB and DJB + CDCA groups than SHAM group at both protein and mRNA levels ($P < 0.05$). Compared to DJB + CDCA group, the expression of Smpd3 and Sptlc2 with DJB group were even lower at both protein and mRNA levels ($P < 0.05$) (Figures 3A, 3B and 3C).

DISCUSSION

In the present study, we performed SHAM, DJB and DJB + CDCA procedures in a HFD/STZ induced diabetic rat model, and for the first time, demonstrated the changes of luminal individual bile acids in the distal small intestine. We also found that the subsequent changes of the bile acids within the distal common limb after DJB elicited inhibitory effect on regional ceramide synthesis and this phenomenon could be partially antagonized by luminal supplementation of FXR activating bile acid CDCA.

DJB was initially designed to investigate the weight loss independent mechanisms of bariatric surgery[3]. This procedure has no effect on weight loss but could induce fast and sustainable amelioration of type 2 diabetes[4]. Consistent with other bariatric procedures[15,16], serum bile acid concentrations were also increased following DJB, and this phenomenon is clearly related to reconstruction of the gastrointestinal tract[5]. *Via* the biliopancreatic limb, bile acids contact the distal small intestine, where luminal bile acid reabsorption mainly occurs, more rapidly and lead to early and increased reabsorption of luminal bile acids in the small intestine. A recent study has proved that in the biliopancreatic limb, increased reabsorption of luminal bile acids has already commenced as a result of highly concentrated bile acids as well as lack of lipids[17]. While in the alimentary limb, only trace amount of luminal bile acids could be detected[4]. Decreased luminal bile acids lead to marked luminal sodium insufficiency, and hence, intestinal uptake of glucose in the alimentary limb is significantly decreased[18], which represents another mechanism in controlling postprandial glucose excursion. The common limb is where food and bile mix up and the major place for intestinal FXR expression. Therefore, we concentrated on bile acid milieu within the common limb rather than the biliopancreatic or alimentary limb because the common limb is the place mostly close to physiological conditions.

To our knowledge, the present study is the first study reporting luminal bile acid changes after DJB. Most clinical and animal studies concentrated on serum or fecal bile acids, as the intestinal lumen is

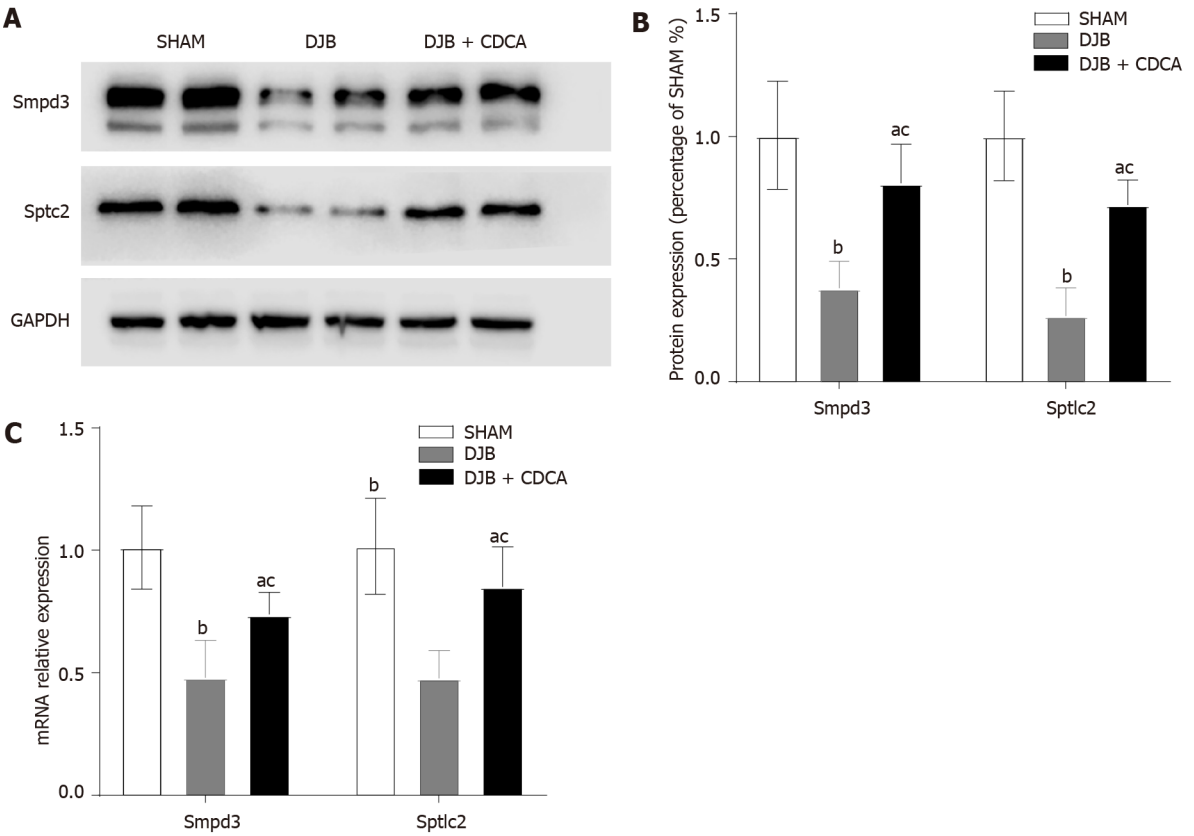

DOI: 10.3748/wjg.v28.i31.4328 **Copyright** ©The Author(s) 2022.

Figure 3 Expression of ceramide synthesis-related enzyme sphingomyelin phosphodiesterase 3 and serine palmitoyltransferase long chain base subunit 2 at protein and mRNA levels. A: Expression of sphingomyelin phosphodiesterase 3 (Smpd3), serine palmitoyltransferase long chain base subunit 2 (Sptlc2) and GAPDH; B: Expression of Smpd3, Sptlc2 at protein; C: Expression of Smpd3, Sptlc2 mRNA levels. $^{a}P < 0.05$, salicylhydroxamic acid *vs* duodenal-jejunal bypass + chenodeoxycholic acid; $^{b}P < 0.05$, salicylhydroxamic acid *vs* duodenal-jejunal bypass; $^{c}P < 0.05$, duodenal-jejunal bypass *vs* duodenal-jejunal bypass + chenodeoxycholic acid. SHAM: Salicylhydroxamic acid; DJB: Duodenal-jejunal bypass; CDCA: Chenodeoxycholic acid; Smpd3: Sphingomyelin phosphodiesterase 3; Sptlc2: Serine palmitoyltransferase long chain base subunit 2.

deep inside and *in vivo* study of luminal contents, particularly in the small intestine, is technically difficult and ethically challenging. Consistent with our previous findings of serum bile acid changes after DJB, the total amount of luminal bile acids and the proportion of FXR-inhibitory bile acids were both increased. These specific changes have at least two clinical relevance. First, concentrated luminal bile acids stimulate TRG5 on the surface of enteroendocrine cells and leads to potentiated GLP-1 secretion[4]; second, increased proportion of FXR-inhibitory bile acids has inhibited expression of FXR downstream pathways and reduced biosynthesis of intestinal-derived ceramides[12]. Compared to TGR5, FXR appears to be a more important and complicated receptor in metabolic regulation; in the absence of FXR, the ability of bariatric surgery to reduce body weight and improve glucose tolerance is substantially reduced while these metabolic benefits are largely preserved when TGR5 is deficient[19-20]. Whole body FXR knock-out mice were associated with elevated serum triglycerides, cholesterols, free fatty acids and severe liver fat accumulation, but were protected from diet- or genetically- induced obesity[21]. In contrast, liver-specific FXR knock-out mice were not protected from diet-induced obesity and insulin resistance[22], suggesting the distinct role of hepatic and intestinal FXR activation in improving glucose tolerance and insulin resistance. In the small intestine, the role of FXR is controversial. After bariatric surgery, increased serum fibroblast growth factor 19 (FGF19) concentrations have been thought to play a role in the remission of human diabetes[15]. And intestinal FXR activation by luminal bile acids has been thought as a major source of increased serum FGF19. However, no direct evidence was available to confirm the state of intestinal FXR activation, and other tissues may also be sources of FGF19. In contrast, more studies support that intestinal FXR activation would damage metabolic homeostasis by reducing energy expenditure and impairing glucose tolerance[12,14,23]. To investigate the direct influence of bile acids on intestinal FXR, bile diversion procedure was reported by three separate studies[4,24,25], including one from our group[4]. Surprisingly, all three studies showed activated intestinal FXR in response to direct bile acid stimulation. However, in contrast, in DJB, the effect of bile acids on intestinal FXR within the common limb was inhibitory. The discrepancy suggests the biliopancreatic limb may have altered the luminal bile acid composition by premature bile acid reabsorption.

Consistent with our hypothesis, both ceramides in the portal vein and in the peripheral circulation were decreased in response to increased proportion of luminal FXR-inhibitory bile acids. Ceramides are signaling molecules and are associated with obesity and insulin resistance at high concentrations[26]. Decreased ceramides inhibits the expression of SREBP-1 in the liver and alleviates hepatic fat accumulation, thus increasing hepatic insulin sensitivity[12]. Our previous study found that DJB suppressed hepatic *de novo* lipogenesis and alleviates liver fat accumulation by inhibiting SREBP-1. However, the mechanisms underlying were unknown. Based on results from the present study, we have unveiled at least one mechanism accounting for alleviated hepatic fat accumulation. Therefore, manipulation of luminal bile acid composition towards FXR-inhibitory trend may have metabolic beneficial effects.

The present study has several limitations. First, bile acids are mixture with a variety of individual bile acids. As bile acids are mainly conjugated with taurine in rodents[27], we only tested luminal unconjugated and taurine-conjugated bile acids. Second, CDCA is not dissolved in water and we used CDCA suspension for gavage, which may have compromised CDCA absorption to a certain degree. Third, the results from the present study were based on a diabetic rat model and should be interpreted with caution due to species gap.

CONCLUSION

In conclusion, DJB significantly changes luminal bile acid composition with increased proportion of FXR-inhibitory bile acids and reduce serum ceramide levels. There observations suggest a novel mechanism of bile acids in metabolic regulation after DJB.

ARTICLE HIGHLIGHTS

Research background

Bile acids have proved to be signaling molecules in mediating metabolic benefits and circulating bile acids were found to be increased following duodenal-jejunal bypass (DJB). However, whether and how the bile acids take effect in the amelioration of metabolic disorders after DJB remain unknown.

Research motivation

Circulating bile acids reflect the amount of bile acids within the gut. It has been proved that luminal bile acids take effect *via* Takeda G-protein-coupled receptor 5 and nuclear farnesoid X receptor (FXR). However, different subtypes of bile acids have distinct effect on the downstream pathway of FXR and hence, a further investigation of luminal bile acids after DJB is of great significance.

Research objectives

To investigate changes and mechanisms of luminal bile acids in mediating metabolic benefits following DJB.

Research methods

Salicylhydroxamic acid (SHAM), DJB, and DJB with oral chenodeoxycholic acid (CDCA) supplementation were performed in a high-fat-diet/streptozotocin-induced diabetic rat model. Body weight, energy intake, oral glucose tolerance test, luminal bile acids, serum ceramides and intestinal ceramide synthesis were analyzed at week 12 postoperatively.

Research results

Compared to SHAM, DJB achieved rapid and durable improvement in glucose tolerance and led to increased total luminal bile acid concentrations with preferentially increased proportion of FXR - inhibitory bile acids within the common limb. Intestinal ceramide synthesis was repressed with decreased serum ceramides, and this phenomenon could be partially antagonized by luminal supplementation of FXR activating bile acid CDCA.

Research conclusions

DJB significantly changes luminal bile acid composition with increased proportion FXR-inhibitory bile acids and reduces serum ceramide levels. There observations suggest a novel mechanism of bile acids in metabolic regulation after DJB.

Research perspectives

Mechanisms of bile acids in mediating metabolic benefits after bariatric surgery.

FOOTNOTES

Author contributions: Cheng ZQ and Liu TM were involved in animal surgery, data collection, interpretation, statistical analysis, and writing of the manuscript; Ren PF, Chen C, Wang YL and Dai Y were involved in animal surgery, experimental analysis and assist in writing; Cheng ZQ, Dai Y and Zhang X were involved in conception, design, and coordination of the work; Dai Y and Zhang X are the guarantors of this work; and all authors critically reviewed the manuscript and have approved the publication of this final version of the manuscript.

Institutional animal care and use committee statement: All procedures involving animals were reviewed and approved by the Ethics Committee on Animal Experiment of Shandong University Qilu Hospital (KYLL-2017(ZM)-156).

Conflict-of-interest statement: All the authors report no relevant conflicts of interest for this article.

Data sharing statement: No additional data are available.

ARRIVE guidelines statement: The authors have read the ARRIVE guidelines, and the manuscript was prepared and revised according to the ARRIVE guidelines.

Country/Territory of origin: China

ORCID number: Zhi-Qiang Cheng 0000-0002-6916-747X; Yan-Lei Wang 0000-0002-4227-0274; Yong Dai 0000-0001-6163-8022; Xiang Zhang 0000-0001-7417-6082.

S-Editor: Wang JJ
L-Editor: A
P-Editor: Wang JJ

REFERENCES

1 **Cohen R**, Caravatto PP, Correa JL, Noujaim P, Petry TZ, Salles JE, Schiavon CA. Glycemic control after stomach-sparing duodenal-jejunal bypass surgery in diabetic patients with low body mass index. *Surg Obes Relat Dis* 2012; **8**: 375-380 [PMID: 22410638 DOI: 10.1016/j.soard.2012.01.017]
2 **Ramos AC**, Galvão Neto MP, de Souza YM, Galvão M, Murakami AH, Silva AC, Canseco EG, Santamaría R, Zambrano TA. Laparoscopic duodenal-jejunal exclusion in the treatment of type 2 diabetes mellitus in patients with BMI<30 kg/m^2 (LBMI). *Obes Surg* 2009; **19**: 307-312 [PMID: 18987919 DOI: 10.1007/s11695-008-9759-5]
3 **Rubino F**, Forgione A, Cummings DE, Vix M, Gnuli D, Mingrone G, Castagneto M, Marescaux J. The mechanism of diabetes control after gastrointestinal bypass surgery reveals a role of the proximal small intestine in the pathophysiology of type 2 diabetes. *Ann Surg* 2006; **244**: 741-749 [PMID: 17060767 DOI: 10.1097/01.sla.0000224726.61448.1b]
4 **Zhang X**, Liu T, Wang Y, Zhong M, Zhang G, Liu S, Wu T, Rayner CK, Hu S. Comparative Effects of Bile Diversion and Duodenal-Jejunal Bypass on Glucose and Lipid Metabolism in Male Diabetic Rats. *Obes Surg* 2016; **26**: 1565-1575 [PMID: 26464241 DOI: 10.1007/s11695-015-1925-y]
5 **Zhang X**, Wang Y, Zhong M, Liu T, Han H, Zhang G, Liu S, Wei M, Wu Q, Hu S. Duodenal-Jejunal Bypass Preferentially Elevates Serum Taurine-Conjugated Bile Acids and Alters Gut Microbiota in a Diabetic Rat Model. *Obes Surg* 2016; **26**: 1890-1899 [PMID: 26715331 DOI: 10.1007/s11695-015-2031-x]
6 **Angelin B**, Björkhem I, Einarsson K, Ewerth S. Hepatic uptake of bile acids in man. Fasting and postprandial concentrations of individual bile acids in portal venous and systemic blood serum. *J Clin Invest* 1982; **70**: 724-731 [PMID: 7119112 DOI: 10.1172/jci110668]
7 **Goldspink DA**, Lu VB, Billing LJ, Larraufie P, Tolhurst G, Gribble FM, Reimann F. Mechanistic insights into the detection of free fatty and bile acids by ileal glucagon-like peptide-1 secreting cells. *Mol Metab* 2018; **7**: 90-101 [PMID: 29167062 DOI: 10.1016/j.molmet.2017.11.005]
8 **Wu T**, Bound MJ, Standfield SD, Gedulin B, Jones KL, Horowitz M, Rayner CK. Effects of rectal administration of taurocholic acid on glucagon-like peptide-1 and peptide YY secretion in healthy humans. *Diabetes Obes Metab* 2013; **15**: 474-477 [PMID: 23181598 DOI: 10.1111/dom.12043]
9 **Makishima M**, Okamoto AY, Repa JJ, Tu H, Learned RM, Luk A, Hull MV, Lustig KD, Mangelsdorf DJ, Shan B. Identification of a nuclear receptor for bile acids. *Science* 1999; **284**: 1362-1365 [PMID: 10334992 DOI: 10.1126/science.284.5418.1362]
10 **Mueller M**, Thorell A, Claudel T, Jha P, Koefeler H, Lackner C, Hoesel B, Fauler G, Stojakovic T, Einarsson C, Marschall HU, Trauner M. Ursodeoxycholic acid exerts farnesoid X receptor-antagonistic effects on bile acid and lipid metabolism in morbid obesity. *J Hepatol* 2015; **62**: 1398-1404 [PMID: 25617503 DOI: 10.1016/j.jhep.2014.12.034]

11 **Sayin SI**, Wahlström A, Felin J, Jäntti S, Marschall HU, Bamberg K, Angelin B, Hyötyläinen T, Orešič M, Bäckhed F. Gut microbiota regulates bile acid metabolism by reducing the levels of tauro-beta-muricholic acid, a naturally occurring FXR antagonist. *Cell Metab* 2013; **17**: 225-235 [PMID: 23395169 DOI: 10.1016/j.cmet.2013.01.003]

12 **Jiang C**, Xie C, Lv Y, Li J, Krausz KW, Shi J, Brocker CN, Desai D, Amin SG, Bisson WH, Liu Y, Gavrilova O, Patterson AD, Gonzalez FJ. Intestine-selective farnesoid X receptor inhibition improves obesity-related metabolic dysfunction. *Nat Commun* 2015; **6**: 10166 [PMID: 26670557 DOI: 10.1038/ncomms10166]

13 **Han H**, Hu C, Wang L, Zhang G, Liu S, Li F, Sun D, Hu S. Duodenal-jejunal bypass surgery suppresses hepatic de novo lipogenesis and alleviates liver fat accumulation in a diabetic rat model. *Obes Surg* 2014; **24**: 2152-2160 [PMID: 24898720 DOI: 10.1007/s11695-014-1308-9]

14 **Jiang C**, Xie C, Li F, Zhang L, Nichols RG, Krausz KW, Cai J, Qi Y, Fang ZZ, Takahashi S, Tanaka N, Desai D, Amin SG, Albert I, Patterson AD, Gonzalez FJ. Intestinal farnesoid X receptor signaling promotes nonalcoholic fatty liver disease. *J Clin Invest* 2015; **125**: 386-402 [PMID: 25500885 DOI: 10.1172/JCI76738]

15 **Gerhard GS**, Styer AM, Wood GC, Roesch SL, Petrick AT, Gabrielsen J, Strodel WE, Still CD, Argyropoulos G. A role for fibroblast growth factor 19 and bile acids in diabetes remission after Roux-en-Y gastric bypass. *Diabetes Care* 2013; **36**: 1859-1864 [PMID: 23801799 DOI: 10.2337/dc12-2255]

16 **Myronovych A**, Kirby M, Ryan KK, Zhang W, Jha P, Setchell KD, Dexheimer PJ, Aronow B, Seeley RJ, Kohli R. Vertical sleeve gastrectomy reduces hepatic steatosis while increasing serum bile acids in a weight-loss-independent manner. *Obesity (Silver Spring)* 2014; **22**: 390-400 [PMID: 23804416 DOI: 10.1002/oby.20548]

17 **Ueno T**, Tanaka N, Imoto H, Maekawa M, Kohyama A, Watanabe K, Motoi F, Kamei T, Unno M, Naitoh T. Mechanism of Bile Acid Reabsorption in the Biliopancreatic Limb After Duodenal-Jejunal Bypass in Rats. *Obes Surg* 2020; **30**: 2528-2537 [PMID: 32291708 DOI: 10.1007/s11695-020-04506-3]

18 **Baud G**, Daoudi M, Hubert T, Raverdy V, Pigeyre M, Hervieux E, Devienne M, Ghunaim M, Bonner C, Quenon A, Pigny P, Klein A, Kerr-Conte J, Gmyr V, Caiazzo R, Pattou F. Bile Diversion in Roux-en-Y Gastric Bypass Modulates Sodium-Dependent Glucose Intestinal Uptake. *Cell Metab* 2016; **23**: 547-553 [PMID: 26924216 DOI: 10.1016/j.cmet.2016.01.018]

19 **Ryan KK**, Tremaroli V, Clemmensen C, Kovatcheva-Datchary P, Myronovych A, Karns R, Wilson-Pérez HE, Sandoval DA, Kohli R, Bäckhed F, Seeley RJ. FXR is a molecular target for the effects of vertical sleeve gastrectomy. *Nature* 2014; **509**: 183-188 [PMID: 24670636 DOI: 10.1038/nature13135]

20 **Hao Z**, Leigh Townsend R, Mumphrey MB, Gettys TW, Yu S, Münzberg H, Morrison CD, Berthoud HR. Roux-en-Y Gastric Bypass Surgery-Induced Weight Loss and Metabolic Improvements Are Similar in TGR5-Deficient and Wildtype Mice. *Obes Surg* 2018; **28**: 3227-3236 [PMID: 29770924 DOI: 10.1007/s11695-018-3297-6]

21 **Wang W**, Cheng Z, Wang Y, Dai Y, Zhang X, Hu S. Role of Bile Acids in Bariatric Surgery. *Front Physiol* 2019; **10**: 374 [PMID: 31001146 DOI: 10.3389/fphys.2019.00374]

22 **Watanabe M**, Houten SM, Wang L, Moschetta A, Mangelsdorf DJ, Heyman RA, Moore DD, Auwerx J. Bile acids lower triglyceride levels *via* a pathway involving FXR, SHP, and SREBP-1c. *J Clin Invest* 2004; **113**: 1408-1418 [PMID: 15146238 DOI: 10.1172/JCI21025]

23 **Watanabe M**, Horai Y, Houten SM, Morimoto K, Sugizaki T, Arita E, Mataki C, Sato H, Tanigawara Y, Schoonjans K, Itoh H, Auwerx J. Lowering bile acid pool size with a synthetic farnesoid X receptor (FXR) agonist induces obesity and diabetes through reduced energy expenditure. *J Biol Chem* 2011; **286**: 26913-26920 [PMID: 21632533 DOI: 10.1074/jbc.M111.248203]

24 **Flynn CR**, Albaugh VL, Cai S, Cheung-Flynn J, Williams PE, Brucker RM, Bordenstein SR, Guo Y, Wasserman DH, Abumrad NN. Bile diversion to the distal small intestine has comparable metabolic benefits to bariatric surgery. *Nat Commun* 2015; **6**: 7715 [PMID: 26197299 DOI: 10.1038/ncomms8715]

25 **Goncalves D**, Barataud A, De Vadder F, Vinera J, Zitoun C, Duchampt A, Mithieux G. Bile Routing Modification Reproduces Key Features of Gastric Bypass in Rat. *Ann Surg* 2015; **262**: 1006-1015 [PMID: 25575265 DOI: 10.1097/SLA.0000000000001121]

26 **Bikman BT**, Summers SA. Ceramides as modulators of cellular and whole-body metabolism. *J Clin Invest* 2011; **121**: 4222-4230 [PMID: 22045572 DOI: 10.1172/JCI57144]

27 **Shonsey EM**, Wheeler J, Johnson M, He D, Falany CN, Falany J, Barnes S. Synthesis of bile acid coenzyme a thioesters in the amino acid conjugation of bile acids. *Methods Enzymol* 2005; **400**: 360-373 [PMID: 16399360 DOI: 10.1016/S0076-6879(05)00021-2]

World Journal of Gastroenterology

Submit a Manuscript: https://www.f6publishing.com

World J Gastroenterol 2022 August 21; 28(31): 4338-4350

DOI: 10.3748/wjg.v28.i31.4338

ISSN 1007-9327 (print) ISSN 2219-2840 (online)

ORIGINAL ARTICLE

Basic Study

Duodenal-jejunal bypass increases intraduodenal bile acids and upregulates duodenal SIRT1 expression in high-fat diet and streptozotocin-induced diabetic rats

Hai-Feng Han, Shao-Zhuang Liu, Xiang Zhang, Meng Wei, Xin Huang, Wen-Bin Yu

Specialty type: Gastroenterology and hepatology

Provenance and peer review: Unsolicited article; Externally peer reviewed.

Peer-review model: Single blind

Peer-review report's scientific quality classification

Grade A (Excellent): 0
Grade B (Very good): B, B, B
Grade C (Good): 0
Grade D (Fair): 0
Grade E (Poor): 0

P-Reviewer: Kim M, South Korea; Madadi-Sanjani O, Germany; Nio M, Japan

Received: May 26, 2022
Peer-review started: May 26, 2022
First decision: June 19, 2022
Revised: June 28, 2022
Accepted: July 25, 2022
Article in press: July 25, 2022
Published online: August 21, 2022

Hai-Feng Han, Shao-Zhuang Liu, Xiang Zhang, Meng Wei, Xin Huang, Wen-Bin Yu, Department of General Surgery, Qilu Hospital, Cheeloo College of Medicine, Shandong University, Jinan 250012, Shandong Province, China

Corresponding author: Wen-Bin Yu, MD, PhD, Chief Doctor, Professor, Department of General Surgery, Qilu Hospital, Cheeloo College of Medicine, Shandong University, No. 107 West Wenhua Road, Jinan 250012, Shandong Province, China. wenbin_yu2003@163.com

Abstract

BACKGROUND

The mechanisms underlying diabetes remission after duodenal-jejunal bypass (DJB) remain elusive. In DJB surgery, the duodenum is excluded. However, the duodenum has emerged as an important regulator of glucose homeostasis, and elevated duodenal SIRT1 leads to improved hepatic insulin sensitivity. After DJB, bile acids (BAs) in the duodenum are not mixed and diluted by the ingested food. And activation of BA receptors promotes SIRT1 expression in many tissues. We hypothesized that BA-mediated upregulation of SIRT1 may contribute to diabetic control after DJB.

AIM

To investigate the surgical effects of DJB on duodenal SIRT1 expression and uncover the potential crosslinks between BAs and SIRT1.

METHODS

Twenty diabetic rats were randomly allocated to the sham (n = 10) and DJB (n = 10) groups. Body weight, food intake, fasting blood glucose (FBG), serum and intraduodenal total BA (TBA) levels were measured accordingly. Oral glucose tolerance test (OGTT) and intraperitoneal pyruvate tolerance test (ipPTT) were performed to evaluate the effects of surgeries on systemic glucose disposal and hepatic gluconeogenesis. The key genes of BA signaling pathway in the duodenal mucosa, including farnesoid X receptor (FXR), small heterodimer partner (SHP), and Takeda G-protein-coupled receptor 5 (TGR5) were evaluated by real-time quantitative polymerase chain reaction 8 wk postoperatively. The duodenal SIRT1, AMPK, and phosphorylated AMPK (p-AMPK) levels were evaluated by western blotting. Rat small intestine epithelial IEC-6 cells were treated with

GW4064 and INT-777 to verify the effects of BAs on SIRT1 expression in enterocytes.

RESULTS

The DJB group exhibited body weight and food intake comparable to those of the sham group at all postoperative time points. The FBG level and area under the curve for the OGTT and ipPTT were significantly lower in the DJB group. The DJB group exhibited higher fasting and postprandial serum TBA levels than the sham group at both 2 and 8 wk postoperatively. At 8 wk after surgery, the DJB group showed higher intraluminal TBA concentration, upregulated mRNA expression of FXR and SHP, and elevated protein expression of SIRT1 and p-AMPK in the descending and horizontal segments of the duodenum. Activation of FXR and TGR5 receptors by GW4064 and INT-777 increased the mRNA and protein expression of SIRT1 and promoted the phosphorylation of AMPK in IEC-6 cells.

CONCLUSION

DJB elevates intraduodenal BA levels and activates the duodenal BA signaling pathway, which may upregulate duodenal SIRT1 and further contribute to improved glucose homeostasis after DJB.

Key Words: Duodenal-jejunal bypass; Diabetes mellitus; Bile acids; Sirtuin 1; Duodenum; High-fat diet

Core Tip: The intrinsic mechanisms of diabetes remission after duodenal-jejunal bypass (DJB) surgery are complicated. Duodenal SIRT1 is a novel therapeutic target for diabetes, and increased duodenal SIRT1 is linked to improved hepatic insulin sensitivity and decreased hepatic glucose output. The animal study demonstrated that DJB increased intraduodenal bile acid (BA) levels, activated the BA signaling pathway, and upregulated SIRT1 expression in the duodenal mucosa. Our cell experiments proved that farnesoid X receptor and Takeda G-protein-coupled receptor 5 activation increased SIRT1 expression in rat small intestine epithelial cells, indicating that increased intraluminal BAs and activation of BA receptors contributed to increased duodenal SIRT1 after DJB.

Citation: Han HF, Liu SZ, Zhang X, Wei M, Huang X, Yu WB. Duodenal-jejunal bypass increases intraduodenal bile acids and upregulates duodenal SIRT1 expression in high-fat diet and streptozotocin-induced diabetic rats. *World J Gastroenterol* 2022; 28(31): 4338-4350

URL: https://www.wjgnet.com/1007-9327/full/v28/i31/4338.htm

DOI: https://dx.doi.org/10.3748/wjg.v28.i31.4338

INTRODUCTION

Diabetes is one of the fastest-growing global health issues. The International Diabetes Federation reported that the global prevalence of diabetes in adults was approximately 10.5% in 2021, expected to rise to 12.2% in 2045[1]. Bariatric surgery is much more effective and persistent in diabetes control than conventional medical therapy[2]. Duodenal-jejunal bypass (DJB) is a well-designed experimental procedure investigating the weight-independent anti-diabetic mechanisms of Roux-en-Y gastric bypass (RYGB). It can improve glucose homeostasis in both diabetic rats and patients[3-5], however, the underlying mechanisms remain unclear. A critical anatomical alteration of DJB is the exclusion of the duodenum. In addition, DJB liner, which mimics the duodenal-jejunal exclusion effects of RYGB, also improves glucose homeostasis[6]. Duodenal mucosal resurfacing, an endoscopic procedure that involves circumferential hydrothermal ablation and subsequent regeneration of the duodenal mucosa, elicits dramatic and durable glycemic improvements in patients with type 2 diabetes mellitus (T2DM)[7]. These findings suggest that the bypassed duodenum may play an important role in diabetic control after DJB.

The duodenum was primarily viewed as a digestive organ. However, accumulating evidence demonstrates that the duodenum has emerged as a key regulator of metabolic diseases, including diabetes[8]. The duodenal mucosa is exposed to various endogenous and exogenous chemical stimuli, such as macro- and micronutrients, gastric acid, bile acids (BAs), digestive enzymes, microorganisms, and drugs[9,10]. The duodenum is densely innervated by the enteric autonomous nervous system (ENS). Through chemical sensors located in the mucosa and ENS, the duodenum detects changes in luminal contents and further triggers a gut-brain negative feedback loop to inhibit exogenous nutrient intake and endogenous liver nutrient production[10,11]. In healthy rats, short-term intraduodenal

intralipid infusion inhibits hepatic glucose production (HGP) *via* the gut-brain-liver neural axis. However, this suppressive effect is negated in insulin-resistant rats[12]. Metformin and resveratrol, two well-known anti-diabetic drugs, can activate specific duodenal energy sensors (AMPK and SIRT1, respectively) even before being absorbed into the systemic circulation, and further trigger the gut-brain-liver network to reverse insulin resistance and inhibit HGP[13,14].

SIRT1 is a conserved mammalian nicotinamide adenine dinucleotide (NAD+)-dependent protein deacetylase that acts as a key metabolic sensor in various metabolic tissues, including the liver, skeletal muscle, adipose tissue, and pancreas. It directly links the cellular metabolic status to the regulation of gene expression, thus modulating various cellular processes, such as glucose metabolism, inflammation, and stress response[15,16]. SIRT1 is also expressed in the duodenal mucosa, which is significantly inhibited in high-fat diet (HFD)-fed insulin-resistant rats. Duodenum-specific knockdown of SIRT1 is sufficient to induce hepatic insulin resistance and increase hepatic glucose output in normal chow-fed rats[14]. To the best of our knowledge, the anti-diabetic effects of DJB surgery that could be linked to duodenal SIRT1 have not been investigated.

DJB hinders the duodenum from contacting the ingested chyme, therefore, the BAs released into the duodenum will not be mixed and diluted by food. In addition to their widely known roles in facilitating lipid absorption, BAs have recently been recognized as novel endocrine molecules that modulate glucose, lipids, and energy metabolism[17,18]. Activation of BA receptors, including the nuclear farnesoid X receptor (FXR) and membrane Takeda G-protein-coupled receptor 5 (TGR5), upregulates SIRT1 expression in the liver and brain, respectively[19,20]. These findings raise the possibility that DJB might upregulate duodenal SIRT1 by increasing intraluminal BAs, which might further contribute to the improved glucose homeostasis after DJB. Therefore, this study aimed to investigate the impact of DJB on duodenal BA signaling and SIRT1 expression in HFD and streptozotocin (STZ)-induced diabetic rats, and further explore the roles of BAs in modulating SIRT1 expression.

MATERIALS AND METHODS

Animals

Eight-week-old male Wistar rats were purchased from the Laboratory Animal Center of Shandong University (Jinan, China) and individually housed in ventilated cages in a controlled environment (12 h light/dark cycle, 24 ± 2 °C, humidity 50%-60%). The rats had *ad libitum* access to rodent chow and water. The diabetic rat model was established by HFD (40% fat, Huafukang Biotech, China) feeding for 4 wk to induce insulin resistance, followed by subsequent intraperitoneal injection of low-dose STZ (35 mg/kg, Sigma, United States) to induce mild insulin deficiency and hyperglycemia. After 72 h of STZ administration, 20 diabetic rats with random blood glucose ≥ 16.7 mmol/L were selected and randomly allocated to the sham (n = 10) and DJB (n = 10) groups. All animal protocols were approved by the Ethics Committee on Experimental Animals of Cheeloo College of Medicine, Shandong University.

Surgical procedures

The rats were deprived of solid food but were given free access to water and 10% enteral nutrition powder (Ensure, Abbott Laboratories B.V., Netherlands) two days preoperatively. Complete fasting was initiated 12 h preoperatively. All operations were conducted under anesthesia with 10% chloral hydrate (3 mL/kg). DJB and sham surgeries were performed as previously described[21].

DJB: First, a midline incision was made in the upper abdomen and the duodenum was then transected 1 cm distal to the pylorus and the stump was sealed. Next, the jejunum was transected approximately 10 cm distal to the ligament of Treitz, and the distal limb of the jejunum was anastomosed to the proximal duodenum in an end-to-end manner. Finally, the biliopancreatic limb was anastomosed to the jejunum 15 cm distal to the duodenojejunal anastomosis in a Roux-en-Y manner.

Sham: Sham surgery was performed *via* an incision comparable to that of the DJB group. The intestines were transected at the same sites where enterotomies were performed in DJB, and re-anastomosis was made *in situ*. The operation time was prolonged equally to that of the DJB group to achieve similar surgical and anesthetic stress.

The rats were only given access to water during the first 24 h postoperatively, followed by 10% enteral nutrition powder for three days, and thereafter a standard rodent chow until the end of this study. Body weight and food intake were recorded preoperatively and once a week postoperatively. Fasting blood glucose (FBG) levels were measured at baseline and at 1, 2, 4, 6, and 8 wk postoperatively.

Oral glucose tolerance test

Oral glucose tolerance test (OGTT) was performed 2 and 8 wk postoperatively. The rats were administered with 20% glucose (1 g/kg body weight) by oral gavage after overnight fasting. Blood samples were collected from the tail vein at baseline and at 15, 30, 60, 120, and 180 min after glucose administration to measure blood glucose levels. The area under the curve for the OGTT (AUC_{OGTT}) was

calculated by trapezoidal integration.

Intraperitoneal pyruvate tolerance test

The intraperitoneal pyruvate tolerance test (ipPTT) was conducted 2 and 8 wk postoperatively to evaluate hepatic gluconeogenic capacity and hepatic insulin resistance. After 12 h of fasting, 10% pyruvate solution (1 g/kg body weight) was administered intraperitoneally into conscious rats. Blood glucose levels were monitored at baseline and at 15, 30, 60, and 120 min after injection. The AUC for ipPTT (AUC_{ipPTT}) was calculated using trapezoidal integration.

Systemic and duodenal BAs parameters

Fasting and postprandial systemic total BAs (TBAs) were measured 2 and 8 wk postoperatively. The rats were fasted for 12 h and then administered with 10% Ensure (10 mL/kg body weight) *via* intragastric gavage. Blood samples were collected from the retrobulbar venous plexus into chilled SST tubes at baseline and 60 min after gavage to measure the systemic TBAs.

Eight weeks after the surgery, the rats were euthanized immediately after blood collection. Intestine segments of 0.5 cm length were excised from the descending and horizontal duodenum separately without rinsing. TBAs in the duodenum lumen were extracted by mixing the duodenal segments with 1 mL of 50% tert-butyl alcohol for 1 h at 37 °C. After centrifugation, the supernatant was collected and stored at -80 °C until analysis. BAs were measured with an automatic biochemistry analyzer (Roche Cobas 8000 system) using an enzyme cycling method.

Cell culture

Rat small intestine epithelial IEC-6 cells were purchased from Fuheng Biology (Shanghai, China), and cultured in Dulbecco's Modified Eagle Medium (Gibco, CA, United States) supplemented with 10% fetal bovine serum (Gibco, CA, United States), and maintained under standard culture conditions (in incubators at 37 °C in a 5% CO_2/95% air atmosphere). To investigate the effects of FXR and TGR5 activation on SIRT1, AMPK, and phosphorylated AMPK (p-AMPK) expression, IEC-6 cells were treated with GW4064 (5 μM, 24 h) and INT-777 (10 μM, 1 h) respectively, and the control groups were treated with an equal volume of dimethyl sulfoxide. At the end of the study, cells were harvested for protein and gene expression analyses.

Real-time quantitative polymerase chain reaction

Total mRNA of the duodenal mucosa and IEC-6 cells were extracted using TRIzol Reagent (Cwbio, China). The total mRNA was then reverse-transcribed into cDNA using a HiFiScript cDNA Synthesis Kit (Cwbio, China) according to the manufacturer's instructions. The cDNA was subjected to real-time quantitative polymerase chain reaction (RT-qPCR) quantitation with UltraSYBR Mixture (Cwbio, China) on a RT-qPCR system (Hehui biotech, China). GAPDH was used as an internal control. Primers used in this study are listed in Table 1.

Enzyme-linked immunosorbent assay

The duodenal mucosa was immediately flash-frozen in liquid nitrogen after the rats were euthanized. The cyclic adenosine 3′, 5′-monophosphate (cAMP) concentration in the duodenal mucosa was measured using an enzyme-linked immunosorbent assay kit according to the manufacturer's instructions (Sigma-Aldrich, United States).

Western blotting

Total proteins of the duodenal mucosa and IEC-6 cells were extracted with RIPA lysis buffer (Beyotime, China) and analyzed using a BCA protein assay kit (Beyotime, China). The primary antibodies used in western blotting were SIRT1 (Cell Signaling Technology, United States), AMPK (Cell Signaling Technology, United States), p-AMPK (Cell Signaling Technology, United States), and GAPDH (Proteintech, China). The protein bands were visualized using ECL solution (Millipore, United States), and band densitometry was assessed with ImageJ software.

Statistical analysis

Quantitative data were expressed as mean ± SD. The intergroups differences were evaluated by the Student's *t*-test except for blood glucose levels in the OGTT and ipPTT studies, which were analyzed by two-way repeated measures ANOVA (mixed model ANOVA) followed by Bonferroni's multiple comparison test. All analyses were performed using SPSS (Version 26). The criterion for statistical significance was set at $P < 0.05$.

Table 1 Primer sequence

Gene	Forward (5'-3')	Reverse (5'-3')
SIRT1	GGGAACCTCTGCCTCATCTACAT	CGCCACCTAACCTATGACACAA
AMPK	GAAGATCGGACACTACGTGCT	ACTGCCACTTTATGGCCTGTC
FXR	CATTACAACGCGCTCACCTG	CCCATCTCTCTGCACTTCCT
TGR5	TACTCACAGGGTTGGCACTG	CAAAAGTTGGGGGCCAAGTG
SHP	TCCGGTCCCCAGCATACTTA	GAAAGACTCCAGGCAGTGCT
GAPDH	GATTTGGCCGTATCGGAC	GAAGACGCCAGTAGACTC

FXR: Farnesoid X receptor; SHP: Small heterodimer partner; TGR5: Takeda G-protein-coupled receptor 5.

RESULTS

Effects of DJB on body weight and food intake

Body weight and food intake were comparable between the two groups before operation. Due to surgical stress, unrestored gastrointestinal function, and decreased food intake, the body weight of both groups fell to a minimum point in the first week after surgery. As food intake increased, the body weight of both groups gradually recovered to preoperative levels approximately 4 wk after operation. As a nonrestrictive surgery, the DJB group exhibited similar body weight and food intake as the sham group at all measured time points postoperatively (Figures 1A and B).

DJB rapidly improved glucose homeostasis in diabetic rats

There were no significant differences in FBG levels between the two groups preoperatively. The FBG of the DJB group rapidly and significantly declined as early as one week postoperatively and was maintained at a relatively stable level. While the FBG of the sham group was not alleviated after operation and showed a tendency to deteriorate over time. Compared to the sham group, the DJB group exhibited lower FBG at all postoperative time points (Figure 1C).

Consistent with rapidly reduced FBG, the DJB group showed significantly lower blood glucose excursion and AUC_{OGTT} during the OGTT studies at 2 and 8 wk postoperatively (Figures 1D-F), indicating improved glucose tolerance and increased systemic glucose disposal after DJB. To evaluate the impact of DJB on hepatic gluconeogenic capacity, ipPTT was conducted at 2 and 8 wk postoperatively. As shown in Figures 1G-I, the DJB group exhibited reduced glucose excursion and AUC_{ipPTT} in response to intraperitoneal pyruvate challenge, implying that DJB improved hepatic insulin sensitivity and decreased hepatic glucose output in diabetic rats early after surgery.

DJB increased systemic and intraduodenal TBAs, and activated duodenal BA signaling

Compared with the sham group, the DJB-operated rats exhibited elevated fasting and postprandial serum TBAs at 2 and 8 wk postoperatively (Figure 2A). Altered food and digestive juice flow in the gastrointestinal tract also affected luminal TBAs after DJB. As shown in Figure 2B, the DJB group displayed elevated intraluminal TBAs in both the descending and horizontal duodenum 8 wk postoperatively.

To determine the effects of increased intraduodenal TBAs on duodenal BA signaling, the mRNA levels of FXR, TGR5, and small heterodimer partner (SHP) in the duodenal mucosa were evaluated by RT-qPCR eight weeks after surgery. The mRNA expression of FXR and its target gene SHP were concurrently increased in the duodenal mucosa of the DJB group (Figures 2C and D), indicating that the BAs-FXR-SHP pathway was activated. As a membrane bound receptor, TGR5 activation leads to cAMP accumulation in cells. Although DJB did not enhance TGR5 gene expression in the duodenal mucosa (Figures 2C and D), it increased the cAMP content in the horizontal duodenum (Figure 2E). cAMP also tended to increase in the descending duodenum of the DJB group despite no statistical significance (Figure 2E). These results suggest that the duodenal TGR5 receptor may also be activated after DJB.

DJB increased SIRT1 expression and promoted phosphorylation of AMPK in the duodenal mucosa

The ipPTT studies suggested that hepatic gluconeogenesis was reduced after DJB. Elevated duodenal SIRT1 and p-AMPK are associated with suppressed hepatic glucose output *via* the gut-brain-liver neural loop[13,14]. Therefore, to elucidate the underlying mechanism of improved hepatic insulin sensitivity and glucose homeostasis after DJB, duodenal SIRT1 and p-AMPK expression were investigated by western blotting eight weeks after surgery. As shown in Figure 3, DJB increased SIRT1 expression and promoted phosphorylation of AMPK in both the descending and horizontal parts of the duodenum.

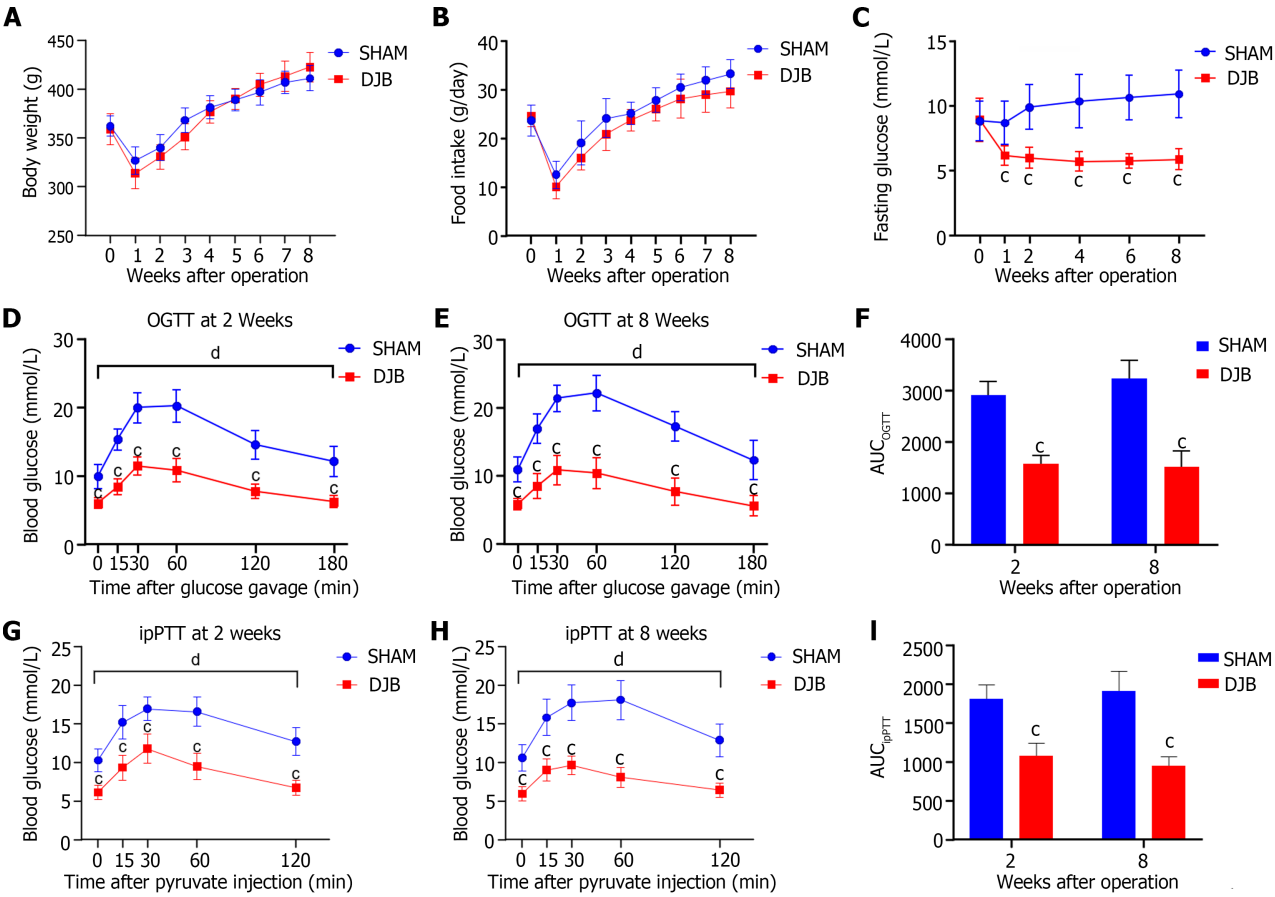

DOI: 10.3748/wjg.v28.i31.4338

Figure 1 Effects of duodenal-jejunal bypass on metabolic parameters. A: Body weight of rats; B: Food intake of rats; C: Fasting blood glucose of rats; D: Oral glucose tolerance test (OGTT) at 2 wk after operation; E: OGTT at 8 wk after operation; F: Area under the curve (AUC) of OGTT at 2 and 8 wk after operation; G: Intraperitoneal pyruvate tolerance test (ipPTT) at 2 wk after operation; H: ipPTT at 8 wk after operation; I: AUC_{ipPTT} at 2 and 8 wk after operation. $^{c}P < 0.001$ duodenal-jejunal bypass (DJB) *vs* sham group by the Student's *t*-test or *post-hoc* Bonferroni's multiple comparison test. $^{d}P < 0.001$, DJB *vs* sham group by mixed model ANOVA. AUC_{OGTT}: Area under the curve of oral glucose tolerance test; AUC_{ipPTT}: Area under the curve of intraperitoneal pyruvate tolerance test; OGTT: Oral glucose tolerance test; ipPTT: Intraperitoneal pyruvate tolerance test; DJB: Duodenal-jejunal bypass.

FXR and TGR5 activation increased SIRT1 expression and promoted phosphorylation of AMPK in IEC-6 cells

To verify whether increased SIRT1 and p-AMPK could be attributed to activated BA signaling in the duodenal mucosa, we treated rat small intestine epithelial IEC-6 cells with FXR and TGR5 agonists, respectively. Upon FXR activation by GW4064, the mRNA expression of FXR, SHP, and SIRT1 were all dramatically upregulated in IEC-6 cells (Figure 4A). Although INT-777 stimulation did not induce TGR5 transcription, it promoted the mRNA expression of SIRT1 (Figure 4B). In line with the increased mRNA expression, the protein levels of SIRT1 were also significantly elevated upon the activation of both BAs receptors (Figures 4C, D, F and G). Although FXR and TGR5 agonists did not increase the gene and protein expression of AMPK, they both promoted AMPK phosphorylation in IEC-6 cells (Figures 4C, E, F and H). These results indicate that the activated BA signaling pathway contributes to the upregulation of SIRT1 and the phosphorylation of AMPK.

DISCUSSION

In this study, we performed DJB and sham surgeries on diabetic rats induced by HFD and STZ, and demonstrated that DJB elevated intraduodenal TBAs, activated the BA signaling pathway and upregulated SIRT1 expression in the duodenal mucosa. By using specific BA receptor agonists, we proved that FXR and TGR5 activation increased SIRT1 expression and promoted phosphorylation of AMPK in rat small intestine epithelial cells, indicating that increased intraluminal BAs and activation of BA receptors contributed to the increased duodenal SIRT1 after DJB.

SIRT1 is an evolutionarily conserved NAD+-dependent deacetylase that belongs to the Sirtuins family (SIRT1-SIRT7)[22]. SIRT1 acts as a key metabolic sensor in the liver, skeletal muscles, adipose tissues, pancreatic islets, and other metabolic tissues. It plays an important role in various aging-related

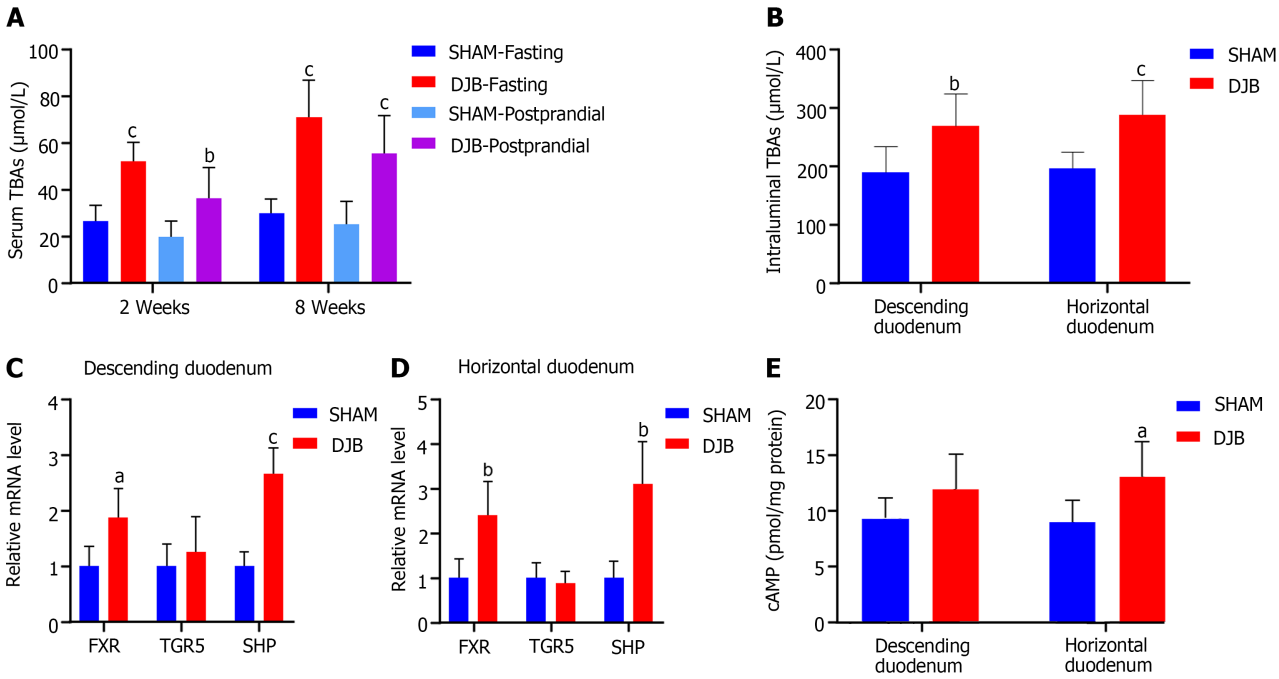

DOI: 10.3748/wjg.v28.i31.4338

Figure 2 Duodenal-jejunal bypass increased serum and intraduodenal total bile acids and activated bile acids signaling in the duodenal mucosa. A: Fasting and postprandial serum total bile acids (TBAs) at 2 and 8 wk after operation; B: Intraluminal TBAs in the descending and horizontal duodenum at 8 wk after operation; C and D: Expression of key genes involved in BA signaling pathway in the mucosa of descending and horizontal duodenum; E: Cyclic adenosine 3',5'-monophosphate concentration in the duodenal mucosa. $^{a}P < 0.05$, $^{b}P < 0.01$, $^{c}P < 0.001$ duodenal-jejunal bypass *vs* sham group. DJB: Duodenal-jejunal bypass; TBAs: Total bile acids; FXR: Farnesoid X receptor; SHP: Small heterodimer partner; TGR5: Takeda G-protein-coupled receptor 5; cAMP: Cyclic adenosine 3',5'-monophosphate.

diseases, including insulin resistance, diabetes, obesity, hepatic steatosis, and cardiovascular diseases [22,23]. Liver-specific deletion of SIRT1 impairs hepatic and systemic insulin sensitivity in mice[24]. Muscular SIRT1 levels are decreased in patients with T2DM and HFD-induced insulin-resistant rats, and overexpression of SIRT1 in skeletal muscle improves muscular insulin sensitivity[25,26]. Adipose tissue-specific ablation of SIRT1 results in increased fat deposition, impaired glucose tolerance and insulin sensitivity in mice[27]. SIRT1 activation protects the function and morphology of residual pancreatic β-cells and induces β-cell regeneration from progenitor cells, thus improving glucose homeostasis[28].

Sleeve gastrectomy (SG) upregulates hepatic SIRT1 and dramatically ameliorates hepatic steatosis in HFD-fed obese mice[29]. RYGB activates the AMPK/SIRT1/PGC-1α pathway in the skeletal muscle of diabetic Zucker fatty rats, which contributes to diabetes remission[30]. Laparoscopic bariatric surgery increases SIRT1 levels in the peripheral blood of patients with obesity and T2DM, which is higher in the effective than in the ineffective group[31]. The effects of bariatric surgeries on duodenal SIRT1 expression have not been investigated previously. Duodenal SIRT1 is a novel therapeutic target for insulin resistance and diabetes. HFD-fed insulin-resistant rats exhibit significantly downregulated SIRT1 in the duodenal mucosa, and duodenum-specific knockdown of SIRT1 is sufficient to induce hepatic insulin resistance in normal chow-fed rats[14]. Our study is the first to demonstrate that DJB promotes SIRT1 expression in the duodenal mucosa. As duodenal SIRT1 activation further inhibits HGP and improves hepatic insulin sensitivity by triggering the gut-hypothalamus-liver neural network[14], we postulate that increased duodenal SIRT1 at least partly accounts for the improved hepatic insulin resistance and glucose homeostasis after DJB.

As an indispensable energy sensor, SIRT1 expression is closely related to energy status and environmental stress[32]. The SIRT1 transcription is usually activated during fasting, which transforms the metabolic status from gluconeogenesis to fat mobilization and fatty acid oxidation[32]. Chen *et al*[33] demonstrated that calorie restriction (CR) increased both pancreatic and hepatic SIRT1 expression in rats. Additionally, Civitarese *et al*[34] reported that CR for 6 mo promoted muscular SIRT1 expression in healthy overweight individuals. In mammalian cells, acute nutrient deprivation increases SIRT1 transcription by activating the Forkhead transcription factor Foxo3a[35]. Although food intake is not reduced after DJB, the duodenum is hindered from contact with ingested food, which might result in a duodenum-specific CR status, thus further inducing duodenal SIRT1 expression. Furthermore, gastric acids are not expelled into the duodenum after DJB, which increases the pH of duodenal content. The deacetylation activity of SIRT1 is pH-dependent, and higher pH attenuates the inhibition of SIRT1 by nicotinamide[36].

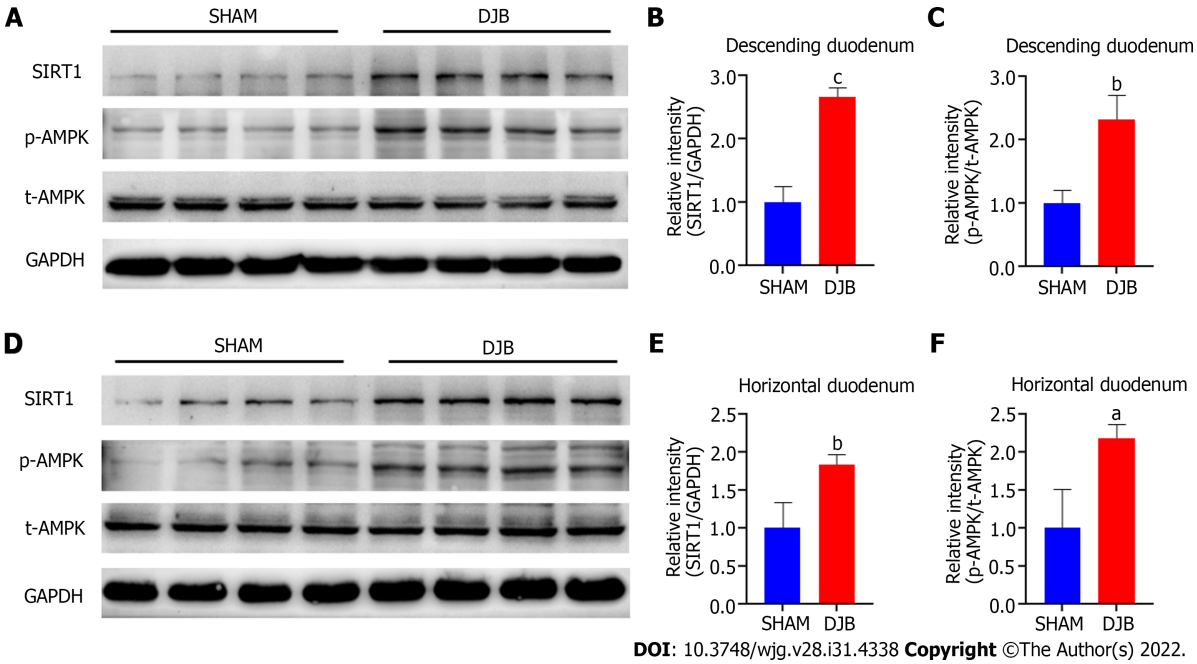

DOI: 10.3748/wjg.v28.i31.4338

Figure 3 Duodenal-jejunal bypass increased SIRT1 expression and promoted phosphorylation of AMPK in the duodenal mucosa. A: Western blot images of SIRT1, phosphorylated AMPK (p-AMPK), and total AMPK (t-AMPK) in the descending duodenum; B and C: The relative intensity of SIRT1 and p-AMPK/t-AMPK in the descending duodenum; D: Western blot images of SIRT1, p-AMPK, and t-AMPK in the horizontal duodenum; E and F: The relative intensity of SIRT1 and p-AMPK/t-AMPK in the horizontal duodenum. $^{a}P < 0.05$, $^{b}P < 0.01$, $^{c}P < 0.001$ duodenal-jejunal bypass *vs* sham group. p-AMPK: Phosphorylated AMPK; t-AMPK: Total AMPK; DJB: Duodenal-jejunal bypass.

Increased intraduodenal BAs might be another key contributor to elevated duodenal SIRT1 after DJB. It is well documented that circulating BAs are increased after numerous metabolic surgeries, including DJB, SG, and RYGB[3,37,38]. By using genetically modified animal models, it has been proven that both FXR and TGR5 are required for the metabolic benefits of SG[39,40]. As demonstrated by our study, DJB not only elevated serum TBAs, but also significantly increased intraduodenal TBAs. Similarly, Ueno *et al* [41] demonstrated that DJB increased conjugated BAs in the bypassed jejunum just distal to the ligament of Treitz. Furthermore, we observed higher SHP mRNA and cAMP concentrations in the duodenal mucosa of DJB-operated rats, indicating that FXR and TGR5 signaling were activated after DJB. Whether causality exists between activated BA signaling and increased SIRT1 in enterocytes has not been investigated.

Numerous studies have suggested that BAs serve as upstream signaling molecules for SIRT1 in various tissues. FXR activation upregulates SIRT1 expression by promoting the transcription of SHP and repressing the transcription of p53 and miR34a in the livers of normal mice[19]. In diabetic *db/db* mice, TGR5 activation increases both the mRNA and protein levels of SIRT1 in the kidneys[42]. Similarly, TGR5 activation upregulates SIRT1 expression in the brains of Sprague Dawley rats[20]. These studies suggest that activation of duodenal FXR and/or TGR5 might account for the increased duodenal SIRT1 after DJB. To verify our hypothesis, we used GW4064 and INT-777 to activate FXR and TGR5 in IEC-6 cells and showed that both agonists increased SIRT1 expression in enterocytes. We also found that GW4064 increased FXR gene expression in IEC-6 cells in accordance with the elevated FXR mRNA in the duodenal mucosa after DJB. Similar changes in FXR mRNA were also observed in mouse mesangial cells after GW4064 stimulation[43].

In addition, we demonstrated that DJB promoted phosphorylation of AMPK in the duodenal mucosa, which might also contribute to improved glucose homeostasis after DJB, as duodenal AMPK activation improves hepatic insulin sensitivity and inhibits hepatic glucose output *via* the gut-hypothalamus-liver neural axis[13]. Jiao *et al*[4] reported that DJB promoted phosphorylation of AMPK in both the liver and skeletal muscle, which contributed to the restoration of normoglycemia after surgery. Likewise, SG enhances AMPK phosphorylation in both the liver and monocytes[44]. Similarly, RYGB exhibits anti-diabetic properties *via* AMPK activation in the liver and Kupffer cells[45]. Actually, as two important energy sensors in cells, AMPK and SIRT1 mutually regulate each other, share many common target molecules, and have similar effects on diverse processes such as glucose and energy metabolism[46]. Our study suggests that activated duodenal AMPK might also be attributed to elevated duodenal BAs because both FXR and TGR5 activation promoted phosphorylation of AMPK in IEC-6 cells.

There are some limitations in our study. First, we only investigated changes in TBAs in the duodenum after DJB. There are numerous components in the BA pool, and different components may exert different metabolic effects. Second, our study did not provide sufficient information on whether

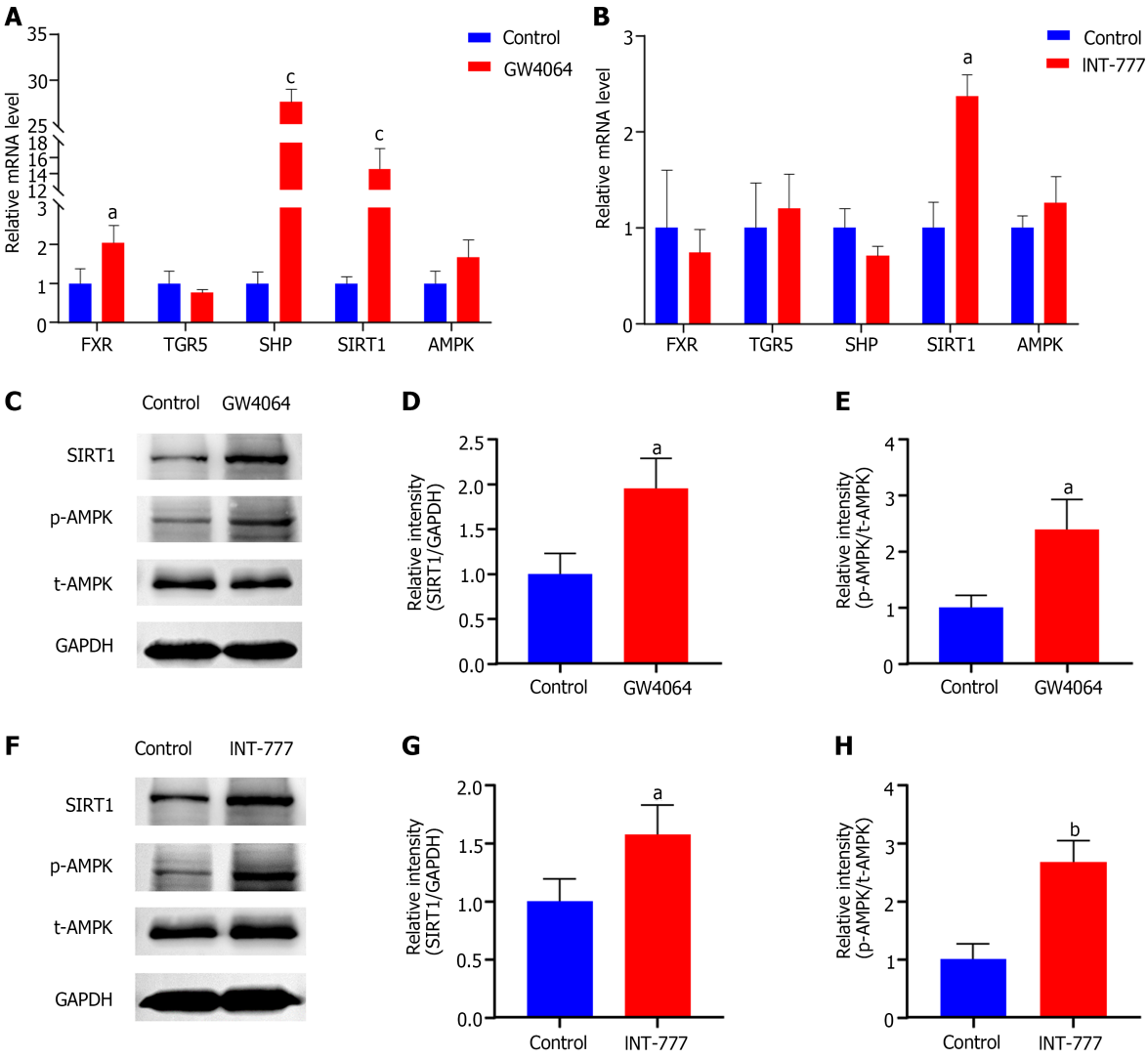

DOI: 10.3748/wjg.v28.i31.4338

Figure 4 Activation of farnesoid X receptor and Takeda G-protein-coupled receptor 5 increased SIRT1 and promoted phosphorylation of AMPK in rat small intestine epithelial IEC-6 cells. A and B: Effects of farnesoid X receptor (FXR) and Takeda G-protein-coupled receptor 5 (TGR5) activation on SIRT1, AMPK, and key genes involved in BA signaling pathway; C: Western blot images of SIRT1, phosphorylated AMPK (p-AMPK), and total AMPK (t-AMPK) in IEC-6 cells after FXR activation; D and E: The relative intensity of SIRT1 and p-AMPK/t-AMPK in IEC-6 cells after FXR activation. F: Western blot images of SIRT1, p-AMPK, and t-AMPK in IEC-6 cells after TGR5 activation; G and H: The relative intensity of SIRT1 and p-AMPK/t-AMPK in IEC-6 cells after TGR5 activation. $^{a}P < 0.05$, $^{b}P < 0.01$, $^{c}P < 0.001$ GW4064 or INT-777 *vs* control group. p-AMPK: Phosphorylated AMPK; t-AMPK: Total AMPK; FXR: Farnesoid X receptor; SHP: Small heterodimer partner; TGR5: Takeda G-protein-coupled receptor 5.

duodenal SIRT1 is indispensable for DJB-induced diabetic control, therefore, duodenum-specific SIRT1 loss- and gain-of-function animal models would be necessary for future studies.

CONCLUSION

DJB upregulates SIRT1 expression in the duodenal mucosa, which may partly account for surgery-induced diabetic control. Increased intraduodenal TBA levels and activated duodenal BA signaling pathway may contribute to the upregulation of duodenal SIRT1 after DJB.

ARTICLE HIGHLIGHTS

Research background

Duodenal-jejunal bypass (DJB) induces rapid and significant amelioration of type 2 diabetes mellitus in various diabetic rat models, while the mechanisms have not been fully elucidated. Duodenal SIRT1

regulates hepatic glucose production and hepatic insulin sensitivity through a gut-brain-liver axis, and activation of bile acid (BA) receptors promotes SIRT1 expression in many tissues. This study aimed at uncovering the roles of duodenal BAs and SIRT1 in the diabetic control after DJB.

Research motivation

To expand and deepen our understanding on the mechanisms underlying diabetes control after DJB, and to provide new ideas and targets for the non-surgical treatment of diabetes in the future.

Research objectives

To investigate the effects of DJB on the duodenal BA signaling pathway and SIRT1 expression in a diabetic rat model, and further reveal the roles of BAs in modulating SIRT1 expression in enterocytes.

Research methods

DJB and sham surgeries were performed on rats with diabetes induced by high-fat diet and low-dose streptozotocin. The effects of surgeries on metabolic parameters were compared accordingly. The intraduodenal BA concentration, the key genes of BA signaling pathway and SIRT1 in the duodenal mucosa were evaluated 8 wk postoperatively. Rat small intestine epithelial IEC-6 cells were treated with GW4064 and INT-777 to verify the effects of BA receptor activation on SIRT1 expression in enterocytes.

Research results

DJB rapidly and dramatically improved glucose homeostasis in the diabetic rats independently of body weight and food intake. DJB increased both systemic and intraduodenal total BAs, activated the BA signaling pathway and promoted SIRT1 expression in the duodenum mucosa. Activation of BA receptors including farnesoid X receptor and Takeda G-protein-coupled receptor 5 increased the mRNA and protein expression of SIRT1 in IEC-6 cells.

Research conclusions

DJB increases intraduodenal BA levels and activates the duodenal BA signaling pathway, which may further contribute to the improved hepatic insulin resistance and glucose homeostasis by upregulating SIRT1 expression in the duodenal mucosa.

Research perspectives

Our findings provide evidence that BA-mediated upregulation of SIRT1 in the duodenum contributes to the diabetic control after DJB. This study also implicates that duodenal BAs and SIRT1 might be potential targets for improving hepatic insulin sensitivity and systemic glucose homeostasis, which lays the groundwork for developing duodenal BA and SIRT1-specific treatments to alleviate diabetes.

ACKNOWLEDGEMENTS

The authors would like to acknowledge Sun M and Liu XM for their skillful technical assistance.

FOOTNOTES

Author contributions: Han HF and Yu WB conceived of the experiments; Liu SZ and Yu WB designed the experiments; Han HF, Zhang X, Wei M, and Huang X carried out the experiments, performed the statistical analyses and wrote the manuscript; and all authors have commented on the initial and final drafts of the manuscript and approved the final version of the article.

Supported by the National Natural Science Foundation of China, No. 81600617, 81700708, 81702647 and 82100853; and the Natural Science Foundation of Shandong Province, No. ZR2020MH246, ZR2021LZL003 and ZR2021QH028.

Institutional animal care and use committee statement: All procedures involving animals were reviewed and approved by the Institutional Animal Care Committee of Cheeloo College of Medicine, Shandong University, (Protocol No. 19085).

Conflict-of-interest statement: All the authors report no relevant conflicts of interest for this article.

Data sharing statement: No additional data are available.

ARRIVE guidelines statement: The authors have read the ARRIVE guidelines, and the manuscript was prepared and revised according to the ARRIVE guidelines.

Country/Territory of origin: China

ORCID number: Hai-Feng Han 0000-0002-1417-9350; Shao-Zhuang Liu 0000-0003-2052-0516; Xiang Zhang 0000-0001-7417-6082; Meng Wei 0000-0002-0402-5083; Xin Huang 0000-0002-6208-4751; Wen-Bin Yu 0000-0001-7111-3780.

S-Editor: Wang JJ
L-Editor: A
P-Editor: Cai YX

REFERENCES

1 **Sun H**, Saeedi P, Karuranga S, Pinkepank M, Ogurtsova K, Duncan BB, Stein C, Basit A, Chan JCN, Mbanya JC, Pavkov ME, Ramachandaran A, Wild SH, James S, Herman WH, Zhang P, Bommer C, Kuo S, Boyko EJ, Magliano DJ. IDF Diabetes Atlas: Global, regional and country-level diabetes prevalence estimates for 2021 and projections for 2045. *Diabetes Res Clin Pract* 2022; **183**: 109119 [PMID: 34879977 DOI: 10.1016/j.diabres.2021.109119]

2 **Khorgami Z**, Shoar S, Saber AA, Howard CA, Danaei G, Sclabas GM. Outcomes of Bariatric Surgery Versus Medical Management for Type 2 Diabetes Mellitus: a Meta-Analysis of Randomized Controlled Trials. *Obes Surg* 2019; **29**: 964-974 [PMID: 30402804 DOI: 10.1007/s11695-018-3552-x]

3 **Zhang X**, Wang Y, Zhong M, Liu T, Han H, Zhang G, Liu S, Wei M, Wu Q, Hu S. Duodenal-Jejunal Bypass Preferentially Elevates Serum Taurine-Conjugated Bile Acids and Alters Gut Microbiota in a Diabetic Rat Model. *Obes Surg* 2016; **26**: 1890-1899 [PMID: 26715331 DOI: 10.1007/s11695-015-2031-x]

4 **Jiao J**, Bae EJ, Bandyopadhyay G, Oliver J, Marathe C, Chen M, Hsu JY, Chen Y, Tian H, Olefsky JM, Saberi M. Restoration of euglycemia after duodenal bypass surgery is reliant on central and peripheral inputs in Zucker fa/fa rats. *Diabetes* 2013; **62**: 1074-1083 [PMID: 23248171 DOI: 10.2337/db12-0681]

5 **Klein S**, Fabbrini E, Patterson BW, Polonsky KS, Schiavon CA, Correa JL, Salles JE, Wajchenberg BL, Cohen R. Moderate effect of duodenal-jejunal bypass surgery on glucose homeostasis in patients with type 2 diabetes. *Obesity (Silver Spring)* 2012; **20**: 1266-1272 [PMID: 22262157 DOI: 10.1038/oby.2011.377]

6 **de Jonge C**, Rensen SS, Verdam FJ, Vincent RP, Bloom SR, Buurman WA, le Roux CW, Schaper NC, Bouvy ND, Greve JW. Endoscopic duodenal-jejunal bypass liner rapidly improves type 2 diabetes. *Obes Surg* 2013; **23**: 1354-1360 [PMID: 23526068 DOI: 10.1007/s11695-013-0921-3]

7 **van Baar ACG**, Holleman F, Crenier L, Haidry R, Magee C, Hopkins D, Rodriguez Grunert L, Galvao Neto M, Vignolo P, Hayee B, Mertens A, Bisschops R, Tijssen J, Nieuwdorp M, Guidone C, Costamagna G, Devière J, Bergman JJGHM. Endoscopic duodenal mucosal resurfacing for the treatment of type 2 diabetes mellitus: one year results from the first international, open-label, prospective, multicentre study. *Gut* 2020; **69**: 295-303 [PMID: 31331994 DOI: 10.1136/gutjnl-2019-318349]

8 **van Baar ACG**, Nieuwdorp M, Holleman F, Soeters MR, Groen AK, Bergman JJGHM. The Duodenum harbors a Broad Untapped Therapeutic Potential. *Gastroenterology* 2018; **154**: 773-777 [PMID: 29428335 DOI: 10.1053/j.gastro.2018.02.010]

9 **Akiba Y**, Kaunitz JD. Duodenal chemosensing and mucosal defenses. *Digestion* 2011; **83** Suppl 1: 25-31 [PMID: 21389725 DOI: 10.1159/000323401]

10 **Rønnestad I**, Akiba Y, Kaji I, Kaunitz JD. Duodenal luminal nutrient sensing. *Curr Opin Pharmacol* 2014; **19**: 67-75 [PMID: 25113991 DOI: 10.1016/j.coph.2014.07.010]

11 **Lam TK**. Neuronal regulation of homeostasis by nutrient sensing. *Nat Med* 2010; **16**: 392-395 [PMID: 20376051 DOI: 10.1038/nm0410-392]

12 **Wang PY**, Caspi L, Lam CK, Chari M, Li X, Light PE, Gutierrez-Juarez R, Ang M, Schwartz GJ, Lam TK. Upper intestinal lipids trigger a gut-brain-liver axis to regulate glucose production. *Nature* 2008; **452**: 1012-1016 [PMID: 18401341 DOI: 10.1038/nature06852]

13 **Duca FA**, Côté CD, Rasmussen BA, Zadeh-Tahmasebi M, Rutter GA, Filippi BM, Lam TK. Metformin activates a duodenal Ampk-dependent pathway to lower hepatic glucose production in rats. *Nat Med* 2015; **21**: 506-511 [PMID: 25849133 DOI: 10.1038/nm.3787]

14 **Côté CD**, Rasmussen BA, Duca FA, Zadeh-Tahmasebi M, Baur JA, Daljeet M, Breen DM, Filippi BM, Lam TK. Resveratrol activates duodenal Sirt1 to reverse insulin resistance in rats through a neuronal network. *Nat Med* 2015; **21**: 498-505 [PMID: 25849131 DOI: 10.1038/nm.3821]

15 **Cao Y**, Jiang X, Ma H, Wang Y, Xue P, Liu Y. SIRT1 and insulin resistance. *J Diabetes Complications* 2016; **30**: 178-183 [PMID: 26422395 DOI: 10.1016/j.jdiacomp.2015.08.022]

16 **Li X**. SIRT1 and energy metabolism. *Acta Biochim Biophys Sin (Shanghai)* 2013; **45**: 51-60 [PMID: 23257294 DOI: 10.1093/abbs/gms108]

17 **Molinaro A**, Wahlström A, Marschall HU. Role of Bile Acids in Metabolic Control. *Trends Endocrinol Metab* 2018; **29**: 31-41 [PMID: 29195686 DOI: 10.1016/j.tem.2017.11.002]

18 **Ahmad TR**, Haeusler RA. Bile acids in glucose metabolism and insulin signalling - mechanisms and research needs. *Nat Rev Endocrinol* 2019; **15**: 701-712 [PMID: 31616073 DOI: 10.1038/s41574-019-0266-7]

19 **Lee J**, Padhye A, Sharma A, Song G, Miao J, Mo YY, Wang L, Kemper JK. A pathway involving farnesoid X receptor and small heterodimer partner positively regulates hepatic sirtuin 1 Levels *via* microRNA-34a inhibition. *J Biol Chem* 2010; **285**: 12604-12611 [PMID: 20185821 DOI: 10.1074/jbc.M109.094524]

20 **Liang H**, Matei N, McBride DW, Xu Y, Tang J, Luo B, Zhang JH. Activation of TGR5 protects blood brain barrier *via* the BRCA1/Sirt1 pathway after middle cerebral artery occlusion in rats. *J Biomed Sci* 2020; **27**: 61 [PMID: 32381096 DOI: 10.1186/s12929-020-00656-9]

21 **Liu S**, Zhang G, Wang L, Sun D, Chen W, Yan Z, Sun Y, Hu S. The entire small intestine mediates the changes in glucose homeostasis after intestinal surgery in Goto-Kakizaki rats. *Ann Surg* 2012; **256**: 1049-1058 [PMID: 23001083 DOI: 10.1097/SLA.0b013e31826c3866]

22 **Zhou S**, Tang X, Chen HZ. Sirtuins and Insulin Resistance. *Front Endocrinol (Lausanne)* 2018; **9**: 748 [PMID: 30574122 DOI: 10.3389/fendo.2018.00748]

23 **Morris BJ**. Seven sirtuins for seven deadly diseases of aging. *Free Radic Biol Med* 2013; **56**: 133-171 [PMID: 23104101 DOI: 10.1016/j.freeradbiomed.2012.10.525]

24 **Wang RH**, Kim HS, Xiao C, Xu X, Gavrilova O, Deng CX. Hepatic Sirt1 deficiency in mice impairs mTorc2/Akt signaling and results in hyperglycemia, oxidative damage, and insulin resistance. *J Clin Invest* 2011; **121**: 4477-4490 [PMID: 21965330 DOI: 10.1172/JCI46243]

25 **Fröjdö S**, Durand C, Molin L, Carey AL, El-Osta A, Kingwell BA, Febbraio MA, Solari F, Vidal H, Pirola L. Phosphoinositide 3-kinase as a novel functional target for the regulation of the insulin signaling pathway by SIRT1. *Mol Cell Endocrinol* 2011; **335**: 166-176 [PMID: 21241768 DOI: 10.1016/j.mce.2011.01.008]

26 **Zhang HH**, Qin GJ, Li XL, Zhang YH, Du PJ, Zhang PY, Zhao YY, Wu J. SIRT1 overexpression in skeletal muscle *in vivo* induces increased insulin sensitivity and enhanced complex I but not complex II-V functions in individual subsarcolemmal and intermyofibrillar mitochondria. *J Physiol Biochem* 2015; **71**: 177-190 [PMID: 25782776 DOI: 10.1007/s13105-015-0396-x]

27 **Li F**, Li H, Jin X, Zhang Y, Kang X, Zhang Z, Xu M, Qian Z, Ma Z, Gao X, Zhao L, Wu S, Sun H. Adipose-specific knockdown of *Sirt1* results in obesity and insulin resistance by promoting exosomes release. *Cell Cycle* 2019; **18**: 2067-2082 [PMID: 31296102 DOI: 10.1080/15384101.2019.1638694]

28 **Wu SY**, Liang J, Yang BC, Leung PS. SIRT1 Activation Promotes β-Cell Regeneration by Activating Endocrine Progenitor Cells *via* AMPK Signaling-Mediated Fatty Acid Oxidation. *Stem Cells* 2019; **37**: 1416-1428 [PMID: 31400234 DOI: 10.1002/stem.3073]

29 **Hua R**, Wang GZ, Shen QW, Yang YP, Wang M, Wu M, Shao YK, He M, Zang Y, Yao QY, Zhang ZY. Sleeve gastrectomy ameliorated high-fat diet (HFD)-induced non-alcoholic fatty liver disease and upregulated the nicotinamide adenine dinucleotide +/ Sirtuin-1 pathway in mice. *Asian J Surg* 2021; **44**: 213-220 [PMID: 32712045 DOI: 10.1016/j.asjsur.2020.05.030]

30 **Huang H**, Aminian A, Hassan M, Dan O, Axelrod CL, Schauer PR, Brethauer SA, Kirwan JP. Gastric Bypass Surgery Improves the Skeletal Muscle Ceramide/S1P Ratio and Upregulates the AMPK/ SIRT1/ PGC-1α Pathway in Zucker Diabetic Fatty Rats. *Obes Surg* 2019; **29**: 2158-2165 [PMID: 30809769 DOI: 10.1007/s11695-019-03800-z]

31 **Wang Y**, Wang DS, Cheng YS, Jia BL, Yu G, Yin XQ, Wang Y. Expression of MicroRNA-448 and SIRT1 and Prognosis of Obese Type 2 Diabetic Mellitus Patients After Laparoscopic Bariatric Surgery. *Cell Physiol Biochem* 2018; **45**: 935-950 [PMID: 29428938 DOI: 10.1159/000487287]

32 **Pardo PS**, Boriek AM. SIRT1 Regulation in Ageing and Obesity. *Mech Ageing Dev* 2020; **188**: 111249 [PMID: 32320732 DOI: 10.1016/j.mad.2020.111249]

33 **Chen YR**, Fang SR, Fu YC, Zhou XH, Xu MY, Xu WC. Calorie restriction on insulin resistance and expression of SIRT1 and SIRT4 in rats. *Biochem Cell Biol* 2010; **88**: 715-722 [PMID: 20651844 DOI: 10.1139/O10-010]

34 **Civitarese AE**, Carling S, Heilbronn LK, Hulver MH, Ukropcova B, Deutsch WA, Smith SR, Ravussin E; CALERIE Pennington Team. Calorie restriction increases muscle mitochondrial biogenesis in healthy humans. *PLoS Med* 2007; **4**: e76 [PMID: 17341128 DOI: 10.1371/journal.pmed.0040076]

35 **Nemoto S**, Fergusson MM, Finkel T. Nutrient availability regulates SIRT1 through a forkhead-dependent pathway. *Science* 2004; **306**: 2105-2108 [PMID: 15604409 DOI: 10.1126/science.1101731]

36 **Rymarchyk S**, Kang W, Cen Y. Substrate-Dependent Sensitivity of SIRT1 to Nicotinamide Inhibition. *Biomolecules* 2021; **11** [PMID: 33670751 DOI: 10.3390/biom11020312]

37 **Wu Q**, Zhang X, Zhong M, Han H, Liu S, Liu T, Wei M, Guo W, Xie H, Hu S, Zhang G. Effects of Bariatric Surgery on Serum Bile Acid Composition and Conjugation in a Diabetic Rat Model. *Obes Surg* 2016; **26**: 2384-2392 [PMID: 26843082 DOI: 10.1007/s11695-016-2087-2]

38 **Patti ME**, Houten SM, Bianco AC, Bernier R, Larsen PR, Holst JJ, Badman MK, Maratos-Flier E, Mun EC, Pihlajamaki J, Auwerx J, Goldfine AB. Serum bile acids are higher in humans with prior gastric bypass: potential contribution to improved glucose and lipid metabolism. *Obesity (Silver Spring)* 2009; **17**: 1671-1677 [PMID: 19360006 DOI: 10.1038/oby.2009.102]

39 **Ryan KK**, Tremaroli V, Clemmensen C, Kovatcheva-Datchary P, Myronovych A, Karns R, Wilson-Pérez HE, Sandoval DA, Kohli R, Bäckhed F, Seeley RJ. FXR is a molecular target for the effects of vertical sleeve gastrectomy. *Nature* 2014; **509**: 183-188 [PMID: 24670636 DOI: 10.1038/nature13135]

40 **Ding L**, Sousa KM, Jin L, Dong B, Kim BW, Ramirez R, Xiao Z, Gu Y, Yang Q, Wang J, Yu D, Pigazzi A, Schones D, Yang L, Moore D, Wang Z, Huang W. Vertical sleeve gastrectomy activates GPBAR-1/TGR5 to sustain weight loss, improve fatty liver, and remit insulin resistance in mice. *Hepatology* 2016; **64**: 760-773 [PMID: 27312543 DOI: 10.1002/hep.28689]

41 **Ueno T**, Tanaka N, Imoto H, Maekawa M, Kohyama A, Watanabe K, Motoi F, Kamei T, Unno M, Naitoh T. Mechanism of Bile Acid Reabsorption in the Biliopancreatic Limb After Duodenal-Jejunal Bypass in Rats. *Obes Surg* 2020; **30**: 2528-2537 [PMID: 32291708 DOI: 10.1007/s11695-020-04506-3]

42 **Wang XX**, Edelstein MH, Gafter U, Qiu L, Luo Y, Dobrinskikh E, Lucia S, Adorini L, D'Agati VD, Levi J, Rosenberg A, Kopp JB, Gius DR, Saleem MA, Levi M. G Protein-Coupled Bile Acid Receptor TGR5 Activation Inhibits Kidney Disease

in Obesity and Diabetes. *J Am Soc Nephrol* 2016; **27**: 1362-1378 [PMID: 26424786 DOI: 10.1681/ASN.2014121271]

43 **Jiang T**, Wang XX, Scherzer P, Wilson P, Tallman J, Takahashi H, Li J, Iwahashi M, Sutherland E, Arend L, Levi M. Farnesoid X receptor modulates renal lipid metabolism, fibrosis, and diabetic nephropathy. *Diabetes* 2007; **56**: 2485-2493 [PMID: 17660268 DOI: 10.2337/db06-1642]

44 **Angelini G**, Castagneto Gissey L, Del Corpo G, Giordano C, Cerbelli B, Severino A, Manco M, Basso N, Birkenfeld AL, Bornstein SR, Genco A, Mingrone G, Casella G. New insight into the mechanisms of ectopic fat deposition improvement after bariatric surgery. *Sci Rep* 2019; **9**: 17315 [PMID: 31754142 DOI: 10.1038/s41598-019-53702-4]

45 **Peng Y**, Li JZ, You M, Murr MM. Roux-en-Y gastric bypass improves glucose homeostasis, reduces oxidative stress and inflammation in livers of obese rats and in Kupffer cells *via* an AMPK-dependent pathway. *Surgery* 2017; **162**: 59-67 [PMID: 28291540 DOI: 10.1016/j.surg.2017.01.012]

46 **Ruderman NB**, Xu XJ, Nelson L, Cacicedo JM, Saha AK, Lan F, Ido Y. AMPK and SIRT1: a long-standing partnership? *Am J Physiol Endocrinol Metab* 2010; **298**: E751-E760 [PMID: 20103737 DOI: 10.1152/ajpendo.00745.2009]

World Journal of Gastroenterology

Submit a Manuscript: https://www.f6publishing.com

World J Gastroenterol 2022 August 21; 28(31): 4351-4362

DOI: 10.3748/wjg.v28.i31.4351

ISSN 1007-9327 (print) ISSN 2219-2840 (online)

ORIGINAL ARTICLE

Retrospective Study

Approaches to reconstruction of inferior vena cava by *ex vivo* liver resection and autotransplantation in 114 patients with hepatic alveolar echinococcosis

Yusufukadier Maimaitinijiati, Tuerganaili AJi, Tie-Min Jiang, Bo Ran, Ying-Mei Shao, Rui-Qing Zhang, Qiang Guo, Mao-Lin Wang, Hao Wen

Specialty type: Gastroenterology and hepatology

Provenance and peer review: Unsolicited article; Externally peer reviewed.

Peer-review model: Single blind

Peer-review report's scientific quality classification

Grade A (Excellent): 0
Grade B (Very good): B, B
Grade C (Good): 0
Grade D (Fair): 0
Grade E (Poor): 0

P-Reviewer: Sánchez JIA, Colombia; Singh N, United States

Received: February 11, 2022
Peer-review started: February 11, 2022
First decision: May 29, 2022
Revised: June 10, 2022
Accepted: July 25, 2022
Article in press: July 25, 2022
Published online: August 21, 2022

Yusufukadier Maimaitinijiati, Tie-Min Jiang, Hao Wen, State Key Laboratory on Pathogenesis, Prevention and Treatment of High Incidence Diseases in Central Asia, The First Clinical College, Xinjiang Medical University, Urumqi 830011, Xinjiang Uygur Autonomous Region, China

Yusufukadier Maimaitinijiati, Tuerganaili AJi, Tie-Min Jiang, Bo Ran, Ying-Mei Shao, Rui-Qing Zhang, Qiang Guo, Mao-Lin Wang, Department of Hepatobiliary Surgery, The First Affiliated Hospital of Xinjiang Medical University, Urumqi 830011, Xinjiang Uygur Autonomous Region, China

Ying-Mei Shao, Hao Wen, Xinjiang Organ Transplant Institution, The First Affiliated Hospital of Xinjiang Medical University, Urumqi 830011, Xinjiang Uygur Autonomous Region, China

Corresponding author: Hao Wen, MD, PhD, Chief Doctor, Professor, State Key Laboratory on Pathogenesis, Prevention and Treatment of High Incidence Diseases in Central Asia, The First Clinical College, Xinjiang Medical University, No. 8 Liyushan South Road, Xinshi District, Xinjiang Uygur Autonomous Region 830011, Xinjiang, China. surgeon0309@126.com

Abstract

BACKGROUND

Hepatic alveolar echinococcosis (AE) is most commonly found in retrohepatic inferior vena cava (RHIVC). *Ex vivo* liver resection and autotransplantation (ELRA) can better realize the radical resection of end-stage hepatic AE with severely compromised hepatocaval confluences, and reconstruction of the affected vessels. Currently, there is a scarcity of information regarding RHIVC reconstruction in ELRA.

AIM

To propose reasonable RHICV reconstruction strategies for *ex vivo* liver resection and autotransplantation.

METHODS

We retrospectively summarized the clinical data of 114 patients diagnosed with hepatic AE who treated by ELRA in our department. A total of 114 patients were

divided into three groups according to the different reconstruction methods of RHIVC: Group A with original RHIVC being repaired and reconstructed (n = 64), group B with RHIVC being replaced (n = 43), and group C with RHIVC being resected without reconstruction (n = 7). The clinical data of patients, including the operation time, anhepatic phase, intraoperative blood loss, complications and postoperative hospital stay, were analyzed and the patients were routinely followed up. The normally distributed continuous variables were expressed as means ± SD, whereas the abnormally distributed ones were expressed as median and analyzed by analysis of variance. Survival curve was plotted by the Kaplan-Meier method.

RESULTS

All patients were routinely followed up for a median duration of 52 (range, 12-125) mo. The 30 d mortality rate was 7.0% (8/114) and 7 patients died within 90 d. Among all subjects, the inferior vena cava (IVC)-related complication rates were 17.5% (11/63) in group A and 16.3% (7/43) in group B. IVC stenosis was found in 12 patients (10.5%), whereas thrombus was formed in 6 patients (5.3%). Twenty-two patients had grade III or higher complications, with the complication rates being 17.2%, 16.3%, and 57.1% in the three groups. The average postoperative hospital stay in the three groups was 32.3 ± 19.8, 26.7 ± 18.2, and 51.3 ± 29.4 d (P = 0.03), respectively.

CONCLUSION

ELRA can be considered a safe and feasible option for end-stage hepatic AE patients with RHIVC infiltration. The RHIVC reconstruction methods should be selected appropriately depending on the defect degree of AE lesions in IVC lumen. The RHIVC resection without any reconstruction method should be considered with caution.

Key Words: *Ex vivo* liver resection; Alveolar echinococcosis; Inferior vena cava; Vascular reconstruction; Liver transplantation; Artificial vessel

Core Tip: We retrospectively summarized and analyzed the clinical data of 114 patients diagnosed with hepatic alveolar echinococcosis (AE) treated by *ex vivo* liver resection and autotransplantation (ELRA) in our department between August 2010 and December 2020. This study is the first and largest cohort to specifically compare the different inferior vena cava (IVC) reconstruction methods in ELRA. We present a more quantitative IVC reconstruction strategy for end-stage hepatic AE patients with retrohepatic IVC infiltration based on the outcomes of this study and our experience.

Citation: Maimaitinijiati Y, AJi T, Jiang TM, Ran B, Shao YM, Zhang RQ, Guo Q, Wang ML, Wen H. Approaches to reconstruction of inferior vena cava by *ex vivo* liver resection and autotransplantation in 114 patients with hepatic alveolar echinococcosis. *World J Gastroenterol* 2022; 28(31): 4351-4362
URL: https://www.wjgnet.com/1007-9327/full/v28/i31/4351.htm
DOI: https://dx.doi.org/10.3748/wjg.v28.i31.4351

INTRODUCTION

Echinococcosis is an infectious zoonotic parasitic disease[1,2]. Notably, 90% of the global burden of this disease occurs in China, and echinococcosis has been a major public health problem in the Northwestern area of China[3,4]. Hepatic alveolar echinococcosis (AE) has been considered invasive growth and systematic metastasis[5,6], but its insidious onset and slow progression usually contribute to the delayed diagnosis. The mortality rate within 10 years after diagnosis is over 90% if the lesion is inadequately or not treated[7-9]. To date, radical surgery combined with albendazole treatment has been considered the best option for AE patients[10,11]. However, it is difficult to perform radical hepatectomy *in vivo* when AE lesion invades the hepatocaval confluence[12]. Generally, only 35%-40% of patients can be treated with conventional radical resection[7]. Fortunately, *ex vivo* liver resection and autotransplantation (ELRA) can better realize the radical resection of end-stage hepatic AE with severely compromised outflow tract, and reconstruction of the affected vessels[13].

Retrohepatic inferior vena cava (RHIVC) is often severely invaded by AE lesions, and resection of the invaded duct segment often presents a variety of irregular shapes, resulting in different inferior vena cava (IVC) reconstruction methods and the complex process. Proper RHIVC reconstruction may simplify graft liver implantation, which is a key element to postoperative recovery. To the best of our

knowledge, there have been few studies on the reconstruction of IVC in ELRA worldwide[14,15], and no clear consensus has been reached on the optimal strategy. This research reported our experience with 114 hepatic AE patients using different IVC reconstruction methods in ELRA. This is the study with the largest sample size to date, which provides a quantitative strategy of IVC reconstruction for end-stage hepatic AE patients with RHIVC infiltration.

MATERIALS AND METHODS

Patients

A total of 114 patients with end-stage hepatic AE who received ELRA at the First Affiliated Hospital of Xinjiang Medical University between August 2010 and December 2020 were retrospectively analyzed. All patients were divided into three groups: Group A was the repaired and reconstructed group (n = 64) that sought reconstruction of the original RHIVC by self-suture or vascular patch, group B was the RHIVC replacement group (n = 43) that completely replaced the RHIVC with substitute vessels, and group C was the RHIVC resection without reconstruction group (n = 7) that excised the invaded RHIVC segment without reconstruction (Table 1).

Medical ethical approval

This study was approved by the Ethics Committee of First Affiliated Hospital of Xinjiang Medical University and conducted in accordance with the Helsinki Declaration[16]. Written and signed informed consent was obtained from all patients or their legal custodians.

Preoperative assessment

All subjects underwent comprehensive preoperative evaluation, including abdominal computed tomography angiography (CTA) and hepatic magnetic resonance imaging, to assess the location of the lesion, the extent of vessel and bile duct involvement. For patients whose CTA results suggested RHIVC severe stenosis or occlusion, IVC digital subtraction angiography was also performed. The predicted autograft liver mass (GLM) was detected by a three-dimensional reconstruction system.

Surgical procedures

More details of the ELRA procedures are reported in our previous study[13]. Here, we focused on the reconstruction of IVC. First, we ligated and resected the IVC between the upward side of the confluence of three hepatic veins and the site at 1 cm above the confluence of renal vein, and removed it together with the liver. Then the RHIVC was reconstructed *in vitro* individually depending on the defect of lumen wall after radical resection of AE lesion. When the defect was less than 120° of the lumen circumference, it was considered that directly suturing the defect of wall did not affect vascular tension or patency, and thus self-suture repair was performed. When the defect was more than 120° of the circumference, we repaired the lumen defect with vascular patches such as ligamentum teres hepatis and internal jugular veins, because direct suturing might lead to stenosis in this case. Moreover, the RHIVC was replaced in patients with extensive defect and being unable to obtain adequate vascular patches. The hepatic veins of autograft liver were anastomosed with an alternative vessel. In this case, the position and angle of anastomosis were relatively freely controlled, which facilitated the increased reflux of hepatic outflow and further improved the recovery of autograft liver function (Figure 1).

Uniquely, for some patients in this study, the preoperative CTA and IVC venography showed that the RHIVC segment was completely occluded, and suitably compensated by the collateral branches. During the operation, we further verified whether the RHIVC was completely occluded and whether the collateral circulation was sufficient. Finally, for the 7 patients, the AE infiltrated segment of IVC was resected without any reconstruction, the proximal end of IVC was anastomosed with autogenous hepatic vein, and the distal end was closed directly (Figure 1).

Postoperative management and follow-up

After surgery, all patients received systemic anticoagulant therapy. Low-molecular-weight heparin was used in the 1st week, and prothrombin time (PT) and international normalized ratio (INR) were closely observed. In the 2nd week, oral tablets were substituted, and patients in group A and group C were recommended to withdraw these drugs 1 mo later when the PT and INR returned to normal levels. Patients in group B, however, needed to continue the medication for a long term and closely observe the coagulation index regularly. Each patient was regularly followed up, and serological tests, liver function tests and CTA scans were performed every 3-6 mo after discharge. Postoperative complications were assessed according to the Clavein-Dindo classification system[17]. All patients were administered with albendazole (10 mg/kg/d) routinely for 2 years[18].

Statistical analyses

The statistical software IBM SPSS 22.0 (IBM Corp, Armonk, NY, United States) was used for data

Table 1 Clinical data of 114 alveolar echinococcosis patients treated by *ex vivo* liver resection and autotransplantation

Characteristics	Group A, *n* = 64	Group B, *n* = 43	Group C, *n* = 7	Total, *n* = 114	*P* value
Sex					0.12
Male	24	21	5	50	
Female	40	22	2	64	
Age in yr	36.9 ± 12.3	36.9 ± 10.5	30.8 ± 14.1	36.2 ± 11.8	0.29
Hepatitis B (+)	3	3	1	7	0.37
Intervention history					0.84
No	30	27	5	62	
Hepatectomy	11	9	1	21	
PTCD or ERCP	17	7	1	25	
Albendazole history	16	11	0	27	0.31
Extrahepatic lesion					0.44
No	51	30	6	87	
Lung	10	9	1	20	
Kidney	1	1	1	3	
Atrium	0	1	0	1	
Brain	4	2	0	6	
Bone	0	1	0	1	

ERCP: Endoscopic retrograde cholangio-pancreatography; PTCD: Percutaneous transhepatic cholangial drainage.

analysis. The normally distributed continuous variables were expressed as means ± SD, whereas the abnormally distributed ones were expressed as medians and analyzed by analysis of variance. Survival curve was plotted by the Kaplan–Meier method. $P < 0.05$ was considered statistically significant.

RESULTS

Patient characteristics

Altogether 114 patients were treated by ELRA, including 50 males (43.9%) and 64 females (56.1%), with an average age of 36.2 ± 11.8 (range, 15-64) years. Preoperative PTCD or ERCP was performed in 25 patients to reduce the bilirubin levels and biliary obstructions. There were 21 patients with a previous history of hepatectomy. Albendazole therapy was administered to 27 patients. The average GLM was 828.3 ± 250.8 g. There were no significant differences in basic clinical data among the three groups ($P > 0.05$; Table 1).

Intraoperative outcomes

Intraoperative reassessment confirmed that AE lesions invaded the RHIVC in all patients, and RHIVC repair or reconstruction was needed. Among them, the self-suture repairing was performed in 52 patients with a defective RHIVC lumen less than 120° of circumference after R0 resection. The lumen defect was repaired with autologous vascular patches in 12 patients whose defect was 120°-180° of wall circumference. Meanwhile, 43 patients had defect exceeding 180° of circumference with extensive range and difficulty in reestablishing with autogenous patches. For these cases, the RHIVC was replaced with artificial vascular grafts ($n = 38$) or allogeneic vascular ($n = 5$). In another 7 patients, preoperative imaging examination indicated that the RHIVC segment was occluded and a collateral circulation network was formed. During the operation, stable systemic hemodynamics with no obvious intestinal congestion was found after the IVC was ligated. Finally, the RHIVC was resected without reconstruction (Figure 2). The average operation time was 16.7 ± 2.9 h for group A, 15.5 ± 3.1 h for group B, and 16.9 ± 4.1 h for group C ($P = 0.56$), and the average anhepatic phase was 418.4 ± 108.3, 383.9 ± 117.0, and 337.4 ± 108.7 min in groups A, B and C ($P = 0.41$; Table 2).

Table 2 Intraoperative outcomes for 114 alveolar echinococcosis patients

	Group A, *n* = 64	Group B, *n* = 43	Group C, *n* = 7	Total, *n* = 114	*P* value
Operative time in h	16.7 ± 2.9	15.5 ± 3.2	16.9 ± 4.2	16.3 ± 3.1	0.56
Anhepatic phase in min	418.4 ± 108.3	383.9 ± 117.0	337.4 ± 108.7	394.0 ± 114.5	0.41
Blood loss in mL	1100 (400-15000)	1000 (400-8000)	2400 (800-14000)	1000 (400-15000)	0.07
Blood transfusion in U	5.8 ± 4.3	5.9 ± 3.9	14.8 ± 9.9	6.4 ± 6.2	0.90
Postoperative hospital stays in d	32.3 ± 19.8	26.7 ± 18.2	51.3 ± 29.4	36.4 ± 21.7	0.03
GLM in g	783.9 ± 233.5	908.6 ± 262.0	740.0 ± 235.6	828.3 ± 250.8	0.14
GLM/SLM, %	65.5 ± 18.9	74.1 ± 20.5	64.1 ± 17.8	68.6 ± 19.8	0.25
Materials (*n*)	Self-suture (52); Ligamentum teres hepatis (11); Internal jugular vein (1)	Artificial vascular (38); Allogeneic vascular (5)	Without reconstruction		

GLM: Graft liver mass; SLM: Standard liver mass.

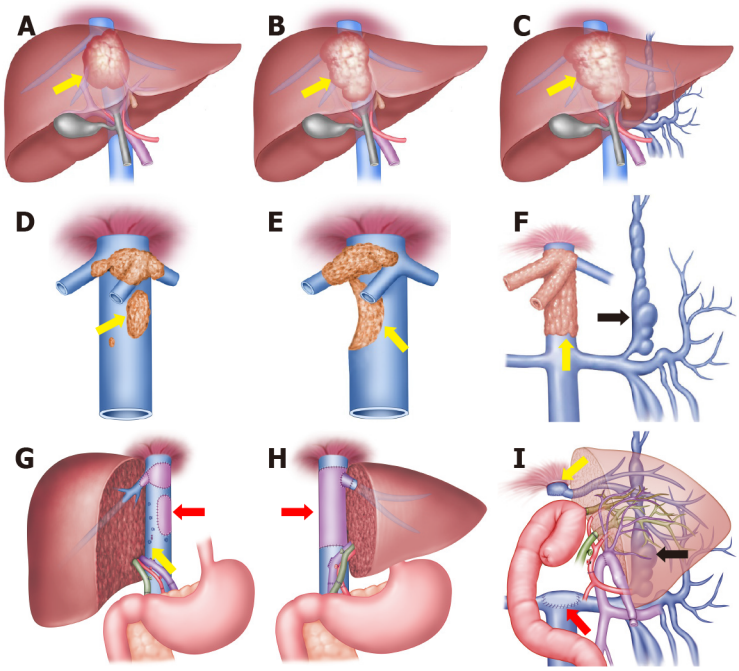

DOI: 10.3748/wjg.v28.i31.4351 **Copyright** ©The Author(s) 2022.

Figure 1 Schematic diagrams of retrohepatic inferior vena cava reconstruction methods. A-C: Hepatic alveolar echinococcosis (AE) lesion invades the hepatocaval confluence; D: Retrohepatic inferior vena cava (RHIVC) is invaded by the AE lesion (yellow arrow); E: RHIVC is extensive invaded (yellow arrow); F: RHIVC completely occluded (yellow arrow), and compensation by the collateral branches (black arrow); G: Self-repairing reconstruction method, showed vascular patch repair (red arrow) and self-suture repair (yellow arrow); H: RHIVC replacement method, showed the RHIVC after replacement (red arrow); I: RHIVC resection without reconstruction method, showed IVC anastomoses with graft liver hepatic vein (yellow arrow) and adrenal vein (red arrow), the collateral circulation branches after operation (black arrow).

Postoperative and follow-up outcomes

All patients were followed up with a median duration of 52 (range, 12-125) mo, except for 1 patient who was lost to follow-up at 6 mo after the operation. No intraoperative death occurred. The 30 d mortality rate was 7.0% (8/114) and another 7 patients died within 90 d (15/114). Among all subjects, the IVC-related complication rates were 17.5% (11/63) in group A and 16.3% (7/43) in group B. IVC stenosis was found in 12 patients (10.5%), and thrombus was formed in 6 patients (5.3%). Twenty-two patients experienced grade III or higher complications according to the Clavin-Dindo classification system, and the complication rates were 17.2%, 16.3% and 57.1%, in the three groups (Table 3). The average

Table 3 Follow-up outcomes for 114 alveolar echinococcosis patients treated by *ex vivo* liver resection and autotransplantation

	Group A, *n* = 64	Group B, *n* = 43	Group C, *n* = 7	Total
Complications				
Clavien-Dindo Grade IIb or lower	27 (42.2%)	19 (44.2%)	3 (42.9%)	49 (43.0%)
Clavien-Dindo Grade IIIa or higher	11 (17.2%)	7 (16.3%)	4 (57.1%)	22 (19.3%)
IVC related complications				
IVC thrombosis	1 (1.6%)	5 (11.6%)	0	6 (5.3%)
IVC stenosis	10 (15.6%)	2 (4.7%)	0	12 (10.5%)
Liver related complications				
Biliary leakage	9 (14.1%)	7(16.3%)	3 (42.9%)	19 (16.7%)
Budd-chiari syndrome	1(1.6%)	1(2.33%)	0	2 (1.8%)
Hepatic dysfunction	8 (12.5%)	3(7.0%)	1 (14.3%)	12 (10.5%)
Pleural effusion	19	10	0	29
Ascites	8	6	3	17
Renal failure	3	0	0	3
Bone marrow suppression	0	0	1	1
Abdominal infection	2	2	1	5

IVC: Inferior vena cava.

postoperative hospital stay was 32.3 ± 19.8 d for group A, 26.7 ± 18.2 d for group B and 51.3 ± 29.4 d for group C (P = 0.03). Obviously, patients in group B obviously required a shorter postoperative hospital stay than the other two groups.

Kaplan-Meier survival analysis curve and log-rank test were used to observe the postoperative survival for the three groups based on the follow-up results. The survival rates of group A and group B were quite close, whereas that of group C was lower, but the differences were not statistically significant (P = 0.81). The early periods after surgery, especially in the 1st month, witnessed the high mortality rate (Figure 3).

DISCUSSION

Hepatic AE is also known as "parasitic cancer," which is ascribed to its tumor-like characteristics with infiltration of vessels or biliary structures and distant metastasis[19]. The insidious onset and slow progression of AE usually contribute to the delayed diagnosis, and hepatic veins and RHIVC are often invaded by the time when treatment is sought in more than half of the patients, thus depriving them of the opportunity for traditional surgical resection[20,21]. In 1986, the Liver Transplantation Center of Bezancon Hospital in France was the first to report allogeneic liver transplantation (ALT) for an end-stage hepatic AE patient[22]. Since then, more successful clinical cases and treatment experience with liver transplantation for end-stage hepatic AE have been reported worldwide[23-26]. However, a shortage of donor livers and a significant recurrence rate have limited the further development of ALT for hepatic AE[24,27]. In 2010, our center first applied ELRA to manage a patient with end-stage hepatic AE[28]. Compared with ALT, this technique requires no graft donor or immunosuppressive treatment, and is more affordable[29,30]. In particular, it is more suitable for patients with severe invasion of RHIVC and intrahepatic veins whose are unresectable by traditional surgical methods. Notably, the corresponding reconstruction of autograft liver RHIVC remains the most challenging step in the ELRA procedures, since no uniform fixed pattern is available and individual design is required. To date, very few studies have investigated the reconstruction of IVC in ELRA worldwide (Table 4), and no clear consensus has been reached on the optimal reconstruction strategy. In this study, we analyzed the largest series of end-stage hepatic AE cases with seriously infringed RHIVC who received ELRA treatment, and discussed the safety and effectiveness of three different IVC reconstruction methods.

Reconstruction options for the RHIVC are assessed individually from preoperative evaluation and intraoperative reassessment of vascular defect. In our center, the repairing and reconstruction method was used when the defect in the RHIVC was less than 180° of the lumen circumference after radical resection of the lesion. The average operation time and anhepatic phase of this pattern were relatively

Table 4 Literature summary of inferior vena cava reconstruction in *ex vivo* liver resection and autotransplantation

Ref.	Number of cases	IVC reconstructed	Reconstructed type	Follow up time in mo	Effect of reconstruction
Wen *et al*[28], 2011	1	No	-	-	-
Hwang *et al*[34], 2012	6	No	-	-	-
Lei *et al*[15], 2015	1	Yes	III	12	Satisfied
Wen *et al*[29], 2016	15	No	-	-	-
Shen *et al*[14], 2018	45	Yes	I and II	22	Satisfied
Aji *et al*[13], 2018	69	No	-	-	-
Du *et al*[37], 2019	8	Yes	III	23	Satisfied
Ran *et al*[32], 2019	1	Yes	III	-	-
Kong *et al*[38], 2019	2	No	-	-	-
Yang *et al*[39], 2020	5	Yes	III	18	Unsatisfied
Zhang *et al*[40], 2020	1	Yes	II	6	Satisfied
Ran *et al*[41], 2021	7	Yes	III	64	Unsatisfied
Jiang *et al*[33], 2021	6	Yes	I	17.5	Satisfied

IVC: Inferior vena cava. Reconstructed type: I: Retrohepatic inferior vena cava (RHIVC) self-repairing reconstruction; II: RHIVC replacement; III: RHIVC resection without reconstruction; -: There is no related description.

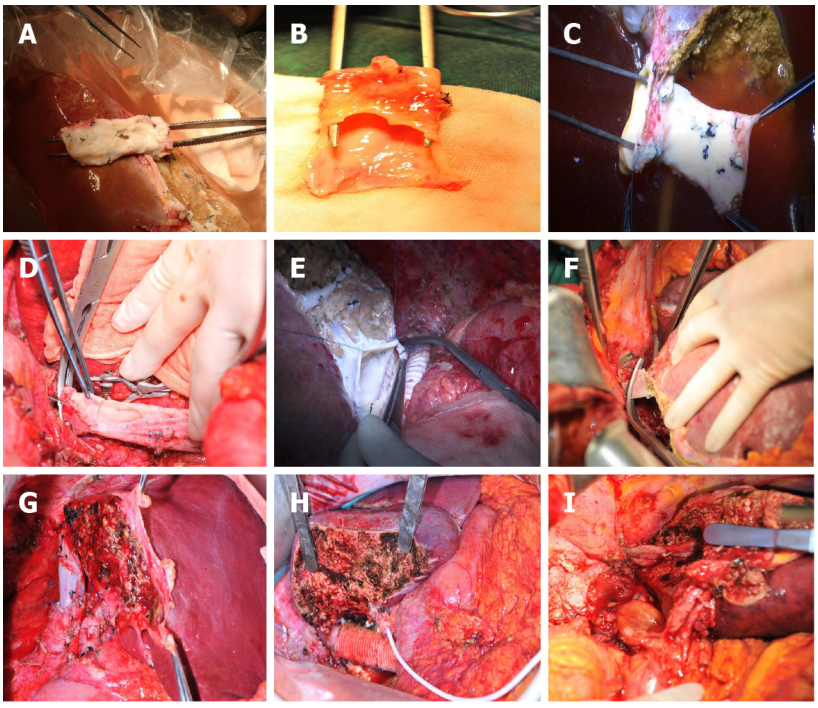

DOI: 10.3748/wjg.v28.i31.4351 **Copyright** ©The Author(s) 2022.

Figure 2 Intraoperative procedures. A: The infiltrated retrohepatic inferior vena cava (RHIVC); B: The large defect of RHIVC after radical resection; C: The RHIVC with self-suture repairing; D: The original RHIVC anastomoses with hepatic vein; E: The artificial blood vessel anastomoses with graft liver hepatic vein; F: The suprahepatic IVC anastomoses with left hepatic vein; G: The autologous RHIVC after reconstruction; H: Artificial RHIVC; I: Anastomotic stoma of suprahepatic IVC and hepatic vein.

longer than the other two methods, which was attributed to the diversity and complexity of this approach. RHIVC stenosis occurred in 10 patients, but only 1 developed lower limb edema, and the symptoms disappeared after balloon dilation. Meanwhile, no clinical symptoms were found in the other 9 patients. It seemed that IVC stenosis after surgery might be related to the longer cold ischemia time and tunica intimal injury during the reconstruction process. In this regard, strict management of the

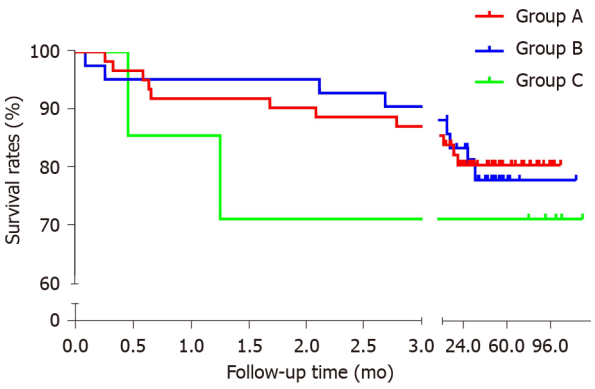

DOI: 10.3748/wjg.v28.i31.4351

Figure 3 Kaplan-Meier survival analysis curve.

reconstruction time and shortening the cold ischemia phase as much as possible are the key factors for preventing IVC stenosis[31]. Based on previous reports[32,33] and our experience, the ligamentum teres hepatis is applied most often as a vascular patch, due to its convenience and strong plasticity. Postoperative patency and prognosis of these patients are satisfactory, suggesting that reconstruction with autogenous materials may be the optimal choice for RHIVC, although the process is complex and demanding.

Generally, replacement of the RHIVC is indicated for patients those with a large defect after resection that cannot be repaired by suture or patch. In the present study, 38 patients had the RHIVC replaced with artificial vessels, and 5 were treated with the cryopreserved allogeneic vascular donated after citizen death (DCD). Due to the shortage of resources, rejection, high preservation requirements and time restrictions, DCD vessels are not the first choice for substitute material. In our center, the expanded polytetrafluoroethylene artificial vessel (Sokang Corp, Shanghai, China)[34] is generally preferred. RHIVC replacement with artificial vascular is not only convenient, but also effectively shortens the anhepatic phase and operation time. On the other hand, artificial vessels are associated with potential risk, including venous thrombosis, artificial vascular malformation, and distortion or stenosis of anastomoses caused by postoperative liver hyperplasia. In our research, thrombosis of artificial vessels occurred in 5 patients, among them, 2 died of liver failure due to simultaneous thrombosis of the IVC and portal vein. Another 3 patients developed lower limb or scrotal edema, and the symptoms recovered after symptomatic treatments, including thrombolysis and anticoagulation. In addition, stenosis of anastomoses was found in 2 patients. As there may not be any clinical means for decreasing the incidence of graft thrombosis and stenosis apart from anti-coagulation and anti-infective treatment, we recommend that replacement of RHIVC with artificial materials should be avoided when it can be reestablished with autogenous materials.

Hepatic AE behaves like a slow-growing "warm cancer," and occlusion and severe stenosis of the IVC is a chronic process, which provides sufficient time for the establishment of collateral circulation. The obstructed blood flow can induce expansion of lumbar vein plexus, azygos vein and hemiazygos vein on both sides of the spine, as well as the formation of a functional collateral circulation network[32] Although the extent of vascular invasion is a vital indicator for the choice of reconstruction method, it remains controversial whether the IVC should be reconstructed for patients with adequate collateral circulation. Blair *et al*[35] proposed that, for low-grade retroperitoneal sarcoma, resection without reconstruction was performed after the establishment of collateral circulation. In addition, Hardwigse *et al*[36] also reported IVC resection without reconstruction in 6 patients with hepatic carcinoma. Unlike malignant tumors, the parasite grows relatively slow, which provides enough time for the organism to form collateral circulation. Among our subjects, 7 received RHIVC resection without reconstruction, since a sufficient collateral path was formed, but the outcomes were unsatisfactory. To be specific, postoperative complications occurred in all 7 patients, and their survival rate was only 71.1%. One patient died of liver failure on the 14th day after operation, and another one died of multiple organ failure caused by severe abdominal infection on the 38th day after operation. There is little previous information available concerning resection without reconstruction of the RHIVC in ELRA (Table 4). Before this study, Du *et al*[37] reported 8 patients receiving IVC resection without reconstruction, thus supporting this approach from the most reported cases at that time. In their subjects, 1 patient died of upper gastrointestinal bleeding, and 3 developed lower extremity or scrotal edema. Comparatively, the complication rate and postoperative hospital stay in our study were relatively high, which might be related to the immature collateral circulation or pathway destruction by excessive traction of diaphragm. It cannot be determined whether these poor outcomes are related to not providing reconstruction, and more studies are needed for further elucidation. To be sure, a comprehensive preoperative evaluation system and a meticulous intraoperative procedure are essential to the success of this method.

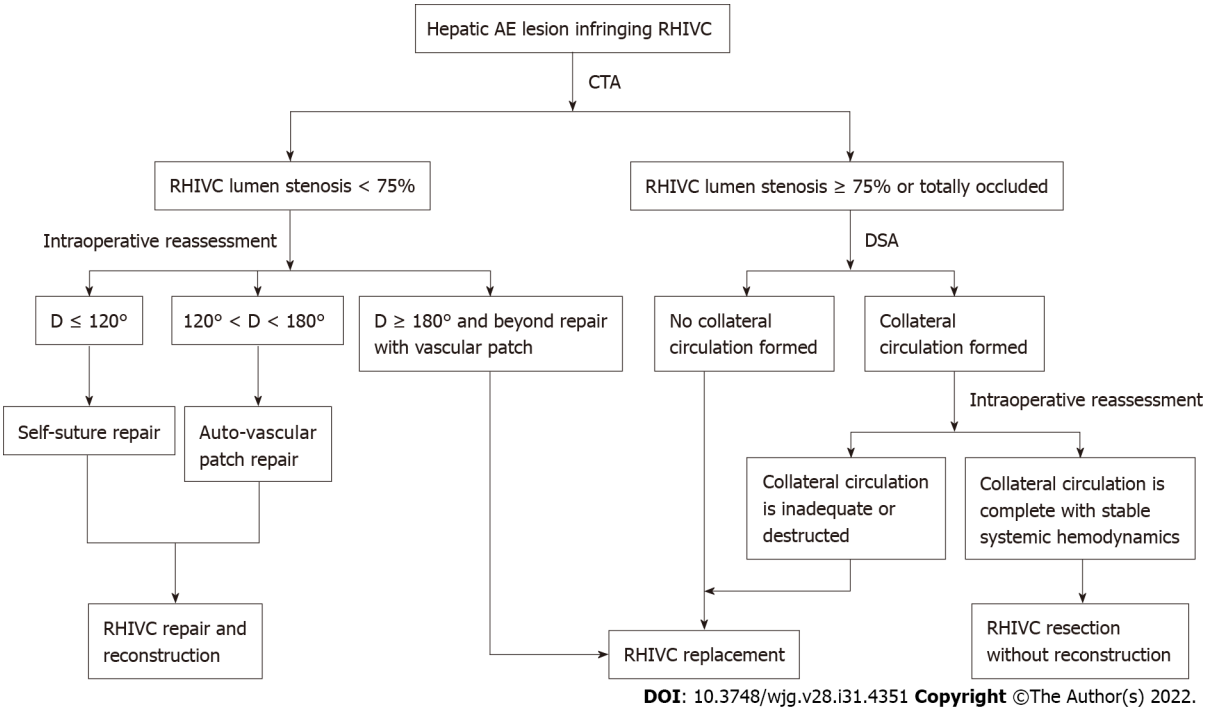

DOI: 10.3748/wjg.v28.i31.4351

Figure 4 Strategy for retrohepatic inferior vena cava reconstruction in *ex vivo* liver resection and autotransplantation. CTA: Computed tomography angiography; D represents the defect of retrohepatic inferior vena cava lumen after resection; DSA: Digital subtraction angiography; RHIVC: Retrohepatic inferior vena cava.

Surgical planning based on a reasonable strategy can improve the success rate of operation and reduce related complications. In this study, although adverse outcomes were not entirely avoided, the postoperative complications and prognosis were acceptable, showing that our approaches were relatively safe and effective on end-stage hepatic AE with infiltrating outflow vessels of the liver. Based on the outcome of the present study and our experience, the following strategies are recommended for IVC reconstruction in hepatic AE patients treated by ELRA: (1) When the wall defect of the IVC after radical resection is less than 120° of the lumen circumference, the self-suture method can be used; (2) If the defect is 120°-180° of circumference, repair with autogenous vascular patches is the optimal choice; (3) When the defect has exceeded 180° of circumference and is difficult to repair by autologous patches, the RHIVC should be replaced. However, the strict anticoagulation therapy must be provided postoperatively; and (4) The RHIVC resection without reconstruction approaches are suitable when the IVC is completely blocked and the collateral circulation is fully formed (Figure 4). Although this study reports a retrospective single-center experience, it is also the largest cohort to specifically compare the different IVC reconstruction methods in ELRA, which can serve as a reference for IVC reconstruction in liver transplantation.

CONCLUSION

In short, ELRA can be considered a safe and feasible option for the end-stage hepatic AE patients with RHIVC infiltration. The RHIVC reconstruction approaches should be selected appropriately according to the lumen defect degree after radical resection. It should be emphasized that RHIVC resection without reconstruction should be considered with caution, and RHIVC reestablishment may be more beneficial for patients with poor compensation. Regrettably, the strategy does not consider the length of the wall defect, since it is related to the location, angle, elasticity and tension of the vessel, all of which are hard to be quantified without a larger dataset of cases. Therefore, prospective, multicenter studies with long-term follow-up are necessary to further evaluate and improve the strategy presented here.

ARTICLE HIGHLIGHTS

Research background

Ex vivo liver resection and auto-transplantation (ELRA) can better realize the radical resection of end-stage hepatic alveolar echinococcosis (AE) with severely compromised hepatocaval confluences, and the

reconstruction of the affected vessels.

Research motivation

There are no clear consensus has been reached on the strategy for retrohepatic inferior vena cava (RHIVC) reconstruction in ELRA.

Research objectives

To provide a strategy of RHIVC reconstruction for end-stage hepatic AE patients with hepatocaval confluence infiltration.

Research methods

The clinical data of 114 patients, including the operation time, anhepatic phase, intraoperative blood loss, complications and postoperative hospital stay, were analyzed and the patients were routinely followed up.

Research results

We found a lower survival rate in group C (resection without reconstruction method) than in groups A (self-suture repairing method) and B (replacement method). Also, the complications rate was higher in group C.

Research conclusions

The RHIVC reconstruction methods should be selected appropriately depending on the defect degree of AE lesions in IVC lumen.

Research perspectives

Our strategies can serve as a reference for IVC reconstruction in liver transplantation.

FOOTNOTES

Author contributions: Maimaitinijiati Y contributed to the conception and design, and drafting of the article; Maimaitinijiati Y and Ran B contributed to the acquisition of data, analysis, and interpretation of data; Jiang TM, Tuerganaili A, and Wen H contributed to the conception and design, and provision of study material; Jiang TM, Zhang RQ, Guo Q, and Wang ML contributed to the data collection; Shao YM did provision of study material; Zhang RQ analyzed the data; Wen H did final approval of the version to be submitted.

Institutional review board statement: The study was approved by the Human Ethics Committee of the First Affiliated Hospital of Xinjiang Medical University and conducted in accordance with the Declaration of Helsinki. All data were analyzed anonymously.

Informed consent statement: Informed written consent was obtained from the patient for publication of this report and any accompanying images.

Conflict-of-interest statement: The authors have no conflicts of interest to declare.

Data sharing statement: The datasets used and analyzed during the current study are available from the corresponding author on reasonable request.

Country/Territory of origin: China

ORCID number: Yusufukadier Maimaitinijiati 0000-0003-2069-9202; AJi Tuerganaili 0000-0001-6737-8874; Tie-Min Jiang 0000-0002-6100-1870; Bo Ran 0000-0002-0241-3410; Rui-Qing Zhang 0000-0003-3022-2555; Ying-Mei Shao 0000-0001-5154-345X; Qiang Guo 0000-0002-5943-4255; Mao-Lin Wang 0000-0001-8944-0894; Hao Wen 0000-0002-6431-9382.

S-Editor: Zhang H
L-Editor: Filipodia
P-Editor: Zhang H

REFERENCES

1 **McManus DP**, Zhang W, Li J, Bartley PB. Echinococcosis. *Lancet* 2003; **362**: 1295-1304 [PMID: 14575976 DOI: 10.1016/S0140-6736(03)14573-4]

2 **Eckert J**, Deplazes P. Biological, epidemiological, and clinical aspects of echinococcosis, a zoonosis of increasing concern. *Clin Microbiol Rev* 2004; **17**: 107-135 [PMID: 14726458 DOI: 10.1128/cmr.17.1.107-135.2004]

3 **Torgerson PR**, Keller K, Magnotta M, Ragland N. The global burden of alveolar echinococcosis. *PLoS Negl Trop Dis* 2010; **4**: e722 [PMID: 20582310 DOI: 10.1371/journal.pntd.0000722]

4 **Piarroux M**, Piarroux R, Giorgi R, Knapp J, Bardonnet K, Sudre B, Watelet J, Dumortier J, Gérard A, Beytout J, Abergel A, Mantion G, Vuitton DA, Bresson-Hadni S. Clinical features and evolution of alveolar echinococcosis in France from 1982 to 2007: results of a survey in 387 patients. *J Hepatol* 2011; **55**: 1025-1033 [PMID: 21354448 DOI: 10.1016/j.jhep.2011.02.018]

5 **Kern P**, Menezes da Silva A, Akhan O, Müllhaupt B, Vizcaychipi KA, Budke C, Vuitton DA. The Echinococcoses: Diagnosis, Clinical Management and Burden of Disease. *Adv Parasitol* 2017; **96**: 259-369 [PMID: 28212790 DOI: 10.1016/bs.apar.2016.09.006]

6 **Vuitton D**. Alveolar echinococcosis of the liver: a parasitic disease in search of a treatment. *Hepatology* 1990; **12**: 617-618 [PMID: 2401464 DOI: 10.1002/hep.1840120329]

7 **Bresson-Hadni S**, Vuitton DA, Bartholomot B, Heyd B, Godart D, Meyer JP, Hrusovsky S, Becker MC, Mantion G, Lenys D, Miguet JP. A twenty-year history of alveolar echinococcosis: analysis of a series of 117 patients from eastern France. *Eur J Gastroenterol Hepatol* 2000; **12**: 327-336 [PMID: 10750654 DOI: 10.1097/00042737-200012030-00011]

8 **Vuitton DA**, Azizi A, Richou C, Vuitton L, Blagosklonov O, Delabrousse E, Mantion GA, Bresson-Hadni S. Current interventional strategy for the treatment of hepatic alveolar echinococcosis. *Expert Rev Anti Infect Ther* 2016; **14**: 1179-1194 [PMID: 27686694 DOI: 10.1080/14787210.2016.1240030]

9 **Brunetti E**, Kern P, Vuitton DA; Writing Panel for the WHO-IWGE. Expert consensus for the diagnosis and treatment of cystic and alveolar echinococcosis in humans. *Acta Trop* 2010; **114**: 1-16 [PMID: 19931502 DOI: 10.1016/j.actatropica.2009.11.001]

10 **Filippou D**, Tselepis D, Filippou G, Papadopoulos V. Advances in liver echinococcosis: diagnosis and treatment. *Clin Gastroenterol Hepatol* 2007; **5**: 152-159 [PMID: 17157079 DOI: 10.1016/j.cgh.2006.08.017]

11 **Vuitton D A**, Bresson-Hadni S. Alveolar echinococcosis: evaluation of therapeutic strategies. *Expert Opin Orphan D* 2014; **67** [DOI: 10.1517/21678707.2014.870033]

12 **Qiu Y**, Yang X, Shen S, Huang B, Wang W. Vascular infiltration-based surgical planning in treating end-stage hepatic alveolar echinococcosis with ex vivo liver resection and autotransplantation. *Surgery* 2019; **165**: 889-896 [PMID: 30591376 DOI: 10.1016/j.surg.2018.11.007]

13 **Aji T**, Dong JH, Shao YM, Zhao JM, Li T, Tuxun T, Shalayiadang P, Ran B, Jiang TM, Zhang RQ, He YB, Huang JF, Wen H. Ex vivo liver resection and autotransplantation as alternative to allotransplantation for end-stage hepatic alveolar echinococcosis. *J Hepatol* 2018; **69**: 1037-1046 [PMID: 30031886 DOI: 10.1016/j.jhep.2018.07.006]

14 **Shen S**, Kong J, Zhao J, Wang W. Outcomes of different surgical resection techniques for end-stage hepatic alveolar echinococcosis with inferior vena cava invasion. *HPB (Oxford)* 2019; **21**: 1219-1229 [PMID: 30782476 DOI: 10.1016/j.hpb.2018.10.023]

15 **Lei JY**, Hao JC, Wang WT, Yan LN, Zhao JC, Huang B, Yuan D. Ex vivo liver resection followed by autotransplantation to a patient with advanced alveolar echinococcosis with a replacement of the retrohepatic inferior vena cava using autogenous vein grafting: a case report and literature review. *Medicine (Baltimore)* 2015; **94**: e514 [PMID: 25700312 DOI: 10.1097/MD.0000000000000514]

16 **World Medical Association**. World Medical Association Declaration of Helsinki: ethical principles for medical research involving human subjects. *JAMA* 2013; **310**: 2191-2194 [PMID: 24141714 DOI: 10.1001/jama.2013.281053]

17 **Dindo D**, Demartines N, Clavien PA. Classification of surgical complications: a new proposal with evaluation in a cohort of 6336 patients and results of a survey. *Ann Surg* 2004; **240**: 205-213 [PMID: 15273542 DOI: 10.1097/01.sla.0000133083.54934.ae]

18 **Wen H**, Vuitton L, Tuxun T, Li J, Vuitton DA, Zhang W, McManus DP. Echinococcosis: Advances in the 21st Century. *Clin Microbiol Rev* 2019; **32** [PMID: 30760475 DOI: 10.1128/cmr.00075-18]

19 **Conraths FJ**, Probst C, Possenti A, Boufana B, Saulle R, La Torre G, Busani L, Casulli A. Potential risk factors associated with human alveolar echinococcosis: Systematic review and meta-analysis. *PLoS Negl Trop Dis* 2017; **11**: e0005801 [PMID: 28715408 DOI: 10.1371/journal.pntd.0005801]

20 **Qian MB**, Abela-Ridder B, Wu WP, Zhou XN. Combating echinococcosis in China: strengthening the research and development. *Infect Dis Poverty* 2017; **6**: 161 [PMID: 29157312 DOI: 10.1186/s40249-017-0374-3]

21 **Bresson-Hadni S**, Koch S, Miguet JP, Gillet M, Mantion GA, Heyd B, Vuitton DA; European group of clinicians. Indications and results of liver transplantation for Echinococcus alveolar infection: an overview. *Langenbecks Arch Surg* 2003; **388**: 231-238 [PMID: 12905036 DOI: 10.1007/s00423-003-0394-2]

22 **Geering K**. Lipase and unspecific esterase activity in the fat body of Aedes aegypti L. *Acta Trop* 1975; **32**: 273-276 [PMID: 1988]

23 **Rajcáni J**, Krobová J, Málková D. Distribution of Lednice (Yaba 1) virus in the chick embryo. *Acta Virol* 1975; **19**: 467-472 [PMID: 1991]

24 **Koch S**, Bresson-Hadni S, Miguet JP, Crumbach JP, Gillet M, Mantion GA, Heyd B, Vuitton DA, Minello A, Kurtz S; European Collaborating Clinicians. Experience of liver transplantation for incurable alveolar echinococcosis: a 45-case European collaborative report. *Transplantation* 2003; **75**: 856-863 [PMID: 12660515 DOI: 10.1097/01.tp.0000054230.63568.79]

25 **Pan GD**, Yan LN, Li B, Lu SC, Zeng Y, Wen TF, Zhao JC, Cheng NS, Ma YK, Wang WT, Yang JY, Li ZH. Liver transplantation for patients with hepatic alveolar echinococcosis in late stage. *Hepatobiliary Pancreat Dis Int* 2004; **3**: 499-503 [PMID: 15567732]

26 **Li F**, Yang M, Li B, Yan L, Zen Y, Wen T, Zao J. Initial clinical results of orthotopic liver transplantation for hepatic alveolar echinococcosis. *Liver Transpl* 2007; **13**: 924-926 [PMID: 17538987 DOI: 10.1002/lt.21187]

27 **Bresson-Hadni S**, Blagosklonov O, Knapp J, Grenouillet F, Sako Y, Delabrousse E, Brientini MP, Richou C, Minello A, Antonino AT, Gillet M, Ito A, Mantion GA, Vuitton DA. Should possible recurrence of disease contraindicate liver transplantation in patients with end-stage alveolar echinococcosis? *Liver Transpl* 2011; **17**: 855-865 [PMID: 21455928 DOI: 10.1002/lt.22299]

28 **Wen H**, Dong JH, Zhang JH, Zhao JM, Shao YM, Duan WD, Liang YR, Ji XW, Tai QW, Aji T, Li T. Ex vivo liver resection followed by autotransplantation for end-stage hepatic alveolar echinococcosis. *Chin Med J (Engl)* 2011; **124**: 2813-2817 [PMID: 22040485]

29 **Wen H**, Dong JH, Zhang JH, Duan WD, Zhao JM, Liang YR, Shao YM, Ji XW, Tai QW, Li T, Gu H, Tuxun T, He YB, Huang JF. Ex Vivo Liver Resection and Autotransplantation for End-Stage Alveolar Echinococcosis: A Case Series. *Am J Transplant* 2016; **16**: 615-624 [PMID: 26460900 DOI: 10.1111/ajt.13465]

30 **Yang X**, Qiu Y, Huang B, Wang W, Shen S, Feng X, Wei Y, Lei J, Zhao J, Li B, Wen T, Yan L. Novel techniques and preliminary results of ex vivo liver resection and autotransplantation for end-stage hepatic alveolar echinococcosis: A study of 31 cases. *Am J Transplant* 2018; **18**: 1668-1679 [PMID: 29232038 DOI: 10.1111/ajt.14621]

31 **Rodrigues MG**, Castro PMV, Almeida TC, Danziere FR, Sergi Filho FA, Zeballos Sempertegui BE, Branez JR, Mota LT, Perosa de Miranda M, Gomes Dos Santos R, Genzini T. Impact of Cold Ischemia Time on the Function of Liver Grafts Preserved With Custodiol. *Transplant Proc* 2021; **53**: 661-664 [PMID: 33139037 DOI: 10.1016/j.transproceed.2020.03.002]

32 **Ran B**, Shao YM, Jiang TM, Zhang RQ, Guo Q, Abulizi A, Yimiti Y, Wen H, Aji T. Resection of retrohepatic inferior vena cava without reconstruction for hepatic alveolar echinococcosis. *Chin Med J (Engl)* 2019; **132**: 1623-1624 [PMID: 31205076 DOI: 10.1097/CM9.0000000000000297]

33 **Jiang T**, Ran B, Guo Q, Zhang R, Duan S, Zhong K, Wen H, Shao Y, Aji T. Use of the ligamentum teres hepatis for outflow reconstruction during ex vivo liver resection and autotransplantation in patients with hepatic alveolar echinococcosis: A case series of 24 patients. *Surgery* 2021; **170**: 822-830 [PMID: 33994007 DOI: 10.1016/j.surg.2021.03.040]

34 **Hwang S**, Jung DH, Ha TY, Ahn CS, Moon DB, Kim KH, Song GW, Park GC, Jung SW, Yoon SY, Namgoong JM, Park CS, Park YH, Park HW, Lee HJ, Lee SG. Usability of ringed polytetrafluoroethylene grafts for middle hepatic vein reconstruction during living donor liver transplantation. *Liver Transpl* 2012; **18**: 955-965 [PMID: 22511404 DOI: 10.1002/lt.23456]

35 **Blair AB**, Reames BN, Singh J, Gani F, Overton HN, Beaulieu RJ, Lum YW, Black JH 3rd, Johnston FM, Ahuja N. Resection of retroperitoneal sarcoma en-bloc with inferior vena cava: 20 year outcomes of a single institution. *J Surg Oncol* 2018; **118**: 127-137 [PMID: 29878363 DOI: 10.1002/jso.25096]

36 **Hardwigsen J**, Baqué P, Crespy B, Moutardier V, Delpero JR, Le Treut YP. Resection of the inferior vena cava for neoplasms with or without prosthetic replacement: a 14-patient series. *Ann Surg* 2001; **233**: 242-249 [PMID: 11176131 DOI: 10.1097/00000658-200102000-00014]

37 **Du Q**, Wang Y, Zhang M, Chen Y, Mei X, Li Y, Zhou Y, Fan H. A new treatment strategy for end-stage hepatic alveolar echinococcosis: IVC resection without reconstruction. *Sci Rep* 2019; **9**: 9419 [PMID: 31263143 DOI: 10.1038/s41598-019-45968-5]

38 **Kong J**, Shen S, Yang X, Wang W. Transhepatic-intrahepatic branches of the portal vein catheterization for ex vivo liver resection and autotransplantation: Two case reports of novel approach to perfuse the liver. *Medicine (Baltimore)* 2019; **98**: e14706 [PMID: 30882634 DOI: 10.1097/MD.0000000000014706]

39 **Yang X**, Wang T, Kong J, Huang B, Wang W. Resection of retrohepatic inferior vena cava without reconstruction in ex vivo liver resection and autotransplantation: a retrospective study. *BMC Surg* 2020; **20**: 56 [PMID: 32209078 DOI: 10.1186/s12893-020-00720]

40 **Zhang Y**, Xie P, Yang C, Yang H, Liu J, Zhou G, Deng S, Lau WY. Percutaneous stenting of left hepatic vein followed by Ex vivo Liver Resection and Autotransplantation in a patient with hepatic alveolar echinococcosis with Budd-Chiari syndrome. *Int J Surg Case Rep* 2020; **68**: 251-256 [PMID: 32199250 DOI: 10.1016/j.ijscr.2020.03.004]

41 **Ran B**, Maimaitinijiati Y, Yasen A, Jiang T, Zhang R, Guo Q, Shao Y, Wen H, Aji T. Feasibility of Retrohepatic Inferior Vena Cava Resection Without Reconstruction for Hepatic Alveolar Echinococcosis. *Am Surg* 2021; **87**: 443-449 [PMID: 33026233 DOI: 10.1177/0003134820951457]

World Journal of Gastroenterology

Submit a Manuscript: https://www.f6publishing.com

World J Gastroenterol 2022 August 21; 28(31): 4363-4375

DOI: 10.3748/wjg.v28.i31.4363

ISSN 1007-9327 (print) ISSN 2219-2840 (online)

ORIGINAL ARTICLE

Retrospective Study

Application of computed tomography-based radiomics in differential diagnosis of adenocarcinoma and squamous cell carcinoma at the esophagogastric junction

Ke-Pu Du, Wen-Peng Huang, Si-Yun Liu, Yun-Jin Chen, Li-Ming Li, Xiao-Nan Liu, Yi-Jing Han, Yue Zhou, Chen-Chen Liu, Jian-Bo Gao

Specialty type: Radiology, nuclear medicine and medical imaging

Provenance and peer review: Unsolicited article; Externally peer reviewed.

Peer-review model: Single blind

Peer-review report's scientific quality classification

Grade A (Excellent): A
Grade B (Very good): B, B
Grade C (Good): C
Grade D (Fair): 0
Grade E (Poor): 0

P-Reviewer: Ferreira GSA, Brazil; Ghoneim S, United States; Okasha H, Egypt; Sato H, Japan

Received: March 16, 2022
Peer-review started: March 16, 2022
First decision: June 11, 2022
Revised: June 11, 2022
Accepted: July 25, 2022
Article in press: July 25, 2022
Published online: August 21, 2022

Ke-Pu Du, Wen-Peng Huang, Yun-Jin Chen, Li-Ming Li, Yi-Jing Han, Yue Zhou, Chen-Chen Liu, Jian-Bo Gao, Department of Radiology, The First Affiliated Hospital of Zhengzhou University, Zhengzhou 450052, Henan Province, China

Si-Yun Liu, Department of Pharmaceutical Diagnostics, General Electric Company Healthcare, Beijing 100176, China

Xiao-Nan Liu, Department of Pathology, The First Affiliated Hospital of Zhengzhou University, Zhengzhou 450052, Henan Province, China

Corresponding author: Jian-Bo Gao, PhD, Academic Research, Chairman, Chief Doctor, Instructor, Department of Radiology, The First Affiliated Hospital of Zhengzhou University, No. 1 East Jianshe Road, Zhengzhou 450052, Henan Province, China.
jianbogaochina@163.com

Abstract

BACKGROUND

The biological behavior of carcinoma of the esophagogastric junction (CEGJ) is different from that of gastric or esophageal cancer. Differentiating squamous cell carcinoma of the esophagogastric junction (SCCEG) from adenocarcinoma of the esophagogastric junction (AEG) can indicate Siewert stage and whether the surgical route for patients with CEGJ is transthoracic or transabdominal, as well as aid in determining the extent of lymph node dissection. With the development of neoadjuvant therapy, preoperative determination of pathological type can help in the selection of neoadjuvant radiotherapy and chemotherapy regimens.

AIM

To establish and evaluate computed tomography (CT)-based multiscale and multiphase radiomics models to distinguish SCCEG and AEG preoperatively.

METHODS

We retrospectively analyzed the preoperative contrasted-enhanced CT imaging data of single-center patients with pathologically confirmed SCCEG (n = 130) and AEG (n = 130). The data were divided into either a training (n = 182) or a test group (n = 78) at a ratio of 7:3. A total of 1409 radiomics features were separately

extracted from two dimensional (2D) or three dimensional (3D) regions of interest in arterial and venous phases. Intra-/inter-observer consistency analysis, correlation analysis, univariate analysis, least absolute shrinkage and selection operator regression, and backward stepwise logical regression were applied for feature selection. Totally, six logistic regression models were established based on 2D and 3D multi-phase features. The receiver operating characteristic curve analysis, the continuous net reclassification improvement (NRI), and the integrated discrimination improvement (IDI) were used for assessing model discrimination performance. Calibration and decision curves were used to assess the calibration and clinical usefulness of the model, respectively.

RESULTS

The 2D-venous model (5 features, AUC: 0.849) performed better than 2D-arterial (5 features, AUC: 0.808). The 2D-arterial-venous combined model could further enhance the performance (AUC: 0.869). The 3D-venous model (7 features, AUC: 0.877) performed better than 3D-arterial (10 features, AUC: 0.876). And the 3D-arterial-venous combined model (AUC: 0.904) outperformed other single-phase-based models. The venous model showed a positive improvement compared with the arterial model (NRI > 0, IDI > 0), and the 3D-venous and combined models showed a significant positive improvement compared with the 2D-venous and combined models ($P < 0.05$). Decision curve analysis showed that combined 3D-arterial-venous model and 3D-venous model had a higher net clinical benefit within the same threshold probability range in the test group.

CONCLUSION

The combined arterial-venous CT radiomics model based on 3D segmentation can improve the performance in differentiating EGJ squamous cell carcinoma from adenocarcinoma.

Key Words: Esophagogastric junction; Squamous cell carcinoma; Adenocarcinoma; X-ray computed tomography; Radiomics

Core Tip: In this study, multiscale and multiphase computed tomography (CT)-based radiomics models were constructed and evaluated to discriminate squamous cell carcinoma and adenocarcinoma of the esophagogastric junction (CEGJ) before operation. The results demonstrated that the combination of multiphase 3D CT radiomics features could improve the differentiation performance than 2D CT radiomics or single-phase-based radiomics. Therefore, radiomics method could help open up a new field for noninvasive diagnosis and personalized management of CEGJ.

Citation: Du KP, Huang WP, Liu SY, Chen YJ, Li LM, Liu XN, Han YJ, Zhou Y, Liu CC, Gao JB. Application of computed tomography-based radiomics in differential diagnosis of adenocarcinoma and squamous cell carcinoma at the esophagogastric junction. *World J Gastroenterol* 2022; 28(31): 4363-4375
URL: https://www.wjgnet.com/1007-9327/full/v28/i31/4363.htm
DOI: https://dx.doi.org/10.3748/wjg.v28.i31.4363

INTRODUCTION

Carcinoma of the esophagogastric junction (CEGJ) is defined as a carcinoma whose center is located within 5 cm above and below the esophagogastric anatomical junction and crosses the esophagogastric junction (EGJ). Due to the short and narrow EGJ site and the up-and-down invasive nature of the CEGJ, its biological behavior is different from that of gastric or esophageal cancer[1-3]. The Siewert staging, which is widely accepted in academia, classifies CEGJ into types I, II, and III based on the distance between the tumor center and the EGJ[4]. Because of the infiltrative growth pattern of the tumor, the distance between the tumor center and the EGJ in CEGJ is difficult to measure accurately, and Siewert staging is often not easy to determine directly. Squamous cell carcinoma of the esophagogastric junction (SCCEG) has different clinicopathological features from adenocarcinoma of the esophagogastric junction (AEG). Based on the results from previous research, mediastinal lymph node metastases are more likely to occur in SCCEG above the EGJ, whereas metastases from the AEG under the EGJ probably appear in the abdomen[5,6]. Differentiating SCCEG from AEG can indicate Siewert stage and whether the surgical route for patients with CEGJ is transthoracic or transabdominal, as well as aid in determining the extent of lymph node dissection. With the development of neoadjuvant therapy,

preoperative determination of pathological type can help in the selection of neoadjuvant radiotherapy and chemotherapy regimens.

Clinically, medical imaging plays a supporting role in pathological classification and tumor staging. Conventional computed tomography (CT), magnetic resonance imaging, and positron emission tomography rely primarily on the visual assessment of the imaging physician and have limitations in early identification of the pathological type of CEGJ. Although histological biopsies are commonly used in clinical practice, some patients have contraindications or low tolerance, and the biopsy sample is limited to the mucosal surface, which may provide an inadequate assessment of the entire tumor status [7]. Therefore, it is important to explore a reliable, practical, and non-invasive preoperative histological staging method for CEGJ, which is clinically important for neoadjuvant radiotherapy, surgical approach selection, and lymph node dissection in CEGJ patients. Radiomics technique uses a combined medical-industrial approach to transform traditional images into digital quantitative features, which has potential for digging the potential biological characteristics and heterogeneity of tumor images and has been widely and non-invasively used in the diagnosis, differential diagnosis, and disease evaluation[8-12]. Radiomics technique has also been studied in the differential diagnosis of squamous lung cancer and adenocarcinoma[13,14]. However, it is still unclear whether radiomics features extracted from CT images would be useful in predicting pathological type in patients with CEGJ.

Both of two-dimensional (2D) cross section or three-dimensional (3D) volume in CT images could be delineated for radiomics feature extraction. The reported radiomics-based gastric cancer studies have either utilized 2D or 3D segmentation[12,15]. However, it remains unclear whether to apply 2D or 3D regions of interest (ROIs) for pathological typing. The selection of 2D or 3D ROIs for outlining can influence radiomics feature values, feature stability, feature screening, and discriminative model performance[16-18]. And the controversy still exists for the performance of diagnosis or prognosis between 2D and 3D radiomics in tumor[16-18].

Therefore, in the current study, we aimed to construct and evaluate the multiscale and multiphase CT-based radiomics to discriminate SCCEG and AEG. The developed CT-based models might provide assistance in the personalized and precise treatment of clinical CEGJ patients, especially in the selection of surgical approach and determination of the extent of lymph node dissection.

MATERIALS AND METHODS

Patient selection

With institutional review board approval (ethical approval number: 2021-ky-1070-002) and waiver of the written informed consent, we retrospectively collected patients with SCCEG confirmed by gastroscopy and surgical pathology at the First Affiliated Hospital of Zhengzhou University from January 2010 to June 2021. The patient enrollment criteria included: (1) CT-enhanced abdominal examination within 30 d before surgery; (2) Complete clinicopathological data available; (3) The lesion covers at least 3 slices on CT cross section, and the maximum plane diameter is not less than 2 cm; and (4) No neoadjuvant chemoradiotherapy prior to CT examination. The exclusion criteria included: (1) Patient's history of other malignant tumors in combination; (2) Poor CT image quality or lack of raw DICOM data; and (3) Combined heart, lung, and other important organ dysfunction which could not allow CT examination to be performed. Finally, 130 patients with SCCEG were included, including 87 males and 43 females, aged 38-89 (65.72 ± 8.84) years, with a disease duration of 5 d to 4 years and main symptoms of dysphagia, obstructive sensation of eating, and abdominal pain. Another 130 patients with AEG who were matched with the SCCEG patients were also recruited, including 93 males and 37 females, aged 31-83 (62.95 ± 9.91) years.

CT image acquisition

Informed consent forms were signed before all patients underwent contrast-enhanced CT scans. CT scans were acquired using a 64-row CT scanner (GE Healthcare, Discovery CT 750 HD, United States) or 256-row CT scanner (GE Healthcare, Revolution CT, United States). Preparation for the examination: fasting for more than 8 h before the examination, intramuscular injection of scopolamine 10-20 mg 15-20 min before the examination to reduce gastrointestinal motility (Hangzhou Minsheng Pharmaceutical PG Roup Co., Ltd. Specifications: 10 mg/mL), and perform breath-holding exercises. Drink 800-1 000 mL of warm water 10 to 15 min before the examination. Scanning parameters: tube voltage 120 kV, tube current using automatic milliampere second technology, pitch 1.375/1.1; field of view (FOV) of 500 mm; 512 mm x 512 mm matrix, scan thickness 0.625mm to 5 mm, scan spacing 0.625mm to 5mm. Scan area: at least encompasses the lower esophagus to the lower border of both kidneys. Enhancement scan: 90-100 mL of non-ionic contrast agent was injected through the elbow vein using a high-pressure syringe (GE Medical Systems, iopromide, 370 mg/mL).

Image processing and segmentation

The arterial- and venous-phase CT images were isotropically resampled with a voxel size of 1 mm × 1 mm × 1 mm by using the trilinear interpolation in the Artificial Intelligence Kit software (A.K, version:

3.3.0.R, GE Healthcare, United States), in order to minimize the effect of different scanning protocols or equipment on quantitative inhomogeneity of histological features[19]. 2D ROIs were outlined along the largest cross-sectional area in the axial plane of CT images. After delineating the tumor cross-sectional area slice-by- slice in the axial plane, 3D ROIs were finally merged into volume of interest (VOI) (Figures 1 and 2). Care should be taken to avoid the gastric cavity and stomach contents, fatty tissue around the stomach wall, and blood vessels when segmenting. The 2D ROI or 3D VOI delineation was conducted by a radiologist (Chen YJ, 6 years of experience in imaging diagnosis). In order to ensure the reliability and reproducibility of the radiomics features, 30 patients were randomly selected to be segmented in a 2D and 3D manner. For inter-observer agreement analysis, when the radiologist (Chen YJ) conducted the first-time whole-dataset segmentation, another radiologist (Huang WP, 7 years of experience in imaging diagnosis) delineated the selected 30 patients at the same period. For intra-observer agreement analysis, the radiologist (Chen YJ) repeatedly conducted the segmentation 1 mo after the first-time delineation.

Radiomics feature extraction

The 2D or 3D radiomics features were extracted with open-source Python package Pyradiomics[20]. There were respectively 1409 radiomics features extracted from 2D or 3D ROIs in the arterial or venous phase. The original images and the transformed images based on different filters were mainly used for feature extraction. A total of 107 features were extracted from the original images, including 18 intensity statistical and 14 shape-based features. There were 75 textural features extracted from Gray Level Cooccurrence Matrix (GLCM), Gray Level Run Length Matrix (GLRLM), Gray Level Size Zone Matrix (GLSZM), Gray Level Dependence Matrix (GLDM), and Neighboring Gray Tone Difference Matrix (NGTDM). In addition, the same number of first-order grayscale statistical features and texture features were extracted based on different transformed images. A total of 744 features were extracted based on wavelet decomposition images with eight filter channels, 279 features were extracted based on Laplacian of Gaussian (LoG) transform images (sigma parameters selected as 1.0 mm, 3.0 mm, and 5.0 mm), and 279 features were extracted based on Local Binary Pattern (LBP) filtered images (2^{nd} order spherical harmonic function, spherical neighborhood operator with radius 1.0 and fine fraction 1)[20]. The features were extracted by discretizing the CT values within the ROIs based on a fixed interval width (bin width = 25 HU). The 2D and 3D radiomics features extracted from the randomly selected patients were used to calculate the intra-/inter-class correlation coefficients (ICCs). 2D or 3D features with intra- and inter-observer ICC values simultaneously greater than 0.75 were retained, which meant that the features with good repeatability were involved in the further analysis[18,21].

Feature selection and model construction

The 260 cases of data were divided into a training group and an internal test group by randomly stratified sampling at a ratio of 7:3. The training group was mainly used for preprocessing parameter determination, and feature screening and modeling, and the same treatment process, parameters, and model were applied to the test group for internal test. The same method was used for feature preprocessing and feature screening in the arterial and venous phase training samples, and independent arterial and venous radiomics models were established. The feature selection and final modeling procedure were performed as follows. The features were first preprocessed by excluding features with variance < 1.0, filling missing values with the median and *Z*-score normalization, and excluding collinear features with a cut-off value of correlation coefficients larger than 0.7. Then the Mann-Whitney *U*-test or *t*-test was used to select features with a significant difference between two classes ($P < 0.05$). The least absolute shrinkage and selection operator (LASSO) logistic regression (minimum binomial deviance) with 10-fold cross validation was conducted to avoid overfitting and the features with non-zero coefficients were retained[22]. Finally, the retained features were inputted into backward stepwise logistic regression with the minimum Akaike Information Criterion (AIC) to develop the regression radiomics model. The "Radscore" of each patient was calculated according to the formula (Radscore = $\beta_0 + \sum\beta_i x_i$, β_0 is a constant term and βi is the regression coefficient of the feature *x*i).

Four independent radiomics models were constructed, including: 2D arterial-phase model ($Radscore^{AP\_2D}$), 2D venous-phase model ($Radscore^{VP\_2D}$), 3D arterial-phase model ($Radscore^{AP\_3D}$), and 3D venous-phase model ($Radscore^{VP\_3D}$). Two combined models were derived based on the established independent model Radscore according to the regression formula (Radscore = $\beta_0 + \sum\beta_i x_i$, β_0 is a constant term and βi is the logistic regression coefficient of the model score *x*i). And the 2D arterial-venous combined model 3 ($Radscore^{AP\_VP\_2D}$) and 3D arterial-venous combined model ($Radscore^{AP\_VP\_3D}$) were established.

Evaluation of model predictive performance

The performance of the models was evaluated by using receiver operating characteristic curve (ROC) analysis to obtain the area under the ROC curve (AUC). The sensitivity, accuracy, negative predictive value, and positive predictive value were calculated based on the cut-off values corresponding to the maximum Youden index to evaluate the discrimination performance of the models. The cut-off values of the training group were applied to the test group to obtain their corresponding ROC parameters in

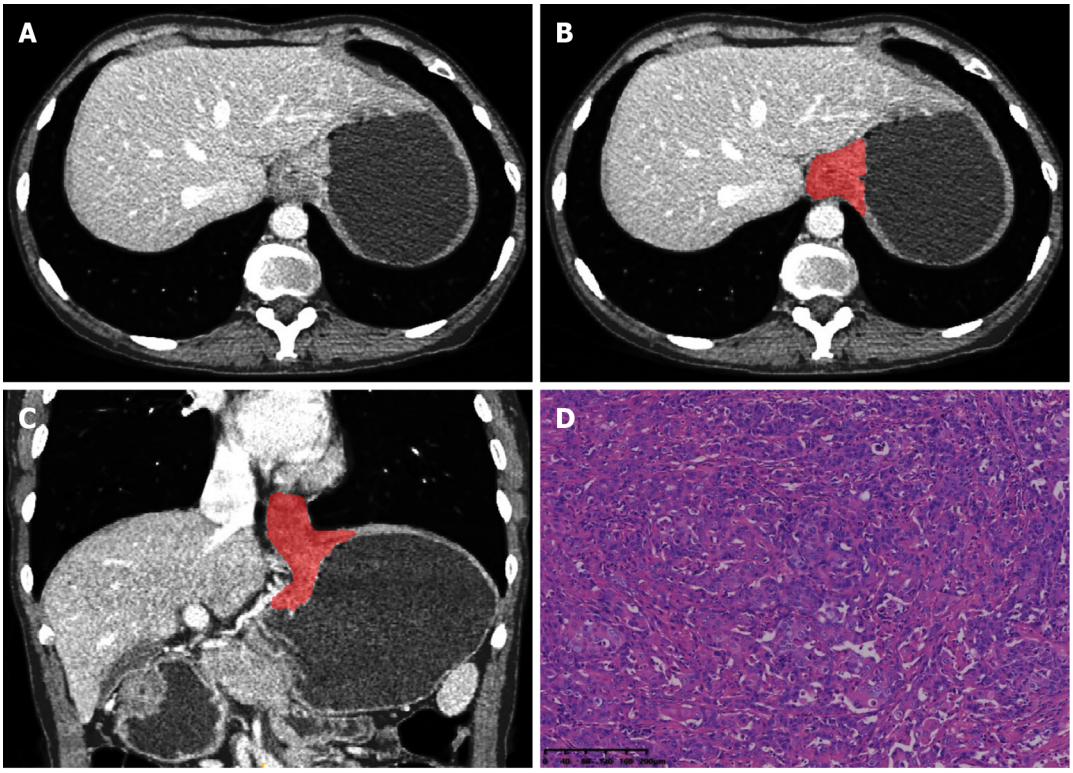

DOI: 10.3748/wjg.v28.i31.4363 **Copyright** ©The Author(s) 2022.

Figure 1 A 43-year-old man with squamous cell carcinoma of the esophagogastric junction. A: Axial computed tomography image in venous phase; B: Schematic diagram of 2D region of interest (ROI) segmentation on ITK-SNAP software; C: Schematic diagram of 3D ROI segmentation on ITK-SNAP software; D: Postoperative pathological image confirming squamous cell carcinoma of the esophagogastric junction (HE staining, × 200).

the test group. The calibration curve analysis and the Hosmer-Lemeshow test were used for evaluating model calibration and the goodness of fit ($P > 0.05$ indicates a good model fit). Delong's test was used to compare the AUC between paired models. Continuous net reclassification improvement (NRI) and integrated discrimination improvement (IDI) were used to assess ability of the models in improving the classification effectiveness[18]. The decision curve analysis (DCA) was used to assess the net clinical benefit or clinical utility of each model at different threshold probabilities.

Statistical analysis

R software (version 3.6.3, http://www.r-project.org) was applied for statistical analyses in the current study. Radiomics features and Radscore are continuous variables, and data normality was tested using kurtosis and skewness values, and comparisons between two groups were made using independent samples *t*-test (for data with a normal distribution) or Mann-Whitney *U* test (for data not following a normal distribution). Categorical variables were tested by chi-square test or Fisher's exact test. A two-sided $P < 0.05$ was considered statistically significant. The optimism of the prediction accuracy of the model was validated using 1000-times Bootstrap in the training group. The following R packages were applied: "icc" for intra-/inter-class correlation coefficient; "glmnet" for logistic regression; "pROC" for ROC analysis; "rmda" for DCA; calibration function in the "rms" package for calibration analysis, and the "PredictABEL" package for NRI and IDI analysis.

RESULTS

Feature screening and model construction

Arterial phase model based on 2D ROI: A total of 175 radiomics features (ICCs > 0.75) were retained among 1409 features. There were 61 and 6 features retained rafter variance and correlation analysis, respectively. Among 6 features screened by univariate analysis and 10-fold cross validation LASSO regression (Figure 3A and B), 5 were further selected by stepwise logistic regression analysis. The Radscore^{AP_2D} is summarized in Supplementary Figure 1. The results of ICCs for individual features are shown in Supplementary Table 1 and the multivariable logistic regression results of features involved in the model are summarized in Supplementary Table 2. ROC curves for single 2D arterial features to identify SCCEG and AEG are shown in Supplementary Figure 2A and The 2D arterial model radiomics

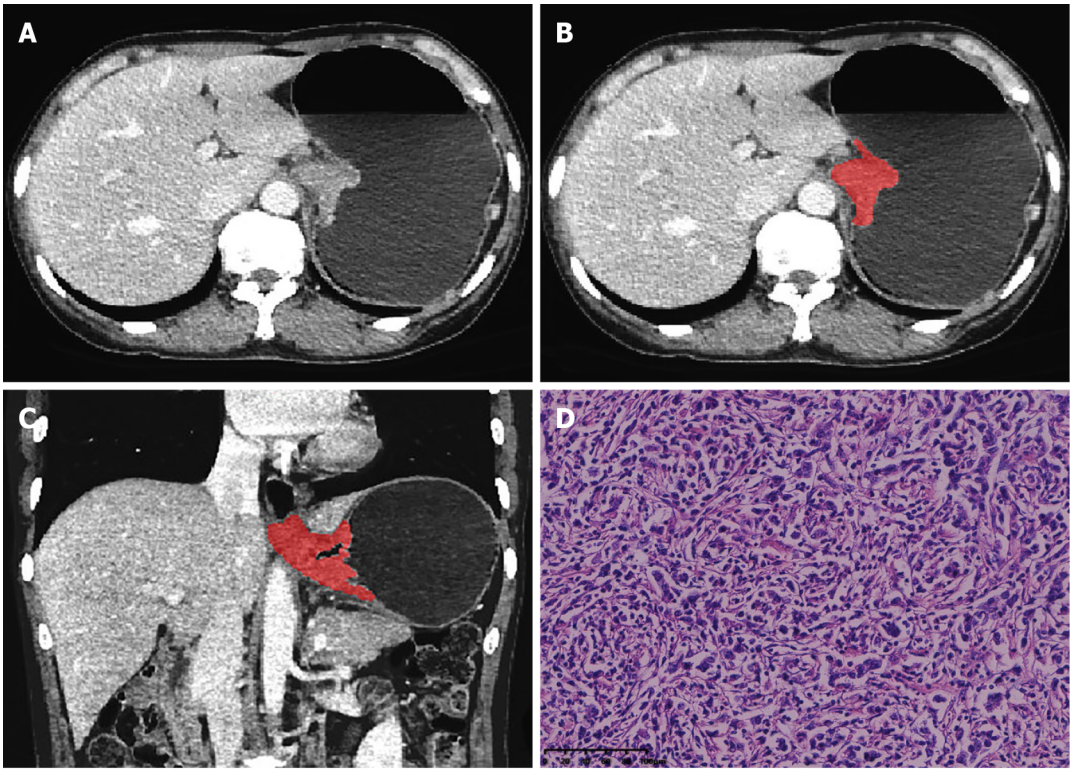

DOI: 10.3748/wjg.v28.i31.4363 **Copyright** ©The Author(s) 2022.

Figure 2 A 56-year-old man with adenocarcinoma of the esophagogastric junction. A: Axial computed tomography image in venous phase; B: Schematic diagram of 2D region of interest (ROI) segmentation on ITK-SNAP software; C: Schematic diagram of 3D ROI segmentation on ITK-SNAP software; D: Postoperative pathological image confirming adenocarcinoma of the esophagogastric junction (HE staining, × 200).

features and the differences of Rad-score^{AP_2D} in the training and test groups are shown in Supplementary Table 3.

Venous phase model based on 2D ROI: A total of 275 radiomics features (ICCs > 0.75) were retained among 1409 features. There were 124 and 12 features kept after variance and correlation analysis, respectively. Among 6 features screened by univariate analysis and 10-fold cross validation LASSO regression (Figure 3C and D), 5 were kept by stepwise logistic regression analysis. The Radscore^{VP_2D} is summarized in Supplementary Figure 3. The results of ICCs for individual features are shown in Supplementary Table 4 and the multivariable logistic regression results of features involved in the model are summarized in Supplementary Table 5. ROC curves for single 2D venous features to identify SCCEG and AEG are illustrated in Supplementary Figure 2C and The 2D venous model radiomics features and the differences of Rad-score^{VP_2D} in the training and test groups are shown in Supplementary Table 6.

Arterial phase model based on 3D ROI: A total of 714 radiomics features (ICCs > 0.75) were retained among 1409 features. There were 358 and 27 features kept after variance and correlation analysis, respectively. Among 15 features screened by univariate analysis and 10-fold cross validation LASSO regression (Figure 3E and F), 10 were kept by stepwise logistic regression analysis. The Radscore^{AP_3D} is summarized in Supplementary Figure 4. The ICCs for individual features are shown in Supplementary Table 7 and the multivariable logistic regression results of features involved in the model are summarized in Supplementary Table 8. ROC curves for single 3D arterial features to identify SCCEG and AEG are shown in Supplementary Figure 2E and the 3D arterial model radiomics features and the differences of Rad-score^{AP_3D} in the training and test groups are summarized in Supple-mentary Table 9.

Venous phase model based on 3D ROI: A total of 774 radiomics features (ICCs>0.75) were retained among 1409 features. There were 355 and 23 features kept after variance and correlation analysis, respectively. Among 8 features screened by univariate analysis and 10-fold cross validation LASSO regression (Figure 3G and H), 7 were kept by stepwise logistic regression analysis, and the Radscore^{VP_3D} is summarized in Supplementary Figure 5. The ICCs result for individual features are shown in Supplementary Table 10 and the multivariable logistic regression results of features involved in the model are summarized in Supplementary Table 11. ROC curves for single 3D venous features to identify SCCEG and AEG are shown in Supplementary Figure 2G and The 3D venous model radiomics features and the differences of Rad-score^{VP_3D} in the training and test groups are summarized in

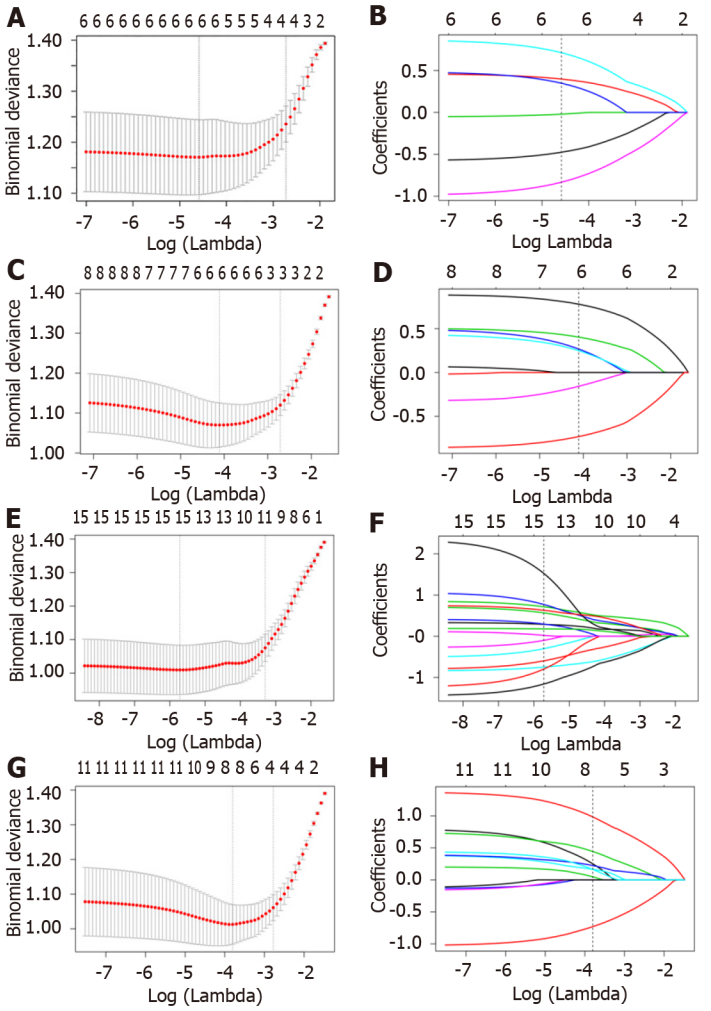

DOI: 10.3748/wjg.v28.i31.4363 **Copyright** ©The Author(s) 2022.

Figure 3 Least absolute shrinkage and selection operator logistic regression feature screening graphs. The radiomics feature screening using the least absolute shrinkage and selection operator regression was performed to select the optimal model parameter λ using 10-fold cross-validation. A, C, E, and G: Graphs of binomial deviation of 2D-arterial model, 2D-venous model, 3D-arterial model, and 3D-venous model with parameter λ, respectively. The dashed lines indicate the selected optimal log(λ) values and the location of one standard error; B, D, F, and H: Graphs of variation of the radiomics characteristic coefficients with log(λ) for 2D-arterial model, 2D-venous model, 3D-arterial model, and 3D-venous model, respectively. The dotted line indicates the location of the selected optimal log(λ) value.

Supplementary Table 12.

2D arterial-venous combined model

By combining Radscore^{AP_2D} and Radscore^{VP_2D}, the 2D arterial-venous combined model was derived and the Radscor^{AP_VP_2D} is described in Supplementary Figure 6.

3D arterial-venous combined model

By combining Radscore^{AP_3D} and Radscore^{VP_3D}, the 3D arterial-venous combined model was derived and the Radscor^{AP_VP_3D} is summarized in Supplementary Figure 7.

In this study, a total of 10 candidate radiomics feature parameters were screened out in 2D arterial and venous phase images, mostly first-order features and texture features extracted based on Log transformed or wavelet transformed images, and the main categories included 4 first-order features, 2 GLRLM features, 2 GLSZM features, 1 GLDM feature, and 1 NGTDM feature. More features were screened out in the 3D arterial phase and venous phase images—17 in total, and the main categories included 6 first-order features, 4 GLDM features, 4 NGTDM features, 1 GLRLM feature, 1 GLSZM feature, and 1 GLCM feature.

Radiomics model performance

The AUC, specificity, sensitivity, accuracy, positive predictive value, and negative predictive value of the 6 models developed in this study to discriminate SCCEG from AEG in the training and test groups

are summarized in Table 1, and the ROC curves are shown in Figure 4. The model optimism was assessed by 1000-times bootstrap as shown in Table 2. It indicated that the 2D-arterial, 2D-venous, 3D-arterial, and 3D-venous model presented a degree of optimism less than 0.1 during repeated sampling. The Delong test results in the training and test groups are shown in Supplementary Table 13. All the 2D models had an AUC greater than 0.800 in the test group, except for the arterial model, which had an AUC of 0.752 in the test group. The AUC values of the venous model were higher than those of the arterial model (0.849 *vs* 0.808 and 0.831 *vs* 0.752) in both the training and test groups. All the 3D models had a higher AUC in the venous model than in the arterial model. In the combined models, both the 3D and 2D models were higher than their independent phase model both in the training and test groups. When comparing the performance between 2D and 3D models, the results showed that no matter for the independent phase model or the multi-phase-combined model, 3D models performed with a higher AUC than 2D models. Among all the models, the 3D-arterial-venous combined model had the highest AUC values of 0.904 and 0.901 in the training and test groups, respectively. As some statistical significance was not obvious during the Delong test, continuous NRI and IDI analyses were performed to evaluate the ability of each model for improving the classification and the results are shown in Supplementary Table 14. In both the training and test groups, the venous model demonstrated a positive improvement in discrimination over the arterial model (NRI > 0, IDI > 0), the 3D-venous model demonstrated a significant positive improvement in discrimination over the 2D-venous model (P < 0.05), both in the 3D model and in the 2D model, the combined model demonstrated a significant positive improvement in discrimination over the arterial model (P < 0.05); the 3D combined model reflected a significant positive improvement in discrimination compared with the 2D combined model (P < 0.05). In addition, the calibration curve (Figure 5) and the results of the Hosmer-Lemeshow test (Supplementary Table 15) indicate that the six models had good calibration. The clinical utility of the model was confirmed by the decision curve (Figure 6), in which the 3D-arterial-venous combined model and the 3D-venous model had higher net benefits in the test group within a threshold probability interval of 0.3-1.

DISCUSSION

In the current study, the multiscale and multiphase CT-based radiomics method was used to preoperatively discriminate SCCEG and AEG. The results showed that the combination of multiphase 3D CT radiomics features could improve the differentiation performance. Therefore, radiomics method could help open up a new field for noninvasive diagnosis and personalized management of CEGJ. Histopathology biopsy is a commonly used clinical method, and these radiomics features are considered to be complementary to histology biopsy but not a complete substitute for histopathology at this time. Repeat biopsy or endoscopic ultrasound deeper biopsies should be recommended if upper endoscopic biopsies are inconclusive or if it conflicts with the results suggested by radiomics features. Radiomics can provide an adequate reference if the patient has contraindications and low tolerance to endoscopic biopsy.

Previous studies have focused on the quantitative parameters of spectral CT. Zhou *et al*[23] found that the normalized iodine concentration, the $K_{40\text{-}70\ keV}$, and the effective atomic number in the arterial phase could identify SCCEG and AEG; the AUC values were 0.720, 0.730, and 0.706, respectively. Radiomics uses mathematically describable imaging features to comprehensively analyze tumor heterogeneity[24], and has not been validated for identifying SCCEG from AEG. Therefore, we tried to use radiomics features to identify the pathological type of CEGJ by comprehensively considering the effectiveness of different phases and segmentation method. In this study, more features were screened out in the 3D models of different phases than in the 2D models, which is related to the fact that the 3D ROIs contain the lesion as a whole and the extracted features have a larger distribution. The results showed that the efficacy of the venous features was higher than that of the arterial features in identifying SCCEG from AEG. Pathologically, squamous carcinoma grows faster and tends to grow in a swelling superposition with denser tissue structure, while adenocarcinoma mostly grows in an appendicular pattern with looser tissue structure[25]. With the prolongation of scanning time, the contrast agent continuously penetrates into the interstitial space of tumor cells, and more textural features appear in the venous phase, which better reflects the heterogeneous characteristics of squamous carcinoma. Tumor vascularization is a kind of biological behavior that reconstructs nutrition connection and promotes tumor development. Pathologic types, tumor origin, and structure of the microvasculature affect the enhancement pattern and radiomics-based parameters.

We found that among the features retained in the venous model, Dependence variance (GLDM) and Large dependence high gray level emphasis (GLDM) had larger weight in the 3D and 2D models, respectively. GLDM mainly describes the degree of dependence between voxel gray levels, and the SCCEG group reflects the high "Dependence variance" of 3D gray levels and the "Large dependence high gray level emphasis" of 2D gray levels, which reflects the large gray level heterogeneity of squamous cancer tissue in 3D features and the high gray level distribution in 2D features from texture features. The uneven distribution of tumor vessels in squamous carcinoma lesions is prone to tumor cell

Table 1 Model performance for differentiating squamous cell carcinoma of the esophagogastric junction and adenocarcinoma of the esophagogastric junction in the training and validation groups

	2D-ROI models			3D-ROI models		
Model	**Artery**	**Venous**	**Artery + venous**	**Artery**	**Venous**	**Artery + venous**
Training group						
AUC	0.808	0.849	0.869	0.876	0.877	0.904
95%CI	0.744-0.872	0.792-0.905	0.818-0.920	0.827-0.926	0.827-0.927	0.861-0.947
Threshold	0.095	-0.101	-0.370	-0.149	-0.352	0.043
Specificity	0.802	0.758	0.681	0.813	0.780	0.879
Sensitivity	0.736	0.802	0.890	0.824	0.857	0.802
Accuracy	0.769	0.780	0.786	0.819	0.819	0.841
NPV	0.753	0.793	0.861	0.822	0.845	0.816
PPV	0.788	0.768	0.736	0.815	0.796	0.869
Validation group						
AUC	0.752	0.831	0.845	0.824	0.879	0.901
95%CI	0.640-0.864	0.742-0.921	0.763-0.928	0.732-0.917	0.798-0.960	0.830-0.973
Threshold	0.095	-0.101	-0.370	-0.149	-0.352	0.043
Specificity	0.795	0.692	0.718	0.769	0.667	0.821
Sensitivity	0.641	0.769	0.769	0.744	0.872	0.795
Accuracy	0.718	0.731	0.744	0.756	0.769	0.808
NPV	0.689	0.750	0.757	0.750	0.839	0.800
PPV	0.758	0.714	0.732	0.763	0.723	0.816

ROI: Region of interest; AUC: Area under the curve; NPV: Negative predictive value; PPV: Positive predictive value.

Table 2 Model optimism estimation by 1000-times bootstrap in the training group

Index	Model	Apparent AUC[1]	AUC Bootstrap-test[2] (mean, 95%CI)	Optimism
1	2D-arterial model	0.808	0.770 (0.767-0.772)	0.050
2	2D-venous model	0.849	0.820 (0.817-0.822)	0.036
3	3D-arterial model	0.876	0.815 (0.812-0.880)	0.080
4	3D-venous model	0.877	0.833 (0.830-0.835)	0.056

[1]The area under the curve of predictive model developed in the whole training dataset.
[2]The averaged model performance in the "out-of-bag" test set after 1000-times bootstrap. AUC: Area under the curve.

degeneration and necrosis, and it is speculated that the grayscale distribution of squamous carcinoma lesions has some complexity in different transformed images. In addition, features prevalent in the arterial and venous models are Busyness (NGTDM), Dependence variance (GLDM), first order grayscale features. NGTDM features can also represent a certain degree of grayscale distribution inhomogeneity. NGTDM describes the difference between adjacent grayscale values and average grayscale values within the quantized distance of the adjacent grayscale difference matrix, and the squamous carcinoma exhibits a high "Busyness", representing rapid intensity changes between pixels and their neighbors and reflecting the heterogeneous nature of the tissue. In addition, the first-order statistical gray value features calculated based on different dimensions and different phases of images were selected into each model simultaneously, indicating that the images of the SCCEG group in different phases and dimensions have lower gray values, which may be attributed to the histopathological inhomogeneity of microvessels within squamous carcinoma, less blood supply than adenocarcinoma, and lower gray statistical values in squamous carcinoma than adenocarcinoma.

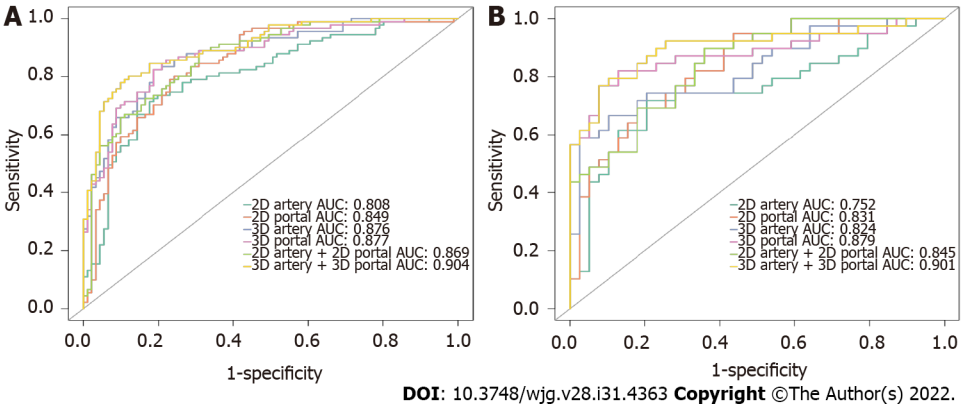

DOI: 10.3748/wjg.v28.i31.4363 **Copyright** ©The Author(s) 2022.

Figure 4 Receiver operating characteristic curves of different models to identify squamous cell carcinoma and adenocarcinoma of the esophagogastric junction. A: Training group; B: Test group.

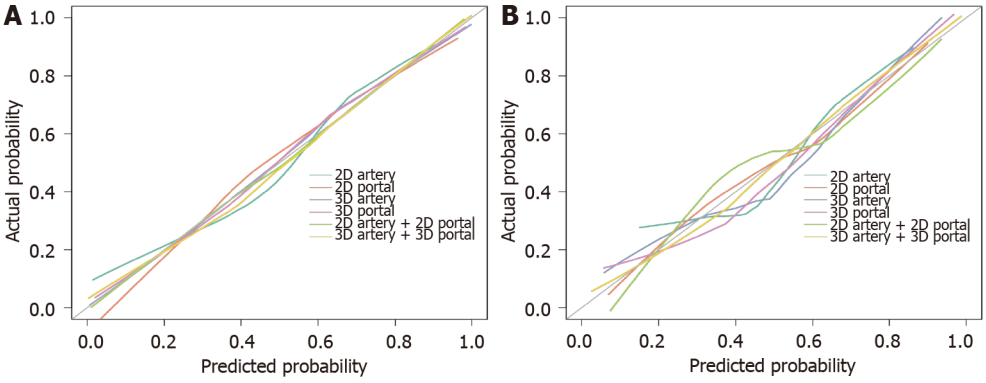

DOI: 10.3748/wjg.v28.i31.4363 **Copyright** ©The Author(s) 2022.

Figure 5 Calibration curves of 2D-arterial model, 2D-venous model, 3D-arterial model, 3D-venous model, 2D arterial-venous combined model, and 3D arterial-venous combined model to identify squamous cell carcinoma of the esophagogastric junction and adenocarcinoma of the esophagogastric junction. A: Training group; B: Test group.

For both of 2D and 3D models, the AUC difference was statistically significant between the arterial-venous combined model and the independent arterial model, while not significant between the arterial-venous combined model and the independent venous model. It suggested that the venous phase might contribute more predictive information compared with the arterial phase. Combining the NRI and IDI index results, the venous model showed a positive improvement in discrimination compared to the arterial model, and the 3D model showed a significant positive improvement in discrimination compared to the 2D model as well.

Most previous radiomics studies varied in the utilization of 2D or 3D segmentation. However, different delineation methods may result in different feature values and predictive performance. The study of different dimensional outlining approaches and the corresponding model performance can guide radiomics practice in related disease areas. Zhao *et al*[15] developed a dual-energy CT–based nomogram for noninvasive identification of the status of HER2 expression in gastric cancer, and both 2D and 3D radiomics nomograms performed well. Huang *et al*[18] found that the efficacy of the 3D model was superior to the 2D model when they developed 2D and 3D radiomics models to predict the aggressiveness of pancreatic solid pseudopapillary tumors. This study showed that in the discrimination of SCCEG and AEG, the use of 3D radiomics-based on CT images will be beneficial to improve the discrimination, but the time required for 3D segmentation was significantly longer than that of 2D, so it is also necessary to consider the improvement and optimization of automatic 3D lesion segmentation.

This study still has some limitations. First, the lesion morphology of CEGJ is not fixed, and manual segmentation methods are required. While the lesion travels along the gastric and esophageal walls in a tortuous manner, the consistency and stability of the annotation will affect the efficacy of the model. In this study, features with ICCs > 0.75 were used for subsequent analysis, which ensured the robustness of the radiomics features to some extent. More candidate semi-automatic or automatic segmentation algorithms would be welcomed to improve clinical efficiency. Second, our study was previously reported to include data on squamous cell carcinoma of the cardia or distal esophagus, but it is still a single-center retrospective study with a small sample size, especially for SCCEG, which inevitably

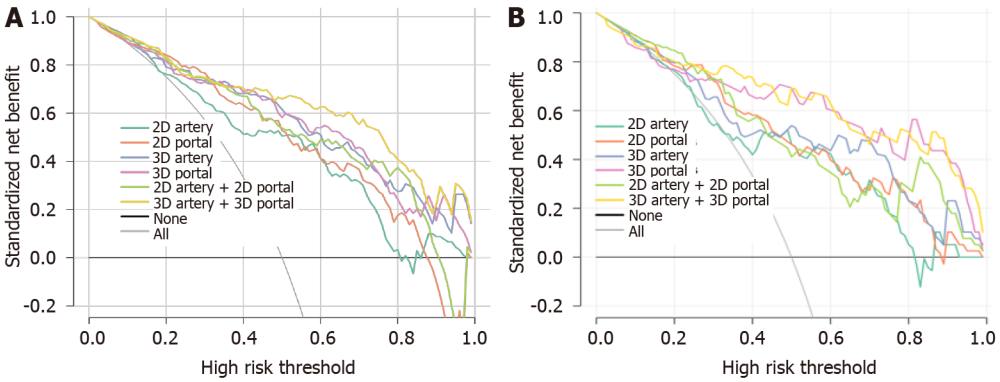

DOI: 10.3748/wjg.v28.i31.4363 **Copyright** ©The Author(s) 2022.

Figure 6 Decision curves for 2D-arterial model, 2D venous model, 3D-arterial model, 3D venous model, 2D arterial-venous combined model, and 3D arterial-venous combined model. A: Training group; B: Test group. The black horizontal line indicates no lesions as squamous cell carcinoma (NONE) and the grey line indicates all lesions as squamous cell carcinoma (ALL). The colored lines of each model respectively illustrate the net benefit brought to each patient. The closer the decision curves to the black and gray curves, the similar the clinical decision net benefit of the model compared with "treat ALL" or "treat NONE" decision. When comparing different models, the higher the model curve within the same threshold probability, the higher the clinical net benefit resulting from the model.

generates selectivity bias when paired with a larger number of AEGs. Future multicenter, prospective, large sample studies are needed to further improve and validate the diagnostic efficacy and generalization ability of the model. In addition, the main purpose of the current study was to evaluate the usefulness of 2D- or 3D-based radiomics methods and clinical data or laboratory test indicators were not included. There is much room for improvement of model reliability, which will be further collected in future studies in order to obtain a more comprehensive understanding.

CONCLUSION

In conclusion, multi-scale and multi-phase radiomics models based on CT imaging data were developed and validated for differentiating SCCEG from AEG before the operation in our study. The 3D radiomics model combining arterial and venous phase images showed encouraging performance than the corresponding 2D model. These models require further validation as decision support tools to guide clinical practice and develop individualized treatment plans for CEGJ patients. Currently, histopathological biopsy is still the common method of diagnosis.

ARTICLE HIGHLIGHTS

Research background

Differentiating squamous cell carcinoma of the esophagogastric junction (SCCEG) from adenocarcinoma of the esophagogastric junction (AEG) can indicate Siewert stage and whether the surgical route for patients with carcinoma of the esophagogastric junction (CEGJ) is transthoracic or transabdominal, as well as aid in determining the extent of lymph node dissection. With the development of neoadjuvant therapy, preoperative determination of pathological type can help in the selection of neoadjuvant radiotherapy and chemotherapy regimens.

Research motivation

Radiomics technique uses a combined medical-industrial approach to transform traditional images into digital quantitative features, which has potential for digging the potential biological characteristics and heterogeneity of tumor images and has been widely and non-invasively used in the diagnosis, differential diagnosis, and disease evaluation. However, to the best of our knowledge, there is no literature that has evaluated whether a radiomics signature derived from computed tomography (CT) images would be useful in predicting pathological type in patients with CEGJ.

Research objectives

In the current study, we proposed a CT radiomics-based classification method by considering the performance of 3D or 2D segmentation and multiple CT imaging phases to discriminate SCCEG and AEG.

Research methods

We retrospectively analyzed the preoperative contrasted-enhanced CT imaging data of single-center patients with pathologically confirmed SCCEG (n = 130) and AEG (n = 130). One thousand four hundred and nine radiomics features were separately extracted from 2D or 3D regions of interest in arterial and venous phases. Totally, 6 logistic regression models were established based on 2D and 3D multi-phase features.

Research results

The venous model showed a positive improvement compared with the arterial model (NRI > 0, IDI > 0), and the 3D-venous and combined models showed a significant positive improvement compared with the 2D-venous and combined models (P < 0.05). Decision curve analysis showed that the combined 3D-arterial-venous model and 3D-venous model had a higher net clinical benefit within the same threshold probability range in the test group.

Research conclusions

The combined arterial-venous CT radiomics model based on 3D segmentation can improve the performance in differentiating EGJ squamous cell carcinoma from adenocarcinoma.

Research perspectives

These models require further validation as decision support tools to guide clinical practice and develop individualized treatment plans for CEGJ patients.

FOOTNOTES

Author contributions: Du KP and Huang WP designed the research; Liu SY and Li LM performed the research; Chen YJ, Han YJ, Zhou Y, and Liu CC collected the data; Du KP and Huang WP analyzed the data and wrote the paper; Gao JB reviewed the paper; and all authors have read and approved the final manuscript.

Institutional review board statement: The study was approved by the Institutional Review Board at the First Affiliated Hospital of Zhengzhou University (No. 2021-ky-1070-002).

Conflict-of-interest statement: The authors declare that they have no competing interests to disclose.

Data sharing statement: All data generated or analyzed during this study are included in this published article.

Country/Territory of origin: China

ORCID number: Ke-Pu Du 0000-0002-3870-7656; Wen-Peng Huang 0000-0002-9104-1494; Si-Yun Liu 0000-0001-5611-382X; Yun-Jin Chen 0000-0002-2147-0912; Li-Ming Li 0000-0002-2910-9742; Yi-Jing Han 0000-0001-7358-0139; Yue Zhou 0000-0001-7781-7228; Chen-Chen Liu 0000-0001-5026-3288; Jian-Bo Gao 0000-0003-2621-3701.

S-Editor: Ma YJ
L-Editor: Wang TQ
P-Editor: Ma YJ

REFERENCES

1 **Sun X**, Wang G, Liu C, Xiong R, Wu H, Xie M, Xu S. Comparison of short-term outcomes following minimally invasive versus open Sweet esophagectomy for Siewert type II adenocarcinoma of the esophagogastric junction. *Thorac Cancer* 2020; **11**: 1487-1494 [PMID: 32239662 DOI: 10.1111/1759-7714.13415]
2 **Wang T**, Wu Y, Zhou H, Wu C, Zhang X, Chen Y, Zhao D. Development and validation of a novel competing risk model for predicting survival of esophagogastric junction adenocarcinoma: a SEER population-based study and external validation. *BMC Gastroenterol* 2021; **21**: 38 [PMID: 33499821 DOI: 10.1186/s12876-021-01618-7]
3 **Xu H**, Zhang L, Miao J, Liu S, Liu H, Jia T, Zhang Q. Patterns of recurrence in adenocarcinoma of the esophagogastric junction: a retrospective study. *World J Surg Oncol* 2020; **18**: 144 [PMID: 32593312 DOI: 10.1186/s12957-020-01917-5]
4 **Ito H**, Inoue H, Odaka N, Satodate H, Suzuki M, Mukai S, Takehara Y, Kida H, Kudo SE. Clinicopathological characteristics and optimal management for esophagogastric junctional cancer; a single center retrospective cohort study. *J*

Exp Clin Cancer Res 2013; **32**: 2 [PMID: 23289488 DOI: 10.1186/1756-9966-32-2]

5 **Huang Q**. Carcinoma of the gastroesophageal junction in Chinese patients. *World J Gastroenterol* 2012; **18**: 7134-7140 [PMID: 23326117 DOI: 10.3748/wjg.v18.i48.7134]

6 **Giganti F**, Ambrosi A, Petrone MC, Canevari C, Chiari D, Salerno A, Arcidiacono PG, Nicoletti R, Albarello L, Mazza E, Gallivanone F, Gianolli L, Orsenigo E, Esposito A, Staudacher C, Del Maschio A, De Cobelli F. Prospective comparison of MR with diffusion-weighted imaging, endoscopic ultrasound, MDCT and positron emission tomography-CT in the pre-operative staging of oesophageal cancer: results from a pilot study. *Br J Radiol* 2016; **89**: 20160087 [PMID: 27767330 DOI: 10.1259/bjr.20160087]

7 **Soo TM**, Bernstein M, Provias J, Tasker R, Lozano A, Guha A. Failed stereotactic biopsy in a series of 518 cases. *Stereotact Funct Neurosurg* 1995; **64**: 183-196 [PMID: 8817805 DOI: 10.1159/000098747]

8 **Bhandari A**, Ibrahim M, Sharma C, Liong R, Gustafson S, Prior M. CT-based radiomics for differentiating renal tumours: a systematic review. *Abdom Radiol (NY)* 2021; **46**: 2052-2063 [PMID: 33136182 DOI: 10.1007/s00261-020-02832-9]

9 **Reginelli A**, Nardone V, Giacobbe G, Belfiore MP, Grassi R, Schettino F, Del Canto M, Cappabianca S. Radiomics as a New Frontier of Imaging for Cancer Prognosis: A Narrative Review. *Diagnostics (Basel)* 2021; **11** [PMID: 34679494 DOI: 10.3390/diagnostics11101796]

10 **Ibrahim A**, Primakov S, Beuque M, Woodruff HC, Halilaj I, Wu G, Refaee T, Granzier R, Widaatalla Y, Hustinx R, Mottaghy FM, Lambin P. Radiomics for precision medicine: Current challenges, future prospects, and the proposal of a new framework. *Methods* 2021; **188**: 20-29 [PMID: 32504782 DOI: 10.1016/j.ymeth.2020.05.022]

11 **Lambin P**, Leijenaar RTH, Deist TM, Peerlings J, de Jong EEC, van Timmeren J, Sanduleanu S, Larue RTHM, Even AJG, Jochems A, van Wijk Y, Woodruff H, van Soest J, Lustberg T, Roelofs E, van Elmpt W, Dekker A, Mottaghy FM, Wildberger JE, Walsh S. Radiomics: the bridge between medical imaging and personalized medicine. *Nat Rev Clin Oncol* 2017; **14**: 749-762 [PMID: 28975929 DOI: 10.1038/nrclinonc.2017.141]

12 **Scapicchio C**, Gabelloni M, Barucci A, Cioni D, Saba L, Neri E. A deep look into radiomics. *Radiol Med* 2021; **126**: 1296-1311 [PMID: 34213702 DOI: 10.1007/s11547-021-01389-x]

13 **Ren C**, Zhang J, Qi M, Zhang Y, Song S, Sun Y, Cheng J. Correction to: Machine learning based on clinico-biological features integrated 18F-FDG PET/CT radiomics for distinguishing squamous cell carcinoma from adenocarcinoma of lung. *Eur J Nucl Med Mol Imaging* 2021; **48**: 1696 [PMID: 33532911 DOI: 10.1007/s00259-021-05226-1]

14 **Tomori Y**, Yamashiro T, Tomita H, Tsubakimoto M, Ishigami K, Atsumi E, Murayama S. CT radiomics analysis of lung cancers: Differentiation of squamous cell carcinoma from adenocarcinoma, a correlative study with FDG uptake. *Eur J Radiol* 2020; **128**: 109032 [PMID: 32361604 DOI: 10.1016/j.ejrad.2020.109032]

15 **Zhao H**, Li W, Huang W, Yang Y, Shen W, Liang P, Gao J. Dual-Energy CT-Based Nomogram for Decoding HER2 Status in Patients With Gastric Cancer. *AJR Am J Roentgenol* 2021; **216**: 1539-1548 [PMID: 33852330 DOI: 10.2214/AJR.20.23528]

16 **Xu L**, Yang P, Yen EA, Wan Y, Jiang Y, Cao Z, Shen X, Wu Y, Wang J, Luo C, Niu T. A multi-organ cancer study of the classification performance using 2D and 3D image features in radiomics analysis. *Phys Med Biol* 2019; **64**: 215009 [PMID: 31561245 DOI: 10.1088/1361-6560/ab489f]

17 **Meng L**, Dong D, Chen X, Fang M, Wang R, Li J, Liu Z, Tian J. 2D and 3D CT Radiomic Features Performance Comparison in Characterization of Gastric Cancer: A Multi-Center Study. *IEEE J Biomed Health Inform* 2021; **25**: 755-763 [PMID: 32750940 DOI: 10.1109/JBHI.2020.3002805]

18 **Huang WP**, Liu SY, Han YJ, Li LM, Liang P, Gao JB. Development of CT-Based Imaging Signature for Preoperative Prediction of Invasive Behavior in Pancreatic Solid Pseudopapillary Neoplasm. *Front Oncol* 2021; **11**: 677814 [PMID: 34079766 DOI: 10.3389/fonc.2021.677814]

19 **Mackin D**, Fave X, Zhang L, Yang J, Jones AK, Ng CS, Court L. Harmonizing the pixel size in retrospective computed tomography radiomics studies. *PLoS One* 2017; **12**: e0178524 [PMID: 28934225 DOI: 10.1371/journal.pone.0178524]

20 **van Griethuysen JJM**, Fedorov A, Parmar C, Hosny A, Aucoin N, Narayan V, Beets-Tan RGH, Fillion-Robin JC, Pieper S, Aerts HJWL. Computational Radiomics System to Decode the Radiographic Phenotype. *Cancer Res* 2017; **77**: e104-e107 [PMID: 29092951 DOI: 10.1158/0008-5472.CAN-17-0339]

21 **Koo TK**, Li MY. A Guideline of Selecting and Reporting Intraclass Correlation Coefficients for Reliability Research. *J Chiropr Med* 2016; **15**: 155-163 [PMID: 27330520 DOI: 10.1016/j.jcm.2016.02.012]

22 **Daghir-Wojtkowiak E**, Wiczling P, Bocian S, Kubik Ł, Kośliński P, Buszewski B, Kaliszan R, Markuszewski MJ. Least absolute shrinkage and selection operator and dimensionality reduction techniques in quantitative structure retention relationship modeling of retention in hydrophilic interaction liquid chromatography. *J Chromatogr A* 2015; **1403**: 54-62 [PMID: 26037317 DOI: 10.1016/j.chroma.2015.05.025]

23 **Zhou Y**, Hou P, Zha K, Liu D, Wang F, Zhou K, Gao J. Spectral Computed Tomography for the Quantitative Assessment of Patients With Carcinoma of the Gastroesophageal Junction: Initial Differentiation Between a Diagnosis of Squamous Cell Carcinoma and Adenocarcinoma. *J Comput Assist Tomogr* 2019; **43**: 187-193 [PMID: 30371624 DOI: 10.1097/RCT.0000000000000826]

24 **Gao X**, Ma T, Cui J, Zhang Y, Wang L, Li H, Ye Z. A CT-based Radiomics Model for Prediction of Lymph Node Metastasis in Early Stage Gastric Cancer. *Acad Radiol* 2021; **28**: e155-e164 [PMID: 32507613 DOI: 10.1016/j.acra.2020.03.045]

25 **Qiang JW**, Zhou KR, Lu G, Wang Q, Ye XG, Xu ST, Tan LJ. The relationship between solitary pulmonary nodules and bronchi: multi-slice CT-pathological correlation. *Clin Radiol* 2004; **59**: 1121-1127 [PMID: 15556595 DOI: 10.1016/j.crad.2004.02.018]

World Journal of Gastroenterology

Submit a Manuscript: https://www.f6publishing.com

World J Gastroenterol 2022 August 21; 28(31): 4376-4389

DOI: 10.3748/wjg.v28.i31.4376

ISSN 1007-9327 (print) ISSN 2219-2840 (online)

ORIGINAL ARTICLE

Retrospective Study

Preoperative contrast-enhanced computed tomography-based radiomics model for overall survival prediction in hepatocellular carcinoma

Peng-Zhan Deng, Bi-Geng Zhao, Xian-Hui Huang, Ting-Feng Xu, Zi-Jun Chen, Qiu-Feng Wei, Xiao-Yi Liu, Yu-Qi Guo, Sheng-Guang Yuan, Wei-Jia Liao

Specialty type: Gastroenterology and hepatology

Provenance and peer review: Unsolicited article; Externally peer reviewed.

Peer-review model: Single blind

Peer-review report's scientific quality classification

Grade A (Excellent): 0
Grade B (Very good): B, B
Grade C (Good): 0
Grade D (Fair): 0
Grade E (Poor): 0

P-Reviewer: Gupta T, India; Hu X, China

Received: April 20, 2022
Peer-review started: April 20, 2022
First decision: June 2, 2022
Revised: June 14, 2022
Accepted: July 20, 2022
Article in press: July 20, 2022
Published online: August 21, 2022

Peng-Zhan Deng, Bi-Geng Zhao, Xian-Hui Huang, Ting-Feng Xu, Zi-Jun Chen, Qiu-Feng Wei, Xiao-Yi Liu, Yu-Qi Guo, Sheng-Guang Yuan, Wei-Jia Liao, Laboratory of Hepatobiliary and Pancreatic Surgery, Affiliated Hospital of Guilin Medical University, Guilin 541001, Guangxi Zhuang Autonomous Region, China

Corresponding author: Wei-Jia Liao, MD, Chief Doctor, Professor, Laboratory of Hepatobiliary and Pancreatic Surgery, Affiliated Hospital of Guilin Medical University, No. 15 Lequn Road, Xiufeng District, Guilin 541001, Guangxi Zhuang Autonomous Region, China.
liaoweijia288@163.com

Abstract

BACKGROUND

Hepatocellular carcinoma (HCC) is the most common primary liver malignancy with a rising incidence worldwide. The prognosis of HCC patients after radical resection remains poor. Radiomics is a novel machine learning method that extracts quantitative features from medical images and provides predictive information of cancer, which can assist with cancer diagnosis, therapeutic decision-making and prognosis improvement.

AIM

To develop and validate a contrast-enhanced computed tomography-based radiomics model for predicting the overall survival (OS) of HCC patients after radical hepatectomy.

METHODS

A total of 150 HCC patients were randomly divided into a training cohort (n = 107) and a validation cohort (n = 43). Radiomics features were extracted from the entire tumour lesion. The least absolute shrinkage and selection operator algorithm was applied for the selection of radiomics features and the construction of the radiomics signature. Univariate and multivariate Cox regression analyses were used to identify the independent prognostic factors and develop the predictive nomogram, incorporating clinicopathological characteristics and the radiomics signature. The accuracy of the nomogram was assessed with the concordance index, receiver operating characteristic (ROC) curve and calibration

curve. The clinical utility was evaluated by decision curve analysis (DCA). Kaplan–Meier methodology was used to compare the survival between the low- and high-risk subgroups.

RESULTS

In total, seven radiomics features were selected to construct the radiomics signature. According to the results of univariate and multivariate Cox regression analyses, alpha-fetoprotein (AFP), neutrophil-to-lymphocyte ratio (NLR) and radiomics signature were included to build the nomogram. The C-indices of the nomogram in the training and validation cohorts were 0.736 and 0.774, respectively. ROC curve analysis for predicting 1-, 3-, and 5-year OS confirmed satisfactory accuracy [training cohort, area under the curve (AUC) = 0.850, 0.791 and 0.823, respectively; validation cohort, AUC = 0.905, 0.884 and 0.911, respectively]. The calibration curve analysis indicated a good agreement between the nomogram-prediction and actual survival. DCA curves suggested that the nomogram had more benefit than traditional staging system models. Kaplan–Meier survival analysis indicated that patients in the low-risk group had longer OS and disease-free survival (all $P < 0.0001$).

CONCLUSION

The nomogram containing the radiomics signature, NLR and AFP is a reliable tool for predicting the OS of HCC patients.

Key Words: Hepatocellular carcinoma; Radiomics; Contrast-enhanced computed tomography; Survival prediction

Core Tip: The prognosis of hepatocellular carcinoma (HCC) patients remains poor even after radical resection. Therefore, a precise and reliable tool to predict the prognosis of HCC patients is urgently needed. We established a predictive model incorporating radiomics features extracted from preoperative contrast-enhanced computed tomography images, alpha-fetoprotein and neutrophil-to-lymphocyte ratio to predict the overall survival of patients with HCC, and the model was visualized *via* a nomogram. The nomogram showed good accuracy for survival prediction.

Citation: Deng PZ, Zhao BG, Huang XH, Xu TF, Chen ZJ, Wei QF, Liu XY, Guo YQ, Yuan SG, Liao WJ. Preoperative contrast-enhanced computed tomography-based radiomics model for overall survival prediction in hepatocellular carcinoma. *World J Gastroenterol* 2022; 28(31): 4376-4389
URL: https://www.wjgnet.com/1007-9327/full/v28/i31/4376.htm
DOI: https://dx.doi.org/10.3748/wjg.v28.i31.4376

INTRODUCTION

Primary liver cancer is the sixth most common malignancy and the third leading cause of cancer-related mortality in the world. Hepatocellular carcinoma (HCC) accounts for 75%-85% of primary liver cancers [1]. Presently, the main therapies for HCC include surgical resection, local ablation, interventional embolization and liver transplantation. For HCC patients with early-stage disease, hepatectomy and liver transplantation are the mainstay curative treatments. Due to the insidious onset and lack of evident clinical symptoms in the early stage, patients with HCC are often diagnosed at an advanced stage. Even after surgical resection, the prognosis of HCC patients remains poor due to postoperative recurrence and metastasis. It has been reported that the recurrence rate within 5 years reaches 60%[2].

Alpha-fetoprotein (AFP) has been widely applied as a biomarker of HCC for diagnosis, monitoring treatment response, assessing prognosis and detecting early recurrence. However, the specificity of AFP for diagnosing HCC is 99%-100%, but the sensitivity is only 20% to 45%[3]. Moreover, nearly 31% of patients with HCC are AFP negative[4]. Therefore, AFP still has limitations as a biomarker of HCC. It has been reported that the tumour microenvironment is closely related to the initiation and progression of HCC[5]. Recent studies have shown that a high density of tumour-infiltrating lymphocytes is associated with favourable outcomes[6]. The neutrophil-to-lymphocyte ratio (NLR) was reported to be an independent prognostic factor for patients with HCC[7,8].

Radiomics is a new method of medical image analysis that uses a series of data-mining algorithms or statistical analysis tools for the high-throughput extraction of quantitative metric features[9,10] to obtain prognostic and predictive information for clinical decision support. It has been recognized that

intratumor heterogeneity is often associated with tumour subtyping and can significantly impact prognosis and response to treatment[11,12]. Traditional radiological analysis is mainly based on naked-eye observation, which primarily focuses on tumour size and anatomical location but ignores intratumor heterogeneity. Radiomics features are able to provide a comprehensive overview of intratumor heterogeneity in a noninvasive manner[13]. Several recent studies indicate that radiomics features may potentially be a useful diagnostic and prognostic biomarker in liver cancer and other tumour types[14-16].

Due to the insufficiency of accurateness and objectiveness for prognostic markers in the prognostic evaluation of HCC patients, a precise and reliable tool to predict the prognosis of HCC patients is urgently needed. In the present study, we aimed to develop and validate a model based on contrast-enhanced computed tomography (CECT) images and clinical-pathologic characteristics to predict the overall survival (OS) of HCC patients.

MATERIALS AND METHODS

This study was composed of the following steps: (1) Patient recruitment and data collection; (2) CECT image acquisition, tumour segmentation, region of interest (ROI) selection, radiomics feature extraction and radiomics signature construction; (3) The radiomics signature and clinical-pathologic characteristics were combined to build a predictive model and visualized *via* a nomogram; and (4) Evaluation of the predictive model using receiver operating characteristic (ROC) curves, calibration curves, decision curve analysis (DCA) and Kaplan–Meier curves.

Patients

This retrospective study was approved by the research ethics committee of the Affiliated Hospital of Guilin Medical University and conducted in accordance with the Declaration of Helsinki. Informed consent was obtained from all patients.

A total of 208 HCC patients who underwent radical resection at the Affiliated Hospital of Guilin Medical University with pathologically confirmed HCC were recruited from January 2014 to September 2017. Among them, 150 individuals fulfilled the inclusion and exclusion criteria (Figure 1). Radical resection was defined as a completed resection of the tumour mass with pathologically confirmed negative margins and no residual tumour or new lesion observed in two observations at an interval of no less than 4 wk. All tumour tissue samples were diagnosed by at least two experienced pathologists independently. All patients underwent CECT scans and haematological examinations before surgery. The 150 enrolled HCC patients were randomly divided into a training cohort (n = 107) and a validation cohort (n = 43) at a ratio of 2.5:1. Demographic and clinical-pathologic data were collected from medical records, including age, sex, alanine aminotransferase, AFP, American Joint Committee on Cancer tumor, node and metastasis (TNM) stage, Barcelona clinic liver cancer (BCLC) stage, hepatitis B surface antigen (HBsAg) and NLR.

Each patient was followed up *via* outpatient review. Routine postoperative examinations, including routine blood tests, liver function tests, renal function tests, serum AFP levels and abdominal ultrasonography, were performed every 2 mo after surgery within 2 years and then every 6 mo thereafter. A CECT scan was recommended if the examination results were abnormal or tumour recurrence was suspected. For patients who did not attend the follow-up visit, follow-up information was obtained by phone. OS was defined as the time from surgery to death or the last follow-up date, while disease-free survival (DFS) was defined as the time from surgery to tumour first intrahepatic and/or extrahepatic recurrence, death, or the last follow-up date.

CECT scan protocols and image preprocessing

Abdominal CECT scans were performed with two scanners: A Lightspeed VCT XT (GE Healthcare, United States) and an Optima CT660 (GE Healthcare, United States). The scanner was operated in cine mode, and the parameters were as follows: tube voltage of 120 kV, automatic tube current modulation with noise index of 8, tube rotation speed of 600 ms, pitch of 0.985:1, collimator of 0.625 mm. Iopromide (Ultravist 300, Bayer-Schering Pharma, Germany) was given intravenously in a volume of 1.5 mL/kg at a rate of 4 mL/s *via* the antecubital vein. The slice thickness and interval of the arterial and portal venous phase images was 5 mm. All images were reconstructed into images with a 1.25 mm slice thickness and 1.25 mm interval. All data were transferred to an advanced workstation (AW 4.7).

All CECT images in this study met the criteria delineated by the American Association for the Study of Liver Disease guidelines[17]. CECT images were exported in digital imaging and communication in medicine (DICOM) format from the picture archiving and communication system database. All DICOM images were converted to neuroimaging informatics technology initiative format by the SimpleITK package (version 1.2.0) of Python software (version 3.7).

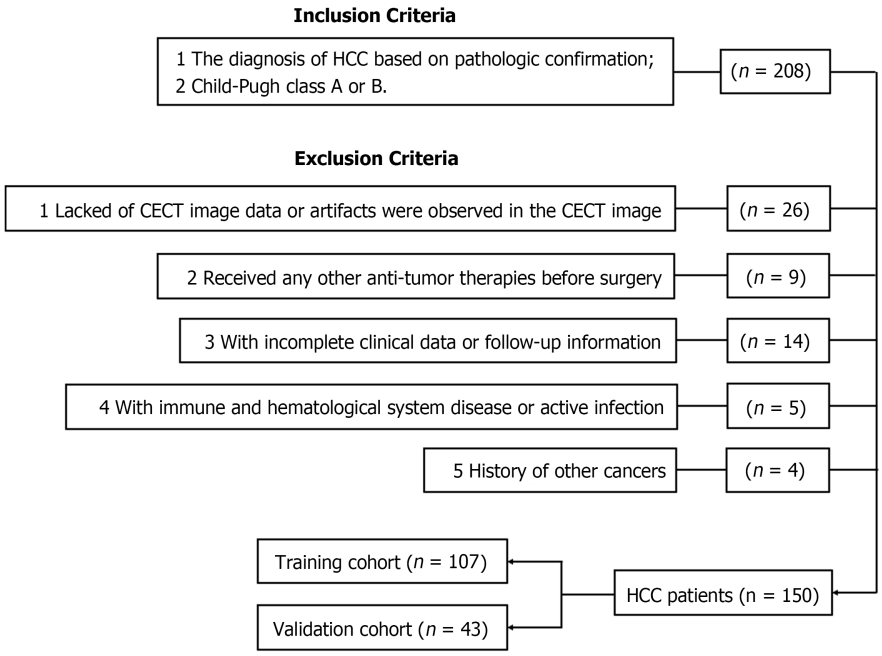

DOI: 10.3748/wjg.v28.i31.4376

Figure 1 Flowchart of the patient selection process. HCC: Hepatocellular carcinoma; CECT: Contrast-enhanced computed tomography.

Radiomics analysis and radiomics signature construction

Tumour segmentation was performed by 3D Slicer software (version 4.11.20210226). ROIs were drawn on each layer of the tumour in the horizontal plane from the upper boundary to the lower boundary. Tumour lesions were semiautomatically outlined on all arterial phase and portal venous phase images, and manual corrections were implemented whenever necessary. The images were reviewed independently by two blinded radiologists with 7 and 8 years of experience, and a third radiologist resolved any discrepancies. For patients with multiple tumours, only the largest tumour was selected.

CECT image normalization and radiomics feature extraction were conducted by the Pyradiomics package (version 3.0.3) of Python software. The radiomics features extracted from ROIs included first order features, shape features (2D and 3D), gray level co-occurrence matrix features, gray level size zone matrix features, gray level run length matrix features, gray level dependence matrix features and neighbouring gray tone difference matrix features. Due to the large number of features, dimensionality reduction was essential. The least absolute shrinkage and selection operator (LASSO) algorithm with a 10-fold cross-validation approach was used to reduce the data dimension in the training cohort. Afterwards, the radiomics score, which was defined as the radiomics signature, was generated by linearly combining the selected radiomics features and their weighted coefficients. The workflow of radiomics analysis and radiomics signature construction is shown in Figure 2A. Afterwards, the concordance index (C-index) and ROC curve analysis were used to estimate the predictive value of the radiomics signature for 1-, 3- and 5-year OS.

Selection of the optimal cut-off value for NLR

According to our previous study[18], the optimal cut-off value for NLR in predicting the prognosis of HCC patients after curative resection was 2.31, which had both maximum sensitivity and specificity [area under the curve (AUC) = 0.723, 95%CI: 0.664–0.777].

Statistical analysis

Normality of distributions was tested by the Shapiro–Wilk test. Clinical-pathologic characteristics were compared by Student's *t* test and are presented as the mean ± SD for continuous variables conforming to a normal distribution. Nonnormally distributed continuous variables were compared using the Wilcoxon signed rank test and are presented as the median with interquartile range. Categorical variables were compared using the Pearson χ^2 test. Univariate and multivariate regression analyses were performed in the training cohort using the Cox proportional hazards model to identify the independent predictors for nomogram construction. The rms and regplot packages were used to establish a nomogram and calibration curve. The ROC curve analysis was performed using the timeROC package. The C-index, ROC curve and calibration curve were used to assess the accuracy of the nomogram. The Kaplan–Meier method and log-rank test were conducted to compare the different survival rates between the low- and high-risk subgroups in different cohorts. We built two predictive models based on BCLC and TNM staging systems. Patients were categorized into stage 0, stage A, stage

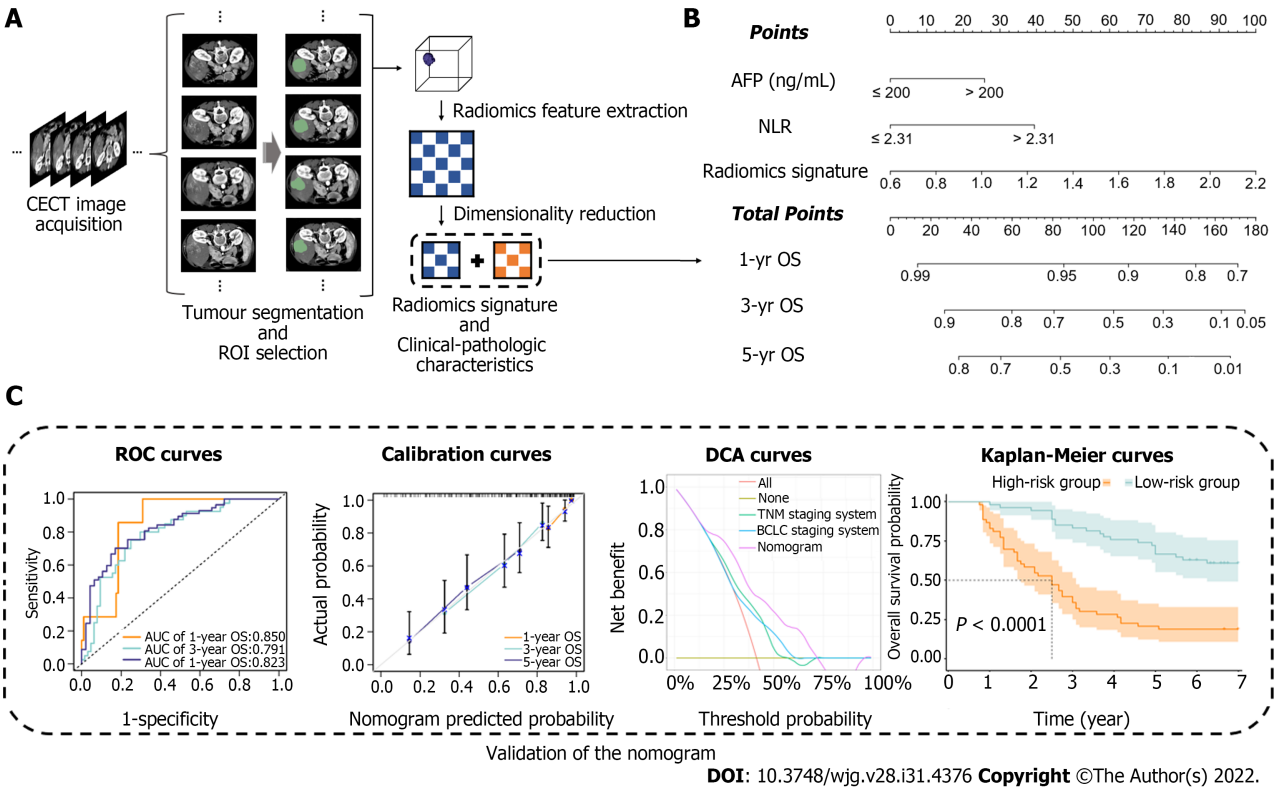

DOI: 10.3748/wjg.v28.i31.4376 **Copyright** ©The Author(s) 2022.

Figure 2 Workflow of model construction and validation. A: Contrast-enhanced computed tomography image acquisition, tumour segmentation, region of interest selection, radiomics feature extraction and radiomics signature construction; B: Combination of the radiomics signature and clinical-pathologic characteristics to build the predictive model, the model was visualized *via* nomogram; C: Evaluation of the predictive model by using receiver operating characteristic curves, calibration curves, decision curve analysis curves and Kaplan–Meier curves. CECT: Contrast-enhanced computed tomography; ROI: Region of interest; AFP: Alpha fetoprotein; NLR: Neutrophil-to-lymphocyte ratio; OS: Overall survival; ROC: Receiver operating characteristic; AUC: Area under the curve; DCA: Decision curve analysis; BCLC: Barcelona Clinic Liver Cancer.

B and stage C according to BCLC staging system; grade I, grade II, grade III and grade IV according to TNM staging system. DCA was conducted to compare the abovementioned two traditional staging systems with the nomogram. All statistical analyses were performed using SPSS software (version 24.0) or R software (version 4.1.2) and accepted as significant at $P < 0.05$.

RESULTS

Demographic and clinicopathological characteristics

A total of 150 HCC patients were enrolled in this study according to inclusion and exclusion criteria, with an average age of 49.9 years (range, 20-75 years), and 130 patients were male. A total of 136 patients were diagnosed with cirrhosis, while 137 patients were classified as Child–Pugh class A. A total of 124 patients were positive for HBsAg. Patients were randomly divided into a training cohort (n = 107) and a validation cohort (n = 43). The demographic and clinical-pathologic characteristics are summarized in Table 1. There were no significant differences in variables between the two cohorts.

Radiomics signature construction

In total, 1926 radiomics features were extracted from the ROIs. Based on the training cohort, radiomics features were reduced to 7 survival-related features by using the LASSO algorithm. The name of the selected features and the formula of the radiomics score are shown in Supplementary Table 1. The C-indices of the radiomics signature for predicting OS in the training and validation cohorts were 0.689 (95%CI: 0.626–0.751) and 0.746 (95%CI: 0.650–0.842), respectively. The ROC curves of the radiomics signature for predicting 1-, 3- and 5-year OS are shown in Figure 3 (AUC = 0.648, 0.753 and 0.807, respectively, in the training cohort; AUC = 0.921, 0.840 and 0.891, respectively, in the validation cohort).

Development and validation of the predictive nomogram

Based on the univariate regression analysis (Table 2), four variables with $P < 0.05$ were enrolled in the multivariate regression analysis. The results of multivariate regression analysis are displayed as forest plots (Figure 4). AFP [hazard ratio (HR), 1.8; 95%CI: 1.06–3.1, P = 0.03], NLR (HR, 2.5; 95%CI: 1.45–4.3, P

Table 1 The demographic and clinical-pathologic characteristics of patients

Variables	Training cohort (*n* = 107)	Validation cohort (*n* = 43)	*P* value
Age, yr (mean ± SD)	49.77 ± 10.57	50.35 ± 11.43	0.766
Sex (male/female)	94/13	36/7	0.501
Alcohol abuse (present/absent)	44/63	19/24	0.731
Tumor number (multiple/single)	22/85	10/33	0.716
Tumor diameter, cm (> 5/≤ 5)	69/38	24/19	0.322
MVI (present/absent)	46/61	17/26	0.698
Cirrhosis (present/absent)	100/7	36/7	0.123
TNM stage (I-II/III-IV)	54/53	18/25	0.340
BCLC stage (0-A/B-C)	61/46	20/23	0.243
WBC, × 10^9/L (median, IQR)	6.05 (5.00-7.3)	6.11 (5.04-8.04)	0.290
Platelets, × 10^9/L (mean ± SD)	190.75 ± 71.91	202.02 ± 79.32	0.401
LYMPH, × 10^9/L (median, IQR)	1.63 (1.19-1.94)	1.74 (1.35-2.04)	0.229
NEUT, × 10^9/L (median, IQR)	3.75 (2.68-4.07)	3.90 (2.85-5.17)	0.385
DB, μmol/L (median, IQR)	5.20 (4.20-5.81)	4.85 (3.68-5.56)	0.077
TB, μmol/L (median, IQR)	12.50 (9.43-15.91)	13.38 (8.93-17.11)	0.840
ALB, g/L (mean ± SD)	38.42 ± 4.30	36.87 ± 5.49	0.069
GLB, g/L (median, IQR)	31.80 (28.80-35.28)	32.22 (29.80-35.44)	0.480
GGT, U/L (mean ± SD)	115.26 ± 136.68	105.49 ± 82.44	0.662
ALT, U/L (median, IQR)	31.00 (21.24-44.14)	27.60 (17.46-42.88)	0.306
AST, U/L (median, IQR)	34.50 (26.55-51.51)	35.40 (25.55-46.02)	0.891
AFP, ng/mL (> 200/≤ 200)	50/57	23/20	0.454
HBsAg (positive/negative)	91/16	33/10	0.225
NLR (> 2.31/≤ 2.31)	50/57	21/22	0.815

IQR: Interquartile range; MVI: Microvascular invasion; TNM: Tumor, node and metastasis; BCLC: Barcelona clinic liver cancer; WBC: White blood cell count; LYMPH: Lymphocyte count; NEUT: Neutrophil count; DB: Direct bilirubin; TB: Total bilirubin; ALB: Albumin; GLB: Globulin; GGT: Gamma-glutamyl transpeptidase; ALT: Alanine transaminase; AST: Aspartate transaminase; AFP: Alpha fetoprotein; HBsAg: Hepatitis B surface antigen; NLR: Neutrophil-to-lymphocyte ratio.

< 0.001) and radiomics signature (HR, 3.7; 95%CI: 1.25–10.7, P = 0.018) were identified as independent predictors of OS. The abovementioned three variables were included to develop the predictive model and visualized *via* a nomogram (Figure 2B). The C-indices of the nomogram in the training and validation cohorts were 0.736 (95%CI: 0.681–0.791) and 0.774 (95%CI: 0.697–0.851), respectively. The AUC values of 1-, 3-, and 5-year OS were 0.850, 0.791 and 0.823, respectively, in the training cohort (Figure 5A) and 0.905, 0.884 and 0.911, respectively, in the validation cohort (Figure 5B). The calibration curves of the nomogram demonstrated good agreement between the predicted and actual survival probabilities (Figure 5C and D).

Evaluation of clinical practicality and risk stratification ability

DCA curves showed that the nomogram received more net benefit than the BCLC staging system model and TNM staging system model in predicting 3- and 5-year OS at reasonable threshold probability (Figure 6).

To further explore the risk stratification ability of the nomogram, we calculated the total points of the nomogram for each patient. The total points conformed to a normal distribution in the training and validation cohorts. Patients were categorized into low- and high-risk subgroups based on whether the total points of the patient were lower (training cohort ≤ 89.8; validation cohort ≤ 66.0) or higher (training cohort > 89.8; validation cohort > 66.0) than the median points of each cohort. Kaplan–Meier curves indicated that patients in the low-risk subgroup had significantly longer OS and DFS, with all P < 0.001 (Figure 7).

Table 2 Univariate Cox regression analysis in the training cohort

Variables	Univariate Cox regression analysis		
	HR	95%CI	*P* value
Age, yr	0.993	0.971-1.016	0.545
Sex (male *vs* female)	0.789	0.376-1.657	0.532
Alcohol abuse (present *vs* absent)	1.133	0.692-1.854	0.620
Tumor number (multiple *vs* single)	1.060	0.594-1.892	0.843
Tumor diameter, cm (> 5 *vs* ≤ 5)	1.147	0.681-1.934	0.606
MVI (present *vs* absent)	1.506	0.921-2.461	0.102
Cirrhosis (present *vs* absent)	1.112	0.404-3.063	0.837
DB, μmol/L (> 6.8 *vs* ≤ 6.8)	1.551	0.766-3.140	0.223
ALB, g/L (> 35 *vs* ≤ 35)	0.677	0.388-1.181	0.169
GGT, U/L (> 50 *vs* ≤ 50)	1.482	0.879-2.499	0.140
ALT, U/L (> 40 *vs* ≤ 40)	1.671	1.002-2.787	0.049
AFP, ng/mL (> 200 *vs* ≤ 200)	2.202	1.340-3.619	0.002
HBsAg (positive *vs* negative)	1.013	0.516-1.991	0.969
NLR (> 2.31 *vs* ≤ 2.31)	3.160	1.901-5.251	< 0.001
Radiomics signature	10.315	3.829-27.786	< 0.001

HR: Hazard ratio; MVI: Microvascular invasion; DB: Direct bilirubin; ALB: Albumin; GGT: Gamma-glutamyl transpeptidase; ALT: Alanine transaminase; AFP: Alpha fetoprotein; HBsAg: Hepatitis B surface antigen; NLR: Neutrophil-to-lymphocyte ratio.

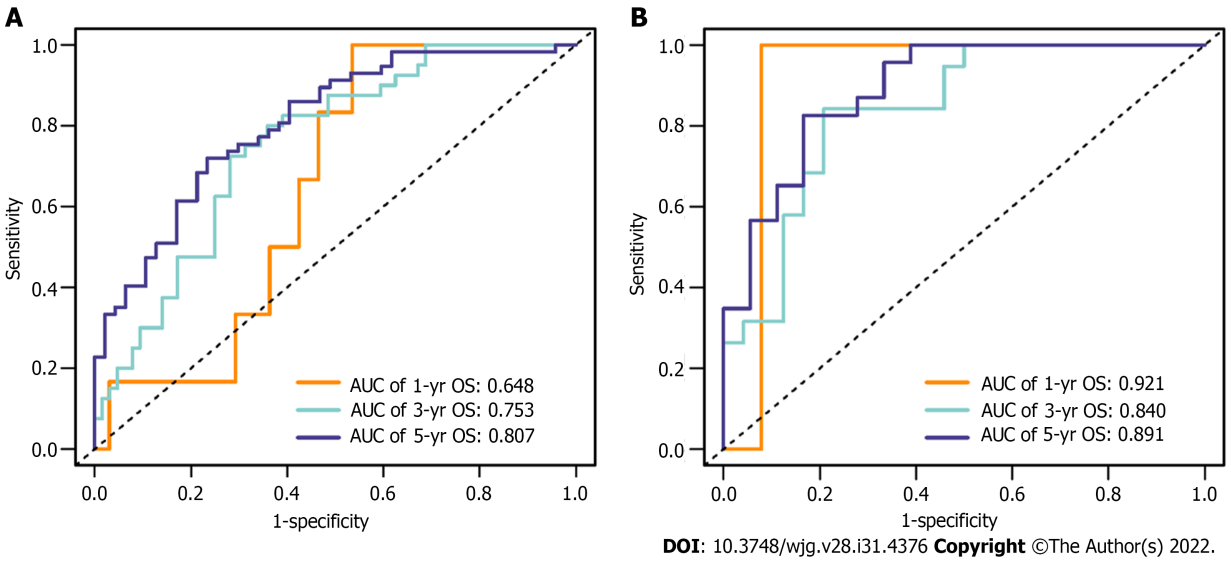

DOI: 10.3748/wjg.v28.i31.4376 **Copyright** ©The Author(s) 2022.

Figure 3 Receiver operating characteristic curves of the radiomics signature for predicting 1-, 3- and 5-year overall survival in the training and validation cohorts. A: Training cohort; B: Validation cohort. OS: Overall survival; AUC: Area under the curve.

DISCUSSION

In this study, we developed a nomogram for predicting the survival of HCC patients after radical hepatectomy. Seven radiomics features were selected from 1926 radiomics features, and then integrated into a single radiomics signature to comprehensively estimate CECT images. We included AFP, NLR and radiomics signature to build the predictive nomogram. The C-indices of the nomogram in the training cohort and validation cohort were 0.736 and 0.774, respectively. The AUCs and the calibration curve indicated satisfactory accuracy in both the training and validation cohorts (AUC of 1-, 3- and 5-year survival = 0.850, 0.791, 0.823 and 0.905, 0.884, 0.911, respectively). The high AUCs of the nomogram

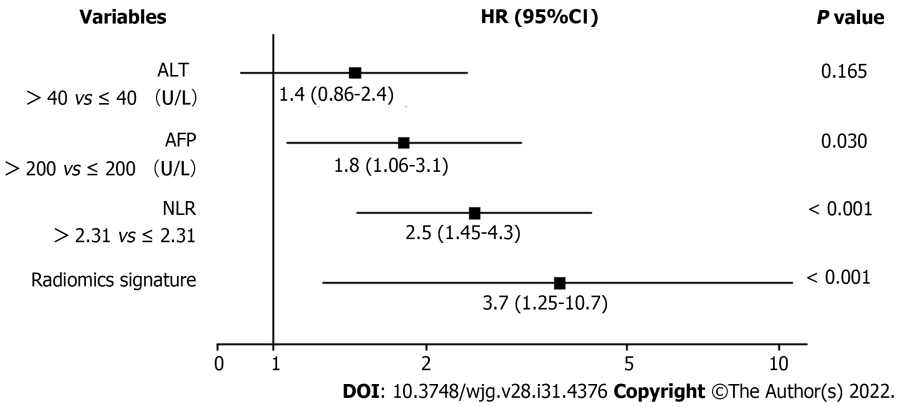

DOI: 10.3748/wjg.v28.i31.4376 **Copyright** ©The Author(s) 2022.

Figure 4 Forest plot of variables with multivariate regression analysis in the training cohort. Variables with a *P* value < 0.05 were considered significantly associated with the overall survival of hepatocellular carcinoma patients. ALT: Alanine transaminase; AFP: Alpha fetoprotein; NLR: Neutrophil-to-lymphocyte ratio; HR: Hazard ratio.

indicate a high accuracy in predicting OS. In DCA, comparing the traditional staging system with our nomogram with respect to predictive ability and clinical practicality, the predictive nomogram was superior to the traditional staging system (BCLC and TNM staging system) in predicting 3- and 5-year survival.

To our knowledge, our radiomics-based model that contains NLR and AFP to predict survival in patients with HCC is entirely novel. A few previous studies[19,20] have investigated the capability of radiomics analysis in predicting the prognosis of HCC patients, and these studies analysed the largest cross-sectional area, whereas entire-tumour analysis was conducted in this study, which can provide more comprehensive information and more effective evaluation of the tumour. Thus, compared with previous studies, radiomics analysis in this study may achieve better performance. Various models combining radiomics features with clinical-pathologic factors to predict prognosis have been developed. Nevertheless, very few studies have enrolled radiomics features and NLR as variables to build a prognostic prediction model for HCC patients. Wang *et al*[21] established an magnetic resonance imaging-based radiomics model incorporating a few clinical factors for predicting the 5-year survival of patients with HCC after radical surgery. The mean AUC in the validation cohort was 0.7578 (95%CI: 0.7056–0.8100).

As precision medicine has developed, accurate prediction of patient prognosis is the principal component of individualized therapy and improving patient prognosis. It has been reported that intratumor heterogeneity is common in a variety of tumours and correlated with clinical outcomes[22]. However, information about intratumor heterogeneity obtained from routine clinical examinations is limited. Radiomics analysis refers to computer-aided data mining of quantitative high-throughput imaging features extracted from medical images[9,10], and it has been reported that radiomics features have potential prognostic value in liver cancer[14], lung cancer[15] and breast cancer[16]. Compared with the interpretation of traditional radiology, radiomics could provide comprehensive information regarding intratumor heterogeneity that may be unable to be obtained by the naked eye of radiologists. To a certain extent, radiomics overcomes these limitations of traditional radiology. As a biomarker associated with HCC, AFP has been widely used for early diagnosis and monitoring of HCC. AFP was considered an independent risk factor for postoperative survival; moreover, patients with low serum AFP levels had longer OS after radical resection. However, AFP still has some limitations in the prognosis prediction of HCC. Prior studies have reported that AFP has no ability to predict prognosis in small HCC (diameter ≤ 3 cm)[23]. Immune cells such as neutrophils, macrophages and lymphocytes within the tumour microenvironment have been confirmed to affect tumour development and progression[24]. There is evidence suggesting that lymphocytes can inhibit tumour proliferation, invasion, and metastasis by enhancing immune surveillance[25]. Moreover, tumour-infiltrating lymphocytes were associated with better outcomes in a variety of tumours, probably linked to tumour infiltration, antitumor activity, lymphocyte induction and inhibition of angiogenesis[26]. One study indicated that neutrophils promote tumour invasion[27]. Neutrophils can inhibit the proliferation of lymphocytes and induce lymphocyte apoptosis[28]. Patients with an elevated NLR level have relative neutrophilia and lymphocytopenia. Therefore, a high NLR indicates a poor prognosis, and this has been confirmed in numerous cancers, including gastric cancer[29], colorectal cancer[30] and pancreatic cancer [31]. To date, there is growing attention to the potential of NLR to be a prognostic biomarker in patients with HCC[32,33]. The NLR is a modality of measuring systemic inflammation that is relatively inexpensive and conveniently obtained from routine preoperative blood tests. In our previous study, the optimal cut-off value of NLR was determined to be 2.31 for predicting the prognosis of patients with HCC, and this was confirmed by not only our previous retrospective trial but also other prospective clinical trials[32]. In summary, NLR is a potential independent predictor for HCC.

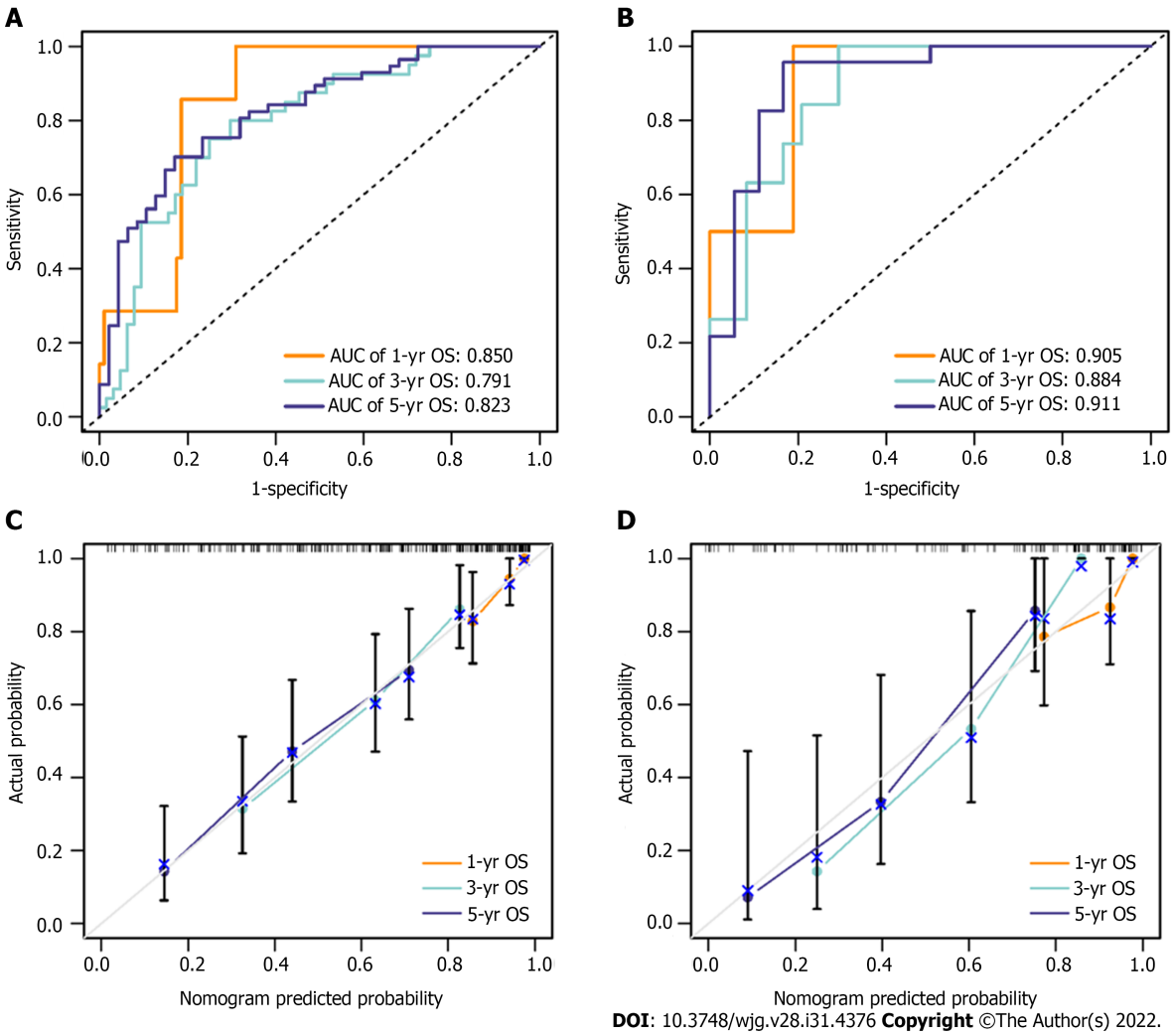

DOI: 10.3748/wjg.v28.i31.4376 **Copyright** ©The Author(s) 2022.

Figure 5 Accuracy of the nomogram for predicting 1-, 3- and 5-year OS in the training and validation cohorts was evaluated by receiver operating characteristic curves and calibration curves. A and B: Receiver operating characteristic curves of the nomogram in the training cohort (A) and validation cohort (B); C and D: Calibration curves of the nomogram in the training cohort (C) and validation cohort (D). In the calibration curve, the nomogram-predicted survival probability is represented on the x-axis, and the actual outcome of overall survival is represented on the y-axis. A closer fit of the coloured lines to the ideal grey line indicates better accuracy in predicting OS. OS: Overall survival; AUC: Area under the curve.

As a standardized and noninvasive imaging modality, CECT is widely utilized for diagnosis, staging, clinical decision-making and treatment response monitoring across numerous cancer types. An advantage of radiomics analysis is that it was performed on existing CECT images as a routine preoperative examination for patients with malignant tumours. Moreover, the variables included in this nomogram were easily acquired from routine blood examinations.

All CECT images were reconstructed with a slice thickness of 1.25 mm, and a previous report showed that slice thickness does not considerably influence the stability of the parameters[34].

The current study has several limitations. First, this study was a single-centre retrospective study. Insufficient data heterogeneity could be a major limitation of single-centre studies. Therefore, more patients from other centres are needed to further validate the reliability and clinical applicability of this prognostic model. Second, HCC is considered to be related to various aetiological factors, including alcohol, aflatoxin, hepatitis B virus and hepatitis C virus. Different aetiologies might result in different outcomes in HCC. Hepatitis B virus was the main aetiology of HCC in the present study. Thus, future studies are required to validate the efficacy and accuracy of this predictive model in HCC with different aetiologies. Third, the different contrast agents or the different injection speeds may affect the quantification of radiomic features[35] and thus affect the accuracy of the model. To overcome this limitation, multi-institutional validation and cross-validation are required in the future. Fourth, regions of interest were outlined semiautomatically and corrected manually when necessary. Hence, a certain degree of selection bias of the ROIs might be created by the different observers. This is a challenging problem for radiomics analysis to eliminate or reduce biases. Fifth, the correlation between radiomics features and biological behaviour remains unknown. Recently, radio-genomics has become an emerging area that integrates radiomics and genomics. Radio-genomics is the discipline that studies the relationship

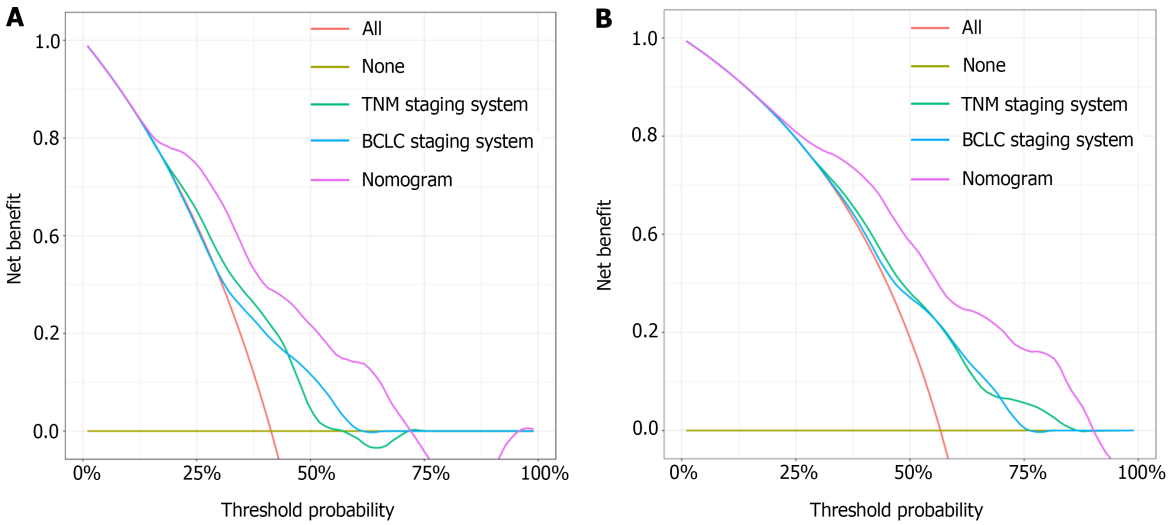

DOI: 10.3748/wjg.v28.i31.4376 **Copyright** ©The Author(s) 2022.

Figure 6 Decision curve analysis was performed in all hepatocellular carcinoma patients to evaluate the clinical practicality of the nomogram for predicting 3- and 5-year overall survival compared with the Barcelona clinic liver cancer staging system model and tumor, node and metastasis staging system model. A and B: Decision curve analysis of the nomogram, Barcelona clinic liver cancer staging system model and tumor, node and metastasis staging system model in predicting 3- (A) and 5-year (B) OS. In the decision curve, the threshold probability is represented on the x-axis, and the net benefit is represented on the y-axis. A higher curve indicates a greater net benefit at any given threshold probability. The decision curve showed that the nomogram adds more net benefit than traditional staging system models. BCLC: Barcelona clinic liver cancer; TNM: Tumor, node and metastasis.

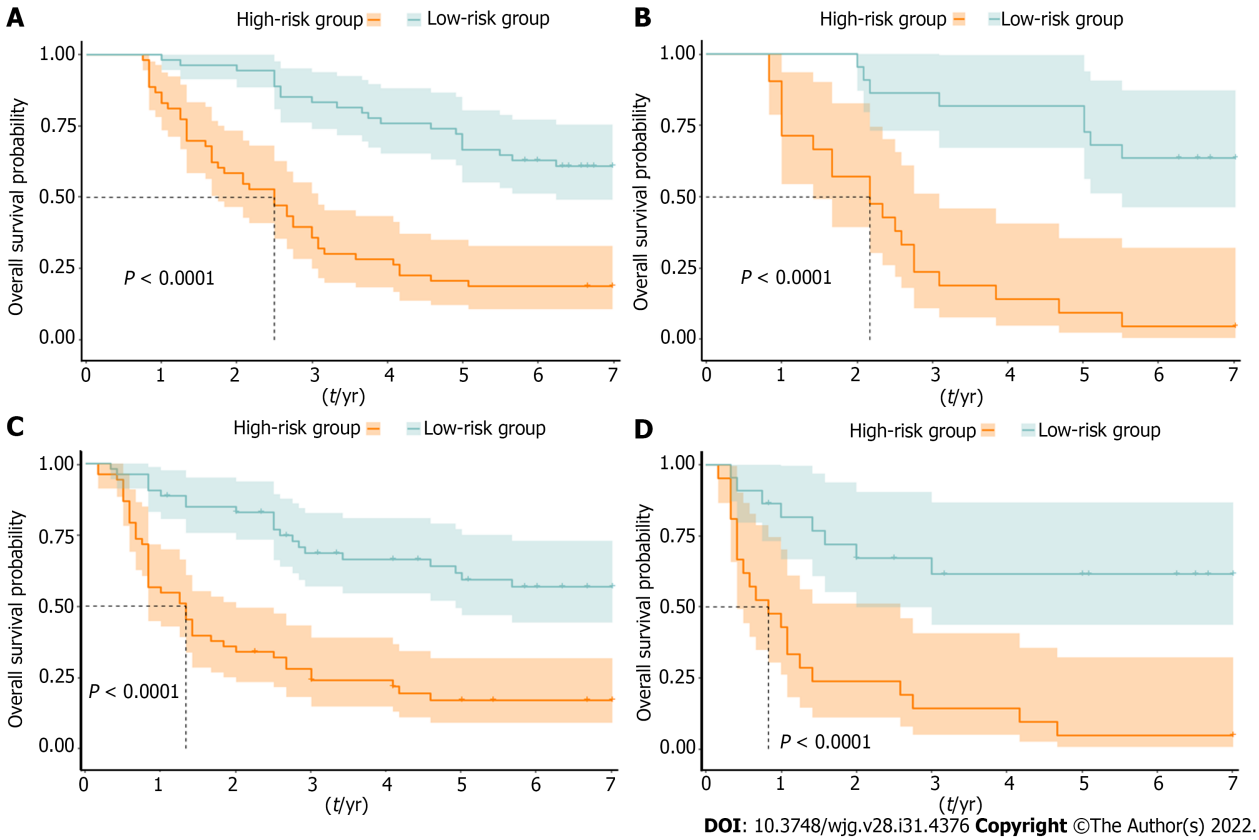

DOI: 10.3748/wjg.v28.i31.4376 **Copyright** ©The Author(s) 2022.

Figure 7 Risk stratification ability of the nomogram was estimated by the Kaplan–Meier method and log-rank test in the training and validation cohorts. A and B: Kaplan–Meier curves between the low- and high-risk subgroups of overall survival in the training cohort (A) and validation cohort (B); C and D: Kaplan–Meier curves between the low- and high-risk subgroups of disease-free survival in the training cohort (C) and validation cohort (D). Patients with hepatocellular carcinoma in the training and validation cohorts were divided into low- and high-risk subgroups according to whether the total points of each patient were lower or higher than the median points of each cohort.

between image phenotypes and genomics, which may contribute to precision medicine development [36]. Further research is still required to determine the potential correlation between radiomics and genomics in HCC. In future studies, we will incorporate genomic characteristics associated with HCC prognosis to construct a more comprehensive radio-genomics predictive model.

CONCLUSION

In conclusion, the nomogram combining the radiomics signature, NLR and AFP may contribute to postoperative outcome prediction and clinical treatment decision-making for HCC patients.

ARTICLE HIGHLIGHTS

Research background

Hepatocellular carcinoma (HCC) is the most common primary liver malignancy. The prognosis of HCC patients remains poor. Radiomics is an artificial intelligent-based method for obtaining prognostic and predictive information which may contribute to clinical outcomes improvement.

Research motivation

Currently, a few studies have analysed the largest cross-sectional area of HCC tumour. In this study, we have analysed the entire-tumour to build a more comprehensive prognostic prediction model with clinical characteristics. We aimed to develop a radiomics model for predicting the overall survival of HCC patients after hepatectomy.

Research objectives

In this study, we aimed to develop a radiomics model based on contrast-enhanced computed tomography (CECT) images for predicting the overall survival of HCC patients after radical hepatectomy.

Research methods

A total of 150 HCC patients were enrolled and randomly divided into a training cohort (n = 107) and a validation cohort (n = 43) at ratio 2.5:1. Radiomics features were extracted from the CECT images. In training cohort, the least absolute shrinkage and selection operator algorithm was applied for radiomics features selection and radiomics signature construction. Univariate and multivariate Cox regression analyses were used to develop the predictive model. The accuracy of the model was assessed with the concordance index, receiver operating characteristic curve and calibration curve. The clinical practicality was evaluated by decision curve analysis. The survival between the low- and high-risk subgroups was compared using Kaplan–Meier methodology.

Research results

In total, seven radiomics features were selected to construct the radiomics signature. Alpha-fetoprotein, neutrophil-to-lymphocyte ratio and radiomics signature were identified as independent risk predictors to build the predictive model. The C-indices of the model in the training and validation cohorts were 0.736 and 0.774, respectively. In receiver operating characteristic curve for predicting 1-, 3-, and 5-year overall survival, area under the curve (AUC) = 0.850, 0.791 and 0.823, respectively in training cohort; AUC = 0.905, 0.884 and 0.911, respectively in validation cohort. The calibration curve analysis indicated a good agreement between the model-prediction and actual survival. Decision curve analysis suggested that the predictive model had more benefit than traditional staging system models. In Kaplan–Meier survival analysis, patients in the low-risk group had longer overall survival and disease-free survival.

Research conclusions

The predictive model is a reliable tool for predicting the overall survival of HCC patients after radical hepatectomy.

Research perspectives

More precise and reliable tool to predict the prognosis of HCC patients is urgently needed. Radiomics is a new method for obtaining prognostic and predictive information. In this study, we aimed to develop a predictive model based on CECT images and clinical-pathologic characteristics to predict the overall survival of HCC patients.

FOOTNOTES

Author contributions: Deng PZ, Zhao BG and Huang XH contributed equally to this work; Liao WJ was the guarantor and designed the study; Deng PZ, Zhao BG, Xu TF, Chen ZJ, Wei QF, and Liu XY participated in the acquisition, analysis, and interpretation of the data; Deng PZ and Huang XH drafted the initial manuscript; Guo YQ, Yuan SG, and Liao WJ revised the article critically for important intellectual content.

Supported by the National Natural Science Foundation of China, No. 81372163; the Science and Technology Planning Project of Guilin, No. 20190218-1; the Openin Project of Key laboratory of High-Incidence-Tumor Prevention & Treatment (Guangxi Medical University), Ministry of Education, No. GKE-KF202101; the Program of Guangxi Zhuang Autonomous Region health and Family Planning Commission, No. Z20210706; and the Innovation and Entrepreneurship Project of University Students in Guangxi, No. 202110601002.

Institutional review board statement: The study was reviewed and approved by the research ethics committee of Affiliated Hospital of Guilin Medical University (Approval NO. 2021WJWZC14).

Informed consent statement: Informed consent was obtained from all patients.

Conflict-of-interest statement: There are no conflicts of interest to report.

Data sharing statement: No additional data are available.

Country/Territory of origin: China

ORCID number: Peng-Zhan Deng 0000-0003-1221-7664; Bi-Geng Zhao 0000-0001-6203-4159; Xian-Hui Huang 0000-0002-4306-1327; Ting-Feng Xu 0000-0003-0303-5471; Zi-Jun Chen 0000-0002-2488-8038; Qiu-Feng Wei 0000-0001-9355-2098; Xiao-Yi Liu 0000-0001-5563-7488; Yu-Qi Guo 0000-0002-6687-6828; Sheng-Guang Yuan 0000-0003-4846-0543; Wei-Jia Liao 0000-0002-8906-8612.

S-Editor: Zhang H
L-Editor: A
P-Editor: Cai YX

REFERENCES

1 **Sung H**, Ferlay J, Siegel RL, Laversanne M, Soerjomataram I, Jemal A, Bray F. Global Cancer Statistics 2020: GLOBOCAN Estimates of Incidence and Mortality Worldwide for 36 Cancers in 185 Countries. *CA Cancer J Clin* 2021; **71**: 209-249 [PMID: 33538338 DOI: 10.3322/caac.21660]
2 **Poon RT**, Fan ST, Lo CM, Liu CL, Wong J. Long-term survival and pattern of recurrence after resection of small hepatocellular carcinoma in patients with preserved liver function: implications for a strategy of salvage transplantation. *Ann Surg* 2002; **235**: 373-382 [PMID: 11882759 DOI: 10.1097/00000658-200203000-00009]
3 **Gupta S**, Bent S, Kohlwes J. Test characteristics of alpha-fetoprotein for detecting hepatocellular carcinoma in patients with hepatitis C. A systematic review and critical analysis. *Ann Intern Med* 2003; **139**: 46-50 [PMID: 12834318 DOI: 10.7326/0003-4819-139-1-200307010-00012]
4 **Zong J**, Fan Z, Zhang Y. Serum Tumor Markers for Early Diagnosis of Primary Hepatocellular Carcinoma. *J Hepatocell Carcinoma* 2020; **7**: 413-422 [PMID: 33376710 DOI: 10.2147/JHC.S272762]
5 **Leonardi GC**, Candido S, Cervello M, Nicolosi D, Raiti F, Travali S, Spandidos DA, Libra M. The tumor microenvironment in hepatocellular carcinoma (review). *Int J Oncol* 2012; **40**: 1733-1747 [PMID: 22447316 DOI: 10.3892/ijo.2012.1408]
6 **Nakagawa S**, Umezaki N, Yamao T, Kaida T, Okabe H, Mima K, Imai K, Hashimoto D, Yamashita YI, Ishiko T, Chikamoto A, Baba H. Survival impact of lymphocyte infiltration into the tumor of hepatocellular carcinoma in hepatitis B virus-positive or non-B non-C patients who underwent curative resection. *Hepatol Res* 2018; **48**: E126-E132 [PMID: 28696046 DOI: 10.1111/hepr.12936]
7 **Liao R**, Tang ZW, Li DW, Luo SQ, Huang P, Du CY. Preoperative neutrophil-to-lymphocyte ratio predicts recurrence of patients with single-nodule small hepatocellular carcinoma following curative resection: a retrospective report. *World J Surg Oncol* 2015; **13**: 265 [PMID: 26328917 DOI: 10.1186/s12957-015-0670-y]
8 **Motomura T**, Shirabe K, Mano Y, Muto J, Toshima T, Umemoto Y, Fukuhara T, Uchiyama H, Ikegami T, Yoshizumi T, Soejima Y, Maehara Y. Neutrophil-lymphocyte ratio reflects hepatocellular carcinoma recurrence after liver transplantation *via* inflammatory microenvironment. *J Hepatol* 2013; **58**: 58-64 [PMID: 22925812 DOI: 10.1016/j.jhep.2012.08.017]
9 **Gillies RJ**, Kinahan PE, Hricak H. Radiomics: Images Are More than Pictures, They Are Data. *Radiology* 2016; **278**: 563-

577 [PMID: 26579733 DOI: 10.1148/radiol.2015151169]
10 **Lambin P**, Rios-Velazquez E, Leijenaar R, Carvalho S, van Stiphout RG, Granton P, Zegers CM, Gillies R, Boellard R, Dekker A, Aerts HJ. Radiomics: extracting more information from medical images using advanced feature analysis. *Eur J Cancer* 2012; **48**: 441-446 [PMID: 22257792 DOI: 10.1016/j.ejca.2011.11.036]
11 **Gerlinger M**, Rowan AJ, Horswell S, Math M, Larkin J, Endesfelder D, Gronroos E, Martinez P, Matthews N, Stewart A, Tarpey P, Varela I, Phillimore B, Begum S, McDonald NQ, Butler A, Jones D, Raine K, Latimer C, Santos CR, Nohadani M, Eklund AC, Spencer-Dene B, Clark G, Pickering L, Stamp G, Gore M, Szallasi Z, Downward J, Futreal PA, Swanton C. Intratumor heterogeneity and branched evolution revealed by multiregion sequencing. *N Engl J Med* 2012; **366**: 883-892 [PMID: 22397650 DOI: 10.1056/NEJMoa1113205]
12 **Tu SM**, Bilen MA, Hess KR, Broaddus RR, Kopetz S, Wei C, Pagliaro LC, Karam JA, Ward JF, Wood CG, Rao P, Tu ZH, General R, Chen AH, Nieto YL, Yeung SC, Lin SH, Logothetis CJ, Pisters LL. Intratumoral heterogeneity: Role of differentiation in a potentially lethal phenotype of testicular cancer. *Cancer* 2016; **122**: 1836-1843 [PMID: 27018785 DOI: 10.1002/cncr.29996]
13 **Aerts HJ**, Velazquez ER, Leijenaar RT, Parmar C, Grossmann P, Carvalho S, Bussink J, Monshouwer R, Haibe-Kains B, Rietveld D, Hoebers F, Rietbergen MM, Leemans CR, Dekker A, Quackenbush J, Gillies RJ, Lambin P. Decoding tumour phenotype by noninvasive imaging using a quantitative radiomics approach. *Nat Commun* 2014; **5**: 4006 [PMID: 24892406 DOI: 10.1038/ncomms5006]
14 **Zheng BH**, Liu LZ, Zhang ZZ, Shi JY, Dong LQ, Tian LY, Ding ZB, Ji Y, Rao SX, Zhou J, Fan J, Wang XY, Gao Q. Radiomics score: a potential prognostic imaging feature for postoperative survival of solitary HCC patients. *BMC Cancer* 2018; **18**: 1148 [PMID: 30463529 DOI: 10.1186/s12885-018-5024-z]
15 **Huang Y**, Liu Z, He L, Chen X, Pan D, Ma Z, Liang C, Tian J. Radiomics Signature: A Potential Biomarker for the Prediction of Disease-Free Survival in Early-Stage (I or II) Non-Small Cell Lung Cancer. *Radiology* 2016; **281**: 947-957 [PMID: 27347764 DOI: 10.1148/radiol.2016152234]
16 **Li H**, Zhu Y, Burnside ES, Drukker K, Hoadley KA, Fan C, Conzen SD, Whitman GJ, Sutton EJ, Net JM, Ganott M, Huang E, Morris EA, Perou CM, Ji Y, Giger ML. MR Imaging Radiomics Signatures for Predicting the Risk of Breast Cancer Recurrence as Given by Research Versions of MammaPrint, Oncotype DX, and PAM50 Gene Assays. *Radiology* 2016; **281**: 382-391 [PMID: 27144536 DOI: 10.1148/radiol.2016152110]
17 **Heimbach JK**, Kulik LM, Finn RS, Sirlin CB, Abecassis MM, Roberts LR, Zhu AX, Murad MH, Marrero JA. AASLD guidelines for the treatment of hepatocellular carcinoma. *Hepatology* 2018; **67**: 358-380 [PMID: 28130846 DOI: 10.1002/hep.29086]
18 **Liao W**, Zhang J, Zhu Q, Qin L, Yao W, Lei B, Shi W, Yuan S, Tahir SA, Jin J, He S. Preoperative Neutrophil-to-Lymphocyte Ratio as a New Prognostic Marker in Hepatocellular Carcinoma after Curative Resection. *Transl Oncol* 2014; **7**: 248-255 [PMID: 24704092 DOI: 10.1016/j.tranon.2014.02.011]
19 **Ahn SJ**, Kim JH, Park SJ, Kim ST, Han JK. Hepatocellular carcinoma: preoperative gadoxetic acid-enhanced MR imaging can predict early recurrence after curative resection using image features and texture analysis. *Abdom Radiol (NY)* 2019; **44**: 539-548 [PMID: 30229421 DOI: 10.1007/s00261-018-1768-9]
20 **Zhou Y**, He L, Huang Y, Chen S, Wu P, Ye W, Liu Z, Liang C. CT-based radiomics signature: a potential biomarker for preoperative prediction of early recurrence in hepatocellular carcinoma. *Abdom Radiol (NY)* 2017; **42**: 1695-1704 [PMID: 28180924 DOI: 10.1007/s00261-017-1072-0]
21 **Wang XH**, Long LH, Cui Y, Jia AY, Zhu XG, Wang HZ, Wang Z, Zhan CM, Wang ZH, Wang WH. MRI-based radiomics model for preoperative prediction of 5-year survival in patients with hepatocellular carcinoma. *Br J Cancer* 2020; **122**: 978-985 [PMID: 31937925 DOI: 10.1038/s41416-019-0706-0]
22 **O'Connor JP**, Rose CJ, Waterton JC, Carano RA, Parker GJ, Jackson A. Imaging intratumor heterogeneity: role in therapy response, resistance, and clinical outcome. *Clin Cancer Res* 2015; **21**: 249-257 [PMID: 25421725 DOI: 10.1158/1078-0432.CCR-14-0990]
23 **Giannini EG**, Marenco S, Borgonovo G, Savarino V, Farinati F, Del Poggio P, Rapaccini GL, Anna Di Nolfo M, Benvegnù L, Zoli M, Borzio F, Caturelli E, Chiaramonte M, Trevisani F; Italian Liver Cancer (ITA. LI.CA) group. Alpha-fetoprotein has no prognostic role in small hepatocellular carcinoma identified during surveillance in compensated cirrhosis. *Hepatology* 2012; **56**: 1371-1379 [PMID: 22535689 DOI: 10.1002/hep.25814]
24 **Joyce JA**, Pollard JW. Microenvironmental regulation of metastasis. *Nat Rev Cancer* 2009; **9**: 239-252 [PMID: 19279573 DOI: 10.1038/nrc2618]
25 **Dunn GP**, Old LJ, Schreiber RD. The immunobiology of cancer immunosurveillance and immunoediting. *Immunity* 2004; **21**: 137-148 [PMID: 15308095 DOI: 10.1016/j.immuni.2004.07.017]
26 **Azimi F**, Scolyer RA, Rumcheva P, Moncrieff M, Murali R, McCarthy SW, Saw RP, Thompson JF. Tumor-infiltrating lymphocyte grade is an independent predictor of sentinel lymph node status and survival in patients with cutaneous melanoma. *J Clin Oncol* 2012; **30**: 2678-2683 [PMID: 22711850 DOI: 10.1200/JCO.2011.37.8539]
27 **Imai Y**, Kubota Y, Yamamoto S, Tsuji K, Shimatani M, Shibatani N, Takamido S, Matsushita M, Okazaki K. Neutrophils enhance invasion activity of human cholangiocellular carcinoma and hepatocellular carcinoma cells: an *in vitro* study. *J Gastroenterol Hepatol* 2005; **20**: 287-293 [PMID: 15683434 DOI: 10.1111/j.1440-1746.2004.03575.x]
28 **Ohtani H**. Focus on TILs: prognostic significance of tumor infiltrating lymphocytes in human colorectal cancer. *Cancer Immun* 2007; **7**: 4 [PMID: 17311363]
29 **Ishizuka M**, Oyama Y, Abe A, Kubota K. Combination of platelet count and neutrophil to lymphocyte ratio is a useful predictor of postoperative survival in patients undergoing surgery for gastric cancer. *J Surg Oncol* 2014; **110**: 935-941 [PMID: 25146385 DOI: 10.1002/jso.23753]
30 **Walsh SR**, Cook EJ, Goulder F, Justin TA, Keeling NJ. Neutrophil-lymphocyte ratio as a prognostic factor in colorectal cancer. *J Surg Oncol* 2005; **91**: 181-184 [PMID: 16118772 DOI: 10.1002/jso.20329]
31 **Stotz M**, Gerger A, Eisner F, Szkandera J, Loibner H, Ress AL, Kornprat P, AlZoughbi W, Seggewies FS, Lackner C, Stojakovic T, Samonigg H, Hoefler G, Pichler M. Increased neutrophil-lymphocyte ratio is a poor prognostic factor in patients with primary operable and inoperable pancreatic cancer. *Br J Cancer* 2013; **109**: 416-421 [PMID: 23799847 DOI:

10.1038/bjc.2013.332]

32 **Oh BS**, Jang JW, Kwon JH, You CR, Chung KW, Kay CS, Jung HS, Lee S. Prognostic value of C-reactive protein and neutrophil-to-lymphocyte ratio in patients with hepatocellular carcinoma. *BMC Cancer* 2013; **13**: 78 [PMID: 23409924 DOI: 10.1186/1471-2407-13-78]

33 **Shiraki T**, Ishizuka M, Kubota K, Kato M, Matsumoto T, Mori S, Shimizu T, Aoki T. An elevated neutrophil-to-lymphocyte ratio predicts a poor postoperative survival in primary hepatocellular carcinoma patients with a normal preoperative serum level of alpha-fetoprotein. *Surg Today* 2019; **49**: 661-669 [PMID: 30806789 DOI: 10.1007/s00595-019-01781-1]

34 **Duda D**, Kretowski M, Bezy-Wendling J. Effect of Slice Thickness on Texture-Based Classification of Liver Dynamic CT Scans. In: Saeed K, Chaki R, Cortesi A, Wierzchoń S, editors. Computer Information Systems and Industrial Management. CISIM 2013: Proceedings of the 12th IFIP TC8 International Conference on Computer Information Systems and Industrial Management. Berlin: Springer, 2013: 96-107 [DOI: 10.1007/978-3-642-40925-7_10]

35 **Kakino R**, Nakamura M, Mitsuyoshi T, Shintani T, Hirashima H, Matsuo Y, Mizowaki T. Comparison of radiomic features in diagnostic CT images with and without contrast enhancement in the delayed phase for NSCLC patients. *Phys Med* 2020; **69**: 176-182 [PMID: 31918370 DOI: 10.1016/j.ejmp.2019.12.019]

36 **Gopal N**, Yazdian Anari P, Turkbey E, Jones EC, Malayeri AA. The Next Paradigm Shift in the Management of Clear Cell Renal Cancer: Radiogenomics-Definition, Current Advances, and Future Directions. *Cancers (Basel)* 2022; **14** [PMID: 35159060 DOI: 10.3390/cancers14030793]

World Journal of Gastroenterology

Submit a Manuscript: https://www.f6publishing.com

World J Gastroenterol 2022 August 21; 28(31): 4390-4398

DOI: 10.3748/wjg.v28.i31.4390

ISSN 1007-9327 (print) ISSN 2219-2840 (online)

ORIGINAL ARTICLE

Retrospective Study

Nationwide retrospective study of hepatitis B virological response and liver stiffness improvement in 465 patients on nucleos(t)ide analogue

Alnoor Ramji, Karen Doucette, Curtis Cooper, Gerald Yosel Minuk, Mang Ma, Alexander Wong, David Wong, Edward Tam, Brian Conway, David Truong, Philip Wong, Lisa Barrett, Hin Hin Ko, Sarah Haylock-Jacobs, Nishi Patel, Gilaad G Kaplan, Scott Fung, Carla S Coffin

Specialty type: Gastroenterology and hepatology

Provenance and peer review: Unsolicited article; Externally peer reviewed.

Peer-review model: Single blind

P-Reviewer: Ferraioli G, Italy; Hua J, China

Received: April 22, 2022
Peer-review started: April 22, 2022
First decision: May 9, 2022
Revised: May 22, 2022
Accepted: July 25, 2022
Article in press: July 25, 2022
Published online: August 21, 2022

Alnoor Ramji, Hin Hin Ko, Department of Medicine, University of British Columbia, Vancouver V6T 1Z3, Canada

Karen Doucette, Mang Ma, Department of Medicine, University of Alberta, Edmonton T6G 2R7, Canada

Curtis Cooper, Department of Medicine, The Ottawa Hospital Research Institute, University of Ottawa, Ottawa ON K1H 8L6, Canada

Gerald Yosel Minuk, Department of Medicine, University of Manitoba, Winnipeg R3E 3J7, Canada

Alexander Wong, Department of Medicine, University of Saskatchewan, Saskatoon S7N 5E5, Canada

David Wong, Scott Fung, Department of Medicine,University Health Network, Toronto M5G 2C4, Canada

Edward Tam, Pacific Gastroenterology Associates, Vancouver V6Z 2K5, Canada

Brian Conway, David Truong, Vancouver Infectious Disease Centre, Vancouver V6Z 2C7, Canada

Philip Wong, Department of Medicine, McGill University, Montreal H3A 0G4, Canada

Lisa Barrett, Department of Microbiology and Immunology, Dalhousie University, Halifax B3H 4R2, Canada

Sarah Haylock-Jacobs, Nishi Patel, Gilaad G Kaplan, Carla S Coffin, Cumming School of Medicine, University of Calgary, Calgary T2N 1N4, Canada

Corresponding author: Alnoor Ramji, MD, Associate Professor, Department of Medicine, University of British Columbia, 2775 Laurel Str, Gordon and Leslie Diamond Health Care, Vancouver V6T 1Z3, Canada. ramji_a@hotmail.com

Abstract

BACKGROUND

Hepatitis B virus (HBV) nucleos(t)ide analog (NA) therapy reduces liver disease but requires prolonged therapy to achieve hepatitis B surface antigen (HBsAg) loss. There is limited North American real-world data using non-invasive tools for fibrosis assessment and few have compared 1st generation NA or lamivudine (LAM) to tenofovir disoproxil fumarate (TDF).

AIM

To assess impact of NA on virological response and fibrosis regression using liver stiffness measurement (LSM) (*i.e.*, FibroScan®).

METHODS

Retrospective, observational cohort study from the Canadian HBV Network. Data collected included demographics, NA, HBV DNA, alanine aminotransferase (ALT), and LSM. Patients were HBV monoinfected patients, treatment naïve, and received 1 NA with minimum 1 year follow-up.

RESULTS

In 465 (median 49 years, 37% female, 35% hepatitis B e antigen+ at baseline, 84% Asian, 6% White, and 9% Black). Percentage of 64 (n = 299) received TDF and 166 were LAM-treated with similar median duration of 3.9 and 3.7 years, respectively. The mean baseline LSM was 11.2 kPa (TDF) *vs* 8.3 kPa (LAM) (P = 0.003). At 5-year follow-up, the mean LSM was 7.0 kPa in TDF *vs* 6.7 kPa in LAM (P = 0.83). There was a significant difference in fibrosis regression between groups (*i.e.*, mean -4.2 kPa change in TDF and -1.6 kPa in LAM, P < 0.05). The last available data on treatment showed that all had normal ALT, but more TDF patients were virologically suppressed (< 10 IU/mL) (n = 170/190, 89%) *vs* LAM-treated (n = 35/58, 60%) (P < 0.05). None cleared HBsAg.

CONCLUSION

In this real-world North American study, approximately 5 years of NA achieves liver fibrosis regression rarely leads to HBsAg loss.

Key Words: Nucleos(t)ide analog therapy; Functional cure; Hepatitis B virus surface antigen loss; Fibrosis regression; Liver stiffness measurement; Transient elastography

Core Tip: In summary in this real-world diverse cohort study of chronic hepatitis B patients in Canada, long-term nucleo(s)ide analog (either 1st or 2nd generation) therapy suppresses hepatitis B virus DNA and improves hepatic inflammation and liver fibrosis, as determined by non-invasive testing (*i.e.*, transient elastography). In patients treated for up to 5 years, none achieved hepatitis B surface antigen loss (functional cure), highlighting the need for improved therapeutic strategies to reduce the life-long burden of antiviral therapy.

Citation: Ramji A, Doucette K, Cooper C, Minuk GY, Ma M, Wong A, Wong D, Tam E, Conway B, Truong D, Wong P, Barrett L, Ko HH, Haylock-Jacobs S, Patel N, Kaplan GG, Fung S, Coffin CS. Nationwide retrospective study of hepatitis B virological response and liver stiffness improvement in 465 patients on nucleos(t)ide analogue. *World J Gastroenterol* 2022; 28(31): 4390-4398

URL: https://www.wjgnet.com/1007-9327/full/v28/i31/4390.htm

DOI: https://dx.doi.org/10.3748/wjg.v28.i31.4390

INTRODUCTION

Hepatitis B virus (HBV) nucleos(t)ide analog (NA) therapy is associated with fibrosis regression, reduced risk of hepatocellular carcinoma (HCC) and improved clinical outcomes[1]. The ultimate goal of HBV therapy is hepatitis B surface antigen (HBsAg) loss and considered a functional cure enabling treatment cessation, but rarely achieved with current NA. Without HBsAg clearance, stopping treatment may lead to severe viral and biochemical flares. Studies of European patients reported HBsAg loss in 20% patients after stopping long-term NA therapy. HBsAg loss among Asian virally suppressed patients was very low (< 5%) suggesting there are important differences among different groups of patients in terms of off-treatment response[2,3]. The approved 2nd generation NA, *i.e.*, entecavir (ETV),

tenofovir disoproxil fumarate (TDF) and tenofovir alafenamide (TAF) potently reduce serum viral load (HBV DNA) but they rarely achieve a functional cure despite prolonged therapy[4]. Studies in large Asian cohorts have compared the effect of NA with a low genetic barrier to drug resistance (*i.e.*, lamivudine, LAM) to higher potency (*i.e.*, ETV, TDF/TAF) NA on liver fibrosis regression and viral response[5]. A single centre Asian study of 124 patients treated with anti-HBV NA documented HBV DNA suppression but all had persistently detectable HBsAg, and none achieved intrahepatic viral marker reduction (*i.e.*, HBV covalently closed circular (ccc) DNA)[5]. A large retrospective Korean study showed lower risk of death or transplantation with ETV compared to LAM but no difference in HCC risk[6]. A recent global study involving 299 centers in 24 countries investigated outcomes after 10 years of follow-up of clinical trial patients treated with ETV or alternative NA[2]. The data revealed that 5305 Chinese ETV recipients maintained virological response with lower risk of HBV-related serious adverse events including HCC. However, approximately 17% of the cohort, and similar rate in other cohorts, continued to identify HBV-related liver disease progression[5,7]. Liver disease complications have also been reported in a Korean study of 440 cirrhotic patients (mostly genotype C) after 5 years of ETV therapy, with a 15% rate of liver disease decompensation in those with > 90% treatment adherence and 41% decompensation in patients with < 90% adherence[8].

There is limited real-world data evaluating the clinical impact of 1st *vs* 2nd generation long-term NA therapy in North American chronic hepatitis B (CHB) patients. These patients maybe characterised by greater diversity and genotype heterogeneity based on a diverse regions of origin. Disparities in access to HBV NA is a global issue. Similarly, in Canada, NA reimbursement criteria vary by provincial or territorial jurisdiction[9]. Until recently, antivirals with a high barrier to resistance such as TDF and ETV were not funded as first line therapies for CHB in two large population provincial health jurisdictions [*i.e.*, British Columbia (BC) and Ontario (ON)][9]. In particular, there were historic differences in reimbursement criteria with LAM utilized as first line in BC and ON, and TDF historically (before 2018) only reimbursed for persons with advanced fibrosis and/or decompensated cirrhosis. In BC and ON, HBV patients could access TDF if they failed LAM, developed resistance or very rarely, had intolerance to LAM. In this retrospective, multi-centre cohort study of 465 CHB patients followed in 8 provinces across Canada, we aim to assess HBV viral response, biochemical remission, liver fibrosis regression and HBsAg sero-clearance after treatment with median 4 years of either a 1st or 2nd line NA therapy.

MATERIALS AND METHODS

This was a retrospective observational cohort study, utilizing the Canadian Hepatitis B Network cohort data from January 1st, 2012-December 1st, 2019. Participating clinics provided data from electronic and/or paper charts. De-identified information was entered into a registry REDCap® database housed at the University of Calgary (U of C) under an approved U of C Conjoint Ethics Research Board (CHREB) protocol (Ethics ID # REB16-0041), and appropriate legal data sharing agreements[10]. Study subjects provided written informed consent to participate, or were included with a waiver of consent, according to local REB approval. Data extracted included demographics (age, sex, ethnicity), antiviral regimens, HBV DNA, hepatitis B e antigen (HBeAg), alanine aminotransferase (ALT) and liver stiffness measurement (LSM) prior to and during therapy. Inclusion: Adult patients >18 years, with known chronic HBV (*i.e.*, HBsAg persistence > 6 mo duration), HBV monoinfected, treatment naïve at baseline, and were on only a single antiviral agent for the study duration. Exclusion: Participants were excluded if they had received previous HBV therapy, had a liver transplant or were co-infected with other hepatotropic viruses (*e.g.*, HCV and HDV) or with HIV. ETV treated patients were also excluded for direct comparison of only two antiviral drugs. Persons who had their antiviral regiment switched (includes LAM-resistant patients switching to TDF) were also excluded. All patients had a minimum of 12 mo follow-up from treatment initiation, with at least annual HBV DNA evaluation using commercial assays (*i.e.*, sensitivity 20 IU/mL or 50 copies/mL, Abbott and/or < 20 IU/mL, Roche) and serial LSM performed using FibroScan® (Echosens, Paris, Fr). Liver fibrosis, based on Metavir staging, was classified as F0-F1 (< 7.3 kPa), F2-F3 (7.3-9.5 kPa) and F4 or cirrhosis (> 9.5 kPa)[11]. CHB management and treatment monitoring was directed by the center physician(s) and based on the Canadian consensus guidelines[12].

Statistical analyses

For all analyses, patients with missing data were excluded. Continuous data were summarized with the mean, 95% confidence interval (CI) and count (n). For comparisons between treatment groups (LAM *vs* TDF) at a given time point, two-tailed *t* test was used. Repeated measures analysis of variance (ANOVA) with post hoc test was used to compare continuous variables at different time points for each treatment group. Categorical data were summarized as proportion using mean % (n/n known). Fisher's exact test was used for comparison between dichotomous data. A linear mixed model was used to identify change over time in a multivariable linear mixed regression analysis. A *P* value of less than 0.05 was considered to be statistically significant. Statistical analyses were performed using SAS/STAT® software, IBM SPSS Statistics 27.0.1.0 and/or GraphPad Prism 9.0.

RESULTS

Characteristics of the study population

The study population included 465 patients who were treatment naïve at baseline. The mean age was 49 (SD 12.9) years, 37% were female, and 35% were HBeAg (+) at baseline. Most were Asian (84%, *n* = 345) (albeit from different East and/or South-East Asian) countries, 9% Black (*n* = 37), and 6% White (*n* = 25). Patients either received TDF (*n* = 299, 65%) or LAM (*n* = 166, 35%) therapies with similar median treatment duration of 3.9 and 3.7 years, respectively. There was no difference between treatment groups in sex or ethnicity. However, TDF treated individuals were more likely to be HBeAg positive (Table 1). Historically, patients from one provincial health jurisdiction (*i.e.*, British Columbia), only had access to TDF as first line therapy if they had cirrhosis. Thus, a greater proportion of persons in the TDF group also had advanced fibrosis (> stage F3/4) at baseline, compared to LAM (Table 1).

Summary of follow-up evaluation and outcomes

The mean baseline LSM prior to treatment was greater in TDF treated recipients (11.2 kPa, 95%CI: 9.9-12.4) than in those receiving LAM (8.3 kPa, 95%CI: 7.2-9.5) (Table 1). At baseline, serum HBV DNA and ALT levels were similar in both groups (Table 1). Compared to baseline, only TDF treated group achieved significant HBV DNA decline at 5 years follow up (p=0.0011) compared to LAM treated group (*P* = 0.37) (Figure 1A).

By year 5, 194/299 (64.9%) TDF patients had undetectable HBV DNA (< 10 IU/mL) than 88/166 (53.0%) LAM patients (*P* = 0.012, Chi-square test, Supplementary Table 1). Furthermore, a higher proportion of TDF treated patients had suppressed HBV DNA (< 10 IU/mL) (*n* = 170/190, 89%) *vs* LAM-treated (*n* = 35/58, 60%) (*P* < 0.05), but none achieved functional cure (HBsAg loss) at the end of the study period.

Both treatment groups had decline in ALT from baseline to 5-year follow-up (*P* = 0.014 for LAM and *P* < 0.0001 for TDF) (Figure 1B). As well, ALT normalization was achieved for both treatment groups by 1-year follow-up. More specifically, by year 5, 167/299 (55.9%) TDF patients achieved ALT normalization compared to 74/166 (44.6%) LAM patients (*P* = 0.020, Chi square test, Supplementary Table 2).

In patients with available serial long-term LSM data, NA treatment also led to improvement in liver inflammation and fibrosis regression with lower mean LSM at 5-year follow-up (7.0 kPa, 95%CI:5.8-8.2 for TDF and 6.7 kPa, 95%CI: 4.9-8.6 for LAM treated patients). Multivariable linear mixed regression with a linear mixed model showed a significant difference in fibrosis regression between antiviral treatment groups. Mean fibrosis regression was greater in TDF treated patients with -4.2 kPa change compared to -1.6 kPa in LAM recipients from baseline, *P* < 0.05 (Figure 2).

As well, by 4-year follow-up, LSM improved by ≥ 1 stage in 92/299 (20.8%) TDF patients compared to 29/166 (17.5%) LAM patients (*P* = 0.002, Chi square test).

Of the 26 HBeAg positive patients that received LAM treatment, 6 patients became HBeAg negative (23.1%). Of the 99 HBeAg positive patients that received TDF treatment, 27 patients (27.3%) achieved HBeAg loss. No data was available on LAM resistance however all patients enrolled in the study were on a single NA agent. It is standard clinical practice to switch to TDF in individuals who developed LAM resistance (and criteria for public formulary drug reimbursement in some provinces). Genotype data was not available in most patients.

DISCUSSION

In this multi-centre, retrospective real-world Canadian study, we assessed clinical outcomes in CHB patients receiving long-term NA therapy. Both 1st generation (LAM) and higher potency antivirals (TDF) reduces HBV DNA and improves liver inflammation and fibrosis based on serial LSM evaluation even after ALT normalization. This study highlights the effectiveness of both antiviral drugs in inducing fibrosis regression in a diverse HBV patient cohort. However, up to 5-year follow-up period no CHB patients achieved HBsAg loss or functional cure. A clinically relevant proportion of patients continued to show low-level viremia, especially if treated with LAM. Persons with LAM- resistance switched to TDF were not included to avoid bias of 2 different regimens. Data on antiviral resistance testing is not available, and it is likely these patients would have been switched to TDF in both BC and ON pharmacare reimbursement criteria. The clinical implications of low-level viremia, especially association with residual HCC risk is unclear and requires further study[13,14].

Many studies including randomized clinical trials, observational cohorts and meta-analyses demonstrate that NA treatment improves clinical outcomes for persons living with chronic hepatitis B [1]. Observational studies from clinical databases also reflect real-world practice and complement clinical trials[15,16]. Single centre real-world Canadian studies have observed reduced HCC risk[17]. The majority of observational studies conducted on long-term NA therapy outcomes were done in HBV-endemic countries with a particular focus on Asia. Canada is non-endemic for HBV but due to high rates of immigration from many endemic regions, CHB remains an important health issue and affects a diverse, multi-ethnic population as persons have from multiple regions and encompasses 40 countries

Table 1 Summary of baseline characteristics of 465 study patients who were treated with either lamivudine or tenofovir disoproxil fumurate enrolled in the Canadian hepatitis B virus network

	LAM treated (*n* = 166)	TDF treated (*n* = 299)	*P* value
Age (yr)	51.6 (49.7-53.6)	47.2 (45.7-48.6)	< 0.001[c]
Male sex	58.4% (97/166)	64.9% (194/299)	0.194
Ethnicity (LAM 88%, *n* = 147/166 known, TDF, 88% *n* = 266/299 known)			
Asian	85.0% (125/147)	82.7% (220/266)	0.582
Black/African/Caribbean	5.4% (8/147)	10.9% (29/266)	0.072
White	6.8% (10/147)	5.6% (15/266)	0.669
Other	2.7% (4/147)	0.4% (1/266)	0.056
Laboratory			
HBeAg positive	24.1% (26/108)	39.9% (99/248)	0.004[b]
HBV DNA (log_{10} IU/mL)	7.5 (6.7-7.7) *n* = 149	7.6 (7.5-7.8) *n* = 269	0.260
ALT (IU/mL)	74.3 (62.0-86.7) *n* = 139	87.8 (76.8-98.7) *n* = 264	0.225
Mean ALT × ULN	2.7 (2.1-3.3) *n* = 139	3.7 (2.9-4.4) *n* = 264	0.077
Fibrosis (baseline)			
Mean Baseline Fibrosis (kPa)	8.3 (7.2-9.5) *n* = 100	11.2 (9.9-12.4) *n* = 184	0.003[b]
F0-F1 Fibrosis (< 7.3 kPa)	53% (53/100)	37.5% (69/184)	0.013[a]
F2-F3 Fibrosis (7.3-9.5 kPa)	25% (25/100)	16.9% (31/184)	0.119
F4 Fibrosis (> 9.5 kPa)	22% (22/100)	45.7% (84/184)	< 0.001[c]

[a]*P* < 0.05.
[b]*P* < 0.01.
[c]*P* < 0.001.
Continuous data are shown as mean (95% CI, n known). Categorical data are shown as mean % (n/n known). For continuous data, a two-tailed *t* test was used. Whereas Fisher's exact test was used for categorical data. LAM: Lamivudine; TDF: Tenofovir disoproxil fumarate; HBV: Hepatitis B virus; ALT: Alanine aminotransferase; HBeAg: Hepatitis B e antigen; ULN: Upper limit of normal.

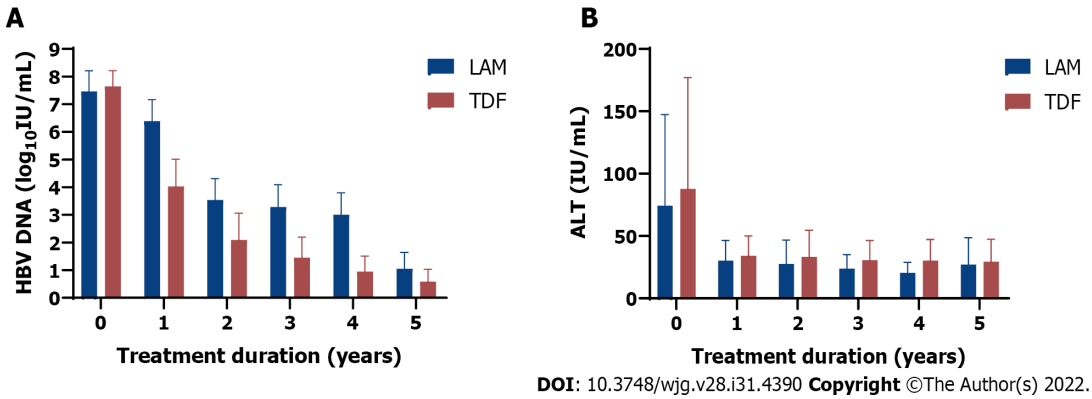

DOI: 10.3748/wjg.v28.i31.4390

Figure 1 Comparison of clinical outcomes in 465 chronic hepatitis B patients receiving 1st generation (lamivudine or LAM, solid bar) *vs* 2nd generation (tenofovir disoproxil fumarate or TDF, dotted bar) hepatitis B virus nucleos(t)ide analog therapy from baseline (pre-treatment) followed for up to 5 years. A: Hepatitis B virus DNA decline (log_{10} IU/mL); B: Mean alanine aminotransferase (IU/mL) decline from baseline after starting lamivudine or tenofovir disoproxil fumarate. Mean with error bars representing standard deviation is plotted. LAM: Lamivudine; TDF: Tenofovir disoproxil fumarate; HBV: Hepatitis B virus; ALT: Alanine aminotransferase.

as based on Canadian HBV Network Data. Compared to other published real-world studies, the data is also relevant/applicable in a single-payer universal health care system with equal access care albeit differences in medication re-imbursement providing for the unique aspect of this study. The Canadian health care system does provide some financial assistance to cover the cost of antiviral therapy, and other associated costs (*i.e.*, physician visits, hospitalization, laboratory monitoring, diagnostic imaging

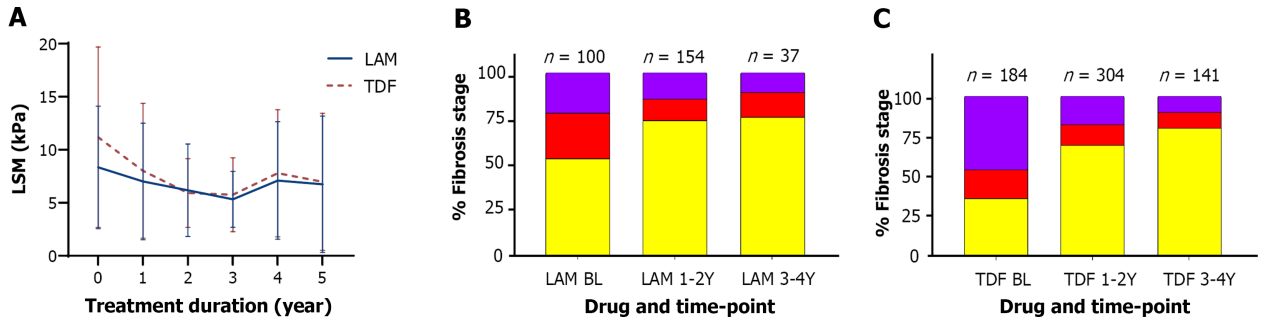

DOI: 10.3748/wjg.v28.i31.4390

Figure 2 Comparison of lamivudine *vs* tenofovir disoproxil fumarate on liver stiffness measurement over time. A: Liver stiffness measurement change from baseline (before treatment) and while on treatment; mean with error bars representing standard deviation is plotted; B and C: Comparison of fibrosis severity at baseline, 1-2 years, and 3-4 years post-treatment for lamivudine (B) and for tenofovir disoproxil fumarate (C). F0-F1 (yellow), F2-F3 (red), and F4 (purple). LSM: Liver stiffness measurement; LAM: Lamivudine; TDF: Tenofovir disoproxil fumarate.

etc.) is reimbursed by provincial health care plans.

Our study is similar to previous published work that highlights the benefits of antiviral treatment in improving liver fibrosis. A systemic review and meta-analysis including 34 published studies of treated and untreated CHB patients also found low rates of NA-induced HBsAg seroclearance, highlighting the need for improved curative therapies[18]. In fact, HBsAg seroclearance generally occurred in untreated individuals with less active disease[18], and is consistent with retrospective data from the Canadian HBV Network of CHB patients comparing outcomes in individuals that remained HBsAg positive *vs* those with HBsAg loss[19].

The current study is limited by retrospective data and missing data at all defined time-points, including serial lab and LSMs, and highlights the limitation of real-world studies (*i.e.*, missed appointments, adherence and incomplete clinician documentation or reporting). We also excluded patients treated with the other approved 2nd generation NA (*i.e.*, ETV) for purposes of the study analysis to compare a single 1st *vs* 2nd generation NA therapy. Moreover, although our cohort was multi-ethnic most patients were Asian, albeit individuals were born in many different east and south-east Asian countries. Additionally, there was missing ethnicity data on 52 patients (11%). Overall, this data represents immigration from up to 40 countries, based on Canadian HBV Network Data. The 2016 Canadian census reported the top Asian countries of birth for recent immigrants are Philippines, India, China, Iran, Pakistan, Syria and South Korea and Syria (www.statcan.gc.ca). There is increasing data on LSM for assessment of liver inflammation and HBV-related fibrosis, although transient elastography is not widely available in resource limited countries compared to other non-invasive fibrosis markers such as aspartate aminotransferase to platelet ratio index (APRI) and Fibrosis4 (FIB4) calculator[20]. It is noteworthy that our analysis represents the largest North American study conducted to date on long-term follow-up with NA therapy utilizing this novel technology.

CONCLUSION

In summary in this real-world diverse cohort study of chronic hepatitis B patients in Canada, long-term nucleo(s)ide analog (either 1st or 2nd generation) therapy suppresses HBV DNA and improves hepatic inflammation and liver fibrosis, as determined by non-invasive testing (*i.e.*, transient elastography). In patients treated for up to 5 years, none achieved HBsAg loss (functional cure), highlighting the need for improved therapeutic strategies to reduce the life-long burden of antiviral therapy.

ARTICLE HIGHLIGHTS

Research background

Therapy of hepatitis B virus (HBV) with nucleos(t)ide analogues (NA) can be associated with fibrosis regression. There are both low and high potency agents approved for therapy and access to these therapies maybe variable. There is limited real-world data comparing these agents on their effect to result in fibrosis regression and long term outcomes.

Research motivation

Although high-potency agents are considered the standard of care, there has been variable access to these agents and indeed ongoing use of these agents in 1st world countries to include Canada. It is thus

important to provide evidence in outcomes to include fibrosis regression between the high and low potency NA's. This study may impact the use of these agents in the future, and allow consideration for switching from low to high potency agents if possible.

Research objectives

To assess HBV viral response, biochemical remission, liver fibrosis regression and hepatitis B surface antigen (HBsAg) sero-clearance after treatment with either a 1st or 2nd line NA therapy. These objectives were realized and the future impact would be the consideration of utilizing 1st *vs* 2nd line NA's. Further, other outcome measure to include HBsAg loss and development of hepatocellular carcinoma (HCC) may be considered.

Research methods

We performed a retrospective observational cohort study utilizing a National network in HBV. Novel aspects that allowed this study is the utilization of a National Network which was able to capture differences in NA utilization based on regional differences of reimbursement. The strength of this study lies in the diversity that the Canadian HBV Network provides. The utilization of liver stiffness by transient elastography in a North American cohort for this objective is also unique.

Research results

As per differences in utilization, a larger proportion of patients with advanced fibrosis were initiated with tenofovir disoproxil fumarate (TDF) compared to LAM. At the end of the study period there were similar stages of fibrosis between the 2 groups. There was an increased fibrosis regression in those treated with a high potency compared to a low-potency NA. More patients in the TDF group also achieved virological suppression, though alanine amino transferase (ALT) normalization was similar.

Research conclusions

In this diverse cohort treatment with low and high potency NA's achieves high rates of viral suppression, ALT normalization and a large proportion achieve fibrosis regression. The strength of national collaboration within a network is exemplified in this study in particular taking advantages of diversity within an overall similar medical system. These differences within a Network can be a powerful tool to answer research questions and can reduce a number of biases inherent when comparing populations/studies between countries or regions.

Research perspectives

The future direction would include potential for long-term outcomes with differential NA usage to include HBsAg loss or seroconversion and any differences in development of HCC albeit in a population with differences in stage of fibrosis at baseline. This study population and Network provides a unique perspective to answer this question.

FOOTNOTES

Author contributions: Ramji A contributed to study design, data contribution, and manuscript draft; Coffin CS contributed to manuscript draft, data contribution, data analysis, and resource support; Haylock-Jacobs S contributed to data analysis and manuscript draft; Patel N and Kaplan GG contributed to data analysis; all other authors contributed to data contribution, manuscript review and feedback.

Institutional review board statement: The study was reviewed and approved by the Conjoint Health Research Ethics Board, No. REB17-2321_REN4.

Conflict-of-interest statement: Dr. Alnoor Ramji and Dr. Carla S Coffin didn't receive at any time payment from a third party for any aspect for the submitted work; there are no relevant conflict of interest; there are no patents related to this work; Dr. Alnoor Ramji and Dr. Carla S Coffin have nothing to disclosure.

Data sharing statement: No data sharing is approved by the institutional ethics board.

Country/Territory of origin: Canada

ORCID number: Alnoor Ramji 0000-0003-4059-8767; Karen Doucette 0000-0002-1660-9166; Gerald Yosel Minuk 0000-0002-

2687-940X; Mang Ma 0000-0003-2587-1788; Alexander Wong 0000-0002-5984-3083; David Wong 0000-0002-1145-1611; Edward Tam 0000-0002-8306-3968; Brian Conway 0000-0001-6821-7829; David Truong 0000-0002-3190-784X; Philip Wong 0000-0002-3446-4116; Hin Hin Ko 0000-0002-2740-2486; Gilaad G Kaplan 0000-0003-2719-0556; Scott Fung 0000-0003-0501-8800; Carla S Coffin 0000-0002-1472-0901.

S-Editor: Chen YL
L-Editor: A
P-Editor: Chen YL

REFERENCES

1 **Lok AS**, McMahon BJ, Brown RS Jr, Wong JB, Ahmed AT, Farah W, Almasri J, Alahdab F, Benkhadra K, Mouchli MA, Singh S, Mohamed EA, Abu Dabrh AM, Prokop LJ, Wang Z, Murad MH, Mohammed K. Antiviral therapy for chronic hepatitis B viral infection in adults: A systematic review and meta-analysis. *Hepatology* 2016; **63**: 284-306 [PMID: 26566246 DOI: 10.1002/hep.28280]
2 **Hou JL**, Zhao W, Lee C, Hann HW, Peng CY, Tanwandee T, Morozov V, Klinker H, Sollano JD, Streinu-Cercel A, Cheinquer H, Xie Q, Wang YM, Wei L, Jia JD, Gong G, Han KH, Cao W, Cheng M, Tang X, Tan D, Ren H, Duan Z, Tang H, Gao Z, Chen S, Lin S, Sheng J, Chen C, Shang J, Han T, Ji Y, Niu J, Sun J, Chen Y, Cooney EL, Lim SG. Outcomes of Long-term Treatment of Chronic HBV Infection With Entecavir or Other Agents From a Randomized Trial in 24 Countries. *Clin Gastroenterol Hepatol* 2020; **18**: 457-467.e21 [PMID: 31306800 DOI: 10.1016/j.cgh.2019.07.010]
3 **Liaw YF**. Undesirable Long-Term Outcome of Entecavir Therapy in Chronic Hepatitis B With Cirrhosis. *Clin Gastroenterol Hepatol* 2020; **18**: 2146-2147 [PMID: 32088301 DOI: 10.1016/j.cgh.2020.02.028]
4 **Liem KS**, Fung S, Wong DK, Yim C, Noureldin S, Chen J, Feld JJ, Hansen BE, Janssen HLA. Limited sustained response after stopping nucleos(t)ide analogues in patients with chronic hepatitis B: results from a randomised controlled trial (Toronto STOP study). *Gut* 2019; **68**: 2206-2213 [PMID: 31462554 DOI: 10.1136/gutjnl-2019-318981]
5 **Wong DK**, Seto WK, Fung J, Ip P, Huang FY, Lai CL, Yuen MF. Reduction of hepatitis B surface antigen and covalently closed circular DNA by nucleos(t)ide analogues of different potency. *Clin Gastroenterol Hepatol* 2013; **11**: 1004-10.e1 [PMID: 23376799 DOI: 10.1016/j.cgh.2013.01.026]
6 **Lim YS**, Han S, Heo NY, Shim JH, Lee HC, Suh DJ. Mortality, liver transplantation, and hepatocellular carcinoma among patients with chronic hepatitis B treated with entecavir vs lamivudine. *Gastroenterology* 2014; **147**: 152-161 [PMID: 24583062 DOI: 10.1053/j.gastro.2014.02.033]
7 **Fan R**, Hou J. Reply. *Clin Gastroenterol Hepatol* 2020; **18**: 2147-2148 [PMID: 32684317 DOI: 10.1016/j.cgh.2020.03.024]
8 **Shin JW**, Jung SW, Lee SB, Lee BU, Park BR, Park EJ, Park NH. Medication Nonadherence Increases Hepatocellular Carcinoma, Cirrhotic Complications, and Mortality in Chronic Hepatitis B Patients Treated With Entecavir. *Am J Gastroenterol* 2018; **113**: 998-1008 [PMID: 29880971 DOI: 10.1038/s41395-018-0093-9]
9 **Congly SE**, Brahmania M. Variable access to antiviral treatment of chronic hepatitis B in Canada: a descriptive study. *CMAJ Open* 2019; **7**: E182-E189 [PMID: 30926602 DOI: 10.9778/cmajo.20180108]
10 **Coffin CS**, Ramji A, Cooper CL, Miles D, Doucette KE, Wong P, Tam E, Wong DK, Wong A, Ukabam S, Bailey RJ, Tsoi K, Conway B, Barrett L, Michalak TI, Congly SE, Minuk G, Kaita K, Kelly E, Ko HH, Janssen HLA, Uhanova J, Lethebe BC, Haylock-Jacobs S, Ma MM, Osiowy C, Fung SK; Canadian HBV Network. Epidemiologic and clinical features of chronic hepatitis B virus infection in 8 Canadian provinces: a descriptive study by the Canadian HBV Network. *CMAJ Open* 2019; **7**: E610-E617 [PMID: 31641059 DOI: 10.9778/cmajo.20190103]
11 **de Lédinghen V**, Vergniol J. Transient elastography (FibroScan). *Gastroenterol Clin Biol* 2008; **32**: 58-67 [PMID: 18973847 DOI: 10.1016/S0399-8320(08)73994-0]
12 **Coffin C**, Fung S, Alvarez F. Management of Hepatitis B Virus Infection: 2018 Guidelines from the Canadian Association for the Study of Liver Disease and Association of Medical Microbiology and Infectious Disease Canada. *Canadian Liver J* 2018; **1**: 156-217 [DOI: 10.3138/canlivj.2018-0008]
13 **Kim JH**, Sinn DH, Kang W, Gwak GY, Paik YH, Choi MS, Lee JH, Koh KC, Paik SW. Low-level viremia and the increased risk of hepatocellular carcinoma in patients receiving entecavir treatment. *Hepatology* 2017; **66**: 335-343 [PMID: 28012257 DOI: 10.1002/hep.28916]
14 **Kim TS**, Sinn DH, Kang W, Gwak GY, Paik YH, Choi MS, Lee JH, Koh KC, Paik SW. Hepatitis B virus DNA levels and overall survival in hepatitis B-related hepatocellular carcinoma patients with low-level viremia. *J Gastroenterol Hepatol* 2019; **34**: 2028-2035 [PMID: 31157456 DOI: 10.1111/jgh.14750]
15 **Kim WR**, Loomba R, Berg T, Aguilar Schall RE, Yee LJ, Dinh PV, Flaherty JF, Martins EB, Therneau TM, Jacobson I, Fung S, Gurel S, Buti M, Marcellin P. Impact of long-term tenofovir disoproxil fumarate on incidence of hepatocellular carcinoma in patients with chronic hepatitis B. *Cancer* 2015; **121**: 3631-3638 [PMID: 26177866 DOI: 10.1002/cncr.29537]
16 **Chon YE**, Park JY, Myoung SM, Jung KS, Kim BK, Kim SU, Kim DY, Ahn SH, Han KH. Improvement of Liver Fibrosis after Long-Term Antiviral Therapy Assessed by Fibroscan in Chronic Hepatitis B Patients With Advanced Fibrosis. *Am J Gastroenterol* 2017; **112**: 882-891 [PMID: 28374814 DOI: 10.1038/ajg.2017.93]
17 **Coffin CS**, Rezaeeaval M, Pang JX, Alcantara L, Klein P, Burak KW, Myers RP. The incidence of hepatocellular carcinoma is reduced in patients with chronic hepatitis B on long-term nucleos(t)ide analogue therapy. *Aliment Pharmacol Ther* 2014; **40**: 1262-1269 [PMID: 25312649 DOI: 10.1111/apt.12990]
18 **Yeo YH**, Ho HJ, Yang HI, Tseng TC, Hosaka T, Trinh HN, Kwak MS, Park YM, Fung JYY, Buti M, Rodríguez M, Treeprasertsuk S, Preda CM, Ungtrakul T, Charatcharoenwitthaya P, Li X, Li J, Zhang J, Le MH, Wei B, Zou B, Le A, Jeong D, Chien N, Kam L, Lee CC, Riveiro-Barciela M, Istratescu D, Sriprayoon T, Chong Y, Tanwandee T, Kobayashi

M, Suzuki F, Yuen MF, Lee HS, Kao JH, Lok AS, Wu CY, Nguyen MH. Factors Associated With Rates of HBsAg Seroclearance in Adults With Chronic HBV Infection: A Systematic Review and Meta-analysis. *Gastroenterology* 2019; **156**: 635-646.e9 [PMID: 30342034 DOI: 10.1053/j.gastro.2018.10.027]

19 **Coffin C**, Haylock-Jacobs S, Doucette K. Association between quantitative hepatitis B surface antigen levels (qHBsAg) and clinical outcomes of ethnically diverse Canadian chronic hepatitis B (CHB) patients: REtrospective and prospectiVe rEAL world evidence study of CHB in Canada (REVEAL- CANADA). The Liver Meeting, Annual Meeting American Association for the Study of Liver Disease; 2021; Canada. Digital Online, 2021 [DOI: 10.15406/jlrdt.2015.01.00007]

20 **Gane EJ**, Charlton MR, Mohamed R, Sollano JD, Tun KS, Pham TTT, Payawal DA, Gani RA, Muljono DH, Acharya SK, Zhuang H, Shukla A, Madan K, Saraf N, Tyagi S, Singh KR, Cua IHY, Jargalsaikhan G, Duger D, Sukeepaisarnjaroen W, Purnomo HD, Hasan I, Lesmana LA, Lesmana CRA, Kyi KP, Naing W, Ravishankar AC, Hadigal S. Asian consensus recommendations on optimizing the diagnosis and initiation of treatment of hepatitis B virus infection in resource-limited settings. *J Viral Hepat* 2020; **27**: 466-475 [PMID: 31785182 DOI: 10.1111/jvh.13244]

World Journal of Gastroenterology

Submit a Manuscript: https://www.f6publishing.com

World J Gastroenterol 2022 August 21; 28(31): 4399-4416

DOI: 10.3748/wjg.v28.i31.4399

ISSN 1007-9327 (print) ISSN 2219-2840 (online)

ORIGINAL ARTICLE

Observational Study

Radiomics and nomogram of magnetic resonance imaging for preoperative prediction of microvascular invasion in small hepatocellular carcinoma

Yi-Di Chen, Ling Zhang, Zhi-Peng Zhou, Bin Lin, Zi-Jian Jiang, Cheng Tang, Yi-Wu Dang, Yu-Wei Xia, Bin Song, Li-Ling Long

Specialty type: Gastroenterology and hepatology

Provenance and peer review: Unsolicited article; Externally peer reviewed.

Peer-review model: Single blind

Peer-review report's scientific quality classification

Grade A (Excellent): A
Grade B (Very good): 0
Grade C (Good): C
Grade D (Fair): 0
Grade E (Poor): 0

P-Reviewer: Granito A, Italy; Hussein R, Egypt

Received: December 14, 2021
Peer-review started: December 14, 2021
First decision: January 27, 2022
Revised: February 5, 2022
Accepted: July 24, 2022
Article in press: July 24, 2022
Published online: August 21, 2022

Yi-Di Chen, Ling Zhang, Zi-Jian Jiang, Cheng Tang, Li-Ling Long, Department of Radiology, The First Affiliated Hospital of Guangxi Medical University, Nanning 530021, Guangxi Zhuang Autonomous Region, China

Zhi-Peng Zhou, Bin Lin, Department of Radiology, Affiliated Hospital of Guilin Medical University, Guilin 541001, Guangxi Zhuang Autonomous Region, China

Yi-Wu Dang, Department of Pathology, The First Affiliated Hospital of Guangxi Medical University, Nanning 5350021, Guangxi Zhuang Autonomous Region, China

Yu-Wei Xia, Department of Technology, Huiying Medical Technology (Beijing), Beijing 100192, China

Bin Song, Department of Radiology, West China Hospital, Sichuan University, Chengdu 610041, Sichuan Province, China

Li-Ling Long, Key Laboratory of Early Prevention and Treatment for Regional High Frequency Tumor, Ministry of Education, Guangxi Medical University, Nanning 530021, Guangxi Zhuang Autonomous Region, China

Li-Ling Long, Guangxi Key Laboratory of Immunology and Metabolism for Liver Diseases, First Affiliated Hospital of Guangxi Medical University, Nanning 530021, Guangxi Zhuang Autonomous Region, China

Corresponding author: Li-Ling Long, MD, Chairman, Chief Doctor, Professor, Department of Radiology, The First Affiliated Hospital of Guangxi Medical University, No. 6 Shuangyong Road, Nanning 530021, Guangxi Zhuang Autonomous Region, China.
cjr.longliling@vip.163.com

Abstract

BACKGROUND

Microvascular invasion (MVI) of small hepatocellular carcinoma (sHCC) (≤ 3.0 cm) is an independent prognostic factor for poor progression-free and overall survival. Radiomics can help extract imaging information associated with tumor pathophysiology.

AIM

To develop and validate radiomics scores and a nomogram of gadolinium ethoxybenzyl-diethyl-enetriamine pentaacetic acid (Gd-EOB-DTPA)-enhanced magnetic resonance imaging (MRI) for preoperative prediction of MVI in sHCC.

METHODS

In total, 415 patients were diagnosed with sHCC by postoperative pathology. A total of 221 patients were retrospectively included from our hospital. In addition, we recruited 94 and 100 participants as independent external validation sets from two other hospitals. Radiomics models of Gd-EOB-DTPA-enhanced MRI and diffusion-weighted imaging (DWI) were constructed and validated using machine learning. As presented in the radiomics nomogram, a prediction model was developed using multivariable logistic regression analysis, which included radiomics scores, radiologic features, and clinical features, such as the alpha-fetoprotein (AFP) level. The calibration, decision-making curve, and clinical usefulness of the radiomics nomogram were analyzed. The radiomic nomogram was validated using independent external cohort data. The areas under the receiver operating curve (AUC) were used to assess the predictive capability.

RESULTS

Pathological examination confirmed MVI in 64 (28.9%), 22 (23.4%), and 16 (16.0%) of the 221, 94, and 100 patients, respectively. AFP, tumor size, non-smooth tumor margin, incomplete capsule, and peritumoral hypointensity in hepatobiliary phase (HBP) images had poor diagnostic value for MVI of sHCC. Quantitative radiomic features (1409) of MRI scans) were extracted. The classifier of logistic regression (LR) was the best machine learning method, and the radiomics scores of HBP and DWI had great diagnostic efficiency for the prediction of MVI in both the testing set (hospital A) and validation set (hospital B, C). The AUC of HBP was 0.979, 0.970, and 0.803, respectively, and the AUC of DWI was 0.971, 0.816, and 0.801 ($P < 0.05$), respectively. Good calibration and discrimination of the radiomics and clinical combined nomogram model were exhibited in the testing and two external validation cohorts (C-index of HBP and DWI were 0.971, 0.912, 0.808, and 0.970, 0.843, 0.869, respectively). The clinical usefulness of the nomogram was further confirmed using decision curve analysis.

CONCLUSION

AFP and conventional Gd-EOB-DTPA-enhanced MRI features have poor diagnostic accuracies for MVI in patients with sHCC. Machine learning with an LR classifier yielded the best radiomics score for HBP and DWI. The radiomics nomogram developed as a noninvasive preoperative prediction method showed favorable predictive accuracy for evaluating MVI in sHCC.

Key Words: Magnetic resonance imaging; Hepatocellular carcinoma; Radiomics; Nomogram

Core Tip: Microvascular invasion (MVI) accounts for approximately 20% of small hepatocellular carcinoma (sHCC) (≤ 3.0 cm) and is a poor independent prognostic factor for progression-free survival and overall survival. However, no studies have been published on the preoperative prediction of the MVI of sHCC. This multi-center study was developed and validated radiomics scores and nomogram of gadoxetic acid-enhanced magnetic resonance imaging (EOB-MRI) for the preoperative prediction of MVI in sHCC. The results demonstrated that AFP and conventional EOB-MRI features have poor diagnostic accuracy for MVI in patients with sHCC. The radiomics scores of HBP and diffusion-weighted imaging can improve the ability to predict MVI. As a noninvasive preoperative prediction method, the radiomics nomogram presented in this study showed a favorable predictive accuracy in evaluating MVI of sHCC, which may help reassess the clinical therapeutic regimen for patients with sHCC.

Citation: Chen YD, Zhang L, Zhou ZP, Lin B, Jiang ZJ, Tang C, Dang YW, Xia YW, Song B, Long LL. Radiomics and nomogram of magnetic resonance imaging for preoperative prediction of microvascular invasion in small hepatocellular carcinoma. *World J Gastroenterol* 2022; 28(31): 4399-4416

URL: https://www.wjgnet.com/1007-9327/full/v28/i31/4399.htm

DOI: https://dx.doi.org/10.3748/wjg.v28.i31.4399

INTRODUCTION

Hepatocellular carcinoma (HCC) is the fourth most common cause of cancer-related death and ranks sixth in terms of incident cases worldwide[1]. HCC is an important public health problem worldwide, and the death rate has increased over the past few years[2,3]. The cut-off size to define small HCC (sHCC) has been adopted as 3.0 cm[4]. Although the prognosis of sHCC is better than other types of HCC, the higher postoperative recurrence rate results in poor long-term outcomes after resection of sHCC[5]. Previous studies have confirmed that tumor size, higher tumor stage, worse histological differentiation, and the presence of microvascular invasion (MVI) are significant risk factors for short-term recurrence of HCC[6-8]. In particular, the incidence of MVI, which is an independent poor prognostic factor for progression-free survival and overall survival of patients with sHCC, is generally about 20% in sHCC[9]. The presence or absence of MVI also suggests the need for different therapeutic options for HCC. Research has indicated that transcatheter arterial chemoembolization combined with intensity-modulated radiotherapy and sorafenib showed obvious clinical benefits in HCC patients with MVI[10]. Enlarged hepatectomy may be necessary for patients with sHCC and MVI.

Pathological examination of postoperative specimens is the gold standard for the diagnosis of MVI [11]. However, postoperative specimens exhibit hysteresis, which is not ideal for guiding treatment. In addition to being an invasive method, biopsy carries some risks of bleeding or tumor seeding[12]. Gadolinium ethoxybenzyl-diethylenetriamine pentaacetic acid (Gd-EOB-DTPA) contrast-enhanced liver magnetic resonance imaging (MRI) is a noninvasive examination used to diagnose a variety of liver diseases[13] and can be used to assess liver function in patients with various stages of liver disease[14]. Gd-EOB-DTPA MRI has been used to predict MVI based on tumor size, non-smooth tumor margin, incomplete capsule, and peritumoral hypointensity in the hepatobiliary phase[15-18]. However, sHCC has a small size, regular margin, complete capsule (or no capsule), and is usually free of peritumoral hypointensity. Therefore, it is difficult to predict the MVI of sHCC using traditional GD-EOB-DTPA MRI features.

Radiomics is an emerging field that attempts to quantify tumor heterogeneity related to the tumor parenchyma and microenvironment, including cellularity, extracellular matrix deposition, angiogenesis, necrosis, and fibrosis[19,20]. Machine learning is a scientific method of algorithms and statistical models that uses computers to interpret or predict patterns and inferences[21]. In many medical situations, medical imaging can be analyzed by machine learning through a series of processes, such as image registration, image segmentation, object detection, classification, and outcome prediction[22,23]. Automated computer algorithms can be used for quantitative image analysis, which can objectively quantify the heterogeneity of an image by measuring the spatial variation in the pixel intensity[24]. Radiomics with quantitative analysis provides a potential method for the diagnosis and prognosis of cancers[25,26]. Although a few studies have explored the feasibility of using radiomics based on computed tomography (CT) or MRI features to predict MVI in HCC[27-29], to our knowledge, previous studies have not investigated the prediction of MVI in sHCC. Therefore, this study aimed to explore the diagnostic value of liver Gd-EOB-DTPA MRI features in MVI of sHCC and to construct and validate the predictive efficacy of radiomics signatures and a nomogram for MVI in sHCC. This study also aimed to confirm the best modeling sequences, including images of T1 weighted imaging (T1WI), T2 weighted imaging (T2WI), diffusion-weighted imaging (DWI), and post-Gd-EOB-DTPA enhancement images of the arterial phase (AP), portal vein phase (PVP), and hepatobiliary phase (HBP), for extracting radiomics signatures by machine learning.

MATERIALS AND METHODS

Study cohort

The ethical review board of our institution approved this multi-center and external validation study (No. 2019 KY-E-134). This study adhered to the principles of the Declaration of Helsinki and the requirement for informed consent was waived. First, we retrospectively searched our institution's (Guangxi Medical University First Affiliated Hospital, Hospital A) departmental electronic database for patients with consecutive hospital visits who had undergone upper-abdomen MRI between January 2016 and June 2020. A total of 221 patients were enrolled who met the following inclusion criteria: (1) Patients received Gd-EOB-DTPA enhanced upper-abdomen MRI and small HCC (tumor size ≤ 3.0 cm) were diagnosed; (2) no macrovascular tumor invasion on MRI *(i.e.*, no tumor thrombus in the hepatic or portal veins); (3) primary HCC were diagnosed by histopathologic examination within two weeks after the MRI examination; and (4) MR images were of sufficient image quality. The exclusion criteria of this study were: (1) Patients who had undergone previous hepatobiliary surgery or liver-directed therapy (*i.e.*, transarterial chemoembolization or ablation); and (2) the lesions were diagnosed other than primary HCC. Second, we continuously recruited 94 and 100 participants as independent external validation sets from two other hospitals (Affiliated Hospital of Guilin Medical University and West China Hospital, Hospital B and C) between July 2020 and August 2021 using the same inclusion and exclusion criteria. All patients underwent hepatectomy and pathologic assessment within two weeks of the MRI

examination. The alpha fetal protein (AFP), Child-Pugh grades (grade A to C), and model for end-stage liver disease (MELD) scores were also analyzed and calculated for all patients (Figure 1).

Histopathologic analysis

Two experienced pathologists performed all the histological analyses in our central pathology laboratory. The Edmondson-Steiner classification was used to identify the major histological grades of HCC. When a tumor within a vascular space was lined by the endothelium, MVI was confirmed to be visible only microscopically, and the sites of positive MVI were documented. All disagreements were resolved by consensus.

MRI examination

All patients underwent 3.0 T MRI with six sequences of Gd-EOB-DTPA enhancement and DWI (Discovery MR750, GE Healthcare, Waukesha, WI, United States; Prisma and MAGNETOM Verio, Siemens Healthcare, Erlangen, Germany), including T1WI, T2WI, DWI, and post-injection phases of EOB as AP, PVP, and HBP. Detailed descriptions of the imaging acquisition protocols are summarized in Supplementary Table 1. For advanced DWI image quality, respiratory triggering, propeller, and resolve technical proposals were adopted.

Conventional radiological features analysis

Conventional radiological features were carefully evaluated based on the Liver Imaging Reporting and Data System (LI-RADS v2018), which included the tumor size, AP hyperenhancement, blood products in mass, capsule, corona enhancement, delayed central enhancement, diffusion restriction, fat or iron in mass more than the adjacent liver, fat or iron sparing in a solid mass, mosaic appearance, hepatobiliary phase hypointensity, hepatobiliary phase isointensity, and nodule-in-nodule appearance. The following MRI features were selected in this study: (1) Tumor size; the maximum diameter was measured on HBP axial images; (2) non-smooth tumor margin, which was defined as nodular with extranodular growth or multinodular confluence; (3) incomplete capsule, the region where the tumor border with liver tissue has no or incomplete capsule on portal venous phase or delayed phase; and (4) peritumoral hypointensity on HBP, wedge-shaped hypointense located outside of the tumor margin on HBP. After independent evaluation by three senior radiologists, discussions were conducted to reach a consensus wherever discrepancies occurred.

RADIOMICS SIGNATURES AND REPRODUCIBILITY ANALYSIS

Segmentation of the volume of interests

The Digital Imaging and Communications in Medicine images were transferred to the Big Data Intelligent Analysis Cloud Platform (Huiying Medical Technology Co., Ltd., Beijing, China). Two experts in liver MRI (senior radiologists with 15 and 25 years of experience) reviewed all images, and a radiologist manually segmented all target lesions who were blinded to the clinical information, creating a segmented volume of interest (VOI). After completion of the VOIs by a junior radiologist, the VOIs were reviewed by a senior radiologist for validation. To minimize the intensity variations caused by different scanning equipment and scanning parameters, these MR images were normalized by the standard deviation (μ-3σ, μ + 3σ) before feature extraction, and all delineated VOIs were automatically analyzed (Figure 2).

As two radiologists measured the radiomics features to assess reproducibility, we calculated the intraclass correlation coefficient (ICC). When the ICC was > 0.80, consistency was considered excellent.

Features extraction

We extracted 1409 quantitative imaging features from VOIs using the cloud platform big data intelligent analysis (http://radcloud.cn/). The features were categorized into four groups. The first-order statistical features were considered as group 1 (including a total of 18 descriptors), which delineated the distribution of voxel intensities in the MR images through common and basic metrics. Group 2 included shape- and size-based features (containing 14 three-dimensional features) that reflected the shape and size of the lesion areas. Group 3 included features of two-order texture, gray-level co-occurrence, and gray-level run-length texture matrices that were used to calculate those features, and 75 texture features were extracted to quantify the heterogeneity of lesions. The higher-order filter features such as group 4, Laplacian, wavelet, logarithmic, and exponential filters were applied to medical images, and then the first-order statistics and texture features were extracted based on the filtered image (1302 filter features).

Features selection

The least absolute shrinkage and selection operator (LASSO) was used to decrease irrelevance and redundancy. We performed a 10-fold cross-validation to select the optimal feature subset in LASSO regression, which was based on binomial deviance minimization criteria from the training cohort with a

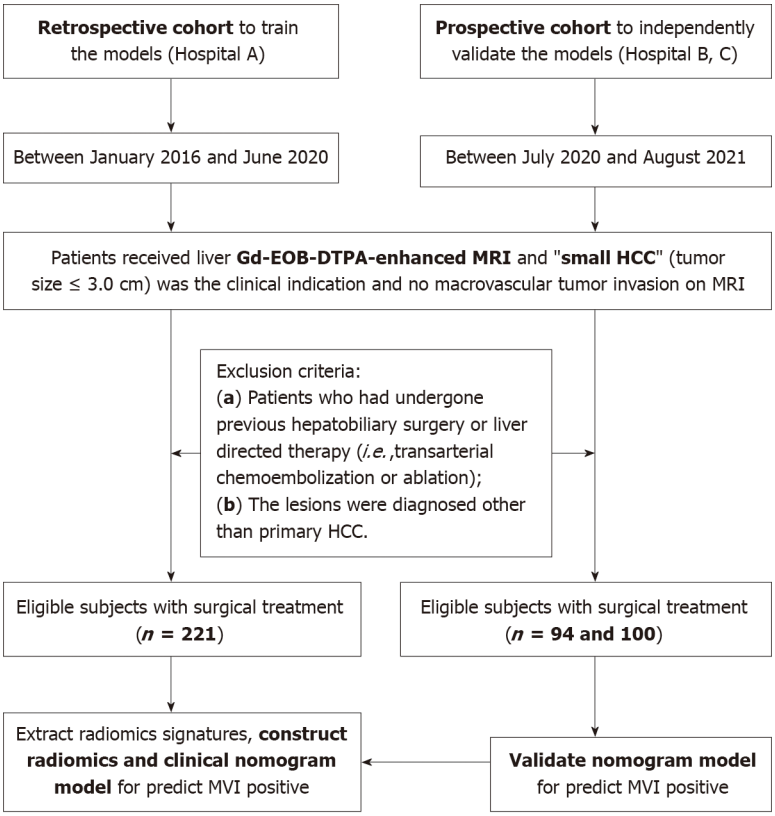

DOI: 10.3748/wjg.v28.i31.4399 **Copyright** ©The Author(s) 2022.

Figure 1 Flow diagram of the study cohort. A total of 415 participants were included in this multi-center study.

maximum iteration of 2000. A variance threshold of 0.8 was used for the selected eigenvalues of the variance.

Model development and validation

The retrospective data (Hospital A) were separated from the training and testing datasets using a random method with a ratio of 7:3, and external data (Hospitals B and C) as the independent validation sets. After feature qualification, based on the selected features, several machine learning classifiers can be used for classification analysis, creating models that can separate or predict MVI-positive data. In this study, radiomics-based LASSO models (machine learning) were constructed using T1WI, T2WI, DWI, AP, PVP, and HBP. We selected K-nearest neighbor (KNN), support vector machine (SVM), extreme gradient boosting (XGBoost), random forest (RF), logistic regression (LR), and decision tree (DT) as the machine learning classifiers, and the effectiveness of the model was improved using the validation method (Figure 2).

Confirmation of radiomics nomogram

R package (version 3.0, http://www.r-project.org/) was used to analyze the radiomics nomogram. Multivariate logistic regression analysis was performed to develop a model for predicting MVI, and all variables associated with MVI at a significant level were candidates for stepwise multivariate analysis. A nomogram was constructed based on the results of the multivariate logistic regression analysis. The receiver operating characteristic (ROC) curve was used to calculate the discrimination performance of the established models, and the values of the area under the curve (AUC) were compared using the Delong non-parametric approach. The calibration of the radiomics model was assessed using calibration curves. External data from the independent validation sets (hospitals B and C) were used to test the performance of the radiomics model. Finally, we constructed decision curves by calculating the net benefits for a range of threshold probabilities.

Statistical analyses

MedCalc 16.2.1 (Ostend, Belgium) and SPSS (version 22.0; Armonk, NY, United States) were used for the statistical analyses. The Kolmogorov-Smirnov method was used to identify the normal distribution of continuous variables. The differences in categorical and continuous variables were compared using the χ^2 test, Fisher's exact test, two-sample *t*-test, or Mann-Whitney *U* test, respectively. ROC analyses were performed to evaluate the predictive performance of MVI for sHCC. The Youden index was used for determining the cut-off values. Then, the AUC, sensitivity, and specificity were calculated, and a *Z*

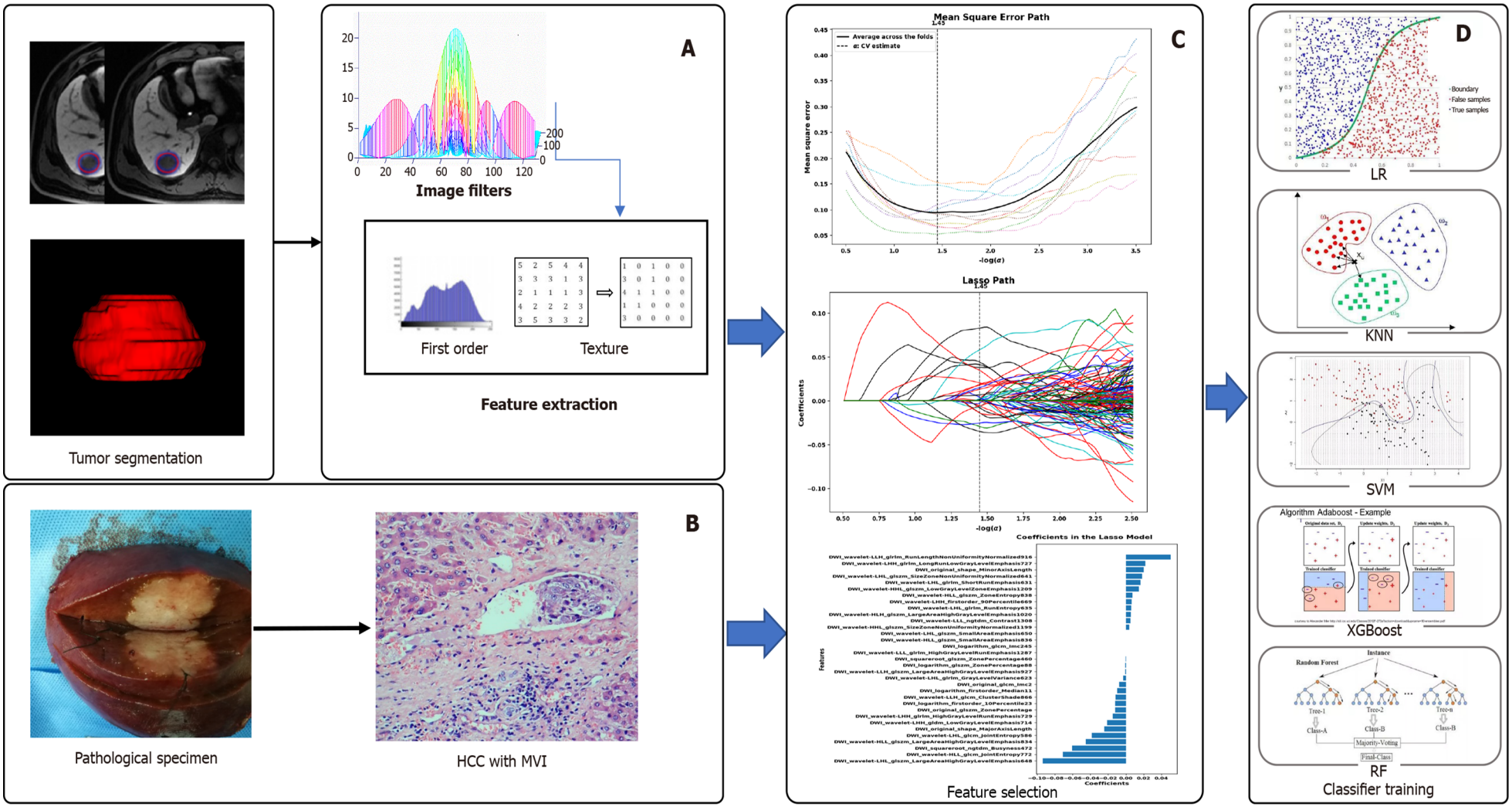

DOI: 10.3748/wjg.v28.i31.4399

Figure 2 Flow diagram for the radiomics of machine learning. A: Construct radiomics models, the volume of interest was delineated by experienced radiologists and three-dimensional images were formed, extracting quantitative features by software; B: Pathologic examination, firstly obtaining specimens of small hepatocellular carcinoma tissue, and then taking pathologic diagnosis for microvascular invasion; C: Data cleaning and dimensions reduction; D: Establishing the model for predicting microvascular invasion by machine learning. LR: Logistic regression; KNN: K-Nearest neighbor; SVM: Support vector machine; RF: Random forest.

test was used to compare the differences between the AUCs. Statistical significance was set at $P < 0.05$.

RESULTS

Patients and serological examinations

A total of 415 patients with qualified sHCC were enrolled in the final study (Figure 1). In hospitals A, B, and C, the mean participant age was 51.2 ± 10.9 (range 29-78) years, 53.04 ± 10.59 (range 28-77) years, and 54.01 ± 10.82 (range 28-85) years, respectively. Histological examination confirmed MVI in 64 (28.9%), 22 (23.4%), and 16 (16.0%) patients. The number of patients with hepatitis B, C and alcoholic hepatitis were 162 (73.3%), 21 (9.5%), 29 (13.1%); 71 (75.6%), 10 (10.6%), 8 (8.5%); and 82 (82.0%), 6 (6.0%), 2 (2.0%), respectively. The numbers of patients with cirrhosis were 173 (78.3%), 69 (73.4%), and 70 (70%), respectively. The median serum AFP levels were 26.10 (range 0.98-25451.00) ng/mL, 9.34 (range 1.09-6740.42) ng/mL, and 31.070 (range 0.713-4587.000) ng/mL, respectively. The median serum total bilirubin levels were 12.5 (range 2.9-64.6) μmol/L, 17.4 (range 3.6-446.9) μmol/L and 13.2 (range 4.4-47.2) μmol/L, respectively. The median direct bilirubin levels were 3.9 (range 1.0-17.0) μmol/L, 4.5 (range 1.0-218.9) μmol/L and 5.50 (range 1.50-26.84) μmol/L, respectively. The MELD scores were 13.9 ± 4.8 (range 7.0-26.9), 13.8 ± 5.8 (range 6.0-35.5) and 11.8 ± 4.5 (range 5.2-25.6). The number of Child-Pugh classes A, B, and C were 205 (93.2%), 13 (5.9%), 2 (0.9%), 81 (86.2%), 12 (12.8%), 1 (1.1%), 86 (86.0%), 13 (13.0%), and 1 (1.0%), respectively. There were 32 (14.5%), 142 (64.3%), 47 (21.2%); 12 (12.8%), 68 (72.3%), 14 (14.9%) and 8 (8.0%), 71 (71.0%), 21 (21.0%) cases that were histological grades I, II, and III, respectively (Table 1).

Conventional radiological features

In the group comparison of MVI-positive and negative, the AFP and tumor size were 33.91 (range 1.4-25451.0) and 22.52 (range 0.98-18929.00) (ng/mL) ($P = 0.026$), 2.34 ± 0.56 and 1.92 ± 0.67 (cm) ($P = 0.036$) in hospital A; 38.97 (range 1.90-6740.40) and 5.43 (range 1.10-2018.79) (ng/mL) ($P = 0.01$), 2.43 ± 0.57 and 2.11 ± 0.66 (cm) ($P = 0.047$) in hospital B; 109.72 (range 0.80-2278.00) and 24.41 (range 0.71-4587.00) (ng/mL) ($P = 0.032$), 2.47 ± 0.43 and 2.21 ± 0.64 (cm) ($P = 0.054$) in hospital C. In the MVI-positive group, the proportion of patients with non-smooth tumor margin, incomplete capsule, and peritumoral hypointensity was 39.7% (27/68) ($P = 0.019$), 40.3% (25/62) ($P = 0.02$), and 51.5% (17/33) ($P = 0.002$) in hospital A; 52.9% (9/17) ($P = 0.003$), 59.5% (25/42) ($P = 0.062$), and 35.7% (5/14) ($P = 0.304$) in hospital B; and 31.3% (10/32) ($P = 0.004$), 14.6% (6/41) ($P = 0.759$), and 63.6% (14/22) ($P = 0.002$) in hospital C (Table 2).

For discriminating MVI-positive, in hospital A, B and C the AUC of AFP was 0.597 [95% confidence interval (CI):0.528-0.662], 0.683 (95%CI):0.528-0.662] and 0.669 (95%CI:0.568-0.760), respectively; the AUC of tumor size was 0.675 (95%CI:0.609-0.736), 0.639 (95%CI:0.553-0.735) and 0.576 (95%CI:0.473-0.675), respectively; the AUC of non-smooth tumor margin was 0.580 (95%CI:0.512-0.646), 0.649 (95%CI:0.544-0.745) and 0.682 (95%CI:0.581-0.771), respectively; the AUC of incomplete capsule was 0.577 (95%CI:0.509-0.643), 0.595 (95%CI:0.489-0.695) and 0.521 (95%CI:0.419-0.622), respectively; the AUC of peritumoral hypointensity on HBP was 0.582 (95%CI:0.514-0.648), 0.551 (95%CI:0.445-0.654) and 0.667 (95%CI:0.565-0.758), respectively (Table 3).

Radiomics signatures

There were 155 and 66 patients with sHCC in the training and test datasets, respectively. The proportions of MVI-positive patients were 27.1% and 29%, respectively. There were no significant differences in patient characteristics between the training and testing cohorts ($P > 0.05$). Among the 1409 radiomics features in each T1WI, T2WI, DWI, AP, PVP, and HBP model, 443, 483, 467, 554, 462, and 453 features were selected based on a variance threshold of over 0.80. After LASSO analysis, five, 22, 33, four, eight, and 30 features were selected for T1WI, T2WI, DWI, AP, PVP, and HBP, respectively.

Robustness analysis results

We found that 70.5% (993/1409) of the features extracted from T1WI images had excellent consistency (ICC > 0.8), and all five features selected for modeling had excellent consistency (ICC median, 0.969; minimum, 0.877; maximum, 1.000). The features of 51.9% (731/1409) extracted from T2WI images had excellent consistency (ICC > 0.8), and most of the 22 features selected for modeling had good consistency (ICC median, 0.701; minimum, 0.41; maximum, 0.94). The features of 60.04% (846/1409) extracted from DWI images had excellent consistency (ICC > 0.8), and most of the 33 features selected for modeling had excellent consistency (ICC median, 0.869; minimum, 0.41; maximum, 0.98). The features of 67.8% (956/1409) extracted from AP images had excellent consistency (ICC > 0.8), and the ICC of the four features selected for modeling were 0.902, 0.884, 0.734, and 0.891. The features of 62.1% (875/1409) extracted from PVP images had excellent consistency (ICC > 0.8), and most of the eight features selected for modeling had excellent consistency (ICC median = 0.844, minimum = 0.500, maximum = 1.000). The features of 82.5% (1163/1409) extracted from HBP images had excellent consistency (ICC > 0.8), and most of the 30 features selected for modeling had excellent consistency (ICC

Table 1 Demographics, alpha fetal protein, bilirubin, tumor characteristics, and microvascular infiltration of the patients with small hepatocellular carcinoma in data sets of three hospitals

Characteristics	Hospital A (*n* = 221)	Hospital B (*n* = 94)	Hospital C (*n* = 100)
Age (yr)	mean ± SD: 51.2 ± 10.9 (range 29-78)	mean ± SD: 53.04 ± 10.59 (range 28-77)	mean ± SD: 54.01 ± 10.82 (range 28-85)
Male/female	189 (85.5%)/32 (14.5%)	84 (89.4%)/10 (10.6%)	85 (85.5%)/15 (15.0%)
Causes of liver disease			
Hepatitis B	162 (73.3%)	71 (75.6%)	82 (82.0%)
Hepatitis C	21 (9.5%)	10 (10.6%)	6 (6.0%)
Alcoholic hepatitis	29 (13.1%)	8 (8.5%)	2 (2.0%)
Others	9 (4.1%)	5 (5.3%)	10 (10.0%)
Cirrhosis			
Present	173 (78.3%)	69 (73.4%)	70 (70%)
Absent	48 (21.7%)	25 (26.6%)	30 (30%)
AFP (ng/mL)	Median: 26.10 (range 0.98-25451.00)	Median: 9.34 (range 1.09-6740.42)	Median: 31.070 (range 0.713- 4587.000)
TBiL (μmol/L)	Median: 12.5 (range 2.9-64.6)	Median: 17.4 (range 3.6-446.9)	Median: 13.2 (range 4.4-47.2)
DBiL (μmol/L)	Median: 3.9 (range 1.0-17.0)	Median: 4.5 (range 1.0-218.9)	Median: 5.50 (range 1.50-26.84)
MELD scores	mean ± SD: 13.9 ± 4.8 (range 7.0-26.9)	mean ± SD: 13.8 ± 5.8 (range 6.0-35.5)	mean ± SD: 11.8 ± 4.5 (range 5.2-25.6)
Child-Pugh classes			
A	205 (93.2%)	81 (86.2%)	86 (86.0%)
B	13 (5.9%)	12 (12.8%)	13 (13.0%)
C	2 (0.9%)	1 (1.1%)	1 (1.0%)
Edmondson-steiner grade			
Grade I	32 (14.5%)	12 (12.8%)	8 (8.0%)
Grade II	142 (64.3%)	68 (72.3%)	71 (71.0%)
Grade III	47 (21.2%)	14 (14.9%)	21 (21.0%)
Tumor size (cm)	mean ± SD: 2.04 ± 0.67 (range 0.60-3.00)	mean ± SD: 2.17 ± 0.42 (range 0.80-3.00)	mean ± SD: 2.20 ± 0.41 (range 0.90-3.00)
MVI			
Positive	64 (28.9%)	22 (23.4%)	16 (16.0%)
Negative	157 (71.1%)	72 (76.6%)	84 (84.0%)

TBiL: Total bilirubin; DBiL: Direct bilirubin; MELD: Model for end-stage liver disease; AFP: Alpha-fetoprotein; MVI: Microvascular infiltration.

median, 0.917; minimum, 0.690; maximum, 1.000).

Predictive performance of the machine learning classifiers

The machine learning classifiers used in this study were KNN, LR, MLP, RF, SVM, and DT. In general, all classifiers achieved satisfactory performance, with LR being the best machine learning method. To predict MVI, T1WI, T2WI, DWI, AP, PVP, and HBP radiomics models were constructed and validated. In the testing set, the AUCs were 0.776 (95%CI: 0.611-0.895), 0.813 (95%CI: 0.651-0.922), 0.971 (95%CI: 0.858-0.999), 0.788 (95%CI: 0.642-0.894), 0.790 (95%CI: 0.630-0.904) and 0.979 (95%CI: 0.911-1.000). In validation hospital B, the AUCs were 0.834 (95%CI: 0.742-0.904), 0.825 (95%CI: 0.732-0.896), 0.816 (95%CI: 0.678-0.876), 0.810 (95%CI: 0.715-0.884), 0.847 (95%CI: 0.758-0.913) and 0.970 (95%CI: 0.912-0.994). In validation hospital C, the AUCs were 0.766 (95%CI: 0.672-0.844), 0.761 (95%CI: 0.669-0.839), 0.801 (95%CI: 0.710-0.871), 0.824 (95%CI: 0.737-0.892), 0.833 (95%CI: 0.748-0.898) and 0.803 (95%CI: 0.680-0.834) (Figure 3, Table 4).

Development and validation of MVI predicting nomogram

The C-indexes of the radiomics and clinic combined nomogram with the model of T1WI, T2WI, DWI, AP, PVP and HBP were 0.771 (95%CI: 0.695-0.836), 0.895 (95%CI: 0.834-0.940), 0.990 (95%CI: 0.957-0.999), 0.774 (95%CI: 0.706-0.833), 0.746 (95%CI: 0.668-0.814) and 0.990 (95%CI: 0.944-0.993) in the training set,

Table 2 Age, gender, alpha-fetoprotein and radiologic features of patients with small hepatocellular carcinoma and relationship with microvascular infiltration

	Hospital A (*n* = 221)			Hospital B (*n* = 94)			Hospital C (*n* = 100)		
	Positive	Negative	*P* value	Positive	Negative	*P* value	Positive	Negative	*P* value
Age (yr)	50.9 ± 10.7	51.3 ± 10.9	0.840	51.7 ± 12.3	53.1 ± 10.1	0.597	53.5 ± 9.1	53.7 ± 11.0	0.958
Gender			0.593			0.443			0.259
Female	8	24		1	9		1	14	
Male	56	133		21	63		15	70	
AFP (ng/mL)	33.91 (range 1.40-25451.00)	22.52 (range 1-18929)	0.026	38.97 (range 1.90-6740.40)	5.43 (range 1.10-2018.79)	0.010	109.72 (range 0.80-2278.00)	24.41 (range 0.71-4587.00)	0.032
Size (cm)	2.34 ± 0.56	1.92 ± 0.67	0.036	2.43 ± 0.57	2.11 ± 0.66	0.047	2.47 ± 0.43	2.21 ± 0.64	0.054
Nonsmooth tumor margin			0.019			0.003			0.004
Absent	37	116		13	64		6	62	
Present	27	41		9	8		10	22	
Capsule			0.020			0.062			0.756
Absent	39	120		21	55		10	49	
Present	25	37		25	17		6	35	
Peritumoral hypointensity			0.002			0.304			0.007
Absent	47	141		17	63		70	8	
Present	17	16		5	9		14	8	

Size: Large tumor size; AFP: Alpha-fetoprotein; MVI: Microvascular infiltration.

respectively; 0.846 (95%CI: 0.594-0.883), 0.917 (95%CI: 0.640-0.915), 0.970 (95%CI: 0.843-0.997), 0.794 (95%CI: 0.615-0.876), 0.831 (95%CI: 0.650-0.916) and 0.971 (95%CI: 0.892-0.999) in the testing set, respectively; 0.895 (95%CI: 0.775-0.925), 0.886 (95%CI: 0.746-0.906), 0.843 (95%CI: 0.685-0.881), 0.886 (95%CI: 0.695-0.899), 0.918 (95%CI: 0.791-0.934) and 0.912 (95%CI: 0.918-0.996) in validation hospital B, respectively; 0.830 (95%CI: 0.667-0.850), 0.808 (95%CI: 0.654-0.867), 0.869 (95%CI: 0.694-0.899), 0.874 (95%CI: 0.674-0.884), 0.870 (95%CI: 0.732-0.887) and 0.808 (95%CI: 0.635-0.892) in validation hospital C, respectively (Figure 4, Table 5).

Decision curve analysis showed adequate performance for radiomics nomogram models for predicting MVI in sHCC. The proposed radiomics model to predict MVI showed a greater advantage than the "clinicoradiological" scheme ($P < 0.05$). There was no significant difference in predictive efficacy between the combination nomogram model and the single radiomics model ($P > 0.05$) (Figure 5).

DISCUSSION

In this multi-center study, we analyzed the clinical and imaging data of 415 patients with sHCC who underwent DWI, Gd-EOB-DTPA-enhanced MRI, and hepatectomy. We used a machine learning approach to construct radiomics signatures and nomogram models for preoperative prediction of MVI and then independently validated the machine learning and nomogram models. Our data showed that clinical and common MRI radiological features, including AFP, tumor size, non-smooth tumor margin, incomplete capsule, and HBP peritumoral hypointensity, have limited diagnostic value for MVI of sHCC. The LR classifier was the best machine learning method, and the radiomics scores of HBP and DWI had great diagnostic efficiency for predicting MVI of sHCC. The nomogram model of combined radiomics scores, APF, and common MRI features exhibited good calibration and discrimination in the training, testing, and independent external validation cohorts.

Gd-EOB-DTPA with a pendant ethoxybenzyl group covalently attached to gadopentetate dimeglumine is a hepatocyte-specific MRI contrast agent that can be taken up by hepatocytes *via* the organic anion transporting polypeptides[30]. Gd-EOB-DTPA, which has dual extracellular and hepatobiliary

Table 3 Diagnostic performance of alpha-fetoprotein and radiologic features for assessing microvascular infiltration of small hepatocellular carcinoma by receiver operating characteristic curve analysis

	AFP	Tumor size	Nonsmooth tumor margin	Incomplete capsule	Peritumoral hypointensity
Hospital A					
AUC	0.597	0.675	0.580	0.577	0.582
95%CI	0.528-0.662	0.609-0.736	0.512-0.646	0.509-0.643	0.514-0.648
P value	0.024	< 0.001	0.024	0.027	0.007
Sensitivity	34.92	70.31	42.19	39.06	26.56
Specificity	81.82	61.15	73.89	76.43	89.81
Hospital B					
AUC	0.683	0.639	0.649	0.595	0.551
95%CI	0.577-0.777	0.553-0.735	0.544-0.745	0.489-0.695	0.445-0.654
P value	0.006	0.035	0.008	0.005	0.304
Sensitivity	63.64	81.82	71.43	95.45	22.73
Specificity	72.06	44.44	88.89	23.61	87.50
Hospital C					
AUC	0.669	0.576	0.682	0.521	0.667
95%CI	0.568-0.760	0.473-0.675	0.581-0.771	0.419-0.622	0.565-0.758
P value	0.016	0.213	0.007	0.759	0.014
Sensitivity	87.50	68.75	62.50	62.50	50.00
Specificity	52.38	54.76	73.81	41.67	83.33

DeLong test for comparison of receiver operating characteristic curve. AFP: Alpha-fetoprotein; AUC: Area under the curve; 95%CI: 95% confidence interval.

properties that provide structural and functional information on liver lesions, can also provide information on nonspecific gadolinium chelates during dynamic enhancement[31,32]. Granito *et al*[33] reported that Gd-EOB-DTPA-enhanced MRI may improve the sensitivity of noninvasive diagnosis of small HCC nodules in patients with cirrhosis, and the double hypointensity in the portal/venous and HBP can be regarded as an MRI pattern, which is highly suggestive of hypovascular hepatocellular carcinoma. This previous study revealed that large tumor size, incomplete capsule, non-smooth tumor margin, peritumoral enhancement on AP, and peritumoral hypointensity on HBP could achieve predictive AUCs of up to 0.85 for MVI of HCC[34]. However, for small HCC (large tumor size ≤ 3 cm), the common MRI radiologic features are smooth tumor margin, complete capsule (or no capsule), and no peritumoral hypointensity in HBP. In this study, the results from three hospitals showed that these conventional MRI radiologic features had limited value in evaluating MVI for sHCC.

Based on these characteristics, we established a Gd-EOB-DTPA MRI radiomics model using machine learning to construct and validate radiomics models for predicting MVI of sHCC. Machine learning has demonstrated capabilities to learn and even master complex tasks, making it useful for computer-aided diagnosis and decision support systems[21]. Radiomics refers to a technique of high-throughput extraction of quantitative imaging features or textures to decode histology and create a high-dimensional dataset[35]. However, it was thought that the parameters of the MRI scanner would not have an obvious influence on the results of radiomics analysis after the images were standardized when a previous multi-center study[36] did not demand the same MRI scanners and parameters. However, to minimize the possible influence of other factors, a unified MRI scanner and image standardization process were used in our study. Furthermore, whole-tumor volume analysis was used to decrease sampling bias.

Although previous studies have verified that the radiomics features of CT imaging could predict MVI status in patients with HCC preoperatively, it has high diagnostic efficiency, and the AUC can reach approximately 0.85[27,37]. In addition, Feng *et al*[38] evaluated Gd-EOB-DTPA-enhanced MRI quantitative features of peri- and intratumoral regions, providing a radiomics model for MVI prediction in patients with HCC. In the validation cohort, the AUC, sensitivity, and specificity were 0.83%, 90.00%, and 75.00%, respectively. However, none of these studies predicted the MVI for sHCC or provided a clinical nomogram. In this study, we extracted radiomics signatures from images of Gd-EOB-DTPA-

Table 4 Receiver operator characteristic curve analysis of radiomics scores with different sequences of magnetic resonance imaging for predict microvascular infiltration of small hepatocellular carcinoma

	T1WI	T2WI	DWI	AP	PVP	HBP
Training set						
AUC	0.740	0.878	0.991	0.763	0.739	0.976
95%CI	0.661-0.808	0.814-0.926	0.958-0.999	0.695-0.823	0.661-0.807	0.940-0.991
P value	< 0.001	< 0.001	< 0.001	< 0.001	< 0.001	< 0.001
Sensitivity	77.08	82.98	95.74	71.43	56.25	89.83
Specificity	68.00	82.00	96.04	79.37	78.22	99.27
Testing set						
AUC	0.776	0.813	0.971	0.788	0.790	0.979
95%CI	0.611-0.895	0.651-0.922	0.858-0.999	0.642-0.894	0.630-0.904	0.911-1.000
P value	0.0004	< 0.001	< 0.001	0.0014	0.0001	< 0.001
Sensitivity	91.67	58.33	100.00	64.29	84.62	100.00
Specificity	57.69	92.00	84.62	93.75	73.08	91.43
Validation Hospital B						
AUC	0.834	0.825	0.816	0.810	0.847	0.970
95%CI	0.742-0.904	0.732-0.896	0.678-0.876	0.715-0.884	0.758-0.913	0.912-0.994
P value	< 0.001	< 0.001	0.0002	< 0.001	< 0.001	< 0.001
Sensitivity	63.64	95.45	71.43	57.14	54.55	95.45
Specificity	94.29	57.75	88.89	88.89	98.61	98.57
Validation Hospital C						
AUC	0.766	0.761	0.801	0.824	0.833	0.803
95%CI	0.672-0.844	0.669-0.839	0.710-0.871	0.737-0.892	0.748-0.898	0.680-0.834
P value	0.0001	0.0003	< 0.001	< 0.001	< 0.001	0.007
Sensitivity	80.00	60.00	90.00	86.67	85.71	83.33
Specificity	70.45	89.01	68.89	68.54	72.83	77.67

T1WI: T1 weighted imaging; T2WI: T2 weighted imaging; DWI: Diffusion weighted imaging; AP: Arterial phase; PVP: Portal vein phase; HBP: Hepatobiliary phase; AUC: Area under the curve; 95%CI: 95% confidence interval.

enhanced MRI and then built the model using T1WI, T2WI, AP, PVP, and HBP. The results illustrated that radiomics has the best modeling in HBP and DWI when the LR and classifier of machine learning are utilized, producing great diagnostic efficiency for predicting MVI. Furthermore, the independent external validation results confirmed this efficiency. This may be because the post-Gd-EOB-DTPA contrast enhancement images provide structural and functional information on HBP lesions. The LR algorithm is used to establish a cost function for a classification or regression problem and then solve the optimal model iteratively through the optimization method.

Our results also demonstrate that the radiomics characteristics of DWI images can accurately predict the MVI of sHCC. DWI is an MRI technology that can reflect the motion of water molecules *in vivo* and can be used to assess tumor cellularity[39]. HCC with MVI is more likely to have higher cellularity and poor differentiation than HCC without MVI[40]. Okamura *et al*[41] suggested that the apparent diffusion coefficient (ADC) value is a valuable predictor of poor differentiation and MVI and is significantly related to tumor recurrence. Kim *et al*[42] illustrated that the tumor-to-liver ADC ratio was a significant independent parameter for the MVI of sHCC and the degree of lymphocyte infiltration. Our research further extracted the radiomics characteristics of the tumor, which were based on DWI images that confirmed that the quantitative characteristics of the radiomics had good performance for predicting the MVI of sHCC.

A nomogram was built in our study, which converted each regression coefficient proportionally in multivariate logistic regression to a 0- to 100-point scale. The effect of features with the absolute value of the highest β coefficient was assigned 100 points. The total points of the independent variables were

Table 5 Predictive performance of the nomogram prediction model for estimating the risk of microvascular infiltration presence in patients with small hepatocellular carcinoma

	Training set	Testing set	Validation Hospital B	Validation Hospital C
T1WI				
C-index	0.771	0.846	0.895	0.830
95%CI	0.695-0.836	0.594-0.883	0.775-0.925	0.667-0.850
P value	< 0.001	0.0014	< 0.001	0.0001
T2WI				
C-index	0.895	0.917	0.886	0.808
95%CI	0.834-0.940	0.640-0.915	0.746-0.906	0.654-0.867
P value	< 0.001	0.0001	< 0.001	0.0015
DWI				
C-index	0.990	0.970	0.843	0.869
95%CI	0.957-0.999	0.843-0.997	0.685-0.881	0.694-0.899
P value	< 0.001	< 0.001	0.0001	< 0.001
AP				
C-index	0.774	0.794	0.886	0.874
95%CI	0.706-0.833	0.615-0.876	0.695-0.899	0.674-0.884
P value	< 0.001	0.0025	< 0.001	< 0.001
PVP				
C-index	0.746	0.831	0.918	0.870
95%CI	0.668-0.814	0.650-0.916	0.791-0.934	0.732-0.887
P value	< 0.001	< 0.001	< 0.001	< 0.001
HBP				
C-index	0.990	0.971	0.912	0.808
95%CI	0.944-0.993	0.892-0.999	0.918-0.996	0.635-0.892
P value	< 0.001	< 0.001	< 0.001	0.0081

T1WI: T1 weighted imaging; T2WI: T2 weighted imaging; DWI: Diffusion weighted imaging; AP: Arterial phase; PVP: Portal vein phase; HBP: Hepatobiliary phase; 95%CI, 95% confidence interval; C-index: Concordance index.

converted to the predicted probabilities. The concordance index (C-index) was used to predict the performance of the nomogram and calibration with 1000 bootstrap samples to decrease the overfitting bias[43]. Our study incorporated six factors: radiomics signatures, APF, tumor size, non-smooth tumor margin, incomplete capsule, and peritumoral hypointensity. Radiomics combined with the clinico-radiological factors nomogram model achieved good concordance indices in predicting MVI in the training and validation cohorts. In particular, the nomogram with HBP and DWI radiomics model showed excellent predictive efficiency in the two external validation datasets, and decision curve analysis further confirmed the clinical usefulness of the nomogram.

Nonetheless, this study had several limitations. First, the included patient population in this study had an inevitable bias in the inter-center distribution, although the application of radiomics and clinical nomogram was ensured by the multi-center nature of this study. To investigate the impact factors of bias on the baseline, we analyzed the age, AFP levels, liver function, and tumor size. Further larger-scale studies with more balanced subjects are needed to validate our results. Second, given the difficulty of collecting scalable medical imaging data for small HCC, many patients with small HCC who underwent transarterial chemoembolization or ablation could not be enrolled in the model of radiomics signatures and clinical nomogram to predict MVI. Given larger medical imaging datasets, deep networks are expected to improve prediction accuracy. Third, due to the lack of prognostic analysis in this study, we analyzed the different prognoses of sHCC patients with positive and negative MVI, which were predicted using a radiomics nomogram.

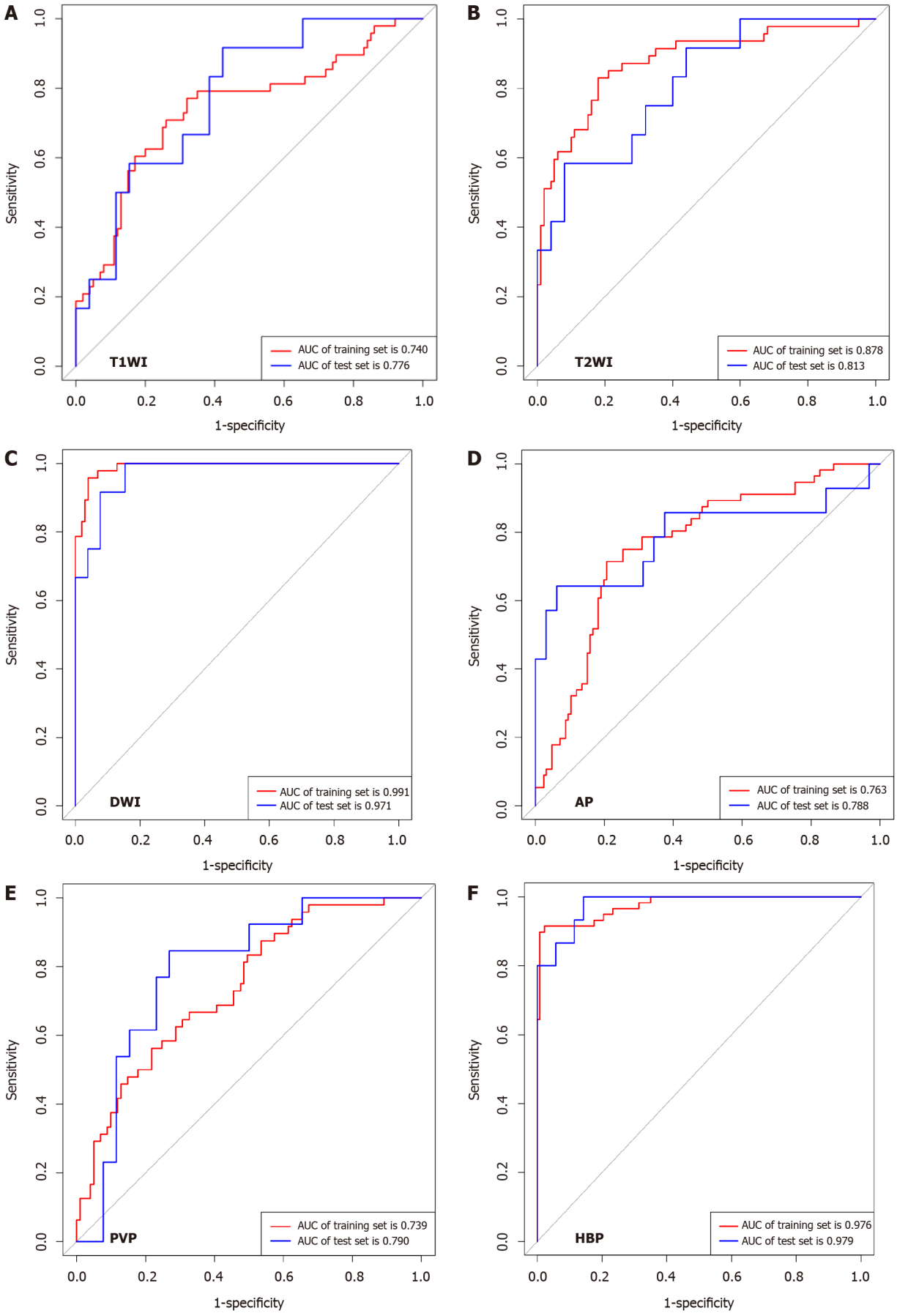

DOI: 10.3748/wjg.v28.i31.4399

Figure 3 Receiver operating characteristic curve of different radiomics models for diagnosis microvascular invasion in small hepato-

cellular carcinoma (testing set). A: T1 weighted imaging [area under curve (AUC) was 0.776; 95% confidence interval (CI): 0.611-0.895]; B: T2 weighted imaging [AUC, 0.813; 95% confidence interval (CI): 0.651-0.922]; C: Diffusion weighted imaging (AUC, 0.971; 95%CI: 0.858-0.999); D: Arterial phase (AUC, 0.788; 95%CI: 0.642-0.894); E: Portal vein phase (AUC, 0.790; 95%CI: 0.630-0.904); F: Hepatobiliary phase (AUC, 0.990; 95%CI: 0.911-1.000). T1W1: T1 weighted imaging; T2W2: T2 weighted imaging; AUC: Area under curve; DWI: Diffusion weighted imaging; AP: Arterial phase; PVP: Portal vein phase; HBP: Hepatobiliary phase.

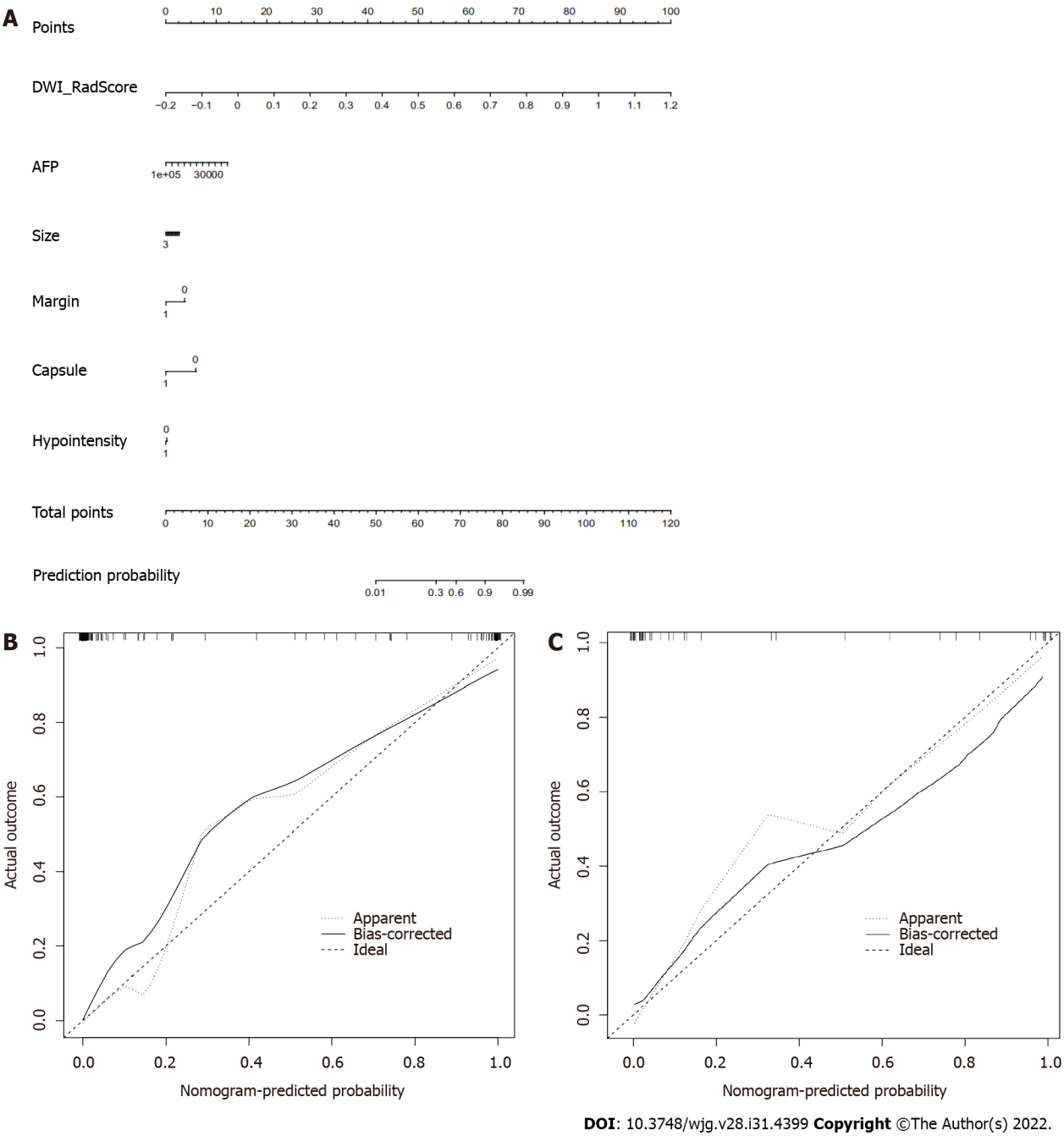

DOI: 10.3748/wjg.v28.i31.4399

Figure 4 Nomogram of diffusion weighted imaging radiomics model to predict microvascular invasion in patients with small hepatocellular carcinoma. A: The nomogram was developed with radiomics signature and clinicoradiological factors. A vertical line was drawn according to the value of radiomics scores to determine the corresponding value of points. Similarly, the points of tumor markers were determined. The total points were the sum of the two points above. Finally, a vertical line was made according to the value of the total points to determine the probability of microvascular invasion (MVI); B: Validity of the predictive performance of the nomogram in estimating the risk of MVI presence in the training cohort; C: Validity of the predictive performance of the nomogram in estimating the risk of MVI presence in the validation cohort. AFP: Alpha-fetoprotein; DWI: Diffusion weighted imaging; Rad_score: Radiomics signatures score.

CONCLUSION

In conclusion, our study revealed that AFP and conventional Gd-EOB-DTPA-enhanced MRI features

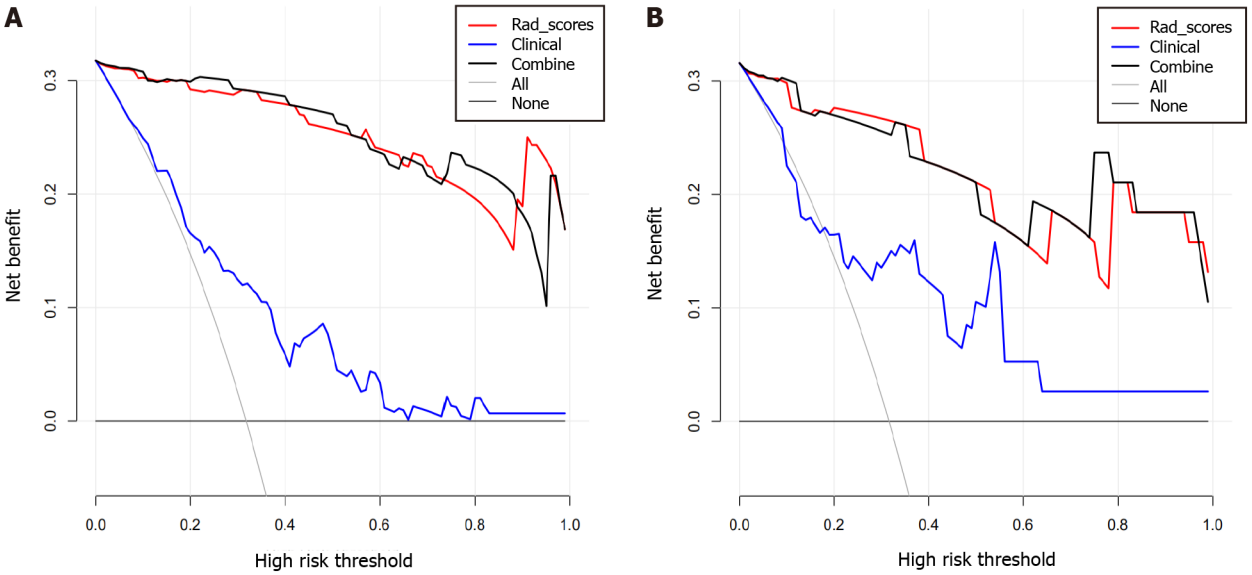

DOI: 10.3748/wjg.v28.i31.4399 **Copyright** ©The Author(s) 2022.

Figure 5 Decision curve analysis. A and B: Decision curve analysis of the prediction model for training (A) and testing (B) cohort. Y-axis represents the net benefit, which is calculated by gaining true positives and deleting false positives. The X-axis is the probability threshold. The curve of the radiomics and combined nomogram over the clinical features that integrated AFP and radiological signatures showed the greatest benefit. AFP: Alpha-fetoprotein; Rad_score: Radiomics signatures score.

have poor diagnostic accuracies for MVI in sHCC. The radiomic signatures of HBP and DWI can further improve the ability to predict MVI. Furthermore, as a noninvasive preoperative prediction method, the radiomics nomogram showed favorable predictive accuracy for evaluating MVI in sHCC, which may help reassess the clinical therapeutic regimen for patients with sHCC.

ARTICLE HIGHLIGHTS

Research background

Microvascular invasion (MVI) of hepatocellular carcinoma (HCC) is an independent poor prognostic factor.

Research motivation

It is difficult to determine MVI of small hepatocellular carcinoma (HCC) (≤ 3.0 cm) by preoperative MRI conventional features.

Research objectives

To develop and validate radiomics scores and nomogram of gadolinium ethoxybenzyl diethylenetriamine pentaacetic acid (Gd-EOB-DTPA)-enhanced magnetic resonance imaging (MRI) for preoperative prediction of MVI in sHCC.

Research methods

Radiomics models of Gd-EOB-DTPA enhanced MRI and diffusion weighted images were constructed and validated by machine learning from data sets of three hospitals. A nomogram prediction model was developed using multivariable logistic regression analysis which included the radiomics scores, radiologic features, and alpha-fetoprotein (AFP) level.

Research results

AFP and MRI conventional features had poor diagnostic value for MVI of small HCC. The nomogram model (combined radiomics and clinic features) exhibited good calibration and discrimination in the testing and two external validation cohorts (in the two external validation cohorts, C-index was 0.912 and 0.808, respectively).

Research conclusions

As a noninvasive preoperative prediction method, the MRI radiomics nomogram shows favorable predictive accuracy for evaluate MVI in sHCC.

Research perspectives

This clinical prediction model may help in the selection of treatment options for small HCC.

ACKNOWLEDGEMENTS

The authors would like to thank Yingying Ezell for the language recheck and editing, Fuling Huang for his technical support, and Huiting Zhang (Siemens Healthineers, Wuhan, Hubei Province, China) for her constructive suggestions during the MRI scanning.

FOOTNOTES

Author contributions: Chen YD and Zhang L contributed equally to this work; Chen YD and Long LL was the guarantor and designed the study; Zhang L, Lin B, Jiang ZJ, Tang C, Dang YW, and Xia YW participated in the acquisition, analysis, interpretation of the data, and drafted the initial manuscript; Zhou ZP and Song B revised the article critically for important intellectual content.

Supported by the National Natural Science Foundation of China, No. 82060310; and Science and Technology Support Program of Sichuan Province, No. 2022YFS0071.

Institutional review board statement: The study was reviewed and approved by The First Affiliated Hospital of Guangxi Medical University Ethical Review Committee, No. 2019 KY-E-65.

Informed consent statement: All study participants, or their legal guardian, provided informed written consent prior to study enrollment.

Conflict-of-interest statement: There are no conflicts of interest to report.

Data sharing statement: The data that support the findings of this study are available in the Baidu Netdisk or our AI Scientific Research Platform (https://mics.radcloud.cn/). Further enquiries can be directed to the corresponding author.

STROBE statement: The authors have read the STROBE Statement—checklist of items, and the manuscript was prepared and revised according to the STROBE Statement—checklist of items.

Country/Territory of origin: China

ORCID number: Yi-Di Chen 0000-0001-6293-4624; Ling Zhang 0000-0001-7270-3555; Yi-Wu Dang 0000-0002-7793-1239; Bin Song 0000-0002-7269-2101; Li-Ling Long 0000-0003-3369-8532.

S-Editor: Chen YL
L-Editor: Filipodia
P-Editor: Yuan YY

REFERENCES

1 **Ghouri YA**, Mian I, Rowe JH. Review of hepatocellular carcinoma: Epidemiology, etiology, and carcinogenesis. *J Carcinog* 2017; **16**: 1 [PMID: 28694740 DOI: 10.4103/jcar.JCar_9_16]
2 **Xu J**. Trends in Liver Cancer Mortality Among Adults Aged 25 and Over in the United States, 2000-2016. *NCHS Data Brief* 2018; 1-8 [PMID: 30044212]
3 **Omata M**, Cheng AL, Kokudo N, Kudo M, Lee JM, Jia J, Tateishi R, Han KH, Chawla YK, Shiina S, Jafri W, Payawal DA, Ohki T, Ogasawara S, Chen PJ, Lesmana CRA, Lesmana LA, Gani RA, Obi S, Dokmeci AK, Sarin SK. Asia-Pacific clinical practice guidelines on the management of hepatocellular carcinoma: a 2017 update. *Hepatol Int* 2017; **11**: 317-370 [PMID: 28620797 DOI: 10.1007/s12072-017-9799-9]
4 **Viganò L**, Laurenzi A, Solbiati L, Procopio F, Cherqui D, Torzilli G. Open Liver Resection, Laparoscopic Liver Resection, and Percutaneous Thermal Ablation for Patients with Solitary Small Hepatocellular Carcinoma (≤ 30 mm): Review of the Literature and Proposal for a Therapeutic Strategy. *Dig Surg* 2018; **35**: 359-371 [PMID: 29890512 DOI:

10.1159/000489836]
5 **Hong YJ**, Kim SH, Choi GH, Kim KS, Choi JS. Long-term outcome after liver resection and clinicopathological features in patients with small hepatocellular carcinoma. *Korean J Hepatobiliary Pancreat Surg* 2011; **15**: 199-205 [PMID: 26421040 DOI: 10.14701/kjhbps.2011.15.4.199]
6 **Chen ZH**, Zhang XP, Wang H, Chai ZT, Sun JX, Guo WX, Shi J, Cheng SQ. Effect of microvascular invasion on the postoperative long-term prognosis of solitary small HCC: a systematic review and meta-analysis. *HPB (Oxford)* 2019; **21**: 935-944 [PMID: 30871805 DOI: 10.1016/j.hpb.2019.02.003]
7 **Lim KC**, Chow PK, Allen JC, Chia GS, Lim M, Cheow PC, Chung AY, Ooi LL, Tan SB. Microvascular invasion is a better predictor of tumor recurrence and overall survival following surgical resection for hepatocellular carcinoma compared to the Milan criteria. *Ann Surg* 2011; **254**: 108-113 [PMID: 21527845 DOI: 10.1097/SLA.0b013e31821ad884]
8 **Choi KK**, Kim SH, Choi SB, Lim JH, Choi GH, Choi JS, Kim KS. Portal venous invasion: the single most independent risk factor for immediate postoperative recurrence of hepatocellular carcinoma. *J Gastroenterol Hepatol* 2011; **26**: 1646-1651 [PMID: 21592228 DOI: 10.1111/j.1440-1746.2011.06780.x]
9 **Du M**, Chen L, Zhao J, Tian F, Zeng H, Tan Y, Sun H, Zhou J, Ji Y. Microvascular invasion (MVI) is a poorer prognostic predictor for small hepatocellular carcinoma. *BMC Cancer* 2014; **14**: 38 [PMID: 24460749 DOI: 10.1186/1471-2407-14-38]
10 **Zhao Y**, Zhu X, Wang H, Dong D, Gao S, Wang W. Safety and Efficacy of Transcatheter Arterial Chemoembolization Plus Radiotherapy Combined With Sorafenib in Hepatocellular Carcinoma Showing Macrovascular Invasion. *Front Oncol* 2019; **9**: 1065 [PMID: 31681599 DOI: 10.3389/fonc.2019.01065]
11 **Renzulli M**, Brocchi S, Cucchetti A, Mazzotti F, Mosconi C, Sportoletti C, Brandi G, Pinna AD, Golfieri R. Can Current Preoperative Imaging Be Used to Detect Microvascular Invasion of Hepatocellular Carcinoma? *Radiology* 2016; **279**: 432-442 [PMID: 26653683 DOI: 10.1148/radiol.2015150998]
12 **Rodríguez-Perálvarez M**, Luong TV, Andreana L, Meyer T, Dhillon AP, Burroughs AK. A systematic review of microvascular invasion in hepatocellular carcinoma: diagnostic and prognostic variability. *Ann Surg Oncol* 2013; **20**: 325-339 [PMID: 23149850 DOI: 10.1245/s10434-012-2513-1]
13 **Golfieri R**, Renzulli M, Lucidi V, Corcioni B, Trevisani F, Bolondi L. Contribution of the hepatobiliary phase of Gd-EOB-DTPA-enhanced MRI to Dynamic MRI in the detection of hypovascular small (≤ 2 cm) HCC in cirrhosis. *Eur Radiol* 2011; **21**: 1233-1242 [PMID: 21293864 DOI: 10.1007/s00330-010-2030-1]
14 **Verloh N**, Utpatel K, Zeman F, Fellner C, Schlitt HJ, Müller M, Stroszczynski C, Evert M, Wiggermann P, Haimerl M. Diagnostic performance of Gd-EOB-DTPA-enhanced MRI for evaluation of liver dysfunction: a multivariable analysis of 3T MRI sequences. *Oncotarget* 2018; **9**: 36371-36378 [PMID: 30555635 DOI: 10.18632/oncotarget.26368]
15 **Huang M**, Liao B, Xu P, Cai H, Huang K, Dong Z, Xu L, Peng Z, Luo Y, Zheng K, Peng B, Li ZP, Feng ST. Prediction of Microvascular Invasion in Hepatocellular Carcinoma: Preoperative Gd-EOB-DTPA-Dynamic Enhanced MRI and Histopathological Correlation. *Contrast Media Mol Imaging* 2018; **2018**: 9674565 [PMID: 29606926 DOI: 10.1155/2018/9674565]
16 **Lei Z**, Li J, Wu D, Xia Y, Wang Q, Si A, Wang K, Wan X, Lau WY, Wu M, Shen F. Nomogram for Preoperative Estimation of Microvascular Invasion Risk in Hepatitis B Virus-Related Hepatocellular Carcinoma Within the Milan Criteria. *JAMA Surg* 2016; **151**: 356-363 [PMID: 26579636 DOI: 10.1001/jamasurg.2015.4257]
17 **Kaibori M**, Ishizaki M, Matsui K, Kwon AH. Predictors of microvascular invasion before hepatectomy for hepatocellular carcinoma. *J Surg Oncol* 2010; **102**: 462-468 [PMID: 20872949 DOI: 10.1002/jso.21631]
18 **Suh YJ**, Kim MJ, Choi JY, Park MS, Kim KW. Preoperative prediction of the microvascular invasion of hepatocellular carcinoma with diffusion-weighted imaging. *Liver Transpl* 2012; **18**: 1171-1178 [PMID: 22767394 DOI: 10.1002/lt.23502]
19 **Davnall F**, Yip CS, Ljungqvist G, Selmi M, Ng F, Sanghera B, Ganeshan B, Miles KA, Cook GJ, Goh V. Assessment of tumor heterogeneity: an emerging imaging tool for clinical practice? *Insights Imaging* 2012; **3**: 573-589 [PMID: 23093486 DOI: 10.1007/s13244-012-0196-6]
20 **Aerts HJ**, Velazquez ER, Leijenaar RT, Parmar C, Grossmann P, Carvalho S, Bussink J, Monshouwer R, Haibe-Kains B, Rietveld D, Hoebers F, Rietbergen MM, Leemans CR, Dekker A, Quackenbush J, Gillies RJ, Lambin P. Decoding tumour phenotype by noninvasive imaging using a quantitative radiomics approach. *Nat Commun* 2014; **5**: 4006 [PMID: 24892406 DOI: 10.1038/ncomms5006]
21 **Erickson BJ**, Korfiatis P, Akkus Z, Kline TL. Machine Learning for Medical Imaging. *Radiographics* 2017; **37**: 505-515 [PMID: 28212054 DOI: 10.1148/rg.2017160130]
22 **Litjens G**, Kooi T, Bejnordi BE, Setio AAA, Ciompi F, Ghafoorian M, van der Laak JAWM, van Ginneken B, Sánchez CI. A survey on deep learning in medical image analysis. *Med Image Anal* 2017; **42**: 60-88 [PMID: 28778026 DOI: 10.1016/j.media.2017.07.005]
23 **Tao Q**, Lelieveldt BPF, van der Geest RJ. Deep Learning for Quantitative Cardiac MRI. *AJR Am J Roentgenol* 2020; **214**: 529-535 [PMID: 31670597 DOI: 10.2214/AJR.19.21927]
24 **Simpson AL**, Adams LB, Allen PJ, D'Angelica MI, DeMatteo RP, Fong Y, Kingham TP, Leung U, Miga MI, Parada EP, Jarnagin WR, Do RK. Texture analysis of preoperative CT images for prediction of postoperative hepatic insufficiency: a preliminary study. *J Am Coll Surg* 2015; **220**: 339-346 [PMID: 25537305 DOI: 10.1016/j.jamcollsurg.2014.11.027]
25 **Li M**, Fu S, Zhu Y, Liu Z, Chen S, Lu L, Liang C. Computed tomography texture analysis to facilitate therapeutic decision making in hepatocellular carcinoma. *Oncotarget* 2016; **7**: 13248-13259 [PMID: 26910890 DOI: 10.18632/oncotarget.7467]
26 **Gillies RJ**, Kinahan PE, Hricak H. Radiomics: Images Are More than Pictures, They Are Data. *Radiology* 2016; **278**: 563-577 [PMID: 26579733 DOI: 10.1148/radiol.2015151169]
27 **Xu X**, Zhang HL, Liu QP, Sun SW, Zhang J, Zhu FP, Yang G, Yan X, Zhang YD, Liu XS. Radiomic analysis of contrast-enhanced CT predicts microvascular invasion and outcome in hepatocellular carcinoma. *J Hepatol* 2019; **70**: 1133-1144 [PMID: 30876945 DOI: 10.1016/j.jhep.2019.02.023]
28 **Bakr S**, Echegaray S, Shah R, Kamaya A, Louie J, Napel S, Kothary N, Gevaert O. Noninvasive radiomics signature based on quantitative analysis of computed tomography images as a surrogate for microvascular invasion in hepatocellular carcinoma: a pilot study. *J Med Imaging (Bellingham)* 2017; **4**: 041303 [PMID: 28840174 DOI: 10.1117/1.JMI.4.4.041303]

29 **Chen Y**, Xia Y, Tolat PP, Long L, Jiang Z, Huang Z, Tang Q. Comparison of Conventional Gadoxetate Disodium-Enhanced MRI Features and Radiomics Signatures With Machine Learning for Diagnosing Microvascular Invasion. *AJR Am J Roentgenol* 2021; **216**: 1510-1520 [PMID: 33826360 DOI: 10.2214/AJR.20.23255]

30 **Kim SH**, Jeong WK, Kim Y, Kim MY, Kim J, Pyo JY, Oh YH. Hepatocellular carcinoma composed of two different histologic types: imaging features on gadoxetic acid-enhanced liver MRI. *Clin Mol Hepatol* 2013; **19**: 92-96 [PMID: 23593616 DOI: 10.3350/cmh.2013.19.1.92]

31 **Lee NK**, Kim S, Kim GH, Heo J, Seo HI, Kim TU, Kang DH. Significance of the "delayed hyperintense portal vein sign" in the hepatobiliary phase MRI obtained with Gd-EOB-DTPA. *J Magn Reson Imaging* 2012; **36**: 678-685 [PMID: 22649000 DOI: 10.1002/jmri.23700]

32 **van Kessel CS**, Veldhuis WB, van den Bosch MA, van Leeuwen MS. MR liver imaging with Gd-EOB-DTPA: a delay time of 10 minutes is sufficient for lesion characterisation. *Eur Radiol* 2012; **22**: 2153-2160 [PMID: 22645040 DOI: 10.1007/s00330-012-2486-2]

33 **Granito A**, Galassi M, Piscaglia F, Romanini L, Lucidi V, Renzulli M, Borghi A, Grazioli L, Golfieri R, Bolondi L. Impact of gadoxetic acid (Gd-EOB-DTPA)-enhanced magnetic resonance on the non-invasive diagnosis of small hepatocellular carcinoma: a prospective study. *Aliment Pharmacol Ther* 2013; **37**: 355-363 [PMID: 23199022 DOI: 10.1111/apt.12166]

34 **Lee S**, Kim SH, Lee JE, Sinn DH, Park CK. Preoperative gadoxetic acid-enhanced MRI for predicting microvascular invasion in patients with single hepatocellular carcinoma. *J Hepatol* 2017; **67**: 526-534 [PMID: 28483680 DOI: 10.1016/j.jhep.2017.04.024]

35 **Lambin P**, Leijenaar RTH, Deist TM, Peerlings J, de Jong EEC, van Timmeren J, Sanduleanu S, Larue RTHM, Even AJG, Jochems A, van Wijk Y, Woodruff H, van Soest J, Lustberg T, Roelofs E, van Elmpt W, Dekker A, Mottaghy FM, Wildberger JE, Walsh S. Radiomics: the bridge between medical imaging and personalized medicine. *Nat Rev Clin Oncol* 2017; **14**: 749-762 [PMID: 28975929 DOI: 10.1038/nrclinonc.2017.141]

36 **Hamerla G**, Meyer HJ, Schob S, Ginat DT, Altman A, Lim T, Gihr GA, Horvath-Rizea D, Hoffmann KT, Surov A. Comparison of machine learning classifiers for differentiation of grade 1 from higher gradings in meningioma: A multicenter radiomics study. *Magn Reson Imaging* 2019; **63**: 244-249 [PMID: 31425811 DOI: 10.1016/j.mri.2019.08.011]

37 **Peng J**, Zhang J, Zhang Q, Xu Y, Zhou J, Liu L. A radiomics nomogram for preoperative prediction of microvascular invasion risk in hepatitis B virus-related hepatocellular carcinoma. *Diagn Interv Radiol* 2018; **24**: 121-127 [PMID: 29770763 DOI: 10.5152/dir.2018.17467]

38 **Feng ST**, Jia Y, Liao B, Huang B, Zhou Q, Li X, Wei K, Chen L, Li B, Wang W, Chen S, He X, Wang H, Peng S, Chen ZB, Tang M, Chen Z, Hou Y, Peng Z, Kuang M. Preoperative prediction of microvascular invasion in hepatocellular cancer: a radiomics model using Gd-EOB-DTPA-enhanced MRI. *Eur Radiol* 2019; **29**: 4648-4659 [PMID: 30689032 DOI: 10.1007/s00330-018-5935-8]

39 **Taouli B**, Koh DM. Diffusion-weighted MR imaging of the liver. *Radiology* 2010; **254**: 47-66 [PMID: 20032142 DOI: 10.1148/radiol.09090021]

40 **Pawlik TM**, Delman KA, Vauthey JN, Nagorney DM, Ng IO, Ikai I, Yamaoka Y, Belghiti J, Lauwers GY, Poon RT, Abdalla EK. Tumor size predicts vascular invasion and histologic grade: Implications for selection of surgical treatment for hepatocellular carcinoma. *Liver Transpl* 2005; **11**: 1086-1092 [PMID: 16123959 DOI: 10.1002/Lt.20472]

41 **Okamura S**, Sumie S, Tonan T, Nakano M, Satani M, Shimose S, Shirono T, Iwamoto H, Aino H, Niizeki T, Tajiri N, Kuromatsu R, Okuda K, Nakashima O, Torimura T. Diffusion-weighted magnetic resonance imaging predicts malignant potential in small hepatocellular carcinoma. *Dig Liver Dis* 2016; **48**: 945-952 [PMID: 27338850 DOI: 10.1016/j.dld.2016.05.020]

42 **Kim JG**, Jang KM, Min GS, Kang TW, Cha DI, Ahn SH. Questionable correlation of the apparent diffusion coefficient with the histological grade and microvascular invasion in small hepatocellular carcinoma. *Clin Radiol* 2019; **74**: 406.e19-406.e27 [PMID: 30826002 DOI: 10.1016/j.crad.2019.01.019]

43 **Steyerberg EW**, Vergouwe Y. Towards better clinical prediction models: seven steps for development and an ABCD for validation. *Eur Heart J* 2014; **35**: 1925-1931 [PMID: 24898551 DOI: 10.1093/eurheartj/ehu207]

World Journal of Gastroenterology

Submit a Manuscript: https://www.f6publishing.com

World J Gastroenterol 2022 August 21; 28(31): 4417-4430

DOI: 10.3748/wjg.v28.i31.4417

ISSN 1007-9327 (print) ISSN 2219-2840 (online)

ORIGINAL ARTICLE

Observational Study

Prevalence and clinical characteristics of autoimmune liver disease in hospitalized patients with cirrhosis and acute decompensation in China

Zi-Xuan Shen, Dan-Dan Wu, Jie Xia, Xian-Bo Wang, Xin Zheng, Yan Huang, Bei-Ling Li, Zhong-Ji Meng, Yan-Hang Gao, Zhi-Ping Qian, Feng Liu, Xiao-Bo Lu, Jia Shang, Hua-Dong Yan, Yu-Bao Zheng, Wen-Yi Gu, Yan Zhang, Jian-Yi Wei, Wen-Ting Tan, Yi-Xin Hou, Qun Zhang, Yan Xiong, Cong-Cong Zou, Jun Chen, Ze-Bing Huang, Xiu-Hua Jiang, Sen Luo, Yuan-Yuan Chen, Na Gao, Chun-Yan Liu, Wei Yuan, Xue Mei, Jing Li, Tao Li, Xin-Yi Zhou, Guo-Hong Deng, Jin-Jun Chen, Xiong Ma, Hai Li

Specialty type: Gastroenterology and hepatology

Provenance and peer review: Unsolicited article; Externally peer reviewed.

Peer-review model: Single blind

Peer-review report's scientific quality classification

Grade A (Excellent): A
Grade B (Very good): B, B
Grade C (Good): 0
Grade D (Fair): 0
Grade E (Poor): 0

P-Reviewer: Haile D, Ethiopia; Hayat U, United States

Received: March 3, 2022
Peer-review started: March 3, 2022
First decision: April 25, 2022
Revised: May 19, 2022
Accepted: July 25, 2022
Article in press: July 25, 2022
Published online: August 21, 2022

Zi-Xuan Shen, Dan-Dan Wu, Wen-Yi Gu, Yan Zhang, Jian-Yi Wei, Xiong Ma, Hai Li, Department of Gastroenterology, Renji Hospital, School of Medicine, Shanghai Jiao Tong University, Shanghai 200127, China

Zi-Xuan Shen, Dan-Dan Wu, Wen-Yi Gu, Yan Zhang, Jian-Yi Wei, Xiong Ma, Hai Li, Shanghai Institute of Digestive Disease, Key Laboratory of Gastroenterology and Hepatology, Chinese Ministry of Health, Shanghai Jiao Tong University, Shanghai 200001, China

Jie Xia, Wen-Ting Tan, Guo-Hong Deng, Department of Infectious Diseases, Southwest Hospital, The Third Military Medical University (Army Medical University), Chongqing 400038, China

Xian-Bo Wang, Yi-Xin Hou, Qun Zhang, Center of Integrative Medicine, Beijing Ditan Hospital, Capital Medical University, Beijing 100102, China

Xin Zheng, Yan Xiong, Cong-Cong Zou, Department of Infectious Diseases, Institute of Infection and Immunology, Union Hospital, Tongji Medical College, Huazhong University of Science and Technology, Wuhan 430022, Hubei Province, China

Yan Huang, Jun Chen, Ze-Bing Huang, Department of Infectious Diseases, Hunan Key Laboratory of Viral Hepatitis, Xiangya Hospital, Central South University, Changsha 410008, Hunan Province, China

Bei-Ling Li, Jun Chen, Xiu-Hua Jiang, Jin-Jun Chen, Hepatology Unit, Department of Infectious Diseases, Nanfang Hospital, Southern Medical University, Guangzhou 510515, Guangdong Province, China

Zhong-Ji Meng, Sen Luo, Yuan-Yuan Chen, Department of Infectious Disease, Taihe Hospital, Hubei University of Medicine, Shiyan 430418, Hubei Province, China

Yan-Hang Gao, Na Gao, Chun-Yan Liu, Department of Hepatology, The First Hospital of Jilin University, Changchun 130031, Jilin Province, China

Zhi-Ping Qian, Wei Yuan, Xue Mei, Department of Liver Intensive Care Unit, Shanghai Public

Health Clinical Centre, Fudan University, Shanghai 201508, China

Feng Liu, Tianjin Institute of Hepatology, Nankai University Second People's Hospital, Tianjin 300102, China

Feng Liu, Jing Li, Tao Li, Department of Infectious Diseases and Hepatology, The Second Hospital of Shandong University, Jinan 250033, Shandong Province, China

Xiao-Bo Lu, Xin-Yi Zhou, Infectious Disease Center, The First Affiliated Hospital of Xinjiang Medical University, Urumqi 830054, Xinjiang, China

Jia Shang, Department of Infectious Diseases, Henan Provincial People's Hospital, Zhengzhou 450003, Henan Province, China

Hua-Dong Yan, Department of Infectious Diseases, Hwamei Hospital, The Second Hospital of Ningbo, University of Chinese Academy of Sciences, Ningbo 315153, Zhejiang Province, China

Yu-Bao Zheng, Department of Infectious Diseases, The Third Affiliated Hospital of Sun Yat-sen University, Guangzhou 510630, Guangdong Province, China

Corresponding author: Hai Li, MD, Professor, Department of Gastroenterology, Renji Hospital, School of Medicine, Shanghai Jiao Tong University, No. 1630 Dongfang Road, Shanghai 200127, China. hai_17@126.com

Abstract

BACKGROUND

Autoimmune liver disease (AILD) has been considered a relatively uncommon disease in China, epidemiological data for AILD in patients with cirrhosis and acute decompensation (AD) is sparse.

AIM

To investigate the prevalence, outcome and risk factors for AILD in cirrhotic patients complicated with AD in China.

METHODS

We collected data from patients with cirrhosis and AD from two prospective, multicenter cohorts in hepatitis B virus endemic areas. Patients were regularly followed up at the end of 28-d, 90-d and 365-d, or until death or liver transplantation (LT). The primary outcome in this study was 90-d LT-free mortality. Acute-on-chronic liver failure (ACLF) was assessed on admission and during 28-d hospitalization, according to the diagnostic criteria of the European Association for the Study of the Liver (EASL). Risk factors for death were analyzed with logistic regression model.

RESULTS

In patients with cirrhosis and AD, the overall prevalence of AILD was 9.3% (242/2597). Prevalence of ACLF was significantly lower in AILD cases (14%) than those with all etiology groups with cirrhosis and AD (22.8%) ($P < 0.001$). Among 242 enrolled AILD patients, the prevalence rates of primary biliary cirrhosis (PBC), autoimmune hepatitis (AIH) and PBC-AIH overlap syndrome (PBC/AIH) were 50.8%, 28.5% and 12.0%, respectively. In ACLF patients, the proportions of PBC, AIH and PBC/AIH were 41.2%, 29.4% and 20.6%. 28-d and 90-d mortality were 43.8% and 80.0% in AILD-related ACLF. The etiology of AILD had no significant impact on 28-d, 90-d or 365-d LT-free mortality in patients with cirrhosis and AD in both univariate and multivariate analysis. Total bilirubin (TB), hepatic encephalopathy (HE) and blood urea nitrogen (BUN) were independent risk factors for 90-d LT-free mortality in multivariate analysis. The development of ACLF during hospitalization only independently correlated to TB and international normalized ratio.

CONCLUSION

AILD was not rare in hospitalized patients with cirrhosis and AD in China, among which PBC was the most common etiology. 90-d LT-free mortality were independently associated with TB, HE and BUN.

Key Words: Prevalence; Autoimmune liver disease; Cirrhosis and acute decompensation; Mortality; Acute-on-chronic liver failure

Core Tip: Autoimmune liver disease (AILD) has been regarded as a relatively rare disease in China. Our study reported that the overall prevalence of AILD was 9.3% hospitalized patients with cirrhosis and acute decompensation, among which primary biliary cirrhosis was the most prevalent type. In AILD patients with cirrhosis and acute decompensation, the etiology types of AILD had no significant effect on short-term mortality, total bilirubin, hepatic encephalopathy (HE) and blood urea nitrogen were independently associated with 90-d mortality in multivariate analysis. Strategies are needed to prevent presence of HE and closely monitor the changes of liver and renal function in clinical practice. These data will be a crucial complement to the public epidemiology research on AILD in Asian-Pacific regions.

Citation: Shen ZX, Wu DD, Xia J, Wang XB, Zheng X, Huang Y, Li BL, Meng ZJ, Gao YH, Qian ZP, Liu F, Lu XB, Shang J, Yan HD, Zheng YB, Gu WY, Zhang Y, Wei JY, Tan WT, Hou YX, Zhang Q, Xiong Y, Zou CC, Chen J, Huang ZB, Jiang XH, Luo S, Chen YY, Gao N, Liu CY, Yuan W, Mei X, Li J, Li T, Zhou XY, Deng GH, Chen JJ, Ma X, Li H. Prevalence and clinical characteristics of autoimmune liver disease in hospitalized patients with cirrhosis and acute decompensation in China. *World J Gastroenterol* 2022; 28(31): 4417-4430
URL: https://www.wjgnet.com/1007-9327/full/v28/i31/4417.htm
DOI: https://dx.doi.org/10.3748/wjg.v28.i31.4417

INTRODUCTION

Autoimmune liver disease (AILD) includes primary biliary cirrhosis (PBC), autoimmune hepatitis (AIH), primary sclerosing cholangitis (PSC) and immunoglobulin G 4-related diseases (IgG4-RD)[1-3]. Some patients display clinical manifestations of two different entities based on clinical and histological features, which is described as "overlap syndrome", among which PBC-AIH overlap syndrome (PBC/AIH) is the most common[4]. AILD has been considered to be a relatively rare etiology of chronic liver disease (CLD) in China where viral hepatitis has a high prevalence. However, recent findings indicated that the prevalence of AILD is increasing in the Asia-Pacific region. In Japan, AIH prevalence increased from 8.7 to 23.9 per 100000 population from 2004 to 2016[5]. In a city in northern China, PBC prevalence rose from 0.5 to 8.0 per 100000 population in the past 10 years[6]. Several studies have illustrated the prevalence and clinical characteristics of AILD in general population[7-9]. Few studies have been conducted to investigate the nature history of AILD, especially in the late stage of CLD-cirrhosis and acute decompensation (AD).

The Chinese Acute on Chronic Liver Failure (CATCH-LIFE) study consisted of two prospective, multicenter cohorts that enrolled hospitalized patients with CLD of various etiologies, most of whom had cirrhosis and complicated with AD. It is nationally representative of hospitalized CLD patients in China. In this study, we used the data from the CATCH-LIFE study to investigate the following: (1) The prevalence and short-term outcome of AILD in patients with cirrhosis and AD; (2) The impact of AILD etiology on mortality; and (3) Risk factors for 90-d mortality in AILD patients with cirrhosis and AD.

MATERIALS AND METHODS

Patients

Data were collected from 2 prospective, observational cohorts of the CATCH-LIFE study which enrolled hospitalized patients with CLD and acute events, from January 2015 to December 2016 and July 2018 to January 2019, respectively. The rationale and design of the cohorts have been described elsewhere[10, 11]. The medical ethics boards of the Shanghai Renji Hospital, approved the study. Written informed consent were obtained from every participant or his or her legal surrogates before enrollment.

Cirrhosis was diagnosed according to a computed tomography/magnetic resonance imaging scan, clinical symptoms, laboratory tests and medical history[12]. AD was defined as ascites, variceal hemorrhage, hepatic encephalopathy (HE), infection and jaundice within 1 mo[13]. The diagnosis of AILD was exclusionary. The following patients were excluded: Coinfections with other viruses [hepatitis A virus, hepatitis B virus (HBV), hepatitis C virus and hepatitis E virus], alcoholic liver disease, nonalcoholic fatty liver disease, schistosomiasis, metabolic liver diseases, chronic drug-induced liver disease, and cryptogenic liver disease.

PBC was defined according to the American Association for the Study of Liver Diseases clinical guidance in 2008[14], with at least 2 of the following: (1) Elevated serum alkaline phosphatase (ALP) [> 1.5 folds the upper limit of normal (ULN)] or gamma glutamyl transpeptidase (GGT) (> 3 ULN); (2) Positive test for antimitochondrial antibodies (AMA) (titer > 1:40); and (3) Compatible liver biopsy suggestive of suppurative destructive cholangitis (ductopenia, cholestasis, fibrosis and portal inflammation). AIH was defined based on simplified criteria (score > 6) proposed by the International

Autoimmune Hepatitis Group in 2008[15]. PBC/AIH overlap syndrome was strictly diagnosed according to the Paris Criteria proposed by Chazouillères *et al*[16] in 1998, which associated PBC and AIH either synchronously or consecutively. Presence of at least 2 of the 3 criteria was required. PBC criteria were the following: (1) ALP > 2 ULN or GGT > 5 ULN; (2) A positive serology for AMA; and (3) A liver biopsy specimen indicating florid bile duct lesions. AIH criteria were the following: (1) Serum alanine transaminase (ALT) > 5 ULN; (2) IgG > 2 ULN or a positive serology for anti-smooth muscle antibodies; and (3) A liver biopsy indicating moderate to severe periportal or periseptal lymphocytic piecemeal interface hepatitis.

Some uncommon etiologies of AILD in this study, such as PSC, PBC-PSC overlap syndrome, AIH-PSC overlap syndrome and IgG4-RD were categorized into a "others" group, as the number of cases of "others" was quite small to allow robust statistical analysis. Acute-on-chronic liver failure (ACLF) was diagnosed based on the European Association for the Study of the Liver (EASL) criteria[17]. Just as follows: (1) ACLF grade 1: Single kidney failure or single cerebral failure with renal dysfunction (1.5 mg/dL < creatinine < 1.9 mg/dL) or other single organ failure [serum bilirubin ≥ 12 mg/dL for liver; (international normalized ratio) INR = 2.5 for coagulation; vasopressors to maintain arterial pressure for circulation; $PaO_2/FiO_2 \leq 200$ or $SpO_2/FiO_2 \leq 214$ for respiration] with renal dysfunction and/or mild HE; (2) ACLF grade 2: The presence of 2 organ failures; and (3) ACLF grade 3: The failure no less than 3 organs.

Data collection

Demographics, medical history, imagological examination and laboratory parameters were obtained from every participant on admission. Participants were regularly followed up for 28 d, 90 d and 365 d until death or liver transplantation (LT). Development of ACLF was assessed on admission and during hospitalization within 28 d, respectively. The primary outcome of this study was 90-d LT-free mortality. The secondary outcome was ACLF development during 28-d hospitalization.

Statistical analysis

Continuous variables were summarized as mean (SD) or median (interquartile range) according to their distribution, while categorical variables were summarized as frequency (proportion). Comparisons between four groups were performed using Kruskal-Wallis test for continuous variables, Chi-square test or Fisher's exact test for categorical variables. The impact of the etiology of AILD on short-term mortality were analyzed using a multivariable logistic regression model, adjusting for potential confounders, including demographics (age, sex) and AD events (HE, gastrointestinal bleeding, infection and ascites). Logistic regression was also used to determine the risk factors for 90-d mortality and ACLF development during hospitalization. Variables with P values less than 0.1 were included in the multivariate logistic regression model[18,19]. All continuous variables were log2 transformed before entering the model. Two-tailed P values of 0.05 were considered statistically significant. Statistical analysis was conducted using R 3.6.2 and SPSS 19.0.

RESULTS

Prevalence of AILD and ACLF in patients with cirrhosis and AD

A total of 3970 patients from CATCH-LIFE study were screened, 2597 of whom had cirrhosis and AD. Eventually, 242 patients conforming the diagnostic criteria of AILD were finally enrolled (Figure 1). In patients with cirrhosis and AD, the overall prevalence of AILD was 9.3% (242/2597). Prevalence of ACLF was significantly lower in AILD cases (14%) than those with all etiology groups with cirrhosis and AD (22.8%) ($P < 0.001$). Distribution of participating centers in this study and number of AILD patients enrolled from each center were displayed in Figures 2A and 2B, respectively. Among the 242 enrolled AILD patients, 234 (96.6%) are from eastern China, where 94% of Chinese population resides; 8 (3.4%) are from western China, where 6% of Chinese population resides. Due to Renji Hospital accounted for 60.3% (146/242) of the total enrolled patients, we further analyzed district distribution of patients enrolled from Renji Hospital. Actually, these patients were from 20 different district all over the country (Figure 2C), the number of patients from each district was shown in Figure 2D. Distribution of patients enrolled from Renji Hospital were also consistent with population density distribution (divided by Hu Line) in China.

Baseline characteristics and outcomes among different etiologies in AILD patients

Baseline characteristics of 242 AILD patients with cirrhosis and AD categorized by etiology are depicted in Table 1. 123 (50.8%) patients showed PBC, 69 (28.5%) displayed AIH, 29 (12.0%) had AIH-PBC overlap syndrome (AIH/PBC) and 21 (8.7%) patients manifested other uncommon etiologies of AILD. Most patients were female (81.0%) and their mean age was 56.04 years. Patients with PBC/AIH had higher white blood cell ($P < 0.001$) and neutrophil-lymphocyte (NL) ratio ($P < 0.001$) levels than patients with PBC, AIH or others. ALT ($P < 0.001$) and AST ($P = 0.04$) levels were higher in the AIH/PBC group.

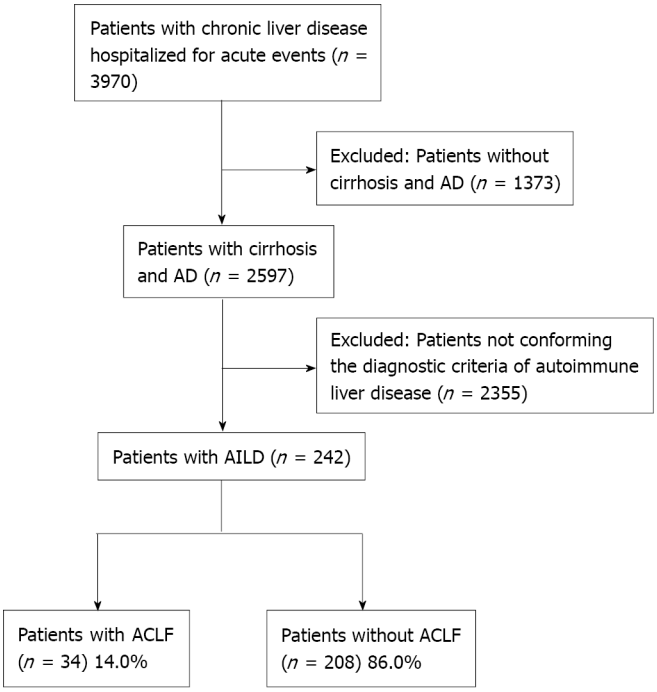

DOI: 10.3748/wjg.v28.i31.4417 **Copyright** ©The Author(s) 2022.

Figure 1 Flow chart of the study. AD: Acute decompensation; AILD: Autoimmune liver disease; ACLF: Acute-on-chronic liver failure.

In addition, the PBC group tended to have lower hemoglobin (P = 0.003) and higher ALP (P < 0.001) levels than other AILD etiologies.

Baseline characteristics of 34 ACLF patients categorized by etiology are shown in Table 2. PBC (41.2%) was still the most common etiology among ACLF patients with AILD, followed by AIH (29.4%), AIH/PBC overlap syndrome (20.6%) and others (8.8%). However, as the number of patients in some subgroups was small, the results may not be robust and require further validation in a larger population. At the end of 28-d and 90-d, no patients were lost to follow up. At the end of 365-d, 3 (1.2%) patients were lost to follow-up. Short-term (28-d, 90-d and 365-d) LT-free mortality of AILD patients with cirrhosis and AD are presented in Figure 3. Generally, among AILD patients with cirrhosis and AD, 90-d LT-free mortality were 17%. AIH/PBC had higher 28-d, 90-d and 365-d mortality, although the results were not statistically significant. Among patients with AILD-related ACLF, 28-d and 90-d mortality were 43.8% and 80.0%, respectively.

The impact of etiology on mortality

To investigate the effect of etiology on short-term (28-d, 90-d and 365-d) LT-free mortality in AILD patients with cirrhosis and AD, we constructed 3 models to gradually control other potential confounding factors (Table 3). Both univariate (unadjusted) and multivariate (adjusted I and adjusted II) analyses showed that compared to PBC, AIH patients were at lower risk for death at 90-d and 365-d, whereas PBC/AIH patients were at higher risk for death at all time periods. However, none of the associations were statistically significant. Subgroup analysis was conducted according to Child Turcotte Pugh and model for end-stage liver disease (MELD) score, there was no heterogeneity in the impact of etiology types on 90-d LT-free mortality in different AILD subgroups, as was shown in Supplementary Figure 1.

Risk factors of short-term mortality in AILD patients with cirrhosis and AD

Logistic regression model was conducted to assess the risk factors for 90-d LT-free mortality. Univariable analysis identified 10 variables on admission correlated with 90-d prognosis: Bacterial infection, HE, total bilirubin (TB), INR, blood urea nitrogen (BUN), albumin, ALT, white blood cell, NL-ratio and sodium (Supplementary Table 1). Variables with P < 0.1 were selected into multivariable model for further analysis. Only HE, TB and BUN were found to be independently associated with 90-d mortality in AILD patients with cirrhosis and AD (Figure 4). We also investigated risk factors for ACLF development during hospitalization (Table 4). 21 ACLF patients diagnosed on admission were excluded from analysis. Multivariable analysis revealed that only TB (P = 0.046) and INR (P = 0.048) independently correlated with ACLF development.

Table 1 Characteristics of autoimmune liver disease patients with cirrhosis and acute decompensation among different etiologies

	PBC	AIH	PBC/AIH	Others	*P* value
	n = 123	*n* = 69	*n* = 29	*n* = 21	
Demographics					
Age	56.00 (48.02, 63.83)	57.47 (49.33, 65.34)	52.62 (45.53, 60.85)	52.94 (41.15, 62.48)	0.28
Male, no. (%)	25 (20.3)	11 (15.9)	4 (13.8)	6 (28.6)	0.51
AD, no. (%)					
Bacterial infection	34 (27.6)	21 (30.4)	13 (44.8)	8 (38.1)	0.30
Ascites	82 (66.7)	42 (60.9)	17 (58.6)	14 (66.7)	0.77
Gastrointestinal bleeding	27 (22.0)	11 (15.9)	4 (13.8)	2 (9.5)	0.42
Hepatic encephalopathy	10 (8.1)	4 (5.8)	6 (20.7)	3 (14.3)	0.11
Jaundice	61 (49.6)	35 (50.7)	19 (65.5)	9 (42.9)	0.38
Laboratory results, median (IQR)					
TB, mg/dL	4.88 (1.60, 10.82)	5.15 (1.86, 11.14)	7.31 (3.04, 23.60)	4.88 (2.05, 11.72)	0.17
INR	1.29 (1.13, 1.52)	1.39 (1.23, 1.64)	1.39 (1.16, 1.49)	1.24 (1.15, 1.44)	0.044
Creatinine, mg/dL	0.65 (0.50, 0.88)	0.64 (0.51, 0.76)	0.67 (0.53, 0.79)	0.67 (0.45, 0.73)	0.51
Blood urea nitrogen, mmol/L	5.38 (3.70, 8.27)	4.73 (3.63, 5.95)	5.37 (3.90, 7.20)	4.50 (3.37, 6.60)	0.26
White blood cell, 10^9/L	4.39 (2.75, 6.34)	4.01 (2.81, 5.78)	6.85 (4.56, 11.76)	3.82 (3.10, 5.72)	0.001
Neutrophil-lymphocyte ratio	2.80 (1.73, 4.29)	2.00 (1.25, 3.25)	3.61 (3.01, 5.67)	2.89 (2.35, 4.86)	< 0.001
Platelet, 10^9/L	0.17 (0.11, 0.30)	0.15 (0.11, 0.25)	0.32 (0.14, 0.45)	0.12 (0.08, 0.30)	0.11
Albumin, g/L	30.30 (25.70, 33.70)	28.50 (25.70, 32.55)	29.90 (26.10, 33.80)	30.40 (28.45, 34.92)	0.262
ALT, IU/L	48.00 (24.50, 80.50)	59.00 (37.00, 116.00)	81.00 (61.00, 148.00)	57.90 (39.00, 85.40)	< 0.001
AST, IU/L	79.60 (48.40, 124.50)	87.00 (52.90, 187.00)	120.70 (79.00, 153.00)	90.00 (39.00, 148.00)	0.037
Hemoglobin, g/L	90.00 (68.00, 110.00)	99.00 (87.00, 119.00)	99.00 (85.00, 115.00)	98.00 (89.00, 112.00)	0.003
ALP, IU/L	208.50 (136.25, 313.00)	143.00 (105.74, 181.70)	175.50 (128.50, 243.00)	202.50 (133.50, 298.85)	< 0.001
GGT, IU/L	105.00 (51.23, 192.50)	86.63 (37.00, 126.00)	106.20 (58.70, 235.25)	122.70 (32.92, 220.22)	0.19
Pre-albumin, mg/L	78.30 (46.80, 113.90)	63.20 (40.93, 83.25)	77.30 (57.75, 97.80)	68.65 (54.75, 88.90)	0.25
Score, median (IQR)					
Child Turcotte Pugh	9.00 (8.00, 10.00)	9.00 (8.00, 10.25)	10.00 (8.00, 11.00)	9.00 (8.00, 11.00)	0.58
MELD	11.00 (7.00, 17.00)	15.00 (11.00, 21.00)	18.00 (14.00, 23.00)	12.00 (10.00, 16.00)	< 0.001
MELD Na	14.00 (7.75, 19.00)	17.00 (12.00, 23.00)	20.50 (15.75, 25.00)	13.00 (10.00, 19.00)	< 0.001
CLIF SOFA	5.00 (3.00, 6.00)	5.00 (3.00, 6.00)	6.00 (3.00, 7.00)	5.00 (4.00, 6.00)	0.44

PBC: Primary biliary cirrhosis; AIH: Autoimmune hepatitis; PBC/AIH: Primary biliary cirrhosis-autoimmune hepatitis overlap syndrome; AD: Acute decompensation; IQR: Interquartile range; TB: Total bilirubin; INR: International normalized ratio; ALT: Alanine transaminase; AST: Aspartate transaminase; ALP: Alkaline phosphatase; GGT: Gamma glutamyl transpeptidase; MELD: Model for end-stage liver disease; CLIF-SOFA: Chronic liver failure-sequential organ failure assessment.

DISCUSSION

The current study is the first nationwide investigation of the prevalence and short-term outcome of end-stage AILD in China, which is a traditional HBV high endemic area. Our study showed that the overall prevalence of AILD was 9.3% in tertiary hospitalized patients with cirrhosis and AD. PBC was responsible for half of AILD cases. The prevalence of ACLF was significantly lower in AILD patients than those with all etiology groups with cirrhosis and AD. Short-term mortality were extremely high in AILD-related ACLF.

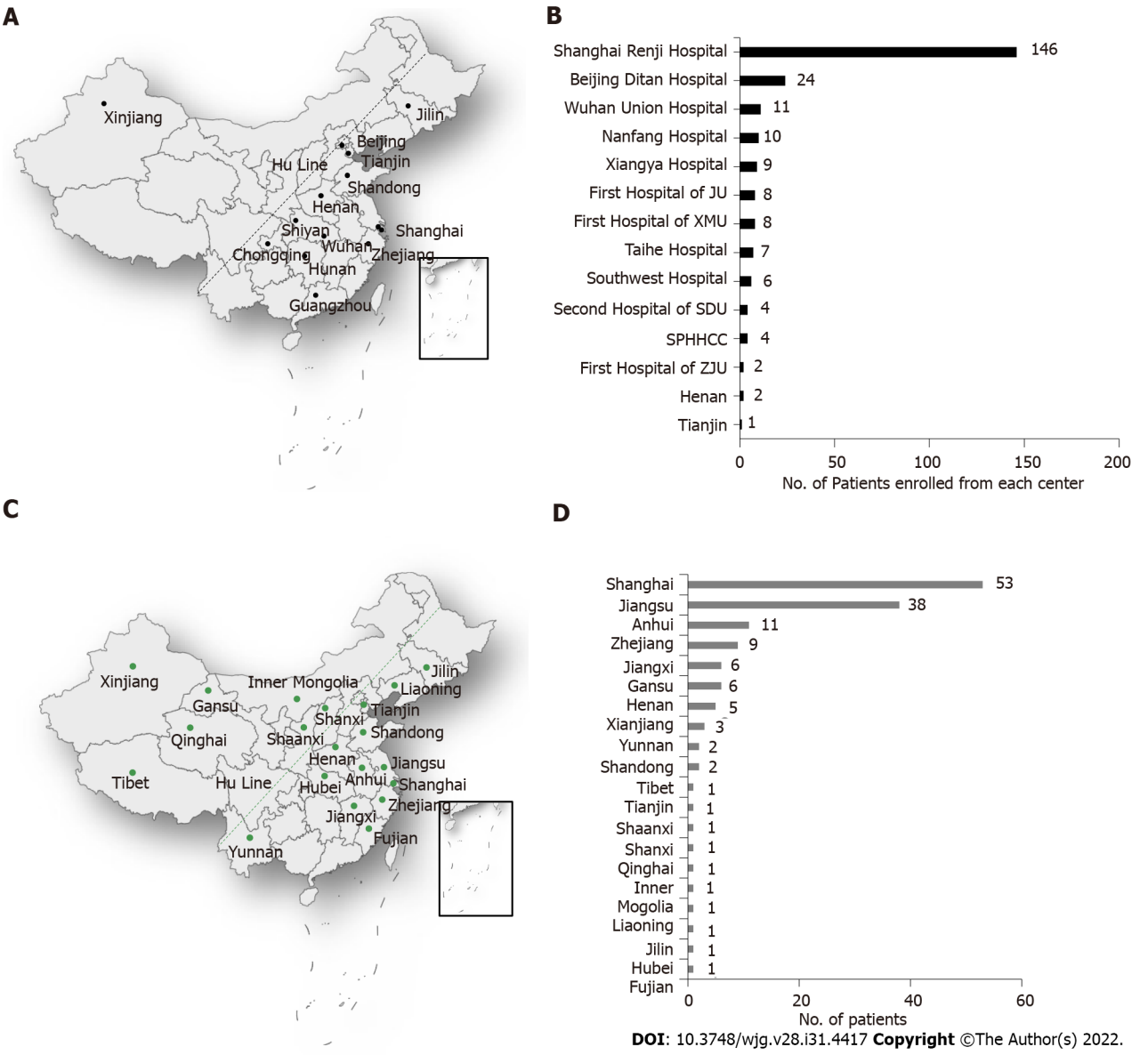

DOI: 10.3748/wjg.v28.i31.4417

Figure 2 Distribution and the number of autoimmune liver disease patients enrolled from each of center and from Renji Hospital. A: District distribution of each enrolled center; B: The number of patients enrolled from center; C: Population distribution of patients from Renji Hospital; D: The number of patients enrolled from each of the 20 districts. Approximately 94% of the total Chinse population resides east of the dividing line (Hu Line) in the figure, and 6% resides west of the line; 13 centers lie in eastern China, and 1 lies in western China.

EASL-CLIF study reported that the prevalence of ACLF was 30.9% in alcohol-related cirrhosis and AD, whereas COSSH study showed that the prevalence of ACLF reached up to 26.2% in patients with HBV-related cirrhosis and AD[17,20]. However, in this study, among 242 AILD patients with cirrhosis and AD, only 34 (14%) had ACLF, the prevalence was significantly lower than that of patients with other etiology types. One plausible explanation may be that AILD patients have distinct clinical characteristics (higher severity, higher prevalence of infection and lower prevalence of organ failures) that differ distinctly from those of patients with other etiologies, which led to lower prevalence of ACLF but higher short-term mortality.

Despite having higher levels of inflammation and liver injury, PBC/AIH had similar short-term mortality rates compared to PBC individually after adjusting for confounding factors. Neuhauser *et al* [21] and Yang *et al*[22] showed that a more aggressive clinical course and worse clinical consequences were observed in patients with PBC/AIH than patients with pure PBC. Based on these results, some experts suggested that PBC/AIH should be identified and aggressively treated. Notably, these studies only evaluate the univariate prognostic value of etiology and did not take confounders into consideration. It is, therefore, likely that they fail to objectively reveal the independent impact of etiology on the prognosis of AILD. PBC, AIH and PBC/AIH are all complex disorders but result in significant morbidity and mortality. Once progressed to liver failure, no effective treatment is clinically available. Herein, our results clearly showed that presence of HE, higher TB and BUN levels, rather than liver disease etiologies, were independently associated with short-term mortality in AILD patients with

Table 2 Characteristics of autoimmune liver disease patients with acute-on-chronic liver failure according to etiology

Variable	PBC	AIH	PBC/AIH	Others	*P* value
	n = 14	*n* = 10	*n* = 7	*n* = 3	
Demographics					
Age, median (IQR)	55.34 (48.88, 58.96)	55.94 (50.00, 64.01)	53.46 (47.97, 63.46)	50.85 (46.87, 58.00)	0.88
Male, no. (%)	6 (42.9)	1 (10.0)	0 (0.0)	2 (66.7)	0.04
AD, no. (%)					
Bacterial infection	7 (50.0)	3 (30.0)	6 (85.7)	2 (66.7)	0.14
Ascites	9 (64.3)	6 (60.0)	5 (71.4)	3 (100.0)	0.61
Gastrointestinal bleeding	1 (7.1)	1 (10.0)	0 (0.0)	1 (33.3)	0.39
Hepatic encephalopathy	4 (28.6)	3 (30.0)	4 (57.1)	2 (66.7)	0.40
Jaundice	10 (71.4)	9 (90.0)	6 (85.7)	2 (66.7)	0.64
Laboratory results, median (IQR)					
TB, mg/dL	16.78 (4.79, 27.10)	12.56 (8.94, 17.64)	23.60 (14.64, 27.52)	14.56 (8.94, 19.29)	0.71
INR	1.57 (1.34, 1.77)	2.64 (1.67, 2.80)	1.49 (1.44, 2.31)	1.50 (1.47, 1.97)	0.35
Creatinine, mg/dL	0.83 (0.79, 2.01)	0.58 (0.50, 0.74)	0.79 (0.75, 0.84)	0.68 (0.36, 1.46)	0.08
Blood urea nitrogen, mmol/L	12.05 (6.04, 20.65)	5.40 (2.74, 8.12)	7.70 (7.20, 9.25)	8.73 (6.92, 21.00)	0.09
White blood cell, 10^9/L	5.55 (3.62, 10.19)	4.57 (3.13, 5.34)	8.82 (6.55, 16.27)	6.71 (4.91, 9.37)	0.08
Neutrophil-lymphocyte ratio	4.55 (3.78, 5.84)	1.80 (1.06, 4.40)	7.64 (5.66, 12.77)	5.40 (4.86, 6.30)	0.05
Albumin, g/L	28.90 (26.75, 33.72)	27.80 (25.38, 31.48)	27.20 (25.05, 28.60)	27.40 (25.00, 31.15)	0.60
ALT, IU/L	105.15 (33.30, 186.90)	59.05 (38.65, 99.47)	113.90 (102.60, 204.10)	69.90 (57.55, 146.65)	0.37
AST, IU/L	121.50 (62.72, 182.23)	99.45 (61.10, 172.75)	153.00 (111.65, 238.05)	34.20 (30.30, 85.15)	0.33
Hemoglobin, g/L	88.00 (40.75, 138.00)	64.00 (33.00, 116.00)	65.00 (46.00, 77.50)	57.00 (55.20, 74.50)	0.89
ALP, IU/L	76.00 (69.00, 96.25)	86.50 (82.00, 90.75)	108.00 (89.00, 127.50)	91.40 (65.80, 102.90)	0.29
GGT, IU/L	187.00 (111.25, 252.80)	149.00 (125.65, 195.00)	153.00 (109.00, 365.00)	NA (NA, NA)	0.76
Pre-albumin, mg/L	89.00 (52.00, 119.57)	106.50 (45.25, 116.50)	63.00 (58.70, 258.60)	NA (NA, NA)	0.85
Albumin, g/L	66.50 (54.60, 115.00)	33.40 (23.55, 60.40)	87.65 (60.35, 91.55)	NA (NA, NA)	0.13
Score, median (IQR)					
Child Turcotte Pugh	9.50 (8.25, 10.75)	12.00 (10.00, 12.75)	11.00 (10.50, 12.50)	11.00 (11.00, 12.50)	0.04
MELD	20.00 (18.00, 22.75)	27.50 (18.50, 28.75)	24.00 (22.00, 28.00)	21.00 (20.50, 23.00)	0.17
MELD Na	21.00 (19.00, 25.00)	26.50 (23.00, 28.75)	29.00 (23.00, 32.00)	41.00 (39.00, 41.50)	0.12
CLIF SOFA	7.00 (6.25, 8.00)	7.00 (7.00, 8.00)	8.00 (6.50, 9.00)	9.00 (8.00, 10.00)	0.32

PBC: Primary biliary cirrhosis; AIH: Autoimmune hepatitis; PBC/AIH: Primary biliary cirrhosis-autoimmune hepatitis overlap syndrome; AD: Acute decompensation; IQR: Interquartile range; TB: Total bilirubin; INR: International normalized ratio; ALT: Alanine transaminase; AST: Aspartate transaminase; ALP: Alkaline phosphatase; GGT: Gamma glutamyl transpeptidase; MELD: Model for end-stage liver disease; CLIF-SOFA: Chronic liver failure-sequential organ failure assessment; NA: Not available.

cirrhosis and AD. Therefore, in clinical management of AILD, physicians are supposed to pay more attention to the presence of HE and closely monitor the changes of liver and renal function.

This study had several strengths. With national samples, our multicenter data provided an overview of epidemiological features of end-stage AILD in China, where it is considered uncommon. Thus, we presented a national view of the disease. Indeed, most of the studies in this field originated from single center or other geographic areas[7,23-25]. We focused on the role of the etiology on short-term mortality. Moreover, we clarified that HE, TB and BUN were significant risk factors of short-term mortality in AILD patients with cirrhosis and AD. These data will be an important complement to the public epidemiological data of AILDs in Asian-Pacific regions.

Table 3 The impact of etiology on liver transplantation-free mortality in acute-on-chronic liver failure patients with cirrhosis and acute decompensation (primary biliary cirrhosis as a reference)

	n	Num of death (percentage)	Unadjusted OR (95%CI), *P* value	Adjusted I[1], OR (95%CI), *P* value	Adjusted II[2], OR (95%CI), *P* value
28-d LT-free mortality					
PBC	111	7 (6.3)	1.0	1.0	1.0
AIH	67	4 (6.0)	0.94 (0.24-3.25), 0.93	0.94 (0.24-3.24), 0.92	1.26 (0.3-4.85), 0.74
PBC/AIH	28	5 (17.9)	3.23 (0.89-11.05), 0.06	3.43 (0.93-11.93), 0.05	2.61 (0.63-10.21), 0.17
Others	19	2 (10.5)	1.75 (0.25-7.99), 0.51	1.75 (0.24-8.13), 0.51	1.46 (0.17-8.28), 0.70
90-d LT-free mortality					
PBC	103	19 (18.4)	1.0	1.0	1.0
AIH	64	8 (12.5)	0.63 (0.25-1.50), 0.31	0.64 (0.25-1.53), 0.33	0.74 (0.27-1.88), 0.54
PBC/AIH	26	7 (26.9)	1.63 (0.57-4.31), 0.34	1.70 (0.59-4.56), 0.30	1.18 (0.36-3.56), 0.77
Others	18	2 (11.1)	0.55 (0.08-2.17), 0.45	0.51 (0.08-2.02), 0.40	0.44 (0.05-2.08), 0.36
365-d LT-free mortality					
PBC	97	30 (30.9)	1.0	1.0	1.0
AIH	63	16 (25.4)	0.76 (0.37-1.54), 0.45	0.76 (0.36-1.53), 0.44	0.81 (0.38-1.68), 0.58
PBC/AIH	23	11 (47.8)	2.05 (0.9-5.20), 0.13	2.06 (0.81-5.24), 0.13	1.72 (0.63-4.61), 0.28
Others	18	5 (27.8)	0.86 (0.26-2.51), 0.79	0.89 (0.26-2.62), 0.84	0.82 (0.24-2.49), 0.74

[1]Adjusted age, gender.
[2]Adjusted age, gender, hepatic encephalopathy, ascites, infection and gastrointestinal bleeding.
OR: Odds ratio; CI: Confidence interval; PBC: Primary biliary cirrhosis; AIH: Autoimmune hepatitis; PBC/AIH: Primary biliary cirrhosis-autoimmune hepatitis overlap syndrome; LT: Liver transplantation.

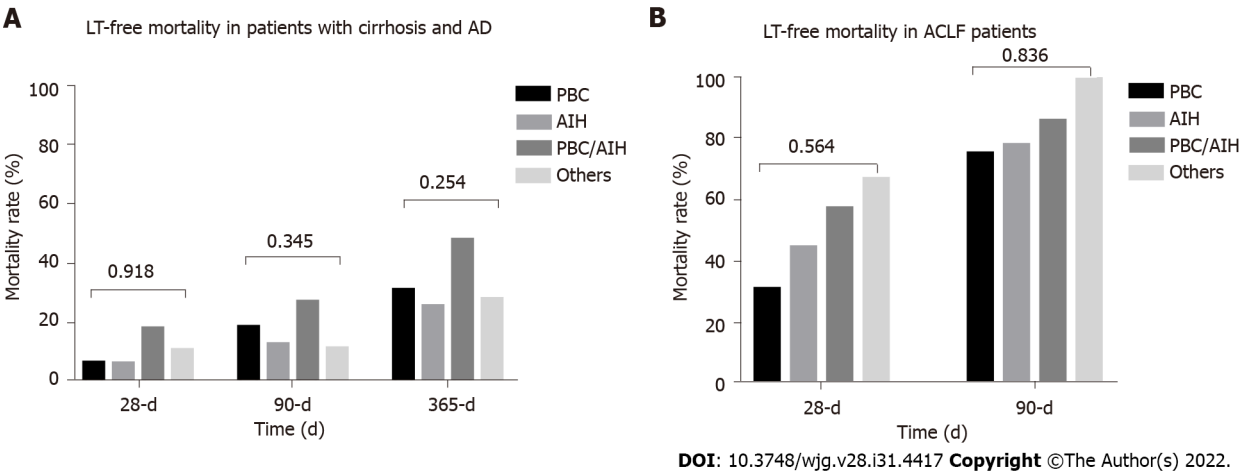

DOI: 10.3748/wjg.v28.i31.4417 **Copyright** ©The Author(s) 2022.

Figure 3 Outcomes of autoimmune liver disease patients with acute decompensated cirrhosis and acute-on-chronic liver failure. A: Liver transplantation (LT)-free mortality in patients with cirrhosis and acute decompensation; B: LT-free mortality in patients with acute-on-chronic liver failure. LT: Liver transplantation; PBC: Primary biliary cirrhosis; AIH: Autoimmune hepatitis; PBC/AIH: Primary biliary cirrhosis-autoimmune hepatitis overlap syndrome; AD: Acute decompensation; ACLF: Acute-on-chronic liver failure.

There were still several limitations in our study. First, since AILD is a relatively rare disease, the number of patients recruited in our study was not quite large, especially ACLF patients. The limited sample size could also slightly reduce the accuracy of the results of risk factor analysis. Second, one of our centers, Renji hospital, is a nationwide center of AILD. Thus, some degree of selection bias could be present in the prevalence rates of AILD due to the participation of this center. However, our further

Table 4 Association of risk factors with acute-on-chronic liver failure development during hospitalization using logistic regression in univariate and multivariate analysis

	OR	95%CI	*P* value
Univariable logistic regression			
Demographic data			
Age	0.96	0.21-6.18	0.96
Male	2.89	0.83-9.17	0.08
Etiology	0.90	0.43-1.70	0.76
Acute decompensation events			
Overt ascites	0.92	0.3-3.14	0.89
Gastrointestinal bleeding	0.74	0.11-2.9	0.7
Bacterial infection	2.22	0.69-6.95	0.17
Hepatic encephalopathy	3.6	0.51-15.95	0.13
Laboratory data			
Total bilirubin	1.68	1.14-2.61	0.012
International normalized ratio	6.53	1.9-28.55	0.006
Creatinine	0.85	0.51-1.87	0.6
Blood urea nitrogen	1.52	0.84-2.63	0.12
Albumin	0.44	0.07-3.19	0.4
ALT	1.25	0.85-1.82	0.24
AST	1.14	0.73-1.75	0.55
White blood cells	0.88	0.45-1.75	0.72
Hemoglobin	0.39	0.11-1.5	0.16
K	1.53	0.13-18.28	0.74
Sodium	0	0-288.55	0.29
Neutrophil-lymphocyte ratio	1.37	0.84-2.23	0.21
ALP	1.15	0.59-2.27	0.7
GGT	0.86	0.54-1.34	0.52
Multivariable logistic regression			
Male	3.24	0.84-11.63	0.07
TB	1.56	1.03-2.47	0.046
INR	4.31	1.15-21.70	0.048

Variables with $P < 0.1$ in univariate analysis were selected into multivariate analysis. Acute-on-chronic liver failure diagnosed on admission was excluded from the analysis. Continuous variables were log transformed before entering the model (base 2). ALT: Alanine transaminase; AST: Aspartate transaminase; ALP: Alkaline phosphatase; GGT: Gamma glutamyl transpeptidase; OR: Odds ratio; CI: Confidence interval; TB: Total bilirubin; INR: International normalized ratio.

analysis showed that patients recruited from Renji Hospital were from 20 different districts all over the country, the population distribution of these patients were also consistent with that of Chinese population density.

CONCLUSION

In conclusion, our study showed that AILD was not rare in China. The etiology of AILD had no significant impact on short-term mortality in AILD patients with cirrhosis and AD. HE, elevated levels of TB and BUN were significantly associated with high 90-d mortality in these patients. Strategies are

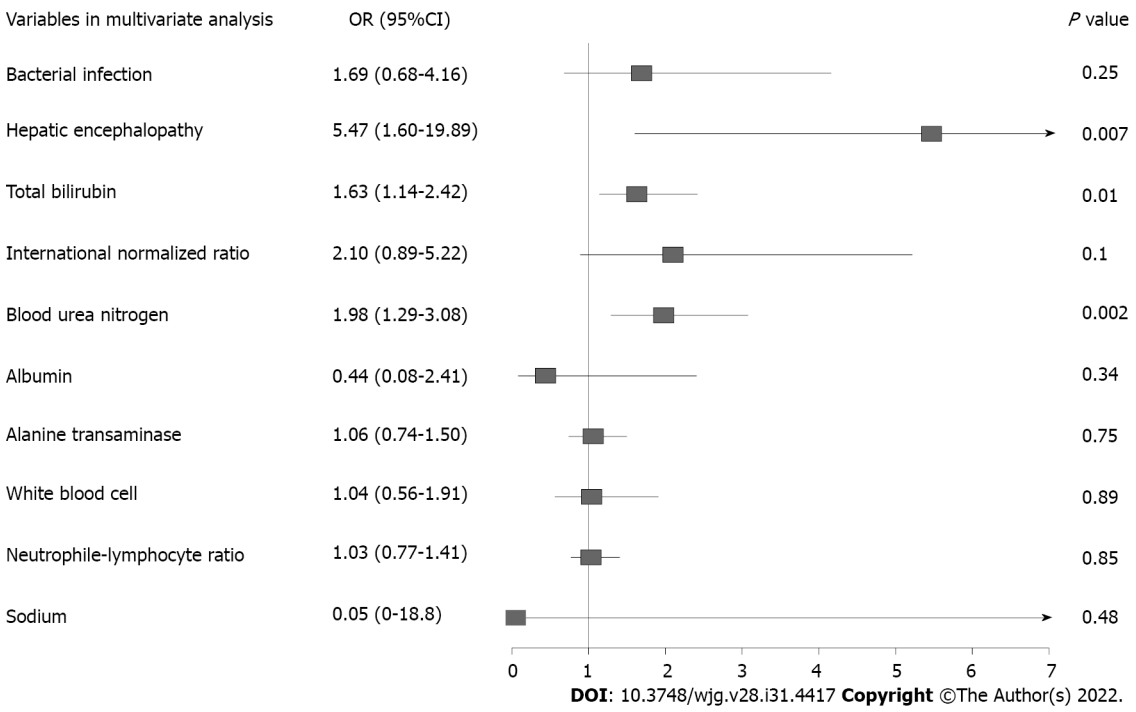

Figure 4 Multivariate analysis of 90-d liver transplantation free mortality in autoimmune liver disease patients with cirrhosis and acute decompensation. OR: Odds ratio; CI: Confidence interval.

needed to the presence of HE and closely monitor the changes of liver and renal function in clinical practice. These data will be a crucial complement to the public epidemiology of AILD in Asian-Pacific regions.

ARTICLE HIGHLIGHTS

Research background

Epidemiological research on autoimmune liver disease (AILD) in patients with end-stage liver disease is sparse in Asian-pacific areas.

Research motivation

This study aimed to provide a national view of epidemiological features of end-stage AILD in China.

Research objectives

To investigate the disease burden and risk factor of short-term mortality in AILD patients with cirrhosis and acute decompensation (AD), and thus provide clues on clinical management.

Research methods

Data were collected from two prospective, multicenter cohorts which enrolled patients with chronic liver disease and acute exacerbation from China. Logistic regression model was conducted to analyze risk factors.

Research results

The overall prevalence of AILD was 9.3% (242/2597) in patients with cirrhosis and AD, among which primary biliary cirrhosis was the most prevalent type. The etiology of AILD had no significant impact on short-term mortality in patients with cirrhosis and AD in univariate and multivariate analysis. Total bilirubin, hepatic encephalopathy (HE) and blood urea nitrogen independently correlated with 90-d LT-free mortality in multivariate analysis.

Research conclusions

AILD was not rare in hospitalized patients with cirrhosis and AD in China. 90-d mortality was independently associated with severity of the disease.

Research perspectives

In clinical management of AILD, strategies are needed to prevent presence of HE and closely monitor the changes of liver and renal function.

ACKNOWLEDGEMENTS

We acknowledge the following Chinese (Acute on) Chronic Liver Failure Consortium members and participants for their hard work. Department of Gastroenterology, Renji Hospital, School of Medicine, Shanghai Jiao Tong University - Shi-Jin Wang, Wen-Yi Gu, Liang Qiao, Yan Zhang; Clinical Research Institute, Shanghai Jiao Tong University School of Medicine, Shanghai, China, Zhang Wei-Tuo; Centre of Integrative Medicine, Beijing Ditan Hospital, Capital Medical University - Qun Zhang, Yi-Xin Hou, Yu-Xin Li, Yun-Yi Huang; Department of Infectious Diseases, Southwest Hospital, Third Military Medical University (Army Medical University) - Jie Xia; Yi Zhou; Bao-Yan Xu; Shu-Ning Sun, Yun-Jie Dan, Wen-Ting Tan; Department of Infectious Disease, Hunan Key Laboratory of Viral Hepatitis, Xiangya Hospital, Central South University - Jun Chen, Ruo-Chan Chen, Xiao-Xiao Liu; Department of Infectious Diseases, Institute of Infection and Immunology, Union Hospital, Tongji Medical College, Huazhong University of Science and Technology - Jing Liu, Ling Xu, Shue Xiong; Hepatology Unit, Department of Infectious Diseases, Nan-fang Hospital, Southern Medical University - Xiu-Hua Jiang, Bei-Ling Li, Cong-Yan Zhu; Department of Hepatology, First Hospital of Jilin University - Chang Jiang, Xiao-Yu Wen, Na Gao, Chun-Yan Liu; Department of Infectious Disease, Taihe Hospital, Hubei University of Medicine - Yuan-Yuan Chen, Sen Luo, Qing Lei; Department of Liver Intensive Care Unit, Shanghai Public Health Clinical Centre, Fudan University - Xue Mei, Liu-Juan Ji, Jie-Fei Wang; Department of Infectious Diseases and Hepatology, Second Hospital of Shandong University - Tao Li, Xuan-Qiong Fang, Zi-Yu Wang; Liver Disease Centre, First Affiliated Hospital of Xinjiang Medical University - Rong-Jiu Zheng, Nan Li; Department of Infectious Disease, Henan Provincial People's Hospital - Hui-Ming Jin; Affiliated Hospital of Logistics University of People's Armed Police Force - Hai Li, Qing Zhang, Xue-Qun Zheng; Department of Infectious Diseases, Affiliated Hospital of Logistics University of People's Armed Police Force - Shao-Yang Wang. We thank all the patients participated in the study.

FOOTNOTES

Author contributions: Shen ZX, Wu DD, Xia J, Wang XB, Zheng X, Huang Y and Li BL contributed equally to this work; Ma X and Li H contributed equally to this work; Li H generated the concept and designed the research; all authors acquired the data; Shen ZX, Wu DD performed statistical analysis; Shen ZX, Wu DD, Xia J, Wang XB generated the results; Shen ZX, Wu DD, Zheng X, Huang Y and Li BL interpreted the results; Shen ZX and Wu DD drafted the manuscript which was revised by Ma X and Li H for important intellectual content; Ma X made important contribution patient recruitment; Li H was responsible for administrative, technical, or material support and study supervision; and all authors have access to the data, approved this final version of the manuscript and are accountable for all aspects.

Supported by Shanghai Hospital Development Commission, No. SHDC2020CR1037B; the National Key R&D Program of China, No. 2017YFC0908100; the National Science and Technology Major Project, No. 2018ZX10302206, 2018ZX10723203 and 2017ZX10202202; Shanghai Municipal Education Commission-Guofeng Clinical Medicine Grant, No. 20152213; the National Natural Science Foundation of China, No. 82170629, 81930061, 81900579, 81970550, 82070613, 82070650, and 81972265; Chongqing Natural Science Foundation, No. CSTC2019jcyj-zdxmX0004; Beijing Municipal Science & Technology Commission, No. Z191100006619033; Local Innovative and Research Teams Project of Guangdong Pearl River Talents Program, No. 2017BT01S131; the Foundation for Innovative Research Groups of Hubei Provincial Natural Science Foundation, No. 2018CFA031; and Guangdong Basic and Applied Basic Research Foundation, No. 2020A1515010052.

Institutional review board statement: The study was conducted in accordance with the Declaration of Helsinki. The Medical Ethics Board of Shanghai Renji Hospital, Shanghai, China, approved the studies (ethics codes: [2014]148k and [2016]142k).

Informed consent statement: Informed consent was obtained from all patients for being included in the study.

Conflict-of-interest statement: All authors declare that they have no conflict of interest in this manuscript.

Data sharing statement: Data are available within 1 year after publication upon reasonable request *via* email: aclf_group@163.com.

STROBE statement: The authors have read the STROBE Statement-checklist of items, and the manuscript was

prepared and revised according to the STROBE Statement-checklist of items.

Country/Territory of origin: China

ORCID number: Zi-Xuan Shen 0000-0003-0122-3954; Dan-Dan Wu 0000-0002-0453-008X; Jie Xia 0000-0002-9580-7186; Xian-Bo Wang 0000-0002-3593-5741; Xin Zheng 0000-0001-6564-7807; Yan Huang 0000-0002-4747-3740; Bei-Ling Li 0000-0002-0633-5632; Zhong-Ji Meng 0000-0003-0401-535X; Yan-Hang Gao 0000-0002-6836-0614; Zhi-Ping Qian 0000-0003-4641-3348; Feng Liu 0000-0001-7060-3710; Xiao-Bo Lu 0000-0001-5532-7551; Jia Shang 0000-0001-9197-8773; Hua-Dong Yan 0000-0003-2792-7490; Yu-Bao Zheng 0000-0002-2630-2563; Wen-Yi Gu 0000-0002-1615-6064; Yan Zhang 0000-0003-0159-9062; Jian-Yi Wei 0000-0003-3897-6896; Wen-Ting Tan 0000-0002-2884-071X; Yi-Xin Hou 0000-0001-8233-7210; Qun Zhang 0000-0002-6365-0030; Yan Xiong 0000-0001-9356-4777; Cong-Cong Zou 0000-0002-9197-055X; Jun Chen 0000-0001-8320-636X; Ze-Bing Huang 0000-0003-0485-1294; Xiu-Hua Jiang 0000-0002-4646-6186; Sen Luo 0000-0001-5846-6717; Yuan-Yuan Chen 0000-0003-3587-7711; Na Gao 0000-0002-8622-9273; Jing Li 0000-0001-5878-6964; Tao Li 0000-0002-2548-5476; Guo-Hong Deng 0000-0003-1263-7220; Jin-Jun Chen 0000-0003-4275-9149; Xiong Ma 0000-0001-9616-4672; Hai Li 0000-0002-3645-6232.

S-Editor: Wang JJ
L-Editor: A
P-Editor: Wang JJ

REFERENCES

1 **Carbone M**, Neuberger JM. Autoimmune liver disease, autoimmunity and liver transplantation. *J Hepatol* 2014; **60**: 210-223 [PMID: 24084655 DOI: 10.1016/j.jhep.2013.09.020]
2 **Floreani A**, De Martin S, Secchi MF, Cazzagon N. Extrahepatic autoimmunity in autoimmune liver disease. *Eur J Intern Med* 2019; **59**: 1-7 [PMID: 30360943 DOI: 10.1016/j.ejim.2018.10.014]
3 **Chang C**, Tanaka A, Bowlus C, Gershwin ME. The use of biologics in the treatment of autoimmune liver disease. *Expert Opin Investig Drugs* 2020; **29**: 385-398 [PMID: 32102572 DOI: 10.1080/13543784.2020.1733527]
4 **Zhang H**, Yang J, Zhu R, Zheng Y, Zhou Y, Dai W, Wang F, Chen K, Li J, Wang C, Li S, Liu T, Abudumijiti H, Zhou Z, Wang J, Lu W, Xia Y, Lu J, Guo C. Combination therapy of ursodeoxycholic acid and budesonide for PBC-AIH overlap syndrome: a meta-analysis. *Drug Des Devel Ther* 2015; **9**: 567-574 [PMID: 25632224 DOI: 10.2147/DDDT.S74515]
5 **Katsumi T**, Ueno Y. Epidemiology and surveillance of autoimmune hepatitis in Asia. *Liver Int* 2022 [PMID: 34990076 DOI: 10.1111/liv.15155]
6 **Zhang L**, Bai SS. Epidemiological survey of hospitalized patients with primary biliary cirrhosis in urban areas of Hohhot. *World Latest Med Information* 2016; **16**: 6-7
7 **Jeong SH**. Current epidemiology and clinical characteristics of autoimmune liver diseases in South Korea. *Clin Mol Hepatol* 2018; **24**: 10-19 [PMID: 29307132 DOI: 10.3350/cmh.2017.0066]
8 **Abe M**, Mashiba T, Zeniya M, Yamamoto K, Onji M, Tsubouchi H; Autoimmune Hepatitis Study Group-Subgroup of the Intractable Hepato-Biliary Disease Study Group in Japan. Present status of autoimmune hepatitis in Japan: a nationwide survey. *J Gastroenterol* 2011; **46**: 1136-1141 [PMID: 21597932 DOI: 10.1007/s00535-011-0421-y]
9 **Lv T**, Chen S, Li M, Zhang D, Kong Y, Jia J. Regional variation and temporal trend of primary biliary cholangitis epidemiology: A systematic review and meta-analysis. *J Gastroenterol Hepatol* 2021; **36**: 1423-1434 [PMID: 33141955 DOI: 10.1111/jgh.15329]
10 **Gu WY**, Xu BY, Zheng X, Chen J, Wang XB, Huang Y, Gao YH, Meng ZJ, Qian ZP, Liu F, Lu XB, Shang J, Li H, Wang SY, Sun X. Acute-on-Chronic Liver Failure in China: Rationale for Developing a Patient Registry and Baseline Characteristics. *Am J Epidemiol* 2018; **187**: 1829-1839 [PMID: 29762630 DOI: 10.1093/aje/kwy083]
11 **Qiao L**, Wang X, Deng G, Huang Y, Chen J, Meng Z, Zheng X, Shi Y, Qian Z, Liu F, Gao Y, Lu X, Liu J, Gu W, Zhang Y, Wang T, Wu D, Dong F, Sun X, Li H. Cohort profile: a multicentre prospective validation cohort of the Chinese Acute-on-Chronic Liver Failure (CATCH-LIFE) study. *BMJ Open* 2021; **11**: e037793 [PMID: 33419900 DOI: 10.1136/bmjopen-2020-037793]
12 **Tsochatzis EA**, Bosch J, Burroughs AK. Liver cirrhosis. *Lancet* 2014; **383**: 1749-1761 [PMID: 24480518 DOI: 10.1016/S0140-6736(14)60121-5]
13 **Zhang Y**, Xu BY, Wang XB, Zheng X, Huang Y, Chen J, Meng ZJ, Gao YH, Qian ZP, Liu F, Lu XB, Shi Y, Shang J, Li H, Wang SY, Yin S, Sun SN, Hou YX, Xiong Y, Li BL, Lei Q, Gao N, Ji LJ, Li J, Jie FR, Zhao RH, Liu JP, Lin TF, Chen LY, Tan WT, Zhang Q, Zou CC, Huang ZB, Jiang XH, Luo S, Liu CY, Zhang YY, Li T, Ren HT, Wang SJ, Deng GH, Xiong SE, Liu XX, Wang C, Yuan W, Gu WY, Qiao L, Wang TY, Wu DD, Dong FC, Hua J. Prevalence and Clinical Significance of Portal Vein Thrombosis in Patients With Cirrhosis and Acute Decompensation. *Clin Gastroenterol Hepatol* 2020; **18**: 2564-2572.e1 [PMID: 32109631 DOI: 10.1016/j.cgh.2020.02.037]
14 **Lindor KD**, Gershwin ME, Poupon R, Kaplan M, Bergasa NV, Heathcote EJ; American Association for Study of Liver Diseases. Primary biliary cirrhosis. *Hepatology* 2009; **50**: 291-308 [PMID: 19554543 DOI: 10.1002/hep.22906]

15 **Hennes EM**, Zeniya M, Czaja AJ, Parés A, Dalekos GN, Krawitt EL, Bittencourt PL, Porta G, Boberg KM, Hofer H, Bianchi FB, Shibata M, Schramm C, Eisenmann de Torres B, Galle PR, McFarlane I, Dienes HP, Lohse AW; International Autoimmune Hepatitis Group. Simplified criteria for the diagnosis of autoimmune hepatitis. *Hepatology* 2008; **48**: 169-176 [PMID: 18537184 DOI: 10.1002/hep.22322]

16 **Chazouillères O**, Wendum D, Serfaty L, Montembault S, Rosmorduc O, Poupon R. Primary biliary cirrhosis-autoimmune hepatitis overlap syndrome: clinical features and response to therapy. *Hepatology* 1998; **28**: 296-301 [PMID: 9695990 DOI: 10.1002/hep.510280203]

17 **Moreau R**, Jalan R, Gines P, Pavesi M, Angeli P, Cordoba J, Durand F, Gustot T, Saliba F, Domenicali M, Gerbes A, Wendon J, Alessandria C, Laleman W, Zeuzem S, Trebicka J, Bernardi M, Arroyo V; CANONIC Study Investigators of the EASL–CLIF Consortium. Acute-on-chronic liver failure is a distinct syndrome that develops in patients with acute decompensation of cirrhosis. *Gastroenterology* 2013; **144**: 1426-1437, 1437.e1 [PMID: 23474284 DOI: 10.1053/j.gastro.2013.02.042]

18 **Jalan R**, Stadlbauer V, Sen S, Cheshire L, Chang YM, Mookerjee RP. Role of predisposition, injury, response and organ failure in the prognosis of patients with acute-on-chronic liver failure: a prospective cohort study. *Crit Care* 2012; **16**: R227 [PMID: 23186071 DOI: 10.1186/cc11882]

19 **Montalvo M**, Mistry E, Chang AD, Yakhkind A, Dakay K, Azher I, Kaushal A, Mistry A, Chitale R, Cutting S, Burton T, Mac Grory B, Reznik M, Mahta A, Thompson BB, Ishida K, Frontera J, Riina HA, Gordon D, Parella D, Scher E, Farkas J, McTaggart R, Khatri P, Furie KL, Jayaraman M, Yaghi S. Predicting symptomatic intracranial haemorrhage after mechanical thrombectomy: the TAG score. *J Neurol Neurosurg Psychiatry* 2019; **90**: 1370-1374 [PMID: 31427365 DOI: 10.1136/jnnp-2019-321184]

20 **Wu T**, Li J, Shao L, Xin J, Jiang L, Zhou Q, Shi D, Jiang J, Sun S, Jin L, Ye P, Yang L, Lu Y, Li T, Huang J, Xu X, Chen J, Hao S, Chen Y, Xin S, Gao Z, Duan Z, Han T, Wang Y, Gan J, Feng T, Pan C, Li H, Huang Y, Xie Q, Lin S, Li L; Chinese Group on the Study of Severe Hepatitis B (COSSH). Development of diagnostic criteria and a prognostic score for hepatitis B virus-related acute-on-chronic liver failure. *Gut* 2018; **67**: 2181-2191 [PMID: 28928275 DOI: 10.1136/gutjnl-2017-314641]

21 **Neuhauser M**, Bjornsson E, Treeprasertsuk S, Enders F, Silveira M, Talwalkar J, Lindor K. Autoimmune hepatitis-PBC overlap syndrome: a simplified scoring system may assist in the diagnosis. *Am J Gastroenterol* 2010; **105**: 345-353 [PMID: 19888204 DOI: 10.1038/ajg.2009.616]

22 **Yang F**, Wang Q, Wang Z, Miao Q, Xiao X, Tang R, Chen X, Bian Z, Zhang H, Yang Y, Sheng L, Fang J, Qiu D, Krawitt EL, Gershwin ME, Ma X. The Natural History and Prognosis of Primary Biliary Cirrhosis with Clinical Features of Autoimmune Hepatitis. *Clin Rev Allergy Immunol* 2016; **50**: 114-123 [PMID: 26411425 DOI: 10.1007/s12016-015-8516-5]

23 **Zhang X**, Chen P, Gao H, Hao S, Yang M, Zhao H, Hu J, Ma W, Li L. Bacterial Infection and Predictors of Mortality in Patients with Autoimmune Liver Disease-Associated Acute-On-Chronic Liver Failure. *Can J Gastroenterol Hepatol* 2018; **2018**: 5108781 [PMID: 29623264 DOI: 10.1155/2018/5108781]

24 **Grønbæk L**, Vilstrup H, Jepsen P. Autoimmune hepatitis in Denmark: incidence, prevalence, prognosis, and causes of death. A nationwide registry-based cohort study. *J Hepatol* 2014; **60**: 612-617 [PMID: 24326217 DOI: 10.1016/j.jhep.2013.10.020]

25 **Choudhuri G**, Somani SK, Baba CS, Alexander G. Autoimmune hepatitis in India: profile of an uncommon disease. *BMC Gastroenterol* 2005; **5**: 27 [PMID: 16098234 DOI: 10.1186/1471-230X-5-27]

World Journal of Gastroenterology

Submit a Manuscript: https://www.f6publishing.com

World J Gastroenterol 2022 August 21; 28(31): 4431-4441

DOI: 10.3748/wjg.v28.i31.4431

ISSN 1007-9327 (print) ISSN 2219-2840 (online)

ORIGINAL ARTICLE

Observational Study

Simple cholecystectomy is an adequate treatment for grade I T1bN0M0 gallbladder carcinoma: Evidence from 528 patients

Jun Shao, Hong-Cheng Lu, Lin-Quan Wu, Jun Lei, Rong-Fa Yuan, Jiang-Hua Shao

Specialty type: Gastroenterology and hepatology

Provenance and peer review: Unsolicited article; Externally peer reviewed.

Peer-review model: Single blind

Peer-review report's scientific quality classification

Grade A (Excellent): A
Grade B (Very good): B
Grade C (Good): 0
Grade D (Fair): 0
Grade E (Poor): 0

P-Reviewer: Mishra TS, India; Sahin TT, Turkey

Received: April 21, 2022
Peer-review started: April 21, 2022
First decision: May 30, 2022
Revised: June 12, 2022
Accepted: July 25, 2022
Article in press: July 25, 2022
Published online: August 21, 2022

Jun Shao, Hong-Cheng Lu, Lin-Quan Wu, Jun Lei, Rong-Fa Yuan, Jiang-Hua Shao, Department of Hepatobiliary Surgery, The Second Affiliated Hospital of Nanchang University, Nanchang 330006, Jiangxi Province, China

Corresponding author: Jiang-Hua Shao, MD, PhD, Chief Doctor, Full Professor, Department of Hepatobiliary Surgery, The Second Affiliated Hospital of Nanchang University, No. 1 Minde Road, Nanchang 330006, Jiangxi Province, China. shao5022@163.com

Abstract

BACKGROUND

T1b gallbladder carcinoma (GBC) is defined as a tumor that invades the perimuscular connective tissue without extension beyond the serosa or into the liver. However, controversy still exists over whether patients with T1b GBC should undergo cholecystectomy alone or radical GBC resection.

AIM

To explore the optimal surgical approach in patients with T1b gallbladder cancer of different pathological grades.

METHODS

Patients with T1bN0M0 GBC who underwent surgical treatment between 2000 and 2017 were included in the Surveillance, Epidemiology, and End Results database. The Kaplan-Meier method and log-rank test were used to analyze the overall survival (OS) and disease-specific survival (DSS) of patients with T1b GBC of different pathological grades. Cox regression analysis was used to identify independent predictors of mortality and explore the selection of surgical methods in patients with T1b GBC of different pathological grades and their relationship with prognosis.

RESULTS

Of the 528 patients diagnosed with T1bN0M0 GBC, 346 underwent simple cholecystectomy (SC) (65.5%), 131 underwent SC with lymph node resection (SC + LN) (24.8%), and 51 underwent radical cholecystectomy (RC) (9.7%). Without considering the pathological grade, both the OS ($P < 0.001$) and DSS ($P = 0.003$) of T1b GBC patients who underwent SC (10-year OS: 27.8%, 10-year DSS: 55.1%) alone were significantly lower than those of patients who underwent SC + LN (10-year OS: 35.5%, 10-year DSS: 66.3%) or RC (10-year OS: 50.3%, 10-year DSS: 75.9%). Analysis of T1b GBC according to pathological classification revealed no

significant difference in OS and DSS between different types of procedures in patients with grade I T1b GBC. In patients with grade II T1b GBC, obvious survival improvement was observed in the OS (P = 0.002) and DSS (P = 0.039) of those who underwent SC + LN (10-year OS: 34.6%, 10-year DSS: 61.3%) or RC (10-year OS: 50.5%, 10-year DSS: 78.8%) compared with those who received SC (10-year OS: 28.1%, 10-year DSS: 58.3%). Among patients with grade III or IV T1b GBC, SC + LN (10-year OS: 48.5%, 10-year DSS: 72.2%), and RC (10-year OS: 80%, 10-year DSS: 80%) benefited OS (P = 0.005) and DSS (P = 0.009) far more than SC (10-year OS: 20.1%, 10-year DSS: 38.1%) alone.

CONCLUSION

Simple cholecystectomy may be an adequate treatment for grade I T1b GBC, whereas more extensive surgery is optimal for grades II-IV T1b GBC.

Key Words: Gallbladder carcinoma; Tumor-node-metastasis; Survival analysis; Tumor grade; Surgical treatment

Core Tip: T1b gallbladder carcinoma (GBC) is defined as a tumor that invades the perimuscular connective tissue without extension beyond the serosa or into the liver. However, controversy still exists over whether patients with T1b GBC should undergo cholecystectomy alone or radical GBC resection. In this study, we included patients with different histological grades of T1b GBC and compared the survival time of patients who underwent simple cholecystectomy, cholecystectomy with lymph node resection, or radical cholecystectomy to explore the optimal surgical approach for these patients.

Citation: Shao J, Lu HC, Wu LQ, Lei J, Yuan RF, Shao JH. Simple cholecystectomy is an adequate treatment for grade I T1bN0M0 gallbladder carcinoma: Evidence from 528 patients. *World J Gastroenterol* 2022; 28(31): 4431-4441

URL: https://www.wjgnet.com/1007-9327/full/v28/i31/4431.htm

DOI: https://dx.doi.org/10.3748/wjg.v28.i31.4431

INTRODUCTION

Gallbladder carcinoma (GBC) is the most common malignant tumor of the biliary tract, accounting for 80%-95% of malignant tumors of the biliary tract. The overall average survival of patients with GBC is only 6 mo, and the 5-year survival rate is < 5%[1,2]. According to global cancer statistics from 2020, 115949 people have been diagnosed with GBC worldwide and 84965 have died from this condition[3]. The treatment effect of adjuvant therapy, chemotherapy, radiotherapy, and targeted therapy on GBC remains unsatisfactory despite recent improvements in diagnosis and treatment methodology, and surgical resection remains the first choice for the treatment of GBC.

Different surgical resection methods are used to treat GBC, based on staging. According to the current tumor-node-metastasis (TNM) staging system of the American Joint Committee on Cancer (AJCC) guidelines, simple cholecystectomy (SC, gallbladder removal alone) is the appropriate treatment for patients with Tis or T1a GBC, radical cholecystectomy (RC, including cholecystectomy, lymph node (LN) dissection, and liver wedge resection) or expanded radical resection of GBC is recommended for patients with T1b-T3 GBC, and surgery is not recommended for T4 GBC[4-6]. However, whether patients with T1b GBC undergo SC or RC had remained controversial for a long time. A previous study found that the long-term survival rate of patients with T1b GBC after SC was equivalent to that after RC [7]. Some studies have also found that the prognosis of patients with T1b who underwent RC of GBC is significantly improved compared to that of patients who underwent cholecystectomy alone[8,9]. Therefore, whether patients with T1b GBC undergo SC or RC remains a clinical problem that surgeons must address.

Recent studies have found that, in addition to TNM staging, tumor pathological grading plays an important role in tumor prognosis and surgical selection. Studies have pointed out that low-grade tumors in the tongue[10], breast[11], and thyroid[12] have a significantly worse prognosis than high-grade tumors in the same locations. Furthermore, studies have pointed out that the median survival of patients with grade I GBC is significantly better than that of patients with grade II-IV GBC, indicating that tumor grade is also an extremely important indicator of the prognosis of GBC[13]. However, a question worthy of discussion is whether pathological classification can be used as the basis for the selection of surgery (SC or RC) in T1b patients.

In the present study, we obtained the treatment and survival data of patients with T1b GBC from the Surveillance, Epidemiology, and End Results (SEER) database[14], analyzed the survival of patients with different histological grades of T1b GBC, and compared the survival of patients who underwent SC, cholecystectomy with LN resection, and RC to assess the optimal surgical approach.

MATERIALS AND METHODS

Data source

The SEER database was established by the National Cancer Institute and contains follow-up information from patients with cancer. We used the SEER-18 database, derived from 18 regional registries representing approximately one-third of the US population, to collect data on patients with GBC between 2000 and 2017, including patient age, sex, histological codes, tumor histology, TNM stage (6th AJCC TNM staging system), tumor grade, surgical information, and patient survival.

Study population

Tumor histology and site codes were used to identify patients in the SEER database with GBC between 2000 and 2017. A total of 15671 patients were included in this study. Patients were excluded from our study for the following reasons: patients did not undergo surgery, patients with GBC other than T1bN0M0, incomplete follow-up data, unknown surgical resection range, tumor grade, or histological data. According to the 6th edition of the AJCC staging system, all T1b patients were staged according to clinical classification based on physical examination, imaging, endoscopy, biopsy, surgical exploration, and other relevant examinations; 528 patients with T1bN0M0 GBC were included (Figure 1). According to the surgical treatment information in the SEER database, patients who underwent SC without LN resection in our study were categorized as SC, those who underwent cholecystectomy with LN resection were categorized as SC + LN, and patients who underwent cholecystectomy and any type of liver resection with extensive LN dissection were categorized as RC. The major outcomes of this study were overall survival (OS) and disease-specific survival (DSS).

Statistical analysis

Both continuous and categorical variables (such as age and sex, tumor grade, tumor histological type, surgical approach, *etc.*) are presented as numbers (n) and percentages (%). Kaplan-Meier survival curves were generated to analyze the OS and DSS between the different groups, and the *P* values for the survival curves were determined using the log-rank test. A multivariate Cox proportional hazards model was built to verify the independent role of prognostic factors, and variables with a *P* value of < 0.1 on the log-rank test were incorporated into the model. The final model was built using a stepwise selection method, and the results were presented as adjusted hazard ratios (HRs) with corresponding 95% confidence intervals (CIs) and *P* values. All *P* values were two-sided, and values of $P < 0.05$ were considered statistically significant. Statistical analyses were performed using the statistical software Statistical Product and Service Solutions (SPSS) IBM (version 19.0).

RESULTS

General characteristics of patients with T1b GBC

In this retrospective study, 528 patients had pathologically confirmed T1bN0M0 GBC between 2000 and 2017. Of these, 385 (72.9%) were women, and 143 (27.1%) were men. The histological types were adenocarcinoma (73.3%), papillary adenocarcinoma (15%), and other tissue types (11.7%). The tumor pathological classification was grade I (30.5%), grade II (50.9%), and grades III and IV (18.6%). Therefore, grade III and grade IV GBC were combined into the same subgroup for analysis in the present study as few patients had grade IV GBC. Among the 528 patients with GBC, 346 underwent SC (65.5%), 131 underwent SC + LN (24.8%), and 51 underwent RC (9.7%) (Table 1).

Univariate analysis performed using the log-rank test revealed that the histological type ($P = 0.059$) and tumor grade ($P = 0.056$) did not significantly affect the 10-year OS of patients with T1b GBC. Younger age ($P < 0.001$) and female sex ($P = 0.007$) were associated with better OS, and patients who underwent RC (50.3%) or SC + LN (35.5%) achieved better OS than those who underwent SC (27.8%) ($P < 0.001$). The 10-year DSS was not significantly affected by histological type ($P = 0.058$), similar to the OS, and DSS rates were significantly higher in younger ($P = 0.023$) and female patients ($P = 0.016$). The DSS was also significantly affected by the extent of surgery, and the 10-year DSS of patients who underwent RC (75.9%) or SC + LN (66.3%) was higher than that of patients who underwent SC (55.1%) ($P = 0.002$). Although tumor grade had no significant effect on the 10-year OS of patients with T1b GBC, we found that the 10-year DSS of patients with grade III and IV tumors (48.9%) was significantly lower than that of patients with grade I (64.7%) or II tumors (62.1%) ($P = 0.002$) (Table 1).

Table 1 General characteristics and survival data for 528 patients with T1b gallbladder cancer

Characteristics	*n* = 528, *n* (%)	10-year survival	
		OS, %	DSS, %
Age, yr			
< 70	220 (41.7)	46.4%	62.7%
≥ 70	308 (58.3)	21.9%	58.9%
		P < 0.001	*P* = 0.023
Gender			
Male	143 (27.1)	13.7	47.5
Female	385 (72.9)	37.8	64
		P = 0.007	*P* = 0.016
Grade			
Grade I	161 (30.5)	33.1	64.7
Grade II	269 (50.9)	32.6	62.1
Grade III, IV	98 (18.6)	28.6	48.9
		P = 0.056	*P* = 0.002
Histological type			
Adenocarcinoma	387 (73.3)	30.5	61.6
Papillary	79 (15.0)	40.2	61.8
Other	62 (11.7)	29	51
		P = 0.059	*P* = 0.058
Surgery			
SC	346 (65.5)	27.8	55.1
SC + LN	131 (24.8)	35.5	66.3
RC	51 (9.7)	50.3	75.9
		P < 0.001	*P* = 0.002

OS: Overall survival; DSS: Disease-specific survival; SC: Simple cholecystectomy; LN: Lymph node resection; RC: Radical cholecystectomy; N: Number.

The impact of different surgical methods on the OS and DSS of patients with T1b GBC, regardless of pathological grade

Kaplan-Meier survival curves were generated for different types of surgery in patients with T1b GBC. The 10-year OS of patients who underwent more extensive surgery, including SC + LN (35.5%) and RC (50.3%), was significantly better than that of patients who underwent SC alone (27.8%) ($P < 0.001$) (Figure 2A). Consistent with OS, we found that the 10-year DSS of patients who underwent SC + LN (66.3%) or RC (75.9%) was significantly higher than that of patients who underwent SC (55.1%) ($P = 0.003$) (Figure 2B).

Using multivariate Cox regression analysis incorporating age, sex, tumor grade, tumor histological type, and surgery type, we confirmed that age, sex, and surgery type were independently associated with OS in patients with T1b GBC. Patients who underwent SC + LN (HR: 0.71, 95%CI: 0.53-0.95, $P = 0.020$) or RC (HR: 0.54, 95%CI: 0.32-0.89, $P = 0.015$) experienced a significant OS benefit compared to patients who underwent SC alone. Independent factors affecting DSS were sex, tumor grade, and surgery type, consistent with OS, and patients who underwent SC + LN (HR: 0.56, 95%CI: 0.37-0.83, $P = 0.020$) or RC (HR: 0.49, 95%CI: 0.27-0.92, $P = 0.015$) had improved DSS compared with patients who underwent SC. Table 2 shows the results of the multivariate Cox regression analysis of patients with T1b GBC based on the 10-year OS and DSS. Based on the above results, we concluded that patients with T1b GBC who underwent RC or SC + LN treatment had better OS and DSS than those who underwent SC, regardless of the pathological grade (Table 2).

Table 2 Multivariate Cox proportional hazards model for 10-year overall survival and disease-specific survival in 528 patients with T1b gallbladder cancer

Variable	10-year overall survival		10-year disease-specific survival	
	HR (95%CI)	*P* value	HR (95%CI)	*P* value
Age, yr				
< 70	Referent		Referent	
≥ 70	2.03 (1.57-2.63)	< 0.001	NA	NA
Gender				
Male	Referent		Referent	
Female	0.71 (0.55-0.91)	0.007	0.62 (0.45-0.87)	0.005
Grade				
Grade I	Referent		Referent	
Grade II	NA	NA	1.21 (0.83-1.76)	0.321
Grade III, IV	NA	NA	2.20 (1.43-3.38)	< 0.001
Histological type				
Adenocarcinoma	Referent		Referent	
Papillary	NA	NA	NA	NA
Other	NA	NA	NA	NA
Surgery				
SC	Referent		Referent	
SC + LN	0.71 (0.53-0.95)	0.020	0.56 (0.37-0.83)	0.004
RC	0.54 (0.32-0.89)	0.015	0.49 (0.27-0.92)	0.025

SC: Simple cholecystectomy; LN: Lymph node resection; RC: Radical cholecystectomy; N: Number; HR: Hazard ratio; CI: Confidence interval; NA: Not available.

The influence of operation methods on OS and DSS in patients with T1b GBC of different pathological grades

To verify the role of tumor grading in choosing the surgical approach for patients with T1b GBC, we divided the 528 patients with GBC into three subgroups based on tumor grade and analyzed the impact of different surgical approaches in each subgroup on 10-year OS and DSS. The type of surgery varied slightly between the different tumor grades, and Figure 2C shows the proportion of different surgical approaches in each subgroup. Of the 161 patients with grade I T1b GBC, 105 underwent SC (65%), 40 underwent SC + LN (25%), and 16 underwent RC (10%); of the 269 patients with grade II T1b GBC, 173 underwent SC (64%), 64 underwent SC + LN (24%), and 32 underwent RC (12%). Of the 98 patients with grade III or IV T1b GBC, 68 underwent SC (69%), 25 underwent SC + LN (26%), and 5 underwent RC (5%) (Figure 2C). Interestingly, no statistically significant differences were observed in OS (P = 0.734) and DSS (P = 0.953) between the different surgical types in patients with grade I T1b GBC (Figure 3A and B). However, an obvious improvement in the OS of patients with grade II T1b GBC who underwent SC + LN (34.6%) or RC (50.5%) was observed compared to that of patients who underwent SC (28.1%) (P = 0.002). The DSS of patients who underwent SC + LN (61.3%) or RC (78.8%) was also much higher than that of patients who underwent SC (58.3%) (P = 0.039) (Figure 3C and D). Moreover, the OS and DSS of patients with grade III and IV T1b GBC were both significantly affected by the type of surgery, and SC + LN (48.5%) or RC (80%) had a far more beneficial effect on OS than SC (20.1%; P = 0.005). Similar to OS, the DSS in patients who underwent SC + LN (72.2%) or RC (80%) was also much higher than that of patients who underwent SC (38.1%) (P = 0.009) (Figure 3E and F). These results show that patients with grade I T1b GBC who undergo SC can attain a survival benefit equivalent to that associated with SC + LN or RC.

The influence of surgical methods on OS and DSS in patients with grade I T1b GBC

To further verify that surgery type did not significantly affect OS and DSS in patients with grade I T1b GBC, we conducted a univariate analysis of 161 patients with grade I T1b GBC. Using the log-rank test, we found that age (P = 0.022) and sex (P = 0.030) significantly affected the OS of patients with grade I

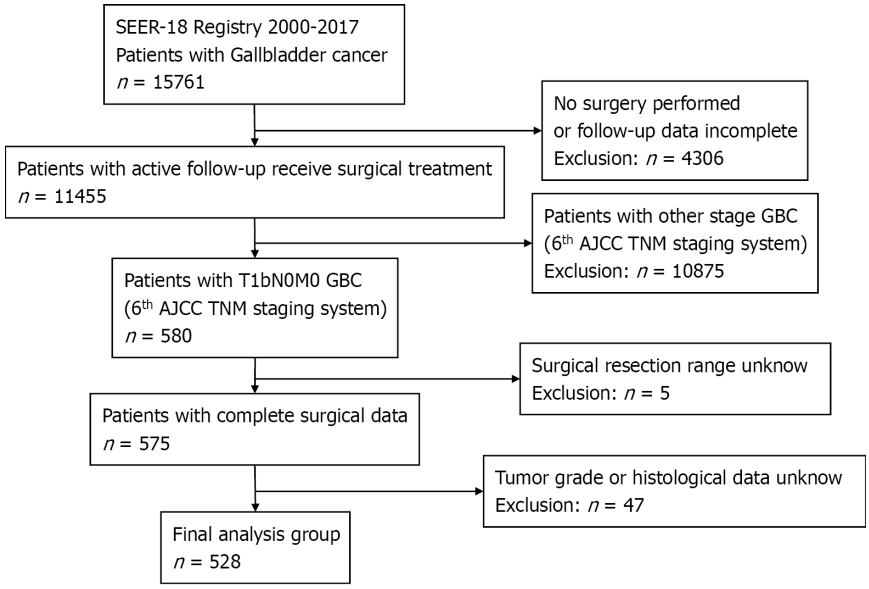

DOI: 10.3748/wjg.v28.i31.4431 **Copyright** ©The Author(s) 2022.

Figure 1 Flow diagram of the study population. A total of 528 patients with T1bN0M0 gallbladder cancer were included in this study.SEER: Surveillance, Epidemiology, and End Results database; AJCC: American Joint Committee on Cancer; TNM: Tumor-node-metastasis; GBC: Gallbladder cancer; N: Number.

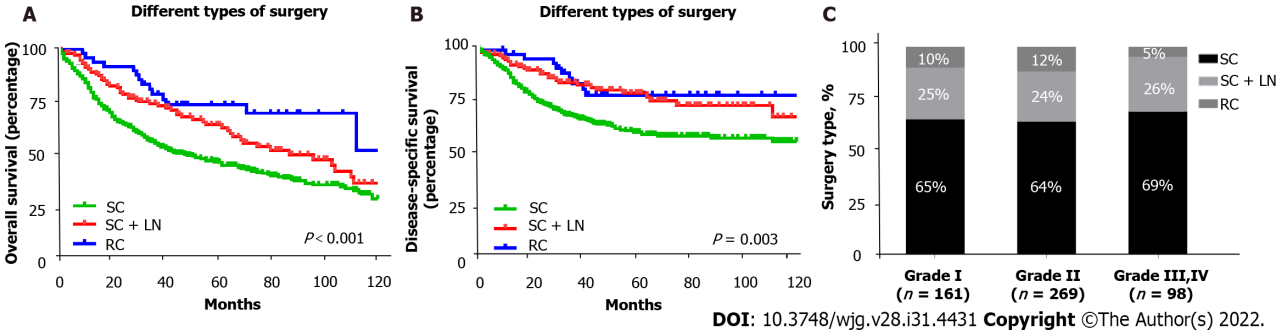

DOI: 10.3748/wjg.v28.i31.4431 **Copyright** ©The Author(s) 2022.

Figure 2 Overall survival and disease-specific survival of 528 patients with T1b gallbladder cancer who received different surgical treatment assessed using Kaplan-Meier analysis, and the proportions of different surgical approaches. A: Overall survival of patients with T1b gallbladder cancer (GBC) received simple cholecystectomy (SC), SC with lymph node resection (SC + LN), or radical cholecystectomy (RC) ($P < 0.001$); B: Disease-specific survival of patients with T1b GBC who received SC, SC + LN, or RC ($P = 0.003$); C: The proportions of different surgical approaches in patients with different pathological grades of gallbladder cancer. SC: Simple cholecystectomy; LN: Lymph node resection; RC: Radical cholecystectomy.

T1b GBC, whereas the histological type of the tumor ($P = 0.799$) and surgical method ($P = 0.734$) had no significant effect on OS. Age ($P = 0.431$), sex ($P = 0.071$), tumor histological type ($P = 0.562$), and surgical method ($P = 0.953$) did not significantly affect DSS in patients with grade I T1b GBC (Table 3).

Subsequently, we performed multivariate Cox regression analysis based on age, sex, tumor grade, tumor histological type, and surgery type and found that age and sex were independent influencing factors for OS in patients with grade I T1b GBC; older age was associated with poor OS (HR: 1.67, 95%CI: 1.07-2.59, $P = 0.023$), and women had better OS (HR: 0.62, 95%CI: 0.40-0.96, $P = 0.031$). The histological type of the tumor and surgical method were not independent factors for OS in patients with grade I T1b GBC. Age, sex, histological tumor type, and surgical method were not independent risk factors for DSS in patients with grade I T1b GBC. Lastly, we verified that the type of surgery did not affect the OS and DSS of 161 patients with grade I T1b GBC (Table 4).

DISCUSSION

The current staging of GBC follows the TNM staging system of the AJCC guidelines, in which primary tumor invasion (T) is a crucial factor in the AJCC staging criteria that determines the surgical approach for GBC[15]. The goal of surgical intervention for GBC is to achieve R0 resection, which is the most important factor in predicting long-term survival. According to the staging system of the AJCC

Table 3 General characteristics and survival data for 161 patients with grade I T1b gallbladder cancer

Characteristics	*n* = 161, *n* (%)	10-year survival	
		OS, %	DSS, %
Age, yr			
< 70	72 (41.7)	65.8	70.6
≥ 70	89 (58.3)	58.0	79.1
		$P = 0.022$[1]	$P = 0.431$
Gender			
Male	49 (27.1)	54.6	72.6
Female	112 (72.9)	63.6	75.9
		$P = 0.030$[1]	$P = 0.071$
Histological type			
Adenocarcinoma	116 (73.3)	62.8	76.2
Papillary	32 (15.0)	60.1	74.6
Other	13 (11.7)	46.2	60.6
		$P = 0.799$	$P = 0.562$
Surgery			
SC	105 (65.5)	60.1	76.1
SC + LN	41 (24.8)	65.2	75.3
RC	15 (9.7)	56.6	67.0
		$P = 0.734$	$P = 0.953$

[1]$P < 0.05$.

OS: Overall survival; DSS: Disease-specific survival; SC: Simple cholecystectomy; LN: Lymph node resection; RC: Radical cholecystectomy; N: Number.

guidelines, Tis refers to the tumor in situ, T1a lesions invade the lamina propria, T1b lesions invade the muscular layer, T2 Lesions invade the connective tissue around the gallbladder muscle without extending to the serosal membrane or liver, T3 tumors perforate the gallbladder serosa or penetrate the liver or one other adjacent organ, and T4 tumors are defined as those that invade the main portal vein, hepatic artery, or two or more adjacent organs[16]. According to the recommendations of the National Comprehensive Cancer Network (NCCN) diagnosis and treatment guidelines, surgical treatment for Tis and T1a GBC should be SC, and RC is the first choice for the treatment of GBC with T1b-T3, whereas surgery is not recommended for T4[17]. Nevertheless, previous studies have also pointed out the controversy in the treatment of T1b, and some studies still reported long-term survival after SC for patients with T1b GBC that is comparable to that after radical resection and did not recommend extended cholecystectomy or radical resection for T1b GBC[18,19]. Therefore, controversy about the surgical treatment of T1b GBC has existed in clinical practice for many years. For example: (1) Should patients with GBC diagnosed as T1b by pathology undergo radical resection; (2) incidental CBC (IGBC) is defined as cholecystectomy for benign gallbladder lesions, but the postoperative pathological diagnosis is GBC[20,21]; and (3) should patients with T1b IGBC undergo another surgical procedure so that RC can be performed?

Tumor grade was categorized as well-differentiated (grade I), moderately differentiated (grade II), poorly differentiated (grade III), or undifferentiated (grade IV), depending on the pathological morphology of the tumor. As an important tumor index, pathological grading plays a crucial role in the prognosis and treatment of many tumors. For example, patients with differentiated T1N0M0 thyroid cancer should undergo total thyroidectomy, whereas patients with undifferentiated T1N0M0 thyroid cancer require total thyroidectomy and LN dissection[22]. However, to our knowledge, the role of tumor grade in the selection of surgical treatment for T1b GBC has not yet been explored. In our study, 528 cases of T1bN0M0 GBC were grouped according to the pathological grade. By analyzing the survival of patients with various pathological grades of GBC following different surgical methods, we found that both DSS and OS of patients with grade II-IV T1b GBC who underwent extensive surgery improved markedly compared to those who underwent SC. However, SC had a comparable survival benefit for both OS and DSS in patients with grade I T1b GBC compared to patients who underwent SC + LN or RC. Using Cox regression analysis, we also found that surgery type was not an independent

Table 4 Multivariate Cox proportional hazards model for 10-year overall survival and disease-specific survival in 161 patients with grade I T1b gallbladder cancer

Variable	10-year overall survival		10-year disease-specific survival	
	HR (95%CI)	*P* value	HR (95%CI)	*P* value
Age, yr				
< 70	Referent		Referent	
≥ 70	1.67 (1.07-2.59)	0.023	NA	NA
Gender				
Male	Referent		Referent	
Female	0.62 (0.40-0.96)	0.031	NA	NA
Histological type				
Adenocarcinoma	Referent		Referent	
Papillary	NA	NA	NA	NA
Other	NA	NA	NA	NA
Surgery				
SC	Referent		Referent	
SC + LN	NA	NA	NA	NA
RC	NA	NA	NA	NA

SC: Simple cholecystectomy; LN: Lymph node resection; RC: Radical cholecystectomy; N: Number; HR: Hazard ratio; CI: Confidence interval; NA: Not available.

factor associated with survival in patients with grade I T1b GBC. These results indicate that the surgery type does not significantly affect OS or DSS in patients with grade I T1b GBC. Patients with grade I T1b GBC who undergo SC alone could obtain a similar survival benefit compared with those treated with SC + LN or RC, and more extensive surgery is the optimal treatment for T1b patients with grade II-IV tumors.

Thus, according to the NCCN guidelines and our research results, we propose the following answers to the two questions given above: (1) For GBC found during the operation, if perioperative frozen pathological examination reveals the TNM stage to be T1b, tumor histopathology should continue to be graded. If the pathological grade is confirmed to be grade I T1b GBC, SC should be performed, and patients with grade II-IV T1b GBC should undergo RC; and (2) for patients with T1b IGBC, the finding should be combined with the pathological grade to decide whether to perform surgery again; patients with grade II-IV T1b IGBC should undergo a second operation and radical resection of GBC to obtain survival benefits. Patients with grade I T1b IGBC do not need to undergo reoperation, which prevents the pain caused by the second operation and saves the patient money in terms of medical expenses.

To the best of our knowledge, this study is the first to use the SEER database, one of the largest population databases, to evaluate the role of tumor grading in choosing surgical approaches for patients with T1b GBC. However, our findings have some unavoidable limitations. First, this study is a retrospective analysis, and the SEER database lists only initial surgical treatment, so patients who underwent subsequent treatment may be included in our study. Furthermore, information on tumor recurrence, metastasis, or progression was also not available in the SEER database. Hence, prospective and multi-center studies of patients with T1b GBC are needed to further verify the impact of surgical methods on the prognosis of T1b patients with different pathological grades to provide a more appropriate, evidence-based rationale for determining the optimal surgical method for patients with T1b GBC of different pathological grades, and patients with grade I T1b GBC who underwent SC should be monitored for tumor recurrence, metastasis, or progression to validate the findings of our study.

CONCLUSION

We demonstrated a comparable survival benefit for patients with grade I T1b GBC who underwent SC, SC + LN or RC, whereas patients with grade II-IV T1b GBC benefit from SC + LN or RC, suggesting that SC may be a suitable treatment for patients with grade I T1b GBC, whereas RC or expanded radical resection is more suitable for those with grade II-IV T1b GBC.

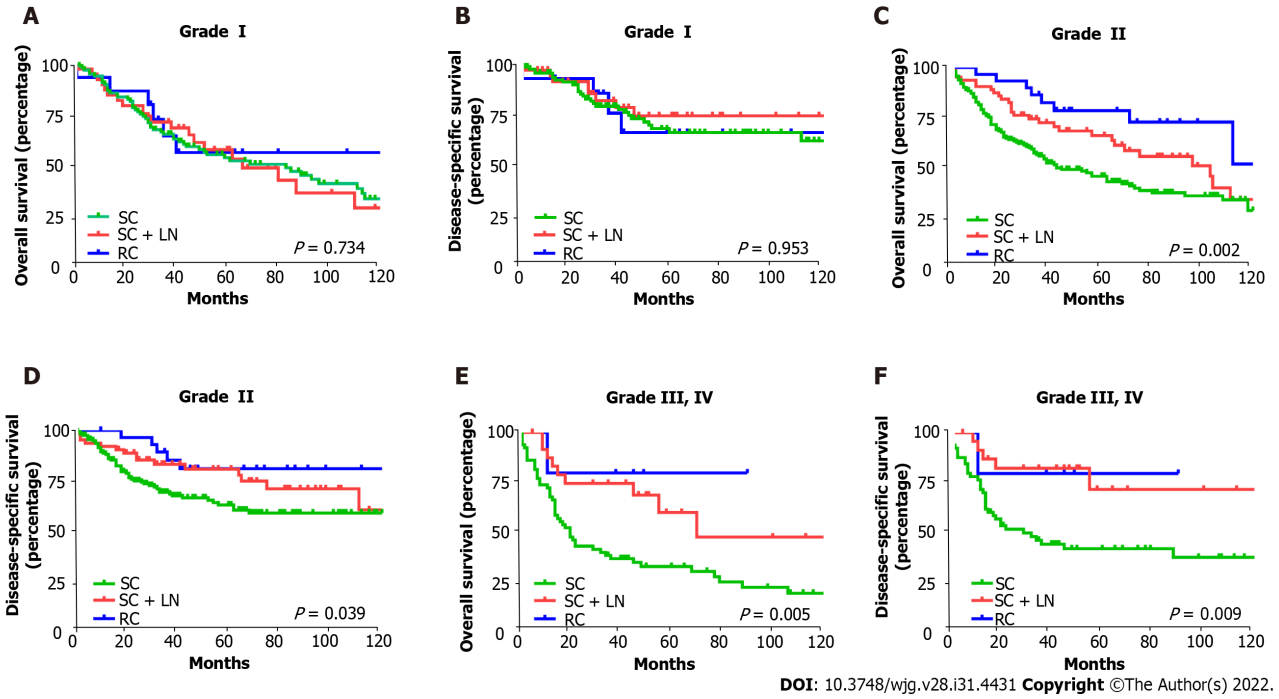

DOI: 10.3748/wjg.v28.i31.4431

Figure 3 The overall survival and disease-specific survival of patients with T1b gallbladder cancer stratified by pathological grades and surgical treatment using Kaplan-Meier analysis. A: Overall survival (OS) of patients with grade I T1b gallbladder cancer (GBC) by type of surgery (P = 0.734); B: Disease-specific survival (DSS) of patients with grade I T1b GBC by type of surgery (P = 0.953); C: OS of patients with grade II T1b GBC by type of surgery (P = 0.002); D: DSS of patients with grade II T1b GBC by type of surgery (P = 0.039); E: OS of patients with grade III, IV T1b GBC by type of surgery (P = 0.005); F: DSS of patients with grade III, IV T1b GBC by type of surgery (P = 0.009). SC: Simple cholecystectomy; LN: Lymph node resection; RC: Radical cholecystectomy.

ARTICLE HIGHLIGHTS

Research background

The surgical treatment of T1b gallbladder cancer has been controversial.

Research motivation

To solve the problem of choosing the surgical treatment for T1b gallbladder cancer.

Research objectives

To explore the optimal surgical approach in patients with T1b gallbladder cancer of different pathological grades.

Research methods

Analysis of survival differences in patients with different pathological grades of T1b gallbladder cancer who received different surgical treatment methods.

Research results

Patients with grade I T1b gallbladder cancer who underwent simple cholecystectomy attained a survival benefit equivalent to that of simple cholecystectomy with lymph node resection or radical cholecystectomy.

Research conclusions

Simple cholecystectomy is an adequate treatment for grade I T1b gallbladder carcinoma (GBC), whereas expanded radical resection is more suitable for grade II-IV T1b GBC.

Research perspectives

Simple cholecystectomy is a suitable treatment for patients with grade I T1b GBC.

ACKNOWLEDGEMENTS

The authors acknowledge the efforts of the SEER Program tumor registries in providing high-quality open resources for research.

FOOTNOTES

Author contributions: Shao J and Lu HC contributed equally to this work; Shao J, Shao JH, and Lu HC were involved in study concept and design, drafting of the manuscript and study supervision; Wu LQ contributed to collect data; Lei J and Yuan RF contributed to analyze the data; Shao JH, Shao J, and Lu HC critically revise the manuscript; all authors have read and approve the final manuscript.

Supported by the National Natural Science Foundation of China, No. 81773126, No. 81560475, and No. 82160486.

Institutional review board statement: The study was reviewed and approved by the Second Affiliated Hospital of Nanchang University Institutional Review Board, No. 74.

Informed consent statement: Patients from the Surveillance, Epidemiology, and End Results (SEER) database consented to participate in any scientific research worldwide.

Conflict-of-interest statement: There are no conflicts of interest to report.

Data sharing statement: The datasets used or analyzed in this study are available from the corresponding author at shao5022@163.com. Patients from the Surveillance, Epidemiology, and End Results (SEER) database consented to participate in any scientific research worldwide.

STROBE statement: The authors have read the STROBE Statement—checklist of items, and the manuscript was prepared and revised according to the STROBE Statement—checklist of items.

Country/Territory of origin: China

ORCID number: Hong-Cheng Lu 0000-0002-7053-6068; Jun Lei 0000-0002-8338-4972; Jiang-Hua Shao 0000-0002-1490-4102.

S-Editor: Chen YL
L-Editor: A
P-Editor: Chen YL

REFERENCES

1 **Lai CH**, Lau WY. Gallbladder cancer--a comprehensive review. *Surgeon* 2008; **6**: 101-110 [PMID: 18488776 DOI: 10.1016/s1479-666x(08)80073-x]
2 **Duffy A**, Capanu M, Abou-Alfa GK, Huitzil D, Jarnagin W, Fong Y, D'Angelica M, Dematteo RP, Blumgart LH, O'Reilly EM. Gallbladder cancer (GBC): 10-year experience at Memorial Sloan-Kettering Cancer Centre (MSKCC). *J Surg Oncol* 2008; **98**: 485-489 [PMID: 18802958 DOI: 10.1002/jso.21141]
3 **Sung H**, Ferlay J, Siegel RL, Laversanne M, Soerjomataram I, Jemal A, Bray F. Global Cancer Statistics 2020: GLOBOCAN Estimates of Incidence and Mortality Worldwide for 36 Cancers in 185 Countries. *CA Cancer J Clin* 2021; **71**: 209-249 [PMID: 33538338 DOI: 10.3322/caac.21660]
4 **Misra MC**, Guleria S. Management of cancer gallbladder found as a surprise on a resected gallbladder specimen. *J Surg Oncol* 2006; **93**: 690-698 [PMID: 16724357 DOI: 10.1002/jso.20537]
5 **Reid KM**, Ramos-De la Medina A, Donohue JH. Diagnosis and surgical management of gallbladder cancer: a review. *J Gastrointest Surg* 2007; **11**: 671-681 [PMID: 17468929 DOI: 10.1007/s11605-006-0075-x]
6 **Kanthan R**, Senger JL, Ahmed S, Kanthan SC. Gallbladder Cancer in the 21st Century. *J Oncol* 2015; **2015**: 967472 [PMID: 26421012 DOI: 10.1155/2015/967472]
7 **Benson AB 3rd**, Abrams TA, Ben-Josef E, Bloomston PM, Botha JF, Clary BM, Covey A, Curley SA, D'Angelica MI, Davila R, Ensminger WD, Gibbs JF, Laheru D, Malafa MP, Marrero J, Meranze SG, Mulvihill SJ, Park JO, Posey JA, Sachdev J, Salem R, Sigurdson ER, Sofocleous C, Vauthey JN, Venook AP, Goff LW, Yen Y, Zhu AX. NCCN clinical practice guidelines in oncology: hepatobiliary cancers. *J Natl Compr Canc Netw* 2009; **7**: 350-391 [PMID: 19406039 DOI: 10.6004/jnccn.2009.0027]

8 **Wagholikar GD**, Behari A, Krishnani N, Kumar A, Sikora SS, Saxena R, Kapoor VK. Early gallbladder cancer. *J Am Coll Surg* 2002; **194**: 137-141 [PMID: 11848630 DOI: 10.1016/s1072-7515(01)01136-x]

9 **Cucinotta E**, Lorenzini C, Melita G, Iapichino G, Currò G. Incidental gall bladder carcinoma: does the surgical approach influence the outcome? *ANZ J Surg* 2005; **75**: 795-798 [PMID: 16173995 DOI: 10.1111/j.1445-2197.2005.03528.x]

10 **Chuang ST**, Chen CC, Yang SF, Chan LP, Kao YH, Huang MY, Tang JY, Huang CM, Huang CJ. Tumor histologic grade as a risk factor for neck recurrence in patients with T1-2N0 early tongue cancer. *Oral Oncol* 2020; **106**: 104706 [PMID: 32330684 DOI: 10.1016/j.oraloncology.2020.104706]

11 **Metzger-Filho O**, Ferreira AR, Jeselsohn R, Barry WT, Dillon DA, Brock JE, Vaz-Luis I, Hughes ME, Winer EP, Lin NU. Mixed Invasive Ductal and Lobular Carcinoma of the Breast: Prognosis and the Importance of Histologic Grade. *Oncologist* 2019; **24**: e441-e449 [PMID: 30518616 DOI: 10.1634/theoncologist.2018-0363]

12 **Ho AS**, Luu M, Barrios L, Balzer BL, Bose S, Fan X, Walgama E, Mallen-St Clair J, Alam U, Shafqat I, Lin DC, Chen Y, Van Eyk JE, Maghami EG, Braunstein GD, Sacks WL, Zumsteg ZS. Prognostic Impact of Histologic Grade for Papillary Thyroid Carcinoma. *Ann Surg Oncol* 2021; **28**: 1731-1739 [PMID: 32808161 DOI: 10.1245/s10434-020-09023-2]

13 **Shibata K**, Uchida H, Iwaki K, Kai S, Ohta M, Kitano S. Lymphatic invasion: an important prognostic factor for stages T1b-T3 gallbladder cancer and an indication for additional radical resection of incidental gallbladder cancer. *World J Surg* 2009; **33**: 1035-1041 [PMID: 19225832 DOI: 10.1007/s00268-009-9950-4]

14 **Doll KM**, Rademaker A, Sosa JA. Practical Guide to Surgical Data Sets: Surveillance, Epidemiology, and End Results (SEER) Database. *JAMA Surg* 2018; **153**: 588-589 [PMID: 29617544 DOI: 10.1001/jamasurg.2018.0501]

15 **Giannis D**, Cerullo M, Moris D, Shah KN, Herbert G, Zani S, Blazer DG 3rd, Allen PJ, Lidsky ME. Validation of the 8th Edition American Joint Commission on Cancer (AJCC) Gallbladder Cancer Staging System: Prognostic Discrimination and Identification of Key Predictive Factors. *Cancers (Basel)* 2021; **13** [PMID: 33535552 DOI: 10.3390/cancers13030547]

16 **Liao X**, Zhang D. The 8th Edition American Joint Committee on Cancer Staging for Hepato-pancreato-biliary Cancer: A Review and Update. *Arch Pathol Lab Med* 2021; **145**: 543-553 [PMID: 32223559 DOI: 10.5858/arpa.2020-0032-RA]

17 **Benson AB 3rd**, D'Angelica MI, Abbott DE, Abrams TA, Alberts SR, Saenz DA, Are C, Brown DB, Chang DT, Covey AM, Hawkins W, Iyer R, Jacob R, Karachristos A, Kelley RK, Kim R, Palta M, Park JO, Sahai V, Schefter T, Schmidt C, Sicklick JK, Singh G, Sohal D, Stein S, Tian GG, Vauthey JN, Venook AP, Zhu AX, Hoffmann KG, Darlow S. NCCN Guidelines Insights: Hepatobiliary Cancers, Version 1.2017. *J Natl Compr Canc Netw* 2017; **15**: 563-573 [PMID: 28476736 DOI: 10.6004/jnccn.2017.0059]

18 **Lee H**, Kwon W, Han Y, Kim JR, Kim SW, Jang JY. Optimal extent of surgery for early gallbladder cancer with regard to long-term survival: a meta-analysis. *J Hepatobiliary Pancreat Sci* 2018; **25**: 131-141 [PMID: 29117469 DOI: 10.1002/jhbp.521]

19 **Kim HS**, Park JW, Kim H, Han Y, Kwon W, Kim SW, Hwang YJ, Kim SG, Kwon HJ, Vinuela E, Járufe N, Roa JC, Han IW, Heo JS, Choi SH, Choi DW, Ahn KS, Kang KJ, Lee W, Jeong CY, Hong SC, Troncoso A, Losada H, Han SS, Park SJ, Yanagimoto H, Endo I, Kubota K, Wakai T, Ajiki T, Adsay NV, Jang JY. Optimal surgical treatment in patients with T1b gallbladder cancer: An international multicenter study. *J Hepatobiliary Pancreat Sci* 2018; **25**: 533-543 [PMID: 30562839 DOI: 10.1002/jhbp.593]

20 **Hickman L**, Contreras C. Gallbladder Cancer: Diagnosis, Surgical Management, and Adjuvant Therapies. *Surg Clin North Am* 2019; **99**: 337-355 [PMID: 30846038 DOI: 10.1016/j.suc.2018.12.008]

21 **Varshney S**, Butturini G, Gupta R. Incidental carcinoma of the gallbladder. *Eur J Surg Oncol* 2002; **28**: 4-10 [PMID: 11869005 DOI: 10.1053/ejso.2001.1175]

22 **Perrier ND**, Brierley JD, Tuttle RM. Differentiated and anaplastic thyroid carcinoma: Major changes in the American Joint Committee on Cancer eighth edition cancer staging manual. *CA Cancer J Clin* 2018; **68**: 55-63 [PMID: 29092098 DOI: 10.3322/caac.21439]

World Journal of Gastroenterology

Submit a Manuscript: https://www.f6publishing.com

World J Gastroenterol 2022 August 21; 28(31): 4442-4455

DOI: 10.3748/wjg.v28.i31.4442

ISSN 1007-9327 (print) ISSN 2219-2840 (online)

META-ANALYSIS

Current standard values of health utility scores for evaluating cost-effectiveness in liver disease: A meta-analysis

Tomohiro Ishinuki, Shigenori Ota, Kohei Harada, Masaki Kawamoto, Makoto Meguro, Goro Kutomi, Hiroomi Tatsumi, Keisuke Harada, Koji Miyanishi, Toru Kato, Toshio Ohyanagi, Thomas T Hui, Toru Mizuguchi

Specialty type: Gastroenterology and hepatology

Provenance and peer review: Invited article; Externally peer reviewed.

Peer-review model: Single blind

Peer-review report's scientific quality classification

Grade A (Excellent): 0
Grade B (Very good): B
Grade C (Good): C
Grade D (Fair): D
Grade E (Poor): 0

P-Reviewer: Jin X, China; Jing X, China; Yeo W, China
A-Editor: Yao QG, China

Received: January 13, 2022
Peer-review started: January 13, 2022
First decision: April 16, 2022
Revised: April 26, 2022
Accepted: July 24, 2022
Article in press: July 24, 2022
Published online: August 21, 2022

Tomohiro Ishinuki, Toru Mizuguchi, Department of Nursing, Surgical Sciences, Sapporo Medical University, Sapporo 0608556, Japan

Shigenori Ota, Goro Kutomi, Toru Kato, Departments of Surgery, Surgical Science and Oncology, Sapporo Medical University, Sapporo 0608543, Japan

Kohei Harada, Department of Radiology, Sapporo Medical University, Sapporo 0608543, Japan

Masaki Kawamoto, Departments of Surgery, Nemuro City Hospital, Nemuro 0870008, Japan

Makoto Meguro, Departments of Surgery, Sapporo Satozuka Hospital, Sapporo 0040811, Japan

Hiroomi Tatsumi, Department of Intensive Care Medicine, Sapporo Medical University, Sapporo 0608543, Japan

Keisuke Harada, Department of Emergency Medicine, Sapporo Medical University, Sapporo 0608543, Japan

Koji Miyanishi, Department of Medical Oncology, Sapporo Medical University, Sapporo 0608543, Japan

Toshio Ohyanagi, Department of Liberal Arts and Sciences, Center for Medical Education, Sapporo Medical University, Sapporo 0608556, Japan

Thomas T Hui, Departments of Surgery, Stanford University School of Medicine, Stanford, 94598, United States

Corresponding author: Toru Mizuguchi, MD, PhD, Professor, Department of Nursing, Surgical Sciences, Sapporo Medical University, S1, W17, Chuo-ku, Sapporo 0608556, Japan.
tmizu@sapmed.ac.jp

Abstract

BACKGROUND

Health utility assessments have been developed for various conditions, including chronic liver disease. Health utility scores are required for socio-economic evaluations, which can aid the distribution of national budgets. However, the standard health utility assessment scores for specific health conditions are largely unknown.

AIM
To summarize the health utility scores, including the EuroQOL 5-dimensions 5-levels (EQ-5D-5L), EuroQol-visual analogue scale, short from-36 (SF-36), RAND-36, and Health Utilities Index (HUI)-Mark2/Mark3 scores, for the normal population and chronic liver disease patients.

METHODS
A systematic literature search of PubMed and MEDLINE, including the Cochrane Library, was performed. Meta-analysis was performed using the RevMan software. Multiple means and standard deviations were combined using the StatsToDo online web program.

RESULTS
The EQ-5D-5L and SF-36 can be used for health utility evaluations during antiviral therapy for hepatitis C. HUI-Mark2/Mark3 indicated that the health utility scores of hepatitis B patients are roughly 30% better than those of hepatitis C patients.

CONCLUSION
The EQ-5D-5L is the most popular questionnaire for health utility assessments. Health assessments that allow free registration would be useful for evaluating health utility in patients with liver disease.

Key Words: Quality of life; EuroQOL 5-dimensions 5-levels; Short from-36; RAND-36; Health Utilities Index-Mark

Core Tip: This study summarized current knowledge about health utility assessments, including the EuroQOL 5-dimensions 5-levels (EQ-5D-5L), EuroQol-visual analogue scale, short from-36, RAND-36, and Health Utilities Index-Mark2/Mark3. The EQ-5D-5L is the most popular questionnaire for health utility assessments. Health utility assessments need to be used widely and routinely.

Citation: Ishinuki T, Ota S, Harada K, Kawamoto M, Meguro M, Kutomi G, Tatsumi H, Harada K, Miyanishi K, Kato T, Ohyanagi T, Hui TT, Mizuguchi T. Current standard values of health utility scores for evaluating cost-effectiveness in liver disease: A meta-analysis. *World J Gastroenterol* 2022; 28(31): 4442-4455
URL: https://www.wjgnet.com/1007-9327/full/v28/i31/4442.htm
DOI: https://dx.doi.org/10.3748/wjg.v28.i31.4442

INTRODUCTION

The quality of health is an important factor when assessing medical management rather than simple survival periods[1,2]. Health utility is an important factor in medical assessments and socio-economic politics[3]. National health budgets have risen steadily in various countries, and governments need to deeply consider the need to maintain a socio-economic balance[4]. Therefore, health benefits should be compared with social costs to avoid national financial collapse.

It is difficult to quantify health quality at regular intervals[5]. We are developing wearable devices that can automatically obtain health data, including data regarding mental health. Some health utility assessments require the use of questionnaires, which are associated with low compliance and involve bothersome calculations[2,6,7]. Before launching our novel health utility assessment tool, we performed this meta-analysis in order to summarize the currently available health utility assessment tools. The most useful questionnaire for evaluating health status depending on liver disease status or sex is unclear. In addition, no universal health utility assessment values for specific liver diseases or the normal population have been reported. Therefore, we conducted a meta-analysis to estimate health utility assessment values for specific populations.

The EuroQOL 5-dimensions 5-levels (EQ-5D-5L) is the simplest instrument for evaluating health utility and has been widely translated into various languages with high reliability and validity[6,8-10]. It only involves five questions and five answering levels. The health utility scores produced by the EQ-5D-5L can be used to calculate quality-adjusted life year (QALY) values[8]. The Health Utilities Index Mark 2/Mark 3 is another instrument for evaluating health utility scores and can also be used to obtain QALY values[11]. However, the Health Utilities Index is complicated, as it involves 45 questions, which take a long time to answer. The short-form 36-item (SF-36) is also widely used to evaluate health quality, although it does not directly involve QALY evaluations[9,12,13].

There are two types of SF-36, and the copyrights to these tools belong to The RAND Corporation (Santa Monica, CA, United States)[14] and QualityMetric (Johnston, RI, United States), respectively[15]. However, most researchers do not actively consider which version they use[12]. Therefore, the exact method and results of such assessments are not always described in the literature (Table 1).

In this meta-analysis, we describe the scores obtained with various health utility indexes (HUIs) in normal healthy populations or patients with different types of liver disease (Table 2)[16-32].

MATERIALS AND METHODS

Literature search

The PICOS scheme was used to set appropriate inclusion criteria. A systematic literature search of PubMed and MEDLINE, including the Cochrane Library, was performed independently by two authors (Ishunuki T and Ota S). The search was limited to human studies whose findings were reported in English. No restrictions were placed on the type of publication, the publication date, or publication status. The search strategy was based on different combinations of words for each database. For the PubMed database, the following combination was used: (("liver"[MeSH Terms] OR "liver"[All Fields] OR "livers"[All Fields] OR "liver s"[All Fields]) AND "qol"[All Fields]) AND (1990/1/1: 3000/12/12[pdat]). For the MEDLINE database, the following combination was used: [quality of life (QOL) and Liver].

Study selection

The two independent authors screened the titles and abstracts of the primary studies identified in the database search. Duplicate studies were excluded. The following inclusion criteria were employed for the meta-analysis: (1) Studies that compared QOL in patients who had liver disease; (2) Studies that compared QOL between male and female patients with liver disease; (3) Studies that reported at least one QOL outcome; and (4) If the same institute reported more than one study, only the most recent or the highest-level study was included.

Data extraction

The same two authors extracted the following primary data: (1) The questionnaires used for each QOL evaluation; (2) The first author, year of publication, and type of study; (3) The etiology of the disease and the number of times each intervention was performed; and (4) The timing of the evaluations.

Statistical analysis

Meta-analyses were performed using the RevMan software (version 5.3.; The Cochrane Collaboration). The mean differences (MD) between groups were calculated for continuous variables. The interquartile ranges of the data were transformed by dividing them by 1.35 to produce alternative standard deviation values. Multiple means and standard deviations were combined using the StatsToDo online web program (https://www.statstodo.com/index.php).

The chi-square test was used to evaluate heterogeneity, and the Cochran Q and I^2 statistics were reported. The I^2 value describes the percentage variation between studies in degrees of freedom. P values of <0.05 were considered significant.

RESULTS

EQ-5D-5L

The EQ-5D-5L has been widely investigated as a tool for evaluating general health in normal populations and patients with different stages of liver disease (Table 3)[17,18,22,25-27,30,32]. Health utility indices should be affected by age, sex, ethics, religion, and geography. However, the EQ-5D-5L produced similar utility indices for groups with different health statuses (Table 3), such as normal healthy individuals (0.8413 ± 0.1905) and hepatitis C virus (HCV)-infected patients with compensated or decompensated cirrhosis (0.8113 ± 0.2261 and 0.7903 ± 0.2182), HCV-infected patients exhibiting a sustained virologic response (SVR) (0.846 ± 0.1816), and patients with hepatocellular carcinoma 0.8127 ± 0.2084).

In general, the EQ-5D-5L produces significantly higher scores in males than in females (Figure 1A) (0.8267 ± 0.229 *vs* 0.7922 ± 0.239; $P < 0.001$). The mean total EuroQol-visual analogue scale score for the general population was found to be 79.796 ± 17.614 in two independent studies (Table 4)[26,30].

SF-36

The SF-36 consists of eight scales, including physical functioning (85.07 ± 15.40); role limitations due to physical health problems (RP)(82.50 ± 25.15); bodily pain (BP) (77.62 ± 17.55); general health perceptions

Table 1 Current health-related outcome for liver disease

Questionnaire	Total	Permission	Company/Organization
EQ-5D-5L	Five questions	Registration required	The EuroQol Research Foundation.
Health Utilities Index Mark 2 or 3	45 questions	Purchase required	Health Utilities Inc.
36-Item Short Form Survey	36 questions	Purchase required	QualityMetric
	36 questions	Free	The RAND Corporation

EQ-5D-5L: EuroQol 5-dimensions 5-levels.

Table 2 List of previous studies and health utility assessments

Ref.	Subjects and countries	EQ-5D-5L	EQ-VAS	HUI-mark	SF-36	Type of SF-36	Others
Jenkinson *et al*[16]	Normal population from United Kingdom				O	RAND®	
Ratcliffe *et al*[17]	Normal population/Liver transplantation patients from United Kingdom	Δ	Δ		O	Not described[1]	
Chong *et al*[18]	Normal population from Canada	O	Δ	Δ	Δ[1]		
Grieve *et al*[19]	Population from United Kingdom	O					
Bondini *et al*[20]	Population from United States			O	Δ[1]		CLDQ
Dan *et al*[21]	Population from United States			O			SF-6D
Björnsson *et al*[22]	Population from Sweden	O			O	Not described[1]	
Hsu *et al*[23]	Population from Vancouver				O	v2	HQLQv2
McDonald *et al*[24]	Population from United Kingdom	O					
Scalone *et al*[25]	Population from United Kingdom	O	Δ				
Vahidnia *et al*[26]	Population from United States	Δ	O				
Kaishima *et al*[27]	Population from Japan	O					
Blanco *et al*[28]	Population from Spain	Δ	O				
Kesen *et al*[29]	HCV patients from Turkey				O	Not described[1]	HADS
Cortesi *et al*[30]	Population from Italy	O	O				
Karimi Sari *et al*[31]	HCV patients from Iran				O	Not described[1]	
Zanone *et al*[32]	HCV patients from Italy	O					

[1]Modified scale excluding from the analyses.

O: The eligible study including the analyses; Δ: The excluding outcomes due to different conditions; EQ-5D-5L: EuroQol 5-dimensions 5-levels; EQ-VAS: EuroQol-visual analogue scale; HUI-mark: Health utility index mark; SF-36: Short from-36; CLDQ: Chronic liver disease questionnaire; SF-6D: Short form 6-dimensions; HQLQv2: Hepatitis Quality of Life® survey version 2; HADS: Hospital anxiety and depression scale; HCV: Hepatitis C virus.

(GH) (63.37 ± 14.16); vitality, energy, or fatigue (VT) (63.37 ± 14.16); social functioning (SF) (86.97 ± 15.13); role limitations due to emotional problems (RE) (83.94 ± 23.57); and general mental health (63.37 ± 14.16). Although the eligible healthy controls differed among countries and age groups, the health utility scores produced by each scale were similar (Table 5)[16,17,22,23].

Compensated liver cirrhosis vs sustained virologic response

Patients with hepatitis C had achieved an SVR exhibited significantly better health utility scores for each SF-36 scale (Figure 2)[22,29,31] and the EQ-5D-5L (Figure 1B)[18,19,22,32] than those with compensated liver cirrhosis (Table 6)[18,19,22,29,31,32]. In particular, significant differences in the scores for RP (61.5 ± 31.6 *vs* 73.3 ± 27.3), GH (64.8 ± 20.9 *vs* 74.8 ± 18.5), VT (70.5 ± 24.0 *vs* 78.1 ± 18.4), RE (56.8 ± 32.0 *vs* 68.1 ± 27.3), and the EQ-5D-5L (0.6863 ± 0.3065 *vs* 0.846 ± 0.1816) were seen between these groups. These results indicate that health utility indices improve by 10%-20% after patients with hepatitis C achieve an SVR.

Table 3 EuroQol 5-dimensions 5-levels

Ref.	Total	Mean	SD
Normal healthy individuals			
Ratcliffe *et al*[17]	3386	0.85	0.03
Chong *et al*[18]	1518	0.821	0.011
Björnsson *et al*[22]	29353	0.819	0.217
Vahidnia *et al*[26]	1565	0.94	0.1
Cortesi *et al*[30]	6800	0.915	0.107
Total	42622	0.8413	0.1905
Compensated cirrhosis with hepatitis C			
Chong *et al*[18]	24	0.74	0.085
Grieve *et al*[19]	40	0.55	0.34
Björnsson *et al*[22]	76	0.749	0.212
Scalone *et al*[25]	222	0.736	0.259
Kaishima *et al*[27]	20	0.824	0.106
Cortesi *et al*[30]	574	0.891	0.119
Zanone *et al*[32]	94	0.68	0.37
Total	1050	0.8113	0.2261
Decompensated cirrhosis with hepatitis C			
Chong *et al*[18]	9	0.66	0.2
Grieve *et al*[19]	64	0.45	0.24
Björnsson *et al*[22]	53	0.565	0.266
Kaishima *et al*[27]	4	0.524	0.25
Cortesi *et al*[30]	523	0.859	0.14
Total	653	0.7903	0.2182
Sustained virologic response			
Chong *et al*[18]	36	0.83	0.065
Grieve *et al*[19]	24	0.82	0.21
Björnsson *et al*[22]	52	0.792	0.209
Zanone *et al*[32]	91	0.89	0.18
Total	203	0.846	0.1816
Hepatocellular carcinoma			
Chong *et al*[18]	15	0.65	0.21
Grieve *et al*[19]	64	0.45	0.24
Scalone *et al*[25]	85	0.777	0.241
Kaishima *et al*[27]	14	0.75	0.057
Cortesi *et al*[30]	545	0.867	0.146
Total	723	0.8127	0.2084

HUI Mark-2/Mark-3

Hepatitis B and C are the main causes of viral-associated chronic liver disease (Figure 3)[20,21]. The health utility scores of hepatitis B patients were significantly better than those of hepatitis C patients (0.6312 ± 0.2867 *vs* 0.8186 ± 0.1886); *i.e.*, there was a roughly 30% difference between the scores of these patients.

Table 4 EuroQol-visual analogue scale in normal healthy individuals

Ref.	Total	Mean	SD
Vahidnia *et al*[26]	1565	87.6	10.6
Cortesi *et al*[30]	6800	78	18.4
Total	8365	79.796	17.614

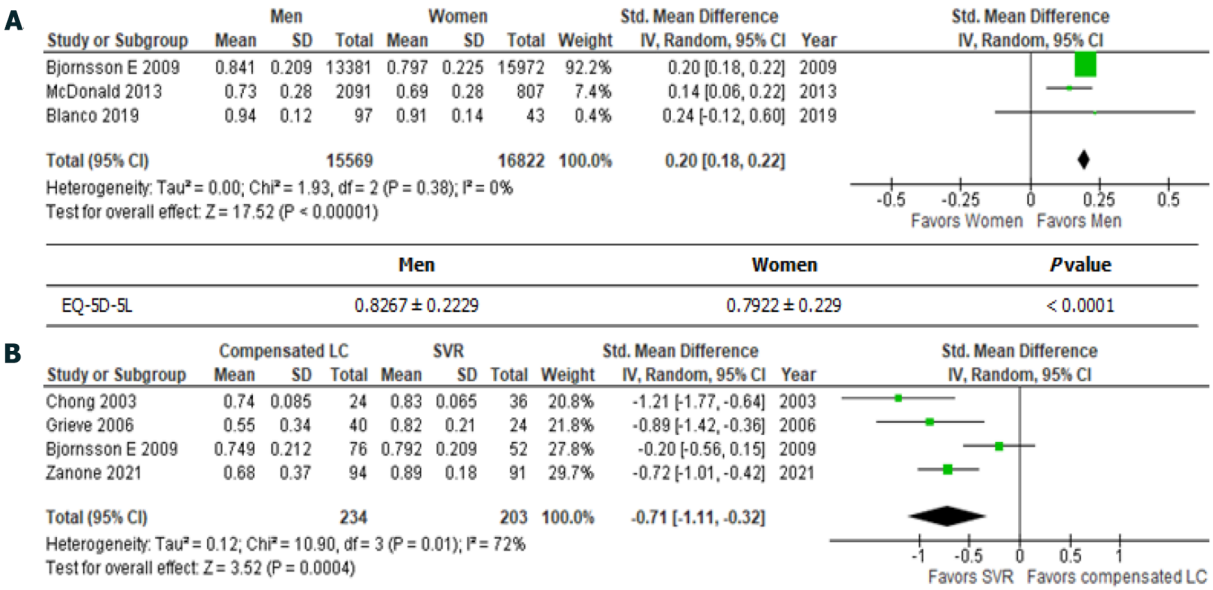

DOI: 10.3748/wjg.v28.i31.4442

Figure 1 EuroQOL 5-dimensions 5-levels. A: Men *vs* women; B: Compensated liver cirrhosis *vs* sustained virologic response. EQ-5D-5L: EuroQol 5-dimensions 5-levels.

DISCUSSION

Which HUI should be used for normal populations or patients with chronic liver disease?

In this meta-analysis, we summarized the findings of previous studies examining health utility evaluations in patients with chronic liver disease. Various questionnaires have been used to evaluate health utility in different populations/at different times. The EQ-5D-5L is the most popular of the questionnaires used to examine health utility scores internationally[17].

One of the concerns regarding the application of health utility scores is their sensitivity[33]. For example, the health utility scores produced by the EQ-5D-5L for patients with compensated cirrhosis and decompensated cirrhosis did not differ significantly (Table 3). On the other hand, the health utility scores for hepatitis C patients with compensated liver cirrhosis and those who achieved an SVR differed significantly according to both the SF-36 and EQ-5D-5L (Table 6). This indicated that both questionnaires are suitable for evaluating health utility in hepatitis C patients after viral elimination. Although the health utility scores derived from the EQ-5D-5L were calculated from 5 questions, the score range of the EQ-5D-5L (123.3%) was greater than that of the SF-36 (105.8%-119.2%). Therefore, the EQ-5D-5L could be suitable for evaluating health utility scores in this specific disease state. On the other hand, EQ-5D-5L-derived health utility scores are based on only five personal factors, mobility, self-care, usual activities, pain/discomfort, and anxiety/depression. Therefore, their sensitivity and any ceiling effects should be validated in each language and ethnic group.

It is well known that the prevailing subtype of viral hepatitis differs depending on the geographic region[34]. Hepatitis B is the prevailing subtype in East Asia[13], whereas hepatitis C is the most common in Western countries[35]. Both types of hepatitis can be controlled by nucleic acid analogs[36]. In this meta-analysis, the HUI scores of hepatitis C patients were roughly 30% lower than those of hepatitis B patients. The differences between hepatitis B and hepatitis C need to be investigated using the EQ-5D-5L and SF-36 in future.

The second concern regarding the use of questionnaires for health assessments relates to the number of questions in each questionnaire. The EQ-5D-5L consists of only five questions[8], whereas the other tools consist of 36[14-16] or 45[11] questions. The number of questions affects study compliance, especially in the elderly[37]. If possible, the number of questions should be minimized.

Table 5 Short from-36: Healthy controls

Ref.	Total	Mean	SD
Physical function			
Björnsson *et al*[22]	339	87	19
Jenkinson *et al*[16] M 60	681	80	22.1
Jenkinson *et al*[16] W 60	684	74.8	23.5
Ratcliffe *et al*[17]	8883	85.4	2.55
Hsu *et al*[23]	9367	85.8	20
Total	19954	85.07	15.40
Role physical			
Björnsson *et al*[22]	339	82	32
Jenkinson *et al*[16] M 60	717	78.8	36.1
Jenkinson *et al*[16] W 60	757	76.8	36.9
Ratcliffe *et al*[17]	9151	83.7	4.4
Hsu *et al*[23]	9367	82.1	33.2
Total	20331	82.50	25.15
Body pain			
Björnsson *et al*[22]	339	72	27
Jenkinson *et al*[16] M 60	724	78.8	23.6
Jenkinson *et al*[16] W 60	779	75	25.1
Ratcliffe *et al*[17]	9214	80	3.05
Hsu *et al*[23]	9367	75.6	23
Total	20423	77.62	17.55
General health			
Björnsson *et al*[22]	339	68	24
Jenkinson *et al*[16] M 60	707	62.9	20.3
Jenkinson *et al*[16] W 60	763	59	21.4
Ratcliffe *et al*[17]	9089	61.1	2.75
Hsu *et al*[23]	9367	65.8	18
Total	20265	63.37	14.16
Vitality, energy, fatigue			
Björnsson *et al*[22]	339	68	24
Jenkinson *et al*[16] M 60	707	62.9	20.3
Jenkinson *et al*[16] W 60	763	59	21.4
Ratcliffe *et al*[17]	9089	61.1	2.75
Hsu *et al*[23]	9367	65.8	18
Total	20265	63.37	14.16
Social function			
Björnsson *et al*[22]	339	88	21
Jenkinson *et al*[16] M 60	729	86.9	22.6
Jenkinson *et al*[16] W 60	783	85.9	22.6
Ratcliffe *et al*[17]	9219	87.8	2.8
Hsu *et al*[23]	9367	86.2	19.8

Total	20437	86.97	15.13
Role emotional			
Björnsson *et al*[22]	339	86	29
Jenkinson *et al*[16] M 60	714	85.8	29.5
Jenkinson *et al*[16] W 60	756	83.3	32.5
Ratcliffe *et al*[17]	9159	83.7	4.4
Hsu *et al*[23]	9367	84	31.7
Total	20335	83.94	23.57
Mental health, emotional, well-being			
Björnsson *et al*[22]	339	50	10
Jenkinson *et al*[16] M 60	697	78	17.5
Jenkinson *et al*[16] W 60	742	74.4	18.5
Ratcliffe *et al*[17]	9014	74.6	2.35
Hsu *et al*[23]	9367	77.5	15.3
Total	20159	75.64	12.23

Table 6 Compensated liver cirrhosis *vs* sustained virologic response

Questionnare	Compensated LC	SVR	*P* value	% improvement
SF-36: Physical function	79.3 ± 19.3	83.9 ± 17.8	0.07	105.8
SF-36: Role physical	61.5 ± 31.6	73.3 ± 27.3	0.004	119.2
SF-36: Body pain	80.8 ± 23.1	85.4 ± 21.3	0.09	105.7
SF-36: General health	64.8 ± 20.9	74.8 ± 18.5	< 0.001	115.4
SF-36: Vitality	70.5 ± 24.0	78.1 ± 18.4	0.002	110.8
SF-36: Social function	77.0 ± 19.0	83.3 ± 15.6	0.05	108.2
SF-36: Role emotional	56.8 ± 32.0	68.1 ± 27.3	< 0.001	119.9
SF-36: Mental health	77.2 ± 16.8	81.3 ± 15.2	0.12	105.3
EQ-5D-5L	0.6863 ± 0.3065	0.846 ± 0.1816	< 0.001	123.3

LC: Liver cirrhosis; SVR: Sustained virologic response; SF-36: Short from-36; EQ-5D-5L: EuroQol 5-dimensions 5-levels.

The last concern is about gaining permission to use such questionnaires for health utility assessments. It takes great effort to develop a questionnaire. However, health utility assessments need to be repeated continuously. In certain human health emergencies, the use of some vaccines has been allowed without patent royalties having to be paid[38]. Commercial companies that own the rights to health assessments should reconsider their policies regarding their use.

CONCLUSION

Health assessments that allow free registration would be useful for evaluating health utility in patients with liver disease. Alternatively, a portable QOL tracker could be used to perform QOL evaluations of any patient-reported outcome, and we are currently developing such a tracker.

A

Study or Subgroup	Compensated LC Mean	SD	Total	SVR Mean	SD	Total	Weight	Std. Mean Difference IV, Random, 95% CI	Year
Bjornsson E 2009	79	22	76	82	21	52	34.6%	-0.14 [-0.49, 0.22]	2009
Kesen 2019	58.51	31.25	27	63.51	28.27	27	24.9%	-0.17 [-0.70, 0.37]	2019
Karimi Sari 2020	83.96	8.49	127	89.08	7.22	127	40.6%	-0.65 [-0.90, -0.40]	2020
Total (95% CI)			230			206	100.0%	-0.35 [-0.73, 0.03]	

Heterogeneity: Tau² = 0.08; Chi² = 6.42, df = 2 (P = 0.04); I² = 69%
Test for overall effect: Z = 1.82 (P = 0.07)

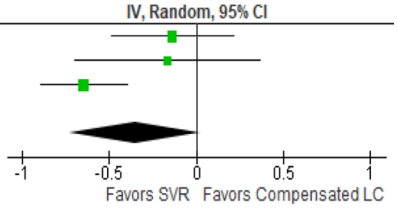

B

Study or Subgroup	Compensated LC Mean	SD	Total	SVR Mean	SD	Total	Weight	Std. Mean Difference IV, Random, 95% CI	Year
Bjornsson E 2009	58	43	76	71	37	52	34.6%	-0.32 [-0.67, 0.04]	2009
Kesen 2019	36.11	42.36	27	52.77	44.03	27	24.4%	-0.38 [-0.92, 0.16]	2019
Karimi Sari 2020	68.54	12.34	127	78.54	11.82	127	40.9%	-0.83 [-1.08, -0.57]	2020
Total (95% CI)			230			206	100.0%	-0.54 [-0.91, -0.17]	

Heterogeneity: Tau² = 0.07; Chi² = 6.01, df = 2 (P = 0.05); I² = 67%
Test for overall effect: Z = 2.88 (P = 0.004)

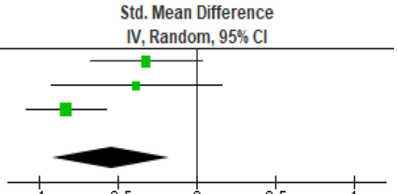

C

Study or Subgroup	Compensated LC Mean	SD	Total	SVR Mean	SD	Total	Weight	Std. Mean Difference IV, Random, 95% CI	Year
Bjornsson E 2009	64	27	76	72	30	52	28.5%	-0.28 [-0.64, 0.07]	2009
Kesen 2019	64.51	19.06	27	66.7	20.21	27	12.5%	-0.11 [-0.64, 0.42]	2019
Karimi Sari 2020	94.27	7.23	127	95.1	6.74	127	59.0%	-0.12 [-0.36, 0.13]	2020
Total (95% CI)			230			206	100.0%	-0.16 [-0.35, 0.03]	

Heterogeneity: Tau² = 0.00; Chi² = 0.59, df = 2 (P = 0.74); I² = 0%
Test for overall effect: Z = 1.70 (P = 0.09)

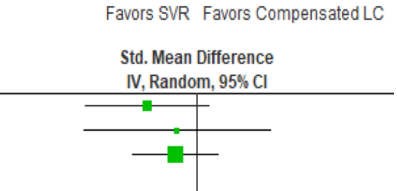

D

Study or Subgroup	Compensated LC Mean	SD	Total	SVR Mean	SD	Total	Weight	Std. Mean Difference IV, Random, 95% CI	Year
Bjornsson E 2009	54	24	76	67	24	52	29.4%	-0.54 [-0.90, -0.18]	2009
Kesen 2019	43.59	19.92	27	53.92	20.84	27	12.9%	-0.50 [-1.04, 0.04]	2019
Karimi Sari 2020	75.73	8.89	127	82.45	7.66	127	57.8%	-0.81 [-1.06, -0.55]	2020
Total (95% CI)			230			206	100.0%	-0.69 [-0.88, -0.49]	

Heterogeneity: Tau² = 0.00; Chi² = 1.97, df = 2 (P = 0.37); I² = 0%
Test for overall effect: Z = 6.94 (P < 0.00001)

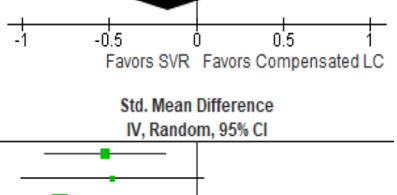

E

Study or Subgroup	Compensated LC Mean	SD	Total	SVR Mean	SD	Total	Weight	Std. Mean Difference IV, Random, 95% CI	Year
Bjornsson E 2009	52	28	76	67	24	52	30.2%	-0.56 [-0.92, -0.20]	2009
Kesen 2019	56.11	19.13	27	60.55	19.38	27	14.9%	-0.23 [-0.76, 0.31]	2019
Karimi Sari 2020	84.6	7.34	127	86.33	7.47	127	54.9%	-0.23 [-0.48, 0.01]	2020
Total (95% CI)			230			206	100.0%	-0.33 [-0.55, -0.12]	

Heterogeneity: Tau² = 0.01; Chi² = 2.35, df = 2 (P = 0.31); I² = 15%
Test for overall effect: Z = 3.03 (P = 0.002)

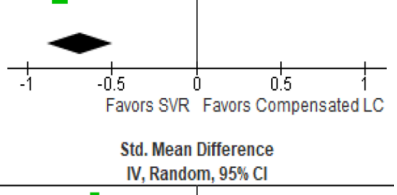

F

Study or Subgroup	Compensated LC Mean	SD	Total	SVR Mean	SD	Total	Weight	Std. Mean Difference IV, Random, 95% CI	Year
Bjornsson E 2009	79	24	76	83	22	52	34.6%	-0.17 [-0.52, 0.18]	2009
Kesen 2019	66.66	26.62	27	73.14	22.91	27	26.5%	-0.26 [-0.79, 0.28]	2019
Karimi Sari 2020	77.92	11.76	127	85.62	7.88	127	38.9%	-0.77 [-1.02, -0.51]	2020
Total (95% CI)			230			206	100.0%	-0.43 [-0.86, 0.00]	

Heterogeneity: Tau² = 0.11; Chi² = 8.27, df = 2 (P = 0.02); I² = 76%
Test for overall effect: Z = 1.94 (P = 0.05)

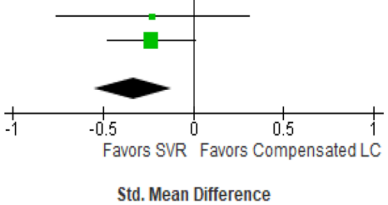

G

Study or Subgroup	Compensated LC Mean	SD	Total	SVR Mean	SD	Total	Weight	Std. Mean Difference IV, Random, 95% CI	Year
Bjornsson E 2009	66	42	76	77	35	52	31.4%	-0.28 [-0.63, 0.08]	2009
Kesen 2019	33.33	41.36	27	58.02	43.94	27	14.6%	-0.57 [-1.12, -0.03]	2019
Karimi Sari 2020	56.33	17.16	127	66.61	16.18	127	54.0%	-0.61 [-0.87, -0.36]	2020
Total (95% CI)			230			206	100.0%	-0.50 [-0.72, -0.29]	

Heterogeneity: Tau² = 0.01; Chi² = 2.35, df = 2 (P = 0.31); I² = 15%
Test for overall effect: Z = 4.55 (P < 0.00001)

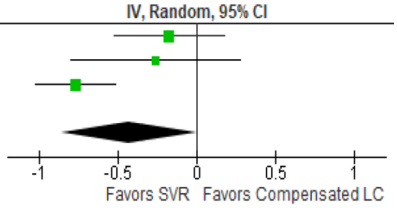

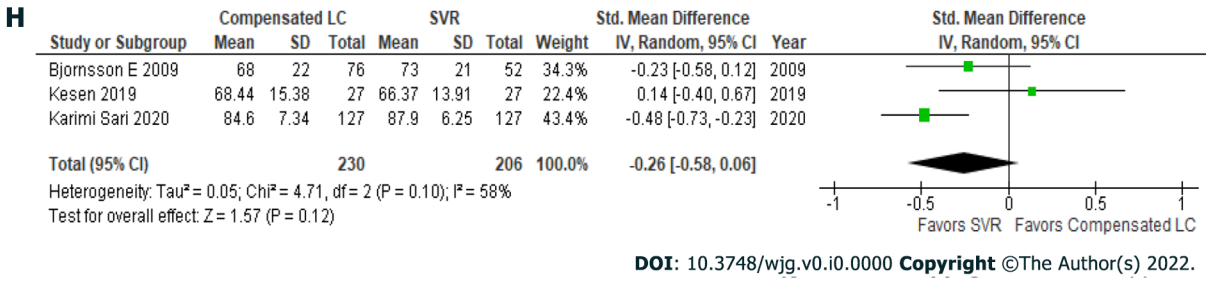

Figure 2 Short from-36: Compensated liver cirrhosis *vs* sustained virologic response. A: Physical function; B: Role physical; C: Body pain; D: General health; E: Vitality; F: Social function; G: Role emotional; H: Mental health.

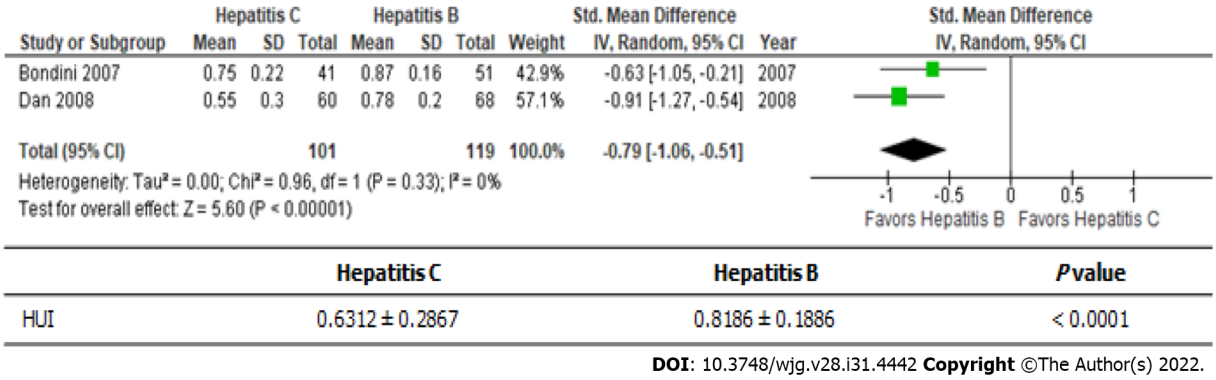

	Hepatitis C	Hepatitis B	*P* value
HUI	0.6312 ± 0.2867	0.8186 ± 0.1886	< 0.0001

DOI: 10.3748/wjg.v28.i31.4442 **Copyright** ©The Author(s) 2022.

Figure 3 Health Utilities Index-Mark2 or 3: Hepatitis C *vs* hepatitis B. HUI: Health Utilities Index.

ARTICLE HIGHLIGHTS

Research background

The most useful questionnaire for evaluating health status depending on liver disease status or sex is unclear.

Research motivation

No universal health utility assessment values for specific liver diseases or the normal population have been reported.

Research objectives

The objective of this study was to conduct a meta-analysis to estimate health utility assessment values for specific populations in the liver disease.

Research methods

A systematic literature search was performed using PubMed and MEDLINE, including the Cochrane Library.

Research results

The short from-36 and EuroQOL 5-dimensions 5-levels (EQ-5D-5L) can be used for health utility evaluations during antiviral therapy for hepatitis C.

Research conclusions

The EQ-5D-5L is the most popular questionnaire for health utility assessments. Health assessments that allow free registration would be useful for evaluating health utility in patients with liver disease.

Research perspectives

Alternatively, a portable quality of life (QOL) tracker could be used to perform QOL evaluations of any patient-reported outcome in future.

ACKNOWLEDGEMENTS

We thank Sandy Tan and Miyako Nara for their valuable discussions and help in preparing this manuscript.

FOOTNOTES

Author contributions: Ishinuki T and Ota S conceptualized and designed the review; Ishinuki T, Harada K, Kawamoto M, and Meguro M searched for and screened the articles; Kutomi G, Tatsumi H, Harada K, and Kato T assessed the articles for eligibility; Miyanishi K and Ohyanagi T carried out the statistical analyses; Hui TT and Mizuguchi T drafted the initial manuscript; Mizuguchi T finalized the manuscript; and all of the authors reviewed and approved the final manuscript as submitted.

Supported by Grants-in-Aid from JSPS KAKENHI, No. JP 20K10404 (to Mizuguchi T) and No. JP 21K10715 (to Ishinuki T); the Hokkaido Hepatitis B Litigation Orange Fund, No. 2059198 (to Mizuguchi T) and No. 2136589 (to Harada K); Terumo Life Science Foundation, No. 2000666; Pfizer Health Research Foundation, No. 2000777; the Viral Hepatitis Research Foundation of Japan, No. 3039838; Project Mirai Cancer Research Grants, No. 202110251; Takahashi Industrial and Economic Research Foundation, No. 12-003-106; Daiichi Sankyo Company, No. 2109540; Shionogi and Co., No. 2109493; MSD, No. 2099412; Takeda Pharmaceutical Company, No. 2000555; Sapporo Doto Hospital, No. 2039118; Noguchi Hospital, No. 2029083; Doki-kai Tomakomai Hospital, No. 2059203; Tsuchida Hospital, No. 2000092; Shinyu-kai Noguchi Hospital, No. 2029083 (to Mizuguchi T); and the Yasuda Medical Foundation, No. 28-1 (to Ishinuki T).

Conflict-of-interest statement: All authors have nothing to disclose.

PRISMA 2009 Checklist statement: The authors have read the PRISMA 2009 Checklist statement, and the manuscript was prepared and revised according to the PRISMA 2009 Checklist statement.

Country/Territory of origin: Japan

ORCID number: Tomohiro Ishinuki 0000-0003-3225-9781; Shigenori Ota 0000-0003-3123-9172; Kohei Harada 0000-0002-3245-6980; Masaki Kawamoto 0000-0002-2800-6207; Makoto Meguro 0000-0002-9170-6919; Goro Kutomi 0000-0003-4557-5126; Hiroomi Tatsumi 0000-0002-9688-6154; Keisuke Harada 0000-0002-7497-6191; Koji Miyanishi 0000-0002-6466-3458; Toru Kato 0000-0002-8520-1949; Toshio Ohyanagi 0000-0001-8335-3087; Thomas T Hui 0000-0003-2717-3983; Toru Mizuguchi 0000-0002-8225-7461.

Corresponding Author's Membership in Professional Societies: The Japanese Society of Gastroenterology.

S-Editor: Ma YJ
L-Editor: A
P-Editor: Ma YJ

REFERENCES

1 **Donabedian A**. Evaluating the quality of medical care. 1966. *Milbank Q* 2005; **83**: 691-729 [PMID: 16279964 DOI: 10.1111/j.1468-0009.2005.00397.x]
2 **Hazawa Y**, Kutomi G, Shima H, Honma T, Ohmura T, Wada A, Mikami T, Hotta M, Narumi M, Ishinuki T, Kuno Y, Meguro M, Takemasa I, Okazaki M, Masuoka H, Asaishi K, Ohyanagi T, Hui TT, Mizuguchi T. The Unique Mental Impacts of Breast-Conserving Surgery and Mastectomy According to a Multi-Centered Cross Sectional Survey Conducted in Japan. *Arch Breast Cancer* 2020; **7**: 119-126 [DOI: 10.32768/abc.202073119-126]
3 **Whitehead SJ**, Ali S. Health outcomes in economic evaluation: the QALY and utilities. *Br Med Bull* 2010; **96**: 5-21 [PMID: 21037243 DOI: 10.1093/bmb/ldq033]
4 **Global Burden of Disease Cancer Collaboration**, Fitzmaurice C, Abate D, Abbasi N, Abbastabar H, Abd-Allah F, Abdel-Rahman O, Abdelalim A, Abdoli A, Abdollahpour I, Abdulle ASM, Abebe ND, Abraha HN, Abu-Raddad LJ, Abualhasan A, Adedeji IA, Advani SM, Afarideh M, Afshari M, Aghaali M, Agius D, Agrawal S, Ahmadi A, Ahmadian E, Ahmadpour E, Ahmed MB, Akbari ME, Akinyemiju T, Al-Aly Z, AlAbdulKader AM, Alahdab F, Alam T, Alamene GM, Alemnew BTT, Alene KA, Alinia C, Alipour V, Aljunid SM, Bakeshei FA, Almadi MAH, Almasi-Hashiani A, Alsharif U, Alsowaidi S, Alvis-Guzman N, Amini E, Amini S, Amoako YA, Anbari Z, Anber NH, Andrei CL, Anjomshoa M, Ansari F, Ansariadi

A, Appiah SCY, Arab-Zozani M, Arabloo J, Arefi Z, Aremu O, Areri HA, Artaman A, Asayesh H, Asfaw ET, Ashagre AF, Assadi R, Ataeinia B, Atalay HT, Ataro Z, Atique S, Ausloos M, Avila-Burgos L, Avokpaho EFGA, Awasthi A, Awoke N, Ayala Quintanilla BP, Ayanore MA, Ayele HT, Babaee E, Bacha U, Badawi A, Bagherzadeh M, Bagli E, Balakrishnan S, Balouchi A, Bärnighausen TW, Battista RJ, Behzadifar M, Bekele BB, Belay YB, Belayneh YM, Berfield KKS, Berhane A, Bernabe E, Beuran M, Bhakta N, Bhattacharyya K, Biadgo B, Bijani A, Bin Sayeed MS, Birungi C, Bisignano C, Bitew H, Bjørge T, Bleyer A, Bogale KA, Bojia HA, Borzì AM, Bosetti C, Bou-Orm IR, Brenner H, Brewer JD, Briko AN, Briko NI, Bustamante-Teixeira MT, Butt ZA, Carreras G, Carrero JJ, Carvalho F, Castro C, Castro F, Catalá-López F, Cerin E, Chaiah Y, Chanie WF, Chattu VK, Chaturvedi P, Chauhan NS, Chehrazi M, Chiang PP, Chichiabellu TY, Chido-Amajuoyi OG, Chimed-Ochir O, Choi JJ, Christopher DJ, Chu DT, Constantin MM, Costa VM, Crocetti E, Crowe CS, Curado MP, Dahlawi SMA, Damiani G, Darwish AH, Daryani A, das Neves J, Demeke FM, Demis AB, Demissie BW, Demoz GT, Denova-Gutiérrez E, Derakhshani A, Deribe KS, Desai R, Desalegn BB, Desta M, Dey S, Dharmaratne SD, Dhimal M, Diaz D, Dinberu MTT, Djalalinia S, Doku DT, Drake TM, Dubey M, Dubljanin E, Duken EE, Ebrahimi H, Effiong A, Eftekhari A, El Sayed I, Zaki MES, El-Jaafary SI, El-Khatib Z, Elemineh DA, Elkout H, Ellenbogen RG, Elsharkawy A, Emamian MH, Endalew DA, Endries AY, Eshrati B, Fadhil I, Fallah Omrani V, Faramarzi M, Farhangi MA, Farioli A, Farzadfar F, Fentahun N, Fernandes E, Feyissa GT, Filip I, Fischer F, Fisher JL, Force LM, Foroutan M, Freitas M, Fukumoto T, Futran ND, Gallus S, Gankpe FG, Gayesa RT, Gebrehiwot TT, Gebremeskel GG, Gedefaw GA, Gelaw BK, Geta B, Getachew S, Gezae KE, Ghafourifard M, Ghajar A, Ghashghaee A, Gholamian A, Gill PS, Ginindza TTG, Girmay A, Gizaw M, Gomez RS, Gopalani SV, Gorini G, Goulart BNG, Grada A, Ribeiro Guerra M, Guimaraes ALS, Gupta PC, Gupta R, Hadkhale K, Haj-Mirzaian A, Hamadeh RR, Hamidi S, Hanfore LK, Haro JM, Hasankhani M, Hasanzadeh A, Hassen HY, Hay RJ, Hay SI, Henok A, Henry NJ, Herteliu C, Hidru HD, Hoang CL, Hole MK, Hoogar P, Horita N, Hosgood HD, Hosseini M, Hosseinzadeh M, Hostiuc M, Hostiuc S, Househ M, Hussen MM, Ileanu B, Ilic MD, Innos K, Irvani SSN, Iseh KR, Islam SMS, Islami F, Jafari Balalami N, Jafarinia M, Jahangiry L, Jahani MA, Jahanmehr N, Jakovljevic M, James SL, Javanbakht M, Jayaraman S, Jee SH, Jenabi E, Jha RP, Jonas JB, Jonnagaddala J, Joo T, Jungari SB, Jürisson M, Kabir A, Kamangar F, Karch A, Karimi N, Karimian A, Kasaeian A, Kasahun GG, Kassa B, Kassa TD, Kassaw MW, Kaul A, Keiyoro PN, Kelbore AG, Kerbo AA, Khader YS, Khalilarjmandi M, Khan EA, Khan G, Khang YH, Khatab K, Khater A, Khayamzadeh M, Khazaee-Pool M, Khazaei S, Khoja AT, Khosravi MH, Khubchandani J, Kianipour N, Kim D, Kim YJ, Kisa A, Kisa S, Kissimova-Skarbek K, Komaki H, Koyanagi A, Krohn KJ, Bicer BK, Kugbey N, Kumar V, Kuupiel D, La Vecchia C, Lad DP, Lake EA, Lakew AM, Lal DK, Lami FH, Lan Q, Lasrado S, Lauriola P, Lazarus JV, Leigh J, Leshargie CT, Liao Y, Limenih MA, Listl S, Lopez AD, Lopukhov PD, Lunevicius R, Madadin M, Magdeldin S, El Razek HMA, Majeed A, Maleki A, Malekzadeh R, Manafi A, Manafi N, Manamo WA, Mansourian M, Mansournia MA, Mantovani LG, Maroufizadeh S, Martini SMS, Mashamba-Thompson TP, Massenburg BB, Maswabi MT, Mathur MR, McAlinden C, McKee M, Meheretu HAA, Mehrotra R, Mehta V, Meier T, Melaku YA, Meles GG, Meles HG, Melese A, Melku M, Memiah PTN, Mendoza W, Menezes RG, Merat S, Meretoja TJ, Mestrovic T, Miazgowski B, Miazgowski T, Mihretie KMM, Miller TR, Mills EJ, Mir SM, Mirzaei H, Mirzaei HR, Mishra R, Moazen B, Mohammad DK, Mohammad KA, Mohammad Y, Darwesh AM, Mohammadbeigi A, Mohammadi H, Mohammadi M, Mohammadian M, Mohammadian-Hafshejani A, Mohammadoo-Khorasani M, Mohammadpourhodki R, Mohammed AS, Mohammed JA, Mohammed S, Mohebi F, Mokdad AH, Monasta L, Moodley Y, Moosazadeh M, Moossavi M, Moradi G, Moradi-Joo M, Moradi-Lakeh M, Moradpour F, Morawska L, Morgado-da-Costa J, Morisaki N, Morrison SD, Mosapour A, Mousavi SM, Muche AA, Muhammed OSS, Musa J, Nabhan AF, Naderi M, Nagarajan AJ, Nagel G, Nahvijou A, Naik G, Najafi F, Naldi L, Nam HS, Nasiri N, Nazari J, Negoi I, Neupane S, Newcomb PA, Nggada HA, Ngunjiri JW, Nguyen CT, Nikniaz L, Ningrum DNA, Nirayo YL, Nixon MR, Nnaji CA, Nojomi M, Nosratnejad S, Shiadeh MN, Obsa MS, Ofori-Asenso R, Ogbo FA, Oh IH, Olagunju AT, Olagunju TO, Oluwasanu MM, Omonisi AE, Onwujekwe OE, Oommen AM, Oren E, Ortega-Altamirano DDV, Ota E, Otstavnov SS, Owolabi MO, P A M, Padubidri JR, Pakhale S, Pakpour AH, Pana A, Park EK, Parsian H, Pashaei T, Patel S, Patil ST, Pennini A, Pereira DM, Piccinelli C, Pillay JD, Pirestani M, Pishgar F, Postma MJ, Pourjafar H, Pourmalek F, Pourshams A, Prakash S, Prasad N, Qorbani M, Rabiee M, Rabiee N, Radfar A, Rafiei A, Rahim F, Rahimi M, Rahman MA, Rajati F, Rana SM, Raoofi S, Rath GK, Rawaf DL, Rawaf S, Reiner RC, Renzaho AMN, Rezaei N, Rezapour A, Ribeiro AI, Ribeiro D, Ronfani L, Roro EM, Roshandel G, Rostami A, Saad RS, Sabbagh P, Sabour S, Saddik B, Safiri S, Sahebkar A, Salahshoor MR, Salehi F, Salem H, Salem MR, Salimzadeh H, Salomon JA, Samy AM, Sanabria J, Santric Milicevic MM, Sartorius B, Sarveazad A, Sathian B, Satpathy M, Savic M, Sawhney M, Sayyah M, Schneider IJC, Schöttker B, Sekerija M, Sepanlou SG, Sepehrimanesh M, Seyedmousavi S, Shaahmadi F, Shabaninejad H, Shahbaz M, Shaikh MA, Shamshirian A, Shamsizadeh M, Sharafi H, Sharafi Z, Sharif M, Sharifi A, Sharifi H, Sharma R, Sheikh A, Shirkoohi R, Shukla SR, Si S, Siabani S, Silva DAS, Silveira DGA, Singh A, Singh JA, Sisay S, Sitas F, Sobngwi E, Soofi M, Soriano JB, Stathopoulou V, Sufiyan MB, Tabarés-Seisdedos R, Tabuchi T, Takahashi K, Tamtaji OR, Tarawneh MR, Tassew SG, Taymoori P, Tehrani-Banihashemi A, Temsah MH, Temsah O, Tesfay BE, Tesfay FH, Teshale MY, Tessema GA, Thapa S, Tlaye KG, Topor-Madry R, Tovani-Palone MR, Traini E, Tran BX, Tran KB, Tsadik AG, Ullah I, Uthman OA, Vacante M, Vaezi M, Varona Pérez P, Veisani Y, Vidale S, Violante FS, Vlassov V, Vollset SE, Vos T, Vosoughi K, Vu GT, Vujcic IS, Wabinga H, Wachamo TM, Wagnew FS, Waheed Y, Weldegebreal F, Weldesamuel GT, Wijeratne T, Wondafrash DZ, Wonde TE, Wondmieneh AB, Workie HM, Yadav R, Yadegar A, Yadollahpour A, Yaseri M, Yazdi-Feyzabadi V, Yeshaneh A, Yimam MA, Yimer EM, Yisma E, Yonemoto N, Younis MZ, Yousefi B, Yousefifard M, Yu C, Zabeh E, Zadnik V, Moghadam TZ, Zaidi Z, Zamani M, Zandian H, Zangeneh A, Zaki L, Zendehdel K, Zenebe ZM, Zewale TA, Ziapour A, Zodpey S, Murray CJL. Global, Regional, and National Cancer Incidence, Mortality, Years of Life Lost, Years Lived With Disability, and Disability-Adjusted Life-Years for 29 Cancer Groups, 1990 to 2017: A Systematic Analysis for the Global Burden of Disease Study. *JAMA Oncol* 2019; **5**: 1749-1768 [PMID: 31560378 DOI: 10.1001/jamaoncol.2019.2996]

5 **Carr AJ**, Gibson B, Robinson PG. Measuring quality of life: Is quality of life determined by expectations or experience? *BMJ* 2001; **322**: 1240-1243 [PMID: 11358783 DOI: 10.1136/bmj.322.7296.1240]

6 **Koide R**, Kikuchi A, Miyajima M, Mishina T, Takahashi Y, Okawa M, Sawada I, Nakajima J, Watanabe A, Mizuguchi T. Quality assessment using EQ-5D-5L after lung surgery for non-small cell lung cancer (NSCLC) patients. *Gen Thorac Cardiovasc Surg* 2019; **67**: 1056-1061 [PMID: 31098867 DOI: 10.1007/s11748-019-01136-0]

7 **Kikuchi A**, Koide R, Iwasaki M, Teramoto M, Satohisa S, Tamate M, Horiguchi M, Niwa N, Saito T, Mizuguchi T. Assessing quality of life using the brief cancer-related worry inventory for gynecological surgery. *World J Obstet Gynecol* 2019; **8**: 1-7 [DOI: 10.5317/wjog.v8.i1.1]

8 **Rabin R**, de Charro F. EQ-5D: a measure of health status from the EuroQol Group. *Ann Med* 2001; **33**: 337-343 [PMID: 11491192 DOI: 10.3109/07853890109002087]

9 **Ishinuki T**, Ota S, Harada K, Tatsumi H, Miyanishi K, Nagayama M, Takemasa I, Ohyanagi T, Hui TT, Mizuguchi T. Health-related quality of life in patients that have undergone liver resection: A systematic review and meta-analysis. *World J Meta-Anal* 2021; **9**: 88-100 [DOI: 10.13105/wjma.v9.i1.88]

10 **Shiroiwa T**, Fukuda T, Ikeda S, Igarashi A, Noto S, Saito S, Shimozuma K. Japanese population norms for preference-based measures: EQ-5D-3L, EQ-5D-5L, and SF-6D. *Qual Life Res* 2016; **25**: 707-719 [PMID: 26303761 DOI: 10.1007/s11136-015-1108-2]

11 **Younossi ZM**, Boparai N, McCormick M, Price LL, Guyatt G. Assessment of utilities and health-related quality of life in patients with chronic liver disease. *Am J Gastroenterol* 2001; **96**: 579-583 [PMID: 11232711 DOI: 10.1111/j.1572-0241.2001.03537.x]

12 **Whitehurst DG**, Engel L, Bryan S. Short Form health surveys and related variants in spinal cord injury research: a systematic review. *J Spinal Cord Med* 2014; **37**: 128-138 [PMID: 24559417 DOI: 10.1179/2045772313Y.0000000159]

13 **de Medeiros MMD**, Carletti TM, Magno MB, Maia LC, Cavalcanti YW, Rodrigues-Garcia RCM. Does the institutionalization influence elderly's quality of life? *BMC Geriatr* 2020; **20**: 44 [PMID: 32024479 DOI: 10.1186/s12877-020-1452-0]

14 **Hays RD**, Sherbourne CD, Mazel RM. The RAND 36-Item Health Survey 1.0. *Health Econ* 1993; **2**: 217-227 [PMID: 8275167 DOI: 10.1002/hec.4730020305]

15 **Ware JE**, Sherbourne CD. The MOS 36-item short-form health survey (SF-36). I. Conceptual framework and item selection. *Med Care* 1992; **30**: 473-483 [PMID: 1593914]

16 **Jenkinson C**, Coulter A, Wright L. Short form 36 (SF36) health survey questionnaire: normative data for adults of working age. *BMJ* 1993; **306**: 1437-1440 [PMID: 8518639 DOI: 10.1136/bmj.306.6890.1437]

17 **Ratcliffe J**, Longworth L, Young T, Bryan S, Burroughs A, Buxton M; Cost-Effectiveness of Liver Transplantation Team. Assessing health-related quality of life pre- and post-liver transplantation: a prospective multicenter study. *Liver Transpl* 2002; **8**: 263-270 [PMID: 11910572 DOI: 10.1053/jlts.2002.31345]

18 **Chong CA**, Gulamhussein A, Heathcote EJ, Lilly L, Sherman M, Naglie G, Krahn M. Health-state utilities and quality of life in hepatitis C patients. *Am J Gastroenterol* 2003; **98**: 630-638 [PMID: 12650799 DOI: 10.1111/j.1572-0241.2003.07332.x]

19 **Grieve R**, Roberts J, Wright M, Sweeting M, DeAngelis D, Rosenberg W, Bassendine M, Main J, Thomas H. Cost effectiveness of interferon alpha or peginterferon alpha with ribavirin for histologically mild chronic hepatitis C. *Gut* 2006; **55**: 1332-1338 [PMID: 15994216 DOI: 10.1136/gut.2005.064774]

20 **Bondini S**, Kallman J, Dan A, Younoszai Z, Ramsey L, Nader F, Younossi ZM. Health-related quality of life in patients with chronic hepatitis B. *Liver Int* 2007; **27**: 1119-1125 [PMID: 17845541 DOI: 10.1111/j.1478-3231.2007.01558.x]

21 **Dan AA**, Kallman JB, Srivastava R, Younoszai Z, Kim A, Younossi ZM. Impact of chronic liver disease and cirrhosis on health utilities using SF-6D and the health utility index. *Liver Transpl* 2008; **14**: 321-326 [PMID: 18306356 DOI: 10.1002/lt.21376]

22 **Björnsson E**, Verbaan H, Oksanen A, Frydén A, Johansson J, Friberg S, Dalgård O, Kalaitzakis E. Health-related quality of life in patients with different stages of liver disease induced by hepatitis C. *Scand J Gastroenterol* 2009; **44**: 878-887 [PMID: 19437190 DOI: 10.1080/00365520902898135]

23 **Hsu PC**, Krajden M, Yoshida EM, Anderson FH, Tomlinson GA, Krahn MD. Does cirrhosis affect quality of life in hepatitis C virus-infected patients? *Liver Int* 2009; **29**: 449-458 [PMID: 19267865 DOI: 10.1111/j.1478-3231.2008.01865.x]

24 **McDonald SA**, Hutchinson SJ, Palmateer NE, Allen E, Cameron SO, Goldberg DJ, Taylor A. Decrease in health-related quality of life associated with awareness of hepatitis C virus infection among people who inject drugs in Scotland. *J Hepatol* 2013; **58**: 460-466 [PMID: 23149064 DOI: 10.1016/j.jhep.2012.11.004]

25 **Scalone L**, Ciampichini R, Fagiuoli S, Gardini I, Fusco F, Gaeta L, Del Prete A, Cesana G, Mantovani LG. Comparing the performance of the standard EQ-5D 3L with the new version EQ-5D 5L in patients with chronic hepatic diseases. *Qual Life Res* 2013; **22**: 1707-1716 [PMID: 23192232 DOI: 10.1007/s11136-012-0318-0]

26 **Vahidnia F**, Stramer SL, Kessler D, Shaz B, Leparc G, Krysztof DE, Glynn SA, Custer B. Recent viral infection in US blood donors and health-related quality of life (HRQOL). *Qual Life Res* 2017; **26**: 349-357 [PMID: 27534773 DOI: 10.1007/s11136-016-1392-5]

27 **Kaishima T**, Akita T, Ohisa M, Sakamune K, Kurisu A, Sugiyama A, Aikata H, Chayama K, Tanaka J. Cost-effectiveness analyses of anti-hepatitis C virus treatments using quality of life scoring among patients with chronic liver disease in Hiroshima prefecture, Japan. *Hepatol Res* 2018; **48**: 509-520 [PMID: 29316059 DOI: 10.1111/hepr.13053]

28 **Blanco JR**, Barrio I, Ramalle-Gómara E, Beltran MI, Ibarra V, Metola L, Sanz M, Oteo JA, Melús E, Antón L. Gender differences for frailty in HIV-infected patients on stable antiretroviral therapy and with an undetectable viral load. *PLoS One* 2019; **14**: e0215764 [PMID: 31071105 DOI: 10.1371/journal.pone.0215764]

29 **Kesen O**, Kani HT, Yanartaş Ö, Aykut UE, Gök B, Gündüz F, Yılmaz Y, Özdoğan OC, Özen Alahdab Y. Evaluation of depression, anxiety and quality of life in hepatitis C patients who treated with direct acting antiviral agents. *Turk J Gastroenterol* 2019; **30**: 801-806 [PMID: 31530524 DOI: 10.5152/tjg.2019.18679]

30 **Cortesi PA**, Conti S, Scalone L, Jaffe A, Ciaccio A, Okolicsanyi S, Rota M, Fabris L, Colledan M, Fagiuoli S, Belli LS, Cesana G, Strazzabosco M, Mantovani LG. Health related quality of life in chronic liver diseases. *Liver Int* 2020; **40**: 2630-2642 [PMID: 32851764 DOI: 10.1111/liv.14647]

31 **Karimi-Sari H**, Hosseini MA, Nikjoo N, Bagheri Baghdasht MS, Alavian SM. Patient-reported outcomes of sleep, mood and quality of life after treatment of chronic hepatitis C infection using direct-acting antiviral agents. *Clin Microbiol Infect* 2020; **26**: 1093.e5-1093.e8 [PMID: 32353413 DOI: 10.1016/j.cmi.2020.04.029]

32 **Zanone MM**, Marinucci C, Ciancio A, Cocito D, Zardo F, Spagone E, Ferrero B, Cerruti C, Charrier L, Cavallo F, Saracco GM, Porta M. Peripheral neuropathy after viral eradication with direct-acting antivirals in chronic HCV hepatitis: A prospective study. *Liver Int* 2021; **41**: 2611-2621 [PMID: 34219359 DOI: 10.1111/liv.15002]

33 **Feng YS**, Kohlmann T, Janssen MF, Buchholz I. Psychometric properties of the EQ-5D-5L: a systematic review of the literature. *Qual Life Res* 2021; **30**: 647-673 [PMID: 33284428 DOI: 10.1007/s11136-020-02688-y]

34 **Jefferies M**, Rauff B, Rashid H, Lam T, Rafiq S. Update on global epidemiology of viral hepatitis and preventive strategies. *World J Clin Cases* 2018; **6**: 589-599 [PMID: 30430114 DOI: 10.12998/wjcc.v6.i13.589]

35 **Nainan OV**, Alter MJ, Kruszon-Moran D, Gao FX, Xia G, McQuillan G, Margolis HS. Hepatitis C virus genotypes and viral concentrations in participants of a general population survey in the United States. *Gastroenterology* 2006; **131**: 478-484 [PMID: 16890602 DOI: 10.1053/j.gastro.2006.06.007]

36 **Holmes JA**, Rutledge SM, Chung RT. Direct-acting antiviral treatment for hepatitis C. *Lancet* 2019; **393**: 1392-1394 [PMID: 30765125 DOI: 10.1016/S0140-6736(18)32326-2]

37 **Uchmanowicz B**, Chudiak A, Mazur G. The influence of quality of life on the level of adherence to therapeutic recommendations among elderly hypertensive patients. *Patient Prefer Adherence* 2018; **12**: 2593-2603 [PMID: 30584283 DOI: 10.2147/PPA.S182172]

38 **Davis BG**. Could You Patent the Sun? *ACS Cent Sci* 2021; **7**: 508-509 [PMID: 34056081 DOI: 10.1021/acscentsci.1c00377]

World Journal of Gastroenterology

Submit a Manuscript: https://www.f6publishing.com

World J Gastroenterol 2022 August 21; 28(31): 4456-4462

DOI: 10.3748/wjg.v28.i31.4456

ISSN 1007-9327 (print) ISSN 2219-2840 (online)

CASE REPORT

Low-grade myofibroblastic sarcoma of the liver misdiagnosed as cystadenoma: A case report

Jie Li, Xin-Yue Huang, Bo Zhang

Specialty type: Gastroenterology and hepatology

Provenance and peer review: Unsolicited article; Externally peer reviewed.

Peer-review model: Single blind

Peer-review report's scientific quality classification

Grade A (Excellent): A
Grade B (Very good): B
Grade C (Good): 0
Grade D (Fair): 0
Grade E (Poor): 0

P-Reviewer: El-Gendy HA, Egypt; Samizadeh B, Iran

Received: May 16, 2022
Peer-review started: May 16, 2022
First decision: June 6, 2022
Revised: June 10, 2022
Accepted: July 25, 2022
Article in press: July 25, 2022
Published online: August 21, 2022

Jie Li, Xin-Yue Huang, Bo Zhang, Department of Ultrasonic Imaging, Xiangya Hospital, Central South University, Changsha 410008, Hunan Province, China

Corresponding author: Bo Zhang, MD, Associate Chief Physician, Deputy Director, Department of Ultrasonic Imaging, Xiangya Hospital, Central South University, No. 87 Xiangya Road, Changsha 410008, Hunan Province, China. zhangbo8095@csu.edu.cn

Abstract

BACKGROUND

Low-grade myofibroblastic sarcoma (LGMS) is a rare malignant tumor. It has no specific clinical manifestations and commonly occurs in the head and neck, extremities and other body parts, with the liver not as its predisposing site.

CASE SUMMARY

We report a case report of a 58-year-old man with right upper abdominal pain for 11 d. Contrast-enhanced computed tomography (CECT), CE magnetic resonance imaging and CE ultrasound (US) all showed a cystic-solid mass in the right liver. As the initial clinical diagnosis was hepatic cystadenoma, surgical resection was performed, and the postoperative pathology indicated hepatic LGMS. The 3-mo follow-up showed favorable recovery of the patient. However, at 7-mo follow-up, two-dimensional US and CECT showed a suspected metastatic lesion in the right-middle abdomen.

CONCLUSION

Hepatic MS is particularly rare and easily misdiagnosed, more cases will contribute to the understanding and the diagnosis accuracy.

Key Words: Myofibroblastic sarcoma; Liver; Cystic-solid mass; Imaging; Diagnosis; Case report

Core Tip: Myofibroblastic sarcoma (MS) is a rare malignant spindle-shaped cell tumor derived from mesenchymal tissue, and it is particularly rare in the liver. Pathological examination is the gold standard for the diagnosis of hepatic MS. There are different biological characteristics of different lesions and protocols for surgical treatment; therefore, we should pay attention to more information conducive to differential diagnosis in order to improve the preoperative diagnosis, and to choose an appropriate surgical approach.

Citation: Li J, Huang XY, Zhang B. Low-grade myofibroblastic sarcoma of the liver misdiagnosed as cystadenoma: A case report. *World J Gastroenterol* 2022; 28(31): 4456-4462
URL: https://www.wjgnet.com/1007-9327/full/v28/i31/4456.htm
DOI: https://dx.doi.org/10.3748/wjg.v28.i31.4456

INTRODUCTION

Myofibroblastic sarcoma (MS) is a rare mesenchymal spindle-shaped cell tumor, first discovered by Mentzel *et al*[1] in 1998. According to the differential degree of myofibroblasts, it can be divided into low, intermediate and high grade. The first two are collectively called low-grade MS (LGMS)[2]. MS is common in the head and neck, limbs and trunk, but it is extremely rare in the liver. So far, there are only four English language reports available. Here, we present a case of LGMS of the liver.

CASE PRESENTATION

Chief complaints

Right upper abdominal pain for 11 d.

History of present illness

A 58-year-old Chinese man presented with right upper abdominal pain without obvious predisposing factors 11 d prior to the visit. The symptom was not associated with eating and body position. He experienced no nausea or vomiting, no chills or fever, and no significant weight loss.

History of past illness

Right inguinal hernia surgery had been performed at another hospital 3 years prior to the present visit.

Personal and family history

No history of hepatitis and family or genetic history was claimed.

Physical examination

Physical examination showed a flat and soft abdomen without tenderness and rebound pain, and no palpable mass was found. The rest of the physical examination showed no abnormalities.

Laboratory examinations

Cholesterol (5.3 mmol/L) and low density lipoprotein (3.78 mmol/L) were elevated. Routine blood, liver function, renal function and prothrombin tests were normal. Complete quantitative detection of hepatitis B was negative. Alpha-fetoprotein (AFP), carcinoembryonic antigen (CEA) and carbohydrate antigen 19-9 (CA19-9) were normal.

Imaging examinations

Abdominal contrast-enhanced computed tomography (CECT) and hepatic vascular imaging showed that there was a cystic-solid hypodense mass with a size of approximate 99 mm × 92 mm in the right liver. Septa, which were slightly enhanced along with the solid parenchyma, were visible in the mass. The right hepatic vein was displaced due to the compression of the mass supplied by the right hepatic artery (Figure 1A-C). Abdominal CE-magnetic resonance imaging and diffusion-weighted imaging (DWI) showed: (1) A cystic-solid mass with low signal on T1-weighted imaging and high signal on T2-weighted imaging in the right liver, about 101 mm × 98 mm in size; (2) multiple uneven septa and fluid-fluid levels in the lesion; (3) DWI and apparent diffusion coefficient showed high signal and high B value, respectively; and (4) after enhancement, solid components and internal septa of the tumor were significantly enhanced accompanied by unenhanced cystic components (Figure 1D-F).

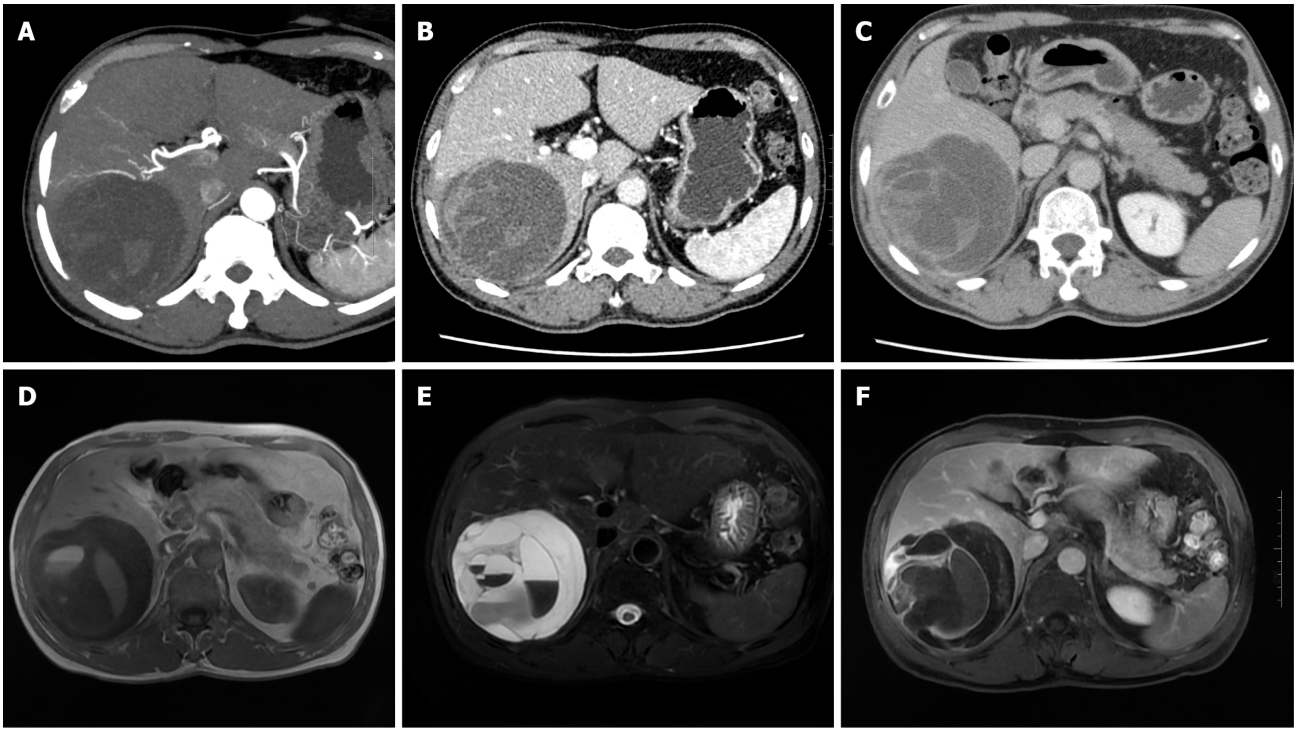

DOI: 10.3748/wjg.v28.i31.4456 **Copyright** ©The Author(s) 2022.

Figure 1 Abdominal contrast-enhanced computed tomography and hepatic vascular imaging examination, and magnetic resonance imaging examination. A: The right hepatic cystic-solid mass was supplied by the right hepatic artery, and the twisting of the supplying artery was seen; B and C: The portal phase and delayed phase, respectively; the solid portion and the septum were enhanced, and the intracapsular septum was clearly displayed; D and E: The lesions were low signal on T1-weighted imaging and high signal on T2-weighted imaging, with multiple septa of uneven thickness and fluid-fluid levels; F: After enhancement, the solid components and septa of the mass were significantly enhanced, but the cystic components were not.

Ultrasound (US) examination showed a 123 mm × 98 mm mixed-echo mass with regular shape and clear boundary in the right liver. The anechoic dark area was the main portion of the mass. The parenchymatous septa with uneven thickness were visible in the mass in which no obvious parasitic body sonogram was found. Color Doppler flow imaging showed punctate blood flow signals in the mass. CEUS showed that the peripheral and internal septa of the tumor were hyper-enhanced in the arterial phase, iso-enhanced in the portal and delayed phases, and unenhanced in the anechoic area in these three phases (Figure 2). Based on the above-mentioned examination, the mass was preliminarily identified as hepatic cystadenoma.

FINAL DIAGNOSIS

The postoperative pathology diagnosis of the presented case is LGMS of right liver (Figure 3).

TREATMENT

The patient underwent laparoscopic right hepatectomy under general anesthesia after preoperative investigations were completed.

OUTCOME AND FOLLOW-UP

The patient recovered well after the operation with the surgical incision healed uneventfully. No apparent event was observed at the postoperative 3-mo follow-up. However, at the 7-mo follow-up, two-dimensional ultrasound and CECT showed a 100 mm × 40 mm cystic-solid lesion occurring in the right middle abdomen, which showed similar properties to a liver lesion. The mass wall was enhanced after enhancement (Figure 4). The patient refused further surgery although the clinician initially believed that metastasis had probably occurred.

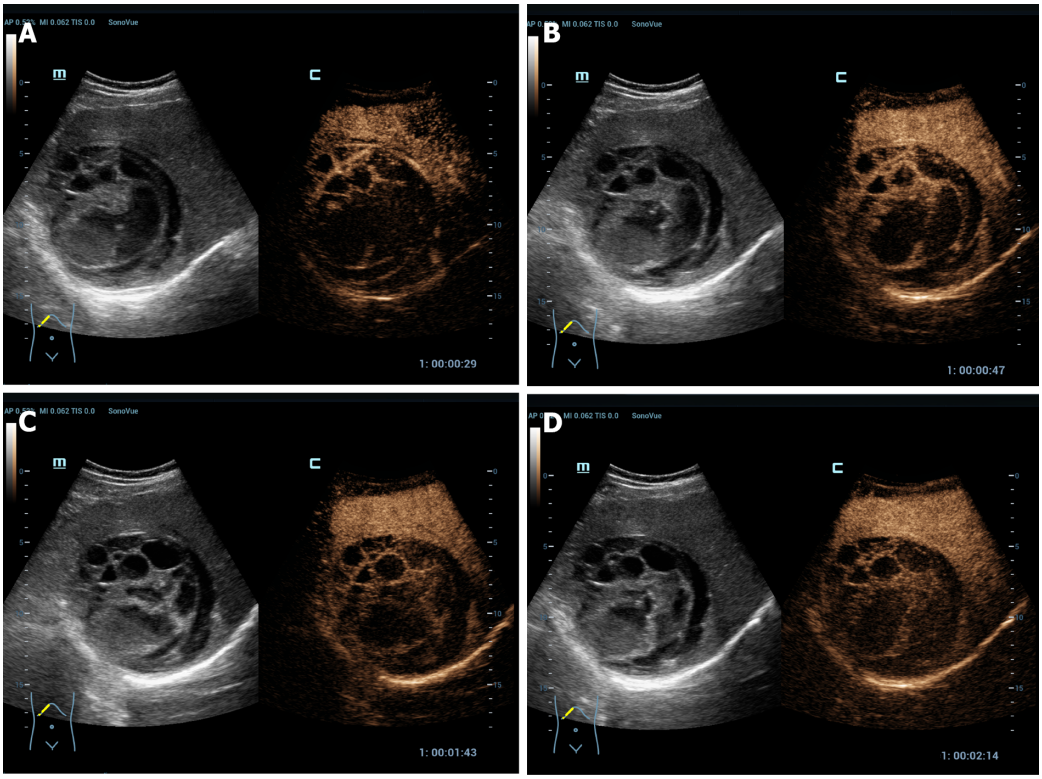

DOI: 10.3748/wjg.v28.i31.4456

Figure 2 Contrast-enhanced ultrasound examination. The peripheral parenchyma and internal septa of the mixed-echo mass showed hyper-enhancement in the arterial phase, and iso-enhancement in the portal and delayed phases. A: Arterial phase; B: Early portal phase; C: Late portal phase; D: Delayed phase.

DISCUSSION

MS is a rare histological type of hepatic sarcoma. Given its rarity, the etiology is not clear, and most of the relevant reports are case reports or case series. Only seven relevant case reports[3-9] were obtained after a comprehensive literature search was conducted by us in CNKI, PubMed and Web of Science databases, involving seven patients (four men, three women; aged 25–38 years, n = 5; > 60 years, n = 2). As described in the WHO classification, males are slightly more predisposed for this disease than females; thus, not surprisingly, the present case was male. Most of the MSs were identified due to the swelling lesion detected or during physical examination. In the literature reports, five of the seven patients presented with abdominal distension and pain, and another two were asymptomatic. As for the present patient, the complaint was right upper abdominal pain. He had no history of hepatitis, although two of the seven patients reported previously had a history of hepatitis B. Serological examination, such as routine blood, liver function, renal function, and AFP and other tumor markers such as CEA, CA19-9 (all of which were in the normal range), was available for six of the seven patients reported previously and for the patient reported here. The remaining patient reported previously had impaired liver function. The lesions reported were mostly located in the right liver, and cystic-solid tumor was found in five cases, but no relevant data were available for the other two cases. For the present case, a cystic-solid tumor located in the right liver was also observed. Among the seven cases reported previously, five were misdiagnosed as liver cancer or hydatid disease as their preliminary clinical diagnosis, while the present case was misdiagnosed as hepatic cystadenoma. Surgical resection was performed in six of the seven patients, and liver lesions were found and biopsy was performed at 3 mo after surgery for the remaining patient initially diagnosed with retroperitoneal inflammatory myofibroblastic tumor. The pathological diagnosis for the current patient was LGMS infiltrated in the liver. Currently, surgical resection of MS is the preferred treatment, although primary treatment, prognosis and follow-up treatment are not clear. More data are needed to obtain reliable conclusions about the role of follow-up treatment such as radiotherapy and chemotherapy.

No specific clinical signs and symptoms were established currently due to the low incidence of hepatic MS, which was generally manifested as abdominal distension or discomfort and/or abnormal liver function, sometimes accompanied by sweating and weight loss. Although there was no clear report on tumor recurrence and metastasis, most hepatic MSs were observed as cystic-solid masses, showing infiltrative and destructive growth.

At present, hepatic MS is mainly diagnosed by histopathology and immunohistochemistry. Under light microscopy, the tumor tissue of the present case was mainly composed of spindle-shaped cells

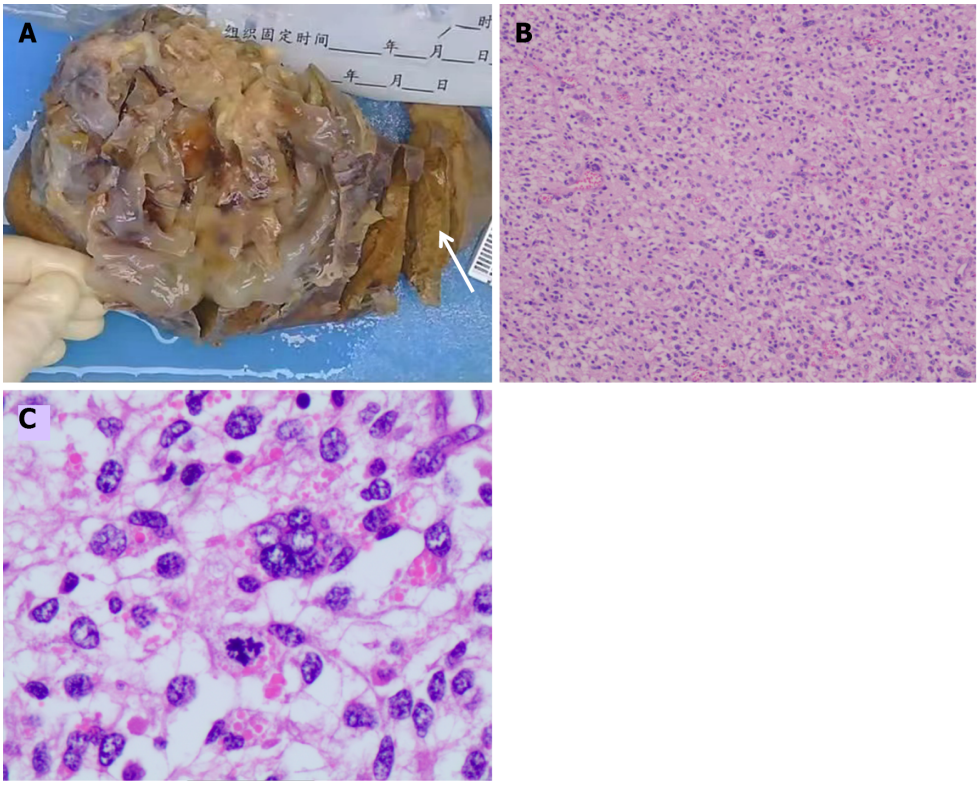

DOI: 10.3748/wjg.v28.i31.4456 **Copyright** ©The Author(s) 2022.

Figure 3 Gross pathology specimen and pathological microscopy. A: A cystic-solid mass was seen with the naked eye, with soft texture and inconspicuous tumor capsule; its cut surface was polycystic, with yellowish jelly-like substances inside the cysts, and the cyst wall thickness was 1 mm-12 mm; no cirrhotic changes were observed in the peripheral liver tissue (arrow); B and C: Spindle-shaped cells are arranged in fascicles under light microscope, eosinophilic cytoplasm with atypia and mitotic figures were seen.

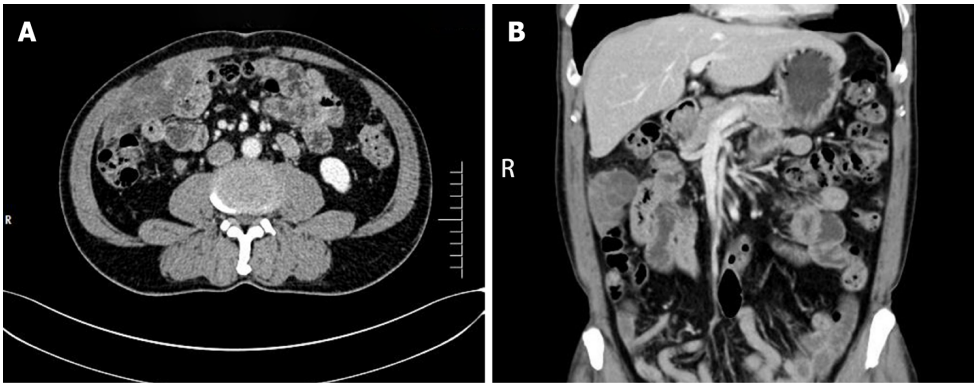

DOI: 10.3748/wjg.v28.i31.4456 **Copyright** ©The Author(s) 2022.

Figure 4 Abdominal contrast-enhanced computed tomography examination at 7-mo follow-up. A and B: The right middle abdomen of the patient in contrast-enhanced computed tomography showed a cystic-solid lesion, with the similar property as a liver lesion. After enhancement, the mass wall was enhanced.

with a diffuse infiltrative distribution. The cytoplasm was eosinophilic and the nucleus was polymorphic. Abnormal mitotic figures were present. The histopathological findings of this case are consistent with those previously reported. In the immunohistochemical study of the cases reported previously, expression of vimentin, smooth muscle actin (SMA) and desmin was commonly observed, along with partially positive actin. No hepatocyte markers, epithelial markers, S100, CD117, CD34, myogenin, pan-cytokeratin (CK-Pan) and h-caldesmon were not found in the tissue[10]. In the of the case reported here, immunohistochemical study was positive for vimentin, SMA and desmin, and negative for HePar-1, Glypican-3, CK-Pan, myogenin, Ard-1, MYOD1, SOX10 and CD31, with an approximately 10% Ki-67 index. As can be seen, the present case is mostly similar to those reported previously for this profile.

To date, due to lack of specific manifestations in imaging examinations, hepatic MS is easily misdiagnosed as liver cancer, hepatic hydatid disease, cystadenoma and other space-occupying lesions, and it is difficult to make a diagnosis in clinical practice as well. The hepatic MS reported here was mainly observed as a cystic-solid mass with well-defined borders and regular morphology. The cystic components within the mass were separated by septa of varying thickness, with a partially visible fluid-fluid levels. After enhancement, the solid portion and septa of the mass were enhanced to different degrees, with inconspicuous regression for the degree and velocity.

CEUS of this case showed that the peripheral and internal septa of the tumor were hyper-enhanced in the arterial phase, isoenhanced in the portal and delayed phases, while in two of the seven cases reported in the literature, the portal and delayed phases were hypo-enhanced. Hence, the CEUS features of hepatic MS require more case data.

Hepatic MS needs to be differentiated from liver cancer (particularly with liquefaction and necrosis), hepatic hydatid disease, and cystadenoma. When liver cancer is accompanied by liquefaction and necrosis, three-phase non-enhanced areas in the lesions may also be found, but most of them are patchy or irregular. Moreover, the substantial portion of the mass shows high enhancement in the arterial phase, and low enhancement in the portal and delayed phases. The process behaves in a fast-in and fast-out mode. In contrast, the non-enhancing area of hepatic MS lesions was separated by the internal septa of the mass, and the parenchyma and internal septa of the mass were not significantly regressed after enhancement. Patients with liver hydatid disease generally have a history of living in pastoral areas or exposure to pathogens. The typical imaging manifestations are mainly cystic masses, showing the mother and daughter sporocysts, with varying degrees of eggshell-like cyst wall calcification, intracystic streamer sign, lily sign, and cyst-within-cyst. Liver cystadenomas are cystic-solid masses with predominantly cystic components, along with mural nodules (papillary-solid components protruding into the cystic cavity on the cyst wall) as specific signs. Mural nodules show nodular enhancement in the portal phase and can continue to enhance in the delayed phase. Imaging examination can clearly show the size, location, border, number, blood supply, and internal and surrounding adjacent tissues of the tumor. However, there is currently no characteristic diagnostic basis for the imaging manifestations of hepatic MS.

The presented case was misdiagnosed for several reasons. First, the patient had no specific clinical history, presentation and abnormal laboratory indexes. Second, the preoperative imaging images were similar to those of cystadenoma. The internal separation of the mass was uniform, the blood flow of the mass was not abundant, and there was no washout after enhancement. Therefore, imaging diagnosis was limited to benign lesions, and malignant behavior was not considered.

In summary, MS of the liver has no characteristic manifestations in clinical performance, serological indicators and imaging findings. Therefore, there is a need to accumulate a large number of cases with complete data to provide meaningful research data for the diagnosis and treatment strategies of MS of the liver.

CONCLUSION

Due to the rarity of hepatic MS, more clinical data and in-depth research are needed to further analyze its pathological mechanism, biomarkers, and imaging manifestations. Improving the understanding of the imaging manifestations of hepatic MS will help improve the preoperative diagnosis rate and assist clinicians in performing precise surgical resection and follow-up treatment.

ACKNOWLEDGEMENTS

We are very grateful to Dr. Jiang Jia-Rui (Department of Pathology, Xiangya Hospital, Central South University) for providing professional guidance to the pathological analysis.

FOOTNOTES

Author contributions: Li J wrote and edited the original draft, reviewed the literature, contributed to data collection and analysis; Huang XY contributed to assist with the patient's CEUS; Zhang B performed the patient's US and CEUS, supervised the report, provided clinical advice, reviewed, and approved the final manuscript.

Informed consent statement: Informed written consent was obtained from the patients for the publication of this report and any accompanying images.

Conflict-of-interest statement: The authors declare that they have no conflict of interest.

CARE Checklist (2016) statement: The authors have read the CARE Checklist (2016), and the manuscript was

prepared and revised according to the CARE Checklist (2016).

Country/Territory of origin: China

ORCID number: Jie Li 0000-0001-8511-8005; Xin-Yue Huang 0000-0001-6546-7427; Bo Zhang 0000-0001-8012-0560.

S-Editor: Chen YL
L-Editor: Kerr C
P-Editor: Chen YL

REFERENCES

1 **Mentzel T**, Dry S, Katenkamp D, Fletcher CD. Low-grade myofibroblastic sarcoma: analysis of 18 cases in the spectrum of myofibroblastic tumors. *Am J Surg Pathol* 1998; **22**: 1228-1238 [PMID: 9777985 DOI: 10.1097/00000478-199810000-00008]
2 **Montgomery E**, Fisher C. Myofibroblastic differentiation in malignant fibrous histiocytoma (pleomorphic myofibrosarcoma): a clinicopathological study. *Histopathology* 2001; **38**: 499-509 [PMID: 11422493 DOI: 10.1046/j.1365-2559.2001.01152.x]
3 **Fang Y**, Yan T, Bi X, Zhang H, Zhou J, Huang Z, Xie Y, Zhang L, Zhao P, Cai J. Clinicopathological and immunohistochemical study of low-grade myofibroblastic sarcoma of the liver-One case report. *Zhongliu Yanjiu Yu Linchuang* 2011; **8**: 250-253 [DOI: 10.1007/s11805-011-0590-8]
4 **Pan Y**, Wu X, Liu J, Muheremu A. Abnormal liver function induced by myofibroblastic sarcoma infiltrating the liver: A case report. *Oncol Lett* 2015; **9**: 798-800 [PMID: 25621053 DOI: 10.3892/ol.2014.2740]
5 **Yi X**, Xiao D, Long X. Myofibroblastic sarcoma in liver: a case report. *Int J Clin Exp Pathol* 2015; **8**: 1073-1076 [PMID: 25755822]
6 **Wen J**, Zhao W, Li C, Shen JY, Wen TF. High-grade myofibroblastic sarcoma in the liver: A case report. *World J Gastroenterol* 2017; **23**: 7054-7058 [PMID: 29097878 DOI: 10.3748/wjg.v23.i38.7054]
7 **Yan T**, Bi X Y, Zhang H T, Zhao J J, Zhang L, Huang Z, Zhou H T, Li C, Cai J Q. A case of malignant myofibroblastic sarcoma of the liver. *Zhongguo Zhongliu Zazhi* 2011; **33**: 477-478 [DOI: 10.1007/s11805-011-0590-8]
8 **Zhang J Y**, Luo Y. Contrast-enhanced ultrasonographic manifestations of hepatic myofibroblastic sarcoma: a case report. *Linchuang Chaosheng Yixue Zazhi* 2021; **23**: 80 [DOI: 10.11152/mu.2013.2066.163.2hhs]
9 **Chen L G**, Li J. A case of spontaneous rupture of liver myofibroblastic sarcoma. *Zhongguo Gandan Waike Zazhi* 2021; **27**: 218-219 [DOI: 10.21037/hbsn-21-102]
10 **Jo VY**, Fletcher CD. WHO classification of soft tissue tumours: an update based on the 2013 (4th) edition. *Pathology* 2014; **46**: 95-104 [PMID: 24378391 DOI: 10.1097/PAT.0000000000000050]

World Journal of Gastroenterology

Submit a Manuscript: https://www.f6publishing.com

World J Gastroenterol 2022 August 21; 28(31): 4463-4466

DOI: 10.3748/wjg.v28.i31.4463

ISSN 1007-9327 (print) ISSN 2219-2840 (online)

LETTER TO THE EDITOR

Evidence-based considerations on bowel preparation for colonoscopy

Konstantinos Argyriou, Adolfo Parra-Blanco

Specialty type: Gastroenterology and hepatology

Provenance and peer review: Unsolicited article; Externally peer reviewed

Peer-review model: Single blind

Peer-review report's scientific quality classification

Grade A (Excellent): 0
Grade B (Very good): B, B, B
Grade C (Good): 0
Grade D (Fair): 0
Grade E (Poor): 0

P-Reviewer: Basson MD, United States; Kobayashi N, Japan; Okasha H, Egypt

Received: December 20, 2021
Peer-review started: December 20, 2021
First decision: March 10, 2022
Revised: March 26, 2022
Accepted: July 24, 2022
Article in press: July 24, 2022
Published online: August 21, 2022

Konstantinos Argyriou, Department of Gastroenterology, University Hospital of Larisa, Larisa GR41334, Greece

Adolfo Parra-Blanco, Department of Gastroenterology, Nottingham University Hospitals NHS Trust, Nottingham NG51PB, United Kingdom

Corresponding author: Konstantinos Argyriou, MD, MSc, PhD, Academic Research, Consultant Physician-Scientist, Department of Gastroenterology, University Hospital of Larisa, Mezourlo, Larisa GR41334, Greece. kosnar2@doctors.org.uk

Abstract

We recently read with interest the article, "Novel frontiers of agents for bowel cleansing for colonoscopy". This is a practical narrative review, which could be of particular importance to clinicians in order to improve their current practice. Although we appreciate the venture of our colleagues, based on our in-depth analysis, we came across several minor issues in the article; hence, we present our comments in this letter. If the authors consider these comments further in their relevant research, we believe that their contribution would be of considerable importance for future studies.

Key Words: Colonoscopy; Bowel preparation; Polyethylene glycol; Post-polypectomy syndrome; Post-polypectomy complications

Core Tip: Colonoscopy is the gold standard investigation for the detection and treatment of colorectal neoplasia. The effectiveness and safety of the procedure mainly depends on the quality of bowel preparation (BP). Although international guidelines underline methods to ensure adequate BP, inadequate BP occurs in approximately one-third of the colonoscopies. The search for an ideal regimen to improve BP remains. The article by the authors addressed this issue successfully, but we detected several minor issues. Therefore, we would like to share our views and opinions on this interesting review.

Citation: Argyriou K, Parra-Blanco A. Evidence-based considerations on bowel preparation for colonoscopy. *World J Gastroenterol* 2022; 28(31): 4463-4466
URL: https://www.wjgnet.com/1007-9327/full/v28/i31/4463.htm
DOI: https://dx.doi.org/10.3748/wjg.v28.i31.4463

TO THE EDITOR

We read with great interest the frontier article, "Novel frontiers of agents for bowel cleansing for colonoscopy"[1]. Although the authors follow the infrastructure of the updated version of the European Society of Gastrointestinal Endoscopy Guideline on bowel preparation (BP) for the main part of their article, they do not make absolutely clear to the reader the way they selected the studies included in their own updated review[2]. Despite this shortcoming, in general the authors summarize the major findings of several reference studies successfully. The salient highlight of this article is that Di Leo *et al* [1] address the issue of BP holistically, from cleansing agents to the multifaceted outcomes of the currently followed BP strategies in specific populations, such as those with congestive heart failure or chronic renal failure, disclosing areas that need to be further investigated. However, we believe that the most striking point of this article is the introduction of the novel term "post colonoscopy syndrome," which sums up all the minor complications that an individual could develop post colonoscopy, worsening his/her quality of life. Therefore, this research has a strong reference and practical value for future studies, overcoming limitations. Nevertheless, through our in-depth reading, we found several shortcomings and anticipate a discussion with the authors.

Initially, we agree with the authors that the assessment of the quality of BP is of utmost importance. Adequate BP is crucial, not only to the efficacy and safety of colonoscopies but also for awarding privileges to the endoscopists[3]. However, there are no universally accepted criteria that endoscopists can use for the assessment of the quality of BP. As a result, at least five quality assessment scales have been currently fully or partially validated and used in daily practice for the assessment of the quality of BP, inducing significant heterogeneity when quality results are compared among different studies. The unanimous approval of a single scale is expected to resolve this issue but is still awaited[3]. By comparing the specific characteristics of all available scales, the authors can disclose areas that need to be further investigated, facilitating endoscopists to reach consensus. However, in this article, the authors only refer to the Ottawa Bowel Preparation Quality Scale, Boston Bowel Preparation Scale and the partially validated Aronchick Scale, excluding other validated scales, such as the Harefield Cleansing Scale, which was the first scale to be developed[3]. This limitation leaves an initial critical step underdiscussed in this review, perpetuating confusion.

In their summary of current evidence, the authors focus on high and low volume polyethylene glycol (PEG)-based preparations, leaving non-PEG-based solutions that have been found to be of equal efficacy to PEG-based formulas under-reviewed. The reason behind this exclusion is not mentioned. However, it constitutes an omission. For example, in this article, the authors do not discuss lactulose, a semi-synthetic derivative of lactose that after fermentation stimulates intestinal motility and increases osmotic pressure within the colon. Accumulated evidence from clinical trials suggest that lactulose has similar efficacy to PEG-based solutions with acceptable safety when used for BP not only in individuals undergoing ambulatory colonoscopy but also in those undergoing colonoscopy for lower gastrointestinal bleeding[4-6]. These results expand the armamentarium of our available solutions for BP; hence, all the relevant information should be supplemented in this review.

In addition to the under-discussed non-PEG based solutions, the authors provided sparse data regarding the safety of using non-PEG based and PEG-based preparations in specific populations. Although the authors quote evidence on the effectiveness and safety of these agents in various patient populations included in this review, their efficacy and safety in patients with liver cirrhosis are not examined. The reason behind this exclusion is not mentioned by the authors, leaving a critical step under-discussed in this review. Patients with cirrhosis demonstrate alterations in physiology and hemodynamics that make them vulnerable to develop electrolyte imbalances during BP[7]. Osmotically balanced solutions have been shown to be effective and safe for the management of hepatic encephalopathy in this patient population[8]. However, little is known regarding their safety when used for BP as patients with liver cirrhosis are often excluded from randomized controlled trials comparing different bowel cleansing agents. In a recent study that examined the safety and efficacy of low volume and high volume PEG based solutions in 166 patients with liver cirrhosis, it was shown that both formulations can be effectively and safely used for BP with low volume formulations showing better acceptability and compliance[9]. Considering the absence of an established BP protocol in patients with liver cirrhosis, we believe that all the relevant information should be included in this review, allowing the reader to acquire a detailed overview of the subject.

Another shortcoming lies at the reference of the agents intended to improve patient experience. More specifically, the authors suggest that the menthol candy drops improve BP in the candy drops-added group compared to controls, with no benefit in side effects. However, in the reference trial, other than

the efficacy, the trial authors state that menthol drops improved nausea (24.5% drops *vs* 4% controls; P = 0.04). Since this finding is important, this detail should be clarified[10].

Finally, the authors attempted to shed light on the pathophysiology of minor post colonoscopy complications that mainly included the symptoms of pain, discomfort and bloating, defined as post colonoscopy syndrome (PCS). We agree that the post BP changes in microbiota composition contribute to the occurrence of PCS. However, we believe that this is the tip of the iceberg. In order to understand the pathophysiology of PCS accurately, researchers should look into the complex mechanisms of abdominal pain and study the impact of BP in all of them[11]. Previous evidence suggested that mucosal changes occurring secondary to colonic over-distension during colonoscopy as well as stress, inflammation, ischemia, pH, bacterial products, immune mediators and neurotransmitters can all be related to visceral pain[12-16]. However, whether BP can have a negative impact is unknown. Future studies should aim to investigate these complex relationships and unravel the exact role of BP in the pathophysiology of PCS, as their results may allow clinicians to mitigate the negative effects and increase the individual acceptance of colonoscopy.

In summary, this review can be a valuable reference study, guiding clinicians in their daily practice. We offer our evidence-based considerations on the shortcomings of this review in an effort to further increase the value of the review and direct more comprehensive future studies. But, whether BP can have a negative impact is unknown. Future studies should aim to investigate these complex relationships and unravel the exact role of BP in the pathophysiology of PCS, as their results may allow clinicians to mitigate the negative effects and increase the individual acceptance of colonoscopy. In summary, this review can be a valuable reference study, guiding clinicians in their daily practice. We offer our evidence-based considerations on the shortcomings of this review in an effort to further increase the value of the review and direct more comprehensive future studies.

FOOTNOTES

Author contributions: Argyriou K and Parra-Blanco A designed and performed the research; Argyriou K wrote this comment; Parra-Blanco A revised the manuscript.

Conflict-of-interest statement: All the authors report no relevant conflicts of interest for this article.

Country/Territory of origin: Greece

ORCID number: Konstantinos Argyriou 0000-0002-2026-9678; Adolfo Parra-Blanco 0030226.

S-Editor: Wang JJ
L-Editor: Filipodia
P-Editor: Wang JJ

REFERENCES

1 **Di Leo M**, Iannone A, Arena M, Losurdo G, Palamara MA, Iabichino G, Consolo P, Rendina M, Luigiano C, Di Leo A. Novel frontiers of agents for bowel cleansing for colonoscopy. *World J Gastroenterol* 2021; **27**: 7748-7770 [PMID: 34963739 DOI: 10.3748/wjg.v27.i45.7748]

2 **Hassan C**, East J, Radaelli F, Spada C, Benamouzig R, Bisschops R, Bretthauer M, Dekker E, Dinis-Ribeiro M, Ferlitsch M, Fuccio L, Awadie H, Gralnek I, Jover R, Kaminski MF, Pellisé M, Triantafyllou K, Vanella G, Mangas-Sanjuan C, Frazzoni L, Van Hooft JE, Dumonceau JM. Bowel preparation for colonoscopy: European Society of Gastrointestinal Endoscopy (ESGE) Guideline - Update 2019. *Endoscopy* 2019; **51**: 775-794 [PMID: 31295746 DOI: 10.1055/a-0959-0505]

3 **Kastenberg D**, Bertiger G, Brogadir S. Bowel preparation quality scales for colonoscopy. *World J Gastroenterol* 2018; **24**: 2833-2843 [PMID: 30018478 DOI: 10.3748/wjg.v24.i26.2833]

4 **Jagdeep J**, Sawant G, Lal P, Bains L. Oral Lactulose vs. Polyethylene Glycol for Bowel Preparation in Colonoscopy: A Randomized Controlled Study. *Cureus* 2021; **13**: e14363 [PMID: 33972914 DOI: 10.7759/cureus.14363]

5 **Menacho AM**, Reimann A, Hirata LM, Ganzerella C, Ivano FH, Sugisawa R. Double-blind prospective randomized study comparing polyethylene glycol to lactulose for bowel preparation in colonoscopy. *Arq Bras Cir Dig* 2014; **27**: 9-12 [PMID: 24676290 DOI: 10.1590/s0102-67202014000100003]

6 **Li CX**, Guo Y, Zhu YJ, Zhu JR, Xiao QS, Chen DF, Lan CH. Comparison of Polyethylene Glycol versus Lactulose Oral Solution for Bowel Preparation prior to Colonoscopy. *Gastroenterol Res Pract* 2019; **2019**: 2651450 [PMID: 31097959 DOI: 10.1155/2019/2651450]

7 **Belsey J**, Epstein O, Heresbach D. Systematic review: oral bowel preparation for colonoscopy. *Aliment Pharmacol Ther* 2007; **25**: 373-384 [PMID: 17269992 DOI: 10.1111/j.1365-2036.2006.03212.x]

8 **Pontone S**, Angelini R, Standoli M, Patrizi G, Culasso F, Pontone P, Redler A. Low-volume plus ascorbic acid *vs* high-volume plus simethicone bowel preparation before colonoscopy. *World J Gastroenterol* 2011; **17**: 4689-4695 [PMID: 22180711 DOI: 10.3748/wjg.v17.i42.4689]

9 **Lee JM**, Lee JH, Kim ES, Lee JM, Yoo IK, Kim SH, Choi HS, Keum B, Seo YS, Jeen YT, Lee HS, Chun HJ, Um SH, Kim CD. The safety and effectiveness of 2-liter polyethylene glycol plus ascorbic acid in patients with liver cirrhosis: A retrospective observational study. *Medicine (Baltimore)* 2017; **96**: e9011 [PMID: 29390432 DOI: 10.1097/MD.0000000000009011]

10 **Sharara AI**, El-Halabi MM, Abou Fadel CG, Sarkis FS. Sugar-free menthol candy drops improve the palatability and bowel cleansing effect of polyethylene glycol electrolyte solution. *Gastrointest Endosc* 2013; **78**: 886-891 [PMID: 23769143 DOI: 10.1016/j.gie.2013.05.015]

11 **Pusceddu MM**, Gareau MG. Visceral pain: gut microbiota, a new hope? *J Biomed Sci* 2018; **25**: 73 [PMID: 30309367 DOI: 10.1186/s12929-018-0476-7]

12 **Sengupta JN**. Visceral pain: the neurophysiological mechanism. *Handb Exp Pharmacol* 2009; 31-74 [PMID: 19655104 DOI: 10.1007/978-3-540-79090-7_2]

13 **Million M**, Wang L, Wang Y, Adelson DW, Yuan PQ, Maillot C, Coutinho SV, Mcroberts JA, Bayati A, Mattsson H, Wu V, Wei JY, Rivier J, Vale W, Mayer EA, Taché Y. CRF2 receptor activation prevents colorectal distension induced visceral pain and spinal ERK1/2 phosphorylation in rats. *Gut* 2006; **55**: 172-181 [PMID: 15985561 DOI: 10.1136/gut.2004.051391]

14 **Ochoa-Cortes F**, Guerrero-Alba R, Valdez-Morales EE, Spreadbury I, Barajas-Lopez C, Castro M, Bertrand J, Cenac N, Vergnolle N, Vanner SJ. Chronic stress mediators act synergistically on colonic nociceptive mouse dorsal root ganglia neurons to increase excitability. *Neurogastroenterol Motil* 2014; **26**: 334-345 [PMID: 24286174 DOI: 10.1111/nmo.12268]

15 **Vanner S**, Greenwood-Van Meerveld B, Mawe G, Shea-Donohue T, Verdu EF, Wood J, Grundy D. Fundamentals of Neurogastroenterology: Basic Science. *Gastroenterology* 2016 [PMID: 27144618 DOI: 10.1053/j.gastro.2016.02.018]

16 **Gayer CP**, Basson MD. The effects of mechanical forces on intestinal physiology and pathology. *Cell Signal* 2009; **21**: 1237-1244 [PMID: 19249356 DOI: 10.1016/j.cellsig.2009.02.011]

World Journal of Gastroenterology

Submit a Manuscript: https://www.f6publishing.com

World J Gastroenterol 2022 August 21; 28(31): 4467-4470

DOI: 10.3748/wjg.v28.i31.4467

ISSN 1007-9327 (print) ISSN 2219-2840 (online)

LETTER TO THE EDITOR

Influence of different portal vein branches on hepatic encephalopathy during intrahepatic portal shunt *via* jugular vein

Xin Yao, Sheng He, Meng Wei, Jian-Ping Qin

Specialty type: Gastroenterology and hepatology

Provenance and peer review: Unsolicited article; Externally peer reviewed.

Peer-review model: Single blind

Peer-review report's scientific quality classification

Grade A (Excellent): A
Grade B (Very good): B
Grade C (Good): C
Grade D (Fair): 0
Grade E (Poor): 0

P-Reviewer: De Gregorio MA, Spain; Kordzaia D, Georgia; Wondmagegn H, Ethiopia

Received: February 11, 2022
Peer-review started: February 11, 2022
First decision: April 5, 2022
Revised: April 7, 2022
Accepted: July 22, 2022
Article in press: July 22, 2022
Published online: August 21, 2022

Xin Yao, Sheng He, Meng Wei, Jian-Ping Qin, Department of Gastroenterology, General Hospital of Western Theater Command, Chengdu 610083, Sichuan Province, China

Corresponding author: Jian-Ping Qin, MD, Chief Doctor, Doctor, Department of Gastroenterology, General Hospital of Western Theater Command, No. 270 Rongdu Road, Chengdu 610083, Sichuan Province, China. jpqqing@163.com

Abstract

This letter is regarding the study titled 'Targeted puncture of left branch of intrahepatic portal vein in transjugular intrahepatic portosystemic shunt (TIPS) to reduce hepatic encephalopathy'. Prior to the approval of TIPS dedicated stents (Viatorr stents) in China in October 2015, Fluency covered stents were typically used. As Fluency covered stents have a strong support force and axial elastic tension, a 'cap' may form if the stent is located too low at the end of the hepatic vein or too short at the end of the portal vein during surgery, leading to stent dysfunction. Since the blood shunted by the stent is from the main trunk of the portal vein, the correlation between the incidence of postoperative hepatic encephalopathy and the location of the puncture target (left or right portal vein branch) is worth discussion. Notably, no studies in China or foreign countries have proven the occurrence of left and right blood stratification after the accumulation of splenic vein and mesenteric blood flow in the main trunk of the portal vein in patients with cirrhotic portal hypertension.

Key Words: Viatorr stent; Portosystemic shunt; Transjugular intrahepatic; Hypertension; portal; Left and right portal vein branches

Core Tip: This Letter to the Editor aims to analyse the effect of establishing a shunt in the left or right portal vein branch in transjugular intrahepatic portosystemic shunt on the incidence of postoperative hepatic encephalopathy in patients with cirrhotic portal hypertension. Based on preliminary clinical experience, it is thought that there is no difference in the incidence of hepatic encephalopathy among patients regardless of the use of a COOK bare stent or Viatorr stent with an inner diameter of 8 mm if a shunt is established in the left or right portal vein branch.

Citation: Yao X, He S, Wei M, Qin JP. Influence of different portal vein branches on hepatic encephalopathy during intrahepatic portal shunt *via* jugular vein. *World J Gastroenterol* 2022; 28(31): 4467-4470
URL: https://www.wjgnet.com/1007-9327/full/v28/i31/4467.htm
DOI: https://dx.doi.org/10.3748/wjg.v28.i31.4467

TO THE EDITOR

We read the article of Luo *et al*[1] titled "Targeted puncture of left branch of intrahepatic portal vein in transjugular intrahepatic portosystemic shunt (TIPS) to reduce hepatic encephalopathy" and are very interested in its conclusions. We think that therapy by "targeted puncture of the left branch of the intrahepatic portal vein in TIPS to reduce hepatic encephalopathy" is worthy of discussion.

First, Luo *et al*[1] performed a retrospective analysis of portal hypertension patients receiving TIPS from January 2000 to January 2013. During this period, a shunt was established using a Fluency stent (BARD, Voisins le Bretonneux, France) or Viatorr stent (W.L. Gore & Associates, Flagstaff, AZ, United States). However, the shunts were established in TIPS mainly using Fluency covered stents in China before the approval of TIPS dedicated stents (Viatorr stents) in China in October 2015. As Fluency covered stents have a strong support force and axial elastic tension, a 'cap' may form if the stent is located too low at the end of the hepatic vein or too short at the end of the portal vein during the operation, thereby leading to stent dysfunction. Since the blood shunted by the stent is from the main trunk of the portal vein, as shown in Figure 2 of Luo *et al*'s paper (the stent is inserted into the main trunk of the portal vein at the end of the portal vein for shunts in both the left and right portal vein branches), the correlation between the incidence of postoperative hepatic encephalopathy and the location of the puncture target (left or right portal vein branch) is worthy of discussion.

As pointed out by Luo *et al*[1], prior studies have reported that the backflow blood from the splenic and superior mesenteric veins is not thoroughly mixed but rather enters the left and right portal vein branches separately, *i.e.*, the blood from the superior mesenteric vein mainly flows into the right branch, while the blood from the splenic vein mainly flows into the left branch[2-3]. In a study on corrosion casting of the portal vein and hepatic artery ramifications in dogs, this study focused on explaining the anatomical features of the hepatic portal vein and hepatic artery in animals instead of the blood flow features of the portal vein system[2]. The author team believes that a substantial difference between animals and humans. In a study using carbon dioxide angiography, iodinated contrast medium was used to replace traditional angiography[3]. This study included chronic liver disease patients receiving percutaneous transhepatic puncture of the portal vein with the tube inserted into the splenic vein; a mechanical injection system was used to inject a total volume of 30 mL of contrast medium at a speed of 5 mL/s. Notably, a difference was observed in blood mixing at the left and right sides of the main trunk of the portal vein. An early study conducted in United States of America found that an increase in the pressure in the portal vein was followed by a decrease in hepatic blood inflow and blood flow rate and grading of liver function due to hepatic sinusoidal obstruction, perisinusoidal fibrosis and portal vein obstruction in cirrhosis was related to the portal blood flow rate; furthermore, portal hypertensive liver function damage was obvious, and the portal blood flow rate was low[4]. In the hyperdynamic splanchnic circulatory state, the progressive decrease in the portal blood flow rate suggests aggravation of hepatic parenchymal lesions and increased portal blood flow resistance. The author team believes that the blood flow rate decreased after splenic vein and mesenteric blood flows accumulated in the main trunk of the portal vein in cirrhotic portal hypertension patients, and so it was necessary to define the presence of different blood flow rates after the blood flows accumulated in the main trunk of the portal vein so as to achieve left and right blood stratification in the natural state. However, it is controversial at home and abroad whether there is difference between splenic vein blood flow velocity and mesenteric blood flow velocity in cirrhotic patients with portal hypertension after the accumulation of the main portal vein in the natural state. In a study conducted in 2020 in China, 15 patients with liver cirrhosis and upper gastrointestinal haemorrhage received TIPS, and blood samples were collected from the left branch, right branch and main trunk of the portal vein during the operation[5]. In these patients, the plasma ammonia concentration (μmol/L) was 96.4 ± 17.6 for the left branch *vs* 113.5 ± 18.4 for the right branch *vs* 106.9 ± 38.7 for the main trunk, without any statistically significant differences ($P > 0.05$). This study provides important evidence for the comparison of blood bacterial metabolites in the left and right branches of the cirrhotic portal vein.

TIPS dedicated stents (Viatorr stents) have been adopted for surgery at the Center since March 2016. In previous studies, COOK bare stents with an inner diameter of 8 mm were used to establish a shunt[6-7]. Although such a stent should be long enough at the end of the portal vein, the shunted blood was from the portal vein branches, so whether a shunt was established in the left or right portal vein branch had no significant effect on the incidence of hepatic encephalopathy. In a study conducted in China in 2020, 120 cirrhotic portal hypertension patients received TIPS using Viatorr stents. Intraoperative portal vein angiography showed that a shunt was established in the left portal vein branch for 52 patients and in the right portal vein branch for 68 patients[8]. There was no statistically significant difference in the

incidence of postoperative hepatic encephalopathy (χ^2 = 0.159, P = 0.69) between the left portal vein and right portal vein branch shunting groups. A recent study reported that the incidence of hepatic encephalopathy decreased significantly by controlling the inner diameter of the stent, *i.e.*, using a Viatorr stent with an inner diameter of 8 mm[9]. The bare area of a Viatorr stent may guarantee a smooth blood flow in the portal vein and prevent more blood not metabolised by the liver from directly entering the systemic circulation.

There is no information in the TIPS guidelines circulated in North America regarding differences in the incidence of postoperative hepatic encephalopathy when shunts are established in different portal vein branches[10-11]. We believe that there are no differences in the incidence of hepatic encephalopathy among postoperative patients when using a Viatorr stent with an inner diameter of 8 mm when the shunt is established in the left or right portal vein branch. As the postoperative medium and long-term efficacy of TIPS are related to clinical procedures, postoperative management of patients and other factors, future studies with larger sample sizes and multicentre randomised controlled trials are warranted.

FOOTNOTES

Author contributions: All authors wrote and edited the manuscript.

Conflict-of-interest statement: The authors declare no competing interests for this manuscript.

Country/Territory of origin: China

ORCID number: Xin Yao 0000-0002-9977-6153; Sheng He 0000-0002-4468-0728; Meng Wei 0000-0001-6197-9812; Jian-Ping Qin 0000-0001-7834-8830.

S-Editor: Chang KL
L-Editor: A
P-Editor: Chang KL

REFERENCES

1 **Luo SH**, Chu JG, Huang H, Zhao GR, Yao KC. Targeted puncture of left branch of intrahepatic portal vein in transjugular intrahepatic portosystemic shunt to reduce hepatic encephalopathy. *World J Gastroenterol* 2019; **25**: 1088-1099 [PMID: 30862997 DOI: 10.3748/wjg.v25.i9.1088]

2 **Ursic M**, Ravnik D, Hribernik M, Pecar J, Butinar J, Fazarinc G. Gross anatomy of the portal vein and hepatic artery ramifications in dogs: corrosion cast study. *Anat Histol Embryol* 2007; **36**: 83-87 [PMID: 17371378 DOI: 10.1111/j.1439-0264.2006.00719.x]

3 **Maruyama H**, Okugawa H, Ishibashi H, Takahashi M, Kobayashi S, Yoshizumi H, Yokosuka O. Carbon dioxide-based portography: an alternative to conventional imaging with the use of iodinated contrast medium. *J Gastroenterol Hepatol* 2010; **25**: 1111-1116 [PMID: 20594227 DOI: 10.1111/j.1440-1746.2010.06248.x]

4 **Ljubicić N**, Duvnjak M, Rotkvić I, Kopjar B. Influence of the degree of liver failure on portal blood flow in patients with liver cirrhosis. *Scand J Gastroenterol* 1990; **25**: 395-400 [PMID: 2186474 DOI: 10.3109/00365529009095505]

5 **Deng LYY**, Chen Y, Ye P, Liao HF, Zhen QL, Xie ZG, Zhao GR, Yao KC. Preliminary analysis of liver-related blood components in portal system *via* TIPS approach. *J Intervent Radiol* 2020; **29**: 608-661 [DOI: 10.3969/j.issn.1008-794X.2020.06.018]

6 **Qin JP**, Jiang MD, Tang W, Wu XL, Yao X, Zeng WZ, Xu H, He QW, Gu M. Clinical effects and complications of TIPS for portal hypertension due to cirrhosis: a single center. *World J Gastroenterol* 2013; **19**: 8085-8092 [PMID: 24307804 DOI: 10.3748/wjg.v19.i44.8085]

7 **Qin JP**, Tang SH, Jiang MD, He QW, Chen HB, Yao X, Zeng WZ, Gu M. Contrast enhanced computed tomography and reconstruction of hepatic vascular system for transjugular intrahepatic portal systemic shunt puncture path planning. *World J Gastroenterol* 2015; **21**: 9623-9629 [PMID: 26327770 DOI: 10.3748/wjg.v21.i32.9623]

8 **Yao X**, Zhou H, Tang SH, Huang S, Chen XL, Qin JP. Effect of intraoperative Viatorr stent implantation for shunting of blood flow in the left or right branch of the portal vein and its effect on clinical outcome in patients with cirrhotic portal hypertension undergoing transjugular intrahepatic portosystemic shunt. *J Clin Hepatol* 2020; **36**: 1970-1974 [DOI: 10.3969/j.issn.1001-5256.2020.09.012]

9 **Yao X**, Zhou H, Huang S, Tang SH, Qin JP. Effects of transjugular intrahepatic portosystemic shunt using the Viatorr stent on hepatic reserve function in patients with cirrhosis. *World J Clin Cases* 2021; **9**: 1532-1542 [PMID: 33728297 DOI:

10.12998/wjcc.v9.i7.1532]

10 **Boyer TD**, Haskal ZJ; American Association for the Study of Liver Diseases. The Role of Transjugular Intrahepatic Portosystemic Shunt (TIPS) in the Management of Portal Hypertension: update 2009. *Hepatology* 2010; **51**: 306 [PMID: 19902484 DOI: 10.1002/hep.23383]

11 **Boike JR**, Thornburg BG, Asrani SK, Fallon MB, Fortune BE, Izzy MJ, Verna EC, Abraldes JG, Allegretti AS, Bajaj JS, Biggins SW, Darcy MD, Farr MA, Farsad K, Garcia-Tsao G, Hall SA, Jadlowiec CC, Krowka MJ, Laberge J, Lee EW, Mulligan DC, Nadim MK, Northup PG, Salem R, Shatzel JJ, Shaw CJ, Simonetto DA, Susman J, Kolli KP, VanWagner LB; Advancing Liver Therapeutic Approaches (ALTA) Consortium. North American Practice-Based Recommendations for Transjugular Intrahepatic Portosystemic Shunts in Portal Hypertension. *Clin Gastroenterol Hepatol* 2021 [PMID: 34274511 DOI: 10.1016/j.cgh.2021.07.018]

World Journal of Gastroenterology

Submit a Manuscript: https://www.f6publishing.com

World J Gastroenterol 2022 August 21; 28(31): 4471-4474

DOI: 10.3748/wjg.v28.i31.4471

ISSN 1007-9327 (print) ISSN 2219-2840 (online)

LETTER TO THE EDITOR

Promising role of D-amino acids in irritable bowel syndrome

Yuka Ikeda, Kurumi Taniguchi, Haruka Sawamura, Ai Tsuji, Satoru Matsuda

Specialty type: Gastroenterology and hepatology

Provenance and peer review: Invited article; Externally peer reviewed.

Peer-review model: Single blind

Peer-review report's scientific quality classification

Grade A (Excellent): 0
Grade B (Very good): B, B
Grade C (Good): C
Grade D (Fair): 0
Grade E (Poor): 0

P-Reviewer: Gobin I; Ji G, China; Mamieva Z, Russia

Received: April 4, 2022
Peer-review started: April 4, 2022
First decision: May 29, 2022
Revised: June 14, 2022
Accepted: July 20, 2022
Article in press: July 20, 2022
Published online: August 21, 2022

Yuka Ikeda, Kurumi Taniguchi, Haruka Sawamura, Ai Tsuji, Satoru Matsuda, Department of Food Science and Nutrition, Nara Women's University, Nara 630-8506, Japan

Corresponding author: Satoru Matsuda, MD, PhD, Professor, Department of Food Science and Nutrition, Nara Women's University, Kita-Uoya Nishimachi, Nara 630-8506, Japan. smatsuda@cc.nara-wu.ac.jp

Abstract

Irritable bowel syndrome (IBS) is an important health care concern. Alterations in the microbiota of the gut-brain axis may be linked to the pathophysiology of IBS. Some dietary intake could contribute to produce various metabolites including D-amino acids by the fermentation by the gut microbiota. D-amino acids are the enantiomeric counterparts of L-amino acids, in general, which could play key roles in cellular physiological processes against various oxidative stresses. Therefore, the presence of D-amino acids has been shown to be linked to the protection of several organs in the body. In particular, the gut microbiota could play significant roles in the stability of emotion *via* the action of D-amino acids. Here, we would like to shed light on the roles of D-amino acids, which could be used for the treatment of IBS.

Key Words: Irritable bowel syndrome; D-amino acid; Gut microbiota; Colitis; Probiotics; Fecal microbiota transplantation

Core Tip: The potential efficacy of D-amino acids for the treatment of irritable bowel syndrome is shown here.

Citation: Ikeda Y, Taniguchi K, Sawamura H, Tsuji A, Matsuda S. Promising role of D-amino acids in irritable bowel syndrome. *World J Gastroenterol* 2022; 28(31): 4471-4474
URL: https://www.wjgnet.com/1007-9327/full/v28/i31/4471.htm
DOI: https://dx.doi.org/10.3748/wjg.v28.i31.4471

TO THE EDITOR

With great interest, we have read the article by Mamieva *et al*[1]. As irritable bowel

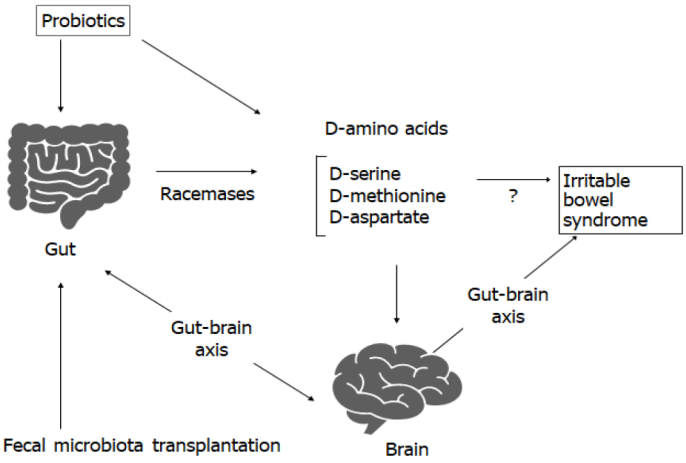

DOI: 10.3748/wjg.v28.i31.4471 **Copyright** ©The Author(s) 2022.

Figure 1 Gut microbiota could contribute to the production of D-amino acids, which might play key roles in irritable bowel syndrome *via* direct action on the gut and/or indirect action through the gut-brain axis with emotional stability. Fecal microbiota transplantation consists of fecal microbiota infusion from a healthy donor into a recipient subject, which has been also shown to be a promising therapy for irritable bowel syndrome. Arrowheads mean stimulation and/or augmentation whereas hammerheads represent inhibition. Note that some critical events such as reactive oxygen species production, immune activation, and/or cytokine-induction have been omitted for clarity.

syndrome (IBS) could exacerbate the patients' quality of life, it is a considerable health care concern. Although the underlying pathophysiological mechanisms are not clear, the role of low-grade inflammation and mucosal immune activation appears to be obvious in the signs of IBS. IBS is a functional gastrointestinal disorder, and some probiotic supplementation may reduce the symptoms[2]. In addition, fecal microbiota transplantation expects recommendations for the treatment of IBS, suggesting that alterations in the gut microbiota-brain axis are linked to the pathophysiology of IBS (Figure 1). It has been revealed that some cytokines and neurotransmitters as well as several microbial metabolites including short chain fatty acids (SCFAs) such as acetate, lactate, butyrate, and propionate produced by the bacteria in the gut could modulate the integrity of brain function[1]. The bidirectional communication between the gut microbiota and the brain is well-known as the gut-brain axis, which could play an important role in the stability of emotion[3]. As shown in the article by Mamieva *et al*[1], the microbiota could influence the pathogenetic factors of IBS through the production of several microbial metabolites. Here, we would like to add the efficacy of D-amino acids for the alteration of IBS condition.

Mice treated with D-serine prior to the induction of colitis exhibited a reduction in the colonic inflammation that was not seen in mice fed L-serine[4]. In addition, D-serine efficiently suppressed the progression of chronic colitis. Therefore, D-serine might have effective properties as a preventive strategy and/or a treatment for colitis[4]. In addition, several studies have shown the significance of D-amino acids in clinical usage[5]. For example, D-methionine protects against the intestinal damage through anti-oxidative and anti-inflammatory effects, which could improve the gut microbiome imbalance by enhancing the growth of beneficial bacteria[6]. Protective effects of low-dose D-serine have been also shown to suppress the renal damage, which may promote the proliferation of kidney epithelial cells[7]. In addition, D-cysteine administration could defend the kidney from ischemia-reperfusion injury, which may be beneficial for the treatment of several renal diseases[8]. Gastroprotective effect with D-cysteine but not with L-cysteine has been shown *via* the effects of decreasing cellular damage, edema, and epithelium loss[9]. Treatment with D-aspartate may bring positive effects in the nervous system[10]. Furthermore, D-cycloserine is a glutamatergic N-methyl-D-aspartate receptor agonist which has been revealed to support the stability of emotion[11]. Furthermore, the activity of ovarian development with D-tryptophan is more effective than that with L-tryptophan[12]. These data suggest that D-amino acids could have beneficial and/or protective effects on various tissues, which might be favorable to the treatment of IBS (Figure 1). In particular, the emotional stability *via* the action of D-amino acids seems to be important[13], because it has been shown that different types of physiological and/or psychological stressors are known to contribute to the development, maintenance, and exacerbation of IBS[14].

The gut microbiota has a large genetic capacity to produce D-amino acids which are utilized as nutrients to support bacterial growth[15]. D-amino acids are essential elements of peptidoglycans in the cell wall of bacteria. Hence, higher levels of D-amino acids have been basically related to the mass of the gut microbiota[16]. Many bacterial species encode specific racemases that can convert L-amino acids to D-amino acids, which are frequently present in the peptidoglycan-containing bacteria in the gut microbiota[17]. Accordingly, the lumen of the gastro-intestinal tract in mammals may be rich in free D-amino acids that might be derived from such bacteria or fermented foods. Probably, the source of D-

amino acids in mammals may mostly be from their gut microbiota. For example, D-alanine production is linked to the relative abundance of bacterial species such as *Enterococcus* and *Lactobacillus* in the gut microbiota[18]. Therefore, the metabolism of D-amino acids in the body might be modified by the alteration of gut bacterial communities affecting the host health and/or homeostasis[19]. Reduction of the amount of several D-amino acids may promote senescence through the increase of reactive oxygen species production[20,21].

FOOTNOTES

Author contributions: Ikeda Y and Matsuda S contributed equally to this work; Ikeda Y, Taniguchi K, Sawamura H, Tsuji A, and Matsuda S designed the research study and wrote the manuscript; and all authors have read and approved the final manuscript.

Conflict-of-interest statement: All authors report no relevant conflicts of interest for this article.

Country/Territory of origin: Japan

ORCID number: Yuka Ikeda 0000-0003-4805-1758; Ai Tsuji 0000-0003-1619-7592; Satoru Matsuda 0000-0003-4274-5345.

S-Editor: Ma YJ
L-Editor: Wang TQ
P-Editor: Ma YJ

REFERENCES

1 **Mamieva Z**, Poluektova E, Svistushkin V, Sobolev V, Shifrin O, Guarner F, Ivashkin V. Antibiotics, gut microbiota, and irritable bowel syndrome: What are the relations? *World J Gastroenterol* 2022; **28**: 1204-1219 [PMID: 35431513 DOI: 10.3748/wjg.v28.i12.1204]
2 **Lee J**, Park SB, Kim HW, Lee HS, Jee SR, Lee JH, Kim TO. Clinical Efficacy of Probiotic Therapy on Bowel-Related Symptoms in Patients with Ulcerative Colitis during Endoscopic Remission: An Observational Study. *Gastroenterol Res Pract* 2022; **2022**: 9872230 [PMID: 35082846 DOI: 10.1155/2022/9872230]
3 **Barberio B**, Zamani M, Black CJ, Savarino EV, Ford AC. Prevalence of symptoms of anxiety and depression in patients with inflammatory bowel disease: a systematic review and meta-analysis. *Lancet Gastroenterol Hepatol* 2021; **6**: 359-370 [PMID: 33721557 DOI: 10.1016/S2468-1253(21)00014-5]
4 **Asakawa T**, Onizawa M, Saito C, Hikichi R, Yamada D, Minamidate A, Mochimaru T, Asahara SI, Kido Y, Oshima S, Nagaishi T, Tsuchiya K, Ohira H, Okamoto R, Watanabe M. Oral administration of D-serine prevents the onset and progression of colitis in mice. *J Gastroenterol* 2021; **56**: 732-745 [PMID: 34148144 DOI: 10.1007/s00535-021-01792-1]
5 **Müller C**, Fonseca JR, Rock TM, Krauss-Etschmann S, Schmitt-Kopplin P. Enantioseparation and selective detection of D-amino acids by ultra-high-performance liquid chromatography/mass spectrometry in analysis of complex biological samples. *J Chromatogr A* 2014; **1324**: 109-114 [PMID: 24315356 DOI: 10.1016/j.chroma.2013.11.026]
6 **Wu CH**, Ko JL, Liao JM, Huang SS, Lin MY, Lee LH, Chang LY, Ou CC. D-methionine alleviates cisplatin-induced mucositis by restoring the gut microbiota structure and improving intestinal inflammation. *Ther Adv Med Oncol* 2019; **11**: 1758835918821021 [PMID: 30792823 DOI: 10.1177/1758835918821021]
7 **Nakade Y**, Iwata Y, Furuichi K, Mita M, Hamase K, Konno R, Miyake T, Sakai N, Kitajima S, Toyama T, Shinozaki Y, Sagara A, Miyagawa T, Hara A, Shimizu M, Kamikawa Y, Sato K, Oshima M, Yoneda-Nakagawa S, Yamamura Y, Kaneko S, Miyamoto T, Katane M, Homma H, Morita H, Suda W, Hattori M, Wada T. Gut microbiota-derived D-serine protects against acute kidney injury. *JCI Insight* 2018; **3** [PMID: 30333299 DOI: 10.1172/jci.insight.97957]
8 **Kimura H**. The physiological role of hydrogen sulfide and beyond. *Nitric Oxide* 2014; **41**: 4-10 [PMID: 24491257 DOI: 10.1016/j.niox.2014.01.002]
9 **Souza LK**, Araújo TS, Sousa NA, Sousa FB, Nogueira KM, Nicolau LA, Medeiros JV. Evidence that d-cysteine protects mice from gastric damage *via* hydrogen sulfide produced by d-amino acid oxidase. *Nitric Oxide* 2017; **64**: 1-6 [PMID: 28137610 DOI: 10.1016/j.niox.2017.01.010]
10 **de Rosa V**, Secondo A, Pannaccione A, Ciccone R, Formisano L, Guida N, Crispino R, Fico A, Polishchuk R, D'Aniello A, Annunziato L, Boscia F. D-Aspartate treatment attenuates myelin damage and stimulates myelin repair. *EMBO Mol Med* 2019; **11** [PMID: 30559305 DOI: 10.15252/emmm.201809278]
11 **Levinson CA**, Rodebaugh TL, Fewell L, Kass AE, Riley EN, Stark L, McCallum K, Lenze EJ. D-Cycloserine facilitation of exposure therapy improves weight regain in patients with anorexia nervosa: a pilot randomized controlled trial. *J Clin Psychiatry* 2015; **76**: e787-e793 [PMID: 26132687 DOI: 10.4088/JCP.14m09299]
12 **Kobayashi K**, Maezawa T, Tanaka H, Onuki H, Horiguchi Y, Hirota H, Ishida T, Horiike K, Agata Y, Aoki M, Hoshi M,

Matsumoto M. The identification of D-tryptophan as a bioactive substance for postembryonic ovarian development in the planarian Dugesia ryukyuensis. *Sci Rep* 2017; **7**: 45175 [PMID: 28338057 DOI: 10.1038/srep45175]

13 **Taniguchi K**, Sawamura H, Ikeda Y, Tsuji A, Kitagishi Y, Matsuda S. D-Amino Acids as a Biomarker in Schizophrenia. *Diseases* 2022; **10** [PMID: 35225861 DOI: 10.3390/diseases10010009]

14 **Raskov H**, Burcharth J, Pommergaard HC, Rosenberg J. Irritable bowel syndrome, the microbiota and the gut-brain axis. *Gut Microbes* 2016; **7**: 365-383 [PMID: 27472486 DOI: 10.1080/19490976.2016.1218585]

15 **Macfarlane GT**, Macfarlane S. Bacteria, colonic fermentation, and gastrointestinal health. *J AOAC Int* 2012; **95**: 50-60 [PMID: 22468341 DOI: 10.5740/jaoacint.sge_macfarlane]

16 **Sasabe J**, Miyoshi Y, Rakoff-Nahoum S, Zhang T, Mita M, Davis BM, Hamase K, Waldor MK. Interplay between microbial D-amino acids and host D-amino acid oxidase modifies murine mucosal defence and gut microbiota. *Nat Microbiol* 2016; **1**: 16125 [PMID: 27670111 DOI: 10.1038/nmicrobiol.2016.125]

17 **Cava F**, Lam H, de Pedro MA, Waldor MK. Emerging knowledge of regulatory roles of D-amino acids in bacteria. *Cell Mol Life Sci* 2011; **68**: 817-831 [PMID: 21161322 DOI: 10.1007/s00018-010-0571-8]

18 **Gilmore MS**, Skaugen M, Nes I. Enterococcus faecalis cytolysin and lactocin S of Lactobacillus sake. *Antonie Van Leeuwenhoek* 1996; **69**: 129-138 [PMID: 8775973 DOI: 10.1007/BF00399418]

19 **Kawase T**, Nagasawa M, Ikeda H, Yasuo S, Koga Y, Furuse M. Gut microbiota of mice putatively modifies amino acid metabolism in the host brain. *Br J Nutr* 2017; **117**: 775-783 [PMID: 28393748 DOI: 10.1017/S0007114517000678]

20 **Nagano T**, Yamao S, Terachi A, Yarimizu H, Itoh H, Katasho R, Kawai K, Nakashima A, Iwasaki T, Kikkawa U, Kamada S. D-amino acid oxidase promotes cellular senescence *via* the production of reactive oxygen species. *Life Sci Alliance* 2019; **2** [PMID: 30659069 DOI: 10.26508/lsa.201800045]

21 **Canteros MG**. D-Arginine as a neuroprotective amino acid: promising outcomes for neurological diseases. *Drug Discov Today* 2014; **19**: 627-636 [PMID: 24252866 DOI: 10.1016/j.drudis.2013.11.010]

Published by **Baishideng Publishing Group Inc**
7041 Koll Center Parkway, Suite 160, Pleasanton, CA 94566, USA
Telephone: +1-925-3991568
E-mail: bpgoffice@wjgnet.com
Help Desk: https://www.f6publishing.com/helpdesk
https://www.wjgnet.com